



A blue-toned scanning electron micrograph (SEM) showing a dense cluster of *Salmonella* bacteria. The bacteria are rod-shaped and appear to be attached to a surface or each other, forming a complex network of filaments.

Heide Schatten
Abraham Eisenstark *Editors*

Salmonella

Methods and Protocols
Second Edition

METHODS IN MOLECULAR BIOLOGY

Series Editor
John M. Walker
School of Life Sciences
University of Hertfordshire
Hatfield, Hertfordshire, AL10 9AB, UK

For further volumes:
<http://www.springer.com/series/7651>

Salmonella

Methods and Protocols

Second Edition

Edited by

Heide Schatten

Department of Veterinary Pathobiology, University of Missouri, Columbia, MO, USA

Abraham Eisenstark

Cancer Research Center, University of Missouri, Columbia, MO, USA

 **Humana Press**

Editors

Heide Schatten
Department of Veterinary Pathobiology
University of Missouri
Columbia, MO, USA

Abraham Eisenstark
Cancer Research Center
University of Missouri
Columbia, MO, USA

ISSN 1064-3745 ISSN 1940-6029 (electronic)
ISBN 978-1-4939-1624-5 ISBN 978-1-4939-1625-2 (eBook)
DOI 10.1007/978-1-4939-1625-2
Springer New York Heidelberg Dordrecht London

Library of Congress Control Number: 2014948260

© Springer Science+Business Media New York 2015

This work is subject to copyright. All rights are reserved by the Publisher, whether the whole or part of the material is concerned, specifically the rights of translation, reprinting, reuse of illustrations, recitation, broadcasting, reproduction on microfilms or in any other physical way, and transmission or information storage and retrieval, electronic adaptation, computer software, or by similar or dissimilar methodology now known or hereafter developed. Exempted from this legal reservation are brief excerpts in connection with reviews or scholarly analysis or material supplied specifically for the purpose of being entered and executed on a computer system, for exclusive use by the purchaser of the work. Duplication of this publication or parts thereof is permitted only under the provisions of the Copyright Law of the Publisher's location, in its current version, and permission for use must always be obtained from Springer. Permissions for use may be obtained through RightsLink at the Copyright Clearance Center. Violations are liable to prosecution under the respective Copyright Law.

The use of general descriptive names, registered names, trademarks, service marks, etc. in this publication does not imply, even in the absence of a specific statement, that such names are exempt from the relevant protective laws and regulations and therefore free for general use.

While the advice and information in this book are believed to be true and accurate at the date of publication, neither the authors nor the editors nor the publisher can accept any legal responsibility for any errors or omissions that may be made. The publisher makes no warranty, express or implied, with respect to the material contained herein.

Printed on acid-free paper

Humana Press is a brand of Springer
Springer is part of Springer Science+Business Media (www.springer.com)

Preface

Since the first edition of this book was published in 2007 significant progress has been made on *Salmonella* and *Salmonella*-host cell interactions spanning a variety of aspects on cellular, molecular, and genetic characterizations. Research on *Salmonella* has generated enormous new interest with the realization that many bacteria have developed resistance to the most common antibiotics and new strategies are in demand to overcome antibiotic resistance of harmful enterobacteria such as *Salmonella*. Typhoid fever caused by *Salmonella* can normally be treated with broad-spectrum antibiotics including tetracycline, chlortetracycline, oxytetracycline, demeclocycline, methacycline, doxycycline, minocycline, and a number of other semisynthetic derivatives but *Salmonella* resistance to antibiotics has increasingly become a problem and new avenues are being explored to discover new antibiotics that interfere with bacterial components while not harming their mammalian host cells. Vaccine development has progressed significantly and includes nanotechnology-based approaches with promising results for effective protection.

Salmonella ranks second in causing food-borne illnesses, and every year millions of people worldwide become ill and many thousands die as a result of infections caused by food-borne pathogens in developed as well as underdeveloped countries. A whole host of basic discoveries have resulted in new approaches to prevent and treat *Salmonella* infections acquired through food contaminations, several of which are featured in the present book.

Aside from research to overcome *Salmonella* infections, genetic manipulations of *Salmonella* have led to a new line of research using genetically modified attenuated *Salmonella* as oral vectors for targeted gene delivery and as tumor-targeting vectors that have been developed for applications in novel cancer therapies.

As in the previous edition, the second edition of this book on *Salmonella* presents detailed methods on a variety of different aspects and has selected those that have provided landmarks in advancing our knowledge on *Salmonella* research. The new edition features new methods including chapters on molecular assays for detection, identification, and serotyping of *Salmonella*, quantitative proteomic identification of host factors involved in *Salmonella* infection, determination of antimicrobial resistance in *Salmonella*, site-directed mutagenesis, chromosomal gene analysis, development of bacterial nanoparticle vaccine, attachment of nanoparticle cargo to biotinylated *Salmonella* for combination bacteriotherapy against tumors, various microscopy methods to analyze *Salmonella* interaction with host cells, in vitro modeling of gallbladder-associated *Salmonella* colonization, analysis of *Salmonella* phages and prophages, and other methods as detailed in the specific chapters of this second edition.

As in the previous edition each chapter provides a short overview of the topic followed by detailed methods and protocols that are normally not described in regular research papers. Genetic manipulation, molecular methods, and molecular imaging are techniques that will be of interest to geneticists, cell and molecular biologists, microbiologists, environmentalists, toxicologists, public health scientists, clinicians in human and veterinary medicine, agriculture, and other researchers who want to become familiar and apply

techniques that are commonly not available in research papers. The methods presented here are in high demand and are expected to continue to be of value to researchers and to incoming investigators in the future. This book will also be of interest to students for the study of various aspects of research on *Salmonella*. Because no recent comprehensive literature of this format is available on *Salmonella*, this book will be of value to a wide variety of researchers. The methods presented are in high demand and are expected to continue to be of value to an increasing number of investigators in the *Salmonella* field.

We are delighted to present the second edition of *Salmonella* protocols depicting specific methods that have impacted *Salmonella* research and we are indebted to Dr. John Walker for inviting this second edition on *Salmonella*, and to the publisher with special thanks to David C. Casey. We are most grateful to our outstanding contributors for sharing their unique and specific expertise and experiences with the scientific community and for revealing details of practical insights that are not generally disseminated in regular research papers. Our sincere thanks to all for their most valuable contributions.

Columbia, MO, USA

*Heide Schatten
Abraham Eisenstark*

Contents

<i>Preface</i>	v
<i>Contributors</i>	ix
1 Luminex® Multiplex Bead Suspension Arrays for the Detection and Serotyping of <i>Salmonella</i> spp.....	1
<i>Sherry A. Dunbar, Vivette Brown Ritchie, Michaela R. Hoffmeyer, Gunjot S. Rana, and Hongwei Zhang</i>	
2 Quantitative Proteomic Identification of Host Factors Involved in the <i>Salmonella typhimurium</i> Infection Cycle	29
<i>Dora Kaloyanova, Mijke Vogels, Bas W.M. van Balkom, and J. Bernd Helms</i>	
3 Determination of Antimicrobial Resistance in <i>Salmonella</i> spp.....	47
<i>Belgode N. Harish and Godfred A. Menezes</i>	
4 Red-Mediated Recombineering of <i>Salmonella enterica</i> Genomes	63
<i>Frederik Czarniak and Michael Hensel</i>	
5 A Method to Introduce an Internal Tag Sequence into a <i>Salmonella</i> Chromosomal Gene.....	81
<i>Weidong Zhao and Stéphane Méresse</i>	
6 Generation and Use of Site-Directed Chromosomal <i>cyaA'</i> Translational Fusions in <i>Salmonella enterica</i>	93
<i>Francisco Ramos-Morales, Elena Cardenal-Muñoz, Mar Cordero-Alba, and Fernando Baisón-Olmo</i>	
7 Detection of Antimicrobial (Poly)Peptides with Acid Urea Polyacrylamide Gel Electrophoresis Followed by Western Immunoblot	105
<i>Edith Porter, Erika V. Valore, Rabin Anouseyan, and Nita H. Salzman</i>	
8 Detecting Non-typhoid <i>Salmonella</i> in Humans by Enzyme-Linked Immunosorbent Assays (ELISAs): Practical and Epidemiological Aspects	117
<i>Katrin G. Kuhn, Hanne-Dorthe Emborg, Karen A Krogfelt, and Kåre Mølbak</i>	
9 Study of the Stn Protein in <i>Salmonella</i> ; A Regulator of Membrane Composition and Integrity	127
<i>Masayuki Nakano, Eiki Yamasaki, Joel Moss, Toshiya Hirayama, and Hisao Kurazono</i>	
10 Development of a Bacterial Nanoparticle Vaccine	139
<i>Carlos Gamazo, Javier Ochoa-Repáraz, Ibai Tamayo, Ana Camacho, and Juan M. Irache</i>	

11	Direct Attachment of Nanoparticle Cargo to <i>Salmonella typhimurium</i> Membranes Designed for Combination Bacteriotherapy Against Tumors	151
	<i>Robert Kazmierczak, Elizabeth Choe, Jared Sinclair, and Abraham Eisenstark</i>	
12	Applications of Microscopy in <i>Salmonella</i> Research	165
	<i>Layla M. Malt, Charlotte A. Perrett, Suzanne Humphrey, and Mark A. Jepson</i>	
13	Live Cell Imaging of Intracellular <i>Salmonella enterica</i>	199
	<i>Alexander Kehl and Michael Hensel</i>	
14	In Vitro Modeling of Gallbladder-Associated <i>Salmonella</i> spp. Colonization	227
	<i>Geoffrey Gonzalez-Escobedo and John S. Gunn</i>	
15	<i>Salmonella</i> Phages and Prophages: Genomics, Taxonomy, and Applied Aspects	237
	<i>Andrea I. Moreno Switt, Alexander Sulakvelidze, Martin Wiedmann, Andrew M. Kropinski, David S. Wishart, Cornelis Poppe, and Yongjie Liang</i>	
	<i>Index</i>	289

Contributors

RABIN ANOUSEYAN • *Department of Biological Sciences, California State University Los Angeles, Los Angeles, CA, USA*

FERNANDO BAISÓN-OLMO • *Departamento de Genética, Facultad de Biología, Universidad de Sevilla, Sevilla, Spain*

BAS W.M. VAN BALKOM • *Department of Nephrology and Hypertension, University Medical Center Utrecht, Utrecht, The Netherlands*

VIVETTE BROWN RITCHIE • *Luminex Molecular Diagnostics, Toronto, ON, Canada*

ANA CAMACHO • *Department of Microbiology, University of Navarra, Pamplona, Spain*

ELENA CARDENAL-MUÑOZ • *Departamento de Genética, Facultad de Biología, Universidad de Sevilla, Sevilla, Spain*

ELIZABETH CHOE • *Cancer Research Center, Columbia, MO, USA; Massachusetts Institute of Technology, Cambridge, MO, USA*

MAR CORDERO-ALBA • *Departamento de Genética, Facultad de Biología, Universidad de Sevilla, Sevilla, Spain*

FREDERIK CZARNIAK • *Abteilung Mikrobiologie, Fachbereich Biologie/Chemie, Universität Osnabrück, Osnabrück, Germany*

SHERRY A. DUNBAR • *Luminex Corporation, Austin, TX, USA*

ABRAHAM EISENSTARK • *Cancer Research Center, Columbia, MO, USA; University of Missouri-Columbia, Columbia, MO, USA*

HANNE-DORTHE EMBORG • *Statens Serum Institut, Copenhagen S, Denmark*

CARLOS GAMAZO • *Department of Microbiology, University of Navarra, Pamplona, Spain*

GEOFFREY GONZALEZ-ESCOBEDO • *Department of Microbiology, Center for Microbial Interface Biology, The Ohio State University, Columbus, OH, USA; Department of Microbial Infection and Immunity, Center for Microbial Interface Biology, The Ohio State University, Columbus, OH, USA*

JOHN S. GUNN • *Department of Microbiology, Center for Microbial Interface Biology, The Ohio State University, Columbus, OH, USA; Department of Microbial Infection and Immunity, Center for Microbial Interface Biology, The Ohio State University, Columbus, OH, USA*

BELGODE N. HARISH • *Department of Microbiology, Jawaharlal Institute of Postgraduate Medical Education and Research (JIPMER), Pondicherry, India*

J. BERND HELMS • *Department of Biochemistry & Cell Biology, Faculty of Veterinary Medicine, Utrecht University, Utrecht, The Netherlands; Institute of Biomembranes (IB), Utrecht University, Utrecht, The Netherlands*

MICHAEL HENSEL • *Abteilung Mikrobiologie, Fachbereich Biologie/Chemie, Universität Osnabrück, Osnabrück, Germany*

TOSHIYA HIRAYAMA • *Department of Bacteriology, Institute of Tropical Medicine, Nagasaki University, Sakamoto, Nagasaki, Japan*

MICHAELA R. HOFFMEYER • *Thermo Fisher Scientific, Inc., Carlsbad, CA, USA*

SUZANNE HUMPHREY • *Department of Biochemistry, School of Medical Sciences, University of Bristol, Bristol, UK*

JUAN M. IRACHE • *Department of Pharmacy and Pharmaceutical Technology, University of Navarra, Pamplona, Spain*

MARK A. JEPSON • *Department of Biochemistry, School of Medical Sciences, University of Bristol, Bristol, UK*

DORA KALOYANOVA • *Department of Biochemistry & Cell Biology, Faculty of Veterinary Medicine, Utrecht University, Utrecht, The Netherlands; Institute of Biomembranes (IB), Utrecht University, Utrecht, The Netherlands*

ROBERT KAZMIERCZAK • *Cancer Research Center, Columbia, MO, USA*

ALEXANDER KEHL • *Abteilung Mikrobiologie, Fachbereich Biologie/Chemie, Universität Osnabrück, Osnabrück, Germany*

KAREN A. KROGFELT • *Statens Serum Institut, Copenhagen S, Denmark*

ANDREW M. KROPINSKI • *Public Health Agency of Canada, Laboratory for Foodborne Zoonoses, Guelph, ON, Canada; Departments of Molecular and Cellular Biology, University of Guelph, Guelph, ON, Canada; Departments of Pathobiology, University of Guelph, Guelph, ON, Canada*

KATRIN G. KUHN • *Statens Serum Institut, Copenhagen S, Denmark*

HISAO KURAZONO • *Department of Animal and Food Hygiene, Obihiro University of Agriculture and Veterinary Medicine, Obihiro, Hokkaido, Japan*

YONGJIE LIANG • *Department of Biological Sciences, University of Alberta, Edmonton, Alberta, Canada; Department of Computing Science, University of Alberta, Edmonton, Alberta, Canada*

LAYLA M. MALT • *Department of Biochemistry, School of Medical Sciences, University of Bristol, Bristol, UK*

GODFRED A. MENEZES • *Department of Clinical Laboratory Sciences, College of Applied Medical Sciences, University of Hail, Hail, Kingdom of Saudi Arabia*

STÉPHANE MÉRESSE • *CIML, Aix-Marseille University, Marseille, France; CNRS, UMR 7280, Marseille, France; INSERM, U631, Marseille, France*

KÅRE MØLBAK • *Statens Serum Institut, Copenhagen S, Denmark*

ANDREA I. MORENO SWITT • *Universidad Andres Bello, Escuela de Medicina Veterinaria, Facultad de Ecología y Recursos Naturales, Santiago, Chile*

JOEL MOSS • *Cardiovascular and Pulmonary Branch, NHLBI, National Institutes of Health, Bethesda, MD, USA*

MASAYUKI NAKANO • *Department of Bacteriology, Institute of Tropical Medicine, Nagasaki University, Sakamoto, Nagasaki, Japan*

JAVIER OCHOA-REPÁRIZ • *Center for Nanomedicine, Sanford-Burnham Medical Research Institute, University of California, Santa Barbara, Santa Barbara, CA, USA*

CHARLOTTE A. PERRETT • *Department of Biochemistry, School of Medical Sciences, University of Bristol, Bristol, UK*

CORNELIS POPPE • *Public Health Agency of Canada, Laboratory for Foodborne Zoonoses, Guelph, ON, Canada*

EDITH PORTER • *Department of Biological Sciences, California State University Los Angeles, Los Angeles, CA, USA; Department of Medicine, David Geffen School of Medicine, University of California, Los Angeles, Los Angeles, CA, USA*

FRANCISCO RAMOS-MORALES • *Departamento de Genética, Facultad de Biología, Universidad de Sevilla, Sevilla, Spain*

GUNJOT S. RANA • *Luminex Corporation, Austin, TX, USA*

NITA H. SALZMAN • *Division of Gastroenterology, Department of Pediatrics, Children's Research Institute, Medical College of Wisconsin, Milwaukee, WI, USA*

JARED SINCLAIR • *Cancer Research Center, Columbia, MO, USA; University of Missouri-Columbia, Columbia, MO, USA*

ALEXANDER SULAKVELIDZE • *Intralytix, Inc., Baltimore, MD, USA*

IBAI TAMAYO • *Department of Microbiology, University of Navarra, Pamplona, Spain*

ERIKA V. VALORE • *Department of Medicine, David Geffen School of Medicine, University of California, Los Angeles, Los Angeles, CA, USA*

MIJKE VOGELS • *Immuno Valley, Utrecht, The Netherlands*

MARTIN WIEDMANN • *Department of Food Science, College of Agriculture and Life Sciences, Cornell University, Ithaca, NY, USA*

DAVID S. WISHART • *Department of Biological Sciences, University of Alberta, Edmonton, AB, Canada; Department of Computing Science, University of Alberta, Edmonton, AB, Canada*

EIKI YAMASAKI • *Department of Animal and Food Hygiene, Obihiro University of Agriculture and Veterinary Medicine, Obihiro, Hokkaido, Japan*

HONGWEI ZHANG • *Luminex Molecular Diagnostics, Toronto, ON, Canada*

WEIDONG ZHAO • *CIML, Aix-Marseille University, Marseille, France; CNRS, UMR 7280, Marseille, France; INSERM, U631, Marseille, France*

Chapter 1

Luminex® Multiplex Bead Suspension Arrays for the Detection and Serotyping of *Salmonella* spp.

Sherry A. Dunbar, Vivette Brown Ritchie, Michaela R. Hoffmeyer, Gunjot S. Rana, and Hongwei Zhang

Abstract

In this chapter we describe two commercially available bead-based molecular assays for detection, identification and serotyping of *Salmonella*. The xTAG® Gastrointestinal Pathogen Panel (GPP) is a qualitative multiplex test for the simultaneous detection of nucleic acids from *Salmonella* plus 14 other gastroenteritis-causing bacteria, viruses, and parasites from stool specimens. xTAG GPP uses the Luminex® xTAG universal array technology for the identification of specific target sequences combined with the xMAP® bead multiplexing platform for detection of the targets that were present in the starting sample. The xMAP Salmonella Serotyping Assay (SSA) is a multiplex nucleic acid-based direct hybridization assay for molecular identification of the serotype of *Salmonella* isolates. In xMAP SSA, target sequences amplified from cultured *Salmonella* isolates are captured by hybridization to sequence-specific capture probes which have been coupled to the multiplexed bead sets. Herein we provide detailed protocols for each of these assays and present data which describe their performance characteristics for detection and serotyping *Salmonella*.

Key words *Salmonella*, Gastrointestinal pathogen, Luminex, Multiplex, Bead suspension array

1 Introduction

Globally there are approximately 1.7 billion cases of diarrheal disease each year [1]. Diarrhea is a leading cause of malnutrition and the second leading cause of death in children under 5 years of age, killing 760,000 children under five each year. In the USA, roughly 48 million people become ill, 128,000 are hospitalized and 3,000 die of foodborne diseases annually [2]. In 2011, the cost for hospitalized patients suffering from gastrointestinal infections in the USA was over \$6.7 billion [3]. Diarrheal disease can be caused by a number of pathogens including viruses, bacteria, and parasites with 20 % of cases due to infection with one (or more) of 31 pathogens known to cause foodborne illness. Gastroenteritis due to *Salmonella* spp. is a considerable burden in both developed and developing countries, with a global burden estimated at 93.8

million cases each year and 155,000 deaths due to nontyphoidal *Salmonella* [4]. Analysis of US surveillance data from 2000 to 2008 has indicated that 58 % of illnesses were caused by norovirus, followed by 11 % caused by nontyphoidal *Salmonella* spp. [5]. Furthermore, nontyphoidal *Salmonella* spp. were the leading cause of hospitalization (35 %) and death (28 %) from diarrheal disease. Twelve of sixteen multi-state foodborne outbreaks caused by bacterial enteric pathogens occurring since 2002 have been caused by *Salmonella* [2].

Due to similarity of symptoms, it is difficult to differentiate among viral, bacterial, and parasitic agents and 80 % of all causes of diarrhea currently go unidentified, which could potentially result in inadequate or inappropriate treatment [6]. Identification of the causal agent in symptomatic patients is important for diagnosis and patient management and can assist in treatment decisions, as appropriate antimicrobial therapy can shorten illness and reduce morbidity in some bacterial and parasitic infections and can be life-saving in invasive infections [7]. For example, selective antimicrobial therapy is indicated for toxigenic *Escherichia coli*, *Shigella*, and *Campylobacter* but is not routinely recommended for *Salmonella*. Conventional diagnostic procedures for gastrointestinal pathogens involve culture, microscopy, and/or stool antigen tests, and include enrichment steps, use of selective culture media, biochemical identification, serotyping, and resistance profiling [8, 9]. Each of these methods has limitations including varying sensitivities, specificities, and turnaround times and can be time-consuming and labor-intensive. Maximal recovery of *Salmonella* from fecal specimens is obtained by using an enrichment broth; however, sensitivity of stool culture for recovery of *Salmonella* spp. is estimated to be only 70 % [10]. Traditional methods may fail to reveal a causative agent and may fail to identify coinfections when testing is only performed for a few suspect pathogens as requested by the physician. *Salmonella* spp., among other enteric pathogens, have been found to be involved in coinfections with rotavirus and other organisms [11, 12].

Further analysis of *Salmonella* isolates by serotyping is commonly performed to facilitate public health surveillance and aid in recognition and investigation of outbreaks. Clinical diagnostic laboratories submit *Salmonella* isolates to state and territorial public health laboratories where they are confirmed and serotyped according to the White–Kauffmann–Le Minor scheme [13]. As of 2007, more than 2,500 *Salmonella* serotypes had been described [14]. In the USA, over 1,000 different *Salmonella* serotypes were reported from 2002 to 2006, however the 100 most common serotypes accounted for about 98 % of the isolates [15]. Traditional serotyping is performed via tube or plate agglutination methods which can be laborious and require subjective interpretation of results. To determine a *Salmonella* serotype, the somatic O antigen and all phases of the motility H antigen must be identified,

requiring phase inversion. Furthermore, the serotype of rough and problematic isolates may not be determined by traditional agglutination methods. This process can be lengthy and may require 3–5 days or longer for full serotype determination, thus delaying the reporting of results to public health data information systems.

In the last two decades, in vitro nucleic acid amplification and molecular detection techniques have transformed the microbiology laboratory. Assays designed to directly detect microbial nucleic acid sequences from patient specimens have allowed for more rapid diagnosis and treatment of infectious diseases with high accuracy and reduced turnaround time as compared to traditional immunological and culture-based methods. Recent reports indicate that molecular methods exhibit high sensitivity and improve detection of gastrointestinal pathogens when used for stool testing [7, 16]. Molecular methods that permit multiplexing have a significant advantage compared to single reaction detection methods in that they allow simultaneous detection and identification of multiple nucleic acid sequences from the same sample. Multiplexed tests reduce the time, labor, and cost of laboratory testing, and in addition to improved efficiency, also have a higher diagnostic yield by the ability to detect multiple infections. Thus, multiplexed molecular assays can be used in a panel-based approach to identify a specific infectious etiology from groups of organisms that present with similar symptoms and can also provide information on coinfections and secondary infections.

Among the various multiplexing technologies available, microsphere or bead-based suspension arrays have emerged as a standard molecular multiplexing technology in the clinical microbiology laboratory and multiplex detection of respiratory viral pathogens by reverse transcription PCR (RT-PCR) has become part of the routine diagnostic algorithm over the last 5 years [17, 18]. Multiplex molecular bead arrays have also been developed for detection and quantitation of viral and bacterial agents of gastroenteritis and are highly sensitive and specific, correlating well with real-time PCR [19–21].

The Luminex® xMAP® multiplexing system incorporates polystyrene beads that are internally dyed with precise amounts of multiple spectrally distinct fluorochromes, creating an array consisting of different bead sets with specific spectral identities. The unique spectral characteristics within individual bead sets allow each bead set to be differentiated from all others in a multiplex. Each bead set can possess a different reactant on its surface which is associated with a specific analyte or target, and thus, they can be combined in a single reaction to measure up to 500 different analytes simultaneously. An additional fluorochrome coupled to a reporter molecule quantifies the biomolecular interaction that has occurred at the bead surface and after completion of assay incubations with a nucleic acid sample and the reporter molecule, the reactions are

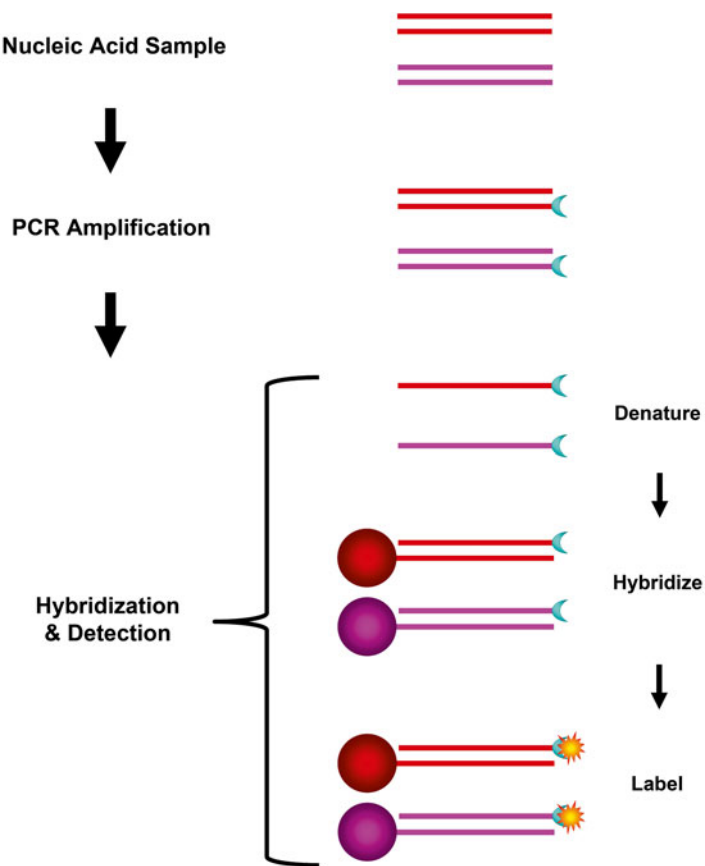


Fig. 1 xMAP® direct hybridization assay format

analyzed within a Luminex reader, classifying the beads based on the bead identity and quantifying the bound fluorophore in the reporter detection channel.

Several assay chemistries have been developed for nucleic acid detection on the xMAP system. One approach is to use direct hybridization of a labeled PCR-amplified target DNA to bead sets bearing oligonucleotide capture probes specific for each sequence (Fig. 1). Another approach is to use a solution-based enzymatic chemistry to simultaneously determine the presence of a specific target sequence and incorporate a unique capture sequence or “tag,” followed by hybridization to complementary “anti-tag” sequences precoupled to the multiplexed bead sets (Fig. 2). Commonly used enzymatic methods for sequence determination rely on the discriminating ability of DNA polymerases and DNA ligases, and include primer extension, oligonucleotide ligation, and target-specific PCR [22–24]. An example of this approach is Luminex’s xTAG® Technology, a proprietary universal tag sorting system consisting of a library of oligonucleotide sequences that have been optimized to be an isothermal set and have minimal

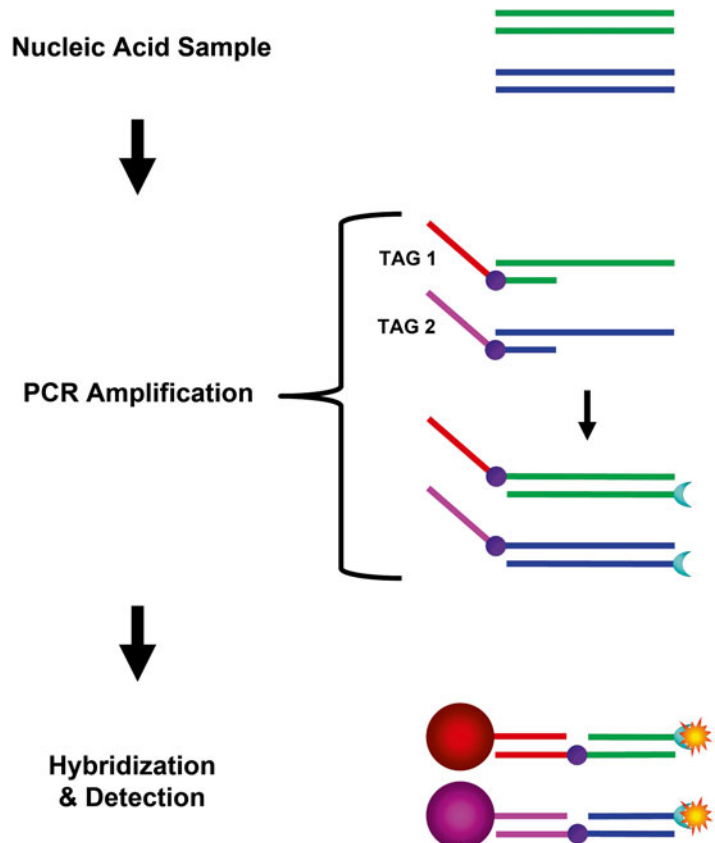


Fig. 2 xTAG® universal array with target-specific PCR assay format

cross-reactivity. Target-specific primers are modified with specific TAG sequences and used in conjunction with MagPlex®-TAG™ Microspheres, which are superparamagnetic beads containing two or three internal fluorescent dyes and precoupled with anti-TAG capture probes. The xTAG universal array platform simplifies assay development and eliminates the need to couple content-specific capture probes to the beads.

In this chapter we describe two multiplex molecular bead array assays for the detection and serotyping of *Salmonella* spp. using the xMAP bead-based array platform. The xTAG Gastrointestinal Pathogen Panel (GPP) is a qualitative test that can simultaneously detect and identify nucleic acids from multiple gastroenteritis-causing viruses, parasites, and bacteria, including *Salmonella* spp., in human stool specimens (Table 1). This assay employs target-specific PCR to simultaneously amplify the target sequences, incorporate a unique TAG sequence for each target and incorporate a biotin label for subsequent detection using the xTAG universal array system. The xMAP Salmonella Serotyping Assay (SSA) is a molecular serotyping assay that detects genes involved in the expression of

Table 1
Pathogen types and subtypes identified by xTAG® GPP^a

Pathogen class	Analytes detected
Bacteria	<i>Campylobacter</i> (<i>C. jejuni</i> , <i>C. coli</i> , and <i>C. lari</i> only) <i>Clostridium difficile</i> Toxin A/B <i>Escherichia coli</i> O157 <i>Enterotoxigenic E. coli</i> (ETEC) LT/ST <i>Shiga-like toxin producing E. coli</i> (STEC) <i>stx1/stx2</i> <i>Salmonella</i> <i>Shigella</i> (<i>S. boydii</i> , <i>S. sonnei</i> , <i>S. flexneri</i> , and <i>S. dysenteriae</i>) <i>Vibrio cholerae</i> <i>Yersinia enterocolitica</i>
Viruses	Adenovirus 40/41 Norovirus GI/GII Rotavirus A
Parasites	<i>Cryptosporidium</i> (<i>C. parvum</i> and <i>C. hominis</i> only) <i>Entamoeba histolytica</i> <i>Giardia lamblia</i>

^aProducts and targets are region-specific and may not be approved in some countries/regions. Contact Luminex at support@luminexcorp.com to obtain appropriate product information for the country of interest

Salmonella serotype-specific antigens. Multiplex PCR is used to amplify *Salmonella* antigen gene target sequences and incorporate a biotin label. The amplified target sequences are then captured by direct hybridization onto bead sets coupled with complementary oligonucleotide capture probes and labeled with fluorescent reporter for detection on the Luminex analyzer.

2 Materials

2.1 Materials

**Provided
with the xTAG GPP
Kit (for 96 Reactions)
(See Notes 1 and 2)**

1. xTAG® GPP Primer Mix, 120 µL×2 vials.
2. xTAG® OneStep Enzyme Mix, 57 µL×4 vials.
3. xTAG® OneStep Buffer, 5×, 1.0 mL×1 vial.
4. xTAG® RNase-Free Water, 1.9 mL×1 vial.
5. xTAG® BSA, 10 mg/mL, 1.0 mL×1 vial.
6. xTAG® MS2 (extraction/internal control), 1.5 mL×2 vials.
7. xTAG® GPP Bead Mix, 1.92 mL×1 vial.
8. xTAG® Reporter Buffer (contains 0.15 M NaCl), 12.0 mL×1 vial.
9. xTAG® 0.22 SAPE, 188 µL×1 vial.
10. Data acquisition protocols for xPONENT® software (versions 3.1, 4.1, and 4.2).
11. xTAG® Data Analysis Software GPP (TDAS GPP).

**2.2 Materials
Required but NOT
Provided
with the xTAG GPP Kit**

1. NucliSENS® easyMAG® System with Specific A 1.0.2 protocol (bioMérieux/#280140, Marcy l'Etoile, France) or QIAamp® MinElute® Virus Spin kit (Qiagen/#57704, Hilden, Germany) or an equivalent nucleic acid extraction method.
2. NucliSENS easyMAG Lysis Buffer, 4×1 L (#280134) or 48×2 mL (#200292).
3. Bertin SK38 Soil Grinding Bead Tubes (Bertin Technologies/#03961-1-006, Aix-en-Provence, France or Luminex Corporation/#GR032C0442, Austin, TX).
4. Luminex® 100/200™ or MAGPIX® analyzer system (with heater block), including xPONENT® software.
5. xMAP analyzer calibration and verification kits.
6. Mini centrifuge (InterScience/#C-1301, St Nom la Bretèche, France) or equivalent.
7. Multichannel pipettes (1–10 µL or 5–50 µL, 50–200 µL).
8. Pipettes (1–1,000 µL).
9. Racks for 1.5 mL and 0.5 mL microcentrifuge tubes.
10. Racks for 0.2 mL thin wall tubes for PCR.
11. Ultrasonic cleaner (sonicator bath) (Cole-Parmer®/#A-08849-00, Vernon Hills, IL) or equivalent.
12. Thermal cycler for 0.2 mL thin wall PCR tubes and 96-well plates.
13. PCR cooler rack capable of holding a temperature range of 0–7 °C for 1 h (Eppendorf/#022510509, Hamburg, Germany) or equivalent.
14. Vortex-Genie® 2 Model G560 (Scientific Industries/#SI-0236, Bohemia, NY).
15. Vortex Adaptor for Vortex-Genie 2 (Mo-Bio Laboratories, Inc./#13000-V1-24, Carlsbad, CA), optional.
16. 10 µL disposable inoculating loops.
17. 0.2 mL thin wall polypropylene tubes for PCR, appropriate for thermal cycler.
18. 1.5 mL polypropylene microcentrifuge tubes.
19. 15 mL and 50 mL polypropylene tubes.
20. Costar® Thermowell® thin-wall polycarbonate 96-well plates (Corning/#6509, Corning, NY) or equivalent.
21. Microseal® ‘A’ film to cover 96-well plate (Bio-Rad Laboratories/#MSA-5001, Hercules, CA).
22. Aerosol resistant tips for pipettes.
23. Reagent reservoirs.

**2.3 Materials
Provided
with the xMAP SSA Kit
(100 Reactions) (See
Note 3)**

1. O-Antigen Microsphere Mix, 3.75×, 1.32 mL×1 vial.
2. H-Antigen Microsphere Mix, 3.75×, 1.32 mL×1 vial.
3. AT Microsphere Mix, 3.75×, 1.32 mL×1 vial.
4. O-Antigen Primer Mix, 280 µL×1 vial.
5. H-Antigen Primer Mix, 280 µL×1 vial.
6. AT Primer Mix, 280 µL×1 vial.
7. Streptavidin-Phycoerythrin (SAPE), 132 µL×1 vial.
8. Assay Buffer, 40 mL×1 vial (*see Note 4*).

**2.4 Materials
Required but NOT
Provided
with the xMAP SSA Kit**

1. Luminex 100/200 analyzer system (with heater block).
2. Vortex.
3. Ultrasonic cleaner (sonicator bath) (Cole-Parmer/#A-08849-00) or equivalent.
4. Thermal cycler for 0.2 mL thin wall PCR tubes (with heated lid).
5. Mini centrifuge.
6. NanoDrop 2000 spectrophotometer (Thermo Scientific, NanoDrop products, Wilmington, DE, USA) or equivalent.
7. Molecular Grade water.
8. Microseal 'A' film (Bio-Rad Laboratories/#MSA-5001).
9. 0.2 mL thin wall polypropylene PCR tubes (USA Scientific/#1402-3900, Orlando, FL).
10. 96-well PCR plates (Bio-Rad Laboratories/#MLL-9601).
11. HotStarTaq Master Mix Kit (Qiagen/#203443, 203445 or 203446).
12. InstaGene matrix (Bio-Rad Laboratories/#732-6030).
13. 1 µL disposable inoculating loops (Thermo Fisher Scientific, Inc./#22-363-604, Waltham, MA).

3 Methods

The xTAG GPP assay workflow includes (1) stool sample preparation and pretreatment, (2) nucleic acid extraction, (3) multiplex RT-PCR, (4) bead hybridization and detection, and (5) data acquisition and analysis (Fig. 3). The xMAP SSA assay serotypes approximately 85 % of the top 100 *Salmonella* serotypes most commonly encountered in testing laboratories and provides partial information for many other serotypes. These serotypes represent more than 90 % of the serotypes routinely encountered in public health laboratories. xMAP SSA consists of three separate tests that determine O and H antigens simultaneously and identify some serotype-specific markers. The O antigen assay detects the following groups: B, C1, C2, D, E, G, and serotype Paratyphi A (ParaA).

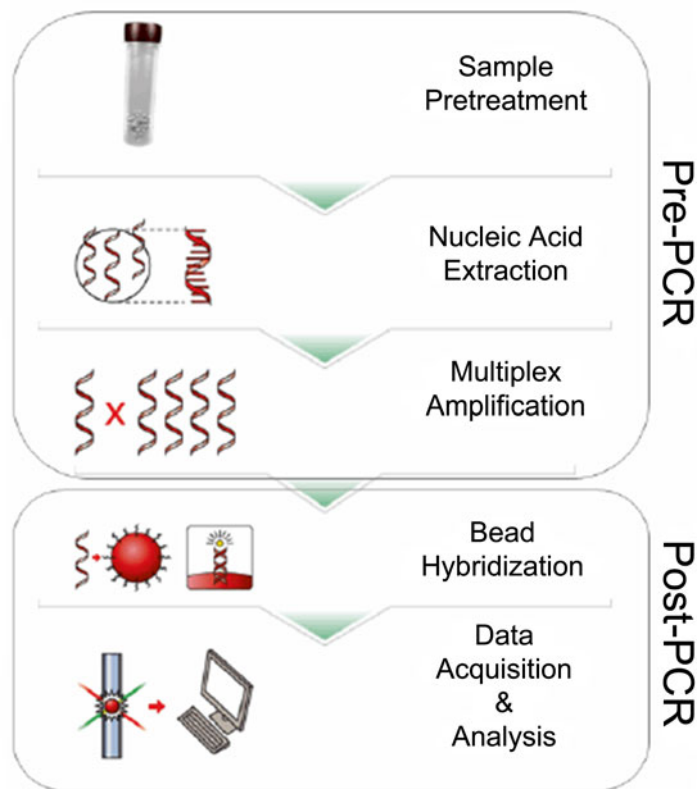


Fig. 3 xTAG® GPP assay workflow

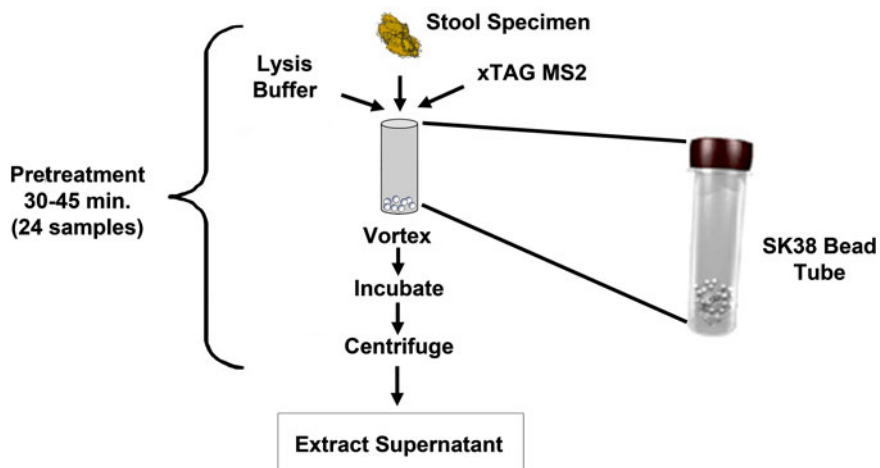
The H antigen assay detects the following antigens: a, b, c, d, j, (e, h), i, k, r, z10, z, z29, z6, y, L-complex, v, z28, EN-complex, x, z15, 1-complex, 2, 5, 6, 7, G-complex, f, (m/g,m), (m/m,t), p, s, t-1*, z51, z4-complex, and z24. The Additional Targets (AT) assay consists of three targets: *sdf*, *fljB*, and *Vi*. The *sdf* and *Vi* targets are specific for *S. enterica* ser. Enteritidis and *S. enterica* ser. Typhi, respectively. The *fljB* target is a positive control for the second motility phase of *Salmonella* (see Note 5). The xMAP SSA assay workflow consists of: (1) DNA extraction and quantification, (2) multiplex PCR, (3) hybridization of the labeled amplicons to the appropriate oligonucleotide probe-coupled microsphere mixture, (4) labeling with SAPE reporter, and (5) analysis on the Luminex 100/200 analyzer at the high reporter gain setting (Fig. 4). The entire protocol and accompanying notes for the xTAG GPP and xMAP SSA assays should be read prior to performing these procedures.

3.1 Specimen Preparation (Pretreatment) for xTAG GPP (See Notes 6–8)

A pretreatment step consisting of bead beating in lysis buffer is required prior to nucleic acid extraction to ensure maximum extraction efficiency, especially for parasites. Pretreatment steps are illustrated in Fig. 5.



Fig. 4 xMAP® SSA assay workflow



Amount of Stool Specimen for Pretreatment

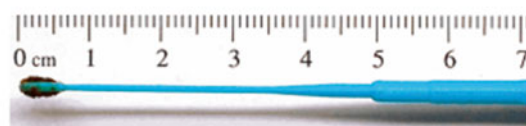


Fig. 5 xTAG® GPP specimen pretreatment workflow

1. Add 1 mL of NucliSENS easyMAG Lysis Buffer to a Bertin SK38 bead tube for each sample and control.
2. Add 10 μ L of xTAG MS2 into all sample pretreatment tubes as an extraction/internal control. Do NOT add xTAG MS2 to the negative (extraction) control tube.
3. Add the stool sample to the bead tube containing the lysis buffer. For solid stool samples (Bristol types 1–5), add approximately 100–150 mg of stool to the bead tube using a 10 μ L disposable inoculating loop, filling the inside of the loop with a “flat” loopful of stool (see Note 9). For liquid stool samples (Bristol types 6–7), add 100 μ L of stool to the bead tube.
4. For the negative extraction control tube, add 100 μ L of Lysis Buffer.
5. Vortex the pretreatment tube for 5 min. If processing multiple samples, a vortex adapter is recommended.
6. Allow the pretreated sample to sit at room temperature for 10–15 min.
7. Centrifuge the pretreatment tubes at 14,000 rpm (20,800 rcf) for 3 min to pellet any insoluble material.
8. Remove 200 μ L of pretreatment supernatant from the middle of the tube for nucleic acid extraction. Avoid aspirating the beads at the bottom of the tube or lipids collected at the top.

3.2 Nucleic Acid Extraction for xTAG GPP (See Note 10)

1. Load the 200 μ L of pretreatment supernatant on to the BioMérieux NucliSENS easyMAG extraction system and use NucliSENS protocol Specific A 1.0.2 for extraction with a 70 μ L elution volume.
2. Alternatively, extract 200 μ L of pretreatment supernatant using the QIAamp MinElute Virus Spin kit and elute nucleic acids in 70 μ L.

3.3 Multiplex RT-PCR/PCR for xTAG GPP

For each sample, 10 μ L of extracted nucleic acid is amplified in a single multiplex RT-PCR/PCR reaction containing 15 μ L Master Mix (25 μ L total reaction volume). Each target or internal control in the sample results in PCR amplicons ranging from 58 to 293 basepairs (not including the 24-nucleotide TAG sequence). During setup, the master mix and samples must be kept on ice or a cold block to avoid nonspecific amplification.

1. Preheat thermal cycler to 53 °C.
2. Thaw and bring to room temperature the xTAG OneStep Buffer (5 \times), xTAG RNase-free water, xTAG GPP Primer Mix, and xTAG BSA.
3. Vortex and mix the xTAG OneStep Buffer for at least 20 s ensuring that any visible precipitates (including clear flakes) are completely dissolved before use. Do NOT centrifuge the xTAG OneStep Buffer.

4. Vortex the xTAG RNase-free water, xTAG GPP Primer Mix, and the xTAG BSA for 2–5 s to mix reagents. Centrifuge for 2–5 s to bring reagents to bottom of the tubes.
5. Place the xTAG OneStep Buffer (5×), xTAG RNase-free water, xTAG GPP Primer Mix, and xTAG BSA on ice or in a pre-cooled cold block to cool in preparation for making the master mix.
6. Remove the xTAG OneStep Enzyme Mix from the freezer when ready to use and return to the freezer immediately after use (alternatively, keep it on a precooled freezer block). Mix the xTAG OneStep Enzyme Mix by inverting and flicking the tube. Centrifuge for 2–5 s to settle reagents to the bottom of the tube.
7. Label the appropriate number of 0.2 mL thin wall PCR tubes. Include one PCR negative control tube for every 30 samples tested. The last tube included in a given run should be a negative control. Put tubes in a precooled PCR cooler rack.
8. Label a 1.5 mL microcentrifuge tube for master mix and place on the ice or in the cold block. Add the reagents in the following order (volumes are indicated for one reaction): 2.5 μ L xTAG RNase-free water, 7.5 μ L xTAG OneStep Buffer (5×), 2.5 μ L xTAG GPP Primer Mix, 0.5 μ L xTAG BSA, 2.0 μ L xTAG OneStep Enzyme Mix (*see Note 11*).
9. Vortex the master mix for 2–5 s to mix reagents. Centrifuge for 2–5 s to settle reagents to the bottom of the tube.
10. Aliquot 15 μ L of the master mix into each of the labeled 0.2 mL PCR tubes racked in the PCR cooler rack.
11. Add 10 μ L of the appropriate extracted nucleic acid sample into each labeled tube. Cap the tube immediately after addition of the sample.
12. Add 10 μ L of xTAG RNase-free water to each negative control tube. Cap the tube immediately after addition of the water.
13. Vortex the PCR tubes for approximately 2 s to mix the reagents and then centrifuge for 2–5 s to settle the reagents to the bottom of the tubes (*see Note 12*). Return the tubes to the PCR cooler rack for transport to the preheated thermal cycler.
14. Place the PCR tubes in a preheated 53 °C thermal cycler and cycle using the following conditions (at block temperature with heated lid enabled): 1 cycle at 53 °C for 20 min; 1 cycle at 95 °C for 15 min; 38 cycles of 95 °C for 30 s, 58 °C for 30 s, 72 °C for 30 s; 1 cycle at 72 °C for 2 min; hold at 4 °C (*see Note 13*).
15. Completed RT-PCR/PCR reactions may be stored at 2–8 °C for up to 12 h until ready to use in hybridization and detection.

3.4 Bead Hybridization and Detection for xTAG GPP

1. Preheat thermal cycler to 60 °C.
2. Thaw and bring to room temperature the xTAG GPP Bead Mix and xTAG Reporter Buffer.
3. Vortex the xTAG 0.22 SAPE for 2–5 s. Dilute the 0.22 SAPE 1:75 with xTAG Reporter Buffer in a polypropylene tube. Each sample requires 75 µL of reporter solution (see Note 14).
4. Close tube and vortex for 10 s to mix. Protect from light until ready to use.
5. Cut the appropriate number of wells from a Costar 96-well plate and label the wells for the hybridization/detection reaction.
6. Vortex the xTAG GPP Bead Mix tube for 10 s and sonicate for 10 s to disperse the beads. Repeat step 6.
7. Aliquot 20 µL of the xTAG GPP Bead Mix into each well.
8. Vortex the tubes of PCR products for 2–5 s and centrifuge for 2–5 s to settle reagents to the bottom of the tubes.
9. Aliquot 5 µL of the PCR product for each sample into the appropriate wells containing the xTAG GPP Bead Mix. Gently pipette up and down 2–3 times to mix (see Note 15).
10. Transfer the reporter solution into a reservoir basin. Using an 8-channel pipette, add 75 µL of the reporter solution into each well. Gently pipette up and down 8 times (see Note 15).
11. Cover the wells/plate with Microseal ‘A’ film.
12. Place the wells/plate in a thermal cycler and incubate using the following conditions (at block temperature with heated lid enabled): 60 °C for 3 min, 45 °C for 45 min, hold at 45 °C.

3.5 Data Acquisition and Analysis for xTAG GPP

The Luminex analyzer should be prepared and ready for data acquisition prior to bead hybridization. Procedures for preparation and calibration are described in the appropriate instrument hardware and software manuals. The xTAG GPP data acquisition protocols and TDAS GPP software (included in the assay kit) must be imported/installed prior to data acquisition and analysis (see Note 16).

3.5.1 Data Acquisition

1. Turn on the Luminex analyzer and start the Luminex xPO-NENT software.
2. Ensure the instrument heater block is in place and set the plate heater temperature to 45 °C. All readings are carried out at 45 °C.
3. Create and save a new batch:
 - (a) On the Batches menu, click *New Batch from Existing protocol*.
 - (b) Fill in the *Batch Name* information by providing a date, batch description, and operator name.

- (c) Navigate to select the *xTAG GPP (LX)* protocol for the Luminex 100/200 System or the *xTAG GPP (MP)* protocol for the MAGPIX System. Click *Next*.
- (d) Select the appropriate wells where the samples will be analyzed and then click *Unknown*. The selected wells are highlighted.
- (e) Enter an appropriate sample ID using the number of samples or patient information. Alternatively, import sample ID by clicking *Import List*.
- (f) Click *Save*. The batch is now saved as a pending batch and ready to run.

4. When the hybridization is complete, remove the Microseal ‘A’ film from the wells/plate and place into the preheated 45 °C heater block. Click *Retract* to retract the holder (*see Note 17*).
5. Select the batch from the pending batches list and click *Run Batch*.
6. After the last sample is read, ensure that the batch data is exported.
7. Remove the wells/plate from the heater block and turn the heater temperature to OFF.
8. Wash and soak the Luminex analyzer, following the standard procedures described in the appropriate Luminex hardware user manual.

3.6 Data Analysis

Once the data is acquired, an output file is created under the Luminex batch run folder. Use the xTAG Data Analysis Software (TDAS) GPP to analyze this file following the procedure below.

1. Verify that the Luminex output file is accessible by the computer where TDAS GPP is installed.
2. Launch TDAS GPP through the *Start* then *All Programs* menu or by double-clicking the desktop icon.
3. Click *Open* on the *File* menu.
4. Browse to the output files by double-clicking the files to add them to the *File names* list box. Ensure that TDAS GPP recognizes the selected files and will analyze them using the xTAG Gastrointestinal Pathogen Panel analysis module.
5. Click *Open*. TDAS GPP will automatically analyze the output data and present the results of the run (*see Note 18*).

3.7 Performance of xTAG GPP for Detection and Identification of *Salmonella*

A detailed and comprehensive description of xTAG GPP clinical studies can be found in the xTAG GPP Kit Package Insert.

3.7.1 Prospective Specimen Data Set

A total of 1,407 prospectively collected stool specimens were tested, of which 28 were positive for *Salmonella* by xTAG GPP. Ten of these specimens were confirmed by culture. Two of the eighteen *Salmonella* xTAG GPP positive, culture-negative specimens were also confirmed as positive by bidirectional sequencing using validated primers targeting genomic regions distinct from the xTAG GPP target regions. Typing results from the ten culture-positive specimens revealed that there were three *S. enterica* ser. Typhimurium, and one each of *S. enterica* ser. Typhi, *S. enterica* ser. Salamae, *S. enterica* ser. Javiana, *S. enterica* ser. Bredeney, *S. enterica* ser. Mississippi, *S. enterica* ser. Heidelberg, and *S. enterica* ser. Muenchen. The overall performance of xTAG GPP for *Salmonella* detection demonstrated a sensitivity of 100 % (10/10) with a 95 % confidence interval (CI) of 72.2–100 %, and a specificity of 98.4 % with a 95 % CI of 97.6–99.0 %.

3.7.2 Preselected Positive Specimen Data Set

A total of 203 archived stool specimens that were positive by reference methods for pathogens that were of low prevalence in the prospective sample set were collected at multiple sites in North America, Africa, and Europe. Of this set, 27 specimens were positive for *Salmonella* by bacterial culture. xTAG GPP detected *Salmonella* in 24 of these specimens, resulting in an 88.9 % (24/27) positive agreement with a 95 % CI of 71.9–96.1 %.

3.7.3 Limit of Detection

The limit of detection (LoD) for *Salmonella* was assessed by analysis of serial dilutions prepared from high titer stocks of *S. enterica* ser. Typhimurium (American Type Culture Collection [ATCC] 13311) in a negative stool matrix. The dilution at the LoD was confirmed with a minimum of 20 replicates. The titer corresponding to the estimated LoD for *Salmonella* was 2.34×10^5 CFU/mL with an average median fluorescent intensity (MFI) of 1377 (CV=17.87 %) for Salmonella Probe 1 and 1005 (CV=25.29 %) for Salmonella Probe 2.

3.7.4 Repeatability and Reproducibility

Repeatability was assessed by testing 20 replicates of each of two analyte concentrations: a very low positive sample at the LoD titer, and a moderate positive sample at a titer generating MFI values 5–10 times above the analyte-specific negative threshold MFI. All replicates for each dilution were examined in a single run starting with sample extraction on the NucliSENS easyMAG system followed by xTAG GPP. For each set of 20 replicates, the same operator performed the testing on the same instrument system, using the same lot of extraction kit and xTAG GPP reagents. Table 2 illustrates the repeatability of the assay for detection of *Salmonella*.

Site-to-site reproducibility was assessed by testing replicates of each of three analyte concentrations: a high negative sample at a titer yielding MFI values not less than 20–30 % of the analyte-specific negative threshold, a low positive sample at a titer

Table 2
Repeatability of xTAG® GPP for *Salmonella* detection

Analyte	Dilution level	Concentration (CFU/mL)	xTAG GPP positive calls	Mean MFI	Mean %CV
Salmonella	Moderate positive	9.38×10^5	20/20	2,100	6.42
	Probe 1 Low positive	2.34×10^5	20/20	1,377	17.87
Salmonella	Moderate positive	9.38×10^5	20/20	1,916	11.20
	Probe 2 Low positive	2.34×10^5	20/20	1,005	25.29

producing MFI values 1–5 times above the analyte-specific negative threshold, and a moderate positive sample at a titer generating MFI values 7–10 times above the analyte-specific negative threshold. Samples were also prepared to simulate coinfections where one microbial target was present at the low positive titer and a second target was present at a high titer (10^5 PFU/mL for viruses and 10^6 CFU/mL or higher for bacteria). Replicates were tested at three sites by two operators at each site, with five runs performed by each operator. Each sample (prepared by dilution of positive stool or pathogen spiked into negative stool) underwent a single pretreatment and extraction on the NucliSENS easyMAG system and extracted material was stored at -70°C until testing. For dual analyte samples, all microbial targets generated a positive call for all replicates when at the high positive concentration, whereas three of six combinations generated a positive call for all replicates when at the low positive concentration. Two of ninety replicates of high positive enterotoxigenic *E. coli* plus low positive *Salmonella* generated a negative call for *Salmonella*, and 4 of 90 replicates of high positive *Salmonella* plus low positive rotavirus generated a negative call for rotavirus. Site-to-site reproducibility for detection of *Salmonella* is shown in Table 3.

3.7.5 Reactivity

Reactivity for *Salmonella* was assessed through empirical testing of a wide range of clinically relevant *Salmonella* strains, serotypes, and isolates representing the temporal and geographical diversity of *Salmonella*. Reactivity was established for a total of 113 unique *Salmonella* samples at a concentration 2–3 times the LoD. The 113 *Salmonella* strains that were detected by xTAG GPP are listed in Table 4 with reference numbers from the ATCC, National Collection of Type Cultures (NCTC), and/or the French National Reference Center (CNR).

3.7.6 Cross-Reactivity

Cross-reactivity was assessed with bacterial, viral, and parasitic pathogens associated with gastrointestinal infections that are not probed by the assay. Potential cross-reactivity was also assessed for commensal flora and non-microbial agents. Organisms were tested

Table 3
Reproducibility of xTAG® GPP for *Salmonella* detection

Sample		High negative		Low positive		Medium positive	
Concentration		3.66×10^3 CFU/mL		1.17×10^5 CFU/mL		9.38×10^5 CFU/mL	
Probe		1	2	1	2	1	2
Site 1	Agreement with expected result (%)	24/30 (80)	29/30 (96.7)	30/30 (100)	29/30 (96.7)	30/30 (100)	30/30 (100)
	Median MFI	75.3	44.5	938.5	591	2,681.3	2,870
	%CV	NA	NA	23.48	37.04	6.01	6.07
Site 2	Agreement with expected result (%)	23/30 (76.7)	22/30 (73.3)	30/30 (100)	30/30 (100)	30/30 (100)	30/30 (100)
	Median MFI	42	30	867	565.5	3,089	3,289
	%CV	NA	NA	28.89	44.35	15.27	13.89
Site 3	Agreement with expected result (%)	30/30 (100)	28/30 (93.3)	30/30 (100)	30/30 (100)	30/30 (100)	30/30 (100)
	Median MFI	65.5	56.3	936	691	2,323.5	2,526.3
	%CV	NA	NA	26.03	34.62	20.44	22.38
Overall	Agreement with expected result (%)	77/90 (85.6)	79/90 (87.8)	90/90 (100)	89/90 (98.9)	90/90 (100)	90/90 (100)
	Median MFI	72.8	48	956	690	2,712.8	2,986.5
	%CV	NA	NA	26.06	40.15	20.01	19.72

NA not applicable

at high positive titers and no cross-reactivity was observed for *Salmonella* (no false positive calls). Of 86 relevant pathogens tested, cross-reactivity was observed for only 2: *Campylobacter fetus* subsp. *fetus* (type strain, ATCC 27374, NCTC 10842) at a concentration of 6.00×10^8 CFU/mL resulted in a positive call for *Campylobacter*, and *E. coli* serotype O124:NM (ATCC 43893) resulted in a positive call for *Shigella*. For the 121 commensal flora tested, only *Salmonella subterranea* (ATCC BAA-836) at a concentration of 6.00×10^8 CFU/mL yielded a false positive call for *Shigella*.

3.8 Extraction and Quantification of *Salmonella* Isolate DNA for xMAP SSA

1. Resuspend the InstaGene matrix by vortex (see Note 19).
2. Add 20 μ L of InstaGene matrix to each 0.2 mL PCR tube.
3. Add a 1 μ L loopful of fresh isolate to the appropriate 0.2 mL PCR tube (see Note 20).
4. Cap the PCR tubes and vortex for 15 s.
5. Place the PCR tubes in a thermal cycler (with heated lid enabled) and incubate under the following conditions: 1 cycle at 56 °C for 10 min, 1 cycle at 100 °C for 5 min, hold at 4 °C (see Note 21).
6. Add 100 μ L of Molecular Grade water to each PCR tube.

Table 4
***Salmonella* spp. recognized by xTAG GPP**

Species	Subspecies	Serotype	Reference numbers for strains tested
<i>S. enterica</i> subsp. <i>enterica</i>	4:i:-		07-7741, CNR; 07-2537, CNR
	Agona		ATCC 51957; 05-960, CNR; 1137/72, CNR
	Anatum		ATCC 9270; 84K, CNR; 08-2926, CNR
	Bareilly		ATCC 9115
	Braenderup		ATCC 700136; 49K, CNR
	Brandenburg		24K, CNR CDC_ <i>Salmonella</i> A
	Cholerasuis		ATCC 7001
	Cholerasuis var. Decatur		2/84, CNR
	Cholerasuis var. Kunzendorf		36K, CNR
	Cholerasuis sensu stricto		34K, CNR
	Corvallis		236K, CNR
	Derby		ATCC 6960; 20K, CNR; 354/67, CNR
	Dublin		05-1078, CNR; 65K, CNR
	Enteritidis		89-323, CNR; 02-131, CNR; 02-9053, CNR; 89-329, CNR; 5-56, CNR; 03-3527, CNR; 02-4884, CNR
	Hadar		ATCC 51956; 02-2760, CNR; 2-74, CNR
	Heidelberg		ATCC 8326; 16K, CNR; 08-2380, CNR
	Infantis		ATCC BAA-1675; 158K, CNR; 05-6334, CNR
	Javiana		4-57, CNR; 214K, CNR
	Kentucky		ATCC 9263; 98K, CNR; 07-6574, CNR; 06-5737, CNR
	Mississippi		1933/77, CNR
	Montevideo		ATCC 8387; 126K, CNR; 06-7410, CNR; 46K, CNR; 06-8080, CNR; 06-8107, CNR; 05-8072, CNR
	Muenchen		ATCC 8388; 54K, CNR
	Newport		ATCC 6962; 05-815, CNR; 50K, CNR; 04-2487, CNR; 01-2174, CNR; 02-7891, CNR
	Oranienburg		ATCC 9239; 42K, CNR
	Panama		ATCC 7378; 73K, CNR
	Paratyphi A		1K, CNR; 06-2065, CNR
	Paratyphi B		ATCC 8759; CIP A214, CNR; 05-4862, CNR; 02-9348, CNR; 5K, CNR; 02-2529, CNR; 6332/88-1, CNR
	Paratyphi B var. Java		ATCC 51962
	Paratyphi B var. L(+) tartrate +		CDC_ <i>Salmonella</i> B
	Paratyphi C		32K, CNR
	Saintpaul		ATCC 9712; 108K, CNR; 05-5166, CNR
	Stanley		ATCC 7308; 15K, CNR; 397K, CNR
	Tennessee		142K, CNR

(continued)

Table 4
(continued)

Species	Subspecies	Serotype	Reference numbers for strains tested
	Thompson	ATCC 8391; 40K, CNR	
	Typhimurium	38 (98) MN, CNR; 49 (98) MN, CNR; 150 (98) MN, CNR; 226 (97) MN, CNR; 31 (98) MN, CNR; 02-1180, CNR; 14-58, CNR; 00-7866, CNR; 75-2099, CNR; 75/67, CNR; SonLai/Hoang63, CNR; 02-3215, CNR; 02-4577, CNR; DK4, CNR; LT2, CNR; 01-1639, CNR; 02-4496, CNR	
	Virchow	ATCC 51955; 41K, CNR; 03-5167, CNR	
subsp. <i>arizonae</i>	53:g,z51:-	SO 8/9, CNR	
subsp. <i>diarizonae</i>	17:z10:e,n,z15	1458/74, CNR	
subsp. <i>salamae</i>	11:l,z28:enx	1368K, CNR	
subsp. <i>houtenae</i>	6,7:z4,z24:-	575K, CNR	
subsp. <i>indica</i>	11:b:1,7	437/68, CNR	
<i>S. bongori</i>	Type strain	ATCC 43975 (NCTC 12419)	
	66:z35:-	1900/76, CNR	

7. Vortex the PCR tubes for 15 s and centrifuge for 5 min.
8. Without disturbing the pellet, carefully remove 50 μ L of the supernatant from each PCR tube and place into a new tube (see Note 22).
9. Quantify the DNA using a NanoDrop spectrophotometer or another comparable DNA quantification method.
10. Dilute the DNA to 100 ng/ μ L using Molecular Grade water (see Note 23).

3.9 PCR for xMAP SSA (See Note 24)

For each sample, 2 μ L of extracted DNA is used in each of three PCR reactions (O, H and AT). During setup, the master mixes and samples should be kept on ice or a cold block to avoid high background in the assay.

1. Thaw the PCR master mix components.
2. Label the appropriate number of 0.2 mL thin wall PCR tubes (three for each sample). Include one no-template control reaction for each of the three master mixes.
3. Briefly vortex and centrifuge the primers and HotStarTaq Master Mix before use.
4. Prepare three separate PCR master mixes (one for the O antigen, one for the H antigen, and one for the AT assay). For one reaction, add the following for each master mix: 12.5 μ L Qiagen HotStarTaq Master Mix, 2.5 μ L appropriate Primer Mix, and 8 μ L Molecular Grade water (see Note 25).
5. For each sample, dispense 23 μ L of each of the three master mixes into a separate PCR tubes.

6. Add 2 μ L of the diluted sample DNA (100 ng/ μ L) to each of the labeled PCR tubes. Cap the tube immediately after addition of the sample.
7. Add 2 μ L of Molecular Grade water to each no-template control tube. Cap the tube immediately after addition of the water.
8. Mix the PCR tubes by vortex and centrifuge for 5 s to ensure all reaction components are at the bottom of the tubes.
9. Place the PCR tubes in the thermal cycler and cycle using the following conditions (with heated lid enabled): 1 cycle at 95 °C for 15 min; 30 cycles of 94 °C for 30 s, 48 °C for 90 s, 72 °C for 90 s; 1 cycle at 72 °C for 10 min; hold at 4 °C.

3.10 Bead Hybridization and Detection for xMAP SSA

1. Vortex and sonicate the bead mixes for 10 s to resuspend the microspheres (*see Note 26*).
2. Prepare the working bead mixes by individually diluting the 3.75 \times stock O, H, and AT bead mixes provided to 1 \times using Assay Buffer (dilute 1:3.75). Each hybridization reaction requires 45 μ L of diluted bead mix (*see Note 27*).
3. For each sample, dispense 45 μ L of each 1 \times bead mix into a separate well in a 96-well PCR plate. Each sample requires three wells, one for each microsphere mix.
4. Add 5 μ L of each PCR product to the wells that contain the corresponding microsphere mix. Add O group PCR products to the wells containing O group microsphere mix, H group PCR products to the wells containing H group microsphere mix, and AT PCR products to the wells containing AT group microsphere mix.
5. Seal the PCR plate with Microseal 'A' film.
6. Transfer the PCR plate to the thermal cycler and incubate under the following conditions (with heated lid enabled): 95 °C for 5 min, 52 °C for 30 min, hold at 52 °C.
7. During the hybridization, set the heater block in the Luminex 100/200 to 52 °C (*see Note 28*).
8. When 10 min are remaining in the hybridization step, prepare a SAPE solution by diluting the 1 mg/mL stock solution 1:167 in Assay Buffer to a final concentration of 6 μ g/mL. Each hybridization reaction requires 50 μ L of diluted SAPE (*see Notes 29 and 30*).
9. When the hybridization is complete, transfer the PCR plate to the preheated 52 °C heater block in the Luminex 100/200 analyzer and carefully remove the Microseal 'A' film. Add 50 μ L of the diluted SAPE (6 μ g/mL) solution to each well (*see Note 31*).
10. Pipette the contents of each well up and down 5 times to mix and retract the PCR plate into the Luminex 100/200 analyzer (*see Note 32*).

11. Incubate the PCR plate in the heater block in the Luminex 100/200 analyzer at 52 °C for 10 min.
12. Analyze the completed reactions on the Luminex 100/200 analyzer calibrated to the high reporter gain setting.

3.11 Data Acquisition and Interpretation for xMAP SSA

The Luminex analyzer should be prepared and ready for data acquisition prior to bead hybridization. Procedures for preparation and calibration are described in the appropriate instrument hardware and software manuals. The xMAP SSA data acquisition protocols and instructions for setting up batches using xMAP SSA protocols are available on the Downloads section of the Luminex website at: <http://www.luminexcorp.com/Downloads/index.htm>.

The xMAP SSA uses the MFI values to make positive or negative calls for each probe or antigen. The raw output file (.csv) is interpreted manually to identify positive probes which are then cross referenced to the White–Kauffmann–Le Minor scheme [13]. In general, any probe with a MFI value greater than 1,000, a signal-to-noise (S/N) of 6 or greater, or both is considered positive.

1. Evaluate the results for the no-template control wells. The MFI value should be less than 300 for any probe in the no-template control reactions (see Note 33).
2. Evaluate the results for each sample. A MFI value equal to or greater than 1,000 for any probe in a sample well is considered positive.
3. Calculate the S/N ratio for each probe for each sample by dividing the MFI value of the probe in the sample well by the MFI value of the same probe in the no-template control well. A S/N ratio of 6 or greater is considered positive (see Note 34).
4. Compare the scored results to the White–Kauffmann–Le Minor scheme to determine the *Salmonella* serotype (see Notes 35 and 36).

3.12 Performance of xMAP SSA for *Salmonella* Serotyping

A panel of 189 *Salmonella* isolates received from six different locations, including poultry producers, food safety testing laboratories, state public health laboratories, and the Centers for Disease Control and Prevention (CDC), were analyzed (Table 5). Serotype identity of these isolates had been previously determined by agglutination by the source laboratory. This panel included one to three isolates each of the top 100 most prevalent *Salmonella* serotypes in the USA (as listed by the CDC), plus additional serotypes. The panel was divided into three subsets for analysis by one of three independent operators and each sample subset was analyzed on a different Luminex 200 analyzer. Data were scored as described above. Of the 189 isolates tested, 185 were correctly serotyped by xMAP SSA, yielding a concordance of 97.8 % to the agglutination method. xMAP SSA could not determine the serotype for four of the *Salmonella* isolates tested. One of these was B:z4:-, which is not

Table 5
Panel of *Salmonella* isolates evaluated by xMAP® SSA

Ranking ^a	Serotype	Number tested	Ranking	Serotype	Number tested
50	Adelaide	2	65	Johannesburg	2
73	Agbeni	1	43	Kentucky	2
15	Agona	2	53	Kiambu	2
76	Alachua	2	92	Kintambo	2
67	Albany	2		Kokomlemle	1
23	Anatum	2	91	Kottbus	1
	B:i:-	1	28	Litchfield	2
	B:z4:- ^b	1		Liverpool	1
84	Bailldon	2	80	Lomalinda	2
	Bandia	1	62	London	2
60	Bardo	2		Madelia	1
22	Bareilly	1	47	Manhattan	2
18	Berta	1	25	Mbandaka	2
52	Blockley	2	90	Meleagridis	2
42	Bovismorbificans	2	39	Miami	2
11	Braenderup	2	57	Minnesota	2
34	Brandenburg	1	13	Mississippi	3
61	Bredeney	2	87	Monschau	1
66	Cerro	1	6	Montevideo	2
68	Chester	2	7	Muenchen ^b	2
89	Choleraesuis	2	45	Muenster	2
93	Corvallis	1	3	Newport	2
77	Cubana	2	98	Nima	1
31	Derby ^b	2	36	Norwich	3
46	Dublin	2	51	Ohio	2
85	Ealing	2	10	Oranienburg	2
79	Eastbourne	2		Orientalis	1
82	Edinburg	1	72	Oslo	2
2	Enteritidis	3	83	Othmarschen	1
40	Gaminara	2	26	Panama	2
38	Give	2	32	Paratyphi A	2

(continued)

Table 5
(continued)

Ranking ^a	Serotype	Number tested	Ranking	Serotype	Number tested
74	Grumpensis	1	27	Paratyphi B ^b	2
78	Haardt	1	16	Paratyphi B var. L 2 (+) tartrate +	
19	Hadar	2	100	Pensacola	1
24	Hartford	2	48	Pomona	2
64	Havana	2	21	Poona	2
4	Heidelberg	2	49	Reading	2
59	Hvittingfoss	2	96	Rissen	1
	I 11:a:-	1	37	Rubislaw	2
	I 4,[5],12:b:-	2	9	Saintpaul	2
	I 4,[5],12:i:-	2	29	Sandiego	2
94	I 9,12:I,z28:-	2	30	Schwarzengrund	1
95	Ibadan	2	35	Senftenberg	2
	II 50:b:z6	1	20	Stanley	2
70	Indiana	2	63	Telelkebir	2
12	Infantis	2	33	Tennessee	2
58	Inverness	2	14	Thompson	2
99	Irumu	1	17	Typhi	2
88	IV 44:z4,z23:-	1	1	Typhimurium	2
	IV 44:z36:-	1	54	Uganda	2

^aIndicates the rank of the serotype within the top 100 serotype list as provided by the CDC^bxMAP SSA result for one isolate of the serotype did not match agglutination results

among the top 100 serotypes. Of the remaining three discordant isolates, other isolates of the same serotype were correctly detected by xMAP SSA.

4 Notes

1. Use caution when handling xTAG GPP kit components. Store kit components under the proper conditions as indicated in the xTAG GPP Kit Package Insert. Reagents have been validated for six freeze-thaws. For a 96-test kit, this assumes a maximum of six batches would be run with reagents provided from a given lot.
2. Do not use the kit or any kit components past the expiry date indicated on the kit carton label. Do not interchange kit

components from different kit lots. Kit lots are identified on the kit carton label.

3. Store kit components under the proper conditions as indicated in the xMAP SSA Kit Package Insert.
4. TMAC (Tetramethylammonium Chloride), a component of the Assay Buffer, is toxic and may be fatal if swallowed. Do not ingest and do not get on skin or clothing. Wash hands thoroughly after handling.
5. Although the Vi antigen may be present in *S. enterica* ser. Paratyphi C and *S. enterica* ser. Dublin, the AT assay Vi target is specific for *S. enterica* ser. Typhi Vi gene sequence. The *fljB* probe may be positive even if the second phase is not detected in the H antigen assay. This implies the presence of a second phase that is not a part of the 35 targets included in the H antigen assay.
6. Stool specimens should be collected as soon after onset of symptoms as possible. Fresh stool specimens should be placed in sterile, leak-proof, wide-mouthed, preservative-free containers.
7. Unpreserved raw stool specimens should be transported to the laboratory at 4 °C. Raw stool specimens should be tested by xTAG GPP as soon as they are received in the laboratory or frozen at -70 °C until testing. Repeat freezing and thawing of specimens is not recommended.
8. Cultured material can be extracted with or without sample pretreatment. Use 200 µL of culture material directly and follow manufacturer's specifications for a given extraction method.
9. Use the recommended amount of stool specimen for best results. Adding too much stool may result in an increased rate of PCR inhibition. Adding too little stool may result in low sensitivity.
10. Leftover pretreated supernatant (in the SK38 bead tube) can be stored at -80 °C for up to 30 days. Extracted nucleic acid can be stored at -80 °C for up to 30 days.
11. When calculating master mix volumes for multiple reactions, include a 10 % overage to account for pipetting variability.
12. Do not over mix. Froth generation during mixing is undesirable. Avoid bubbles in the tube prior to placing in the thermal cycler.
13. The total thermal cycling run time for xTAG GPP should be approximately 2 h and 10 min. Adjust ramp speed as needed to reach the recommended total run time.

14. When calculating reporter solution for multiple reactions, include a 20–25 % overage to account for pipetting variability and reservoir dead volume.
15. When mixing samples, care must be taken to prevent cross-contamination. Pipette up and down using a slow deliberate motion and avoid generating bubbles by keeping the pipette tip immersed in the liquid while mixing.
16. For protocol installation, refer to the *Instructions for Installing the Data Acquisition Protocol* section of the xTAG GPP Kit Package Insert. For TDAS GPP installation, refer to the *Installing TDAS GPP* section of the xTAG GPP Kit Package Insert.
17. Use caution when removing the Microseal 'A' film from the wells to avoid cross-contamination.
18. xTAG GPP includes two *Salmonella* probes to enhance sensitivity for *Salmonella*. Results for *Salmonella* are determined from the two *Salmonella* probes through a dependent call algorithm. TDAS GPP first evaluates the MFI signal for *Salmonella* Probe 1. If the MFI is less than the analyte-specific negative threshold, the sample is negative for *Salmonella*. If the MFI is equal to or greater than the positive threshold, the sample is positive for *Salmonella*. If the MFI for *Salmonella* Probe 1 is equal to or greater than the analyte-specific negative threshold, but less than the positive threshold (Equivocal Zone), TDAS GPP evaluates *Salmonella* Probe 2. If the MFI for *Salmonella* Probe 2 is equal to or greater than the positive threshold in combination with an equivocal MFI for *Salmonella* Probe 1, the sample is positive for *Salmonella*.
19. Ensure that the InstaGene matrix is vortexed thoroughly before use. The matrix tends to settle, reducing the efficiency of the extraction.
20. Use the side of the PCR tube to remove the cells from the loop.
21. These steps can also be performed using heat blocks instead of a thermal cycler.
22. The genomic DNA is in the supernatant. Care should be taken when pipetting as any pelleted material accompanying the DNA may adversely affect PCR efficiency.
23. The diluted DNA may be stored at –20 °C.
24. Primers and PCR reagents should be used in a PCR grade hood to avoid contamination. Do not work with DNA in close proximity to the PCR reagents to avoid contamination of the reagents.
25. When calculating volumes for master mix, include a two reaction overage for every eight reactions to account for pipetting waste.

26. Luminex beads are photosensitive. Avoid prolonged exposure to light. Prepare a fresh dilution of the microsphere mixes before each use. Microsphere mixes are not stable in Assay Buffer for extended periods.
27. Prepare a sufficient volume of the microsphere mixes for the number of wells plus a few reactions overage for pipetting waste.
28. Ensure that the heater block is in place inside the Luminex 100/200 analyzer before turning on the heater.
29. SAPE is photosensitive. Prepare a fresh aliquot of the SAPE solution at the working concentration (6 µg/mL) before each use. SAPE is not stable in Assay Buffer for extended periods. Never freeze the vial of SAPE.
30. Prepare sufficient volume of SAPE reporter solution for the number of reactions plus a 4 reaction overage for every 24 wells to account for pipetting waste.
31. Care should be taken to ensure that the plate remains at target temperature of 52 °C as increase or decrease in temperature may adversely affect results.
32. Mix carefully to prevent formation of bubbles and potential cross-contamination of reactions.
33. In certain cases the MFI value in the no-template control can be greater than 300. The H_f probe is known to have higher background values between 300 and 500 MFI. Therefore the acceptable negative control value for such probes may be higher than 300 MFI.
34. The MFI value for a positive sample may be slightly less than 1,000, or approach but not meet the S/N threshold of 6.0, or both. Each laboratory should establish its own acceptable threshold values.
35. For additional information on interpretation of the results obtained by xMAP SSA, refer to the xMAP SSA Kit Package Insert.
36. The Additional Targets (AT) assay includes several serotype-specific targets. The *fljB* target is a positive control for the second motility phase of *Salmonella* and indicates a second phase of the H antigen exists. Some serotypes or isolates may yield false negative results for *fljB*. Refer to the xMAP SSA Kit Package Insert for a list of serotypes that may have false negative results for *fljB*. A positive signal on the *sdf* probe indicates that the isolate is *S. enterica* ser. Enteritidis. The Vi probe is specific for the Vi gene sequence found in *S. enterica* ser. Typhi.

References

1. World Health Organization (2013) Diarrhoeal disease. Fact sheet no 330. <http://www.who.int/mediacentre/factsheets/fs330/en/index.html>. Accessed 24 June 2014
2. Centers for Disease Control and Prevention (2011) CDC estimates of foodborne illness in the United States. http://www.cdc.gov/foodborneburden/PDFs/FACTSHEET_A_FINDINGS_updated4-13.pdf. Accessed 24 June 2013
3. U.S. Department of Health and Human Services (2011) National statistics on intestinal infections. <http://hcupnet.ahrq.gov/HCUPnet.jsp>. Accessed 24 June 2013
4. Majowicz SE, Musto J, Scallan E et al (2010) The global burden of nontyphoidal *Salmonella* gastroenteritis. *Clin Infect Dis* 50:882–889
5. Scallan E, Hoekstra RM, Angulo FJ et al (2011) Foodborne illness acquired in the United States—major pathogens. *Emerg Infect Dis* 17:7–15
6. Atkinson R, Maguire H, Gerner-Smidt P (2013) A challenge and an opportunity to improve patient management and public health surveillance for food-borne infections through culture-independent diagnostics. *J Clin Microbiol* 51:2479–2482
7. Guerrant RL, Van Gilder T, Steiner TS et al (2001) Practice guidelines for the management of infectious diarrhea. *Clin Infect Dis* 32: 331–350
8. de Boer RF, Alewijn O, Kesztyüs B et al (2010) Improved detection of five major gastrointestinal pathogens by use of a molecular screening approach. *J Clin Microbiol* 48:4140–4146
9. Pawlowski SW, Warren CA, Guerrant R (2009) Diagnosis and treatment of acute or persistent diarrhea. *Gastroenterology* 136:1874–1886
10. Voetsch AC, Van Gilder TJ, Angulo FJ et al (2004) FoodNet estimate of the burden of illness caused by nontyphoidal *Salmonella* infections in the United States. *Clin Infect Dis* 38(Suppl 3):S127–S134
11. Lee WT, Lin PC, Lin LC et al (2012) *Salmonella*/rotavirus coinfection in hospitalized children. *Kaohsiung J Med Sci* 28:595–600
12. Valentini D, Vittucci AC, Grandin A et al (2013) Coinfection in acute gastroenteritis predicts a more severe clinical course in children. *Eur J Clin Microbiol Infect Dis* 32:909–915
13. Grimont PAD, Weill FX (2007) Antigenic formulae of the *Salmonella* serovars 2007, 9th edn. WHO Collaborating Centre for Reference and Research on *Salmonella*, Institut Pasteur, Paris, France. <http://www.pasteur.fr/ip/por-tal/action/WebdriveActionEvent/oid/01s-000036-089>. Accessed 12 Feb 2012
14. Centers for Disease Control and Prevention (2011) National *Salmonella* surveillance overview. U.S. Department of Health and Human Services, CDC, Atlanta, Georgia. http://www.cdc.gov/nationalsurveillance/PDFs/NationalSalmSurveillOverview_508.pdf
15. McQuiston JR, Waters RJ, Dinsmore BA et al (2011) Molecular determination of H antigens of *Salmonella* by use of a microsphere-based liquid array. *J Clin Microbiol* 49:565–573
16. Amar CFL, East C, Maclare E et al (2004) Blinded application of microscopy, bacteriological culture, immunoassays and PCR to detect gastrointestinal pathogens from faecal samples of patients with community-acquired diarrhea. *Eur J Clin Microbiol Infect Dis* 23:529–534
17. Wu W, Tang YW (2009) Emerging molecular assays for detection and characterization of respiratory viruses. *Clin Lab Med* 29:673–693
18. Dunbar SA (2013) Bead-based suspension arrays for the detection and identification of respiratory viruses. In: Tang Y-W, Stratton W (eds) Advanced techniques in diagnostic microbiology, 2nd edn. Springer Science+Business Media, New York, pp 813–833
19. Dunbar SA, Jacobson JW (2007) Quantitative, multiplexed detection of *Salmonella* and other pathogens by Luminex® xMAP™ suspension array. *Methods Mol Biol* 394:1–19
20. Liu J, Kibiki G, Maro V et al (2011) Multiplex reverse transcription PCR Luminex assay for detection and quantitation of viral agents of gastroenteritis. *J Clin Virol* 50:308–313
21. Liu J, Gratz J, Maro A et al (2012) Simultaneous detection of six diarrhea-causing bacterial pathogens with an in-house PCR-Luminex assay. *J Clin Microbiol* 50:98–103
22. Taylor JD, Briley D, Nguyen Q et al (2001) Flow cytometric platform for high-throughput single nucleotide polymorphism analysis. *Biotechniques* 30:661–669
23. Ye F, Li M-S, Taylor JD et al (2001) Fluorescent microsphere-based readout technology for multiplexed human single nucleotide polymorphism analysis and bacterial identification. *Hum Mutat* 17:305–316
24. Gadsby NJ, Hardie A, Claas ECJ et al (2010) Comparison of the Luminex respiratory virus panel fast assay with in-house real-time PCR for respiratory viral infection diagnosis. *J Clin Microbiol* 48:2213–2216

Chapter 2

Quantitative Proteomic Identification of Host Factors Involved in the *Salmonella typhimurium* Infection Cycle

Dora Kaloyanova, Mijke Vogels, Bas W.M. van Balkom, and J. Bernd Helms

Abstract

Quantitative proteomics, based on stable isotope labeling by amino acids in cell culture (SILAC), can be used to identify host proteins involved in the intracellular interplay with pathogens. This method allows identification of proteins subject to degradation or upregulation in response to intracellular infection. It can also be used to study intracellular dynamics (trafficking) of proteins in response to the infection. Here, we describe the analysis of changes in protein profiles determined in Golgi-enriched fractions isolated from cells that were either mock-infected or infected with *Salmonella typhimurium*. Using the SILAC approach we were able to identify 105 proteins in Golgi-enriched fractions that were significantly changed in their abundance as a result of *Salmonella* infection.

Key words Host-pathogen interactions, *Salmonella typhimurium*, SILAC, Cellular fractionation, Golgi membrane enrichment

1 Introduction

In the last decade a powerful quantitative proteomic approach has been developed in which proteins are marked using stable isotope labeling by amino acids in cell culture (SILAC). This technique was developed by Ong et al. [1] in 2002 and makes use of *in vivo* incorporation of stable isotopes allowing mass spectrometry (MS)-based quantitative proteomic analyses. Typically, two cell pools are used for SILAC experiments: one with cells grown in normal medium (containing the “light” amino acids) and one with cells in medium in which one or two essential amino acids are replaced by the “heavy” isotope forms of these amino acids, allowing for the identification of peptides from each sample in MS-MS spectra. After a few cell passages, all proteins produced by the cells in the “heavy” medium have incorporated the “heavy” amino acids. Cells in the “light” and “heavy” medium can then be treated differently, e.g., treated versus non-treated or infected versus non-infected cells.

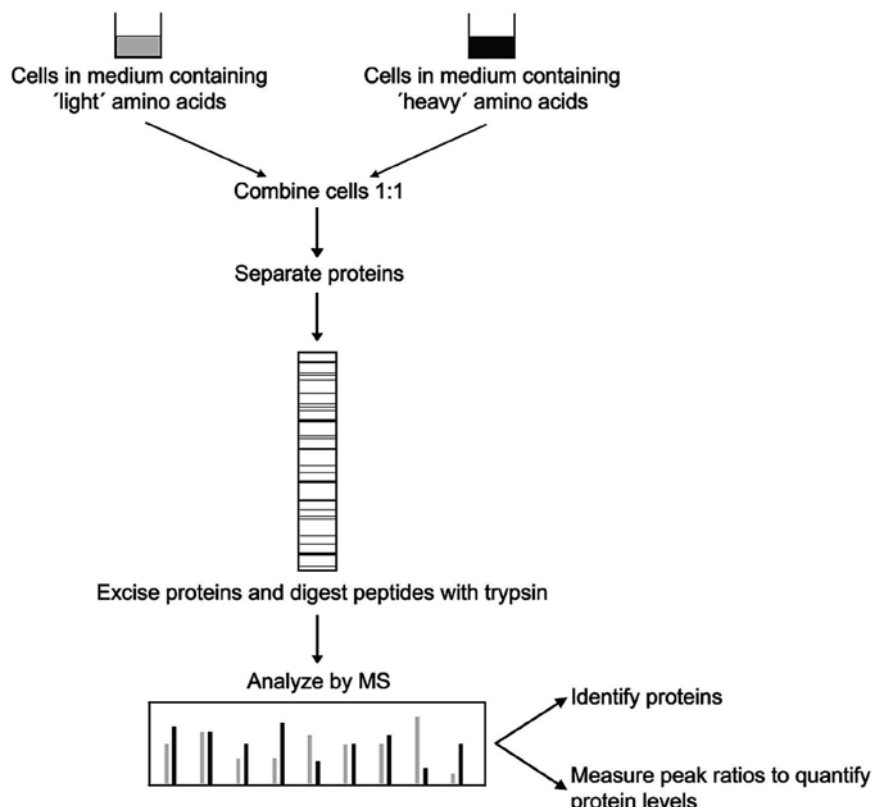


Fig. 1 Stable isotope labeling by amino acids in cell culture (SILAC). Schematic representation of the SILAC procedure. Two cell pools incubated under different conditions are used for SILAC experiments; one pool with cells growing in normal media (containing “light” amino acids) and one pool with cells growing in media containing “heavy” amino acids. Cells from the two pools are combined to a 1:1 ratio, proteins are separated and digested in gel with trypsin. Subsequently, the peptides are applied to a mass spectrometer (MS), analyzed and quantified. Ratios are calculated between the “light” and “heavy” peptides, which reflect differences between protein abundance in the two cell pools. Adapted and modified from Oda et al. [2]

The cells from both treatments are then combined in a 1 to 1 ratio and differences in protein abundance due to the treatment can be assessed and quantified by MS (Fig. 1) [2]. SILAC has become a powerful tool to investigate changes in the host cell proteome upon infection with an intracellular pathogen, allowing elucidation of host–pathogen interactions [3–9].

Most proteomic approaches published so far deal with the analysis of cellular proteomes of total cell lysates rather than specific cellular compartments [6, 7, 9]. However, a major advantage of using quantitative proteomics to study host–pathogen interactions is the ability to fractionate the samples before analysis. In this way, specific compartments of the host cell, such as the organelles that make up the secretory pathway, can be studied.

In this chapter we describe the procedure recently used in our lab [10] to investigate *Salmonella*–host interactions in more detail

by using a quantitative proteomics approach (SILAC) in combination with cell fractionation. We compared the protein profiles of isolated Golgi-enriched fractions from cells that were either infected with *S. typhimurium* or mock-infected. After statistical analysis, 105 proteins were identified that were significantly changed in their abundance in the Golgi-enriched fraction upon *Salmonella* infection. This technique was also previously applied in our laboratory to investigate interactions of coronaviruses with the host secretory pathway [11].

2 Materials

2.1 Cells and Bacteria

1. HeLa cells.
2. Dulbecco's Modified Eagle medium (DMEM; Cambrex).
3. Fetal calf serum (FCS; Life Technologies (Paisley)).
4. Penicillin and streptomycin (pen/strep); both from Life Technologies (Paisley).
5. PBS.
6. Trypsin.
7. T75, T175 flasks (Corning) and 24-well plates (Corning) for cell culture.
8. Luria–Bertani (LB) broth and agar plates (*see Note 1*).
9. Gentamycin (Gibco).

2.2 $^{13}\text{C}^{15}\text{N}$ -Arginine- and $^{13}\text{C}^{15}\text{N}$ -Lysine- Labeling of HeLa Cells

1. DMEM lacking L-arginine and L-lysine (PAN-biotech cat.no. P04-04510S2).
2. L-arginine- $^{13}\text{C}_6^{15}\text{N}_4$ hydrochloride (heavy; Spectra Stable Isotopes, cat.no. 548ARG98).
3. L-lysine- $^{13}\text{C}_6^{15}\text{N}_2$ hydrochloride (heavy; Spectra Stable Isotopes, cat.no. 548LYS98).
4. L-arginine- $^{12}\text{C}_6^{14}\text{N}_4$ hydrochloride (light; Sigma, cat.no. A5131).
5. L-lysine- $^{12}\text{C}_6^{14}\text{N}_2$ hydrochloride (light; Sigma, cat.no. L5626).
6. Dialyzed FCS (Invitrogen, cat.no. 26400-044).
7. Lysisbuffer: 20 mM Tris–HCl, pH 7.6; 150 mM NaCl; 1 % nonidet P-40; 0.5 % NaDOC; 0.1 % SDS; 2 $\mu\text{g}/\text{ml}$ aprotinin; 2 $\mu\text{g}/\text{ml}$ leupeptin; 1 $\mu\text{g}/\text{ml}$ pepstatin; 1 mM PMSF.

2.3 Isolation of Golgi-Enriched Fractions

1. Homogenization buffer: 250 mM sucrose in 10 mM Tris–HCl, pH 7.4.
2. Mixtures of protease inhibitors as tablets (Roche). Each tablet is sufficient for a 50 ml solution.

3. PBS buffer prepared as 10× buffer: 1.37 M NaCl, 81 mM Na₂HPO₄, 15 mM KH₂PO₄ and 27 mM KCl, pH of the 10× buffer is adjusted to pH 7.4.
4. EDTA stock solution: 100 mM EDTA/KOH, pH 7.1.
5. Sucrose solutions: 29 % w/w, 35 % w/w, and 62 % w/w sucrose in 10 mM Tris–HCl, pH 7.4 (*see Note 2*).

2.4 SDS Polyacrylamide Gel Components

1. Laemmli sample buffer: 50 mM TRIS, pH 6.8; 2.5 % β-Mercaptoethanol; 2 % SDS; 0.02 % Bromophenol; 10 % Glycerol.
2. Bio-Rad Gel electrophoresis system.
3. Ingredients for 5 % stacking gel: 30 % Acrylamide/Bis solution; 1 M Tris–HCl, pH 6.8; Demi water; 10 % SDS solution; 10 % Ammonium Persulfate (APS) solution; TEMED.
4. Ingredients for 12 % running gel: 30 % Acrylamide–Bis solution; 1.5 M Tris–HCl, pH 8.8; Demi water; 10 % SDS solution; 10 % APS solution; TEMED.
5. Fixing solution: 5 % acetic acid/30 % methanol.
6. Coomassie staining (GelCode Blue reagent (Pierce)).
7. Destain solution: 30 mM potassium ferricyanide (K₃Fe(CN)₆; 9.9 mg/ml), 100 mM sodium thiosulfate (Na₂S₂O₃·5H₂O; 24.8 mg/ml) (Merck 6516).

2.5 In-Gel Tryptic Digestion

1. 50 mM ammonium bicarbonate, pH 8.5 (NH₄HCO₃; 4 g/L) (Ambic).
2. Acetonitrile (AcN).
3. 6.5 mM DTT (1 mg/ml in 50 mM ammonium bicarbonate, pH 8.5) (ICN 194821).
4. 54 mM iodoacetamide (10 mg/ml in 50 mM ammonium bicarbonate, pH 8.5) (Sigma 16125).
5. Trypsin: Dissolve 100 µg Trypsin in 1 ml 0.1 M HCl (store in 10–50 µl aliquots at –80 °C). During the experiment, dilute stock 10× with 50 mM bicarbonate (10 ng/µl final concentration) just before addition to gel piece.

3 Methods

Carry out all procedures at room temperature unless otherwise specified.

3.1 Cell Culture

This step describes how the HeLa cells are cultured and kept in culture before performing experiments. Specific requirements for HeLa cells, necessary for the experiments, are described in the paragraphs of the respective experiments.

1. DMEM medium, used for the cell culture, is supplemented with 10 % fetal calf serum (FCS), 100 IU of penicillin/ml, and 100 µg of streptomycin/ml (pen/strep).
2. HeLa cells are grown in T75 flasks and incubated overnight in an incubator at 37 °C/5 % CO₂.
3. When 80 % confluence is reached, cells are trypsinized using trypsin (see Note 3) and plated in other flasks or plates (see Note 4).

3.2 *Salmonella* Infection

This step describes how an infection of HeLa cells with *Salmonella* bacteria is performed in general [12]. Specific adjustments made in the experiments are described in the protocols of these experiments.

1. *S. typhimurium* cultures are grown in LB broth for 16–18 h at 37 °C with continuous shaking. On the day of the experiment, bacteria from the overnight culture are diluted 33 times in LB broth and incubated for another 3.5 h to reach the exponential phase as described before [13] (see Note 5).
2. To follow a synchronized population of intracellular bacteria, HeLa cells are infected with *Salmonella* at a multiplicity of infection (MOI) of 100, for 15 min at 37 °C in DMEM with 10 % FCS (see Note 6).
3. Cells are washed thoroughly with PBS and incubated in DMEM with addition of 100 µg/ml gentamycin (Gibco) for 1 h to kill all extracellular bacteria (see Note 7).
4. The medium is replaced by DMEM with 10 % FCS and 10 µg/ml gentamycin and the infection is continued for 5 h.

3.3 ¹³C¹⁵N-Arginine- and ¹³C¹⁵N-Lysine- Labeling of HeLa Cells

This step describes how labeling of HeLa cells works in general. Before performing SILAC experiments, it must be ensured that cells are labeled completely and how many passages this takes to accomplish. Therefore, this should be tested using the protocol below. Upon complete incorporation of labeled amino acids, the protocol described here results in peptide mass shifts of 8 and 10 amu for each lysine and arginine in the peptide, respectively.

1. For the ¹³C¹⁵N-arginine- and ¹³C¹⁵N-lysine-labeling of HeLa cells, cells are cultured in specialized medium: DMEM lacking L-arginine and L-lysine, which is reconstituted with the heavy amino acids, L-arginine-¹³C₆¹⁵N₄ hydrochloride and L-lysine-¹³C₆¹⁵N₂ hydrochloride (referred to as heavy medium). As a control for the extent of labeling, cells are also cultured in medium with the normal, light amino acids, L-arginine-¹²C₆¹⁴N₄ hydrochloride and L-lysine-¹²C₆¹⁴N₂ hydrochloride (referred to as light medium) (see Note 8).
2. The heavy and light culture media are supplemented with dialyzed FCS and pen/strep (see Note 9).

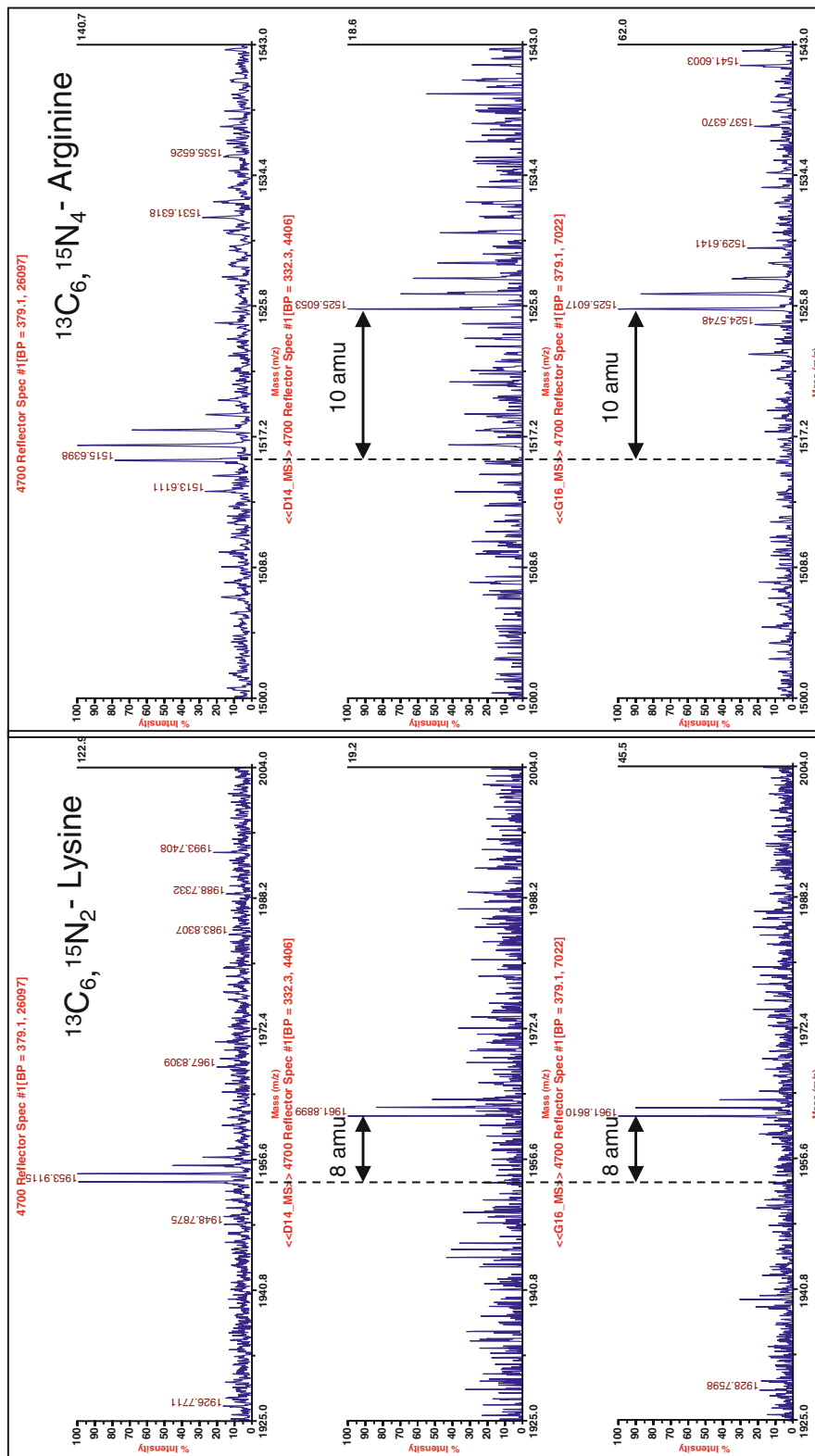


Fig. 2 Maldi TOF analysis to investigate incorporation of SIlAC labels. To investigate whether incorporation of labeled AA in the protein is complete after 1 (top), 2 (middle), or 3 (bottom panel) cell passages, trypsinized Fig. 2 (continued) proteins (from a single gel band) were analyzed by Maldi TOF. For both the heavy Lysine (left) as the heavy Arginine, right) complete incorporation can already be observed after 2 passages, indicated by the absence of the original peptide peaks (displayed in upper panels) and the appearance of the peptide peaks corresponding to the labeled peptides (+8 amu for Lysine, +10 amu for Arginine, both indicated). The labeling is maintained in passage 3

3. Cells are passaged in fresh medium when 80–90 % confluence is reached. The extent and efficiency of the stable isotope labeling of the HeLa cells are checked using MALDI-TOF-TOF analysis as shown previously [8] (see Note 10).
4. When the mass spectrometry analysis shows that the incorporation of the $^{13}\text{C}^{15}\text{N}$ amino acids is complete (Fig. 2), the SILAC experiments can be performed. In our case, incorporation was complete after 1 or 2 passages, but for practical reasons, cells that had been passaged six times in the heavy medium were used in the SILAC experiments.

3.4 SILAC Experiments; *Salmonella* *Typhimurium* Infection

The SILAC procedure, which was described by Ong et al. [1], are performed with certain adjustments as we describe below and as was published previously [10, 11].

1. Two pools of HeLa cells are used that have been passaged six times in either the heavy or the light medium.
2. The HeLa cells are grown in T175 flasks (Corning) until confluence of 80–90 % was reached (approximately 1×10^7 cells per flask).
3. Cells from eight culture flasks are used per experiment, four flasks per labeling condition.
4. In each SILAC experiment, cells cultured either in the light or the heavy medium are mock-infected or infected with WT *S. typhimurium* at a MOI of 100 for 6 h (see Note 11). In our case a 6 h infection is used since that is the time point when *Salmonella* reaches the Golgi apparatus.

3.5 SILAC Experiments; Isolation of a Golgi-Enriched Fraction

1. Six hours post infection (p.i.), the *Salmonella*-infected cells are harvested in homogenization buffer and combined in a 1:1 ratio with the mock-infected cells (see Note 12).
2. A Golgi-enriched fraction is isolated from the cells using an established method [11, 14, 15].
 - (a) Cells from 8 culture flasks are trypsinized and harvested at $500 \times g$ for 10 min and washed twice in cold PBS with subsequent centrifugation at $500 \times g$ for 10 min.
 - (b) The pellet is washed with cold homogenization buffer and the cells are spun down at $500 \times g$ for 10 min (see Note 13).
 - (c) The pellet is resuspended in 5 volumes of cold homogenization buffer (see Note 14), followed by homogenization using a Balch homogenizer (Fig. 3) [16].
 - (d) Cells are homogenized with the Balch homogenizer (gap size 9 μm) with approximately 50–60 strokes (see Note 15).
 - (e) Post nuclear supernatant (PNS) is obtained after centrifugation of the cell homogenate at $600 \times g$ for 10 min at 4 °C.



Fig. 3 Balch homogenizer. To keep the homogenate at 4 °C, precool the homogenizer for 15 min on ice. Depending of the volume of PNS use a suitable syringe size (from 1 to 10 ml). The volume of the PNS to be homogenized should not exceed half of the maximum volume of the syringe [16]

- (f) To 12 ml of PNS, 11 ml of 62 % (w/w) sucrose solution and 250 ml of 100 mM EDTA (pH 7.1) are added to obtain a homogenate with 37 % (w/w) sucrose concentration (*see Note 16*).
- (g) Four milliliter of this homogenate is placed into a SW40 tube (Beckman) and overlaid with a 5 ml 35 % (w/w) and a 4 ml 29 % (w/w) layer of sucrose solution (in 10 mM Tris, pH 7.4) (*see Note 17*).
- (h) This gradient is centrifuged for 2 h and 40 min at 100,000 $\times g$.
- (i) Approximately 1 ml of a Golgi-enriched fraction is collected at the interphase of 35–29 % sucrose layers (*see Note 18*).
- (j) For further analysis, the collected membranes are pelleted by centrifugation for 30 min at 100,000 $\times g$ at 4 °C after the addition of 4 volumes of PBS to 1 volume of the Golgi-enriched fraction. Alternatively, the collected membranes are stored at -80 °C (*see Note 19*). Golgi-enrichment of the isolated fraction is verified by western blot analysis using established organelle marker proteins.

3.6 SDS-PAGE and Coomassie Staining

1. Golgi-enriched membranes (80 µg protein) are dissolved in Laemmli sample buffer containing 10 mM DTT and heated for 5 min at 95 °C (*see Note 20*).
2. Clean the glass plates of the Bio-Rad Gel Electrophoresis system. Prepare the 12 % running gel by mixing 1.98 ml 30 % Acrylamide/Bis, 1.25 ml 1.5 M Tris-HCl, pH 8.8, 1.7 ml demi water, 50 µl 10 % SDS, 50 µl APS, and 3 µl TEMED and cast the gel between the glass plates into the cassette. Allow space for the stacking gel, gently overlay it with water, and let it solidify for 45 min at room temperature.
3. Prepare the 5 % stacking gel by mixing 170 µl 30 % Acrylamide/Bis, 130 µl 1 M Tris-HCl pH 6.8, 700 µl demi water, 10 µl 10 % SDS, 10 µl APS, and 1 µl TEMED. Remove the water from the solid running gel and cast the stacking gel on top of the running gel and insert a 10-well gel comb immediately without introducing air bubbles. Let it solidify for 30 min at room temperature.
4. Remove the comb and add loading standard to the first lane. Samples are loaded in the other lanes of the gel. Electrophoresis is performed at 100 V (15 mA) for 5 min until the samples have entered the stacking gel. Then continue at 150–200 V (20–30 mA) until the dye front has reached the bottom of the running gel (*see Note 21*).
5. After the electrophoresis run, open the glass plates using a spatula, leaving the gel on one of the glass plates. Carefully remove the gel from the plate by rinsing the plate and the gel in deionized water. Transfer the gel into a container filled with fixing solution and fix the gel for 30–45–60 min.
6. After fixation, rinse the gel with ultrapure Milli-Q (MQ) water and stain using GelCode Blue reagent for 45–60 min. After this, distain the gel using MQ water and incubate for 60 min (for publication quality pictures refresh MQ and distain overnight).
7. Each gel lane is cut into 24 equally sized slices (*see Note 22* and Fig. 4) and each slice is transferred into an Eppendorf tube.

3.7 Mass Spectrometry

The 24 gel slices are subjected to in-gel tryptic digestion as described below (*see Note 23*) and before [8]:

1. Add 100 µl AcN per tube, leave it for a few seconds and then remove it from the tube.
2. Reduction of proteins is performed by adding with 100 µl DTT (6.5 mM in 50 mM ambic) and incubation at room temperature for 60 min.

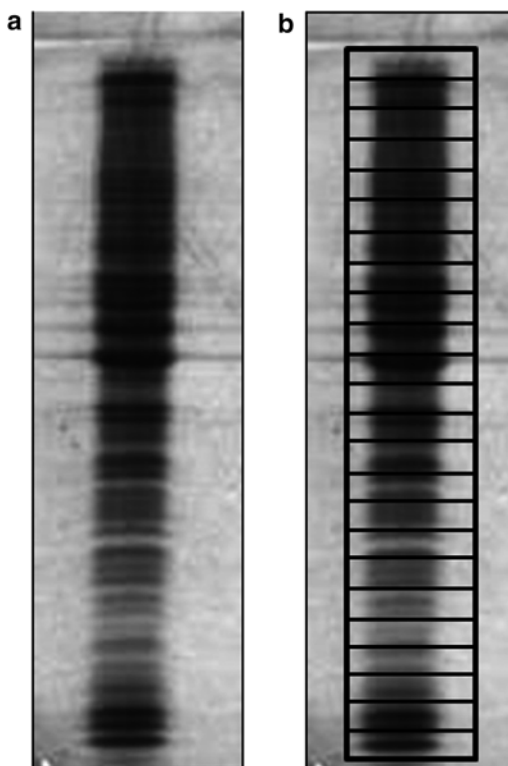


Fig. 4 SDS-PAGE protein profile of a Golgi-enriched fraction after a gel electrophoresis. Separation separation of 80 µg of proteins from a purified Golgi fraction. (a) Coomassie GelCode Blue stained gel. (b) Illustration of the size of the 24 gel slices used for MS analysis

3. Remove the DTT and add 100 µl AcN per tube, leave it for a few seconds and then remove it again from the tube.
4. Alkylate the proteins by adding 100 µl iodoacetamide (54 mM in 50 mM ambic) and incubating at room temperature for 60 min in the dark.
5. Shrink the gel slice by adding (and removing) 100 µl AcN, swell the slice by adding (and removing) 100 µl ambic and shrink again by adding (and removing) 100 µl AcN.
6. Dry the samples in the air (leave cups open).
7. Add 10 µl of diluted trypsin (10 ng/µl final concentration) and incubate on ice for 60 min. Remove supernatant (if there is any) and add 50 µl ambic to cover the gel pieces. Digest the peptides overnight at 37 °C.
8. 20–80 % of the supernatants obtained after the digestion is used for LC-MS/MS analysis on a Thermo Finnigan FT-ICR equipped with a 7 Tesla magnet coupled to an Agilent Series 1100 binary pump system (Agilent Technologies).

- Peptide mixtures are trapped on an in-house packed 5 cm×100 µm AquaTM C18 reversed phase column (Phenomenex) at a flow rate of 5 µl/min (*see Note 24*).
- Peptide separation is achieved on an 15 cm×75 µm AquaTM C18 reversed phase column using a gradient of 0–70 % solution B (solution A=0.1 M acetic acid; solution B=80 % [v/v] acetonitrile, 0.1 M acetic acid) in 60 min at a constant flow rate of 200 nl/min (*see Note 25*).

3.8 Mass Spectrometry Data Analysis

- Finnigan *.raw files are converted to *.dta files using BioWorks software, version 3.1 SR1 (Thermo Electron Corporation).
- For this process the program is set to track the scan limits automatically and calculate for peptides with a mass from 300 to 5,000 amu, automatically detecting the charge state and MS level (MS or MS/MS). The threshold was set to 100 counts.
- Subsequently, Mascot generic files were generated through in-house developed software.
- These files were used to search the IPI_Human 3.36 database [17] on an in-house Mascot server [4] allowing up to 2 missed cleavages, a peptide mass tolerance of 50 ppm and a fragment mass tolerance of 0.8 Da (*see Note 26*).
- Peptide modifications allowed in the searches were carbamidomethyl modification of cysteine (fixed) and oxidation of methionine, tryptophan, and histidine (variable) (*see Note 27*).
- Proteins matching the criteria for at least two reliable peptides (rank 1; unique; individual score higher than 29 [1 % false positive rate]), and with a protein score higher than 64 were considered as positive identified proteins.
- Raw data files and Mascot html results pages were loaded into the MSQuant program [5] adapted for SILAC-based quantitative analysis.
- All quantified peptides are verified by manual inspection of the spectra used for quantification. To identify statistically significant (and removing) different protein abundances between samples ($p < 0.05$), data from 3 independent experiments were loaded into the StatQuant program for statistical analysis [18] (*see Note 28*).

4 Notes

- For 200 ml LB broth, dissolve 2 g tryptone, 1 g yeast extract, 2 g sodium chloride in 200 ml deionized water. For agar plates, add 3 g agar to the mixture. Autoclave for 20 min and allow the solution to cool to 55 °C. Store the liquid LB broth at

room temperature or 4 °C. For agar plates, pour approximately 15 ml into petri dishes and let solidify at room temperature. Store the plates at 4 °C.

2. For 29 % w/w sucrose solution dissolve 65.08 g sucrose in 200 ml of 10 mM Tris, pH 7.4; for the 35 % w/w: 80.60 g sucrose in 200 ml of 10 mM Tris, pH 7.4 and for the 62 % w/w sucrose: 161 g sucrose in 200 ml of 10 mM Tris, pH 7.4. Prepare the solutions in advance and dissolve with rotation ON at 4 °C. Sucrose solutions can be stored at -80 °C.
3. Medium is removed from the cells and cells are washed by rinsing them carefully with PBS, 2 ml of trypsin is added to the cells and the flask is incubated in the incubator at 37 °C/5 % CO₂ for a few minutes. Cells are removed from the surface by carefully tapping the flask. Add medium (10 ml) and transfer the cells into a 15 ml tube (Corning). Cells are centrifuged at 500 ×*g* for 5 min. Resuspend the cell pellet in 1 ml medium and the cell density is determined by cell counting under the microscope using a cell counter. A specific number of cells (see Note 4) is transferred to new flasks or plates in medium and incubated in the incubator at 37 °C/5 % CO₂.
4. Different volumes of DMEM and number of HeLa cells are used, depending on the type of plate, indicated at the specific steps of the protocol.
5. For overnight cultures, add 1 *Salmonella* colony (from a freshly grown agar plate) into 4 ml LB broth in a 15 ml tube (Corning) and incubate for 16–18 h at 37 °C with continuous shaking. Add 1 ml of the overnight culture to 32 ml of LB broth in a 50 ml tube (Corning) and incubate for another 3.5 h at 37 °C with continuous shaking to reach the exponential phase, as described before [13].
6. HeLa cells are infected with *Salmonella* at a multiplicity of infection (MOI) of 100. This means that 100 times more bacteria than HeLa cells are added to the cells. For this, the bacteria from the 33 ml culture are centrifuged for 15 min at 1,000 ×*g* after which the pellet is resuspended in 1 ml DMEM supplemented with 10 % FCS (no pen/strep!). By performing a growth curve of *Salmonella*, we determined that after 3.5 h the concentration of bacteria in the 33 ml culture 3.5 h is 8.3×10^8 bacteria/ml. The growth curve of *Salmonella* should be repeated for the strain that is used in the experiments. Since the number of HeLa cells is known (specified in the specific steps of the protocol), the volume of bacteria that corresponds with an MOI of 100 can be calculated. HeLa cells are carefully rinsed with PBS and incubated in DMEM, supplemented with 10 % FCS (no pen/strep) and the right amount of bacteria. Cells are

incubated for 15 min at 37 °C. During these 15 min, the *Salmonella* bacteria attach to the HeLa cells.

7. After the attachment of the bacteria to the cells, the medium is removed from the cells and the cells are washed with PBS (adding and removing of 15 ml of PBS) to get rid of cell debris and any loose bacteria. Cells and bacteria are then incubated in medium containing 100 µg/ml gentamycin. The stock solution of gentamycin has a concentration of 10 mg/ml. Therefore, this solution should be diluted 1,000 times in DMEM/10 % FCS.
8. The “heavy” amino acids L-arginine-¹³C₆¹⁵N₄ hydrochloride and L-lysine-¹³C₆¹⁵N₂ hydrochloride, or the “light” amino acids L-arginine-¹²C₆¹⁴N₄ hydrochloride and L-lysine-¹²C₆¹⁴N₂ are added to specialized DMEM lacking L-arginine and L-lysine, at a final concentration of 84 mg/L and 146 mg/L for arginine and lysine, respectively. Instead of using commercially available normal “light” DMEM, we choose to add the light amino acids to specialized DMEM lacking L-arginine and L-lysine. In this way, we prepared the heavy and light media in exactly the same manner.
9. 10 % Dialyzed FCS and 100 IU of penicillin/ml and 100 µg of streptomycin/ml are added to specialized DMEM. Dialyzed FCS is used because dialysis depletes FCS of small molecules such as amino acids, hormones and cytokines while avoiding the precipitation of serum proteins. In this way, “normal” L-arginine and L-lysine remains absent in specialized DMEM.
10. To check the incorporation of the “heavy” amino acids into the cells, MALDI-TOF-TOF analysis is performed as described [8]. For this analysis, cells passaged in light and heavy medium are trypsinized, centrifuged for 10 min at 500 ×*g* and pellets are resuspended in 1 ml lysis buffer (20 mM Tris-HCl, pH 7.6, 150 mM NaCl, 1 % nonidet P-40, 0.5 % NaDOC, 0.1 % SDS, 2 µg/ml aprotinin, 2 µg/ml leupeptin, 1 µg/ml pepstatin, 1 mM PMSF). After an incubation on ice for 10 min, the nuclei are spun down by centrifugation for 5 min at 600 ×*g* at 4 °C, and the supernatant is used for MALDI-TOF-TOF analysis.
11. For the SILAC experiments 4 T175 flasks with 1 × 10⁷ cells are infected with *Salmonella* at a MOI of 100. Therefore, 100 × 10⁷ bacteria are needed per flask, which is 400 × 10⁷ bacteria in total. Since the 1:33 culture contains 8.3 × 10⁸ *Salmonella*/ml, 400 × 10⁷ bacteria corresponds with 4.8 ml of bacterial culture. This volume of bacteria is taken and centrifuged for 5 min at 1,000 ×*g* after which the pellet is resuspended in 40 ml of DMEM/10 % FCS. 10 ml is added per flask and infection is

carried out as described in Subheading 3.2. The other 4 flasks are mock-infected. In that case, the same procedure is followed but instead of *Salmonella* bacteria, DMEM is used. The SILAC experiments must be repeated at least three times; 2 experiments in which the “heavy” cells are infected with *Salmonella* and 1 experiment in which the “light” cells are infected.

12. After *Salmonella* infection, remove the medium from the cells, and wash the cells carefully with PBS. Add 5 ml homogenization buffer per flask. Using cell scrapers harvest the cells from the flasks and combine them in a 1:1 ratio in a 50 ml tube. Centrifuge the cells at $500 \times g$ for 10 min (4 °C). In order to wash the cells, resuspend the pellet in cold Homogenization Buffer (HB) and transfer them to a 15 ml tube (10 min, $500 \times g$, 4 °C). Measure the volume of the pellet and add four times HB with protease inhibitors, incubate on ice.
13. Carefully remove the HB as the pellet is loose after this step.
14. It is important to estimate as good as possible the volume of the pellet and to add not more than 5 volumes (of the pellet estimated volume) of HB to ensure sufficiency and reproducibility of the homogenization.
15. Check the homogenization efficiency at the microscope using a vital stain such as Trypan Blue after every 10–20 strokes. In general 50–60 strokes are needed to ensure disruption of about 90 % of the cells. However, the number of strokes are dependent of the pressure given by the operator. Be careful not to homogenize the cells excessively as too harsh conditions may affect the integrity of intracellular membranes and contaminate your preparation.
16. If the sucrose concentration is out of the range 36.5–37.5 (w/w), adjust by adding either 10 mM Tris–HCl buffer (pH 7.4) or sucrose solution (2 M). Use the following formulas to calculate the required volume:

$$\frac{V_{\text{original}} \times (C_{\text{wanted}} - C_{\text{original}})}{(C_{\text{stock solution}} - C_{\text{wanted}})} = V_{\text{to add}}$$

When the sucrose concentration is higher than 37.5:

When sucrose concentration of the homogenate is lower than 36.5:

$$\frac{V_{\text{original}} \times (C_{\text{wanted}} - C_{\text{original}})}{(C_{\text{wanted}})} = V_{\text{to add}}$$

V_{original} = Volume of homogenate solution after the addition of 62 % (w/w) sucrose.

$V_{\text{to add}}$ = Volume to add of either 2 M sucrose solution or 10 mM Tris–HCl buffer.

C_{original} = Sucrose concentration (in M) of homogenate solution after adding 62 % (w/w) sucrose.

C_{wanted} = Desired concentration of sucrose (i.e., 37 % (w/w)).

$C_{\text{stock solution}}$ = Stock solution of sucrose (2 M).

17. When preparing the sucrose gradient use a bent pipet tip to slowly overlay the sucrose layers without disturbing the interfaces. The interfaces have to be easily recognized after layering. Only then the floated Golgi-enriched fraction is easy to see and collect.
18. After centrifugation carefully remove the tube from the centrifuge bucket. Use a syringe with a needle of 22G to puncture the tube and to collect the Golgi-enriched band (*see Fig. 5*).
19. Determine the protein concentration of the collected fraction (usually 0.15 $\mu\text{g}/\mu\text{l}$), aliquot the Golgi fraction into Eppendorf tubes, snap-freeze the tubes in liquid nitrogen and then store at -80°C .
20. Protein concentration of the Golgi-enriched fraction is measured using the Bradford protein assay. The volume corresponding to 80 μg of protein is added to an Eppendorf tube, centrifuged at maximal speed for 10 min (4°C). Pellet is resuspended in 20 μl of Laemmli sample buffer containing 10 mM DTT and heated for 5 min at 95°C . Samples are cooled on ice.

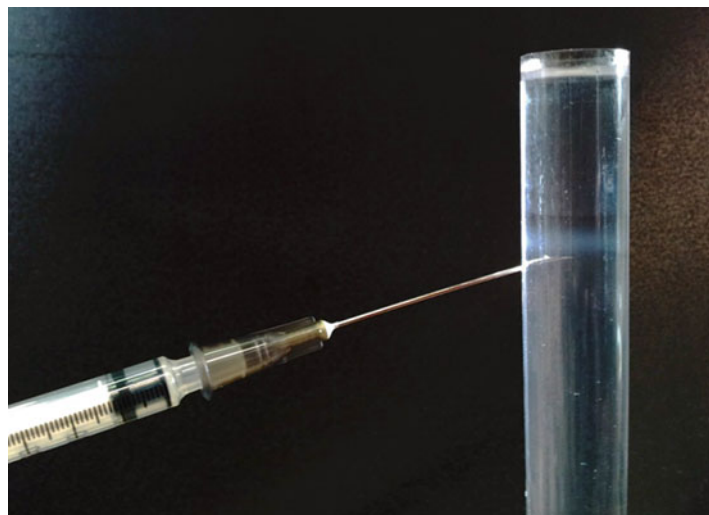


Fig. 5 Floated Golgi-enriched fraction. After flotation an opalescent band at the interface between 35 and 29 % sucrose will be visible. Collect the band by using 1 ml syringe with a 22G needle. The collected fraction is about 1 ml and has a protein concentration of about 0.15 $\mu\text{g}/\mu\text{l}$. The sucrose concentration is about 30 % (w/w)

21. Adding a drop of sample buffer to un-used wells will help to form straight dye front during the electrophoresis.
22. After Coomassie staining, each gel lane is cut into 24-equally sized pieces, using a razor blade. Cut around the edges of the complete lane and remove this lane from the gel. Next, equally divide the lane into 24 pieces (see Fig. 4). Transfer each piece into a Eppendorf tube.
23. DTT is added to reduce cysteines and to disrupt sulfur bridges. Iodoacetamide is added to prevent the formation of new sulfur bridges. The cycle with AcN and Ambic dehydrates and rehydrates the minced gel slices for washing and absorbance of reagents and trypsin in the gel slices. During this cycle, the solutions have only to be added for a few seconds, after which the solutions can be removed again.
24. In this step, the peptides derived from trypsin-digested proteins are loaded onto the trapping column. This step can be compared to the loading of proteins into the stacking gel when performing a SDS-PAGE gel. No separation takes place at this step.
25. After loading of all peptides onto the column, valves are switched and the gradient from solution A to B starts running. More complex samples, e.g., samples containing peptides from various proteins, require longer run times. Peptides are eluted from the trapping column, with the most hydrophilic peptides coming off first, and the most hydrophobic peptides coming off last.
26. In the identification of peptides, some room for error (incorrect measurements of peptide and peptide fragment masses) is allowed. The more accurate the mass spectrometer can determine peptide and fragment mass, the smaller the error will be, yielding higher confidence in identifications.
27. During preparation of peptide mixtures, some peptide modifications can occur. As such modifications affect peptide (and fragment) mass, and mass changes have to be taken into account to deduce to identity of each peptide and fragment. All cysteine residues in the sample are reduced and subsequently alkylated using iodoacetamide, yielding a mass addition of 57.02146 amu on *each* cysteine. Oxidation, which can occur but does not necessarily affect all methionine, tryptophan or histidine residues, yields a mass change of 15.99491 amu.
28. Nowadays, many programs for quantitative analysis of mass spectrometry are available. Many of them have the option to calculate differential quantities based on different labeling methods such as SILAC, iTRAQ or label-free quantitation. Also protein identification is integrated, generating a robust quantitative proteomics analysis pipeline.

References

- Ong SE, Blagoev B, Kratchmarova I, Kristensen DB, Steen H, Pandey A et al (2002) Stable isotope labeling by amino acids in cell culture, SILAC, as a simple and accurate approach to expression proteomics. *Mol Cell Proteomics* 1(5):376–386
- Oda Y, Huang K, Cross FR, Cowburn D, Chait BT (1999) Accurate quantitation of protein expression and site-specific phosphorylation. *Proc Natl Acad Sci U S A* 96(12):6591–6596
- Mannova P, Fang R, Wang H, Deng B, McIntosh MW, Hanash SM et al (2006) Modification of host lipid raft proteome upon hepatitis C virus replication. *Mol Cell Proteomics* 5(12):2319–2325
- Perkins DN, Pappin DJ, Creasy DM, Cottrell JS (1999) Probability-based protein identification by searching sequence databases using mass spectrometry data. *Electrophoresis* 20(18):3551–3567
- Schulze WX, Mann M (2004) A novel proteomic screen for peptide-protein interactions. *J Biol Chem* 279(11):10756–10764
- Shi L, Chowdhury SM, Smallwood HS, Yoon H, Mottaz-Brewer HM, Norbeck AD et al (2009) Proteomic investigation of the time course responses of RAW 264.7 macrophages to infection with *Salmonella enterica*. *Infect Immun* 77(8):3227–3233
- Shui W, Gilmore SA, Sheu L, Liu J, Keasling JD, Bertozzi CR (2009) Quantitative proteomic profiling of host-pathogen interactions: the macrophage response to *Mycobacterium tuberculosis* lipids. *J Proteome Res* 8(1):282–289
- van Balkom BW, van Gestel RA, Brouwers JF, Krijgsveld J, Tielens AG, Heck AJ et al (2005) Mass spectrometric analysis of the *Schistosoma mansoni* tegumental sub-proteome. *J Proteome Res* 4(3):958–966
- Vester D, Rapp E, Gade D, Genzel Y, Reichl U (2009) Quantitative analysis of cellular proteome alterations in human influenza A virus-infected mammalian cell lines. *Proteomics* 9(12):3316–3327
- Vogels MW, van Balkom BW, Heck AJ, de Haan CA, Rottier PJ, Batenburg JJ et al (2011) Quantitative proteomic identification of host factors involved in the *Salmonella typhimurium* infection cycle. *Proteomics* 11(23):4477–4491
- Vogels MW, van Balkom BW, Kaloyanova DV, Batenburg JJ, Heck AJ, Helms JB et al (2011) Identification of host factors involved in coronavirus replication by quantitative proteomics analysis. *Proteomics* 11(1):64–80
- Steele-Mortimer O (2008) Infection of epithelial cells with *Salmonella enterica*. *Methods Mol Biol* 431:201–211
- Beuzon CR, Meresse S, Unsworth KE, Ruiz-Albert J, Garvis S, Waterman SR et al (2000) *Salmonella* maintains the integrity of its intracellular vacuole through the action of SifA. *EMBO J* 19(13):3235–3249
- Balch WE, Dunphy WG, Braell WA, Rothman JE (1984) Reconstitution of the transport of protein between successive compartments of the golgi measured by the coupled incorporation of N-acetylglucosamine. *Cell* 39(2 Pt 1):405–416
- Brugger B, Sandhoff R, Wegehingel S, Gorgas K, Malsam J, Helms JB et al (2000) Evidence for segregation of sphingomyelin and cholesterol during formation of COPI-coated vesicles. *J Cell Biol* 151(3):507–518
- Balch WE, Rothman JE (1985) Characterization of protein transport between successive compartments of the golgi apparatus: asymmetric properties of donor and acceptor activities in a cell-free system. *Arch Biochem Biophys* 240(1):413–425
- Kersey PJ, Duarte J, Williams A, Karavidopoulou Y, Birney E, Apweiler R (2004) The international protein index: an integrated database for proteomics experiments. *Proteomics* 4(7):1985–1988
- van Breukelen B, van den Toorn HW, Drugan MM, Heck AJ (2009) StatQuant: a post-quantification analysis toolbox for improving quantitative mass spectrometry. *Bioinformatics* 25(11):1472–1473

Chapter 3

Determination of Antimicrobial Resistance in *Salmonella* spp.

Belgode N. Harish and Godfred A. Menezes

Abstract

Infections with *Salmonella* are an important public health problem worldwide. *Salmonella* are one of the most common causes of food-borne illness in humans. There are many types of *Salmonella* but they can be divided into two broad categories: those that cause typhoid and those that do not. The typhoidal *Salmonella* (TS), such as *S. enterica* subsp. *enterica* serovars Typhi and *S. Paratyphi* only colonize humans and are usually acquired by the consumption of food or water contaminated with human fecal material. The much broader group of non-typhoidal *Salmonella* (NTS) usually results from improperly handled food that has been contaminated by animal or human fecal material. Antimicrobials are critical to the successful outcome of invasive *Salmonella* infections and enteric fever. Due to resistance to the older antimicrobials, ciprofloxacin [fluoroquinolone (FQ)] has become the first-line drug for treatment. Nevertheless, switch to FQ has led to a subsequent increase in the occurrence of salmonellae resistant to this antimicrobial agent. The exact mechanism of this FQ resistance is not fully understood. FQ resistance has driven the use of third-generation cephalosporins and azithromycin. However, there are sporadic worldwide reports of high level resistance to expanded-spectrum cephalosporins (such as ceftriaxone) in TS and in NTS it has been recognized since 1988 and are increasing in prevalence worldwide. Already there are rare reports of azithromycin resistance leading to treatment failure. Spread of such resistance would further greatly limit the available therapeutic options, and leave us with only the reserve antimicrobials such as carbapenem and tigecycline as possible treatment options. Here, we describe the methods involved in the genotypic characterization of antimicrobial resistance in clinical isolates of salmonellae.

Key words *Salmonella*, Fluoroquinolones, Cephalosporins, Clinical and laboratory standards institute, Mutations, *gyrA*, β -Lactamases

1 Introduction

On a global scale it has been estimated that *Salmonella* is responsible for an estimated three billion human infections each year. The World Health Organization (WHO) has estimated that annually typhoid fever accounts for 21.7 million illnesses (217,000 deaths) and paratyphoid fever accounts for 5.4 million of these cases. Infants, children, and adolescents in south-central and Southeastern Asia experience the greatest burden of illness [1]. However, infection by

the NTS serovars is estimated to cause a large burden worldwide, with a higher morbidity rate than mortality. The NTS are primarily food-borne zoonotic pathogens causing acute gastroenteritis in humans all over the world [1].

A suitable antibiotic is essential for the treatment of patients with invasive *Salmonella* infections and should commence as soon as clinical diagnosis is made. The utility of chloramphenicol for the treatment of typhoid fever was an unexpected discovery. Chloramphenicol has a broad spectrum of activity. Chloramphenicol interferes with microbial protein synthesis by binding to the prokaryotic 50S ribosomal subunit [2]. Chloramphenicol has the drawbacks of a high relapse rate, a high rate of continued and chronic carriage, bone marrow toxicity, and high mortality rates. Ampicillin and trimethoprim-sulfamethoxazole are used as alternative antibiotics. Ampicillin inhibits the enzymes necessary for peptidoglycan synthesis and triggers membrane associated autolytic enzymes. Trimethoprim and sulfamethoxazole inhibit various stages in folate metabolism and prevent synthesis of bacterial DNA. There was emergence of plasmid-mediated chloramphenicol resistance in the typhoid bacillus. The chloramphenicol-resistant strains from outbreaks showed combination resistance to streptomycin, sulfonamides, and tetracyclines (R-type CSSuT), encoded by a plasmid of the H1 incompatibility group (now termed HII) [3].

The plasmid was thermosensitive and encoded chloramphenicol acetyl transferase (catA1); not long after genes encoding resistance to ampicillin (*bla*_{TEM-1}) and trimethoprim/sulfamethoxazole (*dfrA14* and *sul2* respectively) are also acquired [4]. Resistance to all first line antimicrobials—ampicillin, trimethoprim-sulfamethoxazole, and chloramphenicol—is defined as multidrug resistance (MDR) [5]. Chloramphenicol acetyl transferase inactivates the drug by adding 2 acetyl groups to it [2]. A second mechanism of resistance to chloramphenicol is based on the loss of an OMP [6]. Ampicillin resistance is mediated by the production of β -lactamases (usually TEM-1, and therefore inhibited by clavulanic acid). MDR strains are more resistant to amoxicillin-clavulanic acid than sensitive isolates and so other mechanisms may be involved as well. Trimethoprim-sulfamethoxazole resistance is mediated by alteration in the enzyme targets dihydrofolate reductase and dihydropteroate synthase respectively [2].

Resistance to the older antimicrobials, chloramphenicol, ampicillin, and trimethoprim-sulfamethoxazole (co-trimoxazole), termed multidrug resistant (MDR) isolates has been present for many years. In this respect, the fluoroquinolone (FQ) ciprofloxacin has become the first-line drug for treatment, particularly since the global emergence of *S. Typhi* isolates that MDR. Treatment failures have been defined in strains displaying decreased ciprofloxacin susceptibility (DCS) [ciprofloxacin minimum inhibitory concentration (MIC) of 0.125–1.0 μ g/mL] [7]. However, for

ciprofloxacin susceptible isolates, the Clinical and Laboratory Standards Institute (CLSI) in 2012 has revised the breakpoints from $\leq 1 \mu\text{g}/\text{mL}$ to $\leq 0.06 \mu\text{g}/\text{mL}$.

Nalidixic acid resistance has been a reliable indicator of such isolates, which has become common in many regions. Nevertheless, switch to ciprofloxacin has led to a subsequent increase in the occurrence of typhoidal salmonellae resistant to this antimicrobial agent [8].

In salmonellae, quinolone resistance is usually associated with mutations in the quinolone resistance-determining region (QRDR) of the A subunit target site of DNA gyrase, though the presence of plasmid-mediated quinolone resistance *qnr* genes and *aac(6')*-*Ib-cr* has also been described in quinolone-resistant non-Typhi *Salmonella*. Recent reports confirm the *qnrS1* and *qnrB2* from *S. Typhi*, demonstrating the role of plasmid-mediated FQ resistance. The exact mechanism of this DNA gyrase-mediated resistance in *S. Typhi* is not fully understood, though various studies have found that single point mutations in this region confer resistance to nalidixic acid and hence reduced susceptibility to FQs. In contrast, high-level ciprofloxacin resistance may be due to either (a) the cumulative impact of mutations in many genes, (b) decreased membrane permeability, (c) active efflux pump, and/or (d) the presence of plasmid-encoded *qnr* genes [9].

FQ resistance has driven the use of third-generation cephalosporins, such as ceftriaxone and other agents for the management of enteric fever. Worldwide, there are sporadic reports of high level resistance to expanded-spectrum cephalosporins (such as ceftriaxone) in typhoidal salmonellae, due to the presence of CTX-M-15 and SHV-12 extended spectrum β -lactamases (ESBLs). NTS serovars have been found to possess a wide variety of ESBL enzymes, including TEM, SHV, PER, CTX-M, as well as plasmid mediated AmpC β -lactamase enzymes (e.g., CMY, DHA, ACC-1). FQ and ESBL mediated resistance are major problems in the effective treatment of bacterial infections, both in the community and in the nosocomial setting [1].

Here, we describe the determination of predominant molecular mechanisms of antimicrobial resistance to antimicrobials in use for salmonellae.

2 Materials

2.1 Bacterial Isolates

Bacterial isolates are identified by standard biochemical methods as *Salmonella* spp. (see Note 1). The identification was confirmed using specific antisera (Murex Biotech, England).

2.2 PFGE Reagents

1. EET buffer: 100 mM Na₂ EDTA, 10 mM EGTA, 1 M Tris-HCl, pH 8.0 (see Note 2).

2. Lysis solution: EET buffer, lysostaphin 100 µg/ml.
3. Proteinase-K solution (60 mg/ml): Proteinase-K, 10 mM Tris-HCl, 10 mM NaCl.
4. “depro” solution: EET buffer, Proteinase-K, SDS 1 %.
5. T₁₀E_{0.1} buffer: 10 mM Tris-HCl, 0.1 mM Na₂ EDTA.
6. T₁₀E₁ buffer: 10 mM Tris-HCl 1 mM Na₂ EDTA.
7. TBE buffer 0.5×: 0.045 M Tris-HCl, 0.045 M Boric acid, 0.001 M EDTA.

3 Methods: Molecular-Biological Studies

3.1 Preparation of Template DNA

A single bacterial colony from an overnight grown culture is suspended in 100 µl of sterile Milli-Q water and boiled for 5 min. The suspension is centrifuged at 8,000 rpm for 10 min. The supernatant containing bacterial DNA is used as template for PCR, (see Note 3).

3.2 Quinolone Resistance

The mechanism of quinolone resistance is determined by investigating mutations in the QRDRs of DNA gyrase (*gyrA* and *gyrB*) and DNA topoisomerase IV (*parC* and *parE*) genes [10–12]. The sequences of the primers and the thermocycling conditions used are as follows;

gyrA: Template DNA is amplified by PCR with the use of oligonucleotide primers;

5'-ATGAGCGACCTTGCAGAGAAATTACACCG-3' and

5'-TTCCATCAGCCCTTCAATGCTGATGTCTTC-3'. The program for amplification includes a step of initial denaturation at 95 °C for 2 min, followed by 35 cycles of 94 °C for 30 s, 70 °C for 60 s, and 72 °C for 90 s and a final extension step at 72 °C for 5 min.

gyrB: Template DNA is amplified by PCR with the use of oligonucleotide primers;

5'-GGACAAAGAAGGCTACAGCA-3' and

5'-CGTCGCGTTGTACTCAGATA-3'. The program for amplification includes a step of initial denaturation at 95 °C for 5 min, followed by 30 cycles of 94 °C for 15 s, 53 °C for 20 s, and 72 °C for 1 min and a final extension step at 72 °C for 5 min.

parC: Template DNA is amplified by PCR with the use of oligonucleotide primers;

5'-ATGAGCGATATGGCAGAGCG-3' and

5'-TGACCGAGTTCGCTAACAG-3'. The program for amplification includes a step of initial denaturation at 94 °C for 3 min, followed by 30 cycles of 94 °C for 30 s, 55 °C for 30 s, and 72 °C for 30 s and a final extension step at 72 °C for 10 min.

parE: Template DNA is amplified by PCR with the use of oligonucleotide primers;

5'-GACCGAGCTGTCCTGTGG-3' and

5'-GCGTAAC TGCA CGGGTCA-3'. The program for amplification includes a step of initial denaturation at 94 °C for 3 min, followed by 30 cycles of 94 °C for 30 s, 55 °C for 30 s, and 72 °C for 30 s and a final extension step at 72 °C for 10 min.

The PCR is performed in a final reaction volume of 25 µl containing 10 mM Tris-HCl (pH 8.3); 50 mM KCl, 3.0 mM MgCl₂; 6.6 pmol of each primer, 1 U of Taq polymerase, dNTP 0.2 mM each, and 1 µl of template DNA. The PCR products are loaded in 1 % wt/vol agarose gel prepared in Tris-borate-EDTA buffer and detected by ethidium bromide staining after electrophoresis. The PCR products are stored at -20 °C.

3.3 Restriction Fragment Length Polymorphisms (RFLP) Analysis as a Screening Method for *gyrA* Mutations

The amplified 620-bp fragment of the *gyrA* gene has three *HinfI* restriction sites, one of which lies at Ser 83. Therefore, *HinfI* restriction digestion of the PCR product is done to detect mutation at Ser 83. A volume of 20 µl of the PCR product is digested with 10 U of *HinfI* (Fermentas, USA) at 37 °C. The restriction fragments are run on 2 % agarose gel prepared in Tris-borate-EDTA buffer and detected by ethidium bromide staining after electrophoresis [13], (see Note 4).

3.4 Sequence Analysis of *gyrA*, *gyrB*, *parC*, and *parE* PCR Products

Sequencing is performed with both forward and reverse primers (same as used for the PCR) on Thermal Cycler and analyzed in an automatic DNA sequencer. DNA sequences are analyzed by using commercial software (Lasergene; DNAStar, Inc., Madison, Wis.). The BLASTN program is used for database searching (<http://www.ncbi.nlm.nih.gov/BLAST/>). The QRDR DNA sequences are compared with those of *S. Typhi* strain Ty2 (GenBank accession no. AE014613), (see Notes 5 and 6).

3.5 Screening for *qnr* Genes

Plasmid-mediated quinolone resistance, *qnr* (*qnrA*, *qnrB*, and *qnrS*) [14] is detected using sequences of the primers and the thermocycling conditions, as follows:

Template DNA is amplified by simplex PCR with the use of oligonucleotide primers:

qnrA, 5'- TTCAGCAAGAGGATTCTCA-3' and

5'-GGCAGCACTATTACTCCCAA-3';

qnrB, 5'-CCTGAGCGGCACTGAATTAT-3' and

5'-GTTTGCTGCTGCCAGTCGA-3';

qnrS, 5'-CAATCATACATATCGGCACC-3' and

5'-TCAGGATAAACAAACAATACCC-3'.

The program for amplification includes a step of initial denaturation at 94 °C for 5 min, followed by 35 cycles of 94 °C for 30 s, 54 °C for 90 s, and 72 °C for 60 s and a final extension step at 72 °C for 5 min. Control strains are used for the detection methods. The PCR is performed in a final reaction volume of 25 µl containing 10 mM Tris–HCl (pH 8.3); 50 mM KCl, 3.0 mM MgCl₂; 6.6 pmol of each primer, 1 U of Taq polymerase, dNTP 0.2 mM each, and 1 µl of template DNA. The PCR products are loaded in 1 % wt/vol agarose gel prepared in Tris–borate–EDTA buffer and detected by ethidium bromide staining after electrophoresis.

3.6 Screening for *aac(6')-Ib-cr* Gene [15]

PCR screening for *aac(6')-Ib-cr* gene is performed using sequences of the primers and the thermocycling conditions as follows;

Template DNA is amplified by simplex PCR with the use of oligonucleotide primers;

aac(6')-Ib.1,

5'-ATATGCGGATCCAATGAGCAACGCAAAACAAAG
TTAG-3' and

5'-ATATGCGAATTCTTAGGCATCACTGCGTGT
CGCTC-3';

aac(6')-Ib.2, 5'-TTGCAATGCTGAATGGAGAG-3' and

5'-CGTTTGGATCTTGGTGACCT-3';

aac(6')-Ib.qnrA, 5'-TTGCGATGCTCTATGAGTGG-3' and

5'-CTCGAATGCCTGGCGTGT-3'.

The program for amplification includes a step of initial denaturation at 94 °C for 5 min, followed by 35 cycles of 94 °C for 30 s, 54 °C for 90 s, and 72 °C for 60 s and a final extension step at 72 °C for 5 min. Known positive control strains are included in each run. The PCR is performed in a final reaction volume of 25 µl containing 10 mM Tris–HCl (pH 8.3); 50 mM KCl, 3.0 mM MgCl₂; 6.6 pmol of each primer, 1 U of Taq polymerase, dNTP 0.2 mM each, and 1 µl of template DNA. The PCR products are loaded in 1 % wt/vol agarose gel prepared in Tris–borate–EDTA buffer and detected by ethidium bromide staining after electrophoresis.

3.7 Isoelectric Focusing of β -Lactamase Enzymes

Isoelectric focusing of β -lactamase enzymes is performed using the following procedure. Briefly, an overnight culture of the relevant isolate is made in 5 ml Brain Heart Infusion (BHI) broth with 100 µg/ml ampicillin. After overnight incubation the culture is diluted 20 times in 5 ml fresh BHI and incubated at 37 °C for 4 h and with shaking at 200 rpm. The culture tubes are centrifuged for 5 min at 4,000 rpm at 4 °C, the pellet resuspended in 200 µL 50 mM Tris–HCl pH 7.4. Five microliters of lysozyme solution is added (40 mg/mL), and mix rotated for 60 min at 37 °C.

After 60 min, 10 µL of 0.5 M EDTA is added and the mix rotated for further 10 min at room temperature. The mix is centrifuged for 5 min at 14,000 rpm and the supernatant transferred to a clean tube. The isoelectric point (pI) of the β -lactamase is determined by isoelectric focusing, applying the supernatants of crude cell extracts to Phast gels (GE HealthCare, Fairfield, CT, USA) with a pH gradient of 3–9 in a Phast system (GE HealthCare). Extended-spectrum β -lactamases (ESBLs) with known pI values (TEM-1, SHV-2) are included as pI markers [16].

3.8 Molecular Detection of β -Lactamase Genes

Non-typhoidal salmonellae are initially screened (optional) for the presence of TEM and SHV β -lactamases using a commercially available antimicrobial resistance gene microarray (Check-Points BV, The Netherlands).

PCR screening is performed to identify genes coding for β -lactamases; bla_{TEM} , bla_{SHV} , bla_{OXA-1} group, bla_{CTX-M} and $ampC$ [17–21].

S. Typhi isolates with ampicillin MIC of ≥ 256 µg/mL and all NTS are screened for these genes. Known positive controls are included in all PCR protocols.

The sequences of the primers and the thermocycling conditions used are as follows:

bla_{TEM} : Template DNA is amplified by PCR with the use of oligonucleotide primers;

5'-ATAAAATTCTTGAAGACGAAA-3' and

5'-GACAGTTACCAATGCTTAATCA-3'. The PCR is performed in a final reaction volume of 25 µL containing 10 mM Tris–HCl (pH 8.3); 50 mM KCl, 3.0 mM MgCl₂; 6.6 pmol of each primer, 1 U of Taq polymerase, dNTP 0.2 mM each, and 1 µL of template DNA. The program for amplification includes a step of initial denaturation at 94 °C for 5 min, followed by 35 cycles of 94 °C for 30 s, 54 °C for 90 s, and 72 °C for 60 s and a final extension step at 72 °C for 5 min. The PCR products are loaded in 1 % wt/vol agarose gel prepared in Tris–borate–EDTA buffer and detected by ethidium bromide staining after electrophoresis.

bla_{SHV} : Template DNA is amplified by PCR with the use of oligonucleotide primers;

5'-CGCCGGGTTATTCTTATTGTCCGC-3' and

5'-TCTTTCCGATGCCGCCAGTCA-3'. The PCR is performed in a final reaction volume of 25 µL containing 10 mM Tris–HCl (pH 8.3); 50 mM KCl, 3.0 mM MgCl₂; 6.6 pmol of each primer, 1 U of Taq polymerase, dNTP 0.2 mM each, and 1 µL of template DNA. An Eppendorf thermocycler is used for amplification. The program for amplification included a step of initial denaturation at 94 °C for 5 min, followed by 30 cycles

of 94 °C for 30 s, 68 °C for 30 s, and 72 °C for 50 s and a final extension step at 72 °C for 10 min. The PCR products are loaded in 1 % wt/vol agarose gel prepared in Tris–borate–EDTA buffer and detected by ethidium bromide staining after electrophoresis.

*bla*_{OXA-1} group: Template DNA is amplified by PCR with the use of oligonucleotide primers:

5'-GGATAAAACCCCCAAAGGAA-3' and

5'-TGCACCAGTTTCCCATACA-3'. The PCR is performed in a final reaction volume of 25 μ l containing 10 mM Tris–HCl (pH 8.3); 50 mM KCl, 3.0 mM MgCl₂; 6.6 pmol of each primer, 1 U of Taq polymerase, dNTP 0.2 mM each, and 1 μ l of template DNA. The program for amplification includes a step of initial denaturation at 94 °C for 5 min, followed by 30 cycles of 94 °C for 25 s, 60 °C for 40 s, and 72 °C for 50 s and a final extension step at 72 °C for 5 min. The PCR products are loaded in 1 % wt/vol agarose gel prepared in Tris–borate–EDTA buffer and detected by ethidium bromide staining after electrophoresis.

*bla*_{CTX-M}: After initial optimization (simplex PCR), template DNA is amplified by multiplex PCR, with the use of oligonucleotide primers:

group 1, 5'-AAAAATCACTGCGCCAGTTC-3' and

5'-AGCTTATTCTATCGCCACGTT-3';

group 2, 5'-CGACGCTACCCCTGCTATT-3' and

5'-CCA GCGTCAGATTTTCAGG-3';

group 9, 5'-CAAAGAGAGTGCAACGGATG-3' and

5'-ATTGGAAAGCGTTCATCACC-3'.

Fragments of alleles encoding enzymes of groups 8 and 25 are amplified with two specific forward primers and a shared reverse primer:

5'-TCGCGT TAAGCGGATGATGC-3' (group 8 forward);

5'-GCACGATGACATTGGG-3' (group 25 forward); and

5'-AACCCACGATGTGGGTAGC-3' (groups 8/25 reverse).

The PCR is performed in a final reaction volume of 50 μ l containing 25 mM Tris–HCl, 50 mM KCl, 1.5 mM MgCl₂, 0.2 mM each dNTP, 20 pmol of each primers, 2.5 U Taq polymerase, and 5 μ L template DNA. The program for amplification includes a step of initial denaturation at 94 °C for 5 min, followed by 35 cycles of 94 °C for 2 min, 60 °C for 1 min and 72 °C for 2 min and a final extension step at 72 °C for 10 min. The PCR products are loaded in 1 % wt/vol agarose gel prepared in Tris–borate–EDTA buffer and detected by ethidium bromide staining after electrophoresis (Bio-Rad, USA).

ampC: Template DNA is amplified by multiplex PCR, (see Note 7) with the use of oligonucleotide primers:

MOXM, 5'-GCTGCTCAAGGAGCACAGGAT-3' and
 5'-CACATTGACATAGGTGTGGTGC-3';
CITM, 5'-TGGCCAGAACTGACAGGCAAA-3' and
 5'-TTTCTCCTGAACGTGGCTGGC-3';
DHAM, 5'-AACTTTCACAGGTGTGCTGGT-3' and
 5'-CCGTACGCATACTGGCTTGC-3';
ACCM, 5'-AACAGCCTCAGCAGCCGGTTA-3' and
 5'-TTCGCCGCAATCATCCCTAGC-3';
EBCM, 5'-TCGGTAAAGCCGATGTTGCGG-3' and
 5'-CTTCCACTGCCGCTGCCAGTT-3';
FOXN, 5'-AACATGGGTATCAGGGAGATG-3' and
 5'-CAAAGCGCGTAACCGGATTGG-3'.

Each reaction contains 20 mM Tris-HCl (pH 8.4); 50 mM KCl; 0.2 mM each deoxynucleoside triphosphate; 1.5 mM MgCl₂; 0.6 μ M primers MOXMF, MOXMR, CITMF, CITMR, DHAMF, and DHAMR; 0.5 μ M primers ACCMF, ACCMR, EBCMF, and EBCMR; 0.4 μ M primers FOXMF and FOXMR; and 1.25 U of Taq DNA polymerase. Template DNA (2 μ l) is added to 48 μ l of the master mixture. The PCR program consists of an initial denaturation step at 94 °C for 3 min, followed by 25 cycles of DNA denaturation at 94 °C for 30s, primer annealing at 64 °C for 30s, and primer extension at 72 °C for 1 min. After the last cycle, a final extension step at 72 °C for 7 min is added. The PCR products are loaded in 2 % wt/vol agarose gel prepared in Tris-borate-EDTA buffer and detected by ethidium bromide staining after electrophoresis. AmpC β -lactamase control strains are used.

3.9 Sequence Analysis

Sequencing of the β -lactamases gene PCR products is performed using both forward and reverse PCR primers and standard methods. The BLASTN program is used for database searching (<http://www.ncbi.nlm.nih.gov/BLAST/>). Additional sequencing primers are required for *bla*_{TEM} PCR product sequencing (Lagging strand 7, 5'-TTACTGTCATGCCATCC-3' and Lagging strand 3, 5'-AGAGAATTATGCAGTGC-3'). PCR primers corresponding to sequences downstream (ORF 1) of the *bla*_{CTX-M} genes (M3 int upp, 5'-TCACCCAGCCTAACCTAAG-3' and ORF1 pol M3, 5'-GCACCGACACCCTCACACCT-3' are also used. Finally, PCR products of *bla*_{CTX-M} are subjected to sequencing using primers, CTX-M-1 fw multi 5'-AAAAATCACTGCGCCAGTTC-3', CTX-M-1 multi (REV)F seq 5'-AACGTGGCGATGAATAAGCT-3', and ORF1 pol M3 5'-GCACCGACACCCTCACACCT-3' [9], (see Note 8).

3.10 Screening for Plasmids in Non-typhoidal *Salmonellae*

The presence of individual plasmid types is determined by PCR screening of *II*, *FIA*, *FIB*, *FII*, *A/C*, *HII*, *FrepB*, *K/B*, and *B/O* replicons [22], (see Note 9).

After initial optimization (simplex PCR), template DNA is amplified by multiplex PCR, with the use of oligonucleotide primers for *II*, *FIA*, *FIB*, *FII*, *A/C* replicons. Simplex PCR is performed for the following replicons, *HII*, *FrepB*, *K/B*, and *B/O*.

The sequences of the primers and the thermocycling conditions used are as follows:

Template DNA is amplified by PCR with the use of oligonucleotide primers:

II, 5'-CGAAAGCCGGACGGCAGAA-3' and
 5'-TCGTCGTTCCGCCAAGTTCGT-3';
FIA, 5'-CCATGCTGGTTCTAGAGAAGGTG-3' and
 5'-GTATATCCTTACTGGCTTCCGCAG-3';
FIB, 5'-GGAGTTCTGACACACGATTTCCTG-3' and
 5'-CTCCCGTCGCTTCAGGGCATT-3';
FII, 5'-CTGTCGTAAGCTGATGGC-3' and
 5'-CTCTGCCACAAACTTCAGC-3';
A/C, 5'-GAGAACCAAAGACAAAGACCTGGA-3' and
 5'-ACGACAAACCTGAATTGCCTCCTT-3';
HII, 5'-GGAGCGATGGATTACTTCAGTAC-3' and
 5'-TGCCGTTTCACCTCGTGAGTA-3';
FrepB, 5'-TGATCGTTAAGGAATTTC-3' and
 5'-GAAGATCAGTCACACCATCC-3';
K/B, 5'-GCGGTCCGGAAAGCCAGAAAAC-3' and
 5'-TCTTTCACGAGCCCGCCAAA-3';
B/O, 5'-GCGGTCCGGAAAGCCAGAAAAC-3' and
 5'-TCTGCGTTCCGCCAAGTTCGA-3'.

Because of the high level of homology between the *K* and *B/O* replicons the same forward primer is used in both these simplex PCRs. The PCR is performed in a final reaction volume of 25 μ l containing 10 mM Tris-HCl (pH 8.3); 50 mM KCl, 3.0 mM MgCl₂; 6.6 pmol of each primer, 1 U of Taq polymerase, dNTP 0.2 mM each, and 1 μ l of template DNA. An Eppendorf thermocycler is used for amplification.

Touchdown PCR (uses a cycling program with varying annealing temperatures) is employed. It is a useful method to increase the specificity of PCR. The annealing temperature in the initial cycle should be 5–10 °C above the T_m of the primers. In subsequent cycles, the annealing temperature is decreased in steps of 1–2 °C/cycle until a temperature is reached that is equal to, or 2–5 °C

below, the Tm of the primers. Touchdown PCR enhances the specificity of the initial primer-template duplex formation and hence the specificity of the final PCR product. Thermocycling conditions are initial denaturation at 94 °C for 4 min, followed by 15 cycles of 94 °C for 30 s, 70 °C for 1 min and 72 °C for 2 min. In the subsequent cycles, 20 cycles of 94 °C for 30 s, 55 °C for 1 min, 72 °C for 2 min and a final extension step at 72 °C for 10 min. The PCR products are loaded in 1 % wt/vol agarose gel prepared in Tris–borate–EDTA buffer and detected by ethidium bromide staining after electrophoresis. Control plasmid strains are used.

3.11 Detection of Class 1 Integrons in NTS

The presence or absence of class 1 integrons is determined using 5'-CS and 3'-CS primers specific for the variable regions of integrons [23]. The sequences of the primers and the thermocycling conditions used are as follows:

Template DNA is amplified by PCR with the use of oligonucleotide primers:

5'- GGCATCCAAGCAGCAAG-3' and

5'-AAGCAGACTTGACCTGA-3'. The PCR is performed in a final reaction volume of 25 µl containing 10 mM Tris–HCl (pH 8.3); 50 mM KCl, 3.0 mM MgCl₂; 6.6 pmol of each primer, 1 U of Taq polymerase, dNTP 0.2 mM each, and 1 µl of template DNA. An Eppendorf thermocycler is used for amplification. The program for amplification includes a step of initial denaturation at 94 °C for 4 min, followed by 35 cycles of 94 °C for 1 min, 55 °C for 2 min and 72 °C for 2 min and a final extension step at 72 °C for 7 min. The PCR products are loaded in 1 % wt/vol agarose gel prepared in Tris–borate–EDTA buffer and detected by ethidium bromide staining after electrophoresis.

3.12 PCR Targeting the Flagellin Gene (*fliC*) of Ceftriaxone Resistant *S. Typhi* to Confirm the Identity of the Isolate

PCR targeting the flagellin gene (*fliC*) of ceftriaxone resistant *S. Typhi* to confirm the identity of the isolate Nested PCR targeting the flagellin gene of *S. Typhi* is used to confirm the identity of the isolate.

Primers Used

ST1 (5'-TATGCCGCTACATATGATGAG-3') and

ST2 (5'-TTAACGCAGTAAAGAGAG-3'), which are used for regular PCR to amplify a 495 bp fragment, corresponded to nucleotides 1036–1056 and 1513–1530, respectively, in the flagellin gene of *S. Typhi*.

For nested PCR,

ST3 (5'ACTGCTAAAACCCTACT-3') and

ST4 (5'-TGGAGACTTCGGTCGCGTAG-3') are used to amplify a 363 bp fragment [24].

PCR Conditions

For regular PCR, a 25 μ l amplification mixture containing 10 μ l of commercial master mix, 7 μ l of Milli-Q water, 2 μ l ST1 and 2 μ l ST2 primers with 4 μ l of the extracted DNA is used. Using a thermal cycler, the reaction mixture is subjected to 40 cycles of 2 min each at 94 °C for denaturation followed by annealing at 57 °C for 15 s and elongation at 72 °C for 1 min. A final elongation of 7 min duration is done at 72 °C.

Nested PCR

A 1 in 5 diluted amplified product from the regular PCR is used as template for nested PCR. Amplification conditions are similar to the first round PCR except annealing at a higher temperature at 63 °C at 15 s.

The sequencing of the flagellin gene product is carried out and analyzed.

3.13 Genotyping

- (a) Pulsed Field Gel Electrophoresis (PFGE): Briefly, isolates are incubated overnight at 37 °C in 7 ml Mueller Hinton broth. After incubation, 1 ml of bacterial cells are harvested, pelleted, and washed three times using 1 ml EET buffer, before being adjusted to a cell density of 0.5 at 560 nm. A 100 μ L of cell suspension and 100 μ L of 1.4 % PFGE grade agarose in EET buffer are mixed and poured into PFGE plug molds. The plugs are incubated at 4 °C for 30 min to harden and 1 ml of lysozyme is added before incubation at 37 °C for 3 to 4 h. Lysozyme is removed from the plugs and 1 ml each of deproteinizing solution is added prior to overnight incubation at 37 °C. Next, the plugs are washed six times every 30 min with T10E1 buffer, and then soaked in T10E0.1 buffer for 30 min. Restriction digestion is carried out using 40 U of *Xba*I (Fermentas) at 37 °C for typhoidal salmonellae and using 40 U each of both *Xba*I and *Spe*I (Fermentas) at 37 °C, for non-typhoidal salmonellae. PFGE is performed in a 1 % agarose gel in a CHEF DR-II system (Bio-Rad) with the following conditions 0.5× Tris–Borate–EDTA buffer, 140 °C, 6 V/cm for 22 h (with switch times ranging from 5 to 40 s). Lambda ladder PFGE marker (Bio-Rad) is used as a molecular weight standard.
- (b) Enterobacterial Repetitive Intergenic Consensus (ERIC PCR): Extracted DNA is amplified by PCR with the use of oligonucleotide primers: ERIC-1: 5'-ATGTAAGCTCCTGGGGA TTCAC-3' and ERIC-2: 5'-AAGTAATGACTGGGGTG AGCG-3'. The PCR is performed in a final reaction volume of 25 μ l containing 10 mM Tris–HCl (pH 8.3); 50 mM KCl, 3.0 mM MgCl₂; 6.6 pmol of each primer, 1 U of Taq polymerase, dNTP 0.2 mM each, and 1 μ l of template DNA. An Eppendorf

thermocycler is used for amplification. The program for amplification includes a step of initial denaturation at 95 °C for 7 min, followed by 30 cycles of 95 °C for 30 s, 50 °C for 1 min, and 65 °C for 8 min and a final extension step at 65 °C for 16 min. The PCR products are loaded in 2 % wt/vol agarose gel prepared in Tris-borate-EDTA buffer and detected by ethidium bromide staining after electrophoresis [25].

4 Notes

1. Biochemical characterization: H_2S production is a variable factor (there are exceptions) as far as typhoidal salmonellae are concerned; one should not rule out or rule in any serotype of salmonellae based on H_2S production.
2. EET buffer (PFGE reagent preparation): Both EDTA and EGTA dissolved at pH 8.0. It is preferred to adjust the pH starting with NaOH pellets and continue with 4 N NaOH for the “fine tuning”. EGTA = ethylene glycol-bis (beta aminoethylene)-N, N, N', N' tetra acetic acid. EGTA is a sodium chelate and does not bind magnesium.
3. Template DNA: The supernatant should be quantified for DNA or run electrophoresis and seen for the intensity of the band. If the DNA is not found, the sediment from the centrifuged tube could be checked for DNA.
4. Restriction fragment length polymorphisms (RFLP) analysis as a screening method for *gyrA* mutations: PCR-RFLP of the *gyrA* gene of typhoidal salmonellae also revealed an unusual and stable RFLP that points to the existence of mixed genotypes. The *gyrA* gene locus has never been used as an epidemiological marker, so it is unclear whether strain variation can be manifested in this gene. It is possible that these mixed genotypes may be an outcome of evolving FQ resistance; they may very well represent the efforts of typhoidal salmonellae to acquire an FQ resistant phenotype.
5. In typhoidal salmonellae, mutations found in the gene outside of the QRDR of *gyrA* are not associated with quinolone resistance. Meanwhile, more studies are warranted in order to determine whether such mutations, when present alone, confer resistance or DCS in vitro.
6. Despite mutations in the *gyrA* and *parC* genes being the most commonly found and well characterized in conferring quinolone resistance, mutations in the *gyrB* and *parE* genes have also been described, although their contribution, if any, to the resistance phenotype seems to be lesser. It may be important to

include both *gyrB* and *parE* genes in routine sequencing in order to clarify the possible role of these secondary mutations.

7. The *ampC* gene screening PCR is initially optimized using simplex PCR.
8. There are sporadic reports of high resistance to ceftriaxone in typhoidal salmonellae, where ESBLs and AmpC β -lactamase has been reported.
9. The presence of individual plasmid types are determined by PCR screening, where the control strains are made use of for optimizing the test.

References

1. Harish BN, Menezes GA (2011) Antimicrobial resistance in typhoidal salmonellae. Indian J Med Microbiol 29(3):223–229
2. Yu VL, Merigan TC Jr, Barriere SL (eds) (1999) Antimicrobial therapy and vaccines. William & Wilkins, Baltimore, MD
3. Rowe B, Ward LR, Threlfall EJ (1997) Multidrug-resistant *Salmonella typhi*: a worldwide epidemic. Clin Infect Dis 24(Suppl 1):S106–S109
4. Smith HW, Parsell Z, Green P (1978) Thermosensitive H1 plasmids determining citrate utilization. J Gen Microbiol 109(2): 305–311
5. Wain J, Kidgell C (2004) The emergence of multidrug resistance to antimicrobial agents for the treatment of typhoid fever. Trans R Soc Trop Med Hyg 98(7):423–430
6. Toro CS, Lobos SR, Calderon I, Rodriguez M, Mora GC (1990) Clinical isolate of a porin-less *Salmonella typhi* resistant to high levels of chloramphenicol. Antimicrob Agents Chemother 34(9):1715–1719
7. Parry CM, Thuy CT, Dongol S, Karkey A, Vinh H, Chinh NT et al (2010) Suitable disk antimicrobial susceptibility breakpoints defining *Salmonella enterica* serovar Typhi isolates with reduced susceptibility to fluoroquinolones. Antimicrob Agents Chemother 54:5201–5208
8. Harish BN, Menezes GA, Sarangapani K, Parija SC (2008) A case report and review of the literature: Ciprofloxacin resistant *Salmonella enterica* serovar Typhi in India. J Infect Dev Ctries 2(4):324–327
9. Menezes GA, Harish BN, Khan MA, Goessens WH, Hays JP (2012) Antimicrobial resistance trends in blood culture positive *Salmonella* Typhi isolates from Pondicherry, India, 2005–2009. Clin Microbiol Infect 18(3):239–245
10. Renuka K, Kapil A, Kabra SK, Wig N, Das BK, Prasad VV et al (2004) Reduced susceptibility to ciprofloxacin and *gyrA* gene mutation in North Indian strains of *Salmonella enterica* serotype Typhi and serotype Paratyphi A. Microb Drug Resist 10(2):146–153
11. Giraud E, Brisabois A, Martel JL, Chaslus-Dancla E (1999) Comparative studies of mutations in animal isolates and experimental in vitro- and in vivo-selected mutants of *Salmonella* spp. suggest a counterselection of highly fluoroquinolone-resistant strains in the field. Antimicrob Agents Chemother 43(9):2131–2137
12. Lindgren PK, Karlsson A, Hughes D (2003) Mutation rate and evolution of fluoroquinolone resistance in *Escherichia coli* isolates from patients with urinary tract infections. Antimicrob Agents Chemother 47:3222–3232
13. Brown JC, Shanahan PM, Jesudason MV, Thomson CJ, Amyes SG (1996) Mutations responsible for reduced susceptibility to 4-quinolones in clinical isolates of multi-resistant *Salmonella typhi* in India. J Antimicrob Chemother 37(5):891–900
14. Wu JJ, Ko W, Tsai SH, Yan JJ (2007) Prevalence of plasmid-mediated quinolone resistance determinants *QnrA*, *QnrB*, and *QnrS* among clinical isolates of *Enterobacter cloacae* in a Taiwanese hospital. Antimicrob Agents Chemother 51(4):1223–1227
15. Robicsek A, Strahilevitz J, Jacoby GA, Macielag M, Abbanat D, Park CH et al (2006) Fluoroquinolone-modifying enzyme: a new adaptation of a common aminoglycoside acetyltransferase. Nat Med 12(1):83–88
16. Paterson DL, Rice LB, Bonomo RA (2001) Rapid method of extraction and analysis of extended spectrum β -lactamases from clinical strains of *Klebsiella pneumoniae*. Clin Microbiol Infect 7:709–711
17. Mabilat C, Goussard S (1993) PCR detection and identification of genes for extended spectrum β -lactamases. In: Persiang DH, Smith

TF, Tenover FC, white TJ (Eds). Diagnostic molecular Microbiology: principles and applications. Washington DC: American Society of Microbiology. pp. 553–559

- 18. Tasli H, Bahar IH (2005) Molecular characterisation of TEM and SHV derived extended spectrum beta lactamases in hospital based Enterobacteriaceae in Turkey. *Jpn J Infect Dis* 58:162–167
- 19. Karisik E, Ellington MJ, Pike R, Warren RE, Livermore DM, Woodford N (2006) Molecular characterisation of plasmids encoding CTX-M-15 β -lactamase from *Escherichia coli* strains in the United Kingdom. *J Antimicrob Chemother* 58:665–668
- 20. Woodford N, Fagan EJ, Ellington MJ (2006) Multiplex PCR for rapid detection of genes encoding CTX-M extended-spectrum β -lactamases. *J Antimicrob Chemother* 57:154–155
- 21. Pérez-Pérez FJ, Hanson ND (2002) Detection of plasmid-mediated AmpC beta-lactamase genes in clinical isolates by using multiplex PCR. *J Clin Microbiol* 40(6):2153–2162
- 22. Carattoli A, Bertini A, Lilla L, Falbo V, Hopkins K, Threlfall EJ (2005) Identification of plasmids by PCR-based replicon typing. *J Microbiol Methods* 63(3):219–228
- 23. Levesque C, Piche L, Larose C, Roy PH (1995) PCR mapping of integrons reveals several novel combination of resistance genes. *Antimicrob Agents Chemother* 39:185–191
- 24. Khan S, Harish BN, Menezes GA, Acharya NS, Parija SC (2012) Early diagnosis of typhoid fever by nested PCR for flagellin gene of *Salmonella enterica* serotype Typhi. *Indian J Med Res* 136(5):850–854
- 25. Chmielewski R, Wieliczko A, Kuczkowski M, Mazurkiewicz M, Ugorski M (2002) Comparison of ITS Profiling, REP- and ERIC-PCR of *Salmonella Enteritidis* isolates from Poland. *J Vet Med B Infect Dis Vet Public Health* 49:163–168

Chapter 4

Red-Mediated Recombineering of *Salmonella enterica* Genomes

Frederik Czarniak and Michael Hensel

Abstract

The mutagenesis of enterobacterial genomes using phage λ Red recombinase functions is a rapid and versatile experimental tool. In addition to the rapid generation of deletions in the genome of *Salmonella enterica*, variations of the method allow site-directed mutagenesis, generation of reporter fusions, generation of chimeric genes, or transplantation of regulatory elements directly in the chromosome. We describe the application of these approaches with focus on practical aspects and critical steps.

Key words Genetic manipulation, Recombineering, Reporter fusion, In-frame deletion, Genetic transplantation

1 Introduction

1.1 Mutagenesis in *Salmonella enterica* Serovar *Typhimurium*

Mutagenesis of *Salmonella enterica* is an essential tool for the investigation of *Salmonella* pathogenesis. Many previous approaches relied on random mutagenesis, e.g., by transposons, and selection of mutant strains with altered virulence phenotypes. Today, the availability of genome sequences of a large number of *Salmonella* spp. isolates and the broad knowledge on virulence functions favors targeted rather than random mutagenesis approaches. For example, the characterization of virulence genes located on *Salmonella* Pathogenicity Islands (SPI), or genes encoding metabolic functions, is necessary to understand the molecular mechanisms of manipulations of host cells by *Salmonella* and its unique pathogenic lifestyle. The analyses usually include the generation of specific mutations and the subsequent comparison of virulence properties of the mutant strains to that of the isogenic wild-type strain. A considerable effort in these studies is the generation of sets of isogenic mutant strains lacking one or several target genes, harboring in-frame deletions or generation of the C- or N-terminal protein fusions.

Here we describe a set of highly efficient methods for genetic manipulation of *Salmonella* spp. The basic method is on techniques developed in the groups of Don Court [1] and Barry Wanner [2] for *Escherichia coli* K-12 (*E. coli*). This allows a rapid and precise one-step inactivation of selected target genes and was already used to create a genome-wide set gene-specific mutant strains of *E. coli*, named the Keio collection [3]. The original approaches were slightly modified for use in *Salmonella* and have advanced further over the last years [4–6]. Red-mediated recombineering protocols are available for generation of scarless chromosomal mutations, allelic exchange, and generation of reporter fusions.

1.2 Red-Mediated Recombination

For efficient mutagenesis of *Salmonella* spp., the phage λ Red recombination system is used. Genes *red $\alpha\beta\gamma$* were cloned into a low-copy plasmid under control of an arabinose-inducible promoter (pKD46), thus reducing unwanted Red activity and recombination events under non-inducing conditions [2]. The λ Red system harbors the genes necessary for homologous recombination, i.e., *red α* encoding a 5' to 3' exonuclease, *red β* encoding for a single-strand annealing protein, and *red γ* encoding an inhibitor of RecBCD exonuclease [7].

Several template plasmids are available for creating linear targeting DNA fragments containing the antibiotic resistance cassette of interest. These are pKD4 or pKD13 harboring the kanamycin resistance gene (*aph*), or pKD3 harboring the chloramphenicol resistance gene (CAT), and different priming sites upstream and downstream of the targeting cassette [2]. Furthermore, two FRT sites are flanking the antibiotic resistance gene, providing the option for FLP-mediated excision after successful recombination.

1.3 Generic Recombineering Procedure

The first step is the design of a pair of bi-specific oligonucleotides composed of about 5' 40 nt homologous to the selected target region in the genome, and a template-specific sequence of about 3' 20 nt for amplification of the targeting DNA fragment (Fig. 1). After amplification of the targeting cassette, the linear double-stranded DNA is introduced by electroporation into *S. Typhimurium* cells harboring pKD46. Mediated by arabinose-induced activity of the Red system, the linear DNA fragment is then integrated into the genome at a defined position by homologous recombination (Fig. 1). Yeast FLP recombinase-mediated recombination is used as an optional step to cure the recombinant clones from the antibiotic resistance genes. For this purpose, the newly generated *S. Typhimurium* mutant strains are electroporated with pCP20, leading to expression of FLP. FLP recognizes FRT sites and causes excision of the introduced resistance cassette by leaving an FRT scar of 82 or 85 bp [8].

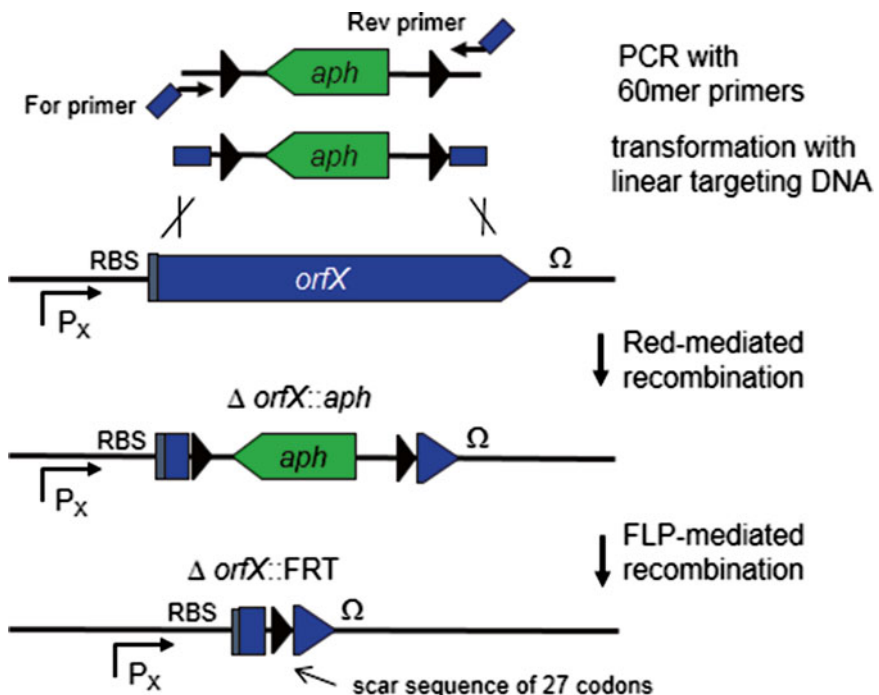


Fig. 1 Basic procedure for Red recombineering. The target gene (*orfX*) is shown as *blue symbol* and promoter (P_x), ribosome-binding site (RBS) and terminator (Ω) of the gene are indicated. A gene cassette consisting of an antibiotic resistance gene (for example kanamycin resistance gene *aph*, *green symbols*) flanked by FRT sites (*black triangles*) is amplified by a primer set. Primers consist of 60mer oligonucleotides with sequences complementary to the target gene (*dark blue bars*) and to the gene cassette (*arrows*). The linear targeting DNA is electroporated into a *Salmonella* spp. target strain expressing Red functions. Red-mediated recombination replaces *orfX* by the targeting DNA, resulting in a gene deletion tagged by the resistance gene ($\Delta orfX::aph$). If required, the antibiotic resistance gene may be deleted FLP-mediated recombination between FRT sites, resulting in an antibiotic sensitive strain with a gene deletion tagged by a remaining FRT scar ($\Delta orfX::FRT$)

1.4 Insertion of Epitope Tags and Reporter Genes

An extension of Red-mediated recombination was the recombineering of epitope tags to the 3' end of chromosomal genes of interest [9]. This modification allowed the fusion of tags such as 6His, FLAG, Myc, or HA that can be used for detection of proteins or protein purification (Fig. 2a). A further use of the gene fusion approach is the introduction of promoter-less reporter genes that allows the in-frame fusion of a variety of genes encoding reporter enzymes or fluorescent proteins to genes of interest in the *Salmonella* spp. genome [5] (Fig. 2b). For example, this approach was used for luciferase reporter gene fusion for analyses of the SsrAB regulon [10], and the rapid generation of *phoA* and *bla* fusions for the determination of membrane topologies of subunits of a protein secretion system [11]. Reporter genes can be fused to any position of the target gene, allowing precise analysis of regulatory elements or versatile generation of protein fusions.

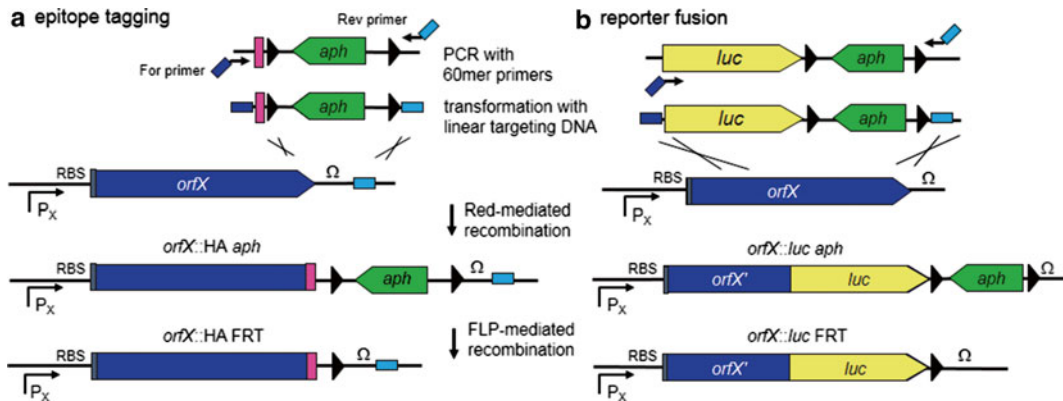


Fig. 2 Workflow for fusions to epitope tags or reporter genes. (a) Red recombineering is used to generate in-frame fusions of various sequences encoding epitope tags (magenta bars) to the 3' end of the gene of interest. (b) A similar strategy is used to generate fusions of reporter genes (for example luciferase, *luc*, yellow symbols) to a gene of interest. Red recombineering allows generation of protein fusions as depicted, as well as positioning of a promoter-less reporter gene under control of a promoter of interest. Primers consist of 60mer oligonucleotides with sequences complementary to target genes (dark blue bars), or downstream of target genes (light blue bars), and to the gene cassette (arrows)

1.5 Insertion of Gene Cassettes and Genetic Transplantation

Red-mediated recombination is also used to integrate expression cassettes into defined positions in the *Salmonella* chromosome (Fig. 3). For this approach, the generic gene cassettes were modified by introduction of foreign genes, for example for expression of vaccine antigens [12] or sigma factors [13]. This way, strains are generated with stable single-copy chromosomal integrations of expression cassettes that are cured of antibiotic resistance genes.

1.6 Scarless Mutagenesis

It is possible to avoid FRT scars using a modified method that deploys positive selection for the loss of selection markers. We initially applied the selection for loss of tetracycline resistance using selection of recombinant clones on Bochner-Maloy plates [6]. This approach requires two rounds of recombineering: (1) the insertion of the *tetRA* resistance cassette in the target region of the genome, and (2) the replacement of the *tetRA* cassette by mutant allele of the target gene or any kind of gene cassette (Fig. 4a). The resulting strains are devoid of tetracycline resistance and any other resistance marker as well as of any undesired foreign sequences. The known disadvantages of this approach are the small time window for selection of Tet-sensitive recombinants on Bochner-Maloy plates [14, 15], and the requirement for two rounds of Red-mediated recombineering.

As an alternative positive selection approach, the loss of a recognition site for the meganuclease I-SceI has been deployed [4] (Fig. 4b). Gene cassettes containing the recognition site for intron-encoded endonuclease I-SceI from *Saccharomyces cerevisiae* are first recombined into the target location of the *Salmonella* genome. The 18 bp I-SceI recognition sequence is absent from *Salmonella* genomes. Next, plasmid pWRG99 encoding I-SceI under control

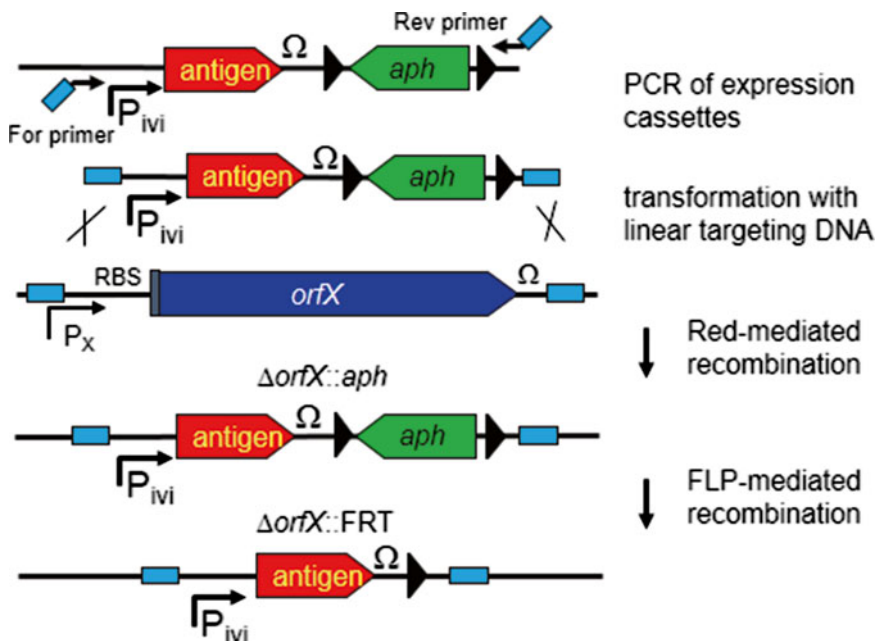


Fig. 3 Workflow for insertion of expression cassettes. Red-mediated recombineering is used to insert gene cassettes consisting of the *aph* resistance gene flanked by FRT sites and a foreign gene (*red*, for example encoding a vaccine antigen) under control of a regulated promoter (P_{vi}). Insertion of expression cassettes may lead to deletion of target genes as depicted, but may also be designed to avoid disruption of chromosomal genes

of an inducible promoter is introduced. Expression of I-*SceI* causes DNA double-strand breaks (DSB), which are lethal to most cells [16]. The replacement of the I-*SceI* site by Red-mediated introduction of a mutant allele or gene cassette can remove the I-*SceI*, thus protecting recombinant clones from I-*SceI*-mediated killing. The I-*SceI* selection approach allowed the generation of point mutations in the chromosomal genes of *Salmonella*. The approach is versatile, but also requires careful selection of recombinant clones against non-recombinant background clones.

2 Materials

General materials and reagents required for Red recombineering are listed in Table 1. Plasmid required for Red recombineering as listed in Table 2:

Oligonucleotides:

1. Synthetic oligonucleotides for generation of target constructs are usually 60mers: of 40 nt or more 5' sequence complementary to the target sequence in the *Salmonella* genome and

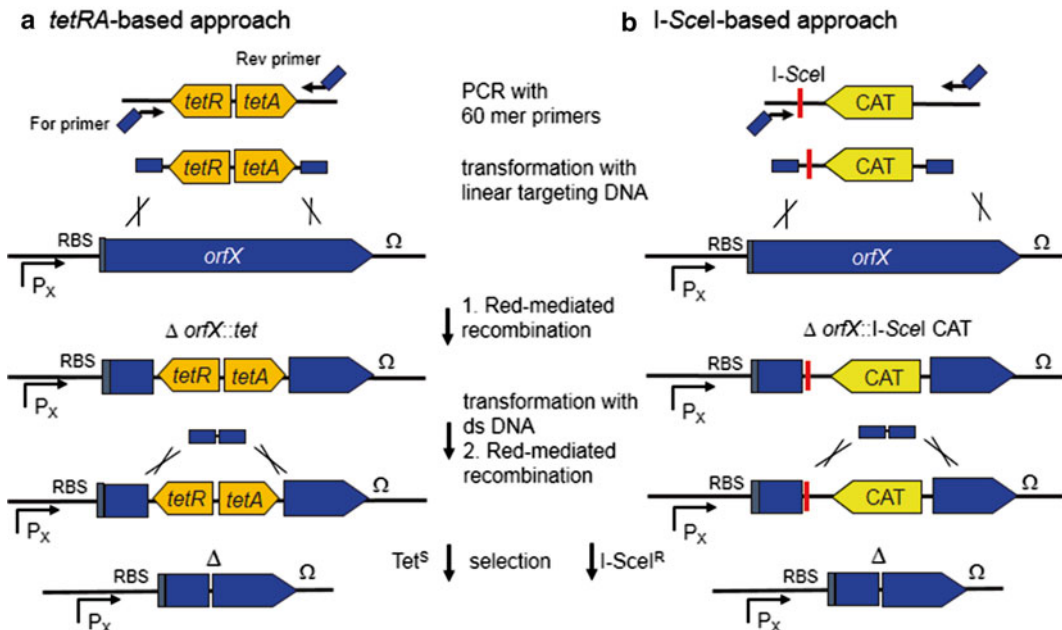


Fig. 4 Workflow for scarless Red recombineering. In approach (a), the tetracycline resistance cassette *tetRA* is amplified and inserted into a target gene by Red-mediated recombination. In approach (b), the first recombination is performed for insertion of a cassette consisting of the chloramphenicol resistance gene (CAT) and a recognition site for the meganuclease I-SceI (red bar). The resulting strains are electroporated with double-stranded (ds) DNA (e.g., annealed oligonucleotides, synthetic DNA) and a second Red-mediated recombination is performed, replacing the *tetRA* cassette (a) or the I-SceI CAT cassette (b). Recombinant clones are selected for sensitivity to tetracycline on Bochner-Maloy plates (a), or by selection for resistance to I-SceI-induced double-strand breaks (b). The mutant alleles comprise in-frame deletion, insertions, or codon exchanges

20 nt or more 3' sequence complementary to the target construct template.

2. Further oligonucleotides for PCR-based confirmation of successful recombination and scarless mutagenesis: The sequence depends on target gene sequence and position of mutation.
3. For scarless mutagenesis approaches, double-stranded DNA is generated by annealing of two complementary, 5' phosphorylated oligonucleotides of 80 nt or more.

3 Methods

3.1 Methods for Red-Mediated Recombination (Basic Approach)

Protocol 1: Generation of linear DNA fragments

1. Use appropriate template plasmid for generation of target constructs containing chloramphenicol or kanamycin resistance genes. For amplification use oligonucleotides made up of a 40 nt long homolog region for the gene of interest and 20 nt specific for the used template DNA.

Table 1
Materials for Red-mediated recombineering in *Salmonella* spp

Item	Supplier/reference	Concentration, composition, remarks
PC and DNA analysis software	Clone Manager, Serial Cloner or other suppliers	From planning recombineering, design of oligonucleotides
Thermocycler	Biometra (Analytic Jena), or other suppliers	Gradient cycler recommended for optimizing PCR parameters
Incubators	Various	At 30 °C, 37 °C, 42 °C, proper control of permissive temperature for ts plasmids, water bath shaker recommended for 30 °C
Glassware	Various	For preparation of competent cells, take care to use detergent-free flasks
Antibiotics	Sigma, Roth, or others	100 mg/ml stock 100 mg/ml stock 34 mg/ml stock in EtOH abs 50 mg/ml stock in 70 % EtOH 1 mg/ml
- Carbenicillin		
- Kanamycin		
- Chloramphenicol		
- Tetracycline		
- Anhydrotetracycline		
L-Arabinose	Sigma	1 M stock, filter sterilized, store aliquots at -20 °C
LB broth	Yeast extract, Bacto tryptone from BD	Per liter: 10 g Bacto tryptone, 5 g Bacto yeast extract, 10 g NaCl. For arabinose induction of Red functions, absence of glucose in LB broth is critical
LB agar	Bacto Agar, BD	Per liter: LB broth and 15 g agar. Fresh plates should be used for selecting clones after recombineering
SOC medium	[20]	Per liter: 20 g Bacto tryptone, 5 g Bacto yeast extract, 0.5 g NaCl, add 10 ml of 250 mM KCl, dissolve in 800 ml H ₂ O _d , adjust to pH 7.0 by adding 5 N NaOH, add H ₂ O _d to 1,000 ml, sterilize by autoclaving (store at room temperature), when the temperature is 60 °C, add 20 ml 1 M glucose and 5 ml 2 M MgCl ₂ . Prepare aliquots of 40 ml and store at -20 °C

(continued)

Table 1
(continued)

Item	Supplier/reference	Concentration, composition, remarks
Terrific broth (TB)	[20]	Per liter: 12 g Bacto tryptone, 24 g Bacto yeast extract, 4 ml glycerol, add H_2O_d to 900 ml, autoclave. After cooling to 60 °C, add 100 ml 0.17 M KH_2PO_4 , 0.72 M K_2HPO_4 (prepare stock by 2.31 g KH_2PO_4 and 12.54 g of K_2HPO_4 in 90 ml of H_2O_d ; after the salts have dissolved, adjust the volume of the solution to 100 ml with H_2O_d and sterilize by autoclaving for 20 min)
Bochner-Maloy agar	[17]	Flask A: 5 g Tryptone, 5 g yeast extract, 50 mg chlortetracycline, 15 g agar, 900 ml H_2O_d , add a magnetic stirring bar to facilitate mixing of solutions after autoclaving. Flask B: 10 g NaCl, 10 g $NaH_2PO_4 \times H_2O$, 100 ml H_2O_d . Autoclave for 20 min, let the solutions cool to about 60 °C, and mix solutions A and B. Prior to pouring of plate, add 12 mg Fusaric acid (Sigma, F6513-1G) dissolved in 50 µl DMSO, and 5 ml 20 mM $ZnCl_2$ ($ZnCl_2$ should be filter sterilized and can be stored for several weeks) Freshly prepared for selection of clones
PCR reagents	Various	For control PCR
- Taq polymerase	HF mix (Fermentas, Thermo), Phusion NEB	Proofreading activity required
- High-fidelity polymerase	Various	
- dNTPs		
DNA purification kits	Qiagen or other suppliers	

Table 2
Plasmids for Red recombineering in *Salmonella*

Designation	Relevant characteristics	Reference
Helper plasmids		
pKD46	P_{BAD} λ <i>redαβγ</i> ts <i>ori</i> , Amp ^R	[2]
pCP20	FLP helper plasmid encoding FLP recombinase ts <i>ori</i> , Amp ^R	[8]
pWRG99	pKD46 with I- <i>SceI</i> endonuclease under tetracycline-inducible promoter, ts <i>ori</i> , Amp ^R	[4]
Template plasmids		
pKD3	FRT-flanked CAT cassette	[2]
pKD4	FRT-flanked <i>aph</i> cassette	[2]
pKD13	FRT-flanked <i>aph</i> cassette, in-frame scar	[2]
pWRG100	pKD3 with I- <i>SceI</i> recognition site Amp ^R , Cm ^R	[4]
p2795	Basic vector for generation of template vectors, FRT-flanked <i>aph</i>	[12]
p3121	Firefly <i>luc</i> in p2795	[5]
p3126	<i>phoA</i> in p2795	[5]
p3138	<i>lacZ</i> in p2795	[5]
p3174	GFTmut3 in p2795	[5]
p3253	<i>araC</i> P_{BAD} in p2795	This work
p3773	<i>tetR</i> P_{tetA} in p2795	This work

2. Run PCR using the following cycling conditions (see Note 1):

Initial denaturation, 95 °C, 4.5 min
 30 cycles of denaturation, 95 °C, 45 s; annealing, 58 °C, 45 s; elongation, 72 °C, X min (1 min per kb of template) (see Note 2)
 Final elongation, 72 °C, 10 min
3. Purification of PCR product (Qiagen PCR purification kit or other suppliers).
4. Optional: *DpnI* digest to remove residual template plasmid (NEB/Fermentas) (see Note 3).

Protocol 2: Preparation of competent cells (standard procedure)

1. Grow target *Salmonella* strain harboring pKD46 overnight at 30 °C in LB containing 50 µg/ml carbenicillin.
2. Inoculate 50 ml culture LB+50 µg/ml carbenicillin using 500 µl overnight culture and add L-arabinose at a final concentration of 10 mM (use flask with baffles).

3. Incubate at 30 °C with agitation at 160 rpm to OD₆₀₀ of about 0.6 (0.5–0.8).
4. Keep the cells on ice and use pre-chilled solutions, tubes, and centrifuges for the following steps. Transfer the culture to 50 ml Falcon tubes and incubate on ice for 20 min followed by centrifugation for 10 min at 7,000 × *g* at 4 °C.
5. Discard supernatant, resuspend pellet in 50 ml ice-cold ddH₂O, and incubate on ice for 20 min followed by centrifugation for 10 min at 7,000 × *g* at 4 °C.
6. Discard supernatant, resuspend pellet in 25 ml ice-cold ddH₂O, and incubate on ice for 20 min followed by centrifugation for 10 min at 7,000 × *g* at 4 °C.
7. Discard supernatant, resuspend pellet in 2 ml ice-cold 10 % glycerol, and incubate on ice for 20 min followed by centrifugation for 10 min at 7,000 × *g* at 4 °C.
8. Discard supernatant and resuspend pellet in 500 µl ice-cold 10 % glycerol.
9. Use cells for electroporation (keep on ice) or store aliquots of competent cells at -70 °C (*see Note 4*).

Protocol 3: Preparation of competent cells (alternative rapid method) (see Note 5)

1. Grow overnight culture of required strains in LB under appropriate selection.
2. Inoculate 3 ml “terrific broth” (TB) medium in glass test tube with overnight culture at a ratio of 1:100.
3. Incubate in roller drum to log phase (about OD₆₀₀ of 1.5).
4. Transfer 1.5 ml culture in sterile Eppendorf tube, and keep in ice for all subsequent steps.
5. Centrifuge for 40 s at 13,000 rpm at 4 °C in microfuge (max. speed).
6. Decant supernatant, and resuspend pellet in 1.5 ml ice-cold H₂O_{dd} by mixing on a vortex mixer.
7. Centrifuge for 40 s at 13,000 rpm at 4 °C in microfuge.
8. Decant supernatant, and resuspend pellet in 1.0 ml ice-cold H₂O_{dd} by mixing.
9. Centrifuge for 40 s at 13,000 rpm at 4 °C in microfuges.
10. Decant supernatant, and resuspend pellet in 1.0 ml ice-cold 10 % glycerol by mixing.
11. Centrifuge for 40 s at 13,000 rpm at 4 °C in microfuges.
12. Decant supernatant, remove remaining puffer with pipette tip. Resuspend pellet in 50 µl ice-cold 10 % glycerol by pipetting up and down.
13. Use directly for electroporation.

Protocol 4: Transformation and selection (see Note 6)

1. Transfer competent cells (~40 μ l) into pre-chilled electroporation cuvette and add appropriate amount of purified PCR product (usually 1–4 μ l, but other volumes are possible). Gently mix suspension by pipetting.
2. Electroporation: 2.5 kV, 200 Ω , 25 μ F for cuvettes with 2 mm gap width (alternative settings: EC2 for Bio-Rad Micropulser).
3. Recover cells immediately in pre-warmed SOC medium and incubate for 1 h at 37 °C with shaking.
4. Spread up to 100 μ l bacterial suspension on appropriate selection plates. Incubate overnight at 37 °C. Optional: Centrifuge the remaining suspension at 13,000 rpm in a microfuge for 40 s, discard most of the supernatant, and resuspend pellet in residual medium. Plate concentrated suspension on selection plates.
5. Pick resistant colonies and purify on LB plates containing appropriate antibiotic. This incubation may be done at 42–44 °C to counter select pKD46.
6. Perform colony PCR to confirm insertion of the resistance cassette at desired position using a reverse primer binding within the resistance cassette and forward primer binding upstream of target gene.
7. Streak confirmed clones on fresh LB plates containing appropriate antibiotics and in parallel on LB plates containing carbenicillin to check the absence of pKD46. Grow cultures at 37 °C.
8. Pick colonies with antibiotic resistance introduced by Red recombination and sensitivity to carbenicillin, inoculate a fresh culture in 3 ml medium containing selective antibiotic, and incubate overnight at 37 °C.
9. Prepare frozen stocks by adding dimethyl sulfoxide to 7 % final concentration.
10. Prior to further experimental use, the mutant allele should be transferred into a fresh strain background using P22 transduction according to standard procedures [17].

Protocol 5: Deletion of resistance markers using FLP recombinase

1. Prepare electro-competent cells of mutant strains as described in Protocols 2 or 3. Culture cells at 37 °C with appropriate antibiotic (no arabinose required).
2. Transform cells by electroporation with pCP20 as described in Protocol 4. Plate suspension on LB plates containing carbenicillin and incubate at 30 °C overnight (see Note 7).
3. Select positive clones and purify twice on LB plates without antibiotics at 37 °C.

4. Check selected clones again for sensitivity against appropriate antibiotics and perform colony PCR to confirm deletion of resistance marker. Use forward and reverse primers flanking the region of interest.
5. Prepare stock cultures as described in Protocol 4.

3.2 Methods for Red-Mediated Recombineering of Scarless Deletions

Protocol 6: tetRA-based approach

Generation of target strain

1. As template for amplification of *tetA* and *tetR*, use genomic DNA of a strain harboring a Tn10dTc insertion or a plasmid harboring cloned *tetRA*. For PCR, use oligonucleotides each 60 nt long with 40 nt 5' homologous sequence for genes of interest and 20 nt 3' sequence specific for *tetRA*.
2. Further steps are performed as described in Protocol 1 and competent cells of target strains harboring pKD46 are prepared as described in Protocols 2 or 3.
3. Electroporation and selection are performed as described in Protocol 4 using tetracycline for selection at a final concentration of 20 µg/ml at 37 °C.
4. Purify resulting clones on LB agar containing 20 µg/ml tetracycline. Incubate at 37 °C to 42 °C to select for loss of pKD46.
5. Confirm resistance to tetracycline by checking growth inhibition on Bochner-Maloy plates for 24 h at 42 °C and parallel streaking on LB plates containing tetracycline (see Note 8).

Generation of double-stranded DNA

3.3 Transformation and Scarless Knockout or in-Frame Deletion

6. Design oligonucleotides for the desired deletion, exchange, or insertion of sequences. The target site is flanked by at least 40 nt of sequence complementary to the target site for allowing homologous recombination by Red recombinase. Oligonucleotides should be 5' phosphorylated after synthesis.
7. Prepare stock solutions of oligonucleotides at 500 pmol. Mix equal amounts of forward and reverse oligonucleotides. Incubate mixture to 95 °C for 15 min and allow the mixture to cool to room temperature overnight. Proper annealing may be checked by agarose electrophoresis.
8. If non-phosphorylated oligonucleotides were used, perform enzymatic phosphorylation reaction (e.g., DNA End Repair Kit, Fermentas Thermo).
9. Introduce pKD46 into *tetRA*-resistant target strain as described in Protocol 2 or 3.
10. Electroporate cells using synthetic double-stranded DNA as described in Protocol 4. We routinely use 2–3 µl of anneal oligonucleotides at 500 pmol; however, the optimal amount of

DNA may be determined empirically. Prepare mock-transformed cells for a control of background growth on selection plates.

11. Select for tetracycline-sensitive clones by plating on freshly prepared Bochner-Maloy plates. Incubate at 42 °C for at least 24 h. Compare growth of cells electroporated with DNA to mock-transformed cell in order to select colonies with faster growth than background colonies.
12. Select about 20–25 single colonies and re-streak on Bochner-Maloy plates. Incubate at 42 °C for at least 24 h.
13. Re-streak single colonies on LB plates and incubate at 37 °C overnight.
14. Confirm oligonucleotide-mediated exchange and loss of *tetRA* by colony PCR. If available, perform diagnostic restriction enzyme digest to confirm the mutation.

Protocol 7: I-SceI approach

Generation of target strain

1. For amplification of a gene cassette containing CAT and the recognition site for I-SceI, use pWRG100 as template plasmid. Oligonucleotides are designed containing at least 40 nt 5' target gene-specific sequence for homologous recombination and 20 nt 3' sequence complementary to pWRG100.
2. Perform PCR amplification as described in Protocol 1. Competent cells of target strains harboring pKD46 are prepared as described in Protocol 2 or 3.
3. Electroporation and selection are performed as described in Protocol 4 using chloramphenicol for selection at a final concentration of 30 µg/ml at 37 °C.
4. Streak purify clones on LB agar containing 30 µg/ml chloramphenicol at 37–42 °C, and confirm carbenicillin sensitivity
5. Confirm proper insertion of the CAT/I-SceI cassette by colony PCR.
6. Prepare competent cells of confirmed target strains as described in Protocol 2 or 3, and culture at 37 °C without arabinose induction.
7. Transform target strains by electroporation with pWRG99 encoding the λ Red recombinase and the endonuclease I-SceI. Select for carbenicillin resistance and incubate overnight at 30 °C.

Generation of double-stranded DNA

8. As described for Protocol 6.

Transformation and scarless knockout or in-frame deletion

9. Grow target strain harboring pWSK99 at 30 °C in LB containing 50 µg/ml carbenicillin and 10 mM arabinose. Prepare competent cells as described in Protocol 2 or 3.
10. Perform transformation using double-stranded DNA as described in Protocol 6. For selection, use LB plates containing 50 µg/ml carbenicillin and 500 ng/ml anhydrotetracycline (AHTC). Incubate overnight at 30 °C.
11. Select large colonies and purify clones on LB plates containing 50 µg/ml carbenicillin and 500 ng/ml AHTC.
12. Confirm deletion of CAT/I-SceI cassette by colony PCR.
13. To cure the resulting strain from pWRG99, re-streak clones and incubate overnight at 37 °C in the absence of carbenicillin. Check clones for sensitivity against carbenicillin.

4 Further Variations of Red Recombineering

4.1 “Remote Control” of Gene Expression

Red-mediated mutagenesis can easily be used to transfer gene cassettes in order to generate new chromosomal fusions to regulatory elements. For example, we used this approach to put otherwise transcriptionally silent genes for *Salmonella* adhesins under control of experimentally inducible promoters, or under control of promoters that are activated by known environmental stimuli.

Template plasmid p3253 contains a gene cassette consisting of FRT-flanked *aph*, *araC*, and *P_{BAD}* and is used to generate arabinose-inducible gene fusions. Template plasmid p3773 contains a gene cassette consisting of FRT-flanked *aph*, *tetR*, and *P_{tetA}* and allows the generation of gene fusions under control of tetracycline derivatives such as AHTC. We successfully used this approach to control the expression of *sadA*, encoding a trimeric autotransporter adhesin (unpublished data).

Red recombineering using p3253, p3773, or related templates will result in gene fusion and the presence of that *aph* gene or an FRT recombination scar. While these foreign elements are not likely to interfere with the expression of the gene under control of *P_{tetA}* or *P_{BAD}*, the precise analysis of the regulation may require promoter exchanges without integration of any additional DNA.

4.2 Recombineering Using Synthetic DNA

The rapidly decreasing costs for synthesis of double-stranded DNA, and the availability of novel synthesis techniques such as GeneStrings (GeneArt, Thermo Scientific, or other suppliers), render synthetic DNA an attractive alternative to oligonucleotide-based mutagenesis. Synthetic fragments allow the design of sequences otherwise difficult to construct and provide a cost-efficient way to enhance recombination efficiency by generation of longer homologous sequences. We have used synthetic DNA fragments for chromosomal site-directed mutagenesis of the 5 codons encoding the Ca²⁺-binding sites of

bacterial Ig domains in the giant adhesin SiiE, or to swap domains in the N-terminal portion of SiiE (unpublished data). The combination of DNA synthesis and scarless mutagenesis theoretically enables any kind of manipulation of the *Salmonella* genome.

5 Critical Parameters and Observations

5.1 Selection of Target Strains for Mutagenesis

Certain strains of *S. enterica* serovar Typhimurium are not amenable for Red recombineering. While we were able to regenerate hundreds of different mutations in strain NCTC 12023 (isogenic to ATCC 14028), the application of the method to SL1344 as another frequently used strain was very inefficient. The molecular basis of this phenomenon is not clear, but we speculate that the different equipment of *Salmonella* strains with prophages and interference by prophage-encoded functions is a possible explanation. A workaround is Red recombineering in a permissive strain such as NCTC 12023, and subsequent P22 transduction of the mutant allele in the desired strain. However, given that P22 transduction leads to transfer of about 1 % of the genome content, the resulting strain is chimeric rather than fully isogenic.

5.2 Repeated Rounds of Mutagenesis

The FLP-mediated recombination of FRT sites flanking the antibiotic resistance cassettes allows rapid and efficient curing of antibiotic resistance. Cured strains may be used for introduction of additional mutations by further rounds of Red recombineering, or by P22 transduction. We have performed up to four successive rounds of mutagenesis and curing of resistance cassettes. The presence of several FRT scars in the chromosome may allow recombination resulting in larger chromosomal rearrangement. However, we obtained sufficient number of clones with proper modifications of the target genes and absence of detectable chromosomal rearrangements.

6 Concluding Remarks

The generic Red recombination approach and the various modifications described here allow the rapid generation of isogenic *Salmonella* mutant strains for subsequent experimental analyses of *Salmonella* virulence properties and the pathogenic lifestyle. The use of the λ Red recombinase functions alleviates the need for long homologous flanks required for conventional homologous recombination by *Salmonella* recombinase. This allows use of PCR-derived or short synthetic DNA for recombination, similar to methods used in yeast genetics. Combined with P22 transduction [18], *Salmonella* researchers have at hand versatile and modular systems for rapid construction of recombinant strains.

We described a set of modification of the Red recombineering for generation of gene fusions, scarless chromosomal modifications, or genetic transplantations. Red recombineering can easily be adapted to various experimental needs, often by combining the recombination step with well-established selection methods for recombinant clones. The Red recombineering approach also allows the incorporation of recent developments in molecular biology. Due to the rapidly decreasing cost for DNA synthesis, recombineering of larger synthetic DNA fragments into the *Salmonella* chromosome is now feasible. The combination of Red recombineering with the in vitro assembly of large recombinant molecules by Gibson assembly [19] and related approaches may open new avenues to the molecular dissection of *Salmonella* virulence.

7 Notes

1. For generation of target DNA, use polymerase with proofreading activity to avoid unwanted mutations (High Fidelity mix, Fermentas; Phusion, NEB, or similar products).
2. Annealing temperature depends on sequence portion of oligonucleotides complementary to template. Select the highest possible temperature for highest specificity. Calculate $T_m = 2 \times (A + T) + 4 \times (G + C)$. Alternatively, run a gradient PCR and check for optimal annealing temperature.
3. *Dpn*I digestion is usually not required if templates are based on suicide plasmids such as pKD3, pKD4, or pKD13. For template plasmid propagated in *Salmonella* spp. WT, *Dpn*I digestion is recommended to reduce false-positive clones.
4. Although cells may be stored for later use, we observed best performance with freshly prepared cells.
5. This procedure allows the generation of low numbers of competent cells in single aliquots for direct use.
6. Prepare mock-transfected cells to monitor background growth on selection plates.
7. FLP-mediated recombination usually occurs directly after introduction of pCP20. We observed that curing of pCP20 might require repeated rounds of culture on LB plates at 42 °C.
8. Since selection of tetracycline sensitivity is important for the subsequent selection of allelic exchange, it is essential to select tetracycline-resistant clones inhibited in growth on Bochner-Maloy plates.

Acknowledgements

Work in our laboratory was supported by the Deutsche Forschungsgemeinschaft by grants HE1964 and Collaborative Research Center SFB944. We like to thank Dr. Roman Gerlach for fruitful discussions and materials.

References

1. Yu D, Ellis HM, Lee EC, Jenkins NA, Copeland NG et al (2000) An efficient recombination system for chromosome engineering in *Escherichia coli*. Proc Natl Acad Sci U S A 97:5978–5983
2. Datsenko KA, Wanner BL (2000) One-step inactivation of chromosomal genes in *Escherichia coli* K-12 using PCR products. Proc Natl Acad Sci U S A 97:6640–6645
3. Baba T, Ara T, Hasegawa M, Takai Y, Okumura Y et al (2006) Construction of *Escherichia coli* K-12 in-frame, single-gene knockout mutants: the Keio collection. Mol Syst Biol 2(2006):0008
4. Blank K, Hensel M, Gerlach RG (2011) Rapid and highly efficient method for scarless mutagenesis within the *Salmonella enterica* chromosome. PLoS One 6:e15763
5. Gerlach RG, Hölzer SU, Jäckel D, Hensel M (2007) Rapid engineering of bacterial reporter gene fusions by using Red recombination. Appl Environ Microbiol 73:4234–4242
6. Gerlach RG, Jäckel D, Hölzer SU, Hensel M (2009) Rapid oligonucleotide-based recombination of the chromosome of *Salmonella enterica*. Appl Environ Microbiol 75: 1575–1580
7. Maresca M, Erler A, Fu J, Friedrich A, Zhang Y et al (2010) Single-stranded heteroduplex intermediates in lambda Red homologous recombination. BMC Mol Biol 11:54
8. Cherepanov PP, Wackernagel W (1995) Gene disruption in *Escherichia coli*: Tc^R and Km^R cassettes with the option of Flp-catalyzed excision of the antibiotic-resistance determinant. Gene 158:9–14
9. Uzzau S, Figueiroa-Bossi N, Rubino S, Bossi L (2001) Epitope tagging of chromosomal genes in *Salmonella*. Proc Natl Acad Sci U S A 98: 15264–15269
10. Xu X, Hensel M (2010) Systematic analysis of the SsrAB virulon of *Salmonella enterica*. Infect Immun 78:49–58
11. Wille T, Wagner C, Mittelstadt W, Blank K, Sommer E et al (2014) SiiA and SiiB are novel type I secretion system subunits controlling SPI4-mediated adhesion of *Salmonella enterica*. Cell Microbiol 16(2):161–178
12. Husseiny MI, Hensel M (2005) Rapid method for the construction of *Salmonella enterica* Serovar Typhimurium vaccine carrier strains. Infect Immun 73:1598–1605
13. Karlinsey JE, Hughes KT (2006) Genetic transplantation: *Salmonella enterica* serovar Typhimurium as a host to study sigma factor and anti-sigma factor interactions in genetically intractable systems. J Bacteriol 188:103–114
14. Bochner BR, Huang HC, Schieven GL, Ames BN (1980) Positive selection for loss of tetracycline resistance. J Bacteriol 143:926–933
15. Maloy SR, Nunn WD (1981) Selection for loss of tetracycline resistance by *Escherichia coli*. J Bacteriol 145:1110–1111
16. Monteilhet C, Perrin A, Thierry A, Colleaux L, Dujon B (1990) Purification and characterization of the *in vitro* activity of I-Sce I, a novel and highly specific endonuclease encoded by a group I intron. Nucleic Acids Res 18: 1407–1413
17. Maloy SR, Stewart VL, Taylor RK (1996) Genetic analysis of pathogenic bacteria. Cold Spring Harbor Laboratory Press, Cold Spring Harbor, NY
18. Schmieger H (1972) Phage P22-mutants with increased or decreased transduction abilities. Mol Gen Genet 119:75–88
19. Gibson DG, Young L, Chuang RY, Venter JC, Hutchison CA 3rd et al (2009) Enzymatic assembly of DNA molecules up to several hundred kilobases. Nat Methods 6:343–345
20. Sambrook J, Fritsch EF, Maniatis T (1989) Molecular cloning: a laboratory manual. Cold Spring Harbor Laboratory, Cold Spring Harbor, NY

Chapter 5

A Method to Introduce an Internal Tag Sequence into a *Salmonella* Chromosomal Gene

Weidong Zhao and Stéphane Méresse

Abstract

Epitope tags are short peptide sequences that are particularly useful for the characterization of proteins against which no antibody has been developed. Influenza hemagglutinin (HA) tag is one of the most widely used epitope tags as several valuable monoclonal and polyclonal antibodies that can be used in various techniques are commercially available. Therefore, adding a HA tag to a protein of interest is quite helpful to get rapid and cost less information regarding its localization, its expression or its biological function. In this chapter, we describe a process, derived from the Datsenko and Wanner procedure, which allows the introduction of an internal 2HA tag sequence into a chromosomal gene of the bacterial pathogen *Salmonella*.

Key words Epitope tag, Hemagglutinin (HA), *Salmonella*, Chromosomal gene

1 Introduction

Bacteria of the species *Salmonella enterica* are intracellular pathogens that express a type III secretion system encoded by the *Salmonella* pathogenicity island 2 (T3SS-2). This secretion system supports the translocation into infected host cells of proteins known as T3SS-2 effectors [1, 2]. These proteins manipulate host cells functions to facilitate the intracellular survival and replication of bacteria [3]. SifA is a T3SS-2 effector that is crucial for virulence in mice [4]. At the cellular level, this effector is required for the stability of *Salmonella*-containing vacuoles (SCV) and promotes the formation of membranous tubules named *Salmonella*-induced filaments (Sif) [4]. Our attempts to produce antibodies against this important protein have failed. Thus, the introduction of a HA tag coding sequence into the *sifA* gene has been useful to follow the delivery of SifA into host cells, its localization and its interaction with host proteins [5].

The HA epitope is a nonapeptide sequence (YPYDVPDYA) of the human influenza virus hemagglutinin protein (HA1 protein).

It has been established that multiple copy in tandem of a given epitope enhances tremendously the detection of the tagged protein [6]. As far as the detection of *Salmonella* effectors is concerned, a modification with two copies of the HA tag (2HA) has given satisfactory results for the detection of these proteins by immunofluorescence or by Western blotting [7].

Several *Salmonella* effectors have been successfully studied by adding a C-terminal 2HA tag [8, 9]. In this case a simple recombination between a PCR product and the last part of the appropriate chromosomal gene is used to generate a strain expressing a C-terminally 2HA tagged T3SS-2 effector from the chromosome. Yet the C-terminus of SifA is not suitable for modification. Therefore, Brumell and coworkers have developed a plasmid encoding SifA with an internal 2HA tag [5]. As compared to the C-terminal tagging, creating a strain expressing a protein with an internal tag from the chromosome is far more challenging. Hence, most studies have used a $\Delta sifA$ strain carrying a plasmid for the expression of SifA-2HA. But the presence of a plasmid can have important functional consequences of the bacterial fitness and on the level of protein expressed by the plasmid. Thus, we have generated a *Salmonella* strain expressing SifA with an internal 2HA tag from the chromosome and under its natural promoter. The procedure used to generate this strain, and which is applicable for tagging other genes, is described in this chapter.

The method is based on a protocol for gene disruption described by Datsenko and Wanner [10], which consist in the replacement of a chromosomal gene sequence by a selectable antibiotic resistance gene. This replacement results from the homologous recombination between the targeted chromosomal sequences and a PCR product coding for an antibiotic resistance cassette. The latter is obtained by amplification of an appropriate plasmid using primers with homology extensions to adjacent sequences of the targeted gene. The antibiotic resistance cassette is flanked by FRT (FLP recognition target) sequences, which offer the possibility to further excise it (Fig. 1a). The recombination requires the phage lambda Red recombinase, which is synthesized by *Salmonella* under the control of an inducible *ara* promoter.

As previously mentioned, the gene disruption method has been modified in order to express C-terminally tagged gene products [9]. For this purpose, the antibiotic resistance cassette is amplified with primers that carry short extensions homologous to the last portion of the targeted gene, excluding the stop codon, and to a region immediately downstream from the gene. In addition, the coding sequences for the tag and a stop codon are included in the 5' primer (Fig. 1b).

The C-terminally tagged SifA is not functional and this problem probably exists for other bacterial effectors or proteins. The specific reasons why this modification alters the functionality

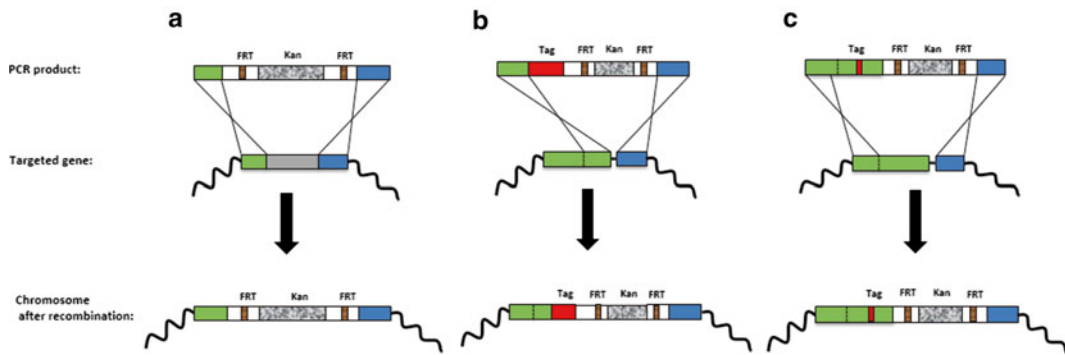


Fig. 1 Strategy for (a) disruption of the gene of interest by homologous recombination, (b) introduction of the C-terminal tag sequence to a gene, (c) introduction of an internal tag sequence into a chromosomal gene. (a) The PCR product contains region homologous to the adjacent sequences (in green and blue) of the targeted gene (in gray). After recombination, a kanamycin resistance gene has replaced the targeted gene. (b) A PCR product carries short extensions homologous to the very last part of the targeted gene (in green) and to a region immediately downstream from it (in blue). In addition a sequence coding for a tag is introduced upstream of the antibiotic resistance cassette. After recombination, a C-terminal tag sequence (in red) and a kanamycin gene are added to bacterial chromosome. (c) A PCR product carries a tagged gene (in green with a red tag) and a sequence homologous to a region downstream of the gene (in blue). The recombination allows a replacement of targeted gene by the same gene carrying an internal tag (in red)

of SifA are unknown but several potential problems can be evoked. This could be the non-secretion and/or non-translocation owing to an improper protein folding. Tags can also modify the interaction or the recognition by other proteins, a chaperone for example or possibly the host target.

Considering that SifA with an internal 2HA tag (SifA-2HA) and expressed from a plasmid is fully functional as it complements a $\Delta sifA$ mutant, we constructed a strain expressing this modified protein from the chromosome and under its natural promoter using a three steps procedure (Fig. 1c).

2 Materials

2.1 Molecular Biology

2.1.1 Plasmid Constructs

1. Plasmids: pACYC184, pKD46, pKD4, and pCP20.
2. Total DNA extracted from *Salmonella typhimurium*.
3. DNA polymerase kit from Invitrogen.
4. PCR product purification kit from Qiagen.
5. Gel extraction kit from Qiagen.
6. Restriction enzymes HindIII, SalI, XhoI, and ClaI from NEB.
7. T4 DNA ligase from Invitrogen.
8. DH₅α competent *E. coli*.
9. λpir competent *E. coli*.

10. Luria–Bertani (LB) broth, Miller (Difco/BRL).
11. Tetracycline stock solution (100 mg/ml), Ampicillin stock solution (100 mg/ml), Kanamycin stock solution (100 mg/ml).
12. Plasmid mini-preps Kit from Promega.

2.1.2 Recombination

1. Arabinose from Sigma.
2. DpnI from NEB.
3. PCR purification Kit from Qiagen.

3 Methods

This method requires a PCR amplification of a DNA module composed of the SifA-2HA gene coding sequence and an antibiotic cassette flanked by FRT sequences and its further recombination with the *Salmonella* chromosome. The initial step is the creation of a plasmid carrying an internal 2HA tagged *sifA*, following the procedure described by Brumell et al. [5]. Using this plasmid as template, the *sifA-2HA* is amplified by PCR and cloned into a suitable restriction enzyme site in 5' of the kanamycin resistance cassette of the pKD4 plasmid [10]. A subsequent PCR is carried out using primers with extensions that are homologous to the adjacent regions of *sifA* gene. The PCR product is then transformed into a *Salmonella* strain containing the pKD46 plasmid that expresses the lambda red recombinase under the control of an arabinose inducible promoter. This yields the bacterial strain expressing SifA-2HA from the chromosome.

3.1 Step 1: Construction of the SifA-2HA Plasmid

The low-copy plasmid pACYC184 was used to clone SifA and to further introduce a 2HA tag between the amino acid residues 136 and 137 of SifA. Primers SifA1 (5'-AGC AAG CTT ACA CGC ATC CAG GCA TGA AGT TTA TTC-3') and SifA2 (5'-ACG TGT CGA CTT ATA AAA AAC AAC ATA AAC AGC CGC TTT G-3') were employed to amplify *sifA* and its upstream promoter from *S. typhimurium* DNA. The PCR product was digested by HindIII and SalI, purified, and cloned into the corresponding sites in pACYC184. A subsequent inverse PCR of the resulting plasmid was carried out with SifA3 (5'-CCG CTC GAG ATT TTA AAA TCG CAT CCA CAA ATG ACG GCC-3') and SifA4 (5'-CCG CTC GAG CGC ATA ATC CGG CAC ATC ATA CGG ATA CGC ATA ATC CGG CAC ATC ATA CGG ATA ATC CGG GCG ATC TTT CAT TAA AAA ATA AAG-3'). This PCR product was then digested with XhoI and ligated with T4 DNA ligase, which yielded plasmid pSifA-2HA.

3.1.1 PCR

A 50 μ l PCR is performed using 50 ng of total *Salmonella* 12023 DNA as template and 0.2 μ M of oligos SifA1 and SifA2. The PCR

is run according the Taq polymerase supplier's protocol using the following program: 4 min at 94 °C/45 s at 94 °C/45 s at 58 °C (see Note 1)/1.25 min at 68 °C/Cycle 20 times back to step 2/10 min at 68 °C.

This should amplify a fragment of about 1,330 bp. In order to get enough PCR product for further steps, four tubes of PCR reactions are performed.

3.1.2 Digestion and Ligation

1. The PCR product are pooled and purified using a PCR purification kit according the manufacturer's protocol and eluted in 10 µl TE. DNA concentration is checked by measuring the OD_{260nm}. The purified PCR product and the plasmid pACYC184 are digested as follows:

Purified PCR product or pACYC184	1.0 µg
HindIII (10 units)	1.0 µl
SalI (10 units)	1.0 µl
10× Enzyme buffer	5.0 µl
H ₂ O	to 50 µl

2. The samples are placed at 37 °C for 3 h.
3. The digested PCR product and pACYC184 are run on a 1 % agarose gel and the 1,330 bp (PCR) and 3,600 bp (plasmid) fragments are purified according to the protocol of the Gel extraction kit.
4. DNA concentration is checked by measuring the OD_{260nm}.
5. Ligation of the PCR fragment with pACYC184 is performed as follows:

Purified PCR	2.0 µg
Purified pACYC184 fragment	1.0 µg
T4 DNA ligase	2.0 µl
Buffer	2.0 µl
H ₂ O	to 20 µl

3.1.3 Transformation

1. The ligation product (5 µl) is mixed with 50 µl of competent *E. coli*. DH₅α cells and incubated: On ice for 30 min. 42 °C for 1 min. On ice for 2 min.
2. Pre-warmed LB (0.5 ml) is added immediately, and bacteria are incubated 1 h at 37 °C under shaking.
3. Hundred microliters of the transformed bacteria is spread on a LB-agar plate supplemented with 100 µg/ml tetracycline.
4. The LB-agar plate is placed at 37 °C overnight.

5. One colony is picked up from LB-agar plate and grown in 5 ml LB medium supplemented with tetracycline (100 µg/ml), overnight at 37 °C, and under vigorous shaking.
6. Plasmid is extracted from bacteria using a Plasmid mini-preps Kit and according to the manufacturer's protocol.
7. The pSifA plasmid is quantified by measuring the OD_{260nm} and sent for sequencing.

3.1.4 Inverse PCR

In order to add an internal 2HA tag between amino acid residues 136 and 137, an inverse PCR with pSifA as template and primers SifA3 and SifA4 is performed using the Taq DNA polymerase and the following program: 4 min at 94 °C/45 s at 94 °C/45 s at 58 °C (see Note 1)/5.5 min at 68 °C/Cycle 20 times back to step 2/10 min at 68 °C. SifA3 and SifA4 both contain a Xhol restriction enzyme site and are designed to introduce a 2HA tag sequence. The PCR fragment is of about 4,750 bp.

3.1.5 Digestion and Ligation

1. Four tubes of 50 µl PCR product are collected and purified using a PCR purification kit (see Subheading 3.1.2).
2. The purified PCR product is quantified by measuring the OD_{260nm} and digested as follows.

Purified PCR product	1.0 µg
XhoI (10 units)	1.0 µl
10× Buffer	5 µl
H ₂ O	to 50 µl

3. The samples are placed at 37 °C for 3 h.
4. The digested PCR product is run on a 1 % agarose gel and the 4,750-bp fragments is purified according to the protocol of the Gel extraction kit.
5. The isolated DNA is quantified by measuring the OD_{260nm}.
6. The self-ligation of the purified PCR fragment is performed as follows:

Purified PCR product	1.0 µg
T4 DNA ligase	1.0 µl
10× Buffer	2 µl
H ₂ O	to 20 µl

7. The sample is placed at 16 °C for 14 h.

3.1.6 Transformation

The self-ligated plasmid is transformed into competent DH₅α *E. coli* cells (see Subheading 3.1.3). Four colonies are picked up for mini-prep and sequencing.

3.2 Step 2: Construction of the pKD4-SifA-2HA Plasmid

Primers O-WZ01 (5'-ACGT ATC GAT GCG CCC GCA GTT GAG ATA AAA AGG G-3') and O-WZ02 (5'-ACGT ATC GAT TTA TAA AAA ACA ACA TAA ACA GCC GCT TTG-3') both containing a ClaI restriction enzyme site were used to amplify *sifA-2HA* from psifA-2HA. This PCR product was then digested with ClaI and cloned directly into the corresponding sites in pKD4, which yields pKD4-SifA-2HA.

3.2.1 PCR

About 50 ng pSifA-2HA is used as template to run a PCR using primers O-WZ01 and O-WZ02 (see Subheading 3.1.1). This should amplify a fragment of about 1,150 bp. Four tubes of 50 μ l PCR reaction are run.

3.2.2 Digestion and Ligation

1. Four tubes of 50 μ l PCR product are pooled and purified using a PCR purification kit (see Subheading 3.1.2).
2. The purified PCR product is quantified by measuring the OD_{260nm} .
3. The purified PCR product and the plasmid are digested as follows.

Purified PCR product or pKD4	1.0 μ g
ClaI (10 units)	1.0 μ l
10 \times Buffer	5 μ l
100 \times BSA	0.5 μ l
H ₂ O	to 50 μ l

4. The samples are placed at 37 °C for 3 h.
5. The digested PCR product is run on a 1 % agarose gel and the 1,150 bp (PCR fragment) and 3,260 bp (pKD4) fragments are purified according to the protocol of the Gel extraction kit.
6. The purified DNA fragments are quantified by measuring the OD_{260nm} .
7. The ligation of purified PCR and pKD4 fragments is performed as follows:

Purified PCR product	1 μ g
Purified pKD4	1 μ g
T4 DNA ligase	1 μ l
10 \times Buffer	2 μ l
H ₂ O	to 20 μ l

8. The sample is placed at 16 °C for 14 h.

3.2.3 Transformation

1. Ligated product (5 μ l) is transformed into λ pir competent *E. coli* according to the protocol described above (see Subheading 3.1.3).
2. The transformed bacteria are spread on a LB-agar plate supplemented with 100 μ g/ml kanamycin. The LB-agar plate is placed at 37 °C overnight.
3. A colony PCR with primers O-WZ01 and O-WZ04 (O-WZ04 is partially homologous to a region downstream the kanamycin resistance gene of pKD4, see Subheading 3.3) is performed to check if *sifA*-2HA has been ligated in pKD4 in the proper orientation (see Subheading 3.1.1). Twenty colonies are screened.
4. Four PCR positive colonies are picked and grown in 5 ml LB medium supplemented with kanamycin (100 μ g/ml) overnight at 37 °C. Plasmids are extracted from bacteria using a Plasmid mini-preps Kit according to the manufacturer's protocol.
5. The pKD4-SifA-2HA plasmid is quantified by measuring the OD_{260nm} and sent for sequencing.

3.3 Step 3: Homologous Recombination

A DNA module is amplified by PCR using pKD4-SifA-2HA as template and primers O-WZ03 (5'-CTG ATT GCC AGT CTCT TTT AAA AAT TAT ATT ACA TCC GAT GCG CCC GCA GTT GAG ATA AAA AGG G-3') and O-WZ04 (5'-GGC CAT TTA AAT GAC TAT TCT CAT CCG ATC CGG TCA TAT GCG GCC ATA TGA ATA TCC TCC TTA G-3'). These primers have extensions that are homologous to regions adjacent to *sifA*. The purified PCR product is introduced into a *Salmonella* strain carrying the pKD46 plasmid, which expresses the lambda red recombinase. The recombinant bacteria (12023 *sifA*-2HA::Km^r) are selected on Kanamycin.

3.3.1 PCR

Eight tubes of 50 μ l PCR reaction are run using 20 ng pKD4-SifA-2HA as template and primers O-WZ03 and O-WZ04 (see Subheading 3.1.1).

3.3.2 Template Digestion

1. The PCR template is eliminated by adding 2 μ l DpnI to the PCR product and incubating for 1 h at 37 °C.
2. The PCR products are pooled, purified using a PCR purification kit according the manufacturer's protocol, and stored at -20 °C.

3.3.3 Homologous Recombination

1. To prepare electrocompetent bacteria, wild-type *Salmonella* are grown overnight in 2 ml LB at 37 °C under vigorous shaking. Bacteria are diluted 1:100 in 50 ml LB and incubated under the same conditions until the OD_{600nm} reaches a value of 0.6. Bacteria are pelleted at 8,000 \times g for 10 min at 4 °C,

washed successively with 25 ml and 12.5 ml ice-cold water and finally resuspended in 500 μ l ice-cold water.

2. Wild-type *Salmonella* (50 μ l) are electroporated in a 0.2 cm chilled electroporation cuvette with about 100 ng of pKD46 plasmid. A pulse of 25 μ F/2.5 kV/200 Ω is applied. 800 μ l warm LB medium are added and the bacteria are incubated for 1 h at 37 °C. Then, bacteria are spread on LB-agar plates containing 100 μ g/ml Ampicillin. Plates are incubated overnight at 30 °C (pKD46 shows temperature-sensitive replication).
3. The *Salmonella* strain carrying the pKD46 plasmid is grown in 2 ml LB medium supplemented with ampicillin (100 μ g/mL), overnight at 30 °C, and under vigorous shaking.
4. The strain is subcultured at a dilution of 1:100 in 50 ml LB medium supplemented with ampicillin (100 μ g/ml) and 10 mM arabinose (for the induction of the lambda red recombinase genes), at 30 °C for about 3.5 h until OD_{600nm} has reached a value of 0.6. Then, electrocompetent bacteria are prepared as described above.
5. The wild-type *Salmonella* strain carrying the pKD46 plasmid is electroporated with purified PCR product according to the protocol described above. Bacteria are spread on LB-agar plate containing 100 μ g/ml kanamycin. The plates are placed overnight at 37 °C.
6. To purify the clones obtained, a single colony is picked and streak on another LB-agar plate supplemented with 100 μ g/ml kanamycin.
7. To check if the transformants have undergone a homologous recombination at the expected place of the chromosome, a PCR is performed, using the primers CFSifA (5'-CGC GAA GCT CTC AGG TTT TAT AC-3') and CRsifA2 (5'-CAA CAA ATT GCC AGA CGA GCG GG-3'). This should amplify a fragment of about 3 kbp.
8. To remove pKD46, the strain is grown overnight at 43 °C in LB medium under vigorous shaking. The bacteria are then spread on a LB plate without antibiotic and incubated at 37 °C overnight. Different colonies are tested for kanamycin resistance and ampicillin sensitivity to isolate the strain that does not contain pKD46 (see Note 2).

4 Validation of the 12023 *sifA-2HA::Kmr* Strain

In order to examine the expression and the secretion of SifA-2HA, the 12023 *sifA-2HA::Kmr* strain is grown into a minimal medium (MgM-MES), which is designed to induce expression of the

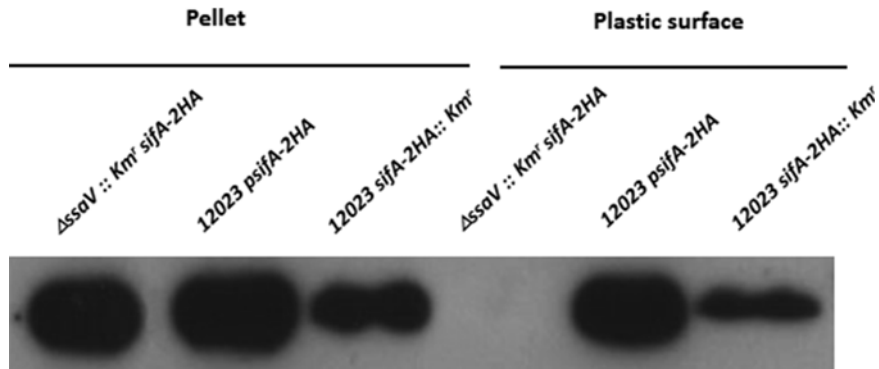


Fig. 2 Western blotting analysis of expression and secretion of SifA-2HA. Strains were grown in Minimal Medium. Bacterial pellet (expression) and plastic surface (secretion) fractions were collected and analyzed by Western blotting using a mouse monoclonal antibody against HA tag. As control an *ssaV*::*Km'* mutation was transduced in a 12023 *sifA*-2HA strain. The resulting bacteria (Δ *ssaV*::*Km'* *sifA*-2HA) expresses a non-functional type three secretion system and is unable to secrete SifA-2HA. The expressions and secretions from a plasmid (pSifA-2HA) and from the chromosome (12023 *sifA*-2HA) are compared

T3SS-2 effectors [11]. Further, the secretion of effectors is promoted by a shift of pH. The biological activities of translocated SifA-2HA are tested in HeLa cells infected with 12023 *sifA*-2HA::*Km'* strain by confocal microscopy.

4.1 Test of the Secretion of SifA in Minimal Medium

Various bacterial strains are cultured overnight in 2 ml LB and further subcultured in MgM-MES (pH 5.0) for 4 h at a dilution of 1:50. Cultures are spun down and the pellets are collected and resuspended into 6 ml pre-warmed MgM-MES at 7.2 in a 50 ml Falcon plastic tube. Bacterial cells are incubated for another 1.5 h at 37 °C. Bacteria are collected by centrifugation. The plastic surface of each 50 ml tube is washed with PBS and incubated with 50 µl of SDS-PAGE protein loading buffer for 1 h under the same conditions. This fraction contains secreted effectors that tend to bind to the plastic surface. The samples were collected and run on a 12 % acrylamide gel and transferred onto a PVDF membrane for Western blotting using a mouse monoclonal anti-HA antibody. Figure 2 shows that SifA-2HA is expressed from the chromosome and secreted.

4.2 Test of Translocation: Visualization of SifA-2HA by Immunofluorescence Analysis of Infected HeLa Cells

HeLa cells were infected with *Salmonella* 12023 *sifA*-2HA::*Km'* for 14 h. Infected cells were then fixed and immunostained for LAMP-1 and for the HA epitope and analyzed by confocal microscopy. Figure 3 shows that SifA-2HA is translocated and localizes on the *Salmonella*-containing vacuole and on associated tubules. The presence of LAMP1-positive tubules indicates this SifA-2HA is fully functional.

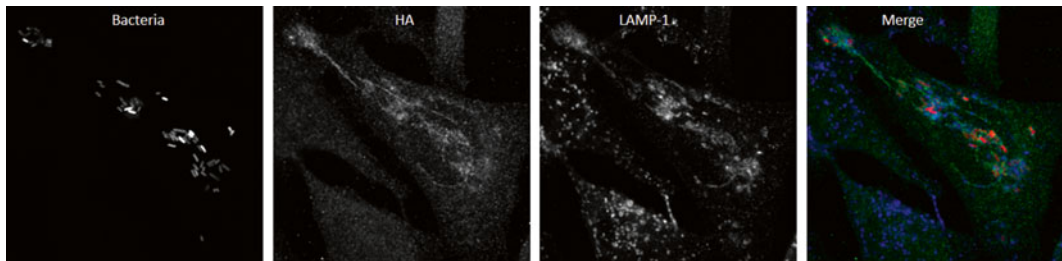


Fig. 3 Translocated SifA-2HA localizes on vacuoles and on associated tubules and induces the formation of LAMP1-positive tubules. HeLa cells were infected with the 12023 *sifA-2HA:Kmr* strain expressing GFP for 14 h. Fixed cells were immunostained for HA and LAMP1 and imaged by confocal microscopy for *Salmonella* (GFP in red), HA (in green), and LAMP1 (in blue) (Color figure online)

5 Notes

1. The annealing temperature varies according to the nucleotide sequence of the primer.
2. Usually, 80 % of the clones are resistant to kanamycin and 20 % sensible to ampicillin after clone purification.

Acknowledgments

W.Z. was supported by the China Scholarship Council (CSC Grant). The authors thank Aude-Agnès Blanchoin for her excellent technical assistance.

References

1. Ochman H, Groisman EA (1996) Distribution of pathogenicity islands in *Salmonella* spp. *Infect Immun* 64:5410–5412
2. Hensel M, Shea JE, Gleeson C et al (1995) Simultaneous identification of bacterial virulence genes by negative selection. *Science* 269:400–403
3. Figueira R, Holden DW (2012) Functions of the *Salmonella* pathogenicity island 2 (SPI-2) type III secretion system effectors. *Microbiology* 158:1147–1161. doi:[10.1099/mic.0.058115-0](https://doi.org/10.1099/mic.0.058115-0)
4. Stein MA, Leung KY, Zwick M et al (1996) Identification of a *Salmonella* virulence gene required for formation of filamentous structures containing lysosomal membrane glycoproteins within epithelial cells. *Mol Microbiol* 20:151–164. doi:[10.1111/j.1365-2958.1996.tb02497.x](https://doi.org/10.1111/j.1365-2958.1996.tb02497.x)
5. Brumell JH, Goosney DL, Finlay BB (2002) SifA, a type III secreted effector of *Salmonella* typhimurium, directs *Salmonella*-induced filament (Sif) formation along microtubules. *Traffic* 3:407–415
6. Zhang L, Hernan R, Brizzard B (2001) Multiple tandem epitope tagging for enhanced detection of protein expressed in mammalian cells. *Mol Biotechnol* 19:313–321. doi:[10.1385/MB:19:3:313](https://doi.org/10.1385/MB:19:3:313)
7. Henry T, Couillault C, Rockenfeller P et al (2006) The *Salmonella* effector protein PipB2 is a linker for kinesin-1. *Proc Natl Acad Sci U S A* 103:13497–13502. doi:[10.1073/pnas.0605443103](https://doi.org/10.1073/pnas.0605443103)
8. Freeman JA, Ohl ME, Miller SI (2003) The *Salmonella enterica* serovar *typhimurium* translocated effectors SseJ and SifB are targeted to

the *Salmonella*-containing vacuole. *Infect Immun* 71:418–427

9. Schroeder N, Henry T, de Chastellier C et al (2010) The virulence protein SopD2 regulates membrane dynamics of *Salmonella*-containing vacuoles. *PLoS Pathog* 6:e1001002. doi:[10.1371/journal.ppat.1001002](https://doi.org/10.1371/journal.ppat.1001002)

10. Datsenko KA, Wanner BL (2000) One-step inactivation of chromosomal genes in *Escherichia coli* K-12 using PCR products. *Proc Natl Acad Sci U S A* 97:6640–6645. doi:[10.1073/pnas.120163297](https://doi.org/10.1073/pnas.120163297)

11. Brown NF, Szeto J, Jiang X et al (2006) Mutational analysis of *Salmonella* translocated effector members SifA and SopD2 reveals domains implicated in translocation, subcellular localization and function. *Microbiology* 152:2323–2343. doi:[10.1099/mic.0.28995-0](https://doi.org/10.1099/mic.0.28995-0)

Chapter 6

Generation and Use of Site-Directed Chromosomal *cyaA'* Translational Fusions in *Salmonella enterica*

Francisco Ramos-Morales, Elena Cardenal-Muñoz,
Mar Cordero-Alba, and Fernando Baisón-Olmo

Abstract

CyaA from *Bordetella pertussis* is a calmodulin-dependent adenylate cyclase. Fusions to the catalytic domain of CyaA (CyaA') are useful tools to detect translocation of type III secretion system effectors from gram-negative pathogens like *Salmonella enterica*. These fusions are usually generated using plasmids with strong promoters. Here, we describe a protocol to insert the CyaA'-encoding sequence in a specific site in the bacterial chromosome in order to get a monocopy fusion whose expression is driven by the native promoter. We also describe the procedure to detect translocation of a CyaA' fusion into mammalian cells.

Key words Type III secretion, Effectors, Translocation, CyaA, cAMP, *Salmonella*, Chromosomal translational fusions

1 Introduction

Type III secretion systems (T3SSs) are molecular devices that allow secretion and translocation of proteins, known as effectors, from bacteria to eukaryotic cells [1]. These systems are major virulence factors that are present in many gram-negative pathogens of animal and plants including members of the genera *Escherichia*, *Pseudomonas*, *Salmonella*, *Shigella*, and *Yersinia*. Some T3SS effectors are known to interfere with biological processes and signal transduction pathways in the host cells through their enzymatic activities and physical interactions. However, the targets of most effectors are unknown. Effectors are targeted to the T3SS by a signal that is usually located within the N-terminal 20–30 amino acids and whose sequence is not universally conserved. The lack of conservation hampers the identification of effectors.

Salmonella enterica has two T3SSs, T3SS1 and T3SS2, encoded in *Salmonella* pathogenicity islands 1 and 2 (SPI1 and SPI2), respectively. At least 7 effectors are secreted through T3SS1,

22 through T3SS2, and 9 through both systems. Some of these effectors are encoded in SPI1 or SPI2, but most of them are encoded outside these islands [2].

A useful technique was developed some years ago to study the secretion of T3SS effectors [3, 4]. This method is based on the catalytic adenylate cyclase domain of CyaA from *Bordetella pertussis*, contained within the first 400 amino acids of this protein. Adenylate cyclase catalyzes conversion of ATP into cyclic AMP (cAMP) but this particular adenylate cyclase is dependent on calmodulin. Since calmodulin is present in eukaryotic host cells but absent from bacterial cells, the secretion of an effector fused to this fragment of CyaA (CyaA') can be monitored by measuring the levels of cAMP in infected cells. Generation of CyaA' translational fusions is usually carried out using specific plasmid vectors [5–7]. Transposons have been used to generate fusions randomly distributed throughout the chromosome of *S. enterica* as a tool to identify new effectors [8, 9]. Here, we describe a protocol, based on the Red recombination system from bacteriophage λ [10, 11], to generate a CyaA' translational fusion in a specific location in the chromosome of *S. enterica*. As an example, we use the *Salmonella* effector SseK1 and we describe also the procedure to detect translocation of the fusion to mammalian cells. The same protocol is applicable to any effector and to other bacteria and host cell types.

2 Materials

2.1 Bacterial Cultures

1. Bacterial strains: *S. enterica* serovar Typhimurium strain 14028 (wild type, ATCC). *Escherichia coli* strain S17-1 λ pir (*recA pro hsdR* RP4-2-Tc::Mu-Km::Tn7 λ pir).
2. Plasmids: pUTmini-Tn5cyaA' (suicide delivery plasmid for mini-Tn5cyaA') [12]; pKD46 (*bla* PBAD *gam* *bet* *exo* pSC101 oriTS) [10].
3. Culture medium: LB (Formedium) and LPM (80 mM 2-(*N*-morpholino) ethanesulfonic acid (pH 5.8), 5 mM KCl, 7.5 mM $(\text{NH}_4)_2\text{SO}_4$, 0.5 mM K_2SO_4 , 0.1 % casamino acids, 38 mM glycerol, 337.5 mM K_2HPO_4 - KH_2PO_4 (pH 7.4) and 8 mM MgCl_2). Supplements: 1.5 % agar for solid medium, 100 $\mu\text{g}/\text{ml}$ ampicillin (Ap), 50 $\mu\text{g}/\text{ml}$ kanamycin (Km), 0.2 % L-arabinose.
4. Incubators and shaking incubators at 30 and 37 °C.
5. Toothpicks and round sticks.

2.2 Generation of Chromosomal cyaA' Fusion

1. Oligonucleotides (see Note 1):

SseK1P1: 5'-CAGTCAGTTACGCAAAGTTCATGGGCGA
GGCATGTGCAGCTGCAGCAATCGCATCAGGC-3'

SseK1P2: 5'-ATATTATGTATTCAATAGCATGATTATT
GCCATTCCGTTAGAAAAACTCATCGAGC-3'

SseK1E1: 5'-TTAATTGCTCACTGGCAGGG-3'

SseK1E2: 5'-GCACTGCGATTAAAGTGG-3'

CyaArev: 5'-CCTTGATGCCATCGAGTACG-3'

2. Thermocycler, buffers, and DNA polymerases for high fidelity PCR (KAPA HiFi PCR kit, Kapa Biosystems), and conventional Taq polymerase (MyTaq Red, Bioline).
3. TAE buffer for DNA electrophoresis: 5 mM EDTA, 0.2 M Tris-acetate, pH 8.0.
4. Agarose (iNtRON Biotechnology), horizontal electrophoresis apparatus (gTPbio), power supply (EPS 301, GE Healthcare), handheld 302 nm UV light lamp (UVP).
5. Refrigerated microcentrifuge (Eppendorf) and 1.5 ml tubes. Refrigerated centrifuge (Beckman-Coulter) and 50 ml centrifuge tubes.
6. Electroporation apparatus (ECM630, BTX) and 2 mm gap electroporation cuvettes.

2.3 Reconstruction and Verification of the Fusion

1. Phages: P22 HT 105/1 *int201*. P22 H5: clear plaque mutant.
2. P22 broth: 100 ml LB broth, 2 ml 50× E salts (sterilized with CHCl₃), 1 ml sterile 20 % glucose, 0.1 ml P22 HT 105/1 *int201* lysate (sterilized with CHCl₃).
3. 50× E salts (for 300 ml): 1.4 g anhydrous MgSO₄, 30 g citric acid, 196 g K₂HPO₄·3H₂O, 52 g NaNH₄HPO₄·4H₂O (see Note 2).
4. EBU plates: 100 ml LB, 0.5 ml 50 % glucose, 1 ml 25 % K₂HPO₄, 0.125 ml 1 % Evans blue, 0.250 ml 1 % sodium fluorescein (also known as uranine).
5. 4× Laemmli sample buffer: 250 mM Tris-HCl (pH 6.8), 8 % SDS, 40 % glycerol, 8 % betamercaptoethanol, 0.02 % bromophenol blue.
6. Polyacrylamide gels, vertical electrophoresis apparatus (Miniprotean, Bio-Rad) and buffers, anti-CyaA antibody (Santa Cruz Biotechnology), anti-DnaK antibody (Assay Designs), anti-mouse IgG (Bio-Rad). Prestained SDS-PAGE standards (Bio-Rad).
7. Hybond ECL nitrocellulose membrane (GE Healthcare). Transfer buffer: 48 mM Tris, 39 mM glycine, 1.3 mM SDS, 20 % methanol. Trans-Blot Turbo Transfer System (Bio-Rad).

2.4 Mammalian Cell Culture and cAMP Measurement

1. Mammalian cells: HeLa cells (human epithelial, ECACC no. 93021013) and RAW264.7 cells (murine macrophages, ECACC no. 91062702).

2. Culture medium for mammalian cells (Biowest): DMEM high glucose (4.5 g/l) with sodium pyruvate, without L-Glutamine, supplemented with L-Glutamine (4 mM) and fetal bovine serum (FBS) (10 % v/v).
3. Other cell culture reagents: Penicillin G sodium salt, 0.06 g/l; streptomycin sulfate, 0.1 g/l (Biowest) were added for routine culture but not for experiments involving infection with *Salmonella*. Trypsin-EDTA (PAA). Gentamicin (PAA).
4. Plasticware for cell culture: Tissue-culture treated culture dishes 100 mm × 20 mm (Corning); cell scrapers (PAA). Serological pipettes (LabClinics).
5. Equipment for mammalian cell culture: Cell culture hood (Telstar). Humid CO₂ incubator (Biotech). Water bath (Reypa). Centrifuge (Beckman Coulter). Refrigerator and freezer (Liebherr). Cell counter (Neubauer). Inverted microscope (Hund Wetzlar). Cryostorage container (Thermo Scientific). Autoclave (Selecta).
6. Colorimetric cAMP direct immunoassay kit (Arbor Assays).
7. Microplate shaker. Colorimetric 96-well microplate reader capable of reading OD at 450 nm.

3 Methods

3.1 Generation of Chromosomal *cyaA*' Fusion

1. Amplify a fragment of plasmid pUTmini-Tn5*cyaA*' containing DNA encoding the catalytic domain of CyaA from *B. pertussis* and a gene conferring Km resistance. Use oligonucleotides SseK1P1 and SseK1P2 (Fig. 1) (see Note 3) as primers and a high-fidelity polymerase (see Note 4). PCR mix: 20 µl of 5× KAPAHiFi buffer (final concentration 1×), 3 µl of dNTP mix (10 mM each dNTP; final concentration 0.3 mM), 3 µl of forward primer (10 µM; final concentration 0.3 µM), 3 µl of reverse primer (10 µM; final concentration 0.3 µM), 1 µl of KAPAHiFi DNA Polymerase (1 U/µl), up to 100 µl of PCR grade water, bacterial colony as template. Thermocycler conditions: (1) 95 °C for 3 min; (2) 30 cycles at 98 °C for 20 s, 60 °C for 15 s, 72 °C for 1.5 min; (3) 72 °C for 5 min.
2. Electrophorese the PCR product in 0.8 % agarose in TAE buffer. Visualize the specific band under a UV lamp. Cut the band with a scalpel and translate it into a 1.5-ml microcentrifuge tube. Extract the DNA from agarose using an appropriate purification protocol (e.g., Wizard SV Gel and PCR Clean-Up System, Promega) to get the DNA in a final volume of 40 µl.
3. Using a sterile round stick (see Note 5) pick a colony of *S. enterica* 14028/pKD46 from an LB plate supplemented with Ap. Suspend in 5 ml of LB with Ap and incubate at 30 °C

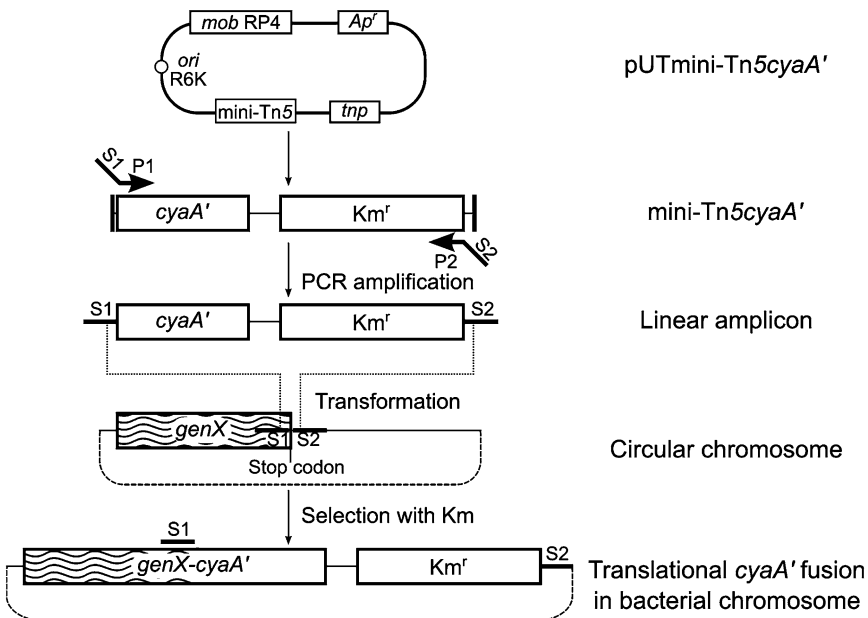


Fig. 1 Schematic representation of the protocol to generate a *cyaA'* fusion in a bacterial chromosome. In addition to the mini-transposon, the plasmid contains a *bla* gene that confers resistance to ampicillin (*Ap'*), a *tnp* gene that codes for Tn5 transposase, the R6K origin of replication (*oriR6K*), and the RP4 *oriT* region for conjugation (*mobRP4*). P1 and P2 are the priming sites for amplification of a fragment of pUT-miniTn5cyaA'. S1 and S2 refer to specific homology regions necessary for insertion of the amplified fragment into a defined site in the chromosome

(*see Note 6*) overnight in a shaking platform at 180 rpm in a tube in a tilted position.

4. Inoculate 25 ml of LB with *Ap* and arabinose with 1 ml of the overnight culture, in a 100 ml flask. Incubate at 30 °C under agitation (200 rpm) until the culture reaches an $OD_{600} \approx 0.6$ (about 3 h). Transfer the culture to a prechilled 50 ml conical tube and pellet the bacteria by centrifugation at $3,900 \times g$, for 5 min, at 4 °C. Discard the supernatant and resuspend the pellet carefully in 1 ml ice-cold distilled, sterile water and then add 24 ml ice-cold distilled, sterile water. Centrifuge and repeat the procedure twice. Finally resuspend in 600 μ l ice-cold distilled, sterile water, and keep on ice (*see Note 7*).
5. Mix 100 μ l of electrocompetent cells (previous step) with 4 μ l of the purified PCR product (obtained in **step 2**) in a chilled microcentrifuge tube. Transfer the mix to the bottom of a chilled 2 mm gap electroporation cuvette. As negative control use 100 μ l of bacteria without added DNA. Keep the cuvettes on ice until electroporation.
6. Dry quickly the external surface of the electrodes with toilet paper. Tap repeatedly the cuvette on the table to ensure that

the cells are at the bottom and without air bubbles. Electroporate at 2.5 kV, 200 Ω , 25 μ F, add immediately 900 μ l of LB, transfer to a 10 ml test tube, and incubate at 37 °C for 1 h with shaking (*see Note 8*).

7. Plate 100 μ l on an LB plate containing 50 μ g/ml of Km. Pellet the remaining bacteria by centrifugation, remove supernatant, except about 100 μ l, resuspend and plate on LB with Km.
8. Incubate at 37 °C for 24 h until obtaining colonies. Tens of colonies are expected. Pick some of them onto a new plate and incubate at 37 °C for 24 h (*see Note 9*).

3.2 Verification of the Fusion

Two kinds of verifications are described: (1) PCR tests to verify the structure and the position of the fusion; (2) Western blot to assess the level of production of the fusion protein.

1. Set up two PCR reactions for each strain using a conventional Taq polymerase (MyTaq Red). Use external oligonucleotides (SseK1E1 and SseK1E2 in this example) as primers in reaction 1 and direct external (SseK1E1) and CyaArev for reaction 2. Use a colony or half a colony as template in each reaction. Use the original wild-type strain as control. PCR mix: up to 25 μ l of PCR grade water, 5 μ l of 5 \times MyTaq Red Reaction Buffer (final concentration 1 \times), 1 μ l of forward primer (10 μ M, final concentration 0.4 μ M), 1 μ l of reverse primer (10 μ M, final concentration 0.4 μ M), bacterial colony or half a colony as template, and 0.3 μ l of MyTaq Red DNA Polymerase (5 U/ μ l). Thermocycler conditions: (1) 95 °C for 1 min; (2) 30 cycles at 95 °C for 15 s, 60 °C for 15 s, 72 °C for 1 min; (3) 72 °C for 2 min.
2. Electrophores the PCR product in 0.8 % agarose in TAE buffer and visualize the specific bands on a UV transilluminator.
3. Compare the sizes of amplified bands. The size of the band obtained using external primers (reaction 1) should be about 3 kb larger in the strain carrying the fusion when compared with the control strain. Reaction 2 should yield no band in the control and a band of the appropriate size in the strain with the fusion (1.2 kb in the SseK1 example).
4. Prepare lysates for Western blot analysis. Suggested conditions for bacterial cultures are: (1) to favor expression of T3SS1 and associate effectors, inoculate a fresh colony in 5 ml LB with 0.3 M NaCl in a capped 10 ml plastic tube, incubate at 37 °C for 15 h without shaking; (2) to favor expression of T3SS2 and associate effectors, prepare an overnight LB culture, centrifuge 1 ml of this culture, discard supernatant, wash with 1 ml of LPM medium, repeat three times, and finally resuspend in 1 ml of LPM; dilute 200 μ l of this washed culture in 5 ml LPM and incubate at 37 °C for 15 h with shaking. For a culture with

an OD₆₀₀ of about 0.8 (see Note 10), pellet 1 ml by centrifugation, discard supernatant, and resuspend the pellet in 50 µl of 4× Laemmli sample buffer. Boil for 5 min, centrifuge briefly, and store at -20 °C.

5. Electrophoresis 20 µl of the protein extract in a 12 % polyacrylamide gel (see Note 11). Use a well to load 5 µl of prestained standards. Transfer proteins to a nitrocellulose membrane. Immunoblot using anti-CyaA (1:500) as primary antibody and anti-mouse IgG (1:5,000) as secondary antibody. Compare the size of the band obtained with the expected size taking into account that the CyaA' fragment adds about 43 kDa.

3.3 Reconstruction of the Fusion

It is advisable to make a phage P22 lysate on the strain with the correct fusion and use it to transfer the antibiotic resistance gene and the linked *cyaA'* fusion into a fresh wild-type background.

1. Get an overnight culture of the strain with the fusion in 5 ml of LB with Km. Mix 200 µl of this culture with 800 µl of P22 broth in a 1.5 ml microtube. Incubate at 37 °C with shaking 4–24 h. Centrifuge 1 min at 15,000 × g. Transfer supernatant to a new tube, add 200 µl of chloroform and mix in vortex to kill remaining bacteria. This lysate can be stored at 4 °C for years (adding chloroform could be necessary periodically). If the chloroform is not at the bottom of the tube, centrifuge for 2 min at 15,000 × g before using the lysate (upper aqueous phase).
2. Prepare an overnight culture of the wild-type strain 14028 in LB. To transduce the fusion into wild-type bacteria, mix 10 µl of the P22 lysate with 100 µl of the culture in a 1.5 ml microtube and incubate at 37 °C for 30–90 min. Plate in LB with 50 µg/ml Km and 1 mM EGTA (see Note 12). Incubate at 37 °C overnight.
3. Select some transductants and streak them to get isolated colonies on EBU plates. Incubate overnight at 37 °C and keep light-colored colonies (see Note 13).
4. To check that these light-colored colonies are not lysogens, cross-streak them against phage H5: using a 0.1 ml pipette spread a small amount of a H5 lysate on a line in the center of a EBU plate; allow to dry for 5 min; streak a colony perpendicular across the H5 streak. Phage-free *Salmonella* will lyse after the contact with H5, whereas lysogens, being immune to phage, will look healthy on both sides of the H5 streak (see Note 14).

3.4 CyaA Activity Assay

1. Grow mammalian cells (epithelial HeLa cells, RAW264.7 macrophages) in DMEM with glutamine, FBS, and antibiotics at 37 °C in a CO₂ incubator.

2. Detach cells with a cell scraper (macrophages) or by trypsinization (epithelial cells). Count cells in a hemocytometer and dilute to 150,000 cells per ml of culture medium. Add 1 ml of cell suspension per well into a 24-well plate and incubate at 37 °C for 24 h in a CO₂ incubator.
3. Prepare *Salmonella* cultures in triplicate (wild type as control and strain expressing the CyaA' fusion) for infection of HeLa cells under invasive conditions (LB 0.3 M NaCl, 15 h, 37 °C, without shaking) and for infection of macrophages under noninvasive conditions (LB, 24 h, 37 °C, with shaking) (*see Note 15*).
4. Infect eukaryotic cells with bacteria at a multiplicity of infection of 75 or 25 bacteria per epithelial cell or macrophage, respectively (*see Note 16*): aspirate media, wash twice with 500 µl of PBS, and add 1 ml of fresh DMEM with glutamine and FBS (but without antibiotics); add bacteria. Optional step: centrifuge the plate at 200 ×*g* during 5 min.
5. Incubate at 37 °C in the CO₂ incubator for the desired period of time. For incubations up to 2 h go to **step 7**.
6. One hour post-infection aspirate media, wash twice with 500 µl of PBS, and add 1 ml of fresh DMEM with glutamine and FBS and 100 µg/ml of gentamicin. One hour later repeat this procedure but adding gentamicin at a concentration of 16 µg/ml (*see Note 17*).
7. To measure the concentration of cAMP in the infected cultures follow the instructions of the kit (Arbor Assays or other colorimetric cAMP direct immunoassay kit) as explained in the next steps.
8. Aspirate media, wash twice with 500 µl of PBS, and lyse cells by adding sample diluent (dilute 1:4 with distilled water before use according to the kit instructions) and incubating at 37 °C in the CO₂ incubator for 10 min.
9. Transfer the contents of each well to a microtube and centrifuge at 15,000 ×*g* for 2 min (*see Note 18*).
10. Determine the number of wells to be used from the microtiter plate coated with donkey anti-sheep IgG provided in the kit and use the regular format for the assay following exactly the protocol provided with the kit (*see Note 19*): add 25 µl of plate primer into all wells used; add 75 µl of sample diluent into the nonspecific binding (NSB) wells; add 50 µl of sample diluent into wells to act as maximum binding wells (Bo); add 50 µl of samples into wells in the plate; add 25 µl of the DetectX cAMP conjugate to each well; add 25 µl of the DetectX cAMP antibody to each well, except the NSB wells; gently tap the sides of the plate to mix reagents; cover with plate sealer; shake at room temperature for 2 h (*see Note 20*); aspirate the plate and wash each well four times with 300 µl of

1. Design primers with specific homology extensions S1 and S2, and priming sites P1 and P2
2. PCR-amplify the region containing *cyaA'* and the gene conferring Km' from S17-λpir/pUT-miniTn5*cyaA'*
3. Transform pKD46-containing *Salmonella* grown at 30°C with arabinose
4. Verify the fusion by PCR with external primers and by Western blot with anti-CyaA
5. Transfer the fusion to a fresh wild-type background by P22-mediated transduction
6. Infect mammalian cell culture with bacteria expressing the fusion
7. Measure cAMP in the infected culture to test translocation of the fusion

Fig. 2 Overview of the steps necessary to generate and test a chromosomal *cyaA'* fusion

wash buffer; tap the plate dry on clean absorbent towels; add 100 µl of the TMB substrate to each well; incubate at room temperature for 30 min without shaking; add 50 µl of the stop solution to each well; read optical density at 450 nm from each well in a plate reader.

11. Subtract the OD value for the NSB from all OD values and calculate the percent of OD relative to the maximum (Bo). A standard curve should be created with known cAMP concentrations according to the kit protocol in order to transform the relative data into cAMP concentrations values (see Note 21). Samples and standards should be prepared in triplicate.
12. An overview of the protocols described in this chapter is presented in Fig. 2.

4 Notes

1. Specific primers should be designed for the gene of interest. Oligonucleotides for *sseK1* are given as an example. The portions of the oligonucleotides that are common to generate any other CyaA' fusion using this method are marked in bold and underlined.
2. Each salt is added successively to 150 ml distilled water and dissolved with stirring and heating (but not boiling). Then distilled H₂O is added to reach a total volume of 300 ml. 5 ml of chloroform (CHCl₃) is added as a preservative.

3. These oligonucleotides include 40-nucleotide homology extensions and 20-nucleotide priming sequences for pUTmini-Tn5 $cyaA'$. The extensions allow recombination of the PCR products with the *Salmonella* chromosome and insertion of $cyaA'$ and the antibiotic resistance gene in a specific site. In this example, extensions are homologous to the region immediately preceding the translation stop signal of *sseK1* (P1) and to a region immediately downstream from it (P2) in order to get an in-frame translational *sseK1-cyaA'* fusion (the stop codon is deleted).
4. As template, pick a fragment of a fresh colony of *E. coli* S17-1 λ pir carrying pUTmini-Tn5 $cyaA'$ with a toothpick and add it to the PCR mix. As an alternative, if there are amplification problems, boil a colony for 3 min in 30 μ l distilled water and then use 1 μ l as template.
5. Sterile loops can be used, but we prefer reusable autoclaved wooden round sticks (1.5 mm diameter, 145 mm long) to pick colonies, inoculate liquid media, or streak bacterial cultures on agar plates.
6. Plasmid pKD46 is a low-copy number, temperature-sensitive replicon that carries bacteriophage λ red genes (γ , β , and *exo*) under the control of an arabinose-inducible promoter. *Salmonella* strains carrying the plasmid should be cultured at 30 °C to permit its replication. Arabinose is added when the production of the Red recombinase is needed (before electroporation). This system mediates recombination between the chromosome and PCR fragments with short homology extensions. The Red plasmid is cured by growth at 37 °C.
7. Bacteria could be prepared for electroporation previously and stored at -80 °C using 10 % glycerol instead of water. However, we get better results with freshly prepared electrocompetent cells using this quick procedure. It is very important to keep the bacteria at 4 °C throughout this procedure.
8. The typical pulse time duration is about 5 ms. Sometimes arcing occurs, the pulse time duration is reduced and the procedure should be repeated. Arcing is rare under the conditions described and is not dangerous for the user. To reduce the probability of arcing, the salt concentration should be low. Some users report that high temperature may also increase the risk of arcing, therefore avoid touching the aluminum electrodes with your fingers.
9. The pUT plasmid, used as template, is a conditional replicon (*oriR6K*) that requires the *pir* gene product for replication (that is the reason to propagate this plasmid in the permissive *E. coli* S17-1 λ pir strain). Therefore, treatment with *Dpn*I to eliminate methylated template is not necessary, since antibiotic-resistant

Salmonella transformants resulting just from acquisition of the plasmid are not expected.

10. The volume of culture and sample buffer is relativized according to the OD₆₀₀ to facilitate comparison between samples and fusion proteins. In addition, immunoblot is also carried out using anti-DnaK (1:10,000) as primary antibody and anti-mouse IgG (1:5,000) as secondary antibody, as internal loading control. An extract of a wild-type strain (without CyaA' fusion) should be used as negative control.
11. Handmade or premade gels (Mini-Protean TGX precast gels, Bio-Rad) can be used.
12. Although selection of transductants can be carried out in plates without EGTA, the addition of EGTA chelates Ca²⁺, preventing P22 adsorption and decreasing reinfection of transductants.
13. Some of the transductants may have also been infected with P22 and have become pseudolysogens that undergo lysis and produce dark blue colonies in EBU plates.
14. The *int* mutation present in the strain of P22 used here prevents formation of true lysogens. But sometimes revertants arise that form lysogens that cannot be reinfected with P22. These lysogens are not lysed by H5.
15. Infection with invasive *Salmonella* (expressing T3SS1) induces early apoptosis in macrophages and should be avoided if translocation of the CyaA' fusion is going to be monitored several hours post-infection.
16. The number of mammalian cells per well should be about 300,000 if 150,000 were seeded the previous day. The number of bacteria can be estimated based on the OD₆₀₀ of the cultures. By serial dilutions, plating and colony counting we have calculated that an OD₆₀₀=0.7 corresponds to 2.4×10^8 colony forming units per ml, but it should be calculated for every strain, laboratory or spectrophotometer.
17. Gentamicin is used to kill extracellular bacteria. It is supposed not to enter inside the host cell, however the risk of entry increases with the time of incubation and therefore its concentration is decreased for long incubations.
18. Centrifugation is not essential but can contribute to eliminate cell debris. Only 50 μ l from the supernatant are used for cAMP measurements. Samples can be stored at -80 °C until all the samples have been collected and are ready to start the assay protocol.
19. All components of the kit are stored at 4 °C but should be placed at room temperature 30–60 min before use.

20. We use an Edmund Bühler GmbH shaker model KM-2 set at maximum speed (420 rpm).
21. Software to estimate the sample values from a linear fit of the standards values should be used. An example is the TREND function in Microsoft Excel.

Acknowledgments

The work in the laboratory is supported by grant SAF2010-15015 and SAF2013-46229-R from the Spanish Ministry of Science and Innovation and the European Regional Development Fund and grant P08-CVI-03487 from the Consejería de Economía, Innovación y Ciencia, Junta de Andalucía, Spain. ECM is a recipient of a postdoctoral fellowship from Consejería de Economía, Innovación y Ciencia, Junta de Andalucía, Spain, and FBO is a recipient of an FPI fellowship from the Spanish Ministry of Science and Innovation.

References

1. Galán JE, Wolf-Watz H (2006) Protein delivery into eukaryotic cells by type III secretion machines. *Nature* 444:567–573
2. Ramos-Morales F (2012) Impact of *Salmonella enterica* type III secretion system effectors on the eukaryotic host cell. *ISRN Cell Biol* 2012, Article ID 787934
3. Sory MP, Boland A, Lamberton I, Cornelis GR (1995) Identification of the YopE and YopH domains required for secretion and internalization into the cytosol of macrophages, using the *cyaA* gene fusion approach. *Proc Natl Acad Sci U S A* 92:11998–12002
4. Sory MP, Cornelis GR (1994) Translocation of a hybrid YopE-adenylate cyclase from *Yersinia enterocolitica* into HeLa cells. *Mol Microbiol* 14:583–594
5. Cardenal-Muñoz E, Ramos-Morales F (2011) Analysis of the expression, secretion and translocation of the *Salmonella enterica* type III secretion system effector SteA. *PLoS One* 6:e26930
6. Cordero-Alba M, Bernal-Bayard J, Ramos-Morales F (2012) SrfJ, a *Salmonella* type III secretion system effector regulated by PhoP, RcsB, and IolR. *J Bacteriol* 194:4226–4236
7. Valinsky L, Nisan I, Tu X, Nisan G, Rosenshine I, Hanski E, Barash I, Manulis S (2002) A host-specific virulence protein of *Erwinia herbicola* pv. *gypsophila* is translocated into human epithelial cells by the Type III secretion system of enteropathogenic *Escherichia coli*. *Mol Plant Pathol* 3:97–101
8. Baisón-Olmo F, Cardenal-Muñoz E, Ramos-Morales F (2012) PipB2 is a substrate of the *Salmonella* pathogenicity island 1-encoded type III secretion system. *Biochem Biophys Res Commun* 423:240–246
9. Geddes K, Worley M, Niemann G, Heffron F (2005) Identification of new secreted effectors in *Salmonella enterica* serovar Typhimurium. *Infect Immun* 73:6260–6271
10. Datsenko KA, Wanner BL (2000) One-step inactivation of chromosomal genes in *Escherichia coli* K-12 using PCR products. *Proc Natl Acad Sci U S A* 97:6640–6645
11. Uzzau S, Figueiroa-Bossi N, Rubino S, Bossi L (2001) Epitope tagging of chromosomal genes in *Salmonella*. *Proc Natl Acad Sci U S A* 98: 15264–15269
12. Tu X, Nisan I, Miller JF, Hanski E, Rosenshine I (2001) Construction of mini-Tn5cyaA' and its utilization for the identification of genes encoding surface-exposed and secreted proteins in *Bordetella bronchiseptica*. *FEMS Microbiol Lett* 205:119–123

Chapter 7

Detection of Antimicrobial (Poly)Peptides with Acid Urea Polyacrylamide Gel Electrophoresis Followed by Western Immunoblot

Edith Porter, Erika V. Valore, Rabin Anouseyan, and Nita H. Salzman

Abstract

Antimicrobial (poly)peptides (AMPs) are ancient key effector molecules of innate host defense and have been identified in mammals, insects, plants, and even fungi (Nakatsuji and Gallo, *J Invest Dermatol*, 132: 887–895, 2012). They exhibit a cationic net charge at physiological pH and are rich in hydrophobic amino acids (Dufourc et al., *Curr Protein Pept Sci*, 13: 620–631, 2012). Their mode of action has been best investigated in bacteria. When assuming secondary structure the cationic and hydrophobic amino acids are sequestered creating a bipartitioned molecule in which the cationic amino acids mediate initial electrostatic interaction with the negatively charged bacterial surface and the hydrophobic amino acids mediate embedding into the bacterial membranes followed by a multitude of effects interfering with bacterial viability (Nicolas, *FEBS J*, 276: 6483–6496, 2009; Padovan et al., *Curr Protein Pept Sci*, 11: 210–219, 2010). However, immunomodulatory, antitumor, and other effects have been added to the ever increasing list of AMP functions (Pushpanathan et al., *Int J Pept*, 2013: 675391, 2013). Several classes of AMPs have been distinguished based on structure, namely anti-parallel beta-sheet, alpha-helical, circular, as well as disulfide bridge connectivity (Bond and Khalid, *Protein Pept Lett*, 17: 1313–1327, 2010). Many of the AMPs undergo posttranslational modification including further proteolysis. Biochemical analysis at the protein level is of great interest for a wide range of scientists and important when studying host–pathogen interaction, for example *Salmonella* invasion of the small intestine. Acid-urea polyacrylamide gel electrophoresis (AU-PAGE) followed by Western immunoblotting is an important tool for the identification and quantification of cationic AMPs. The protocol for these procedures outlined here describes, in detail, the necessary steps; including pouring the AU-gels, preparing the test samples, performing the electrophoretic separation and protein transfer to the membrane, and conducting the immunodetection using an alkaline phosphatase/NBT/BCIP system. A standard SDS-PAGE in comparison with AU-PAGE and the corresponding Western immunoblot are depicted in Fig. 1.

Key words Defensins, Mucosal immunity, Cationic peptides, Innate defense

1 Introduction

Antimicrobial peptides including defensins are small, typically less than 100 amino acids in length and less than 10 kDa in size, cationic, and hydrophobic. Antimicrobial polypeptides like lysozyme are

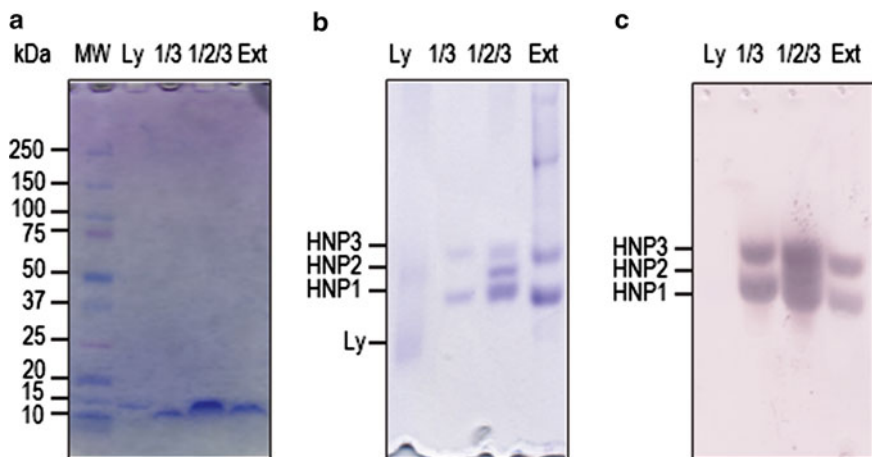


Fig. 1 A comparison between the separation of antimicrobial (poly)peptides by 4–20 % SDS-PAGE and 12.5 % AU-PAGE. Human milk lysozyme (Ly), and mixtures of HNP1 and 3 (1/3), HNP1–3 (1/2/3), and neutrophil granule extract (Ext) were separated by SDS-PAGE (a) or AU-PAGE (b) and Coomassie stained. A Western blot of the AU-PAGE gel was probed using a polyclonal antibody cross-reactive against HNP1–3 (c). For Ly, 1 μ g was loaded. For HNP1–3, 0.4 μ g per peptide per lane was loaded for Coomassie-stained PAGE and 200 ng per peptide per lane for Western immunoblot; Ext: the equivalent of granules from 40,000 neutrophils per lane was loaded for Coomassie-stained PAGE and from 4,000 neutrophils per lane for Western immunoblot; MW: molecular weight marker. Ly was previously purified from human milk [9]. HNPs and neutrophil granule extract were kindly provided by the Ganz lab (UCLA). Identification of HNP1, -2, and -3 in neutrophil granule extract is based on electrophoretic mobility [5]

somewhat larger with a molecular weight around 14 kDa and additional functional domains [1]. Diverse antimicrobial peptide family members are found within a species and often even within a cell such as the presence of multiple defensins in Paneth cells [2] and human neutrophils [3]. These often differ only by a few amino acids in length, and thus, SDS-PAGE typically cannot resolve the various forms of these peptides. In contrast, acid urea (AU)-PAGE operates at a low pH and separates proteins primarily based on their cationic charge, allowing better resolution of peptides that differ only slightly in molecular size but much more in overall net charge. For example human neutrophil peptides HNP1, -2, and -3 differ by only 1 amino acid in their N terminus [3] yet can be clearly distinguished by AU-PAGE [4, 5]. An additional factor influencing the electrophoretic mobility is the shape of the molecule. Since proteins are reversibly denatured in AU-PAGE they can be recovered from the gel and subsequently subjected to functional assays [6, 7]. Like SDS-PAGE, AU-PAGE can be coupled to Western immunoblot allowing for the specific identification of the AMPs [8]. In the following section, we describe the preparation of AU-poly acrylamide gels, sample preparation and electrophoretic separation, transfer and fixation to a membrane followed by probing with specific antibodies using a colorimetric detection system.

The properties of AU-PAGE are then demonstrated by showing electrophoretic separation of archived human neutrophil granule extract by AU-PAGE and subsequent immunodetection compared to a corresponding SDS-PAGE separated granule extract. As shown in Fig. 1, 4–20 % SDS-PAGE is unable to resolve lysozyme, HNP1–3, and human neutrophil granule extract, and all proteins migrate nearby the position of the 15 kDa marker. In contrast, 12.5 % AU-PAGE clearly differentiates lysozyme (14 kDa) from human neutrophil peptides HNP1–3 (~3.5 kDa), separates all three HNPs and can resolve several proteins in neutrophil granule extract. Of note, the larger but more cationic lysozyme (pI 9.28) migrates faster than HNP1, 2, and 3 (pI 8.68, 8.67, and 8.33, respectively). Although HNP3 differs from HNP1 in only one amino acid, it is clearly separated in AU-PAGE. HNP3 contains at its N terminus the anionic amino acid aspartic acid instead of alanine [10], and is, therefore, less cationic and thus slower in AU-PAGE. HNP2 lacks the N terminal amino acid from HNP1 and HNP3 and migrates between HNP1 and HNP3 according to its slightly reduced cationic charge. The corresponding Western immunoblot probing for HNP1–3 (the polyclonal antibodies are cross-reactive with these highly homologous HNPs) mirrors the distinct separation of the three HNPs and demonstrates the predominant presence of HNP1 and HNP3 in neutrophil granule extract.

2 Materials

2.1 AU-PAGE

1. Urea, molecular biology grade (*see Note 1*).
2. Glacial acetic acid (HoAc).
3. *N,N,N,N'*-tetramethyl-ethylenediamine (TEMED).
4. Solution A, 60 % acrylamide-1.6 % bis-acrylamide in dH₂O. Acrylamide powder is neurotoxic and must be handled with gloves and mask, and weighed and dissolved under a fume hood. For 200 mL, weigh out 120 g acrylamide, 3.2 g bis-acrylamide (alternatively, use a prepared mix of 37.5:1 mix of acrylamide:bis-acrylamide, e.g. from BioRad; Cat# 161-0125), add 76.8 mL dH₂O, let dissolve (which may take several hours), and add dH₂O to a final volume of 200 mL. Transfer to a clean glass bottle, wrap the bottle in aluminum foil, and store at room temperature (RT).
5. Solution B, 43.2 % HoAc, 4 % TEMED (v/v). For 50 mL, aliquot 21.6 mL HoAc into a glass bottle containing 26.4 mL of dH₂O, add 2 mL of TEMED (this is an exothermic reaction and fumes will be produced; prepare under a fume hood). Wrap the bottle with aluminum foil and store at RT.
6. APS, 10 % ammonium persulfate. Weigh out 1 g ammonium persulfate and add to 10 mL dH₂O (*see Note 2*).

7. AU-PAGE sample buffer, 9 M urea in 5 % HoAc with methyl green. For 25 mL, weigh out 13.5 g urea and add to 10 mL dH₂O in a glass beaker containing a stirrer and dissolve (this is an endothermic reaction), deionize with resin (see Note 3) for 20 min, filter the solution through Whatman paper No. 4 into a clean glass container, add 1.25 mL HoAc and stir to mix for about a minute, bring the volume to 25 mL with dH₂O and add methyl green dye to produce a medium blue-green color (a few grains). Once fully dissolved aliquot the sample buffer in microfuge tubes and store at -20 °C (see Note 4).
8. Electrophoresis buffer, 5 % HoAc. Add 50 mL HoAc to 950 mL dH₂O.
9. Vertical electrophoresis unit and power supply that allows running at constant current and constant voltage.

2.2 Western Immunoblot

1. Immobilon PSQ® membrane (Millipore), a PVDF membrane with a pore size of 0.1 µm. Alternatively, you can use ImmobilonP (Millipore), a PVDF membrane with a pore size of 0.2 µm (see Note 5).
2. Tris buffered saline, high salt (TBS-HS), 20 mM Tris, 500 mM NaCl, pH 7.5 (see Note 6). For 1 L weigh out 29.22 g of NaCl and dissolve in 800 mL of dH₂O, add 20 mL of 1 M Tris, pH 7.5, stir for a few minutes, and then bring the volume to 1 L with dH₂O. Alternatively, you can add to 20 mL of 1 M Tris, pH 7.5, 100 mL of 5 M NaCl, and 880 mL of dH₂O.
3. Tris buffered saline, low salt (TBS-LS), 20 mM Tris, pH 7.4, 0.9 % NaCl (see Note 7). For 1 L weigh out 9 g of NaCl and dissolve in 800 mL of dH₂O in a beaker with a stir bar, add 20 mL of 1 M Tris, pH 7.4, stir for a few minutes, bring the volume to 1 L with dH₂O and mix well.
4. Phosphate buffered saline, PBS, 10 mM sodium phosphate buffer, pH 7.4, 0.9 % NaCl (see Note 8). For 1 L weigh out 9 g of NaCl, dissolve in 800 mL of dH₂O in a beaker with a stir bar, add 100 mL of 100 mM sodium phosphate buffer, pH 7.4, stir for a few minutes, bring the volume to 1 L with dH₂O, and mix well.
5. Transfer buffer, 0.7 % HoAc, 10 % methanol. For 1 L measure 893 mL dH₂O and transfer into a beaker, add 7 mL of HoAc and stir for a few minutes to mix, add 100 mL of methanol, and stir to mix well.
6. Fixing solution, 0.05 % glutaraldehyde in TBS-HS. Dilute a 25 % glutaraldehyde solution 1:500 in TBS-HS, for example add 0.2 mL of 25 % glutaraldehyde to 99.8 mL of TBS-HS.
7. Blocking buffer, 0.75 % milk (nonfat milk powder such as Carnation®) in PBS. Weigh out 0.75 g and dissolve in 100 mL PBS.

8. Antibody diluent, 0.25 % milk (nonfat milk powder such as Carnation®) in PBS, supplemented with 0.01 % thiomersal as microbicide (*see Note 9*). To 50 mL of blocking buffer add 98.5 mL of PBS and 1.5 mL of a 1 % thiomersal solution.
9. Wash buffer, 0.1 % (w/v) bovine serum albumin (BSA) in TBS-LS. Weigh out 1 g of BSA and add to 1 L of TBS-LS. Stir at low speed to dissolve without generating foam.
10. Alkaline phosphatase (AP) buffer, 100 mM NaCl, 5 mM MgCl₂, 100 mM Tris base, pH 9.8. Add 10 mL of a 5 M NaCl and 2.5 mL of a 1 M MgCl₂ solution to 400 mL of dH₂O, stir, add 6.055 g of Tris Base and dissolve, adjust the pH to 9.8 with HCl, and bring to a final volume of 500 mL with dH₂O. Store at 4 °C but equilibrate to RT prior to use.
11. Developing solution, nitroblue tetrazolium salt (NBT)/5-Bromo-4-Chloro-3-indolyl phosphate (BCIP) in AP buffer. In separate containers, dissolve 1 g NBT in 70 % dimethylformamide (*see Note 10*) and 100 mg BCIP in 2 mL of 100 % dimethylformamide. Store both working solutions wrapped in aluminum foil at 4 °C. Immediately prior to use, add 396 µL NBT working solution and 198 µL BCIP working solution to 60 mL AP buffer.

3 Methods

3.1 Gel Pouring

1. Place mini gel plates (8 cm × 10 cm) and spacers into the gel casting system according to manufacturer's instructions (*see Note 11*).
2. For four 12.5 % mini gels (0.75 mm thickness), weigh out 9.6 g urea, add 13.5 mL dH₂O to dissolve (this reaction is endothermic), add 6.7 mL solution A, 4 mL solution B, and 0.6 mL 10 % APS.
3. *Immediately* pour the gel solution into the caster using a 25 mL pipette which is directed onto a corner of the caster. Fill gel solution to the top of the front plate and insert the matching combs. Add more gel solution as needed to accommodate any losses during comb insertion.
4. Cover the gels with plastic wrap and allow polymerization to occur over night at RT (*see Note 12*).

3.2 Pre-run to Remove Excess Urea from the Gel

1. Remove gels carefully from the casting tray. Using a razor blade clean off excess polyacrylamide and clean plates from the outside with a moist Kimwipe.
2. Carefully remove the combs and briefly rinse the wells with dH₂O using a water wash bottle. This will remove any unpolymerized acrylamide.

3. Shake off excess water and place the gel in the electrophoresis apparatus.
4. Add 5 % HoAc to the upper buffer chamber only until the wells are filled and verify that the gels are not leaking, and then add 5 % HoAc to the lower buffer chamber.
5. Just before loading samples rinse out the wells to remove urea and entrapped air bubbles using a syringe with a 22 g needle filled with 5 % HoAc.
6. Dilute AU-PAGE sample buffer 1:3 in 5 % HoAc (e.g. 50 μ L sample buffer plus 100 μ L 5 % HoAc) and load 10 μ L into each well.
7. Connect the apparatus to the power supply unit with *reversed polarity*. The cathode connection must be plugged into the anode connection and the anode connection into the cathode connection on the power supply unit (*see Note 13*).
8. Apply a voltage of 110 V and run the gels until the dye front has exited from the gel (*see Note 14*), about 30–60 min.
9. Dismantle electrophoresis apparatus, briefly rinse gel cassettes and gel wells with dH₂O, then pat dry.
10. Gels can be immediately used for gel electrophoresis or stored for up to 10 days in a humid chamber at 4 °C (*see Note 15*).

3.3 Gel Electrophoresis

1. Place the gel in an electrophoresis apparatus.
2. Add 5 % HoAc to the upper buffer chamber only until the wells are filled and verify that the gels are not leaking, and then add 5 % HoAc to the lower buffer chamber.
3. Just before loading samples rinse out the wells to remove urea and entrapped air bubbles using a syringe with a 22 g needle filled with 5 % HoAc.
4. Prepare samples as follows: lyophilize the desired amount of protein and dissolve in 5 μ L 5 % HoAc (or use 1–2 μ L of the test sample and add 5 % HoAc to a final volume of 5 μ L), add 3 μ L of AU-PAGE sample buffer (*see Notes 16–18*).
5. Briefly mix the samples by sliding the tubes across a microfuge rack, briefly centrifuge tubes to collect all material and load everything while avoiding loading of air bubbles.
6. Connect the apparatus to the power supply unit with *reversed polarity*. The cathode connection must be plugged into the anode connection and the anode connection into the cathode connection on the power supply unit (*see Note 13*).
7. Start electrophoresis at 80 V and increase voltage to 100 V once samples have fully entered the gel and about 5–10 min later to 130 V.

8. Depending on the electrophoretic mobility of the (poly) peptides of interest run the gels until the dye front has reached the bottom of the gel or up to 30 min after the dye front has left the gel.

9. Dismantle electrophoresis apparatus, briefly rinse gel cassettes and gel wells with dH₂O, and then pat dry.

3.4 Protein Transfer to Membrane Using a Semidry Blotting Technique

1. While electrophoresis is reaching its end, using a sharp razor blade, cut the PSQ® membrane, with the protective sheets still present, into the appropriate size as needed.
2. Remove the protective sheets. Always handle the membrane with the utmost care. Only use blunt forceps to handle the membrane and only touch the corners or side borders of the membrane to avoid damage and artifacts in the area of interest.
3. Label with a pencil the front side of the membrane that will face the gel, e.g. date, in an area that will not be in contact with the gel.
4. Place the membrane into a clean tray and briefly saturate the membrane with 100 % methanol, decant the methanol, add precooled transfer buffer (*see Note 19*), and equilibrate the membrane in transfer buffer for about 5 min (*see Note 20*).
5. Cut eight sheets of Whatman No 4 filter paper to be slightly larger than the membrane and pre-wet in transfer buffer.
6. After completion of the electrophoresis run remove the gel from the electrophoresis apparatus and carefully separate glass plates from the gel and cut one corner of the gel for orientation.
7. Set up the transfer sandwich as follows: four sheets of pre-wetted filter paper, the gel (flipped so that lane one from the left side is now on the right side, *see Note 21*), the membrane, and four sheets of pre-wetted filter paper. Carefully place the next layer onto the previous layer with a rolling movement thereby avoiding the entrapment of air. Remove any residual air bubbles by adding a small amount of transfer buffer on top of the sandwich and gently rolling a serological pipette over the sandwich. Once placed onto the gel, never move the membrane until the transfer has been completed, otherwise, the membrane will bind proteins unrelated to the sample obscuring sample specific proteins.
8. Remove excess liquid and connect the apparatus to the power outlet using *reversed polarity* (for wet or semidry transfer).
9. Allow transfer to occur for 20 min at constant Ampere and 1.5 mA/cm² gel (120 mA for an 8 × 10 cm² gel).
10. Turn off power source and disassemble apparatus.
11. Take a corner of the filter paper with blunt forceps, gently lift the filter paper off the membrane, and discard the filter paper.

12. With a blunt forceps grip a corner of the membrane, gently roll the membrane off the gel and transfer it into a tray containing fixing solution (*see Note 22*).
13. Incubate the membrane for 10–30 min in fixing solution at RT on a rocker. During this time prewarm the blocking solution to 37 °C and stain the gel with Coomassie to assess the degree of protein transfer.
14. Briefly rinse membrane with dH₂O and subsequently wash the membrane with TBS-HS for 5 min at RT to remove residual fixing solution.

3.5 Immunoblot

1. Transfer the membrane to a tray containing the prewarmed blocking solution (about 25–50 mL per membrane, depending on the size of the container) and incubate for 30 min at 37 °C (*see Note 23*).
2. Pour off the blocking solution, add the primary antibody (specific for the target (poly)peptide) diluted as needed in antibody diluent, to the same tray without washing, and incubate overnight, rocking at RT. You need at least 20 mL for one ~8 cm × 10 cm sized membrane.
3. Pour off the primary antibody solution and rinse twice with dH₂O to quickly remove the majority of the primary antibody. Transfer the membrane to a new tray and wash the membrane a total of three times for 10 min each in 1 % BSA-TBS-LS. Change the tray again after the second wash (*see Note 24*).
4. Transfer membrane into a new tray containing alkaline phosphatase-conjugated secondary antibody diluted as needed in antibody diluent, and incubate for 1 h at RT on the rocker. You need at least 20 mL antibody solution for one ~8 cm × 10 cm sized membrane. During the incubation time equilibrate the AP buffer to RT.
5. Wash as described above in **step 3**.
6. Briefly rinse the membrane in dH₂O followed by a 5 min wash in TBS-HS. During this time prepare the NBT-BCIP developing solution.
7. Transfer the membrane into the developing solution and allow the entire membrane to become dark before stopping the reaction by transferring the membrane into a tray containing dH₂O. Upon drying the background will lighten up again and only the specific bands will remain colored.
8. Remove the membrane, place it onto Whatman filter paper no 4, and allow to completely dry before imaging. The membrane may be stored after covering with a plastic wrap in a cool and dry area.

4 Notes

1. Use high-quality urea, for example from Sigma-Aldrich.
2. APS solution can be stored for maximal 10 days in the refrigerator but best results are achieved with freshly prepared APS.
3. To deionize with resin, add about 1/2 scoop (1–2 g) of AG 501-X8 Resin (BioRad, Hercules, CA), stir at RT for 10–15 min, and remove resin by filtering the solution through Whatman paper no 4.
4. The AU-PAGE sample buffer can only go through a few freeze-thaw cycles and therefore, it is advisable to prepare 0.5 mL aliquots that are stored at –20 °C.
5. The ImmobilonP membrane may produce sharper bands. However, the larger pore size may allow small peptides to run through the membrane and exit during the transfer. Therefore, the transfer time should be carefully controlled when using ImmobilonP membranes.
6. For 1 L of a 1 M Tris, pH 7.5, weigh out 127 g of Tris–HCl and 23 g of Tris-base, dissolve in 800 mL dH₂O, adjust the pH to 7.5 with HCl or NaOH as needed, and bring up to 1 L with dH₂O.
7. Prepare a 1 M Tris stock as described in **Note 6** but adjust to pH 7.4.
8. To prepare 100 mM sodium phosphate buffer pH 7.4, mix 100 mM NaH₂PO₄ with 100 mM Na₂HPO₄ at a ratio of 19:81 (v:v). Dilute further as needed.
9. Prepare 100 mL of a 1 % stock solution of thiomerosal (ethyl-mercurithiosalicylic acid sodium salt) in dH₂O, and keep in a glass bottle wrapped in aluminum foil at RT (good for several months). Dilute 100-fold as needed. Thiomerosal contains mercury and is toxic and needs to be labeled as “poison”.
10. If you use NBT-salt then dissolve NBT in dH₂O instead of dimethylformamide.
11. It is important to have very clean plates for pouring the gels. For example, wipe clean glass and metal plates alternating with methanol and distilled water using clean Kimwipes until under careful inspection the glass plates are spotless. Furthermore, we recommend using the Mighty Small Multiple Gel Caster, for SE 250, from GE Healthcare Life Sciences (Piscataway, NJ). We found that gels do not polymerize easily when using the dual caster by GE Healthcare Life Sciences and often gel solution has to be re-added during the polymerization process. If you want to increase sensitivity you can pour thicker gels and load more sample per well.

12. If the gels are slow to polymerize you can try to deionize the dissolved urea solution with two to three scoop full of resin as described in **Note 3**.
13. In AU-PAGE all proteins are maximally positively charged due to the low pH of the 5 % HoAc buffer. Thus, voltage must be applied in a reversed way compared to SDS-PAGE where all proteins are in a negatively charged stage.
14. If you are very pressed for time, you can pre-run until the dye is only half way through the gel. However, this will produce suboptimal results and is not recommended.
15. The gels can be stored before or after the pre-run for up to 10 days at 4 °C in a humid chamber when wrapped properly. Wrap each gel individually. Place the gel on a clear plastic wrap, do not fill the wells with water because this would wash out the urea, place a moist towel onto the top glass plate, and then wrap the gel tightly. Alternatively, you can place the gels into a zip lock bag and then store in a humid chamber. When using the gels, briefly rinse the wells with distilled water, shake off the liquid and pat dry to remove excess moisture.
16. If your samples contain too much salt the color of the loading dye will turn yellow and the electrophoretic mobility will be negatively impacted. In that case ensure that empty wells surround such samples so that the mobility of neighboring samples is not affected and try further diluting your samples or removing salts by e.g. dialysis or gel filtration prior to loading.
17. If you work with very low protein concentrations and it is likely that peptide will be bound to the wall of the test tube add 0.1 % nonfat milk powder to the 5 % acetic acid to dissolve the peptide. Prepare a 10 % nonfat milk stock in dH₂O and dilute the stock 100-fold into 5 % HoAc. Alternatively, you can use 0.5 % BSA in 5 % HoAc as peptide solvent.
18. Band sharpness can be increased by reducing the volume for dissolving the proteins to 2 µL, adding only 1.5 µL of the AU-PAGE sample buffer and loading the sample very slowly, thereby ensuring that the sample will settle concentrated at the bottom of the well.
19. Precooling the transfer buffer to 4 °C prior to use helps to produce a more even transfer and sharper separation.
20. Never squirt or pour any fluid directly on the membrane. This will cause artifacts.
21. By flipping the gel during the transfer the orientation of the lanes on the membrane will be the same as the original orientation of the lanes on the gel. This will facilitate analysis of the results.

22. The fixing step may affect the immunoreactivity of the peptides of interest. An alternative fixative is 10 % formalin vapor. For this obtain a sealable container, place into it an empty pipette tip rack, place on top of the rack 2 or 3 layers of Whatman No 4 filter paper moistened with TBS-HS and place the membrane onto the filter paper with the protein side facing up, pour 10 % formalin solution (diluted in TBS-HS) into the container to a height of about 1 cm, close the container and incubate the membrane in the vapor for 30 min. All steps have to occur under a fume hood.
23. You can use square petri dishes as incubation trays, empty clean pipette boxes, or dedicated blotting containers from e.g. Research Products International Corp.
24. Changing the trays frequently will help reduce background staining.

Acknowledgements

E.P. is supported by SC1NIH grant GM096916. NHS is supported by GM099526, AI097619, and DK088831.

References

1. Nakatsuji T, Gallo RL (2012) Antimicrobial peptides: old molecules with new ideas. *J Invest Dermatol* 132:887–895
2. Lehrer RI, Rosenman M, Harwig SS et al (1991) Ultrasensitive assays for endogenous antimicrobial polypeptides. *J Immunol Methods* 137: 167–173
3. Martinez Rodriguez NR, Eloi MD, Huynh A et al (2012) Expansion of Paneth cell population in response to enteric *Salmonella enterica* serovar Typhimurium infection. *Infect Immun* 80:266–275
4. Harwig SS, Park AS, Lehrer RI (1992) Characterization of defensin precursors in mature human neutrophils. *Blood* 79:1532–15537
5. Greenwald GI, Ganz T (1987) Defensins mediate the microbicidal activity of human neutrophil granule extract against *Acinetobacter calcoaceticus*. *Infect Immun* 55:1365–1368
6. Harwig SS, Chen NP, Park AS et al (1993) Purification of cysteine-rich bioactive peptides from leukocytes by continuous acid-urea-polyacrylamide gel electrophoresis. *Anal Biochem* 208:82–86
7. Porter EM, Bevins CL, Ghosh D et al (2002) The multifaceted Paneth cell. *Cell Mol Life Sci* 59:156–170
8. Linzmeier R, Michaelson D, Liu L et al (1993) The structure of neutrophil defensin genes. *FEBS Lett* 321:267–273
9. Martinez JG, Waldon M, Huang Q et al (2009) Membrane-targeted synergistic activity of docosahexaenoic acid and lysozyme against *Pseudomonas aeruginosa*. *Biochem J* 419: 193–200
10. Selsted ME, Harwig SS, Ganz T et al (1985) Primary structures of three human neutrophil defensins. *J Clin Invest* 76:1436–1439

Chapter 8

Detecting Non-typhoid Salmonella in Humans by Enzyme-Linked Immunosorbent Assays (ELISAs): Practical and Epidemiological Aspects

Katrin G. Kuhn, Hanne-Dorthe Emborg, Karen A Krogfelt, and Kåre Mølbak

Abstract

Salmonellosis caused by non-typhoid *Salmonella* serotypes is one of the most common causes of food-borne illness throughout the world. The diagnosis is primarily by culture and more recently molecular methods, whereas the use of serological methods for diagnosis of *Salmonella* infections is limited by high running costs as well as low sensitivity and specificity. Fast and reliable immunoassays for detection of *S. typhi* subunit antigens are commercially available, but there is no international consensus of similar tests for non-typhoid salmonellosis. Most immunoassays for non-typhoid human *Salmonella* diagnosis are developed in-house and used in-house for research or regional surveillance purposes. Only few laboratories use serology for the diagnosis of *Salmonella*-associated complications such as arthritis. Considering the current burden of disease, the development of a validated and standardized, commercially available antibody assay for diagnosing non-typhoid human salmonellosis can be of great benefit for diagnostic and surveillance purposes throughout the world.

Key words *Salmonella*, Non-typhoid, Antibodies, Commercially available ELISA, Sero-diagnosis, Sero-incidence, Infectious disease surveillance

1 Serology and *Salmonella* Infections

Infections with *Salmonella* (*S. enterica*) are one of the most important sources of human gastroenteritis throughout the world. *Salmonella* serotypes are characterized as typhoid and non-typhoid types, where the former is restricted to humans and can produce a serious and potentially fatal illness known as typhoid (enteric) fever. Non-typhoid salmonellosis is due to infection by a large variety of different zoonotic serovars and is primarily transmitted by ingestion of contaminated food. The primary illness pattern consists of acute self-limiting gastroenteritis, but serious post-infection complications or sequelae such as septicemia, reactive arthritis or aortic aneurysms may occur. Non-typhoid *Salmonella* serotypes are responsible for an estimated annual 200 million to 1.3 billion

cases and 3 million deaths worldwide compared to 16–20 million cases and 200,000 deaths of typhoid fever [1, 2].

The gold standard for diagnosing any *Salmonella* infection is bacteriological culture, usually from feces. However, viable bacteria may sometimes only be present for a few days or too much time has passed since infection, and in these cases detection by culture is not valid. In such circumstances, serological antibody assays are usually applied to provide evidence of infection.

Serological diagnosis of *Salmonella* infections has classically been performed using the Widal tube agglutination test which has formed the basis of typhoid serodiagnosis for more than a century [3]. However, the Widal test is limited by poor sensitivity, an inability to discriminate between different antibody classes and cross-reactivity with other *Salmonella* species. Furthermore, it is time consuming and expensive in practice. Alternative and newer serological methods such as lateral flow rapid tests (LFRTs) or microarrays are expensive to purchase or require several pre-assay steps of purification and amplification. In comparison ELISAs are quantitative, samples do not need pre-assay handling and the overall running costs are lower. ELISAs have the potential of being semi-automated and may be applied for surveillance and research purpose, and have the advantage of being sensitive after the acute phase of infection when culture or detection of *Salmonella*-DNA by molecular methods has low sensitivity. Furthermore, serological tests can be applied to examine past infections in persons without a history of illness and may on this basis be used to measure the “force of transmission” in a population which may be different from the actual rate of illness.

Considering the need for rapid screening of patients with suspected typhoid salmonellosis, the ELISA technique was an optimal candidate for serological diagnosis of *Salmonella* infections and early attempts to use the outer membrane lipopolysaccharide (LPS) in ELISAs showed promising results for detecting antibodies in human sera. LPS-specific immunoglobulin G (IgG) persists for up to 12 months after infection, while IgM and IgA disappear after 2–4 months in most patients. The kinetics of antibody decay have been determined and seem to follow the expected sigmoidal curve [4]. Using the flagellum as detecting antigen has also been tested but with little success [5]. On this basis, it seems likely that an LPS-based ELISA which detects IgG, IgM and IgA responses can provide a specific, sensitive, fast, easy, and reliable assay for routine analyses of human sera.

Today, commercially available *Salmonella*-specific ELISAs are routinely used in veterinary and food sectors across Europe and in the States—not for diagnosis of infection in individual animals but rather as tools in control and surveillance programs. Common for all these tests is that they cannot be directly applied to human samples. In South-East Asia, several commercially available assays exist for fast diagnosis of typhoid salmonellosis, but these will only

detect *S. typhi* and not zoonotic Salmonella species. The potential for using ELISAs to diagnose human infection with non-typhoid Salmonella is promising, but knowledge about the current availability and application of such tests is scarce.

1.1 Use of ELISAs to Detect Salmonella Antibodies in Human Sera

Kuhn et al. [6] reviewed the literature review in order to identify all possible variants of Salmonella ELISAs. The review lists eight publications which describe assays to detect human non-typhoid salmonellosis.

All reported assays used LPS from a single Salmonella serovar (mostly *S. enteritidis* or *S. typhimurium*) separately, and four assays also showed results for a mixture of *S. enteritidis* and *S. typhimurium* LPS. The sensitivity of the assays ranged from 78 to 100 % and specificity ranged from 90 to 97 %. All assays were applied to culture-confirmed Salmonella cases as well as a group of controls (either healthy or with another infection/illness). Cross-reactivity with other bacteria such as *Escherichia coli*, *Yersinia enterocolitica*, *Campylobacter* spp. and *Helicobacter pylori* (which also cause gastrointestinal symptoms) was investigated on four occasions and found to be 17–59 %.

The literature review identified only one commercially available antibody assay for detection of non-typhoid Salmonella in human sera, namely the “IMTEC-Salmonella-Antibodies Screen (IgG/IgA/IgM)/Antibodies IgA” which is based on pooled antigens from *S. enteritidis* and *S. typhimurium* and uses high IgA titers as a marker for the diagnosis of reactive arthritis. These principles are similar to those reported for some of the other assays described in the literature review. The sensitivity of the commercially available test was reported by the manufacturers as 88.5 %, however, no further studies evaluating its design or general use were identified.

Contrastingly, at least four standardized and validated antibody assays exist for the diagnosis of infections due to *Salmonella typhi*. These are primarily used in endemic areas of the developing world where typhoid fever is a serious problem and its relatively high mortality rate makes rapid and accurate diagnosis crucial.

Most likely, a standardized test for identifying non-typhoid Salmonella antibodies in human sera has not yet been developed because of practical rather than technical issues. Some laboratories are using their own in-house tests with acceptable success rates and do not see a need to purchase a standardized one. Additionally, some institutions may even consider the ELISA an old fashioned test, in comparison to other methods. The development of a standardized ELISA requires significant and challenging ground-work and extensive production of new standards and controls. However, given the fact that ELISAs have obvious advantages over other serological methods and that standardized tests have already been successfully developed, these practical issues should be considered of minor importance.

1.2 The Practicality of Developing a Standardized Assay for Sero-Diagnosis of Non-typhoid *Salmonella* in Humans

Based on the literature review, it was suggested that LPS-based ELISA can be a suitable candidate for a standardized, commercially available method of detecting non-typhoid *Salmonella* antibodies in human sera. Encouragingly, LPS antigens of *S. typhimurium* and *S. enteritidis* are commercially available and were indeed used to develop several of the assays reviewed. An acceptable method for detection of non-typhoid human salmonellosis could therefore be a pooled ELISA containing a mixture of LPS from *S. enteritidis* (serogroup D) and *S. typhimurium* (serogroup B) as also suggested recently [7]. The choice of LPS is geographically determined and must reflect the circulation of serovars in the human population. An ELISA based on *S. typhimurium* and *S. enteritidis* LPS would cover 70–90 % of all reported *Salmonella* isolates in Europe [8]. A test designed for use in the United States would need to contain the same mixture but also LPS from *S. Newport* (group C) which is responsible for almost 10 % of reported *Salmonella* cases here [9]. *S. Heidelberg* (group B), the fourth most common type in the US, will be captured by the *S. typhimurium* (also group B) antigens.

The ELISA must be validated on a number of known positive sera and a group of controls, both negative and with other known infections, such as *Yersinia enterocolitica* and *Helicobacter pylori*, to test for cross-reactivity. For this, at least 100 *Salmonella* patients, 100 negative controls and 100 patients with other infections are needed. The assay performance should be assessed with reference to sensitivity and specificity, relative to the chosen cut-off as well as the purpose of the test. For diagnostic purposes, including reactive arthritis, a high specificity is needed in order to avoid high predictive value of a positive result. In practice, a specificity of 95 % or more is required. For surveillance and public health purposes, a correct classification of the individual patient becomes less important and a sensitivity and specificity of 85 % will be sufficient. A preliminary suggested cut-off for a standardized non-typhoid *Salmonella* ELISA could be 10 % Optical Densities (OD) as used in many of the assays reviewed.

1.3 The Epidemiological Implications of Developing a Standardized *Salmonella* ELISA

Standardized ELISAs are today not widely used for routine diagnosis of non-typhoid *Salmonella* in humans or for public health surveillance. As described, most laboratories use their own in-house assays which are not available commercially. If a consensus was reached to develop, validate and routinely use a commercial ELISA for non-typhoid human *Salmonella* detection, it would allow estimation of infections in groups of individuals who would otherwise not have been diagnosed: i.e. slightly symptomatic and asymptomatic persons as well as those with a non-culturable fecal sample. From a broader epidemiological perspective, using ELISAs for diagnosing bacterial infections can therefore create a more realistic estimate of the seroconversion rate. Current figures of *Salmonella* incidence represent only a small fraction of total cases, as they

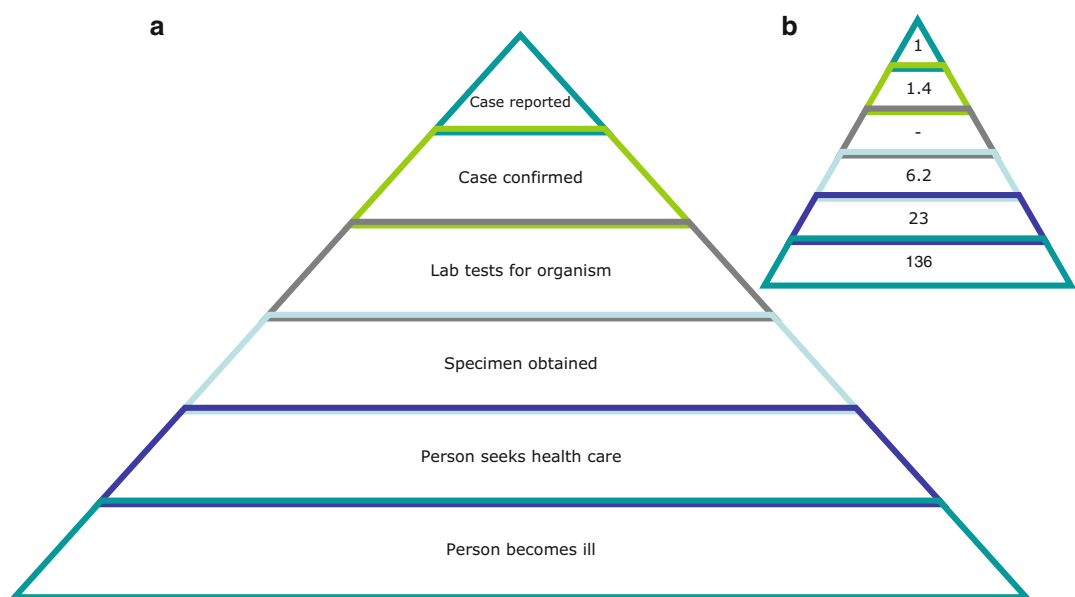


Fig. 1 (a) Burden of illness pyramid illustrating the chain of events in food-borne disease reporting and the imbalance between actual cases and number of cases reported. (b) Example for gastrointestinal illness in England in 1999 (number of persons) from Wheeler et al. [11]

mostly reflect the health-seeking behavior of patients as well as the tendency of physicians to request a stool culture (Fig. 1). A population-based method has been developed [10] to estimate the incidence of seroconversion, using *Salmonella* antibody titers in sera from Danish general population surveys. This method accurately predicted the increasing trend of culture-confirmed cases in the 1980s and showed that the incidence (including asymptomatic infections) in 1 year could have been 100-fold higher than reported. Such an approach demonstrates the promise for using serological results to measure the force of infection and ultimately compare different national surveillance systems as well as evaluate the impact of food safety programs on the incidence of human infections.

In 2008, a total of 131,468 cases of human salmonellosis were reported from the European Union, making it the second most commonly reported zoonotic disease in humans, only surpassed by *Campylobacter* [8]. Considering the burden of this disease, the implications for travel and trade with food and animals, and the fact that many patient samples may not be culturable, the development of a commercial antibody assay to detect *Salmonella* in human sera is now very timely. Evidence from typhoid fever diagnosis and the veterinary sector has shown that it is feasible to develop a rapid, cheap and potentially accurate commercial antibody assay for *Salmonella*. We suggest that now is the time to take the next step and reach an international consensus for the development of an ELISA to diagnose non-typhoid human *Salmonella* infections.

2 Suggested Protocol for a Standardized ELISA (Europe)

Indirect ELISA on human serum using mixed LPS antigens from *Salmonella typhimurium* and *Salmonella enteritidis*. IgA, IgM, and IgG antibodies are measured separately through HRP/TMB enzymatic reactions. The ELISA is performed routinely at Statens Serum Institut, Denmark, and has been accepted by the European Centre for Disease Control and Prevention (ECDC).

2.1 Materials

1. NUNC F96 Microwell Clear Polystyrene, Polysorp® Microtitre plates.
2. Antigens: *Salmonella typhimurium* and *Salmonella enteritidis* LPS in a 1:1 ratio (see Note 1).
3. Sample, standard, and control sera (see Note 2).
4. Coating buffer: 0.1 M sodium carbonate buffer, pH 9.60 in sterile MilliQ water including 0.5 % NaN₃, 0.2 % phenol red for visual confirmation of pH stability. Adjust to pH 9.60 ± 0.02.
5. Wash buffer: PBS-T, pH 7.40. Made with deionized water, 1 sachet PBS (Sigma,), 0.01 % Tween 20. Adjust to pH 7.40 ± 0.02 (see Note 3).
6. Dilution buffer: PBS-T with phenol red. 2 ml 0.5 % phenol red for visual confirmation of pH stability. Adjust to pH 7.40 ± 0.02 (see Note 3).
7. Secondary antibody: HRP labeled rabbit anti-human antibodies.
 - (a) Anti IgA (Dako) 1:500 in dilution buffer.
 - (b) Anti IgM (Dako) 1:1,000 in dilution buffer.
 - (c) Anti IgG (Dako) 1: 2,500 in dilution buffer.
Used the same day at room temperature.
8. Substrate. TMB-One (Kem-En-Tec).
9. Stop-solution. 1 M sulfuric acid.

3 Methods

1. Coating. Stock of *Salmonella* LPS antigen mix at 10 mg/ml is diluted to 1 µg/ml in cold coating buffer (5 °C).
Three Polysorp plates are coated with the diluted antigen using 100 µl per well. The three plates are closed with a lid, wrapped in aluminum foil and incubated overnight in a refrigerator (2–8 °C).
2. Washing. All wash-steps consist of 3–5 successive wash cycles with 250 µl wash buffer per well.
3. Blocking. After washing, 250 µl wash buffer is added to each well on each plate. The plates are closed with a lid and incubated for 30 min (±5 min) at room temperature, no shaking.

4. Dilution of sera. Samples and the two controls are diluted 1:400 in the dilution controls buffer. The standard is first diluted 100-fold. Seven additional dilutions of the standard are then made by successive twofold dilutions (e.g. 1 ml plus 1 ml), making an 8-step dilution series of the standard from 1:100–1:12,800.
5. After incubation, the plates are washed again with 250 µl wash buffer. Then 100 µl of the dilution (see above) of each sample, control or standard is added per well in duplicates. For the blank control, 100 µl dilution buffer is added to the well(s) (see Note 4). The plates are closed with a lid and incubated for 30 min (±5 min) at room temperature, no shaking.
6. The plates are washed and 100 µl of the diluted secondary antibody is added per well. One plate receives only anti IgA, one receives only anti-IgM and one receives only anti-IgG. The plates are incubated for 30 min (±5 min) at room temperature, no shaking.
7. The plates are washed and 100 µl per well of TMB-One is added to each plate. Plates are incubated for exactly 15 min at room temperature without shaking.
8. The enzymatic reaction is stopped by addition of 100 µl per well of 1 M sulfuric acid.
9. Optical density for the plates is read at 450 nm with a reference reading at 630 nm (620 or 650 nm can be used as well).
10. The Optical Density (OD) results from the dilution series of the standard serum is compared to the mean OD results from the same standard serum obtained from at least ten previous runs.

By plotting the current results of the standard serum against the mean expected results for each dilution point—a linear graph should be obtained. The slope of the curve determines how the current results should be corrected in order to minimize day-to-day variations. Results are only valid if the correction is less than 20 % (see Note 5, Fig. 2).
11. The cut-off point should be determined before the assay is set up (see Note 6).

4 Notes

1. To make the antigens, the contents of one ampoule of *Salmonella typhimurium* LPS (Sigma) and one ampoule of *Salmonella enteritidis* LPS (Sigma) are mixed and adjusted to a final concentration of 1 mg/ml. Aliquots are stored frozen at minus 20 °C.

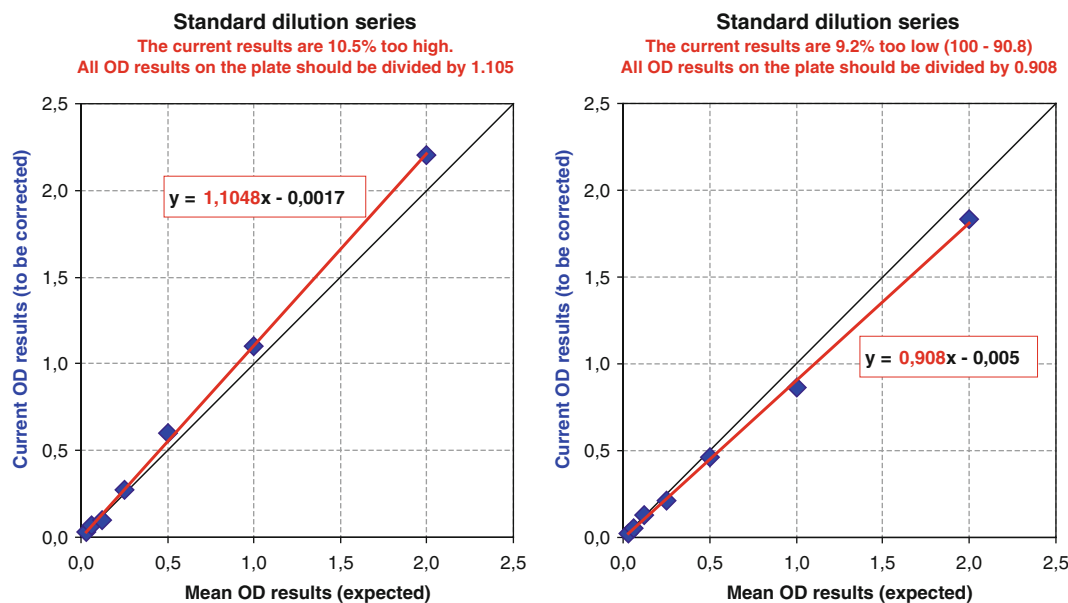


Fig. 2 Correcting current OD results in order to minimize day-to-day variations

2. Along with the sample sera of interest, three types of control sera should be used:
 - (a) Standard: pooled serum from individuals with *Salmonella typhimurium* or *Salmonella enteritidis* infection as confirmed by fecal culturing. Sera are chosen for high values of Salmonella LPS-specific IgA, IgM and IgG antibodies.
 - (b) Positive control: pooled serum from individuals (or from a single individual) with *Salmonella typhimurium* or *Salmonella enteritidis* infection as confirmed by fecal culturing. Sera are chosen for high values of Salmonella LPS-specific IgA, IgM, and IgG antibodies.
 - (c) Negative control: pooled serum from individuals with no detection of anti-Salmonella LPS-specific IgA, IgM, or IgG serum antibodies, and no detection of antibodies against other enteric pathogens as *Yersinia enterocolitica*, *Campylobacter*, and *E. coli*.
3. Wash buffer and dilution buffer should be stored at room temperature and used within a week. Coating buffer should be refrigerated and cold when used.
4. Standard, controls, samples and blanks are placed in the same pattern on all three plates. An example of plate layout is shown below.

	1	2	3	4	5	6	7	8	9	10	11	12
A	Std 100×	Std 100×	blank									
B	Std 200×	Std 200×	Neg	Neg	S7	S7	S14	S14	S21	S21	S28	S28
C	Std 400×	Std 400×	S1	S1	S8	S8	S15	S15	S22	S22	S29	S29
D	Std 800×	Std 800×	S2	S2	S9	S9	S16	S16	S23	S23	S30	S30
E	Std 1,600×	Std 1,600×	S3	S3	S10	S10	S17	S17	S24	S24	S31	S31
F	Std 3,200×	Std 3,200×	S4	S4	S11	S11	S18	S18	S25	S25	S32	S32
G	Std 6,400×	Std 6,400×	S5	S5	S12	S12	S19	S19	S26	S26	Pos	Pos
H	Std 12,800×	Std 12,800×	S6	S6	S13	S13	S20	S20	S27	S27	Neg	Neg

Std refers to standard sera.

Neg is negative control.

Pos is positive control.

Each S1, S2...S27 refers to the individual sample sera to be tested for antibodies.

5. Individual sample results are only valid if the CV value for the duplicate analysis is below 20 %. Moreover, the positive and negative control sera should give results that are interpreted as “positive” and “negative”, respectively, according to the chosen cut-off values.
6. The cut-off should be determined for each country/region separately.
By analyzing 100 sera or more (50 as minimum) from healthy individuals (or blood donors) with the current antigen batch, the 95 percentile is a valid choice for cut-off for each antibody class.
A gray-zone of e.g. $\pm 20\%$ is recommended for each antibody class.

Acknowledgements

Acknowledgements are due to Tine Dalby and Charlotte Sværke Jørgensen at Statens Serum Institut, Denmark, for invaluable help with developing and validating the Salmonella ELISA protocol.

The work was partly financially supported by The European Centre for Disease Prevention and Control (framework contract ECDC/09/032) and the EU Network of Excellence for research on the prevention and control of zoonoses MEDVETNET (Contract no. FOOD-CT-2004-506122).

References

1. Boyle EC, Bishop JL, Grassl GA, Finlay BB (2007) *Salmonella*: from pathogenesis to therapeutics. *J Bacteriol* 189:1489–1495
2. Coburn B, Grassl GA, Finlay BB (2007) *Salmonella*, the host and disease: a brief review. *Immunol Cell Biol* 85:112–118
3. Widal GF (1896) Sérodiagnostic de la fièvre typhoïde. *Bull Mem Hop Paris* 13:561–566
4. Strid MA, Dalby T, Mølbak K, Krogfelt KA (2007) Kinetics of the human antibody response against *Salmonella enterica* Serovars Enteritidis and Typhimurium determined by lipopolysaccharide enzyme-linked immunosorbent assay. *Clin Vaccine Immunol* 14:741–747
5. Dalby T, Strid MA, Beyer NH, Blom J, Mølbak K, Krogfelt KA (2005) Rapid decay of *Salmonella* flagella antibodies during human gastroenteritis: a follow up study. *J Microbiol Methods* 62:233–243
6. Kuhn KG, Falkenhorst G, Ceper TH, Dalby T, Ethelberg S, Mølbak K, Krogfelt KA (2012) Detecting non-typhoid *Salmonella* in humans by ELISA: a literature review. *J Med Microbiol* 61:1–7
7. Falkenhorst G, Ceper TH, Strid MA, Mølbak K, Krogfelt KA (2013) Serological follow-up after non-typhoid *salmonella* infection in humans using a mixed lipopolysaccharide. *Int J Med Microbiol* 303:533
8. EFSA (2010) The Community Summary Report on trends and sources of zoonoses, zoonotic agents and food-borne outbreaks in the European Union in 2008. *EFSS J* 8:1496–1906
9. Hendriksen RS, Vieira AR, Karlsmose S, Lo Fo Wong DMA, Jensen AB, Wegener HC, Aarestrup FM (2011) Global monitoring of *Salmonella* serovar distribution from the World Health Organisation Global Foodborne Infections Network Country Data Bank: results of quality assured laboratories from 2001 to 2007. *Foodborne Pathog Dis* 8:1–14
10. Simonsen J, Strid MA, Mølbak K, Krogfelt KA, Linneberg A, Teunis P (2008) Sero-epidemiology as a tool to study the incidence of *Salmonella* infections in humans. *Epidemiol Infect* 136:895–902
11. Wheeler JG, Sethi D, Cowden JM, Wall PG, Rodrigues LC, Tompkins DS, Hudson MJ, Roderick PJ (1999) Study of infectious intestinal disease in England: rates in the community, presenting to general practice, and reported to national surveillance. *BMJ* 318:1046–1050

Chapter 9

Study of the Stn Protein in *Salmonella*; A Regulator of Membrane Composition and Integrity

**Masayuki Nakano, Eiki Yamasaki, Joel Moss,
Toshiya Hirayama, and Hisao Kurazono**

Abstract

Our studies were undertaken to develop new insights into the function of the *Salmonella* Stn protein. An analysis of total cell membrane protein fraction suggested the possibility that Stn associates with OmpA. This possibility was confirmed by immunogold labeling using anti-OmpA antibody and far-western blotting. From these results, we conclude that Stn regulates membrane composition and integrity in *Salmonella*.

Key words *Salmonella*, Stn protein, Bacterial membrane, Electron microscopy, Immunogold stain

1 Introduction

Salmonella is a major food-borne pathogen; infection results in severe clinical manifestations including acute gastroenteritis and typhoid fever. Several virulence factors produced by *Salmonella* have been identified and their biological activities characterized. Two sets of type III secretion systems are required for *Salmonella* virulence, which include invasion into intestinal epithelial cells and survival in macrophages [1].

In addition to these secretion systems, it has been proposed that *Salmonella* enterotoxin (Stn) is a putative virulence factor responsible for enterotoxic activity [2, 3]. The *stn* gene was cloned for the first time from *S. enterica* serovar Typhimurium and the gene product was shown to be associated with enterotoxic activity in a murine ileal loop model [3]. However, Stn activities responsible for *Salmonella* virulence and the molecular mechanisms underlying its action in the host cells have not been elucidated.

When we evaluated the effects of Stn on *Salmonella* virulence using experimental animal model and cultured cell systems, we found that Stn was not associated with the *Salmonella* virulence

including enterotoxic activity [4]. These findings are consistent with other reports [5–7] and we therefore concluded that Stn does not function as a virulence factor. To evaluate the function of Stn in *Salmonella*, we next characterized the functions of Stn activities using several molecular techniques. In these studies, we found new insights into Stn function. Based on our data, it appears that Stn regulates membrane composition and integrity [4].

Here, we describe the various molecular techniques used in this study.

2 Materials

2.1 Preparation of Membrane Protein Fractions

This procedure is based primarily on a previously described method with some modifications [8].

1. Luria-Bertani (LB) broth: 1 % tryptone, 0.5 % yeast extract, 1 % NaCl (pH 7.0).
2. Phosphate-buffered saline (PBS) tablet (MP Biomedicals, Solon, OH, USA).
3. Protease inhibitor cocktail (Roche, Indianapolis, IN, USA).
4. PBS containing 2 % Triton X-100.
5. SDS sample buffer (2×): 20 % glycerol, 125 mM Tris–HCl, pH 6.8, 4 % SDS, and 0.01 mg/ml of bromophenol blue. Add 2-mercaptoethanol to 10 % volume in this buffer before use (the final concentration of 2-mercaptoethanol in the 1× SDS sample buffer is 5 %).
6. 10 % SDS-polyacrylamide resolving gel (10 ml): 2.5 ml of 40 % acrylamide/bis-acrylamide solution, 2.5 ml of 1.5 M Tris–HCl, pH 8.8, 0.1 ml of 10 % SDS, 0.1 ml of 10 % ammonium persulfate (APS), 0.01 ml of *N,N,N',N'*-tetramethylmethylenediamine (TEMED) and distilled water to a volume of 10 ml. Mix well and pour this gel solution in the gel cassette, allowing space for a stacking gel.
7. 5 % Stacking gel (5 ml): 0.625 ml of 40 % acrylamide/bis-acrylamide solution, 0.625 ml of 1 M Tris–HCl, pH 6.8, 0.025 ml of 10 % SDS, 0.025 ml of 10 % APS, 0.005 ml of TEMED and distilled water to a final volume of 5 ml. When the polymerization of resolving gel is completed, pour the stacking gel solution and insert a gel comb immediately.
8. Running buffer (pH 8.3): 25 mM Tris base, 192 mM glycine, 0.1 % SDS in distilled water.
9. Staining buffer: 0.25 % Coomassie Brilliant Blue R-250, 40 % methanol, 7 % acetic acid, in distilled water. Mix all reagents and pass the solution through a paper filter.
10. Destaining buffer: 0.75 % acetic acid, 0.5 % methanol in distilled water.

2.2 Electron Microscopy

1. 2 % glutaraldehyde buffer: 2 % glutaraldehyde, 0.02 M sodium cacodylate, 0.6 % NaCl, and 0.02 % ruthenium red in 0.1 M phosphate buffer (pH 7.4). Store at 4 °C.
2. 1.5 % osmium tetroxide buffer: 1.5 % osmium tetroxide, 0.02 M sodium cacodylate, and 0.6 % NaCl.
3. Quetol 653 (Nissin EM, Tokyo, Japan).
4. Quetol 653 mixture: mix quetol 653 and propylene oxide (6:4, v/v).
5. Uranyl acetate buffer (pH 4.5): 6 % uranyl acetate and 0.4 % citrate buffer.

2.3 Immunogold Staining

1. LR-Gold resin (Nissin EM).
2. QCU-3 (Nissin EM).
3. Primary antibody solution: Add murine anti-OmpA antibody in blocking buffer before use (see Note 1).
4. Secondary antibody solution: Add goat anti-mouse IgG (10 nm diameter of conjugated gold particle; BBI Solutions, Cardiff, UK) in blocking buffer before use (see Note 2).
5. Blocking buffer: 5 % skim milk, 0.01 % Tween 20 in 0.02 M phosphate buffer (pH 7.4).
6. Washing buffer: 5 % Blocking One (Nacalai tesque, Kyoto, Japan), 0.01 % Tween 20 in 0.02 M phosphate buffer (pH 7.4).
7. Reynold's lead citrate solution (50 ml): Dissolve 1.33 g of lead nitrate and 1.76 g of sodium citrate in distilled water. Add 8 ml of 1 M NaOH and adjust to 50 ml with distilled water.
8. 6 % uranyl acetate: Dissolve 6 g of uranyl acetate in 100 ml methanol.

2.4 Preparation of Recombinant Stn Protein

1. illustra bacteria genomicPrep Mini Spin Kit (GE Healthcare, Buckinghamshire, UK).
2. *Bam*HI and *Sal*II (TaKaRa Bio, Shiga, Japan).
3. pCold TF (Takara Bio).
4. *Escherichia coli* BL21(DE3) (Merck, Darmstadt, Germany).
5. Ni Sepharose High Performance (GE Healthcare).
6. Binding buffer No. 1 (pH 7.4): 20 mM sodium phosphate, 0.5 M NaCl, 20 mM imidazole (see Note 3).
7. Elution buffer No. 1 (pH 7.4): 20 mM sodium phosphate, 0.5 M NaCl, 0.5 M imidazole (see Note 3).

2.5 Preparation of Recombinant OmpA Protein

1. pQE30 (QIAGEN, Hilden, Germany).
2. *Sph*I and *Hind*III (Takara Bio).
3. *E. coli* M15[pREP4] (QIAGEN).

4. Binding buffer No. 2 (pH 7.4): 20 mM sodium phosphate, 40 mM imidazole, 0.5 M NaCl, pH 7.4 (see Note 3).
5. Elution buffer No. 2 (pH 7.4): 20 mM sodium phosphate, 40 mM imidazole, 0.5 M NaCl, 0.5 M imidazole (see Note 3).

2.6 Far-Western Blotting

1. PVDF membranes: Immobilon-P (Millipore, Billerica, MA, USA).
2. Blotting buffer: 25 mM tris(hydroxymethyl)aminomethane, 192 mM glycine, 0.1 % SDS, 20 % methanol.
3. TBST: 10 mM Tris-HCl, pH 7.5, 150 mM NaCl, 0.05 % Tween-20.
4. TBST containing 6 M guanidine-HCl (pH 7.5): Dissolve guanidine in TBST and adjust pH to 7.5 with HCl (see Note 4).
5. Blocking solution: Dissolve 5 % skim milk in TBST.
6. Probe solution: Add 10 µg of purified recombinant Stn protein in blocking solution.
7. Anti-TF monoclonal antibody (TaKaRa Bio).
8. First antibody solution: Add 5 µg of anti-TF monoclonal antibody in 5 ml of blocking solution (see Note 5).
9. Goat anti-mouse IgG antibody (HRP-conjugated; Santa Cruz, CA, USA).
10. Second antibody solution: Add 0.5 µg of anti-mouse IgG antibody in 5 ml of blocking solution (see Note 5).
11. ECL Prime Western Blotting Detection Reagent (GE Healthcare).

3 Methods

3.1 Preparation of Membrane Protein Fraction

1. Culture *Salmonella* in 2 ml of LB broth at 37 °C for 16 h with shaking.
2. Harvest bacteria by centrifugation (1,000×*g*, 10 min at room temperature) and remove the supernatant carefully using a pipette (see Note 6). To remove the bacterial debris, wash bacteria once with 1 ml of PBS and centrifuge again. Remove the supernatant completely using a pipette and resuspend the pellet in 1 ml of PBS. Adjust cell density of the suspension to OD₆₀₀ = 1.0 with PBS using a spectrophotometer.
3. Add 300 µl of bacterial suspension in 30 ml of LB medium and incubate at 37 °C with shaking (120–150 rpm) until bacteria are in log-phase (OD₆₀₀ = 1.0) or stationary phase (see Note 7). Harvest bacteria by centrifugation (16,100×*g*, 20 min at 4 °C) and discard the supernatant. Resuspend the pellet in 1 ml ice-cold PBS containing protease inhibitor cocktail and incubate on ice for 10 min.

4. Disrupt bacteria by sonication on ice (six cycles of 10 s with 1 min break) and remove the unbroken cells by centrifugation ($2,000 \times g$, 10 min at 4 °C) (see Note 8).
5. Transfer the supernatant carefully and centrifuge again ($16,100 \times g$, 30 min at 4 °C). Discard the supernatant and dissolve the pellet in 1 ml PBS containing 2 % Triton X-100.
6. Incubate at 37 °C for 30 min and centrifuge ($16,100 \times g$, 30 min at room temperature) to recover the insoluble protein fraction. After centrifugation, discard the supernatant and wash the pellet with 1 ml PBS followed by centrifugation ($16,100 \times g$, 5 min at room temperature). Remove the supernatant and dissolve the pellet in 100–300 µl PBS.
7. Mix with prepared membrane protein fraction (3–5 µg/tube) and SDS sample buffer. Heat at 100 °C for 5 min and centrifuge the heated samples at $5,000 \times g$ for 10 s. Load the samples on a 10 % gel and run the gel in the running buffer until the loading dye runs to the bottom of the gel. Excise the gel from the gel cassette and stain the gel using Coomassie Brilliant Blue for 20–30 min with gentle shaking. Then, rinse the gel with destaining buffer until the protein bands are seen clearly (Fig. 1).

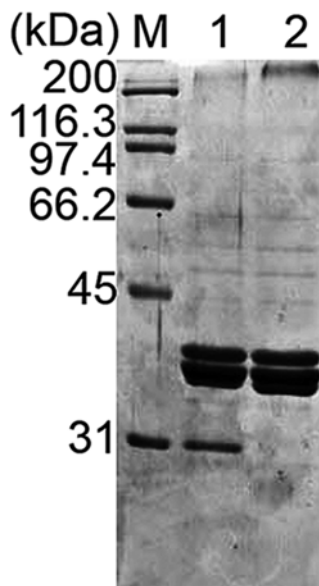


Fig. 1 SDS-PAGE of the membrane protein fraction. Membrane protein fractions were prepared as described in Subheading 3.1. Proteins (5 µg/lane) were loaded on a 10 % gel and the gel was stained with Coomassie Brilliant Blue. In this study, we constructed a *stn* gene-deleted *Salmonella* strain (lane 2) by homologous recombination [4] and this mutant strain was used as a reference strain and compared with wild-type *Salmonella*. M, protein marker; lane 1, wild-type *Salmonella*; lane 2, *stn* gene-deleted *Salmonella* (this figure was reproduced from [4] with permission from Company of Biologists)

3.2 Examination of *Salmonella* Morphology by Electron Microscopy

1. Culture bacteria in 10 ml of LB medium at 37 °C for 16 h with shaking. Harvest bacteria by centrifugation (300×*g*, 10 min at 4 °C) and discard the supernatant carefully (see Note 6).
2. Keep bacteria at 4 °C for 10 min and add 2 ml of 2 % glutaraldehyde buffer very slowly. Incubate at 4 °C for 2 h and remove the supernatant by a pipette. Add 1 ml of 1.5 % osmium tetroxide buffer very slowly and incubate at 4 °C for 1.5 h.
3. Remove osmium tetroxide buffer carefully and wash once with 0.02 M sodium cacodylate. Dehydrate bacteria in graded ethanol series (50, 70, 80, 90, and 100 % at 4 °C for 1 h per each). Then, dehydrate in acetone at room temperature for 60 min and saturate the bacterial cells in propylene oxide for 20 min (see Note 9).
4. Dehydrated specimens are saturated in quetol 653 mixture for 16 h and then remove propylene oxide by placing in the desiccator for 2 days. Embed the specimens in quetol 653 and polymerize the resins by an Ultraviolet Polymerizer (Dosaka EM, Kyoto, Japan) at 37 °C for 2 h followed by incubation at 60 °C for 2 days.
5. Sections were prepared with an Ultramicrotome (80 nm thick; Leica EM UC6, Leica Microsystems, Wetzlar, Germany). Double staining is performed using uranyl acetate buffer for 30 min and then lead citrate for 15 min respectively. Specimens are imaged by JEM-1230 electron microscope at 80 kV (JEOL, Tokyo, Japan) (Fig. 2).

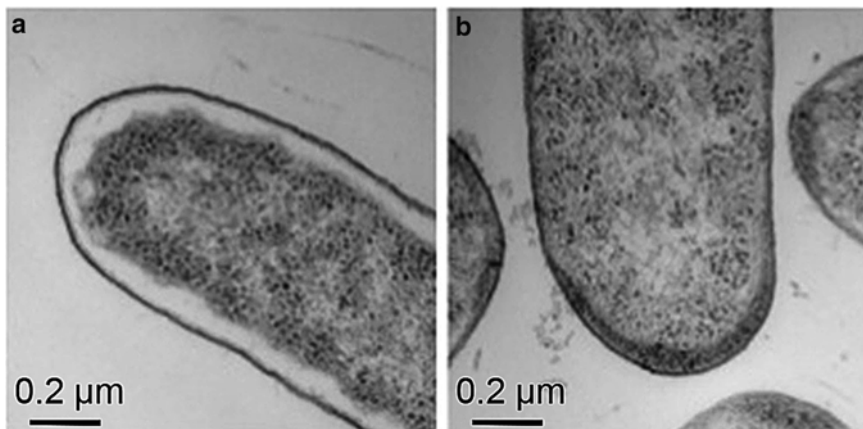


Fig. 2 Transmission electron microscopic analysis of *Salmonella* strains. Each of the pictures is imaged as a representative example of *Salmonella* morphology in ultrathin sections (magnification: 12,000×). **(a)** wild-type *Salmonella*; **(b)** *stn* gene-deleted *Salmonella* (this figure was reproduced from [4] with permission from Company of Biologists)

3.3 Immunogold Stain

1. Culture bacteria on a LB agar plate at 37 °C for 16 h. Mount bacteria from the agar plate on an anoxic copper sheet and fix bacteria using 0.2 % glutaraldehyde at -80 °C [9]. Dehydrate bacteria in ice-cold acetone for 2 days and warm up gradually to room temperature. Strip bacteria from the copper sheet and put into acetone for 40 min at room temperature with gentle shaking.
2. Saturate dehydrated bacteria into a solution of LR-Gold resin containing 3 % QCU-3 and acetone (7:3, v/v) at 20 °C for 24 h with gentle shaking in the dark room and then dry the samples with an evaporator (oil-sealed rotary vacuum pump, ULVAC Kiko, Miyazaki, Japan) for 2 days. Saturate samples in LR-Gold resin containing 3 % QCU-3 at 20 °C for 2 days with gentle shaking in the dark room (see Note 10). Replace segments in fresh LR-Gold resin containing 3 % QCU-3 and polymerize the resins using an Ultraviolet Polymerizer at 4 °C for 4 days.
3. The sections are prepared using an Ultramicrotome (90 nm thick).
4. Immerse the sections in blocking buffer and incubate at 37 °C (or room temperature) for 40 min. Rinse the sections for 30 s with washing buffer and immerse in primary antibody solution. Incubate at 4 °C overnight (ca. 16–18 h) (see Note 11).
5. Rinse the sections carefully four times using washing buffer and incubate in secondary antibody solution at room temperature for 1 h. Remove excess antibody and wash the sections twice with washing buffer. To remove skim milk from the sections, rinse three times with distilled water.
6. Incubate the sections in 1 % osmic acid at room temperature for 3 min and rinse three times with distilled water. Incubate the sections in 6 % uranyl acetate at room temperature for 2 min and rinse twice with distilled water. Stain the sections using Reynold's lead citrate solution [10] at room temperature for 2 min and rinse twice with distilled water.
7. Carry out carbon deposition on the sections using a vacuum evaporator (15 nm thick; JEOL). Specimens are imaged by a JEM-1230 electron microscope at 80 kV (Fig. 3).

3.4 Preparation of Recombinant Stn Protein

1. Culture *Salmonella* in 2 ml of LB medium at 37 °C for 16 h with shaking (150 rpm) and purify genomic DNA using illu-trabacteria genomicPrep Mini Spin Kit according to the manufacturer's instruction.
2. Amplify the *stn* gene by PCR using primers stn-F (5'-GGATC CTTGTTAACCTGTTGTCG-3') and stn-R (5'-GTCGA CTTACTGGCGTTTTGGCA-3') [4]. Digest DNA using

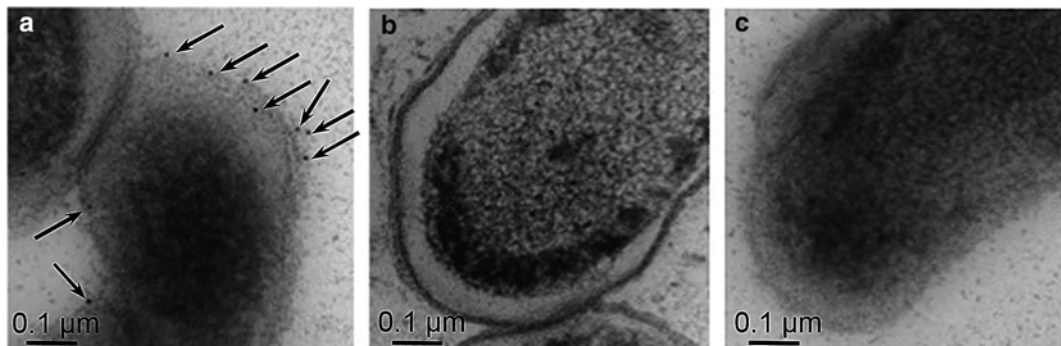


Fig. 3 Immunogold labeling of OmpA using anti-OmpA antibody. This analysis was performed using murine anti-OmpA antibody as a primary antibody and goat anti-mouse IgG antibody conjugated with gold particles as a secondary antibody respectively (magnification: 20,000 \times). Arrows indicate the gold particles bound to OmpA protein. These data show the location of OmpA protein. (a) wild-type *Salmonella*; (b) *stn* gene-deleted *Salmonella*; (c), wild-type *Salmonella* using normal mouse serum for control reaction (this figure was reproduced from [4] with permission from Company of Biologists)

*Bam*HI and *Sal*II according to the manufacturer's instructions: PCR product is then cloned into *Bam*HI and *Sal*II sites of pCold TF (see Note 12). Introduce the modified plasmid into *Escherichia coli* BL21(DE3) according to the manufacturer's instructions (see Note 13).

3. Culture *E. coli* strain containing the plasmid in 30 ml of LB medium supplemented with 50 μ g/ml ampicillin and 1 % glucose at 30 °C until cell density is OD₆₀₀ = 0.6.
4. Incubate the culture at 15 °C for 30 min immediately without shaking and then add isopropyl β -D-1-thiogalactopyranoside (IPTG; final concentration at 0.5 mM). Incubate further at 15 °C for 20–24 h with shaking (see Note 14).
5. Harvest bacteria by centrifugation (20,000 \times g, 20 min, 4 °C) and remove the supernatant completely. Keep the bacteria at -20 °C until use.
6. Dissolve the pellet in 10 ml of cold binding buffer No. 1 containing protease inhibitor cocktail and incubate on ice. Disrupt the bacterial cells by sonication (six cycles of 20 s with a 3 min break on ice) (see Note 8).
7. Harvest unbroken bacteria and bacterial debris by centrifugation (20,000 \times g, 20 min, 4 °C) and transfer the supernatant with a pipette. To remove unbroken cells, pass the supernatant through a syringe filter (0.45 μ m).
8. Add 1 ml of Ni Sepharose High Performance in the cell lysate and incubate at 4 °C for 15 h with vigorous shaking (see Note 15). Pour the slurry down in the empty column (0.8 \times 4 cm; Bio-Rad, Hercules, CA, USA) and wash the resin with 30 ml

of binding buffer No. 1. Elute recombinant proteins in 2 ml of elution buffer No. 1.

9. Verify the contents of the eluted sample by SDS-PAGE (see Note 16).

3.5 Preparation of Recombinant OmpA Protein

1. Amplify the *ompA* gene by PCR using primers omp-F (5'-CG CATGCGCTCCGAAAGATAACAC-3') and omp-R (5'-TAA GCTTTAAGCCTGCGGCTGAGTTAC-3') [4]. Digest DNA using *Sph*I and *Hind*III according to the manufacturer's instructions. PCR product is then cloned into *Sph*I and *Hind*III sites of pQE30 (see Note 12). Introduce the plasmid construct into *E. coli* M15[pREP4] according to the manufacturer's instructions.
2. Culture the bacteria in 100 ml of LB medium supplemented with 100 µg/ml ampicillin, 25 µg/ml kanamycin, and 1 % glucose at 25 °C until bacteria reach an OD₆₀₀ = 0.6. Add IPTG (final concentration: 1 mM) and incubate further at 25 °C for 20 h with shaking (150 rpm).
3. Harvest bacteria by centrifugation (5,000×*g*, 20 min, room temperature) and discard the supernatant. Wash the pellet once with 5 ml of PBS and centrifuge again. Discard the supernatant and keep the pellet at -20 °C until use.
4. Resuspend the pellet in 10 ml of binding buffer No. 2 containing 4 M urea and protease inhibitor cocktail and incubate on ice. Disrupt the bacteria by sonication (six cycles of 20 s with 3 min break on ice) and centrifuge (20,000×*g*, 20 min, 4 °C) (see Note 8). To remove the unbroken cells and debris, pass the supernatant through a syringe filter (0.45 µm).
5. Pack the Ni Sepharose High Performance resin into an empty column and apply the sample to the column (see Note 17). Wash the column with binding buffer No. 2 containing 4 M urea by gravity flow (10 column volumes×2) and elute recombinant OmpA protein with elution buffer No. 2 containing 4 M urea (1 ml×5 tubes). Verify the contents of the eluted protein by SDS-PAGE.
6. Dialyze the samples with elution buffer No. 2 containing 2 M urea for 4 h at 4 °C and replace with elution buffer No. 2 containing 1 M urea for 4 h. Then, dialyze with elution buffer No. 2 and finally replace with binding buffer No. 2. Transfer the samples to a new tube and centrifuge (20,000×*g*, 10 min, 4 °C). Transfer the supernatant and store at 4 °C until used.

3.6 Interaction Between Stn and OmpA Analyzed by Far-Western Blotting

1. Load OmpA protein (1 µg/lane) on a 10 % gel and run the gel at 20 mA until loading dye runs to the bottom of gel.
2. Excise the gel from the gel cassette and transfer the proteins to a PVDF membrane in blotting buffer using mini transblot electrophoretic transfer cell (Bio-Rad) at 100 V for 1 h according to the manufacturer's instruction.

3. After blotting is completed, put the membrane in a tray and wash once with TBST for 1 min at room temperature. Discard the buffer and add TBST containing 6 M guanidine-HCl. Incubate at room temperature for 20 min with vigorous shaking (*see Note 18*). Then, wash in TBST containing 3 M guanidine-HCl for 5 min; then in TBST containing 1.5 M guanidine-HCl for 5 min; in TBST containing 0.75 M guanidine-HCl for 5 min; in TBST containing 0.375 M guanidine-HCl for 5 min; and then in TBST containing 0.1875 M guanidine-HCl for 5 min at room temperature (*see Note 4*). Finally, wash the membrane in TBST for 5 min at room temperature.
4. Put the membrane in blocking solution for 1 h at room temperature with vigorous shaking. Wash the membrane twice with TBST for 5 min and soak in probe solution. Incubate at 4 °C for 16 h with vigorous shaking and wash the membrane three times with TBST for 10 min at room temperature.
5. Soak the membrane in first antibody solution and incubate at 4 °C for 16 h. Wash the membrane with three changes of TBST for 10 min at room temperature and soak in second antibody solution followed by incubation for 1 h at room temperature (*see Note 11*).
6. Wash the membrane with three times changes of TBST for 10 min at room temperature. Drain excess TBST from the washed membrane and place it on a sheet of plastic wrap. Add ECL Prime Western Blotting Detection Reagent to the membrane and incubate for 3 min at room temperature. Drain excess detection reagent and detect the signals using FUJIFILM Luminescent Image Analyzer LAS-1000plus (Fujifilm, Tokyo, Japan) (Fig. 4).

4 Notes

1. We prepared murine polyclonal anti-OmpA antibody for this study. It is important to verify the appropriate concentration or volume of antibody.
2. Several types of gold particles are available from different companies. You should verify which is more suitable for your work.
3. Pass this buffer through a filter to remove debris and then store at 4 °C.
4. All other TBST containing guanidine-HCl buffers are adjusted to pH 7.5.
5. Prepare this solution just before use to maintain the quality of antibody.
6. This bacterial pellet is unstable. It is important to not disturb the pellet when you remove the supernatant.

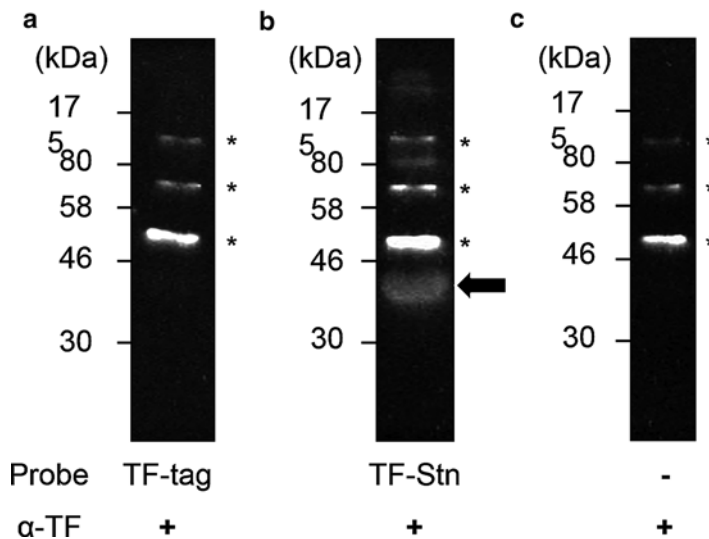


Fig. 4 Interaction between Stn and OmpA. Recombinant OmpA protein was separated by SDS-PAGE and far-western blotting was performed using recombinant Stn protein as a probe (TF-Stn; panel **b**). TF-tag fragment was used as a probe for the negative control (**a**) and this fragment was purified in the same manner as Stn protein using an empty pCold-TF plasmid. Panel (**c**) was carried out as a control reaction for the verification of the quality of anti-TF antibody. Arrow indicates the specific signal for the Stn-OmpA complex and asterisks represent the nonspecific signals with anti-TF antibody. TF, trigger factor-tag (this figure was reproduced from [4] with permission from Company of Biologists)

7. In general, *Salmonella* strains grow rapidly in LB medium at 37 °C and therefore *Salmonella* in the log-phase state passes quickly to the next cell phase. Check the concentrations of *Salmonella* by a spectrophotometer at OD₆₀₀.
8. When you operate the sonication machine, place the samples on ice to prevent an elevation in temperature.
9. When you use this chemical, you should work in the fume hood.
10. Remove the supernatant with a pipette since this bacterial pellet is very unstable.
11. The optimal experimental conditions should be determined to reduce unexpected signals.
12. After cloning of the target gene into the plasmid, confirm the entire DNA sequence of the cloned gene by sequence analysis.
13. Many recombinant expression systems using *E. coli* strain have been available.
14. Cold shock is essential for expression of recombinant protein using pCold TF.

15. Prepare the resin before use according to the manufacturer's manual. This step is carried out to increase the binding ability of recombinant Stn proteins to the resin. If you notice that many unexpected proteins are present in the final eluted fraction, the incubation time should be reduced.
16. Eluted samples must be kept at 4 °C until used. We attempted to digest the recombinant Stn protein by protease to remove the tag fragment, but digested Stn proteins were precipitated in the reaction and therefore we could not obtain a soluble form of digested Stn proteins.
17. Before using the resin, it should be prepared according to the manufacturer's instructions.
18. The incubation time is critical since proteins are denatured readily in the presence of 6 M gunanidine.

Acknowledgement

This work was supported by the Global Center of Excellence Program on Integrated Global Control Strategy for the Tropical and Emerging Infectious Diseases from the Ministry of Education, Culture, Sports, Science and Technology of Japan. JM was supported by the Intramural Research Program, National Institutes of Health, National Heart, Lung, and Blood Institute.

References

1. Grassl G, Finlay BB (2008) Pathogenesis of enteric *Salmonella* infections. *Curr Opin Gastroenterol* 24:22–26
2. Chopra AK, Peterson JW, Chart P et al (1994) Molecular characterization of an enterotoxin from *Salmonella typhimurium*. *Microb Pathog* 16:85–98
3. Chopra AK, Huang JH, Xu X et al (1999) Role of *Salmonella* enterotoxin in overall virulence of the organism. *Microb Pathog* 27:155–171
4. Nakano M, Yamasaki E, Ichinose A et al (2012) *Salmonella* enterotoxin (Stn) regulates membrane composition and integrity. *Dis Model Mech* 5:515–521
5. Lindgren SW, Stojiljkovic I, Heffron F (1996) Macrophage killing is an essential virulence mechanism of *Salmonella typhimurium*. *Proc Natl Acad Sci U S A* 93:4197–4201
6. Watson PR, Galyov EE, Paulin SM et al (1998) Mutation of *invH*, but not *stn*, reduces *Salmonella*-induced enteritis in cattle. *Infect Immun* 66:1432–1438
7. Wallis TS, Wood M, Watson P et al (1999) Sips, Sops, and SPIs but not *stn* influence *Salmonella* enteropathogenesis. *Adv Exp Med Biol* 473:275–280
8. Sittka A, Pfeiffer V, Tedin K et al (2007) The RNA chaperone Hfq is essential for the virulence of *Salmonella typhimurium*. *Mol Microbiol* 63:193–217
9. Ichinose A, Watanabe K, Senba M et al (2011) Demonstration of pneumococcal capsule under immunoelectron microscopy. *Acta Med Nagasaki* 56:1–4
10. Reynold ES (1963) The use of lead citrate at high pH as an electron-opaque stain in electron microscopy. *J Cell Biol* 17:208–212

Chapter 10

Development of a Bacterial Nanoparticle Vaccine

Carlos Gamazo, Javier Ochoa-Repáraz, Ibai Tamayo, Ana Camacho, and Juan M. Irache

Abstract

A simple procedure for obtaining protective antigens from Gram-negative bacteria and their encapsulation into immunomodulatory nanoparticles is described. A heat treatment in saline solution of whole bacteria rendered the release of small membrane vesicles containing outer membrane components and also superficial appendages, such as fractions of fimbriae and flagella. The immunogenicity of these antigens may be improved after encapsulation into poly(anhydride) nanoparticles made from the copolymer of methyl vinyl ether and maleic anhydride (Gantrez AN®).

Key words Nanoparticles, Outer membrane, OMV, Gram-negative bacteria, Vaccine, Acellular vaccine, *Salmonella*

1 Introduction

Subcellular vaccines containing immunodominant bacterial antigens are pushing as the right vaccinal choice [1]. The primary goal of this approach is to identify and purify single protective antigens from pathogens avoiding the selection of immunosuppressive and tolerogenic pathogenic components. The understanding of pathogenesis and current advances in genomics and proteomics are facilitating the identification of specific antigens from most known pathogens that could be essential in inducing appropriate protective immune responses. Several procedures are available in order to obtain crude extracts or purified antigenic complexes from pathogens. In the particular case of gram-negative bacteria, the most relevant antigens characterized thus far are structural components of the outer membrane (OM). Fragments of the outer membrane spontaneously bleb to the external milieu as vesicles (OMVs) [2]. It has been suggested that these OVM are used by gut bacteria such as *Escherichia coli* and *Salmonella* strains as signal delivery mechanism that facilitate host–microbe interactions in the gut [3, 4]. Moreover, OVM from resident bacteria have been proposed as

essential regulators of gut immune homeostasis. For instance, *Bacteroides fragilis* releases the immunomodulator polysaccharide A within OMV that are recognized by dendritic cells through toll-like receptor-2 and induce protective responses against experimental colitis in mice [5]. These OMV can be easily recovered during in vitro culture [5]. Moreover, the release of OMV can be forced by treating the cells with heat under saline conditions [6, 7]. As a result of both spontaneous and enforced release, vesicles enriched in the major bacterial surface antigens can be obtained.

The immunogenicity and bioavailability of these antigens may be enhanced with adjuvants and/or a delivery system [8]. Nanoparticles are submicron-sized delivery systems that may protect antigens from chemical degradation in the gastrointestinal tract, and facilitate targeting and their presentation to relevant immune cells in inductive sites of the mucosal immune system [9]. Their basic colloidal properties, degradation, and thus the release of the antigen(s) depend on the polymer composition utilized for their formulation. These nanoparticle delivery systems have been proposed to improve the mucosal bioavailability of antigens allowing a single dose. Herein, we describe a simple procedure for the preparation of a nanoparticle-based vaccine containing membrane vesicles isolated from pathogenic strains of *Salmonella enterica* as a model

2 Materials

All solutions are prepared using ultrapure water and analytical grade reagents. Reagents are stored at room temperature (unless indicated otherwise). All chemical reagents were purchased from Sigma-Aldrich Company (St. Louis, MO, USA), unless indicated otherwise. Final products are lyophilized and stored at room temperature.

2.1 Bacterial Growth and Antigen Extraction

1. *Salmonella enterica* serovar. Enteritidis growth: Trypticase-soy broth (Biomérieux, SA, Marcy l'Etoile, France) on a rotatory shaker at 37 °C.
2. Saline isotonic solution: 150 mM NaCl in water.
3. Membrane-based Tangential Flow Filtration (TTF): 300-kDa size-pore tangential filtration concentration unit (EMD Millipore, Billerica, MA USA).

2.2 Protein and Lipopolysaccharide Content Determination

1. Protein content determination by Lowry method:
 - (a) Dilution buffer: 0.4 % CuSO₄·5H₂O, 0.4 % NaOH, 2 % Na₂CO₃, 0.16 % sodium tartrate and 1 % sodium dodecyl sulfate (SDS).

- (b) Folin-Phenol reactive (Panreac Química SL, Barcelona, Spain): 50 % reactive in water.
- (c) Standard curve: Bovine serum albumin.
- 2. Protein content determination by microbicinchoninic acid (microBCA) protein assay kit (Pierce, Rockford, CA, USA).
- 3. Lipopolysaccharide (LPS) content by determination of 2-keto-3-deoxyoctonate (kdo) content:
 - (a) Oxidation buffer: 0.042 N Periodic acid in 1.25 N H₂SO₄.
 - (b) Stop reactive: 2 % Sodium arsenite in 0.5 N HCl.
 - (c) Kdo detection buffer: 0.3 % Thiobarbituric acid in water and dimethylsulfoxide (DMSO).
 - (d) Standard curves: pure kdo and D-deoxiribose.

2.3 SDS **Polyacrylamide Gel** **Components**

- 1. 15%acrylamide-Bis-acrylamide (37.5:1) (Bio-Rad Laboratories, Hercules, CA) in 125 mM Tris-HCl, pH 6.8 adjusted with HCl.
- 2. Electrode buffer: 30 mM Tris-HCl pH 8.3, adjusted with HCl, 192 mM glycine and 0.1 % SDS.
- 3. SDS-PAGE running buffer: 30 mM Tris-HCl, pH 8.3, 192 mM glycine, 0.1 % SDS.
- 4. SDS lysis buffer: 62.5 mM Tris-HCl pH 6.8, 10 % glycerol, 2 % SDS, 5 % β-mercaptoethanol, and 0.002 % bromophenol blue. Store the aliquots at -20 °C.
- 5. Periodate-silver staining buffer:
 - (a) Fixation buffers: 50 % methanol and 10 % acetic acid in water, 7.5 % methanol and 5 % acetic acid.
 - (b) Oxidation buffer: for protein staining protocol, 10 % glutaraldehyde in water. For the LPS staining protocol the samples are pretreated with 0.7 % paraperiodic acid 7.5 % methanol, and 5 % acetic acid in water.
 - (c) Staining buffer: 4 % AgNO₃, 0.75 % NaOH and 1.4 % NH₃ in water.
- 6. Comassie blue staining:
 - (a) Incubation buffer: 3 % Trichloroacetic acid in water.
 - (b) Staining buffer: 0.25 % Coomassie blue (Thermo Fisher Scientific, Rockford, IL, USA) in 50 % methanol and 10 % acetic acid in water.
- 7. SDS-PAGE staining molecular mass standard: Rainbow RPN756 (GE Healthcare Bio-Science, Pittsburg, PA, USA) containing myosin (220 kDa), phosphorylase B (97 kDa), bovine serum albumin (66 kDa), ovalbumin (45 kDa), carbonic anhydrase (30 kDa), trypsin inhibitor (20.1 kDa) and lysozyme (14.3 kDa).

2.4 Immunoblotting Components

1. Transfer buffer: 0.2 M glycine; 24 mM Tris-HCl 10 % methanol (pH 8.3) in water. Store at 4 °C.
2. Nitrocellulose membrane: (Gelman Sciences-Fisher Scientific, Dallas, TX, USA).
3. Semidry electroblotter (Bio-Rad Laboratories, Richmond, CA, USA).
4. Blocking buffer (5 % skimmed milk in 10 mM phosphate-buffered saline (pH 7.4)).
5. Antibody dilution buffer (1 % skimmed milk with 0.15 % Tween-20 in 10 mM phosphate-buffered saline (pH 7.4)).
6. Incubation solution: H₂O₂, 4-chloro, 1-naphthol.

2.5 Nanoparticle Formulation

1. Polymer solution: copolymer of methyl vinyl ether and maleic anhydride (PVM/MA) (Gantrez®AN 119; M.W. 200 kDa; Ashland Inc. Covington, KY, USA) in acetone.
2. Cryoprotectant: 5 % sucrose in water.

2.6 Nanoparticle Characterization

1. Particle size and zeta potential of using a Zetamaster analyzer system (Malvern Instruments Ltd., Worcestershire, UK).
2. Zeta potential solution: 0.1 mM KCl solution in water adjusted to pH 7.4 with HCl.
3. Loading capacity buffer: 0.1 N NaOH in water. Nanoparticle disruption done using the Misonix Microson™ Ultrasonic cell disruptor (VWR International, Arlington Heights, IL, USA).
4. Büchi rotavapor R-144 (Büchi, Flawil, Switzerland) to remove the organic solvents.
5. Degradation of nanoparticles for the determination of the structural integrity and antigenicity of HE/OMVs using 2 mL of a mixed of dimethylformamide:acetone (1:3). Ultra Plus Field Emission Scanning Electron Microscope (Carl Zeiss, Hertfordshire, UK).
6. Electron microscopy staining: 4 % Uranyl acetate (Agar scientific, Essex, UK) and lead citrate (Agar scientific). Hitachi 1100 transmission electron microscope (Hitachi Scientific Instruments, Mountain View, CA, USA).

3 Methods

3.1 Bacterial Strain and Growth Conditions

In this example, the antigenic complex is obtained from *S. Enteritidis* grown in trypticase-soy broth on a rotary shaker at 37 °C for 24 h (other conditions may be applied).

3.2 Antigenic Extraction

3.2.1 Heat Saline Antigenic Extract (HE) (Fig. 1a)

Two different methods for antigen extraction are described below.

1. Grow bacteria in trypticase-soy broth on a rotary shaker at 37 °C for 24 h.
2. Harvest cell by centrifugation (12,000×*g*, 10 min).
3. Resuspend cells in saline solution (10 g of packed cells per 100 mL) and heat at 100 °C in flowing steam for 15 min. *See Note 1.*
4. Cells are pelleted by centrifugation at 12,000×*g*, for 15 min.
5. The supernatant containing the HE extract is dialyzed for 2 days at 4 °C against deionized water, with several changes of water per day.
6. Centrifuge the dialyzed material for 5 h at 100,000×*g*. *See Note 2.*
7. Resuspend the pellet (HE extract) in deionized water, lyophilize, and store at room temperature.

Alternatively, from **step 5**, the supernatant of cultured bacteria may be purified, dialyzed, and concentrated by diafiltration (300-kDa tangential filtration concentration unit (EMD Millipore)). The final product is recovered in the retentate fraction and collected by centrifugation at 40,000×*g*, for 2 h. The resulting pellet is finally resuspended in deionized water and lyophilize.

3.2.2 Outer Membrane Vesicles (OMVs) (Fig. 1b)

1. Grow bacteria in trypticase-soy broth on a rotary shaker at 37 °C for 24 h. *See Note 3.*
2. Remove the bacteria by centrifugation at 12,000×*g* for 15 min.

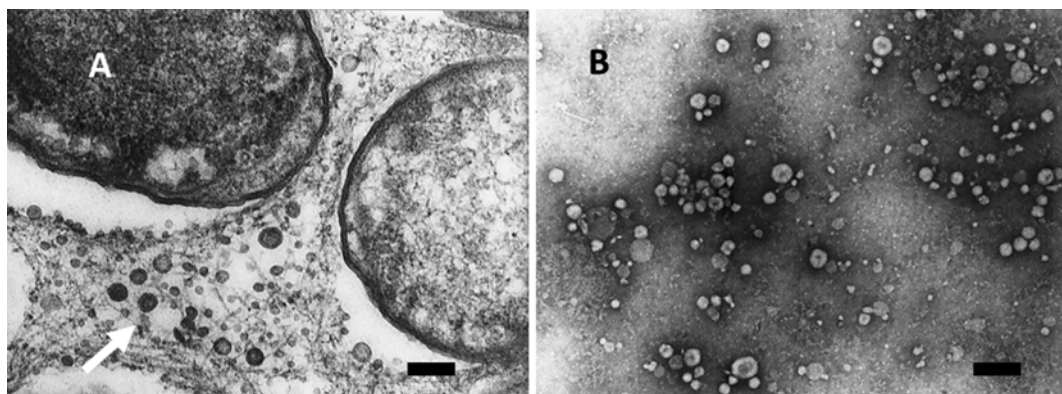


Fig. 1 Electron microscopy of OMVs (a) and HE (b) from *Salmonella enterica* serovar. Enteritidis. Electron micrographs were performed using positive stain of ultrathin sections (a) or negative staining (b). Panel (a) shows several OMVs naturally released from the bacteria. Panel (b) shows the vesicles released from bacteria after heat treatment (*see the text for more information*). The bars correspond to 200 nm

3. The supernatant containing OMVs is dialyzed for 2 days at 4 °C against deionized water, with several changes of water per day.
4. Centrifuge the dialyzed material for 5 h at 100,000×*g*. *See Note 2.*
5. Resuspend the pellet (OMV extract) in deionized water, lyophilize, and store at room temperature.

Alternatively, from **step 5**, the supernatant of cultured bacteria may be purified, dialyzed, and concentrated by diafiltration (300-kDa tangential filtration concentration unit (Millipore)). The final product is recovered in the retentate fraction and collected by centrifugation at 40,000×*g*, for 2 h. The resulting pellet is finally resuspended in deionized water and lyophilize.

3.3 Characterization of the Antigenic Extracts

1. Total protein content determination: Total protein content may be quantified by the method of Lowry [10], with bovine serum albumin as standard.
2. Lipopolysaccharide (LPS) content determination: LPS content may be quantified by the determination of 2-keto-3-deoxyoctonate (kdo) content, performed by the method of Warren [11] as modified by Osborn [12].
3. Dodecyl Sulfate Polyacrylamide Gel Electrophoresis (SDS-PAGE): Protein and LPS profiles may be determined by SDS-PAGE by the method of Laemmli [13] followed by staining with Coomassie blue [14] or with the alkaline silver-glutaraldehyde method for proteins [15], or for LPS [16].
4. Immunoblotting: The antigenicity of HE and OMV components may be analyzed by immunoblotting, carried out as described by Towbin [17] using an appropriate specific antiserum (*see Note 4*), with the following modifications:
 - (a) After SDS-PAGE, transfer the gel in a transfer buffer (0.2 M glycine; 24 mM Tris-HCl; 10 % methanol [pH 8.3]) to nitrocellulose by using a semidry electroblotter (Bio-Rad Laboratories) (200 mA; 5 V; 30 min).
 - (b) Place the membrane in blocking buffer (5 % skimmed milk in 10 mM phosphate-buffered saline [pH 7.4]) overnight at room temperature.
 - (c) Incubated for 4 h at room temperature with serum diluted 1:100 in primary buffer (1 % skimmed milk with 0.15 % Tween-20 in 10 mM phosphate-buffered saline [pH 7.4]).
 - (d) After 4 h, wash the membrane five times in blocking buffer without skimmed milk.

- (e) Incubate the membrane for 1 h at room temperature with the appropriate immuno-conjugate: peroxidase-conjugated diluted 1:1,000 in the antibody dilution buffer.
- (f) Repeat **step 4**.
- (g) Membrane is developed by incubation in a solution containing H_2O_2 and 4-chloro, 1-naphtol for 20 min in the dark.

3.4 Preparation and Characterization of Nanoparticles (Figs. 2 and 3)

Poly(anhydride) nanoparticles are prepared by a modification of the solvent displacement method [7, 18].

1. Dissolve 100 mg of the copolymer of methyl vinyl ether and maleic anhydride (PVM/MA) (Gantrez[®]AN 119; M.W. 200 kDa) in 4 mL acetone under magnetic stirring at room temperature.
2. On the other hand, disperse 4 mg of HE or OMVs by ultrasonication with the probe of the Misonix MicrosonTM cell disruptor in 1 mL acetone for 1 min.
3. This suspension is, then, added to the solution of the copolymer and the mixture is homogenized for 30 min at 25 °C by agitation.
4. Nanoparticles are produced by addition of 10 mL of an ethanol-water solution (1:1 by volume) in the acetone phase containing the copolymer and the antigen (Fig. 1)
5. Continue the agitation during 15 min (see **Note 5**).
6. Remove organic solvents under reduced pressure (Büchi rotavapor R-144).

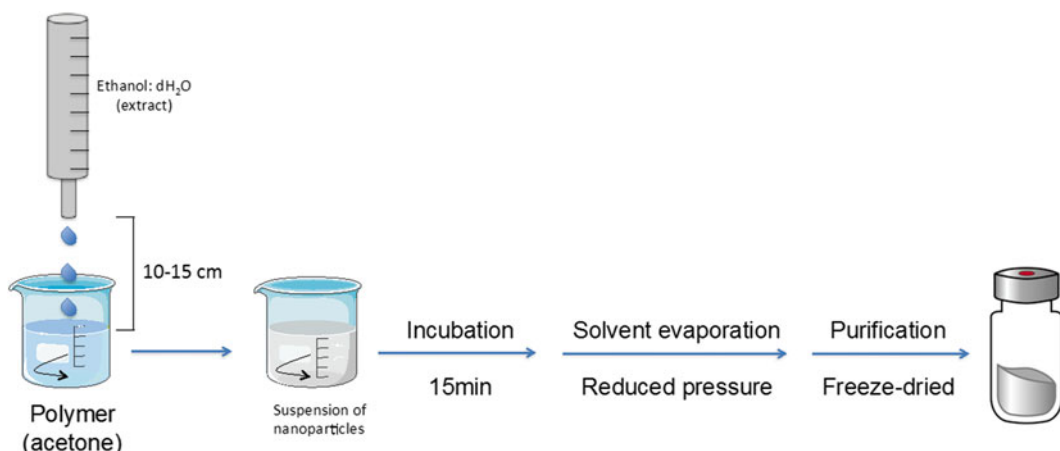


Fig. 2 Schematic representation of the preparative process of poly(anhydride) nanoparticles

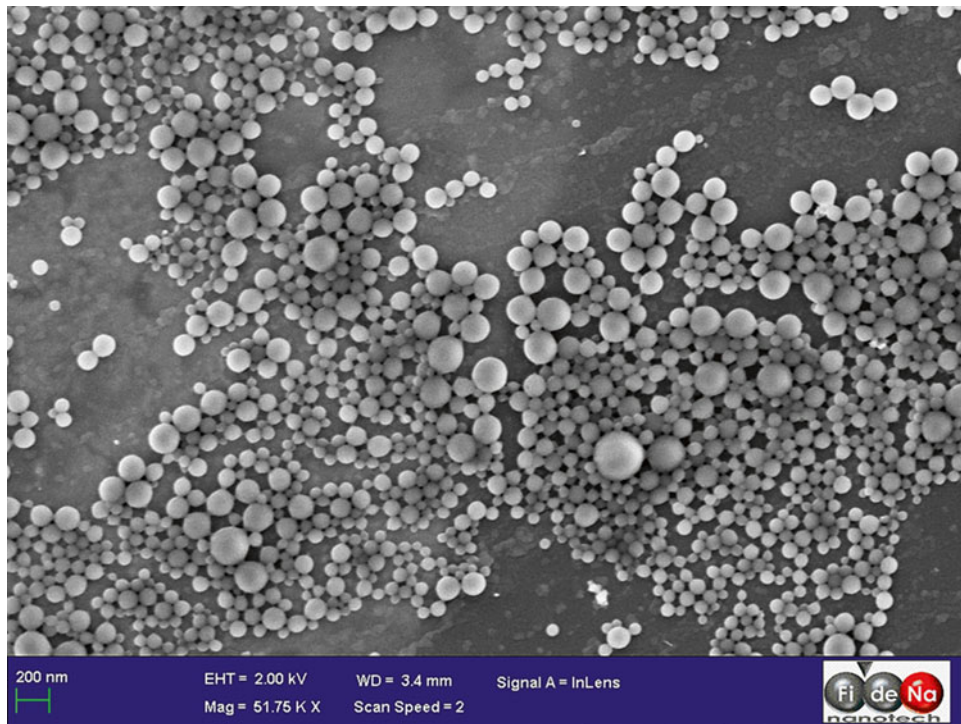


Fig. 3 Scanning electron microphotograph of poly(anhydride) nanoparticles containing the antigenic extract (HE) from *Salmonella Enteritidis*

7. Nanoparticles are centrifuged ($27,000 \times g$, 20 min, 4 °C) in order to eliminate the unloaded antigen and the residual copolymer.
8. The supernatants are collected and the pellet dispersed in water and centrifuged again.
9. The pellet is finally dispersed in an aqueous solution of sucrose 5 % w/v and, then, freeze-dried.
10. Empty nanoparticles may be produced in the same way but in the absence of HE or OMVs.

3.5 Characterization of Nanoparticles

The particle size and the zeta potential of nanoparticles may be determined by photon correlation spectroscopy (PCS) and electrophoretic laser doppler anemometry, respectively, using a Zetamaster analyzer system (Malvern Instruments Ltd.).

1. The diameter of the nanoparticles is determined after dispersion in ultrapure water and measured at 25 °C by dynamic light scattering angle of 90°.
2. The zeta potential is determined as follows: 200 µL of the samples is diluted in 2 mL of a 0.1 mM KCl solution adjusted to pH 7.4.

3. The morphology of the vesicles may be examined by Field Emission Scanning Electron Microscope (Carl Zeiss, model Ultra Plus). For this purpose freeze-dried formulations are resuspended in ultrapure water and centrifuged at $27,000 \times g$ for 20 min at 4 °C. Then, obtained pellets containing nanoparticles are mounted on TEM grids.
4. The yield of the nanoparticles preparation process is determined by gravimetry (*see Note 6*).

3.6 Loading Capacity of Nanoparticles

The ability of PVM/MA nanoparticles to entrap the antigenic complex is directly determined after degradation of loaded nanoparticles with NaOH.

1. Disperse antigen-loaded poly(anhydride) nanoparticles (15 mg) in water vortexing 1 min and centrifuge ($27,000 \times g$, 15 min).
2. Resuspend the pellet in NaOH 0.1 N, sonicate for 1 min (Microson™ Ultrasonic cell disruptor) and incubate for 1 h to assess the total delivery of the associated antigen.
3. Determine the amount of antigen released from the nanoparticles using microbicinchoninic acid (microBCA) protein assay (Pierce) (*see Note 7*).

3.7 Determination of the Structural Integrity and Antigenicity of HE/OMVs

To examine the structure of the antigens, western-blot analysis is used as a qualitative tool complementing the quantification performed by microBCA [7].

1. Disperse 15 mg of loaded nanoparticles in water, vortexing 1 min, and centrifuge ($27,000 \times g$, 15 min).
2. Resuspend the pellet in 2 mL of a mixed of dimethyl-formamide: acetone (1:3) (-80 °C, 1 h) and centrifuge ($27,000 \times g$, 15 min).
3. Resuspend the pellet in acetone (-80 °C, 30 min) and centrifuge ($27,000 \times g$, 15 min) (*see Note 8*).
4. Resuspend the extract in SDS-PAGE loading buffer and analyzed by SDS-PAGE and immunoblotting using an appropriate antiserum (*see Note 4*).

3.8 Electron Microscopy

1. Resuspend the heat extract (HE) in deionized water and stain with 4 % Uranyl acetate (Agar scientific) for 15 min.
2. Add lead citrate (Agar scientific) for 15 min.
3. Examine the sample with a Hitachi 1100 transmission electron microscope (Hitachi Scientific Instruments) operating at 100 kV.

4 Notes

1. Saline solution (9 g/L)
2. Previous to the centrifugation, the supernatant can be frozen and thawed in order to induce vesicles fusion and thus facilitate subsequent harvesting by centrifugation.
3. At this point, and for safety reasons, it may be interesting to inactivate the bacteria. Thus, we suggest the employment of a solution of binary ethylenimine and formaldehyde (6 mM BEI-0, 06 % FA, 6 h, 37 °C). BEI is prepared as a 0.1 M solution by cyclization of 0.1 M 2-bromoethylamine hydrobromide (Sigma) in 0.175 M NaOH solution for 1 h [19].

After BEI treatment, aliquots of 1 mL are directly spread onto TSA plates, incubated at 37 °C and inspected for growth during 7 days. Full bactericidal activity is considered when no colonies appear after 7 days incubation.

In the case you have remaining BEI, it has to be hydrolyzed before discarding by the addition of 1 M Na-thiosulfate solution at 10 % of the volume of the BEI.

4. This step is performed as a quality control of the antigenicity conservation after bacterial antigenic extraction and/or after nanoparticle encapsulation process.
5. This is recommended to maintain the suspension of nanoparticles under magnetic stirrer in order to allow the stabilization of the system.
6. Poly(anhydride) nanoparticles, freshly prepared, are freeze-dried in the absence of cryoprotectant. Then, the yield is calculated as the difference between the initial amount of materials used to prepare nanoparticles and the weight of the freeze-dried carriers.
7. In order to avoid interferences of the process, calibration curves are made with degraded blank nanoparticles, and all measurements are performed in triplicate.
8. On this step, acetone must be removed carefully. Otherwise, it is very easy to lose the pellet and consequently, the released antigen from the nanoparticles.

If there is some acetone on the vial, it is necessary to evaporate de acetone. Since this volume is very low, we recommend leaving the vial open for 10 min.

Acknowledgment

This work was supported by a FIS grant PI12/01358 Ministerio de Sanidad y Consumo/FIS from Spain.

References

1. Cozzi R, Scarselli M, Ferlenghi I (2013) Structural vaccinology: a three-dimensional view for vaccine development. *Curr Top Med Chem* 13:2629–2637
2. Mashburn-Warren LM, Whiteley M (2006) Special delivery: vesicle trafficking in prokaryotes. *Mol Microbiol* 61:839–846
3. Hodges K, Hecht G (2012) Interspecies communication in the gut, from bacterial delivery to host-cell response. *J Physiol* 590:433–440
4. Fahie M, Romano FB, Chisholm C et al (2013) A non-classical assembly pathway of *Escherichia coli* pore-forming toxin cytolysin A. *J Biol Chem* 288:31042–31051
5. Shen Y, Giardino Torchia ML, Lawson GW et al (2012) Outer membrane vesicles of a human commensal mediate immune regulation and disease protection. *Cell Host Microbe* 12:509–520
6. Ochoa-Reparaz J, Garcia B, Solano C et al (2005) Protective ability of subcellular extracts from *Salmonella Enteritidis* and from a rough isogenic mutant against salmonellosis in mice. *Vaccine* 23:1491–1501
7. Ochoa J, Irache JM, Tamayo I et al (2007) Protective immunity of biodegradable nanoparticle-based vaccine against an experimental challenge with *Salmonella Enteritidis* in mice. *Vaccine* 25:4410–4419
8. Reed SG (2013) Vaccine adjuvants. *Expert Rev Vaccines* 12:705–706
9. Irache JM, Esparza I, Gamazo C et al (2011) Nanomedicine: novel approaches in human and veterinary therapeutics. *Vet Parasitol* 180:47–71
10. Lowry OH, Rosebrough NJ, Farr AL et al (1951) Protein measurement with the Folin phenol reagent. *J Biol Chem* 193:265–275
11. Warren L (1959) The thiobarbituric acid assay of sialic acids. *J Biol Chem* 234:1971–1975
12. Osborn MJ (1963) Studies on the gram-negative cell wall. I. Evidence for the role of 2-Keto- 3-deoxyoctonate in the lipopolysaccharide of *Salmonella typhimurium*. *Proc Natl Acad Sci U S A* 50:499–506
13. Laemmli UK (1970) Cleavage of structural proteins during the assembly of the head of bacteriophage T4. *Nature* 227:680–685
14. Fairbanks G, Steck TL, Wallach DF (1971) Electrophoretic analysis of the major polypeptides of the human erythrocyte membrane. *Biochemistry* 10:2606–2617
15. Merril CR, Switzer RC, Van Keuren ML (1979) Trace polypeptides in cellular extracts and human body fluids detected by two-dimensional electrophoresis and a highly sensitive silver stain. *Proc Natl Acad Sci U S A* 76:4335–4339
16. Tsai CM, Frasch CE (1982) A sensitive silver stain for detecting lipopolysaccharides in polyacrylamide gels. *Anal Biochem* 119:115–119
17. Towbin H, Staehelin T, Gordon J (1979) Electrophoretic transfer of proteins from polyacrylamide gels to nitrocellulose sheets: procedure and some applications. *Proc Natl Acad Sci U S A* 76:4350–4354
18. Arbos P, Wirth M, Arangoa MA et al (2002) Gantrez AN as a new polymer for the preparation of ligand-nanoparticle conjugates. *J Control Release* 83:321–330
19. Camacho AI, Souza-Reboucas J, Irache JM et al (2013) Towards a non-living vaccine against *Shigella flexneri*: from the inactivation procedure to protection studies. *Methods* 60:264–268

Chapter 11

Direct Attachment of Nanoparticle Cargo to *Salmonella typhimurium* Membranes Designed for Combination Bacteriotherapy Against Tumors

Robert Kazmierczak, Elizabeth Choe, Jared Sinclair,
and Abraham Eisenstark

Abstract

Nanoparticle technology is an emerging approach to resolve difficult-to-manage internal diseases. It is highly regarded, in particular, for medical use in treatment of cancer due to the innate ability of certain nanoparticles to accumulate in the porous environment of tumors and to be toxic to cancer cells. However, the therapeutic success of nanoparticles is limited by the technical difficulty of fully penetrating and thus attacking the tumor. Additionally, while nanoparticles possess seeming-specificity due to the unique physiological properties of tumors themselves, it is difficult to tailor the delivery of nanoparticles or drugs in other models, such as use in cardiac disease, to the specific target. Thus, a need for delivery systems that will accurately and precisely bring nanoparticles carrying drug payloads to their intended sites currently exists. Our solution to this engineering challenge is to load such nanoparticles onto a biological “mailman” (a novel, nontoxic, therapeutic strain of *Salmonella typhimurium* engineered to preferentially and precisely seek out, penetrate, and hinder prostate cancer cells as the biological delivery system) that will deliver the therapeutics to a target site. In this chapter, we describe two methods that establish proof-of-concept for our cargo loading and delivery system by attaching nanoparticles to the *Salmonella* membrane. The first method (Subheading 1.1) describes association of sucrose-conjugated gold nanoparticles to the surface of *Salmonella* bacteria. The second method (Subheading 1.2) biotinylates the native *Salmonella* membrane to attach streptavidin-conjugated fluorophores as example nanoparticle cargo, with an alternative method (expression of membrane bound biotin target sites using autodisplay plasmid vectors) that increases the concentration of biotin on the membrane surface for streptavidin-conjugated nanoparticle attachment. By directly attaching the fluorophores to our bacterial vector through biocompatible, covalent, and stable bonds, the coupling of bacterial and nanoparticle therapeutic approaches should synergistically lead to improved tumor destruction.

Key words *Salmonella*, Nanoparticle, Gold, Biotin, Autodisplay, Tumor, Cancer

1 Introduction

Developing a site-specific approach to cancer therapy is a vital issue in maximally eliminating tumors while minimizing the destruction of noncancerous cells. Nanoparticles have shown promising

clinical applications by addressing this issue through multiple features, including their biocompatibility, selective toxicity to tumors, and specificity in targeting cancer cells due to the leaky vasculature unique to tumors [1–4]. While originally developed for imaging and detection purposes, current research seeks to take advantage of the therapeutic properties of nanoparticles themselves. Gold nanoparticles, for example, have proven valuable when coupled with laser therapies to preferentially, thermally ablate tumors [5], and have additionally been shown to be functional as an adjuvant for the immune system [6], illustrating their inherent desirable properties in treating cancer.

However, current issues hindering nanoparticles from maximal success in cancer therapy include the high interstitial pressure characteristic of tumor cells, opposing and limiting the radial extent of diffusion of nanoparticles from the blood stream into the tumor despite the tumor's enhanced permeability [4]. Additionally, colloidal instability of nanoparticles in storage is a nonnegligible concern, as aggregates have vastly different properties than individual particles, creating the potential for the loss of therapeutic value [7]. Most current approaches to remedying relatively poor penetration of pure nanoparticles involve taking advantage of the ability to biofunctionalize the nanoparticles themselves with tumor-targeting peptides [4]. Our approach to addressing both issues is to couple therapeutic nanoparticles with bacterial-based cancer therapies ("bacteriotherapy"), leading to an overall increase in tumor homing and destruction capabilities.

While nanotherapies are at the forefront of current cancer research, bacterial-based cancer therapies have been studied as early as the late nineteenth-century, when Coley experimented with *Streptococcus* to evoke immune responses from his tumor-bearing patients [8]. In current research, the focus of bacterial-based therapies has shifted to *Listeria*, *Bifidobacteria*, and *Salmonella*. These bacteria, when injected into tumors, preferentially invade and replicate within them, subsequently inhibiting their growth or destroying them entirely [9, 10]. The development of a successful combination bacteriotherapy could lead to treatments with specificity and precision, avoiding the often negative side effects of nonspecific cancer treatments resulting from destruction of healthy cells and tissue. Additionally, it has been shown that such treatments successfully manage more aggressively metastasizing and further-developed cancer, unlike many forms of chemotherapy [11–13].

Salmonella typhimurium has proven to be a promising cancer therapeutic candidate due to its tumor-targeting and killing abilities [10, 12]; however, wild-type strains are notorious for causing septic side effects in several animal hosts due to their ability to

escape the macrophages of the immune system and infect the human body [14]. Luckily, genetically altered bacterial therapies with reduced toxicity have been developed, successfully colonizing nonresponsive tumors in Phase I human clinical trials [15]. Current research demonstrates that regular administrations of low *Salmonella* eliminate tumors in mouse models while minimizing the incidence of toxic side effects [12]. However, *Salmonella* therapy is not without its shortcomings as well. As documented by Forbes et al. [11] and Toso et al. [15], while colonization of tumors is successfully achieved, adequate tumor regression has yet to be seen in clinical trials for reasons outlined in [11]. Nevertheless, its extreme tumor homing abilities even in advanced metastases [12] make *Salmonella* a model vector candidate for coupling with therapeutic nanoparticles or other delivery systems [16–19] which in turn may compensate for any inadequate dispersion of *Salmonella* in tumors due to their own accumulative properties. Creating a dual approach to fighting tumors builds upon each individual approaches, leading to a synergistic effect of overall enhanced tumor destruction.

Scientists at The Cancer Research Center (CRC) engineered therapeutic *Salmonella* strain CRC2631 (CRC1674 *aroA*::Tn10, $\Delta rfaH$::pKD4, $\Delta thyA$::pKD4, where CRC1674 is LT2 *bisD2550* (archived 1958, “resuscitated” 1999)), derived from archival wild-type *Salmonella typhimurium* LT2 [20] and kept in sealed agar stabs for over 40 years. Phage transduction and recombineering was used to minimize the septic side effects of wild-type *Salmonella* strains while preserving its tumor-targeting and killing capabilities. Strain CRC2631 was intraperitoneally injected into a 6-month-old transgenic adenocarcinoma of mouse prostate (TRAMP) mouse prostate cancer model and the bacterial cells preferentially colonized tumor tissues at ratios of 1,000:1 over spleen and liver reservoirs during the 24-h incubation period [21]. Initial low-dosage studies established that weekly, low-dose injections of CRC2631 do not produce ill effects in immunocompromised mice and prolong survival of TRAMP mice.

The goal of constructing a viable and stable nanoparticle-coated *Salmonella* strain CRC2631 was to obtain greater tumor invasion and destruction abilities than individual nanoparticle and bacterial therapies alone. Nanoparticle-coated *Listeria* and *Escherichia coli* membranes have been used to carry antibody-attached particles, demonstrating the potential of the membrane-bound strategy [22, 23]. This report describes two methods to directly attach nanoparticles to the therapeutic *Salmonella enterica* serovar Typhimurium (*S. typhimurium*) strain CRC631 engineered in our lab without the use of specific antibodies. We expect these methods to be generally applicable for use with other bacterial membranes.

1.1 Introduction: Attachment of 4–16 nm Sucrose- Gold Nanoparticles (AuNP) to *Salmonella* Membrane via Sucrose Conjugation

1.2 Introduction: Surface Biotinylation of *Salmonella* Using Biotin Ligase (BirA) for Direct Attachment of Streptavidin- Associated Nanoparticles

Initial studies, described in Subheading 3.1 below, were performed attaching sucrose-conjugated gold nanoparticles to *Salmonella* membranes. Although the method successfully associated *Salmonella* with sucrose-conjugated gold nanoparticles *in vitro* (Fig. 1), the sucrose-conjugated gold nanoparticle/*Salmonella* membrane protocol was put aside for the novel approach to merging the bacterial and nanoparticle therapeutic approaches using the biotin–streptavidin bond, which eliminated membrane–nanoparticle stability concerns. This method is described in Subheading 1.2.

This method establishes the capability of the biotin–streptavidin approach to directly attach cargo onto our therapeutic *Salmonella* (CRC2631), although we expect the protocol to be applicable to bacterial membranes in general. This method is designed to attach biotin molecules to the *Salmonella* membrane surface using Biotin Ligase (BirA). We began by biotinyling the native membrane surface of *Salmonella* strain CRC 2631; the biotin on the surface of the bacteria was then complexed with streptavidin-conjugated fluorophore nanoparticles, effectively creating direct membrane surface attachment of the fluorophore nanoparticle cargo. This attachment is permanent in the time scale of therapeutic practicality, as the biotin–streptavidin complex is currently the strongest known noncovalent biological interaction [24–26]. Surprisingly, we found that the native *Salmonella* membrane has a significant amount of native BirA target sites for biotin attachment. We evaluated successful surface attachment of fluorophore cargo through fluorescence-activated cell sorting (FACS) analysis (Fig. 2a), and FACS analyses were performed after 3 days to demonstrate stable surface attachment of streptavidin-conjugated nanoparticles (Fig. 2b). We also explored an alternate protocol utilizing an “autodisplay” plasmid vector (pJM22) [27] that expresses a membrane-associated protein that we engineered to display a BirA peptide target site (GLNDIFEAQKIEWHE) at the membrane

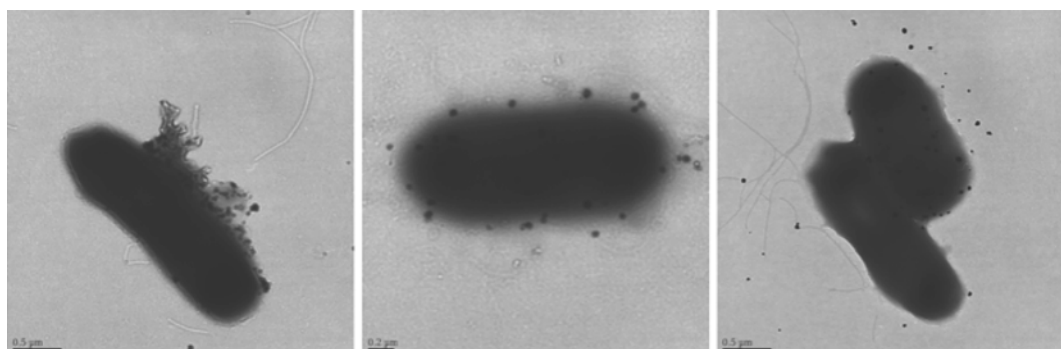


Fig. 1 TEM illustrates plausibility of gold nanoparticle conjugation with CRC 2631 (4 μ L in PBS on carbon-coated copper grid). Large ovoid objects are *Salmonella* bacteria with sucrose-conjugated gold nanoparticles present as small black particles on the periphery of the *Salmonella*

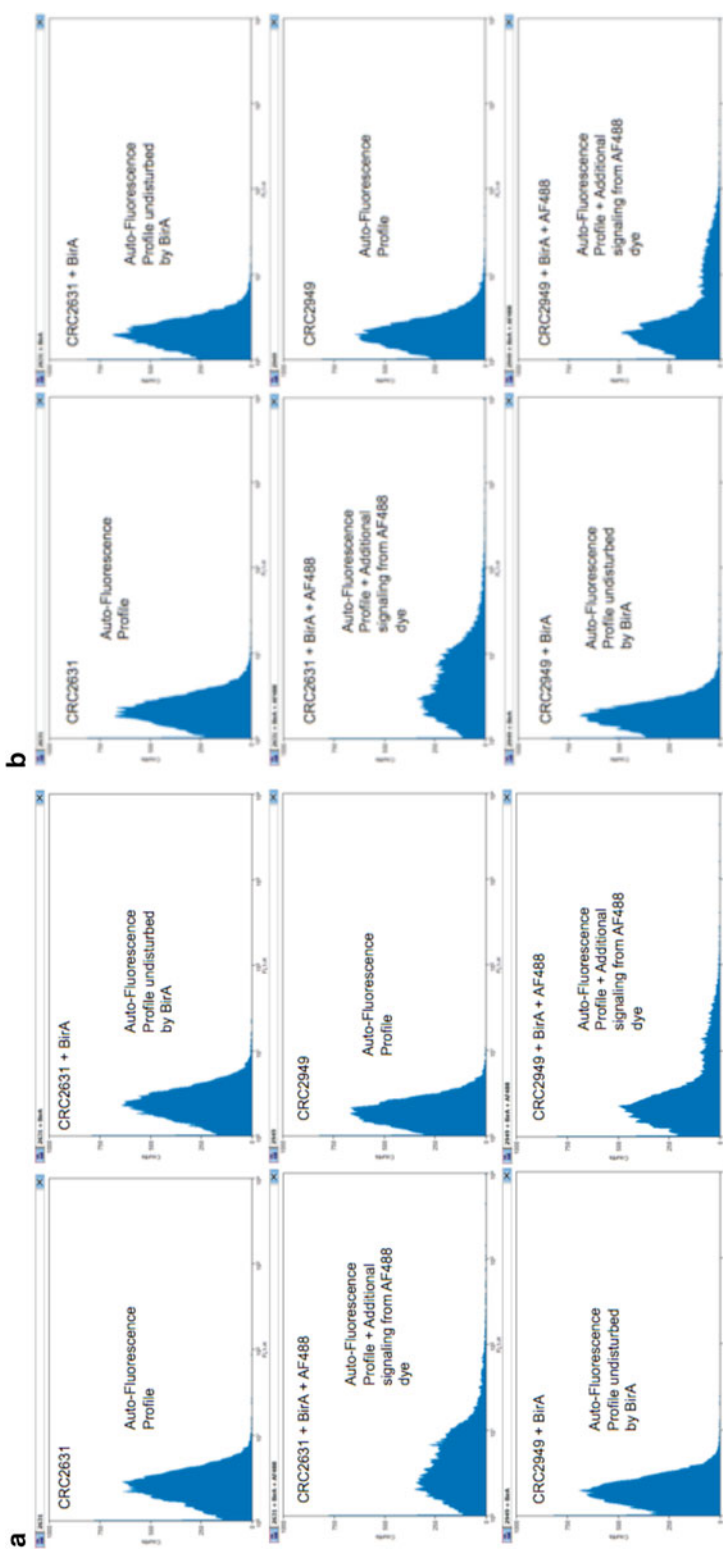


Fig. 2 FACS data collected on (a) day 1 and (b) day 3. Cell sorting was performed on a BD FACScan with a 488 nm argon laser. Biotinylated CRC 2631 and 2949 (CRC 2631 with pJM22-BirA autodisplay vector) was incubated with streptavidin-conjugated Alexa Fluor 488 dye (Invitrogen) for 10 min in PBS-Mg before unbound dye was washed off. Plots illustrate (y-axis) cell counts versus (x-axis) intensity of Alexa Fluor 488 emission wavelength. The following controls were used for the FACS assay: autofluorescence control (CRC 2631 and CRC 2949 alone), BirA-treated autofluorescence control (CRC 2631 and CRC 2949 treated with BirA), and BirA-treated bacteria incubated with AF488 fluorescence tag followed by two washes and suspension in 500 μ L PBS-Mg. The higher intensity signal only occurs due to increasing concentration of the fluorophore. Note the addition of extra BirA target sites by addition of the pJM22-BirA autodisplay vector substantially increases the intensity of the AF488 signal, indicating bacterial subpopulations with greater biotin-streptavidin association (CRC2631 + BirA + AF488 versus CRC2949 + BirA + AF488). Cells were stored at 4 °C after initial assay until reading was performed 72 h later (day 3)

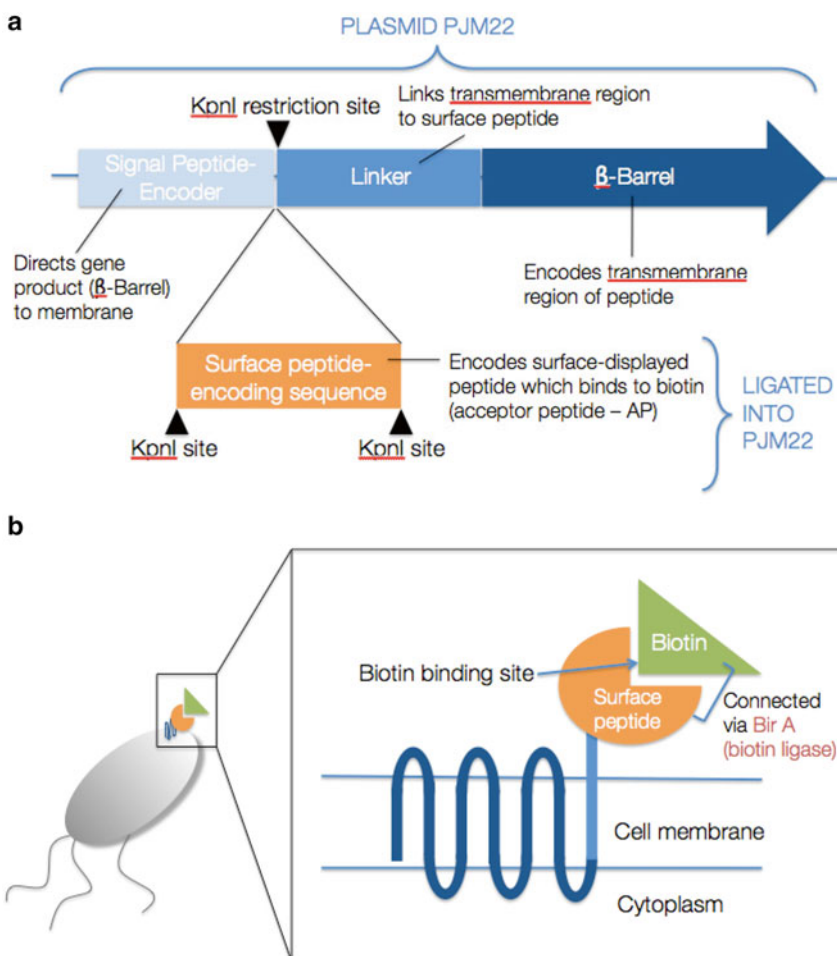


Fig. 3 pJM22-BirA autodisplay vector construction schematic of the membrane protein construct containing the BirA target peptide at (a) plasmid level and (b) cellular level

surface (pJM22-BirA) (Fig. 3). Expression of the autodisplay vector in CRC2631 resulted in a subpopulation with increased streptavidin-conjugated fluorophore signal using FACS assays (Fig. 2), indicating that there were more biotin target sites available for attachment. We recommend using the autodisplay or similar membrane display protocols if there are insufficient biotin ligase target sites present in the bacterial membrane being examined.

2 Materials

2.1 Attachment of 4–16 nm Sucrose-Gold Nanoparticles (AuNP) to *Salmonella* Membrane via Sucrose Conjugation

1. Bacteria: *Salmonella typhimurium* strain CRC2631 (LT2 *bisD2550 aroA::Tn10*, Δ *rfaH::pKD4*, Δ *thyA::pKD4*) is derived from wild-type *Salmonella typhimurium* strain LT2 and used in this protocol.
2. Luria-Bertani (LB) broth agar plates: 25 g/L LB powder, 200 mg powdered thymine, 15 g/L agar in 1 L deionized water.

Autoclave at 121 °C, 15 lb pressure for 15 min immediately after mixing to sterilize. Pour 15 mL aliquots into sterile petri dishes and allow to solidify at room temperature. Store at 4 °C until needed.

3. Luria-Bertani (LB) liquid media: 25 g/L LB powder, 200 mg powdered thymine in 1 L deionized water. Autoclave at 121 °C, 15 lb pressure for 15 min immediately after mixing to sterilize.
4. 4–16 nm gold nanoparticles in ultrapure water solution: supplied by manufacturer (Nanoparticle Biochem, Inc) and described in [28].
5. Sucrose in ultrapure water solution: supplied by manufacturer (Nanoparticle Biochem, Inc) and described in [28].
6. Phosphate-buffered saline (PBS): Dissolve 9.88 g of Sodium Chloride (81 %), Sodium Phosphate Dibasic (14 %), Potassium Phosphate Monobasic (3.0 %), and Potassium Chloride (2 %) powder in 1 L deionized water. Autoclave at 121 °C, 15 lb pressure for 15 min immediately after mixing to sterilize. pH 7.3–7.5.

2.2 Surface Biotinylation of *Salmonella* Using Biotin Ligase (BirA) for Direct Attachment of Streptavidin-Associated Nanoparticles

1. Bacteria: *Salmonella typhimurium* strain CRC2631 (LT2 *hisD2550 aroA::Tn10*, Δ *rfaH::pKD4*, Δ *thyA::pKD4*) and CRC2949 (CRC2631 pJM22-BirA) is derived from wild-type *Salmonella typhimurium* strain LT2 and used in this protocol. CRC2949 is used to demonstrate enhancement of biotinylation by autodisplay vector expression of BirA target membrane surface peptides.
2. Luria-Bertani (LB) liquid media: 25 g/L LB powder, 200 mg powdered thymine in 1 L deionized water. Autoclave at 121 °C, 15 lb pressure for 15 min immediately after mixing to sterilize.
3. Phosphate-buffered saline (PBS): Dissolve 9.88 g of Sodium Chloride (81 %), Sodium Phosphate Dibasic (14 %), Potassium Phosphate Monobasic (3.0 %), and Potassium Chloride (2 %) powder in 1 L deionized water. Autoclave at 121 °C, 15 lb pressure for 15 min immediately after mixing to sterilize. pH 7.3–7.5.
4. 1 M Magnesium Chloride (MgCl₂): 0.926 g of MgCl₂ in 5 mL deionized water. 0.2 μ m Filter sterilize.
5. PBS-Mg: 1 mL of 1 M MgCl₂ in 200 mL of PBS (5 μ L 1.0 M MgCl₂/1 mL PBS).
6. PBS-Mg/1 % pre-dialyzed BSA: 1 g BSA (Invitrogen 6003, fatty acid-free) in 10 mL PBS-Mg, 0.2 μ m filter sterilized (makes a 10 % stock). Add 1 mL of the 10 % stock to 9 mL of PBS-Mg to make the 1 % working concentration (Note 1.)

7. Streptavidin-conjugated Alexa Fluor (488 nm) (“AF488”) (Invitrogen) in PBS-Mg: To suspend in PBS-Mg, place AF488 (1 mg/mL, or 1.54 mM) in Slide-A-Lyzer MINI Dialysis Unit, 20 K MWCO (Thermo Scientific) and put in beaker containing 500 mL PBS-Mg. Dialyze for 1 h at room temp in dark conditions and collect AF488. Store at 4 °C. (See Note 2.)
8. “Biomix A”: 0.5 M Bicine buffer pH 8.3 (Avidity, Inc).
9. “Biomix B”: 100 mM ATP, 100 mM MgO(Ac)₂, 500 µM Biotin (Avidity, Inc).
10. Biotin Ligase (BirA): Purchased from Avidity or isolated [24], 1 mg/mL in PBS. Store at -20 °C.
11. Autodisplay plasmid vector pJM22-BirA (this study): Transform into desired bacterial background for expression of membrane-associated protein with membrane surface BirA target peptide GLNDIFEAQKIEWHE. Select for plasmid retention in strain with 50 µg/mL Ampicillin antibiotic (Sigma).

3 Method

3.1 Attachment of 4–16 nm Sucrose-Gold Nanoparticles (AuNP) to *Salmonella* Membrane via Sucrose Conjugation

1. Preparation of bacteria: All *S. typhimurium* were grown on nutrient Luria-Bertani (LB) broth agar plates supplemented with 200 µg/mL thymine at 37 °C overnight. Plates were stored at 4 °C for up to 4 weeks.
2. Inoculate one volume (3 mL) LB growth media supplemented with 200 µg/mL thymine with a single colony of *Salmonella* strain grown on LB broth agar plates. Incubate in 37 °C dry shaker overnight.
3. Prepare 4–16 nm sucrose-gold nanoparticles. Manufacturer’s protocol:
 - (a) Put 6 mL of pale yellow gold nanoparticle solution on hot plate with stir bar. Heat with stirring to 90–95 °C.
 - (b) Add 100 µL of sucrose solution to gold nanoparticle solution and continue stirring with heat for 15 s (solution will turn from pale yellow to red). Move solution to non-warm stirrer and allow cooling while stirring (30 min). (See Note 3).
4. Pellet culture at 1,485 ×*g* for 5 min. Remove supernatant.
5. Resuspend in one volume sterile phosphate-buffered saline (PBS) and vortex.
6. Normalize optical density of *Salmonella* to 0.2 (600 nm absorbance).

7. Add 1 mL prepared sucrose-gold nanoparticles for every 10 mL of optically normalized culture. Incubate in 37 °C dry shaker overnight. (See Note 4).

Our initial approach to attaching CRC 2631 to nanoparticles involved incubation with sucrose-coated gold nanospheres (whose manufacture is outlined by Qi et al. [28]). Overnight cultures of CRC 2631 grown in LB + thymine broth were spun at $1,485 \times g$ for 5 min and resuspended in PBS until an optical density of 0.2 was reached. The solution was incubated with the sucrose-coated nanoparticles overnight, from which 4 μ L were applied to carbon-coated copper grids for TEM imaging with a JEOL 1400 microscope. While we determined that the colloidal instability of the sucrose nanoparticles compromised the experimental practicality of the approach, we confirmed that CRC 2631 is capable of bearing a sucrose-conjugated gold nanoparticle load and that successful conjugation is qualitatively verifiable via transmission electron microscopy (see Fig. 1).

3.2 Surface Biotinylation of *Salmonella* Using Biotin Ligase (BirA) for Direct Attachment of Streptavidin-Associated Nanoparticles

1. Preparation of bacteria: All *S. typhimurium* were grown on nutrient Luria-Bertani (LB) broth agar plates supplemented with 200 μ g/mL thymine at 37 °C overnight. Plates were stored at 4 °C for up to 4 weeks.
2. Inoculate one volume (2 mL) LB growth media supplemented with 200 μ g/mL thymine with a single colony of *Salmonella* strain grown on LB broth agar plates. Incubate in 37 °C dry shaker overnight. Our tested example strains are CRC2631 and CRC2949.
3. Centrifuge bacterial cells for 1 min at $15,682 \times g$ in an eppendorf tube centrifuge. Discard supernatant.
4. Resuspend bacterial cells in 0.5 mL of PBS-Mg. (See Note 5.)
5. Biotinylate the *Salmonella* membranes using the following reaction volumes:
 - (a) Mix in the following order:
 - 20 μ L bacterial cell culture in PBS-Mg. (See Note 5.)
 - 5 μ L 10 \times Biomix A.
 - 5 μ L 10 \times Biomix B.
 - 15 μ L PBS-Mg.
 - 5 μ L BirA enzyme (1 mg/mL) (See Note 5.)
 - (b) Incubate tubes for 60 min at 23 °C.
6. Wash bacterial cells twice with one volume of 4 °C PBS-Mg (Washing bacterial cells: Centrifuge bacterial cells at $15,682 \times g$ for 1 min and remove supernatant, then resuspend bacterial cells in the initial volume of buffer (PBS-Mg).)

7. Mix 50 μ L biotinylated bacterial cells with 1 μ L prepared streptavidin-conjugated AF488. (See Note 5.)
8. Incubate at 4 °C for 10 min.
9. Wash and resuspend bacterial cells twice in one volume of PBS-Mg. (See Note 6.)
10. Optional: Fix bacterial cells (Fixation: centrifuge bacterial cells at 15,682 $\times g$, remove supernatant and resuspend in one volume of fixative solution) with 4 % paraformaldehyde fixative in PBS-Mg for 10 min if needed for cell sorting requirements. If preparing live cells for testing, do not fix.
11. Centrifuge cells at 15,682 $\times g$ for 1 min and remove supernatant. Resuspend cells in 500 μ L PBS-Mg for FACS analysis with a 488 nm argon laser.

Complexes of *Salmonella* membrane-bound biotin with streptavidin-conjugated fluorescent tags (CRC2631, CRC2949) was indicated in the FACS analysis by a shift in signal intensity created by the fluorescent dye (Fig. 2). The intensity of signal binding per bacterial cell is indicative of the potential amount of nanoparticle load we can attach to each bacterial cell. Increased fluorescence in the labeled CRC2949 population is indicative that the pJM22-BirA plasmid is successfully displaying additional BirA target peptides on the bacterial surface for biotin (and subsequent nanoparticle) attachment. Comparison of FACS data from bacterial cells alone versus bacterial cells labeled with biotin confirms that biotinylation of the bacterial membrane does not change the fluorescence profile. Thus, the FACS profile obtained from bacteria + BirA-mediated membrane biotinylation + AF488 streptavidin-conjugated fluorescent tags is a reliable indicator of streptavidin binding and successful membrane surface attachment. Profile similarities between FACS assays from samples analyzed 3 days apart illustrate no significant degradation of signal strength during that period (Fig. 2). The AF488 signal loss over the duration of the two FACS assays was minimal, as expected due to the high stability of the streptavidin-linked bonds. Thus, the preliminary FACS studies show that our biotinylated membrane-fluorescent nanoparticle construct is stable.

We have created a novel proof-of-concept combination therapy construct by adhering streptavidin-conjugated nanoparticles directly to biotinylated therapeutic *Salmonella typhimurium* membranes for potential use in tumor targeting and destruction. In previous studies, we demonstrated that *Salmonella* strain CRC 2631 is an excellent candidate for nanoparticle delivery due to its tumor-targeting properties [19, 21] and its low toxicity during repeated therapeutic administrations.

These studies illustrate that nanoparticle cargo is not only loadable directly onto the *Salmonella* membrane (see Note 7),

but that the amount that is loaded can be quantified via FACS analysis as long as a marker is attached to the cargo. Cell sorting facilitates collection of *Salmonella* populations with specific concentrations of therapeutic nanoparticle cargo loads, allowing precise control of dosage levels. Our conjugation approach involves the biotinylation of the bacterial membrane using biotin ligase (BirA) enzyme followed by attachment of streptavidin-conjugated cargo. We demonstrate that biotinylation can be additionally enhanced by an autodisplay vector system that puts a biotin ligase peptide target on the membrane surface. This is shown by the increased population of high-intensity AlexaFluor488 binding signal events in the CRC2949 strain that contains the pJM22-BirA engineered autodisplay plasmid, indicating additional BirA target sites for biotinylation and subsequent streptavidin-AF488 conjugation (Fig. 2). We have demonstrated this conjugation to be stable over the course of 3 days; thus, long-term attachment stability does not appear to be a concern for this approach as it is in other conjugation methods [29].

4 Notes

1. All PBS, PBS-Mg, and PBS-Mg/1%BSA stocks can be prepared ahead and stored at 4 °C.
2. Remember to calculate and adjust AF488 concentrations after dialyzing buffer.
3. Stability of sucrose-gold nanoparticles is 24 h from time of synthesis due to nanoparticle aggregation. Synthesize only what is needed for the current experiment.
4. If attaching secondary substrate to gold nanoparticles after bacterial attachment, wash *Salmonella*-AuNP conjugates in one volume of PBS before continuing experiment.
5. When performing new studies, be sure to vary the amount of BirA used to ensure you are saturating the biotinylation sites on the membranes, and the amount of streptavidin conjugates for the biotinylated sites.
6. Determine the minimum number of post-attachment washes to required remove any nonspecific binding. Two washes in PBS-Mg were sufficient for our protocols.
7. We do not know what binding targets BirA (biotin ligase) is biotinyling on the wild-type *Salmonella* membrane. We are investigating to confirm our biotin attachment mechanism, whether by BirA attachment to our synthetic surface display peptide or through native BirA sites on CRC 2631, through the following strategies: (1) running a motif-based sequence

analysis (ScanProsite from ExPASy) of LT2 genome (from which CRC 2631 is derived) to search for alignment with BirA target consensus sequences predicted to be on the membrane surface [30] and (2) immunolabeling pJM22-BirA autodisplay surface protein to determine contributions of FACS signal from BirA attachment to surface peptide versus endogenous binding sites. Our plasmid contains the ~13 kDa cholera toxin B subunit (CTB) that can be tracked with antibody labeling [31].

Acknowledgements

We thank the Mauer lab for the kind gift of pJM22 autodisplay vector, and the Ting lab for the kind gift of BirA overexpression plasmid pET21a-BirA. We thank Alison Dino and the University of Missouri Cell Core for maintaining cell lines and assistance with cell sort protocols. This work was funded internally by the Cancer Research Center (Columbia, MO).

References

1. Jain S, Hirst DG, O'Sullivan JM (2012) Gold nanoparticles as novel agents for cancer therapy. *Br J Radiol* 85(1010):101–113
2. Kennedy LC et al (2011) A new era for cancer treatment: gold-nanoparticle-mediated thermal therapies. *Small* 7(2):169–183
3. Puvanakrishnan P et al (2012) In vivo tumor targeting of gold nanoparticles: effect of particle type and dosing strategy. *Int J Nanomedicine* 7:1251–1258
4. Ruoslahti E, Bhatia SN, Sailor MJ (2010) Targeting of drugs and nanoparticles to tumors. *J Cell Biol* 188(6):759–768
5. Liu Z et al (2008) Drug delivery with carbon nanotubes for in vivo cancer treatment. *Cancer Res* 68(16):6652–6660
6. Dykman LA (2010) Gold nanoparticles as an antigen carrier and an adjuvant. In: *Nanotechnology science and technology*. Nova, New York, NY, xiv, 54 p
7. Gao J et al (2012) Colloidal stability of gold nanoparticles modified with thiol compounds: bioconjugation and application in cancer cell imaging. *Langmuir* 28(9):4464–4471
8. McCarthy EF (2006) The toxins of William B. Coley and the treatment of bone and soft-tissue sarcomas. *Iowa Orthop J* 26:154–158
9. Bermudes D, Zheng LM, King IC (2002) Live bacteria as anticancer agents and tumor-selective protein delivery vectors. *Curr Opin Drug Discov Devel* 5(2):194–199
10. Nguyen VH et al (2010) Genetically engineered *Salmonella typhimurium* as an imageable therapeutic probe for cancer. *Cancer Res* 70(1):18–23
11. Forbes NS et al (2003) Sparse initial entrapment of systemically injected *Salmonella typhimurium* leads to heterogeneous accumulation within tumors. *Cancer Res* 63(17):5188–5193
12. Hayashi K et al (2009) Cancer metastasis directly eradicated by targeted therapy with a modified *Salmonella typhimurium*. *J Cell Biochem* 106(6):992–998
13. Michl P, Gress TM (2004) Bacteria and bacterial toxins as therapeutic agents for solid tumors. *Curr Cancer Drug Targets* 4(8):689–702
14. Hashim S et al (2000) Live *Salmonella* modulate expression of Rab proteins to persist in a specialized compartment and escape transport to lysosomes. *J Biol Chem* 275(21):16281–16288
15. Toso JF et al (2002) Phase I study of the intravenous administration of attenuated *Salmonella typhimurium* to patients with metastatic melanoma. *J Clin Oncol* 20(1):142–152
16. El-Aneed A (2004) An overview of current delivery systems in cancer gene therapy. *J Control Release* 94(1):1–14

17. Ganai S, Arenas RB, Forbes NS (2009) Tumour-targeted delivery of TRAIL using *Salmonella typhimurium* enhances breast cancer survival in mice. *Br J Cancer* 101(10):1683–1691
18. Seow Y, Wood MJ (2009) Biological gene delivery vehicles: beyond viral vectors. *Mol Ther* 17(5):767–777
19. Vassaux G et al (2006) Bacterial gene therapy strategies. *J Pathol* 208(2):290–298
20. McClelland M et al (2001) Complete genome sequence of *Salmonella enterica* serovar Typhimurium LT2. *Nature* 413(6858):852–856
21. Zhong Z et al (2007) *Salmonella*-host cell interactions, changes in host cell architecture, and destruction of prostate tumor cells with genetically altered *Salmonella*. *Microsc Microanal* 13(5):372–383
22. Akin D et al (2007) Bacteria-mediated delivery of nanoparticles and cargo into cells. *Nat Nanotechnol* 2(7):441–449
23. Fernandes R et al (2011) Enabling cargo-carrying bacteria via surface attachment and triggered release. *Small* 7(5):588–592
24. Chen I et al (2005) Site-specific labeling of cell surface proteins with biophysical probes using biotin ligase. *Nat Methods* 2(2):99–104
25. Green NM (1990) Avidin and streptavidin. *Methods Enzymol* 184:51–67
26. Holmberg A et al (2005) The biotin-streptavidin interaction can be reversibly broken using water at elevated temperatures. *Electrophoresis* 26(3):501–510
27. Maurer J, Jose J, Meyer TF (1997) Autodisplay: one-component system for efficient surface display and release of soluble recombinant proteins from *Escherichia coli*. *J Bacteriol* 179(3):794–804
28. Qi Z et al (2004) Characterization of gold nanoparticles synthesized using sucrose by seeding formation in the solid phase and seeding growth in aqueous solution. *J Phys Chem B* 108(22):7006–7011
29. Haisler WL et al (2013) Three-dimensional cell culturing by magnetic levitation. *Nat Protoc* 8(10):1940–1949
30. Beckett D, Kovaleva E, Schatz PJ (1999) A minimal peptide substrate in biotin holoenzyme synthetase-catalyzed biotinylation. *Protein Sci* 8(4):921–929
31. Paniagua-Solis J et al (1996) Construction of CTB fusion proteins for screening of monoclonal antibodies against *Salmonella typhi* OmpC peptide loops. *FEMS Microbiol Lett* 141(1):31–36

Chapter 12

Applications of Microscopy in *Salmonella* Research

Layla M. Malt, Charlotte A. Perrett, Suzanne Humphrey, and Mark A. Jepson

Abstract

Salmonella enterica is a Gram-negative enteropathogen that can cause localized infections, typically resulting in gastroenteritis, or systemic infection, e.g., typhoid fever, in humans and many other animals. Understanding the mechanisms by which *Salmonella* induces disease has been the focus of intensive research. This has revealed that *Salmonella* invasion requires dynamic cross-talk between the microbe and host cells, in which bacterial adherence rapidly leads to a complex sequence of cellular responses initiated by proteins translocated into the host cell by a type 3 secretion system. Once these *Salmonella*-induced responses have resulted in bacterial invasion, proteins translocated by a second type 3 secretion system initiate further modulation of cellular activities to enable survival and replication of the invading pathogen. Elucidation of the complex and highly dynamic pathogen–host interactions ultimately requires analysis at the level of single cells and single infection events. To achieve this goal, researchers have applied a diverse range of microscopy techniques to analyze *Salmonella* infection in models ranging from whole animal to isolated cells and simple eukaryotic organisms. For example, electron microscopy and high-resolution light microscopy techniques such as confocal microscopy can reveal the precise location of *Salmonella* and its relationship to cellular components. Widefield light microscopy is a simpler approach with which to study the interaction of bacteria with host cells and often has advantages for live cell imaging, enabling detailed analysis of the dynamics of infection and cellular responses. Here we review the use of imaging techniques in *Salmonella* research and compare the capabilities of different classes of microscope to address specific types of research question. We also provide protocols and notes on some microscopy techniques used routinely in our own research.

Key words *Salmonella*, Infection, Imaging, Microscope, Widefield microscopy, Confocal laser scanning microscopy, Fluorescent staining, Live cell imaging, Scanning electron microscopy

1 Introduction

1.1 *Salmonella* Infection

Salmonella is a Gram-negative, flagellated enteropathogen which can cause self-limiting gasteroenteritis or in some cases more severe systemic infections, e.g., typhoid fever and secondary bacteremia. Despite improvements in food safety, *Salmonella* continues to be both a social and economic burden responsible for significant morbidity and mortality worldwide. Nontyphoidal *Salmonella* (NTS)

is estimated to cause 93.8 million serious infections worldwide per year and 155,000 deaths [1], whilst the exclusively human adapted serovars *S. Typhi* and *S. Paratyphi* are estimated to cause more than 27 million cases of typhoid fever, of which over 200,000 are fatal [2]. The virulence of *Salmonella enterica* depends on its ability to enter and survive in host cells. Primary infection occurs in the gut after ingestion of contaminated food or drink. The bacterium travels through the digestive system, surviving the low pH conditions of the stomach, to enter the small intestine. Environmental conditions within the lumen of the small intestine activate *Salmonella* virulence gene expression, promoting cellular invasion. A type 3 secretion system (T3SS) encoded by *Salmonella* pathogenicity island 1 (SPI-1) triggers cellular responses including extensive actin cytoskeleton rearrangement, producing “membrane ruffles” on the surface of the epithelial cell [3, 4] which facilitate bacterial uptake.

Salmonella invade preferentially, but not exclusively, via non-phagocytic M cells present in the epithelium overlaying the gut-associated lymphoid tissue [5–7]. The bacterium exploits the antigen uptake and transport function of M cells as a portal for entry into epithelial cells and subsequent dissemination into other cell types, including macrophages. After initial invasion of host cells, bacteria survive and replicate within a specialized membrane-bound compartment called the *Salmonella*-containing vacuole (SCV). From within this vacuolar niche, and with the aid of a second T3SS encoded by SPI-2, *Salmonella* are able to proliferate and avoid degradation by manipulating membrane trafficking, leading to a divergence from the classical endosome/lysosome pathway.

Understanding the mechanisms underlying *Salmonella*–host cell interactions advances our knowledge in both microbial pathogenesis and cell biology. Use of microscopy in this area has provided researchers with a powerful tool to study the intimate and complex cross-talk between bacteria and host cells at a single cell, and single event, level [8–20]. Live cell and fixed cell microscopy has provided a robust tool for revealing the dynamics of *Salmonella* adherence, membrane ruffling [8–13], SCV biogenesis [8, 9, 14–16] and bacterial replication within infected cells [17–19]. Advances in microscopy, together with the development of fluorescent protein-based reporters has helped delineate signaling and trafficking events in infected cells [8, 13–16, 19, 20]. Similarly, GFP-based reporters and microscopy have advanced understanding of virulence gene expression and the extent of population heterogeneity [21, 22].

There is insufficient space to discuss in detail the intricate relationship between *Salmonella* and host cells but information on these topics can be found elsewhere in this volume and in other comprehensive reviews [4, 23, 24]. Here we will focus on the ways microscopy is contributing to research in this field.

1.2 Applications of Microscopy in *Salmonella* Research

1.2.1 Introduction to Microscopy Techniques

Although we will mainly discuss the use of light microscopy (LM) techniques, including conventional phase contrast, fluorescence, and confocal microscopy, it is worth emphasizing that a much broader range of microscopy techniques has been used to study bacterial morphology and the processes involved in infection. For example, transmission electron microscopy (TEM) provides morphological information on *Salmonella* surface structures such as pili, flagella, and T3SS, even yielding molecular level structural information when high-resolution TEM is coupled with advanced image processing and analysis [25–28]. In conjunction with TEM, immunogold labeling offers a useful biological tool to localize proteins of interest and has been used to locate outer membrane proteins and confirm expression of the Vi capsular polysaccharide in *Salmonella* [29, 30]. Scanning electron microscopy (SEM) is also an invaluable technique for revealing the detailed surface structure of individual bacteria, biofilms, and the changes induced on host cells during infection [5, 7, 11, 31–33]. We will briefly discuss some examples of the use of EM and processing techniques we have employed to examine the morphology of *Salmonella* and of membrane ruffles induced during infection of epithelia (Fig. 1) but refer the reader to other papers for detailed technical aspects of the application of EM to study bacterial infection [34, 35].

Atomic force microscopy (AFM) is also capable of providing high-resolution images of surface structures including those on living bacteria [36, 37] and, although it has yet to be widely used to study *Salmonella* infection, it has been employed to study the morphology of protein secretion and translocation pores of *E. coli*, bacterial motility, and biofilm formation [38–43].

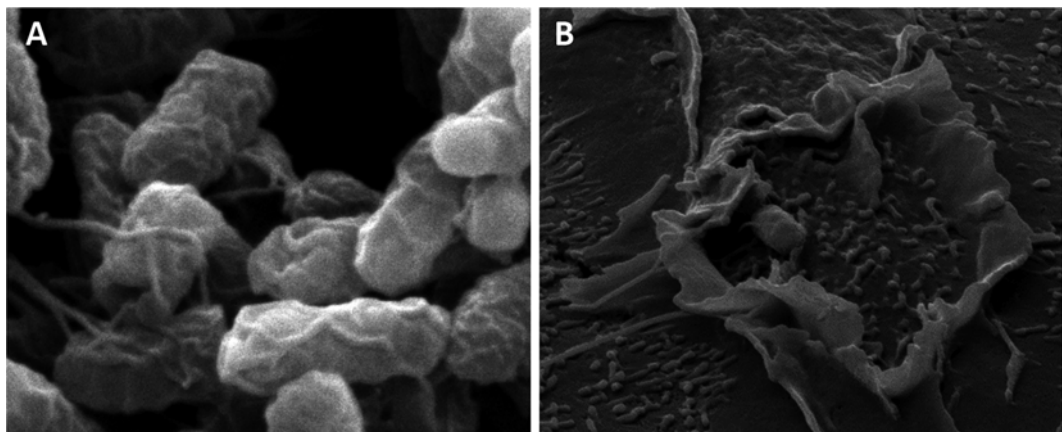


Fig. 1 Scanning electron microscopy (SEM) used to investigate surface structure of *Salmonella* biofilms (panel **a**) and membrane ruffles induced on epithelial cells during infection (panel **b**). Dense *Salmonella* community architecture includes prevalent filamentous material after 48 h growth on plastic coverslips (**a**). Infection of MDCK cells for 15 min with *Salmonella* leads to formation of prominent membrane ruffles (**b**). Panel (**a**): $3.5 \times 2.8 \mu\text{m}$. Panel (**b**): $9 \times 7.2 \mu\text{m}$

Light microscopy techniques are more frequently used to study the interaction of bacteria with cells because they are more readily accessible and, though they fall short of some other techniques in terms of resolution, they are very flexible and can be used to study dynamic processes occurring in living cells. We will discuss some technical aspects of these methods later but will first give a brief introduction to the types of imaging techniques available and how they have been applied to study *Salmonella* infection. Although we are concentrating on the most widely used and accessible techniques it is likely that other techniques will start to become more commonplace in *Salmonella* research. For example, multi-photon (MP) microscopy utilizes the greater penetration of longer wavelength light to study fluorescent entities deep within complex environments and therefore has potential applications in studying the dynamics of host-pathogen interactions during infection of intact tissues as well as intricate biofilm structure [44–46]. This approach was recently used to study *Salmonella*-induced recruitment of dendritic cells into the intestinal epithelium of living mice [47]. Within the past few years, a number of optical and statistical methods have been developed to overcome the traditional diffraction limit to optical resolution improving resolution of LM from 200–250 nm to <100 nm (reviewed in refs. 48, 49). These “super-resolution” microscopy techniques are an area of rapid technological development that will offer new opportunities to bridge the gap between convention LM and EM resolution. Although we are unaware of any publications reporting application of super-resolution microscopy to image *Salmonella*, the recent application of PALM and structured illumination microscopy to image in unprecedented detail the DNA repair machinery, cell wall architecture, and cytokinesis mechanisms in bacteria [50–52] provides proof of principle for their potential application in *Salmonella* research.

Many researchers use a combination of microscopy techniques to address specific questions, reflecting the fact that each has distinct advantages for specific purposes. Having said that, most researchers will not have the luxury of access to a vast range of microscopy systems and here we intend to concentrate primarily on those techniques that are most widely available, namely wide-field microscopy (WFM) and confocal laser scanning microscopy (CLSM).

It is necessary to understand some basic principles underlying LM techniques in order to assess their relative merits for certain applications. The reader requiring more detailed information is referred to other papers dealing with these issues in greater depth [53–55]. WFM can also be referred to as conventional light microscopy and in its simplest form involves a standard upright or inverted microscope (often with fluorescence capabilities) to which a camera (e.g., CCD camera) is added to enable simple image acquisition. The term “widefield” refers to the fact that light is detected

from a broad focal depth so the resulting image approximates that seen by the user through the microscope eyepieces, including both “in-focus” and “out-of-focus” information. WFM imaging systems are highly adaptable, for example they may incorporate shuttering, focus drives, and filter changers to enable the user to automate rapid switching between imaging parameters. These capabilities, together with the high sensitivity of camera systems, which allows rapid image acquisition and minimization of light exposure, makes WFM a popular choice for live cell imaging. Cameras and illumination systems are areas of rapid technological development leading to increased sensitivity, speed, and stability of WFM systems in recent years. This progress seems likely to continue and offers new opportunities for the application of WFM in live cell imaging by optimizing acquisition of quantifiable image data while minimizing the risk of imaging conditions interfering with the cellular processes being investigated.

Since its commercialization in the 1980s, confocal microscopy has become a relatively routine research tool, with CLSM systems in particular being widely available. In CLSM, an image of fluorescence (or reflectance) is acquired point-by-point, or more rarely line-by-line, as a laser is scanned across a field of view. Light emanating from the sample follows a reverse path (is “descanned”) and passes through an aperture (pinhole) to a detector, typically a photomultiplier tube (PMT). In allowing light from only one plane of focus to reach the detector, the confocal aperture facilitates “optical sectioning,” enhancing axial resolution and giving CLSM its major advantage over WFM. Most CLSMs allow simultaneous detection of different fluorophores by selectively directing different wavelengths of emitted light to different detectors. The ability to rapidly switch between excitation wavelengths using an acousto-optic tuneable filter (AOTF) to sequentially excite different fluorophores simplifies separation of their signals and is a standard feature of many modern CLSMs.

When considering CLSM and WFM we are discussing systems with distinct fluorescence imaging capabilities; CLSM providing the best axial resolution achievable with commonly available systems but generally at the cost of sensitivity, speed, increased risk of photodamage, and price. An important caveat to the above generalization is that recent advances in detector and scanning technology have increased the sensitivity and speed of CLSM systems, although these advances are yet to become standard features. It is also worth mentioning an additional type of “confocal” microscopy technique, that of spinning (or Nipkow) disk systems, which in some respects occupy a position in between CLSM and WFM. These systems illuminate specimens with laser light spread across a field of view via an array of pinholes which limit detection to a single level of focus and use a camera to simultaneously detect emitted light from the entire field. Although faster and less prone to inducing photodamage than

conventional CLSMs, which gives them advantages for live cell imaging, spinning disk systems are less flexible in terms of magnification and depth of focus, and provide lower axial resolution than point-scanning confocals. Spinning disk systems offer a very good alternative for imaging at improved axial resolution compared with WFM and have been used extensively for live cell imaging, e.g., of *Salmonella* infection of cultured cells [18, 19] and also for imaging *Salmonella* biofilms [56].

The other principle advantage that CLSM has over WFM and spinning disk systems is that its use of point-scanning allows flexibility over magnification (by “zooming” on a subregion of the specimen). Control of scan geometry also makes CLSM inherently applicable to techniques that require selective illumination of defined areas (photo bleaching, photo activation, uncaging). Selective photobleaching can, for example, be used to study mobility of GFP-tagged cellular proteins in the FRAP (*fluorescence recovery after photobleaching*) technique which has found widespread application in cell biology. For example, FRAP has been used to track the diffusion of effector proteins along *Salmonella*-induced filaments during infection [57]. While addition of photo bleaching lasers to WFM and spinning disk confocals can also enable such techniques on these systems and do this in a way that can be more interactive than CLSM systems, the flexibility of point-scanning systems usually gives them an advantage in this respect.

Up until now we have emphasized increased axial resolution as a major advantage of CLSM but it should always be remembered that this is accompanied by a decrease in sensitivity due to the large proportion of photons that are discarded at the confocal aperture. Moreover, optimal resolution can be a disadvantage where simultaneous detection of fluorescence in a broad depth of field will accelerate data acquisition. Typically, CLSM systems allow the user to open the confocal aperture to increase sensitivity and this is an option well worth exploring whenever sensitivity is favored above optimized resolution, as is usually the case in live cell imaging.

In emphasizing the low axial resolution of WFM systems we have yet to consider improvements that can be made subsequent to image acquisition by image processing. The application of deconvolution algorithms to stacks of WFM images allows reassignment of “out-of-focus” light to its point of origin and can result in marked improvement of image clarity (Fig. 2). WFM coupled with deconvolution can often perform at least as well as CLSM in resolving fluorescent structures, especially when these are of relatively low intensity and samples are relatively thin [58]. However, deconvolution is most effective when stacks of images at relatively narrow focus increments are acquired in a way that optimizes sampling frequency (Nyquist sampling) [54, 58, 59]. Since deconvolution relies on accurate imaging of both in-focus and out-of-focus signal within multiple images, it is reliant on the stability of the imaging

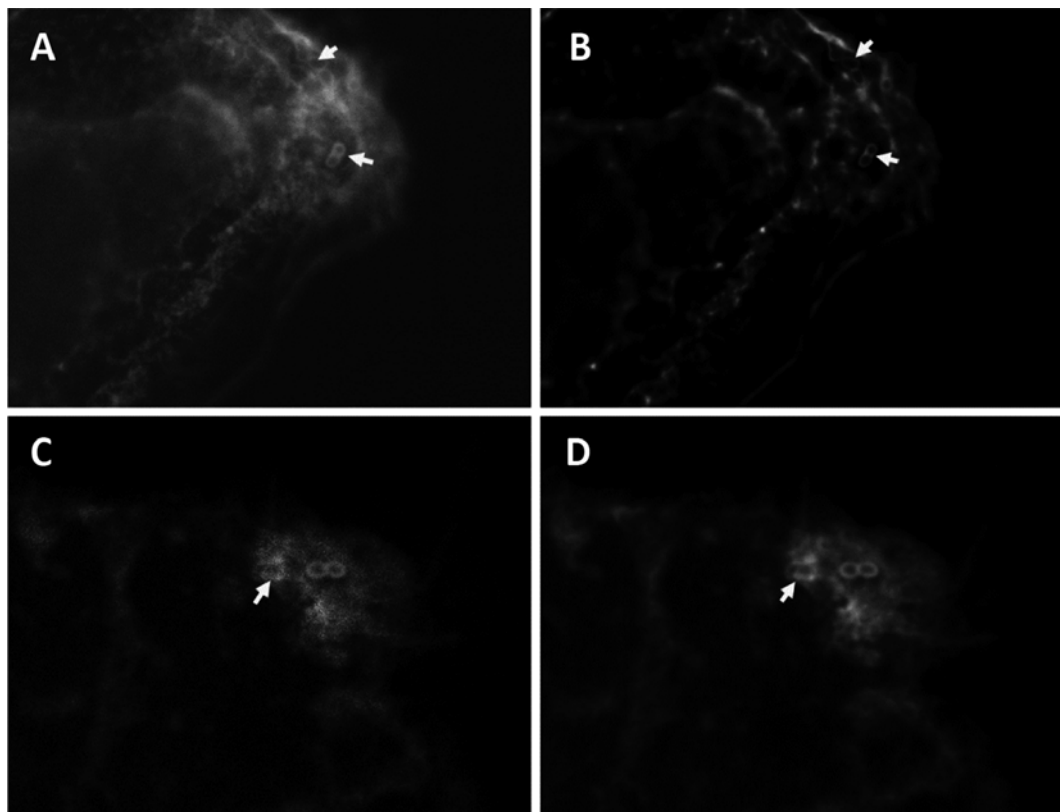


Fig. 2 Comparison of WFM and CLSM imaging and the effects of deconvolution on image clarity. Images of *S. Typhimurium*-infected GFP-actin expressing MDCK cells stained with anti-*Salmonella* antibody and Alexa 555-conjugated secondary antibody to localize bacteria relative to actin cytoskeleton with both channels presented in a single monochrome image. Panel (a): Representative image from a stack of WFM images acquired at 250 nm intervals with a 100 \times oil immersion lens (NA 1.4) throughout the cell depth and beyond with parameters recommended by Huygens software [59]. Panel (b): After deconvolution using Huygens software (and a calculated PSF), a prominent increase in clarity is observed due to removal of out-of-focus fluorescence and increased spatial accuracy within this optical section. Despite the very clear improvement in image clarity, which is especially evident for *Salmonella* localization (arrows), deconvolution has been less effective in removing out-of-focus information from some parts of the actin cytoskeleton due to its highly complex distribution. Panel (c): A representative CLSM image from a stack of 160 nm steps acquired with Leica SP5 AOBS system and a 63 \times glycerine-immersion lens, with pixel size (43 nm) optimized for Nyquist sampling [59] by using the zoom function. Note the improved image clarity compared with the WFM in panel (a) that is especially prominent for the more diffuse actin distribution (arrows). This image nevertheless suffers from a common problem with CLSM imaging, that of low signal-to-noise and a tendency for high-resolution images to appear “speckly.” Panel (d): CLSM image as shown in panel (c) following deconvolution (Volocity software) improves resolution and reduces noise. Field of view approx 42 \times 32 μ m (panels a, b) and approx. 28 μ m \times 21 μ m (panels c, d)

systems and susceptible to any movement of fluorescent entities during stack acquisition. The effectiveness of deconvolution depends on the robustness of the algorithms applied and these vary significantly between commercial software packages. Because deconvolution can be problematic for reasons outlined above, high-resolution images can generally be obtained more simply

using CLSM and this technique is thus preferred by most researchers unless the advantages of WFM outweigh these issues, e.g., when fluorescent signal is necessarily low. It should also be noted that deconvolution can also enhance confocal data by removing remnant out-of-focus information and signal noise that arises from inherent low signal-to-noise ratio of CLSMs (Fig. 2). It is generally accepted that CLSM is likely to out-perform WFM/deconvolution when thicker specimens with more complex distributions of fluorescence are to be imaged, since the contribution of “out-of-focus” fluorescence has a more profound effect on image resolution in such circumstances [54, 58]. For this reason CLSM has distinct advantages when studying *Salmonella* infection of polarized epithelia and intact tissues.

1.2.2 Microscopical Localization of *Salmonella* in Cells and Tissues

Monitoring bacterial invasion and precise localization of *Salmonella* within cells and tissues is a routine requirement in *Salmonella* research. *Salmonella* invasion of epithelial cells in guinea pig ileum was first observed in TEM studies [60] and subsequent studies built on these observations using a combination of light and electron microscopy (SEM and TEM) techniques [5, 6, 61]. Examination of tissues by TEM alone is relatively laborious and for this reason most studies will examine a limited number of cells and thus potentially bias observations and overlook significant events [62]. Therefore, where the optimal resolution of TEM is not required, methods that allow *en face* imaging of extensive areas of epithelium have a distinct advantage in facilitating observation of interactions of *Salmonella* with many cells. For example, CLSM has been used to localize *Salmonella* adhered to and within M cells in intact Peyer’s patch tissue preparations, while parallel studies with SEM—sometimes examining the same cells previously imaged by CLSM in a primitive form of CLEM (correlative light electron microscopy), allowed surface morphology of *Salmonella*-infected epithelial cells to be examined [5, 62, 63]. Similar techniques have also been applied to precisely localize infrequently encountered *Salmonella* within thick sections of intestine and liver [64, 65].

Identification of *Salmonella* using specific antibodies in conjunction with fluorescently labeled secondary antibodies rapidly became the main method for localizing *Salmonella* in relation to cellular components or in specific cell types [66, 67]. Antibody staining has also been used to differentiate between, and quantify, internalized and external bacteria after infection of cells, exploiting the fact that bacteria within intact eukaryotic cells are inaccessible to externally applied antibodies unless the plasma membrane is permeabilized. This method is sometimes regarded as an alternative to the more commonly used, and arguably less laborious, gentamicin-protection assay of bacterial internalization. However, differential immunolabeling of adhered and invaded bacteria has distinct advantages in that adherence and invasion are quantified in the same cells, it provides information on heterogeneity in distribution

of *Salmonella* within cells and it allows simultaneous monitoring of cell damage—cytotoxicity and cell loss being a potential source of serious artifacts in the gentamicin-protection assay. Variations of differential immunolabeling technique have been used. One uses transfer of cells to ice-cold PBS before application of ice-cold antibodies to label external *Salmonella* prior to fixation, and permeabilization with methanol to allow access of antibodies to internalized bacteria in a second round of labeling with a different fluorophore [68, 69]. We have adopted a variation of this technique that allows more flexibility with the timing of labeling by using paraformaldehyde (PFA) to fix, but not permeabilize, cells [22]. The samples can then be labelled with antibodies to localize external bacteria, permeabilized with Triton X-100, then re-stained with antibodies and an alternative fluorophore to label all bacteria (described in Subheading 3.3.2). In our hands, each of these immunolabeling methods has proved more reproducible for assaying bacterial invasion than the gentamicin-protection assay. Immunolabeling to discriminate external and internal bacteria can also be employed along with additional antibodies, or GFP expression, to localize cellular components or transfected cells, enabling quantification of invasion in transfected versus nontransfected cells to investigate the effect on infection of modulating host protein expression [70].

Expression of GFP or alternative fluorescent proteins such as mCherry is now widely used to localize *Salmonella* since it avoids the need for additional labeling steps and enables live cell imaging [18, 19, 71, 72]. Genetic manipulation of bacteria, although arguably more time consuming and technically challenging to engineer, can provide users with real time information which can be applied *in vivo*. Another advantage of this technique is that it provides less complicated sample preparation compared to antibody labeling techniques. GFP labeling has also been used in conjunction with immunolabeling to differentiate internalized bacteria from external ones using a simplified technique based on that described later (Subheading 3.3.2), only requiring fixation and one round of antibody labeling to localize external bacteria, GFP marking both external and internal bacteria [68]. Alternative fluorescent proteins, such as GFP and mCherry, can discriminate between bacterial populations [20] and offer the potential to simultaneously follow infection of distinct *Salmonella* strains during coinfection. It is important to consider the impact that high levels of fluorescent protein expression might have on bacterial fitness and to perform appropriate controls to test for this possibility. Indeed some studies have highlighted adverse effects of plasmid carriage on *Salmonella* infection [72, 73]. Single-copy expression of GFP is less likely to affect bacterial behavior [21].

In addition to providing a method of detecting and enumerating *Salmonella*, GFP expression may be coupled to specific promoters to monitor expression of particular genes or sets of

genes, either microscopically or through the use of flow cytometry or fluorescence-activated cell sorting (FACS). The “differential fluorescence induction” technique of Valdivia and Falkow [74], which utilizes GFP and FACS, identifies promoters whose expression depends on particular environmental stimuli, such as low pH, or are expressed during infection of specific cells or tissues [74, 75]. GFP-promoter constructs have been shown to report gene induction in *Salmonella* as accurately as *lacZ* gene fusions, are being used successfully to monitor gene induction in vitro and during infection of mammalian cells [18, 21, 22] and have the potential to be applied in animal infection models.

Fluorescence microscopy, including CLSM, has also been used to locate translocated effector proteins within infected cells using antibodies to the effector protein itself or, more commonly, epitope tags [76–78]. Use of full length GFP as a means of fluorescently labeling effectors has not been possible since the GFP molecule blocks transfer into host cells. Other methods have recently been devised to measure the rate of translocation of effector proteins that, due in part to the rather small numbers of molecules translocated into host cells, have proved difficult to localize by immunolabeling. For example, *Salmonella* effector translocation has been studied using a sensitive method employing tagging of effector proteins with TEM-1 beta-lactamase. Treatment of cells with a fluorescent lactamase substrate CCF2/AM that is sequestered in the cytoplasm allows detection of TEM-1-tagged proteins translocated into the cells [79]. By effectively amplifying the signal from individual effector molecules this method enhances detection sensitivity and, despite its inability to precisely localize effector proteins (due to diffusion of fluorescent enzyme product) has proven potential as a sensitive single cell assay of translocation. Quantitative immunolabeling of SipA within *Salmonella* after defined periods of interaction with host cells (determined by live cell imaging prior to fixation and labeling) has been used to estimate the rate of transfer of SipA into the host cell [10].

Detection of SopE2 and SptP delivery into host cells has also been examined using the tetracycline-dependent FlAsH tag to fluorescently label effector protein within bacteria and monitor its secretion as loss of signal during infection of host cells [80]. An elegant “split GFP” method was also employed to detect effector delivery, whereby effectors were linked to a small part of GFP, to enable translocation. Reconstitution of full GFP was then enabled by expression of the remaining part of the molecule in host cell cytoplasm so that effector delivery could be effectively monitored by appearance of GFP fluorescence [57].

1.2.3 Imaging Cellular Responses to *Salmonella* Infection

When microscopy methods were first used to study *Salmonella*-infected cells and tissues, it became clear that entry of *Salmonella* into epithelial cells involved major changes in cell morphology.

Formation of the characteristic *Salmonella*-induced “membrane ruffles” was studied extensively using TEM [60, 61, 81] and SEM [61, 62, 69, 82], and fluorescence labeling with LM helped determine how the redistribution of actin and other cytoskeletal proteins promoted formation of these ruffles [3, 61, 67]. With the discovery of the SPI-1 T3SS, attention has turned to unraveling the roles of the various effector proteins in triggering cellular responses associated with bacterial pathogenesis.

Much of the research studying the mechanisms of *Salmonella* invasion has been based on infection of cultured cells. Such model systems have clear advantages in being relatively simple to set up, maintain, genetically manipulate and analyze. However, it is always important to critically consider whether they accurately reflect *in vivo* infection. For example, using nonepithelial and nonpolarized epithelial cells, e.g., HeLa, as a surrogate for epithelia should be interpreted with caution, as these cells do not always mimic the changes occurring in polarized epithelial cells and tissues during *Salmonella* infection.

Although cultured cells are often considered to be relatively homogeneous, *Salmonella* infection of cells is notoriously heterogeneous and this can limit the effectiveness of quantitative analysis unless large samples are imaged and analyzed. This has highlighted the value of scaling up image acquisition and analysis, e.g., by applying high content imaging techniques to mechanistic studies of *Salmonella* invasion and the role of host cell proteins in different stages of the infection cycle [83, 84]. Recent studies utilizing microscopy have also highlighted factors affecting heterogeneous infection of cells, including the role of “skimming” motility in promoting invasion of cells with a prominent profile [12] and the role of vacuolar escape and subsequent replication within subpopulations of cultured epithelial cells [19]. While the use of micropatterned cells may offer some benefits for standardization of cell morphology for some infection studies [13] there remain questions regarding how closely such manipulated cells resemble *in vivo* epithelia.

When studying *Salmonella* infection of polarized epithelial cells, CLSM has distinct advantages over WFM, which is often prone to “out-of-focus” light interfering with image resolution, even if deconvolution is applied. The redistribution of cellular proteins induced by bacterial infection has therefore been monitored by confocal microscopy in a large number of studies in both polarized epithelial cells [85–87] and in intact tissues [1, 62, 65, 87–89]. It is of course not an absolute requirement to use confocal microscopy for all fluorescence imaging and excellent results can be obtained with conventional WFM, especially on flatter cultured cells [76], and spinning disk microscopes [18, 19].

Understanding how *Salmonella* trigger cellular responses relies on studying highly dynamic processes. In the early 1990s, studies using a combination of fluorescence labeling, EM and live cell

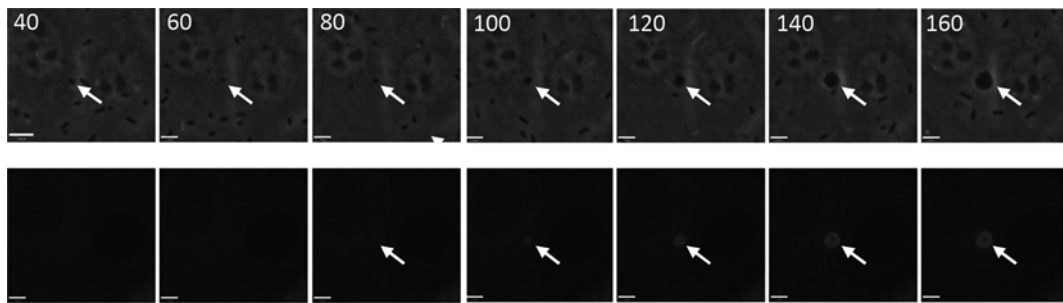


Fig. 3 Use of time-lapse phase contrast and fluorescence WFM to examine membrane ruffle propagation and development in GFP-actin expressing MDCK cells. Representative phase contrast (*top row*) and fluorescence (*bottom*) images of a membrane ruffle generated by wild-type *S. Typhimurium* (SL1344) is shown at distinct points in ruffle development during a 20 min time course. Timestamps on each image indicate relative time compared to the first image in which the bacterium (arrows) responsible for inducing this membrane ruffle attached to cells (0 s). Increased fluorescence due to GFP-actin concentration as *Salmonella* induce membrane ruffling is evident by 80 s following attachment (arrow) and very prominent at 100 s and later time points (arrows), when ruffling is also clearly evident in phase contrast images (arrows). Scale bar = 5 μ m

imaging demonstrated that the triggering of membrane ruffling occurs soon after *Salmonella* adherence to the surface of cells [61]. Several studies have demonstrated the value of live cell imaging in determining the sequence of rapidly occurring events during *Salmonella* invasion, which can be obscured by the nonsynchronized nature of *Salmonella* interaction if studies are limited to the examination of cells fixed at discrete time-points during infection [72, 90]. Live cell imaging is also being supported by developments in image analysis, including tracking algorithms which can semi-automate analysis of complex dynamic processes.

Imaging cellular processes in living cells can frequently reveal facets of bacterial interactions with host cells that would be impossible to determine by other means. This is especially evident when using specific fluorescent probes, e.g., indicators of signaling events and GFP-tagged proteins (e.g., [8, 14, 15]). An example of live cell imaging of *Salmonella* infection of GFP-actin expressing epithelial cells is illustrated in Fig. 3. Such probes enable monitoring of the redistribution of proteins and other cellular changes in real time and have revealed some of the dynamic processes occurring during *Salmonella* invasion. An example from our own research is the identification of cycles of PI(3)P generation on *Salmonella*-containing vacuoles (SCVs) over several minutes, which were revealed by live cell imaging of *Salmonella* invading cells stably expressing GFP-FYVE [8]. Without live cell imaging, the fact that a proportion of SCVs were labelled with PI(3)P would have led to the assumption that this indicated a temporary location rather than the repeated cycles of acquisition and loss identified in this study [8]. Similarly, live cell imaging revealed highly dynamic tubulation of

SCV-associated compartments during early infection of SNX1-GFP expressing epithelial cells which were less evident in fixed cells due to their tendency to be poorly preserved during fixation [15].

Longer-term live cell imaging can also be used to study later events occurring post-invasion; including SPI-2-mediated effects on intracellular trafficking, SCV development and maturation, and bacterial division [16, 19]. However, prolonging the time-course over which images are acquired can be challenging as cells are more prone to damage during such experiments, especially from photo-damage if fluorescent images are acquired. Focus drift during prolonged imaging has also been a common cause of frustration but this can now be largely prevented by use of focus correction devices which detect, and adjust for, movement of a reference point such as reflection from a coverslip. As discussed earlier, WFM has distinct advantages for live cell imaging where the high-intensity excitation required for CLSM is more likely to impair cellular processes. Nevertheless, advances in confocal technology, e.g., spinning disk, hybrid detectors, open up further opportunities for long-term higher resolution imaging [19]. The additional challenges of prolonged imaging have, however, resulted in most studies of longer term infection to date being limited to static imaging techniques [10, 11, 91].

1.2.4 LM Imaging of *Salmonella* Properties and Behavior

A wealth of LM techniques are available to study aspects of *Salmonella* biology aside from infection. Often these are well suited to WFM because they can be applied to bacteria within a narrow focal depth in suspension or on agar-coated coverslips. Motility, growth, and septation can be examined in time-lapse studies which are often limited to phase contrast as a convenient means of locating and potentially tracking bacteria due to high contrast between the bacteria and growth medium. An example of the use of this technique to study septation of filamentous *Salmonella* [92] is illustrated in Fig. 4. The combination of LM with microfluidics apparatus provides detailed information on growth patterns under precisely controlled conditions [93]. Growth of GFP-expressing *Salmonella* has also been studied by WFM to assess the impact of SPI gene expression on growth rates [94]. Further, in addition to using phase contrast microscopy as a simple test of bacterial motility, flagellar dynamics have also been studied in detail following their specific labeling with fluorescent dyes [95, 96].

The integrity and metabolic status of bacteria can also be assessed by fluorescence labeling. The most commonly used technique for assessing viability is the Live/DeadTM BacLightTM kit from Molecular Probes/Invitrogen. This distinguishes “live” and “dead” bacterial cells using two spectrally discrete fluorophores with different permeabilities. One (green) fluorophore is internalized by all cells, while the other (red) dye can only be internalized by cells with compromised membranes, the “dead” population. Live/dead staining has

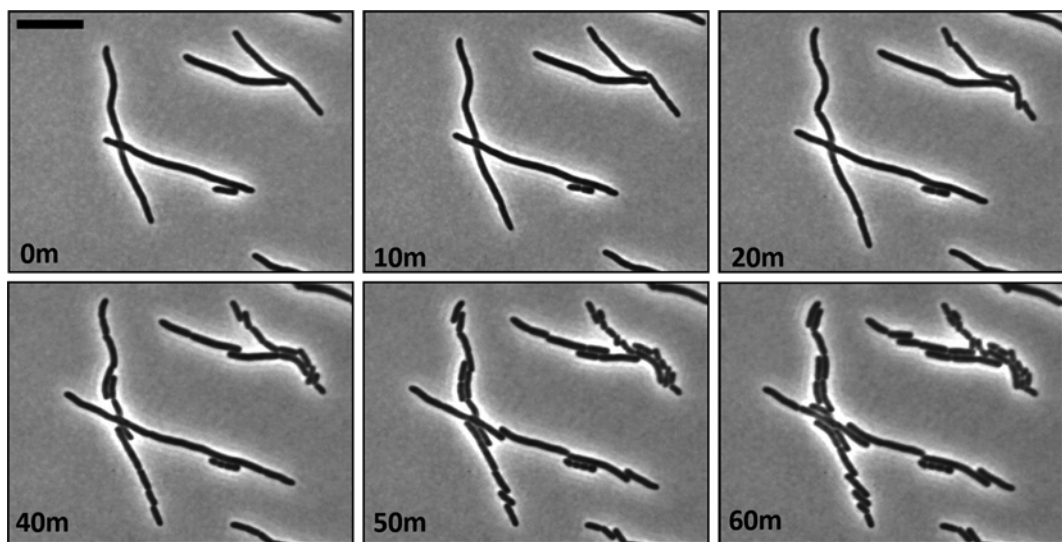


Fig. 4 Septation of filamentous *Salmonella* monitored by phase contrast microscopy following relief from filament-inducing conditions. *Salmonella* on agar disks imaged every 2.5 min to follow the septation process. Figures refer to time intervals (minutes) for each figure. Scale bar represents 10 μ m

been used to monitor *Salmonella* viability under adverse growth conditions [92, 97] and during infection of macrophages [98]. Along with an alternative labeling method that monitors bacterial “vitality” with an insoluble fluorescent product of electron transport chain activity (RedoxSensorTM kit from Molecular Probes/Invitrogen; [99]), it has the potential to find further applications in *Salmonella* research.

2 Materials

2.1 Preparing Cell Monolayers

1. Most of our *Salmonella* infection studies have utilized Madin-Darby canine kidney (MDCK) epithelial cells and the details of culture methods given here are specific for these cells. Infection of other cells, both epithelial, e.g., Caco-2, HeLa, Hep-2, and nonepithelial, e.g., macrophages, COS cells, can be studied using similar methods.
2. Cell culture medium: Minimum Essential Eagle’s Medium, supplemented with 1 % (v/v) GlutaMAX (Gibco, Life Technologies Paisley, UK), 10 % (v/v) fetal calf serum (Biosera, Boussens, France), 1 % (v/v) nonessential amino acids (Gibco) and 100 μ g/ml kanamycin (Sigma-Aldrich, MO, USA) (see Note 1).
3. Glass coverslips: 13 mm diameter, thickness #1 from VWR International (PA, USA), Menzel-Gläser (Braunschweig, Germany) or Corning Inc (NY, USA) (see Notes 2 and 3).
4. 75 % (v/v) ethanol in dH₂O.

2.2 Infecting Cell Monolayers for Immunofluorescence Microscopy

1. Luria-Bertani (LB) broth and LB agar plates, e.g., from Merck Millipore (MA, USA).
2. *Salmonella* strains grown overnight in LB broth, diluted 1:100 in fresh LB and grown in a shaking incubator at 37 °C for 3.5–4.0 h, 150 rpm (see Note 4).
3. Modified Krebs' buffer: 137 mM NaCl, 5.4 mM KCl, 1 mM MgSO₄, 0.3 mM KH₂PO₄, 0.3 mM NaH₂PO₄, 2.4 mM CaCl₂, 10 mM glucose and 10 mM Tris, adjusted to pH 7.4 at 37 °C with HCl (see Note 5).

2.3 Immunofluorescence Microscopy

1. Phosphate buffered saline (PBS), pH 7.4.
2. Fixative: 2 % (w/v) paraformaldehyde (PFA) in PBS (see Note 6).
3. Permeabilization buffer: 0.3 % (v/v) Triton X-100 in PBS.
4. Primary antibody: Either a specific monoclonal or polyclonal antibody generated against an antigen of interest, or an antibody fragment in some cases.
5. Secondary antibodies: Commercial fluorochrome-conjugated antibodies specific for the primary antibody (see Note 7).
6. TRITC-conjugated phalloidin from Sigma (see Note 8).
7. Mounting media: We use Vectashield® mounting media for preservation of fluorescent labeling, usually employing the version supplied with DAPI (Vector Laboratories Inc, CA, USA) (see Note 9).
8. Clear nail varnish.
9. Fluorescence microscope with appropriate fluorescence filters: Leica DMLB2 (Leica, Mannheim, Germany (see Note 10).

2.4 Confocal Laser Scanning Microscope (CLSM)

1. CLSM: Leica TCS SP5 AOBS attached to a Leica DMI6000 inverted epifluorescence microscope (see Note 11).

2.5 Live Cell Imaging

1. Modified Krebs' buffer (see above and Note 5).
2. Imaging dishes: 35 mm diameter (MatTek Corporation, MA, USA).
3. Microscope system and hardware: The systems we routinely use are based on Leica DMIRB inverted microscope. One has a Hamamatsu ORCA ER (12-bit CCD) camera and Prior Scientific filter wheel and shutters. The other has a Photometrics HQ2 camera, a Sutter DG5Plus illumination device, Ludl filter wheels and a PiFoc piezo focus (see Note 12).
4. Image acquisition software: Volocity™ (Improvision/Perkin Elmer, Coventry, UK) or Metamorph (Molecular Devices, Sunnyvale, CA, USA) (see Note 12).
5. Microscope incubation chamber from Solent Scientific (Segensworth, UK) (see Note 13).

2.6 Agar-Disk Imaging Technique

1. 13 mm glass coverslips (thickness #1; VWR).
2. 75 % (v/v) ethanol.
3. 90 mm diameter petri dish (Greiner Bio-one, Frickenhausen, Germany).
4. LB agar.
5. *Salmonella* strains grown as required (see above and Note 3).
6. Metal imaging coverslip chamber for 22 and 24 mm coverslips (custom made).
7. 22 mm glass coverslips (thickness #1; VWR)
8. Microscope system and hardware: Leica DMRB inverted microscope (Leica Microsystems, Mannheim, Germany) with a CCD camera (Hamamatsu) (see Notes 11 and 12).

2.7 Preparation of Bacteria for Scanning Electron Microscopy

1. PBS, pH 7.4.
2. 13 mm glass coverslips (thickness #1).
3. Fixative: 2.5 % (v/v) glutaraldehyde in 100 mM phosphate buffer pH 7.4.
4. Ethanol: 25, 50, 75, 90, and 100 % (v/v) in dH₂O.
5. Hexamethyldisilazane (Sigma-Aldrich, Poole, Dorset, UK).
6. SEM specimen stubs 0.5" (Agar Scientific, Stansted, UK).
7. Specimen carbon adhesive tabs 12 mm (Agar Scientific, Stansted, UK).
8. Gold sputter-coater: Emitech K575x (Quorum Technologies, Lewes, UK).
9. Scanning electron microscope: FEI Quanta 400 SEM (FEI, Eindhoven, Netherlands).

3 Methods

3.1 Preparing Cell Monolayers

1. Place glass coverslips between two pieces of tissue and spray with 75 % ethanol to sterilize. When dry, use forceps sterilized in 75 % ethanol to transfer the coverslips into the appropriate well plate (see Note 14).
2. Seed coverslips in well plates (or filters as appropriate) with epithelial cells. The number of cells used depends on the experimental requirements (see Note 15).
3. Incubate at 37 °C in humidified atmosphere with 5 % (v/v) CO₂ until required confluence reached—generally 2–4 days.

3.2 Infection of Cell Monolayers for Immunofluorescence Microscopy

The following protocol includes volumes and other details specific for infection of cells grown on 13 mm coverslips. These would need to be adjusted for cells grown on other substrates.

1. Wash cells three times with 1 ml prewarmed Krebs' buffer, with the final wash media remaining in the well. Incubation for 10–15 min at 37 °C allows equilibration of the cells in the buffer.
2. Add 50 µl of the log phase *Salmonella* culture to the wells to give a multiplicity of infection (m.o.i) of approximately 50 (see Note 16).
3. Incubate cells for the required time at 37 °C (see Note 17).
4. To remove nonadherent bacteria, extract each coverslip from the well plate with forceps and wash, with moderate agitation, in a beaker of PBS.
5. Place the coverslip in a well of a 12-well plate filled with 1 ml of 2 % PFA, and leave to fix for 45 min (or longer) at 4 °C.

3.3 Fluorescence Microscopy

There are multiple protocols that may be employed for immunofluorescence microscopy depending on which components of the cell/bacteria are to be localized. We introduce two representative protocols which we routinely use; the first for localization of *Salmonella* and F-actin, the second to measure *Salmonella* invasion by separately labeling the adhered and entire bacterial populations associated with cells. In each case, volumes refer to labeling of cells on 13 mm coverslips. Volumes should be increased as required for larger coverslips or permeable supports.

3.3.1 Staining F-Actin and *Salmonella*

1. After fixation in PFA for at least 45 min (overnight if convenient), wash the coverslips in a beaker of PBS and place in a well containing 1 ml of 0.3 % (v/v) Triton X-100 for 10 min to allow permeabilization (see Note 18).
2. Wash coverslip again in PBS and place in a well of 1 ml PBS.
3. Remove excess PBS from the coverslip by blotting with tissue paper (see Note 19) before transferring to an empty well.
4. Incubate cells with 50 µl of primary antibody, in our case goat anti-*Salmonella* CSA-1 antibody (Kirkegaard and Perry Laboratories, MD, USA) diluted 1:200 in PBS, for 45 min at room temperature (RT). Replace the lid on the plate to prevent drying (see Note 19).
5. Add a little PBS to each coverslip to aid its removal from the well plate with forceps. Wash each coverslip in PBS and place in a well of 1 ml PBS, before transferring to an empty well.

6. Incubate cells with 50 μ l of secondary antibody (we use Alexa Fluor[®] 488 anti-goat antibody from Molecular Probes, Life Technologies) and TRITC-conjugated phalloidin (Sigma), diluted in PBS, for 45 min at RT in the dark (replace lid on the plate to prevent drying, and cover with foil to limit photo-bleaching) (*see Note 20*).
7. Remove coverslip from the well plate, wash in PBS, wipe the back of the coverslip and blot with tissue to remove excess liquid.
8. Mount coverslips by placing cell side down on microscope slides with a small drop of mounting media (we generally use Vectashield[®] mounting media with DAPI; *see Note 9*). Remove excess mounting medium by gently overlaying tissue on top of the mounted coverslips.
9. Affix the edges of the coverslip with a minimal amount of clear nail varnish and allow to dry for at least 15 min and/or store at 4 °C, in order to seal and hold the coverslip in place.
10. Store slides in the dark prior to examination in order to reduce photo bleaching.
11. Examine cells using a fluorescence microscope with the appropriate filters and objective lens (*see Note 10*).

3.3.2 Differential Antibody Staining of Adhered/Invaded *Salmonella* (See Note 21)

1. After fixation in PFA, wash coverslip in beaker containing PBS and place in a well containing 1 ml PBS, before transferring to an empty well (**Note 19**).
2. Incubate cells with 50 μ l of primary antibody (anti-*Salmonella* CSA-1 antibody from Kirkegaard and Perry Laboratories) diluted 1:200 in PBS, for 45 min at RT. As no permeabilization step has been performed, only the *Salmonella* adhered to the cell surface are accessible to antibodies at this stage. Place the lid on the well plate to prevent drying (*see Note 20*).
3. Remove coverslip from the well plate, wash in PBS, and place in a well of 1 ml PBS, before transferring to an empty well.
4. Incubate cells with 50 μ l of secondary antibody (we use Alexa Fluor[®] 555 antibody from Molecular Probes, Life Technologies) diluted 1:200 in PBS, for 45 min at room temperature. During this incubation and all subsequent steps, replace lid on the plate to prevent drying and cover with foil to protect fluorophores from bleaching.
5. Remove coverslip, wash in beaker of PBS and place in a well containing 1 ml of 0.3 % (v/v) Triton X-100 for 10 min to permeabilize the plasma membrane.
6. Remove the coverslip from the well plate, wash in PBS, and place in a well of 1 ml PBS, before placing in an empty well.

7. Incubate cells again with 50 μ l of anti-*Salmonella* antibody (as above) diluted 1:200 in PBS, for 45 min at RT. This time both adhered and invaded *Salmonella* will be accessible to antibodies allowing enumeration of all *Salmonella* associated with cells.
8. Remove coverslip from the well plate, wash in PBS, and place in a well of 1 ml PBS, before transferring to an empty well.
9. Incubate cells with 50 μ l of secondary antibody conjugated to a different fluorophore (we use Alexa Fluor[®] 488 anti-goat antibody) diluted 1:200 in PBS, for 45 min at RT. Using a different fluorophore at this stage to label the total population allows the adhered bacteria to be visualized as a separate population, enabling enumeration of adhered and invaded *Salmonella*.
10. Remove the coverslip, wash in PBS, wipe the back of the coverslip and blot edge with tissue to remove excess liquid.
11. Mount coverslips cell side down on microscope slides using a drop of mounting media (we use Vectashield[®] mounting media with DAPI, *see Note 9*). Remove excess mounting medium by gently overlaying tissue on top of the mounted coverslips.
12. To seal and hold the coverslip in place, paint edges of coverslip with a minimal amount of clear nail varnish and leave to dry for 15 min and/or store at 4 °C excluding light.
13. Examine cells with a fluorescence microscope using the appropriate filters and objective lens (*see Note 10*).

3.4 Confocal Laser Scanning Microscopy (CLSM)

Although we have provided a protocol for imaging triple-labelled *Salmonella*-infected MDCK cells using a Leica CLSM system (*see Note 10*) as used to generate Fig. 2, the general principles described are applicable to other CLSM systems.

1. Select 63 \times objective lens (glycerine immersion; 1.3 NA).
2. Examine the slide to locate suitable area for imaging. At this stage it is worth taking care to ensure the image is as clear as expected by eye (*see Note 22*).
3. Select appropriate zoom factor as required (*see Note 23*).
4. The confocal aperture (or “pinhole”) is normally left at the default setting (equivalent to 1 Airy Unit) to optimize resolution (*see Note 24*).
5. Select averaging, e.g., averaging three frames as in Fig. 2, to reduce the effect of detector noise (*see Note 25*).
6. Select appropriate laser power for each fluorophore to allow images of these brightly stained cells to be acquired, with HyD detector settings preferably below 80 % to reduce detector noise. With the CLSM system used, laser powers of <10 % generally provide sufficient signal (*see Note 26*).

7. Using the “TRITC” setting for red fluorophores, locate and select the top and bottom extremes of the cell. This allows a stack of images to be acquired at user-defined intervals within the selected limits (*see Note 27*).
8. After adjusting AOTF setting and PMT voltage for each fluorophore (Alexa 555, GFP and DAPI), and phase contrast (or brightfield or DIC) if required, save these settings to allow sequential imaging of the three fluorophores (*see Note 28*).
9. Choose option for sequential imaging and import previously defined Alexa 555, GFP, and DAPI settings to allow switching between three excitation wavelengths during image capture (*see Note 29*).
10. Acquire image sequence and save as a stack of TIFF files (the default save option), which can be easily exported to other software.

3.5 Live Cell Imaging: Time-Lapse Phase Contrast Microscopy

Although this protocol refers to the phase contrast imaging we routinely perform to examine propagation of membrane ruffles (Fig. 3), the automated imaging can be modified to include fluorescence imaging, e.g., GFP and/or other fluorophores or for differential interference contrast (DIC) imaging (*see Note 30*). The live cell imaging described here can be performed using a reasonably low cost system but faster switching and focussing, and more sensitive cameras are also available (*see Note 11*).

1. Make sure the microscope incubator has been running for at least 30 min, and preferably longer, to allow required temperature to be achieved and stabilized.
2. Wash imaging dishes which cells have been grown in (as described in Subheading 3.1) twice with warm (37 °C) modified Krebs’ buffer.
3. Prewarm imaging dish within microscope incubator. The time taken to move the dish between rooms will be enough for its temperature to drop so it is best to allow 5–10 min on the microscope stage before imaging.
4. Examine cells under phase contrast or GFP optics and select a suitable area for imaging.
5. Open Improvision Velocity software and a previously used automation for the acquisition of images using hardware described in Note 12. We typically set up the automation to capture images at three focal depths (at 1.5 μm increments to ensure data is acquired at correct level and allowing for the possibility of minor stage drift) at 10 s intervals over a 20–30 min time course. Run the automation prior to the start of imaging to allow for trouble-shooting and to optimize the quality of the images obtained, for example by adjusting focus and lamp intensity.

6. Adjust automation to include specific exposure times and focus increments for all channels. These could be standard protocols for established techniques or ones set according to the specific requirements of the sample (see **Note 31**).
7. When ready to start imaging, begin the automation and then, after 1–2 min, add 50 μ l of log phase culture to the Krebs' buffer in the coverslip holder (see **Note 32**).
8. Images can be exported for processing and analysis in the Volocity format to an off-line workstation running Volocity core software. Alternatively images can be exported as a stack of TIFF images for processing with other software.

3.6 Imaging Live Bacteria: Agar-Disk Imaging Technique

This method can be used to examine bacterial suspensions, for example to assess GFP expression, viability or to monitor division (as in Fig. 4).

1. 13 mm coverslips are sterilized by placing them between two pieces of tissue and spraying with 75 % (v/v) ethanol. When dry, forceps sterilized in 75 % ethanol should be used to transfer the coverslips to a sterile petri dish.
2. To make agar disks, 200 μ l of molten LB agar—supplemented with antibiotics if appropriate—is applied to the center of each 13 mm coverslip and allowed to set (Fig. 5).
3. To prepare a sample for imaging, spread 7 μ l of fixed or live bacterial culture onto a 13 mm agar disk and allow it to dry for 1 min at room temperature.
4. Prepare a metal imaging chamber to receive the agar disk by mounting a 22 mm glass coverslip over the rubber O-ring and screwing the base of the imaging chamber tightly against the glass to form a seal.
5. Using sterilized forceps to grasp the glass base of the agar disk, invert it into the imaging chamber with the bacterial sample resting against the large glass coverslip (Fig. 5).
6. To capture phase contrast images of the bacterial sample, mount the imaging chamber onto a Leica DMIRBE inverted microscope with an appropriate 63 \times or 100 \times oil-immersion lens and a CCD camera (as above and see **Notes 10** and **33**). All images and time-lapse sequences should be captured at maximum resolution if possible.

3.7 Preparation of Infected Cells for Scanning Electron Microscopy

This protocol describes how to prepare *Salmonella* cultures for visualization by SEM, however the general principles described here are also applicable to other SEM systems. This protocol is a quick method that is adequate for our requirements but improved results may be obtained in some cases using protocols involving additional fixation steps and/or critical point drying.

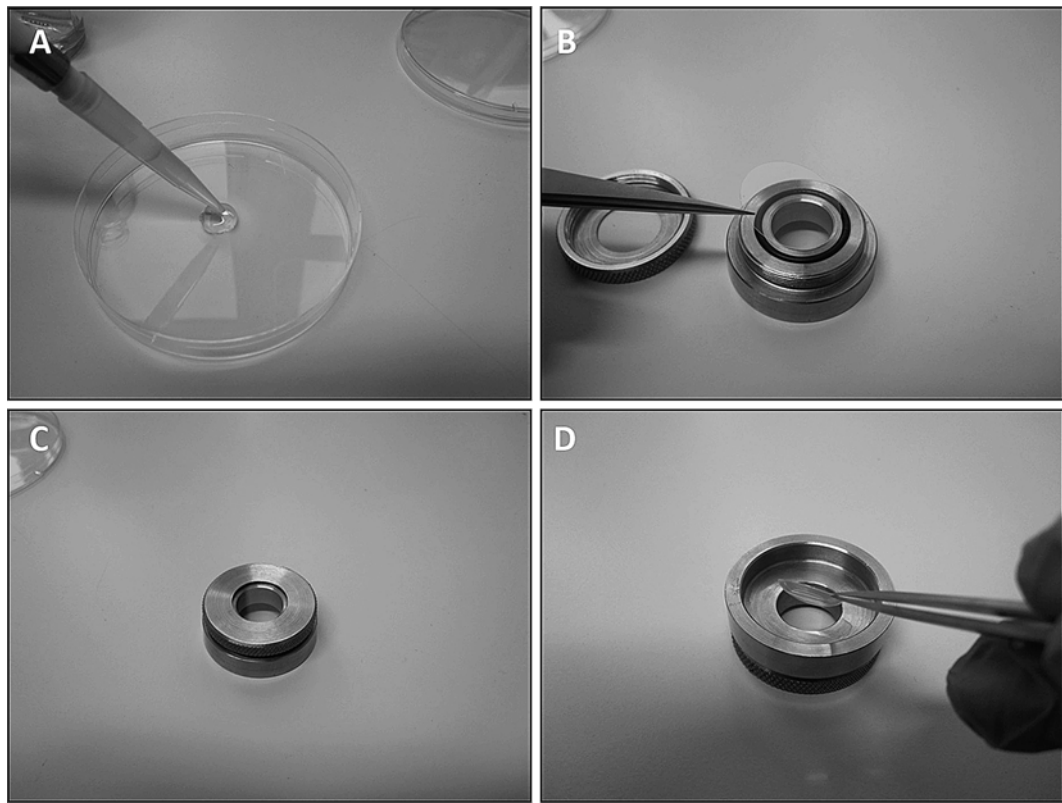


Fig. 5 Agar disk imaging technique. **(a)** 13 mm agar coverslips are prepared by spreading 200 μ l molten LB agar onto sterile 13 mm glass coverslips. Once set, 7 μ l of bacterial sample is spread onto the surface of the agar and allowed to dry for 1 min. **(b)** Using forceps, a 22 mm glass coverslip is mounted onto a metal imaging chamber over the O-ring seal. **(c)** The base of the metal imaging chamber is screwed on tightly against the glass coverslip to form a seal. **(d)** Using forceps, the agar disk is then inverted into a metal imaging chamber, with the bacterial sample resting against the glass coverslip

1. Following infection of monolayers as described in Subheading 3.2 (see Note 17), place coverslips in individual wells filled with 2 % glutaraldehyde in 100 mM phosphate buffer pH 7.4 and leave to fix overnight at 4 °C.
2. To dehydrate the sample, incubate fixed coverslips sequentially in 25, 50, 75, 90, and 100 % ethanol (with the 100 % step repeated) for 20 min at each concentration at room temperature.
3. In a fumehood overlay coverslips with 1 ml hexamethyldisilazane and incubate for 1 h at room temperature.
4. Remove coverslips and transfer to a new 12-well plate and allow residual solvent to evaporate at room temperature.
5. Following solvent evaporation, attach coverslips to SEM stubs with adhesive carbon tabs and coat with gold/palladium using an Emitech sputter coater.
6. Store samples in airtight conditions until examination with an FEI Quanta 400 SEM.

4 Notes

1. Media recipes differ for other cells. Cell culture media and supplements are available from many suppliers.
2. Coverslips are available in a range of thicknesses. Most often we use thickness #1 (130–170 μm) and do not go to any additional lengths to determine the precise thickness of individual coverslips, despite known variability in thicknesses. Microscope manufacturers often specify 170 nm as the optimum coverslip thickness for performance of their objective lenses; so some researchers prefer to purchase thickness #1.5 (160–190 μm) as a result. It should, however, be remembered that many of these will be too thick to allow optimal resolution. Small differences in coverslip thickness are unlikely to significantly affect image quality in most applications, but where optimal resolution is needed, e.g., to ensure optimal precision in deconvolution, some researchers will check the thickness of coverslips. High-performance objective lenses often have correction collars that should be adjusted to the correct coverslip thickness and it is advisable to make fine adjustment to these collars while viewing the effects on image clarity to ensure correct positioning. Multiwell slides, e.g., Lab-Tek, also provide a convenient means of separately treating multiple cell samples on a single slide. At the end of the experiment the chambers are removed and a coverslip placed onto the slide. Cells can also be grown on conventional plasticware if low magnification is sufficient or in multiwall plates with coverslip-quality glass bottoms if high resolution is required.
3. MDCK cells, like some other epithelial cell lines, can form functionally polarized monolayers when grown on permeable supports. The most commonly used permeable culture inserts include Transwell™ (Corning) and Anopore™ (Nalge Nunc International, NY, USA). Epithelial cells able to form polarized layers should be grown on such permeable supports when the effects of *Salmonella* on epithelial properties, such as transport and barrier functions, are to be investigated.
4. Although we mostly use this method to obtain mid-log bacteria with maximal invasiveness, other growth parameters can also be used as required.
5. We use Krebs' buffer as a convenient physiological buffer that avoids the requirement for CO_2 that comes with using bicarbonate-buffered media. Alternatives, which are especially useful for longer-term infection studies, include conventional cell culture media or bicarbonate-free versions of these that incorporate alternative buffering to avoid the requirement for CO_2 . For fluorescence microscopy, avoidance of Phenol Red (which is included in standard cell culture media as a pH indicator) is advisable as this causes substantial background fluorescence.

6. PFA causes less autofluorescence than glutaraldehyde. PFA should be prepared fresh or can be stored in frozen aliquots for many applications. We don't use commercial formaldehyde solutions due to impurities. PFA fixation works well for a large proportion of antigens but in some cases solvent fixation, e.g., methanol, acetone, or mixtures of these, gives superior results. Solvent fixation also has the advantage that it permeabilizes cells and thus eliminates the requirement for this additional step.
7. Indirect immunofluorescence is more commonly used than direct fluorophore conjugation of primary antibodies for a number of reasons including usual scarcity of primary antibodies and the signal amplification and flexibility in fluorophore selection provided by the indirect approach. Secondary antibodies are generally raised in larger animals and are available in a wide variety of fluorophore-conjugates (excited from UV through to red) from suppliers including Jackson Immuno Research Laboratories, Molecular Probes/Invitrogen, and Sigma. In recent years the first generation fluorophores such as fluorescein and rhodamine derivatives have largely been superseded by improved fluorophores, including the extensive range of Alexa Fluor® dyes (350, 488, 555, 594, 633, etc.) and the cyanine dyes (Cy2, Cy3, and Cy5) which have higher quantum yield (brightness) and improved photo-stability.
8. We generally use TRITC-phalloidin, but alternative fluorophore-conjugated versions, e.g., Alexa Fluors®, FITC, Cy5, are available from Sigma, Molecular Probes/Invitrogen, etc.
9. We routinely use Vectashield® supplied with DAPI, unless we specifically want to avoid an additional UV-excited dye interfering with labeling in that part of the spectrum or when we use the far-red alternative TOPRO-3 to avoid the cross-talk between DNA labeling and other fluorophores which is unavoidable when using DAPI. The main advantage of using DAPI-containing mountant is to avoid an additional labeling step and the need to prepare toxic solutions of DAPI or alternative DNA labels. Many researchers instead mount with Mowiol™ containing n-propyl gallate as an anti-fade, which sets hard unlike the Vectashield® we use. A hard-set version of Vectashield® is also available from Vector Laboratories. Other alternative mountants available from other sources include SlowFade Gold™ and ProLong™ from Molecular Probes/Invitrogen. Anti-fade mountants can vary in their effectiveness against photobleaching, and also in the initial intensity of fluorescence. We have not performed a thorough side-by-side comparison of their properties. It is also important to bear in mind that mounting media may not be completely compatible with all fluorophores. For example some users have reported

decreased signal from Cy2 and other cyanine dyes over time when mounted in media containing phenylenediamine as an anti-fade.

10. This can be a relatively simple upright or inverted microscope with fluorescence capabilities. Usually this will have separate fluorescence filter blocks for each fluorophore and be equipped with a range of objective lenses. The major suppliers include Leica, Olympus, Zeiss, and Nikon. All of these produce high-quality optical instruments and choice comes down to personal preferences and practicalities. Details of the Leica upright microscope we use for examining staining are available at <http://www.bris.ac.uk/biochemistry/mrccif/techspecleicadm.html>.
11. We use one of a range of Leica CLSMs. The one used to acquire images in Fig. 2 is a Leica TCS SP5 AOBS tandem scanning CLSM attached to a Leica DMI6000 inverted epifluorescence microscope. Further details of this and our other confocal microscopes are at <http://www.bris.ac.uk/biochemistry/mrccif/equipment.html>. Other suppliers of CLSMs include Zeiss, Olympus, and Nikon.
12. Further details of the WFM system used to acquire images in Fig. 3 are available at: <http://www.bris.ac.uk/biochemistry/mrccif/equipment.html>. Alternative imaging systems, including integrated acquisition and deconvolution systems are available from other companies, e.g., Applied Precision, Leica, Zeiss, Olympus, Molecular Devices, and Media Cybernetics. Each of these has image processing and analysis capabilities. Some researchers prefer to build their own systems, and the open source software, Micro-manager, is now a popular choice for this due to its ability to drive an expanding range of microscope hardware. Similarly, ImageJ, with its extensive range of plug-ins for image processing and analysis is a popular alternative to commercial image analysis software.
13. There are distinct advantages in sample stability (reducing focus drift) by enclosing a large proportion of the microscope in a temperature-controlled environment and ensuring temperature equilibration of cells before imaging, the advantages being more apparent with long-term imaging. Focus control systems, e.g., CRISP from Applied Scientific Instrumentation, Eugene OR, USA, can also be used to correct for any residual focus drift, which is not always possible to eliminate with temperature control devices. Cells in dishes can also be maintained at 37 °C and perfused using on-stage heating devices as supplied by various companies, e.g., Harvard Apparatus, Scientifica, Life Imaging Services, Bioptechs. If using bicarbonate-buffered media it is necessary to have a means of enriching the environment around the cells with CO₂.

14. For fluorescent labeling of fixed cells we favor 13 mm coverslips in 12-well tissue culture plates. For live cell imaging applications we grow cells on 35 mm imaging dishes with 14 mm glass coverslips.
15. We typically seed 13 mm coverslips with 1 ml of 1×10^5 cells/ml or 1 ml of 0.66×10^5 cells/ml so that after 2 and 3 days, respectively, we obtain cells with ~80 % confluence. The same dilutions but 2 ml volumes are used for 35 mm MatTek dishes.
16. This gives a high infection rate which is ideal for live cell imaging and some other experiments. Decreased m.o.i. can be used to provide more realistic infection levels and are preferable for longer-term infection studies. When comparing strains it is important to check that growth characteristics are similar to ensure infection is comparable, i.e. similar numbers of bacteria at equivalent growth state. This can be measured by determining absorbance at 600 nm with volumes adjusted to match m.o.i. for different cultures or more accurately by determining colony forming units (c.f.u.).
17. We routinely examine time points between 5 and 60 min. When later time points after infection are to be examined we use a “pulse-chase” protocol involving initial 15 min infection followed by removal of external *Salmonella*.
18. Alternative detergents, e.g., saponin are used in some protocols. Permeabilization is not required if solvent-fixation is employed.
19. To remove excess PBS from coverslips prior to labeling, dry the back of the coverslip with fine tissue paper and remove excess liquid remaining on the sample surface by tilting the coverslip and holding the edge of the coverslip with tissue paper. This step is used between all staining steps but has been omitted from elsewhere in the protocols for brevity.
20. It is important to stress that the labeling methods described here and in Subheading 3.3.2 are minimalist protocols used for speed and convenience. We know the labeling will be bright and we are not overly concerned with the presence of some nonspecific labeling. This basic protocol does not include any steps to quench autofluorescence or to block nonspecific binding. Several alternative modifications could be employed to decrease nonspecific labeling, the most common being to include BSA or serum from unrelated species (preferably including the same species as that in which secondary antibodies were raised) before and/or during antibody incubations. For example, we have frequently used pre-blocking with 1 % (w/v) BSA (or 5–25 % serum) in PBS as well as addition of 0.1 % BSA (or 5–10 % serum) in the antibody diluents.

21. This is just one alternative method for differentially labeling adhered and invaded *Salmonella*, an alternative is the use of methanol fixation as discussed in Subheading 1.2.2. Although the resulting staining might be cleaner if blocking steps were introduced, this simplified method has proved adequate for our requirements.
22. It is important to optimize image clarity during visual inspection. It is useful to check that there is no additional factor, such as contamination of oil or incorrect objective setting that will compromise image quality. With thicker specimens, e.g., tissues that are more likely to be examined by CLSM than WFM, it can be much harder to determine if the image is optimal because of the level of out-of-focus fluorescence, so it may be worth checking this with a pre-prepared, familiar, and clear specimen such as a standardized slide.
23. In this case, in order to meet the requirements for optimal resolution imaging [59] a zoom factor was selected to obtain 43 nm pixels at $1,024 \times 1,024$ pixel density. It is not always necessary to optimize XY resolution to this extent and it is worth bearing in mind that increasing zoom also increases the light dose per pixel so may be accompanied by increased photo bleaching, and, in the case of live cell imaging, phototoxicity.
24. The confocal pinhole can be opened if required to increase sensitivity, which is especially useful for live cell imaging. Significant increases in signal can be achieved with only minor loss of axial resolution. It is also worth considering the light-collecting properties of the objective lens when applications require optimal signal, e.g., live cell imaging. For example, signal intensity achieved with the oil-immersion lenses available on our CLSM system decreases with increasing magnification such that users will often prefer to use a 40 \times or 63 \times objective lens and zoom rather than choosing 100 \times objective.
25. Depending on the characteristics of the detector, and the amplification applied, there may be additional benefits in noise reduction to be gained from averaging more than three frames. It should be taken into consideration that more averaging comes at the expense of increasing the time taken to acquire stacks, in addition to increasing the light dose received by the sample, with resulting risk of photo-damage. For live cell applications averaging is often limited to fewer frames or completely avoided due to considerations of phototoxicity, as well as movement-based artifacts. Most CLSM systems will now allow line averaging rather than frame averaging, which is particularly useful where movement is likely to affect information within acquired images, as the time between repeated line

scans is negligible compared to the frame interval. We still prefer frame averaging for fixed samples as line averaging can result in decreased signal intensity.

26. Today's CLSM systems generally have acousto-optic tuneable filters (AOTFs) to allow rapid and independent adjustment of illumination intensity from individual laser lines. In the case of fixed (and anti-fade mounted) specimens, the laser power is less critical than for live cell imaging, where it is often necessary to use higher PMT voltages to enable laser power, and hence photo bleaching/damage, to be minimized. We use a color LUT that clearly identifies pixels with intensities 0 or 255 (extremes of 8-bit range) by displaying them as green or blue, respectively. In the case of CLSM there is less advantage to be gained by using 12-bit imaging because, in contrast to WFM, the number of photons detected for each pixel is usually rather small. The image in Fig. 2 was acquired using the Ar laser (488 nm) at 10 % and 561 nm laser at 2 % with detection set at 493–549 nm for GFP and 569–651 nm for Alexa 555. GaAsP (HyD) detectors were used for both channels, at 65 and 74 % gain.
27. Of course it is not always necessary to obtain image stacks, sometimes a single image or at most a small number of sections are all that are required if a limited part of the cell depth contains the required information. In the case of the image shown in Fig. 2, the full depth amounted to an approximately 6 μm stack and step size was set at 126 nm to optimize data acquisition (Nyquist sampling). More often, larger step sizes are selected, e.g., 500 nm, to limit the time required to obtain images, and thereby photobleaching, as well as to limit imaging time, light dose, and file size.
28. This approach has distinct advantages over acquiring images simultaneously, as it usually avoids the cross-talk between fluorophore signals that is almost inevitable if all three fluorophores are excited simultaneously. For example, DAPI emission spectrum overlaps with those of both Alexa Fluor®488 and 555, while the Alexa 488 emission is also likely to contaminate the Alexa 555 channel when labeling with the green fluorophore is relatively intense. With careful selection of fluorophores and balanced labeling intensity, two or more fluorophores can be imaged simultaneously without significant cross-talk, with resulting savings in imaging time.
29. In this case the image stacks were acquired using "line-by-line" sequential imaging where the AOTF is controlled to rapidly switch between excitation lines for every line scanned such that the fluorophores are imaged at millisecond intervals and appear simultaneously on the display panel. Other parameters such as PMT settings, the wavelength range detected, and pinhole size

can be adjusted between fluorophore settings only in the other, slower, and sequential modes i.e. “between frames” and “between stacks” in the Leica confocal software.

30. DIC imaging affords enhanced contrast for some samples compared to phase contrast, although in our hands we have preferred images acquired by phase contrast to monitor ruffle propagation and internalized *Salmonella*. Automated imaging of fluorescence, e.g., GFP, alongside phase contrast is somewhat more straightforward than with DIC, as the DIC optical components reduce detected fluorescence signal intensity. This can be avoided by using a motorized filter cube to switch between DIC and fluorescence filter blocks or by placing the DIC analyzer within an emission filter wheel, though there will be an additional time delay introduced into the time course using this approach. The loss of sensitivity using DIC simultaneously with fluorescence is much greater than the small loss of light transmission caused by the phase ring within phase contrast objectives. Phase contrast also has advantages in facilitating clear discrimination of internalized bacteria which are often more difficult to detect in DIC images.
31. Live cell imaging automations can be customized to switch between, for example, GFP and phase contrast imaging. This can be used to examine the dynamics of intracellular GFP-tagged probes (as in Fig. 3) or GFP-expressing bacteria alongside morphological responses to infection. Automated shuttering of the light source is beneficial to decrease likelihood of photobleaching or phototoxicity compromising data acquisition.
32. In order to compare one strain or growth condition with another it is necessary for the cultures to have been incubated for the same length of time. Therefore, we set up cultures at 45 min intervals, and subsequently the imaging of each culture is timed to allow 20–30 min time courses to be acquired while also allowing time to set the system up for capturing the next time course.
33. This methodology can also be adapted to allow visualization of GFP-expressing bacteria or those stained using a fluorescence stain, for example DAPI or the Molecular probes LIVE/DEAD® *bacLight*™ viability kit for microscopy (Invitrogen Life Technologies, Paisley, UK). To view fluorescent bacteria using this method, stain the bacteria according to the manufacturer’s instructions and apply 7 μ l of stained sample to the agar disk. To prevent bleaching of the fluorescent sample, allow the sample to dry onto the surface of the agar in the dark. In order to visualize the bacterial sample, use a fluorescence microscope with appropriate filters (see Note 10).

Acknowledgements

We would like to thank Alan Leard, Katy Jepson, Tom MacVicar, Joe Beesley, and Jon Jennings for assistance with microscopy, image processing, and protocols. We also acknowledge all our colleagues who have contributed to the studies of *Salmonella* infection and the development of microscopical techniques discussed here. Work in this laboratory as described here was supported by MRC, BBSRC, and Unilever. The University of Bristol Bioimaging Facility was initially established with funding from MRC and its subsequent expansion has been funded by The Wolfson Foundation, University of Bristol and MRC.

References

1. Majowicz SE, Musto J, Scallan E, Angulo FJ, Kirk M, O'Brien SJ, Jones TF, Fazil A, Hoekstra RM (2010) The global burden of nontyphoidal *Salmonella* gastroenteritis. *Clin Infect Dis* 50:882–889
2. De Jong HK, Parry CM, Van der Poll T, Wiersinga WJ (2012) Host-pathogen interaction in invasive *Salmonellosis*. *PLoS Pathog* 8:e1002933
3. Finlay BB, Ruschkowski S, Dedhar S (1991) Cytoskeletal rearrangements accompanying *Salmonella* entry into epithelial cells. *J Cell Sci* 99(Pt 2):283–296
4. Valdez Y, Ferreira RB, Finlay BB (2009) Molecular mechanisms of *Salmonella* virulence and host resistance. *Curr Top Microbiol Immunol* 337:93–127
5. Clark MA, Jepson MA, Simmons NL, Hirst BH (1994) Preferential interaction of *Salmonella typhimurium* with mouse Peyer's patch M cells. *Res Microbiol* 145:543–552
6. Jones BD, Ghori N, Falkow S (1994) *Salmonella typhimurium* initiates murine infection by penetrating and destroying the specialized epithelial M cells of the Peyer's patches. *J Exp Med* 180:15–23
7. Jepson MA, Clark MA (2001) The role of M cells in *Salmonella* infection. *Microbes Infect* 3:1183–1190
8. Pattini K, Jepson M, Stenmark H, Banting G (2001) A PtdIns(3)P-specific probe cycles on and off host cell membranes during *Salmonella* invasion of mammalian cells. *Curr Biol* 11: 1636–1642
9. Unsworth KE, Way M, McNiven M, Machesky L, Holden DW (2004) Analysis of the mechanisms of *Salmonella*-induced actin assembly during invasion of host cells and intracellular replication. *Cell Microbiol* 6:1041–1055
10. Schlumberger MC, Muller AJ, Ehrbar K, Winnen B, Duss I, Stecher B, Hardt WD (2005) Real-time imaging of type III secretion: *Salmonella* SipA injection into host cells. *Proc Natl Acad Sci U S A* 102:12548–12553
11. Perrett CA, Jepson MA (2009) Regulation of *Salmonella*-induced membrane ruffling by SipA differs in strains lacking other effectors. *Cell Microbiol* 11:475–487
12. Misselwitz B, Barrett N, Kreibich S, Vonaesch P, Andritschke D, Rout S, Weidner K, Sormaz M, Songhet P, Horvath P, Chabria M, Vogel V, Spori DM, Jenny P, Hardt WD (2012) Near surface swimming of *Salmonella* Typhimurium explains target-site selection and cooperative invasion. *PLoS Pathog* 8:e1002810
13. Vonaesch P, Cardini S, Sellin ME, Goud B, Hardt WD, Schauer K (2013) Quantitative insights into actin rearrangements and bacterial target site selection from *Salmonella* Typhimurium infection of micropatterned cells. *Cell Microbiol*. doi:10.1111/cmi.12154
14. Hernandez LD, Hueffer K, Wenk MR, Galán JE (2004) *Salmonella* modulates vesicular traffic by altering phosphoinositide metabolism. *Science* 304:1805–1807
15. Bujny MV, Ewels PA, Humphrey S, Attar N, Jepson MA, Cullen PJ (2008) Sorting nexin-1 defines an early phase of *Salmonella*-containing vacuole-remodeling during *Salmonella* infection. *J Cell Sci* 121:2027–2036
16. Ramsden AE, Mota LJ, Münter S, Shorte SL, Holden DW (2007) The SPI-2 type III secretion system restricts motility of *Salmonella*-containing vacuoles. *Cell Microbiol* 9:2517–2529
17. BRAWN LC, HAYWARD RD, KORONAKIS V (2007) *Salmonella* SPI1 effector SipA persists after entry and cooperates with a SPI2 effector to regulate phagosome maturation and

intracellular replication. *Cell Host Microbe* 1:63–75

18. Knodler LA, Vallance BA, Celli J, Winfree S, Hansen B, Montero M, Steele-Mortimer O (2010) Dissemination of invasive *Salmonella* via bacterial-induced extrusion of mucosal epithelia. *Proc Natl Acad Sci U S A* 107:17733–17738
19. Malik-Kale P, Winfree S, Steele-Mortimer O (2012) The bimodal lifestyle of intracellular *Salmonella* in epithelial cells: replication in the cytosol obscures defects in vacuolar replication. *PLoS One* 7(6):e38732
20. Gog JR, Murcia A, Osterman N, Restif O, McKinley TJ, Sheppard M, Achouri S, Wei B, Mastroeni P, Wood JL, Maskell DJ, Cicuta P, Bryant CE (2012) Dynamics of *Salmonella* infection of macrophages at the single cell level. *J R Soc Interface* 9:2696–2707
21. Hautefort I, Proenca MJ, Hinton JC (2003) Single-copy green fluorescent protein gene fusions allow accurate measurement of *Salmonella* gene expression in vitro and during infection of mammalian cells. *Appl Environ Microbiol* 69:7480–7491
22. Clark L, Perrett CA, Malt L, Harward C, Humphrey S, Jepson KA, Martinez Argudo I, Carney LJ, La Ragione RM, Humphrey T, Jepson MA (2011) Differences in *Salmonella enterica* serovar Typhimurium strain invasiveness is associated with heterogeneity in SPI-1 gene expression. *Microbiology* 157:2072–2083
23. Agbor TA, McCormick BA (2011) *Salmonella* effectors: important players modulating host cell function during infection. *Cell Microbiol* 13:1858–1869
24. Figueira R, Holden DW (2012) Functions of the *Salmonella* pathogenicity island 2 (SPI-2) type III secretion system effectors. *Microbiology* 158:1147–1161
25. Galkin VE, Yu X, Bielnicki J, Heuser J, Ewing CP, Guerry P, Egelman EH (2008) Divergence of quaternary structures among bacterial flagellar filaments. *Science* 320:382–385
26. Salih O, Remaut H, Waksman G, Orlova EV (2008) Structural analysis of the Saf pilus by electron microscopy and image processing. *J Mol Biol* 379:174–187
27. Galkin VE, Schmied WH, Schraadt O, Marlovits TC, Egelman EH (2010) The structure of the *Salmonella typhimurium* type III secretion system needle shows divergence from the flagellar system. *J Mol Biol* 396:1392–1397
28. Bergeron JR, Worrall LJ, Sgourakis NG, DiMaio F, Pfuetzner RA, Felise HB, Vuckovic M, Yu AC, Miller SI, Baker D, Strynadka NC (2013) A refined model of the prototypical *Salmonella* SPI-1 T3SS basal body reveals the molecular basis for its assembly. *PLoS Pathog* 9:e1003307
29. Jansen AM, Hall LJ, Clare S, Goulding D, Holt KE, Grant AJ, Mastroeni P, Dougan G, Kingsley RA (2011) A *Salmonella* Typhimurium-Typhi genomic chimera: a model to study Vi polysaccharide capsule function in vivo. *PLoS Pathog* 7:e1002131
30. Nakano M, Yamasaki E, Ichinose A, Shimohata T, Takahashi A, Akada JK, Nakamura K, Moss J, Hirayama T, Kurazono H (2012) *Salmonella* enterotoxin (Stn) regulates membrane composition and integrity. *Dis Model Mech* 5: 515–521
31. Ginocchio CC, Olmsted SB, Wells CL, Galan JE (1994) Contact with epithelial cells induces the formation of surface appendages on *Salmonella typhimurium*. *Cell* 76:717–724
32. Reed KA, Clark MA, Booth TA, Hueck CJ, Miller SI, Hirst BH, Jepson MA (1998) Cell-contact-stimulated formation of filamentous appendages by *Salmonella typhimurium* does not depend on the type III secretion system encoded by *Salmonella* pathogenicity island 1. *Infect Immun* 66:2007–2017
33. Knutson S (2003) Microscopic methods to study STEC. Analysis of the attaching and effacing process. *Methods Mol Med* 73: 137–149
34. Van Putten JP, Weel JF, Grassme HU (1994) Measurements of invasion by antibody labelling and electron microscopy. *Methods Enzymol* 236:420–437
35. Serra DO et al (2013) Microanatomy at cellular resolution and spatial order of physiological differentiation in a bacterial biofilm. *MBio* 4(2):e00103–e00113
36. Muller DJ, Dufrene YF (2011) Atomic force microscopy: a nanoscopic window on the cell surface. *Trends Cell Biol* 21:461–469
37. Dorobantu LS, Goss GG, Burrell RE (2012) Atomic force microscopy: a nanoscopic view of microbial cell surfaces. *Micron* 43:1312–1322
38. Wang HW, Chen Y, Yang H, Chen X, Duan MX, Tai PC, Sui SF (2003) Ring-like pore structures of SecA: implication for bacterial protein-conducting channels. *Proc Natl Acad Sci U S A* 100:4221–4226
39. Ide T, Laarmann S, Greune L, Schillers H, Oberleithner H, Schmidt MA (2001) Characterization of translocation pores inserted into plasma membranes by type III-secreted Esp proteins of enteropathogenic *Escherichia coli*. *Cell Microbiol* 3:669–679
40. GILLIS A, DUPRES V, MAHILLON J, DUFRENE YF (2012) Atomic force microscopy:

a powerful tool for studying bacterial swarming motility. *Micron* 43:1304–1311

41. JONAS K, TOMENIUS H, KADER A, NORMARK S, ROMLING U, BELOVA LM, MELEFORS O (2007) Roles of curli, cellulose and BapA in *Salmonella* biofilm morphology studied by atomic force microscopy. *BMC Microbiol* 7:70

42. OH YJ, CUI Y, KIM H, LI Y, HINTERDORFER P, PARK S (2012) Characterization of curli A production on living bacterial surfaces by scanning probe microscopy. *Biophys J* 103:1666–1671

43. WRIGHT CJ, SHAH MK, POWELL LC, ARMSTRONG I (2010) Application of AFM from microbial cell to biofilm. *Scanning* 32: 134–149

44. MANSSEN LE, MELICAN K, MOLITORIS BA, RICHTER-DAHLFORS A (2007) Progression of bacterial infections studied in real time—novel perspectives provided by multiphoton microscopy. *Cell Microbiol* 9:2334–2343

45. MELICAN K, RICHTER-DAHLFORS A (2009) Multiphoton imaging of host-pathogen interactions. *Biotechnol J* 4:804–811

46. LAKINS MA, MARRISON JL, O'TOOLE PJ, VAN DER WOUDE MW (2009) Exploiting advances in imaging technology to study biofilms by applying multiphoton laser scanning microscopy as an imaging and manipulation tool. *J Microsc* 235:128–137

47. FARACHE J, KOREN I, MILE I, GUREVICH I, KIM KW, ZIGMOND E, FURTADO GC, LIRA SA, SHAKHAR G (2013) Luminal bacteria recruit CD103+ dendritic cells into the intestinal epithelium to sample bacterial antigens for presentation. *Immunity* 38:581–595

48. SCHERMELLEH L, HEINTZMANN R, LEONHARDT H (2010) A guide to super-resolution fluorescence microscopy. *J Cell Biol* 190:165–175

49. CATTONI DI, FICHE JB, NÖLLMANN M (2012) Single-molecule super-resolution imaging in bacteria. *Curr Opin Microbiol* 15:758–763

50. SCHAFFNER MP, LIEW AT, TURNBULL L, WHITCHURCH CB, MONAHAN LG, HARRY EJ (2012) 3D-SIM super resolution microscopy reveals a bead-like arrangement for FtsZ and the division machinery: implications for triggering cytokinesis. *PLoS Biol* 10(9):e1001389

51. TURNER RD, HURD AF, CADBY A, HOBBS JK, FOSTER SJ (2013) Cell wall elongation mode in Gram-negative bacteria is determined by peptidoglycan architecture. *Nat Commun* 4:1496

52. UPHOFF S, REYES-LAMOTHE R, GARZA DE LEON F, SHERRATT DJ, KAPANIDIS AN (2013) Single-molecule DNA repair in live bacteria. *Proc Natl Acad Sci U S A* 110:8063–8068

53. STEPHENS DJ, ALLAN VJ (2003) Light microscopy techniques for live cell imaging. *Science* 300:82–86

54. JEPSON MA (2006) Confocal or wide-field? A guide to selecting appropriate methods for cell imaging. In: Stephens D (ed) *Methods express: cell imaging*. Scion Publishing Ltd (UK), Banbury, pp 17–48

55. WATKINS SA, ST CROIX CM (eds) (2013) *Current protocols select: imaging and microscopy*. Wiley, Hoboken, NJ, USA

56. GRANTCHAROVA N, PETERS V, MONTEIRO C, ZAKIKHANY K, RÖMLING U (2010) Bistable expression of CsgD in biofilm development of *Salmonella enterica* serovar *typhimurium*. *J Bacteriol* 192:456–466

57. VAN ENGELENBURG SB, PALMER AE (2010) Imaging type-III secretion reveals dynamics and spatial segregation of *Salmonella* effectors. *Nat Methods* 7:325–330

58. SWEDLOW JR, HU K, ANDREWS PD, ROOS DS, MURRAY JM (2002) Measuring tubulin content in *Toxoplasma gondii*: a comparison of laser-scanning confocal and wide-field fluorescence microscopy. *Proc Natl Acad Sci U S A* 99: 2014–2019

59. <http://www.svi.nl/NyquistCalculator>

60. TAKEUCHI A (1967) Electron microscope studies of experimental *Salmonella* infection. I. Penetration into the intestinal epithelium by *Salmonella typhimurium*. *Am J Pathol* 50: 109–136

61. FRANCIS CL, STARNBACH MN, FALKOW S (1992) Morphological and cytoskeletal changes in epithelial cells occur immediately upon interaction with *Salmonella typhimurium* grown under low-oxygen conditions. *Mol Microbiol* 6: 3077–3087

62. JEPSON MA, CLARK MA (1998) Studying M cells and their role in infection. *Trends Microbiol* 6:359–365

63. CLARK MA, REED KA, LODGE J, STEPHEN J, HIRST BH, JEPSON MA (1996) Invasion of murine intestinal M cells by *Salmonella typhimurium* *inv* mutants severely deficient for invasion of cultured cells. *Infect Immun* 64: 4363–4368

64. MONAGHAN P, WATSON PR, COOK H, SCOTT L, WALLIS TS, ROBERTSON D (2001) An improved method for preparing thick sections for immuno/histochemistry and confocal microscopy and its use to identify rare events. *J Microsc* 203: 223–226

65. RICHTER-DAHLFORS A, BUCHAN AM, FINLAY BB (1997) Murine salmonellosis studied by confocal microscopy: *Salmonella typhimurium* resides intracellularly inside macrophages and exerts a cytotoxic effect on phagocytes *in vivo*. *J Exp Med* 186:569–580

66. SALCEDO SP, NOURSADEGHI M, COHEN J, HOLDEN DW (2001) Intracellular replication of *Salmonella typhimurium* strains in specific subsets of splenic macrophages *in vivo*. *Cell Microbiol* 3:587–597

67. Zhou D, Mooseker MS, Galan JE (1999) Role of the *S. typhimurium* actin-binding protein SipA in bacterial internalization. *Science* 283:2092–2095

68. Jepson MA, Lang TF, Reed KA, Simmons NL (1996) Evidence for a rapid, direct effect on epithelial monolayer integrity and transepithelial transport in response to *Salmonella* invasion. *Pflugers Arch* 432:225–233

69. La Ragione RM, Cooley WA, Velge P, Jepson MA, Woodward MJ (2003) Membrane ruffling and invasion of human and avian cell lines is reduced for flagellate mutants of *Salmonella enterica* serotype Enteritidis. *Int J Med Microbiol* 293:261–272

70. Hardt WD, Chen LM, Schuebel KE, Bustelo XR, Galan JE (1998) *S. typhimurium* encodes an activator of Rho GTPases that induces membrane ruffling and nuclear responses in host cells. *Cell* 93:815–826

71. Jepson MA, Pellegrin S, Peto L, Banbury DN, Leard AD, Mellor H, Kenny B (2003) Synergistic roles for the Map and Tir effector molecules in mediating uptake of enteropathogenic *Escherichia coli* (EPEC) into non-phagocytic cells. *Cell Microbiol* 5:773–783

72. Mortimer O (2005) Cloning vectors and fluorescent proteins can significantly inhibit *Salmonella enterica* virulence in both epithelial cells and macrophages: implications for bacterial pathogenesis studies. *Infect Immun* 73: 7027–7031

73. Wendland M, Bumann D (2002) Optimization of GFP levels for analyzing *Salmonella* gene expression during an infection. *FEBS Lett* 521:105–108

74. Valdivia RH, Falkow S (1996) Bacterial genetics by flow cytometry: rapid isolation of *Salmonella typhimurium* acid-inducible promoters by differential fluorescence induction. *Mol Microbiol* 22:367–378

75. Bumann D (2002) Examination of *Salmonella* gene expression in an infected mammalian host using the green fluorescent protein and two-colour flow cytometry. *Mol Microbiol* 43:1269–1283

76. Cain RJ, Hayward RD, Koronakis V (2004) The target cell plasma membrane is a critical interface for *Salmonella* cell entry effector-host interplay. *Mol Microbiol* 54:887–904

77. Brumell JH, Kujat-Choy S, Brown NF, Vallance BA, Knodler LA, Finlay BB (2003) SopD2 is a novel type III secreted effector of *Salmonella typhimurium* that targets late endocytic compartments upon delivery into host cells. *Traffic* 4:36–48

78. Brumell JH, Goosney DL, Finlay BB (2002) SifA, a type III secreted effector of *Salmonella typhimurium*, directs *Salmonella*-induced filament (Sif) formation along microtubules. *Traffic* 3:407–415

79. Charpentier X, Oswald E (2004) Identification of the secretion and translocation domain of the enteropathogenic and enterohemorrhagic *Escherichia coli* effector Cif, using TEM-1 beta-lactamase as a new fluorescence-based reporter. *J Bacteriol* 186:5486–5495

80. Van Engelenburg SB, Palmer AE (2008) Quantification of real-time *Salmonella* effector type III secretion kinetics reveals differential secretion rates for SopE2 and SptP. *Chem Biol* 15:619–628

81. Francis CL, Ryan TA, Jones BD, Smith SJ, Falkow S (1993) Ruffles induced by *Salmonella* and other stimuli direct macropinocytosis of bacteria. *Nature* 364:639–642

82. Reed KA, Booth TA, Hirst BH, Jepson MA (1996) Promotion of *Salmonella typhimurium* adherence and membrane ruffling in MDCK epithelia by staurosporine. *FEMS Microbiol Lett* 145:233–238

83. STEINBERG BE, SCOTT CC, GRINSTEIN S (2007) High-throughput assays of phagocytosis, phagosome maturation, and bacterial invasion. *Am J Physiol Cell Physiol* 292:C945–C952

84. Misselwitz B, Dilling S, Vonaesch P, Sacher R, Snijder B, Schlumberger M, Rout S, Stark M, von Mering C, Pelkmans L, Hardt WD (2011) RNAi screen of *Salmonella* invasion shows role of COPI in membrane targeting of cholesterol and Cdc42. *Mol Syst Biol* 7:474

85. Jepson MA, Schlecht HB, Collares-Buzato CB (2000) Localization of dysfunctional tight junctions in *Salmonella enterica* serovar typhimurium-infected epithelial layers. *Infect Immun* 68:7202–7208

86. Criss AK, Ahlgren DM, Jou TS, McCormick BA, Casanova JE (2001) The GTPase Rac1 selectively regulates *Salmonella* invasion at the apical plasma membrane of polarized epithelial cells. *J Cell Sci* 114:1331–1341

87. Raffatellu M, Wilson RP, Chessa D, Andrews-Polymeris H, Tran QT, Lawhon S et al (2005) SipA, SopA, SopB, SopD, and SopE2 contribute to *Salmonella enterica* serotype typhimurium invasion of epithelial cells. *Infect Immun* 73: 146–154

88. Clark MA, Hirst BH, Jepson MA (1998) M-cell surface beta1 integrin expression and invasin-mediated targeting of *Yersinia pseudotuberculosis* to mouse Peyer's patch M cells. *Infect Immun* 66:1237–1243

89. Jepson MA, Clark MA, Simmons NL, Hirst BH (1993) Actin accumulation at sites of attachment of indigenous apathogenic segmented

filamentous bacteria to mouse ileal epithelial cells. *Infect Immun* 61:4001–4004

90. Jepson MA, Kenny B, Leard AD (2001) Role of *sipA* in the early stages of *Salmonella typhimurium* entry into epithelial cells. *Cell Microbiol* 3:417–426

91. Meresse S, Unsworth KE, Habermann A, Griffiths G, Fang F, Martinez-Lorenzo MJ et al (2001) Remodelling of the actin cytoskeleton is essential for replication of intravacuolar *Salmonella*. *Cell Microbiol* 3:567–577

92. HUMPHREYS, MACVICART, STEVENSON A, ROBERTS M, HUMPHREY TJ, JEPSON MA (2011) SulA-induced filamentation in *Salmonella enterica* serovar Typhimurium: effects on SPI-1 expression and epithelial infection. *J Appl Microbiol* 111:185–196

93. Ferry MS, Razinkov IA, Hasty J (2011) Microfluidics for synthetic biology: from design to execution. *Methods Enzymol* 497: 295–372

94. Sturm A, Heinemann M, Arnoldini M, Benecke A, Ackermann M, Benz M, Dormann J, Hardt WD (2011) The cost of virulence: retarded growth of *Salmonella* Typhimurium cells expressing type III secretion system 1. *PLoS Pathog* 7:e1002143

95. Yim L, Betancor L, Martínez A, Bryant C, Maskell D, Chabalgoity JA (2011) Naturally occurring motility-defective mutants of *Salmonella enterica* serovar Enteritidis isolated preferentially from nonhuman rather than human sources. *Appl Environ Microbiol* 77: 7740–7748

96. Hesse WR, Kim MJ (2009) Visualization of flagellar interactions on bacterial carpets. *J Microsc* 233(2):302–308

97. Humphrey S, Clark LF, Humphrey TJ, Jepson MA (2011) Enhanced recovery of *Salmonella* Typhimurium DT104 from exposure to stress at low temperature. *Microbiology* 157: 1103–1114

98. Buchmeier NA, Libby SJ (1997) Dynamics of growth and death within a *Salmonella typhimurium* population during infection of macrophages. *Can J Microbiol* 43: 29–34

99. Freese HM, Karsten U, Schumann R (2006) Bacterial abundance, activity, and viability in the eutrophic River Warnow, northeast Germany. *Microb Ecol* 51:117–127

Chapter 13

Live Cell Imaging of Intracellular *Salmonella enterica*

Alexander Kehl and Michael Hensel

Abstract

During the intracellular phase of the pathogenic lifestyle, *Salmonella enterica* massively alters the endosomal system of its host cells. Two hallmarks are the remodeling of phagosomes into the *Salmonella*-containing vacuole (SCV) as a replicative niche, and the formation of tubular structures, such as *Salmonella*-induced filaments (SIFs). To study the dynamics and the fate of these *Salmonella*-specific compartments, live cell imaging (LCI) is a method of choice. In this chapter, we compare currently used microscopy techniques and focus on considerations and requirements specific for LCI. Detailed protocols for LCI of *Salmonella* infection with either confocal laser scanning microscopy (CLSM) or spinning disk confocal microscopy (SDCM) are provided.

Key words *Salmonella*-containing vacuole, Intracellular pathogen, *Salmonella*-induced filaments, Confocal microscopy

1 Introduction

1.1 *Salmonella* Intracellular Lifestyle

Salmonella enterica is the etiological agent of both acute gastroenteritis and the systemic disease typhoid fever. Whereas for the first the understanding of the invasion event into epithelia, the extracellular fate, is fundamental, for enteric fever knowledge about the intracellular lifestyle is crucial. Although this introduction is not meant as a thorough discussion of the infectious cycle of *Salmonella*, some notable processes will be outlined. For general overviews refer to recent reviews [1, 2].

After oral ingestion and survival of the passage through the acidic stomach, *Salmonella* is able to invade the epithelium in the intestine. The pathogenicity of *Salmonella* is mainly conferred by genes located on the *Salmonella* Pathogenicity Islands (SPI), whereby SPI1 is most important for invasion of non-phagocytic cells. This is mainly mediated by a type III secretion system (T3SS) encoded by SPI1. The SPI1-T3SS translocates so-called effector proteins into host cells that, amongst other activities, rearrange the actin cytoskeleton [3]. In addition, the giant fimbrial adhesion SiiE

acts in cooperation with the SPI1-T3SS to allow *Salmonella* to specifically breach polarized epithelial barriers [4]. SiiE is substrate of a type I secretion system (T1SS) encoded by SPI4.

After entry into host cells, *Salmonella* is able to remodel its compartment into the *Salmonella*-containing vacuole (SCV), which enables the pathogen to withstand the acidic and nutrient-poor environment it is subjected to. The SCV does not follow normal endosomal maturation to late endosomes (LE)/lysosomes [5]. This ability is due to the translocation of a set of effectors by the SPI2-encoded T3SS [6]. During the course of infection, the SCV is positioned in a perinuclear position near the microtubule-organizing center (MTOC) and the Golgi. The SCV matures to a certain degree and acquires over time several LE markers, like Rab7 and lysosome-associated membrane proteins (LAMPs) [7, 8], even though in slightly altered sequences compared to LEs. Other LE markers though, such as the mannose-6-phosphate receptor (M6PR) responsible for the delivery of hydrolases to LEs, are excluded [9]. In this modified organelle, *Salmonella* is able to actively proliferate, representing a hallmark of its pathogenic lifestyle.

Another hallmark is the unique ability of *Salmonella* to induce an extensive network of tubular membrane structures. Whereas for a long time only one type of these structures, the *Salmonella*-induced filaments (SIFs), was known, in recent years a whole bunch of other structures was discovered, including *Salmonella*-induced secretory carrier membrane protein 3 (SCAMP3) tubules (SIST), LAMP1-negative tubules (LNTs), and sorting nexin (SNX) tubules like the spacious vacuole-associated tubules (SVAT) [10]. However, out of these the SIFs are still the best-studied ones, with a membrane composition similar to that of SCV, i.e., being also highly enriched in LAMP1. Although at later time points (≥ 8 h after infection) SIFs form an elaborate but rather rigid network, a highly dynamic behavior, revealed by live cell imaging (LCI), was demonstrated at earlier time points [11, 12]. Here SIFs are rapidly extending, retracting, or branching. SIF dynamics are exemplified in Fig. 1 with various temporal resolutions. Formation of SIF is dependent on several SPI2 effectors, some of them interacting directly or indirectly with the microtubule (MT) cytoskeleton, leading to a close association of MT with SCV and SIF and a possible role in the biogenesis of SIF.

1.2 High-Resolution Microscopic Analysis of Intracellular *Salmonella*

To date, no light microscopy (LM) technique matches the high resolution obtained by electron microscopy (EM), specifically transmission EM (TEM). Although efforts were made to combine the benefits of LM and EM, i.e., observation of dynamic events and ultrastructural information, leading to correlative light and electron microscopy (CLEM) [13], fixation of cells is prerequisite for transition from LCI to TEM. The development of super-resolution techniques like stimulated emission depletion microscopy (STED),

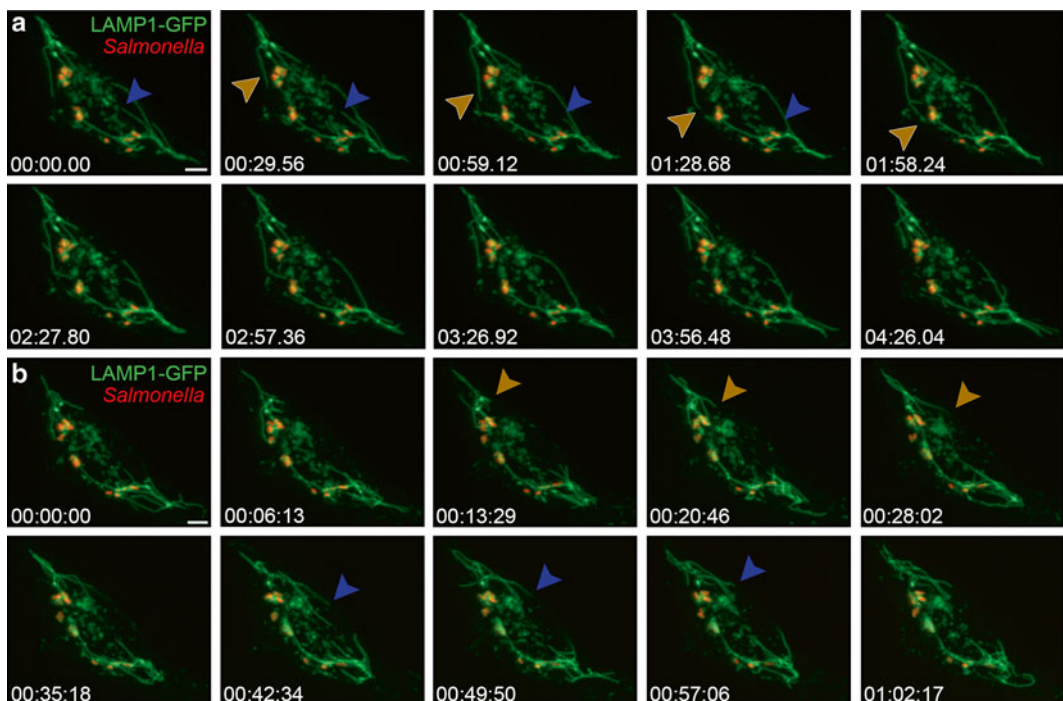


Fig. 1 Short-term and long-term dynamics of SIFs. **(a, b)** HeLa cells stably transfected with LAMP1-GFP were infected with mCherry-expressing wild-type *Salmonella* and imaged with an SDCM (see Note 10) 5 h post infection using 5 % 488 nm laser and 100 ms camera exposure time for GFP and 10 % 561 nm and 100 ms for mCherry, respectively. Shown is a maximum intensity projection (MIP) of a 4.56 μ m Z-stack displayed with “Best Fit” parameters. Extending and retracting SIFs are indicated by *brown* or *blue arrowheads*, respectively. Scale bar, 5 μ m. **(a)** Time-lapse acquisition for 5 min illustrating SIF dynamics in the subminute range; time stamp is given as mm:ss.ff. **(b)** Time-lapse acquisition for 1 h illustrating SIF dynamics in the subhour range; time stamp is given as hh:mm:ss

photo-activated localization microscopy (PALM), and stochastic optical reconstruction microscopy (STORM) pushed the resolution border in LM, but lacked until recently live cell applications. Even though this problem, too, was overcome these applications are still in progress [14–16]. What remains with respect to elevated resolution and compatibility with LCI compared to conventional epifluorescence wide-field microscopy (WFM) is the confocal microscopy, a kind of optical sectioning method. Again, a thorough discussion here is not achievable, but is passed to recent reviews [17, 18]. Thanks to availability of confocal microscopes from several commercial suppliers; such systems are nowadays widely distributed.

Confocal microscopy systems can be divided into two types: confocal laser scanning microscopy (CLSM) and spinning disk confocal microscopy (SDCM). Basic principle of the improved resolution in both cases is the elimination of out-of-focus light by using pinhole apertures, thus excluding this light from detection.

In CLSM systems this is achieved by a single pinhole (or in some cases an extremely narrow slit). In contrast in SDCM systems a so-called rotating Nipkow disk with multiple pinholes is applied.

WFM is a further option of LCI of *Salmonella* intracellular lifestyle. The advantages of WFM include for example inexpensiveness due to simpler setups and higher sensitivity thanks to non-exclusion of light, but the two major ones with respect to LCI are higher acquisition speed and less photobleaching or -toxicity, respectively, of the sample since no laser is utilized (*see* Subheading 1.3). Even the resolution can be optimized by using restorative deconvolution, at least if samples are thin and fulfill the Nyquist sampling during imaging (but this conversely requires higher processing capacities) [19, 20]. So, if high resolution is not necessarily needed, WFM is still a valuable technique.

Nevertheless with thick specimens (meaning more out-of-focus light) and sufficiently high fluorescent signal (making higher sensitivity obsolete) CLSM clearly outperforms WFM. Still CLSM can be troublesome if desiring to combine high resolution with on the one hand weaker signals since in most CLSM systems photomultiplier tubes (PMT) are deployed as light detectors, which have rather low quantum efficiencies (QE) and high noise due to the charge multiplication process, resulting in worse signal-to-noise ratios (S/N); on the other hand one has to accept high resolution with relatively slow acquisition speed. Both problems are circumvented to some degree in SDCM [21].

Whereas SDCM formerly was hampered by insufficient passage of excitation light the introduction of a second microlens disk focusing incoming light into the pinholes of the Nipkow disk by Yokogawa [22] permitted the spread of this technique, also due to the fact that SDCM overcomes some of the problems or disadvantages, respectively, of CLSM. First by applying a rotating disk with multiple pinholes a larger area of a specimen can be scanned simultaneously, thus with a highly increased speed. This reduces remarkably the risk of photobleaching/-toxicity, also due to the fact that using a microlens disk concurrently to the emission the excitation light is confocal. Second, the high frame rate allows the use of charge-coupled device (CCD) cameras which are superior to PMTs with regard to sensitivity/QE. With yet more sensitive (and speed-adapted) back-thinned electron multiplication (EM)CCD cameras excitation light can be even more decreased (if avoiding noise), thus additionally reducing photobleaching/-toxicity (though actually used to compensate for comparatively weak excitation lasers). Only disadvantage of EMCCD cameras is the rather small chip in most cases and thus the reduced resolution, but which also can be avoided by using higher resolution scientific grade CCD cameras.

1.3 Specific Requirements for Live Cell Imaging

If executing LCI, several considerations have to be made beforehand since special requirements are necessary concurrently excluding possibilities normally applicable to fixed imaging setups [23].

Naturally, the most important point concerns the incubation itself or the type of incubation, respectively. Basically one can choose from two types of incubation depending on the sample and microscope used: (1) Box incubation where the complete microscope is heated in a more or less sealed box or (2) cage or stage top incubation where it is only part of the sample stage with special chambers. If using a box solution acquired separately from the microscope one has to make sure that all of the parts surrounded by the box are indeed heatable (which should be the case with most suppliers). The exact buildup of a stage top incubation chamber is heavily varying depending on the culture vessels or sample carriers employed. In most cases one and the same chamber cannot be used for smaller and larger carriers alike, which has to be reasoned in advance. Anyway, with both types of incubation it should also be considered to include humidity- and/or CO₂-supplying devices. Whereas in short-term LCI culture medium evaporation might be negligible, for longer-term LCI a compensation via humidity should be contemplated, because this can cause a severe change of osmolarity. Nevertheless, ideally only a small part of the stage should be humidified to protect the remaining microscope parts from moisture. Likewise a CO₂ supply (mostly via the humidity supply) is inevitable if using a bicarbonate buffer-based culture medium. Nevertheless, this can easily be avoided by replacing with another buffer system, such as bicarbonate-free HEPES-buffered culture medium. In the process one might also use a medium without phenol red (normally used as a pH indicator in bicarbonate buffer-based cell culture media), since phenol-red-containing media affect image acquisition by increasing background noise.

Other major issues in LCI are photobleaching and phototoxicity, i.e., the production of deleterious free-radical species with the risk of oxygen-dependent damage of cellular components. Both artifacts are due to repeated excitation in the same field of the sample. Several approaches can be employed to remedy these problems. With a range of fluorescent proteins (FPs) to tag intracellular targets available by now such ones should be used with suitable properties regarding stability. Whereas enhanced green fluorescent protein (EGFP) still works fairly well concerning brightness and quantum yield (QY) in the green spectral emission range, this does not necessarily hold true for the rest of the spectral range [24]. Of course one is bound to the microscopic setup available regarding the choice of FPs, but apart from the above addressed points the stability is the most important factor to select for in LCI if alternatives are applicable (with EGFP again a rather good choice). Helpful overviews are available [25, 26], but one should be on the qui vive since new FPs are constantly invented.

Another possibility to avoid photobleaching/-toxicity is to increase the speed of acquisition. Again, several actions can be taken in this direction. One is to modify the mode of acquisition by choosing binning (i.e., the integration of arrays of adjacent pixels), and the other is to reduce the chip size of the CCD camera, but both have the disadvantage to reduce at the same time the resolution. One rather easy possibility is to simply concentrate the acquisition on a region of interest (ROI), i.e., not imaging the complete field of view, which will likely lend itself to many cases. If acquiring in three dimensions (3D) additionally the thickness of a Z-stack as well as the single slices themselves can be varied. If not aiming for deconvolution this parameter can be considerably reduced. Nevertheless in long-time experiments possible cell movements in the z-direction should be definitely considered (alleviated either by larger, but more time-consuming Z-stacks or to some extent by suitable focus strategies, *see* below). Furthermore switching of filters or other motorized parts is often not triggerable therefore decreasing speed substantially. One possibility to avoid this is to use band-pass (BP) emission filters (i.e., filters which permit the passage of emission signal from a designated range/band of the spectral range) that feature two separate emission bands, double BP (DBP) filters. This allows the acquisition of two colors without switching filters but only the lasers for excitation. One has only to take care of possible crosstalk (i.e., the unintended excitation of another FP) and/or bleed-through (i.e., the unintended detection of the emission of another FP) of the FPs used. This is demonstrated in Fig. 2b, c, where the bacterial signal is visible in the GFP channel if using a DBP filter instead of single BP filters, since TagRFP-T used here can also be excited at 488 nm. Another option is to use a dual camera setup where the acquisition of two colors is split onto two separate cameras via a beamsplitter. Here not only a change of filters is omitted but even that of lasers, since they are both working at a time, allowing remarkable speeds in acquisition.

Mostly, LCI will include some form of bright field (BF) acquisition, often deploying contrast enhancements such as phase contrast or differential interference contrast (DIC)/Nomarski. One problem in combining BF with fluorescence imaging is the loss of light due to the partial block by the contrast-enhancing parts if they remain in the light path. So apart from manipulation of the fluorescence acquisition this is another parameter for speed optimization (this means the exclusion of phase contrast objectives since this cannot be altered), since switching the microscopic parts from fluorescence to BF/DIC acquisition is principally (if not using triggerable modifications) a highly time-consuming step. Nevertheless, it is often inevitable to delineate cell boundaries, to score cell morphology or to follow cell movement. It is not always required to capture BF images at every time point, but instead it might be sufficient to capture at the beginning and the end of an

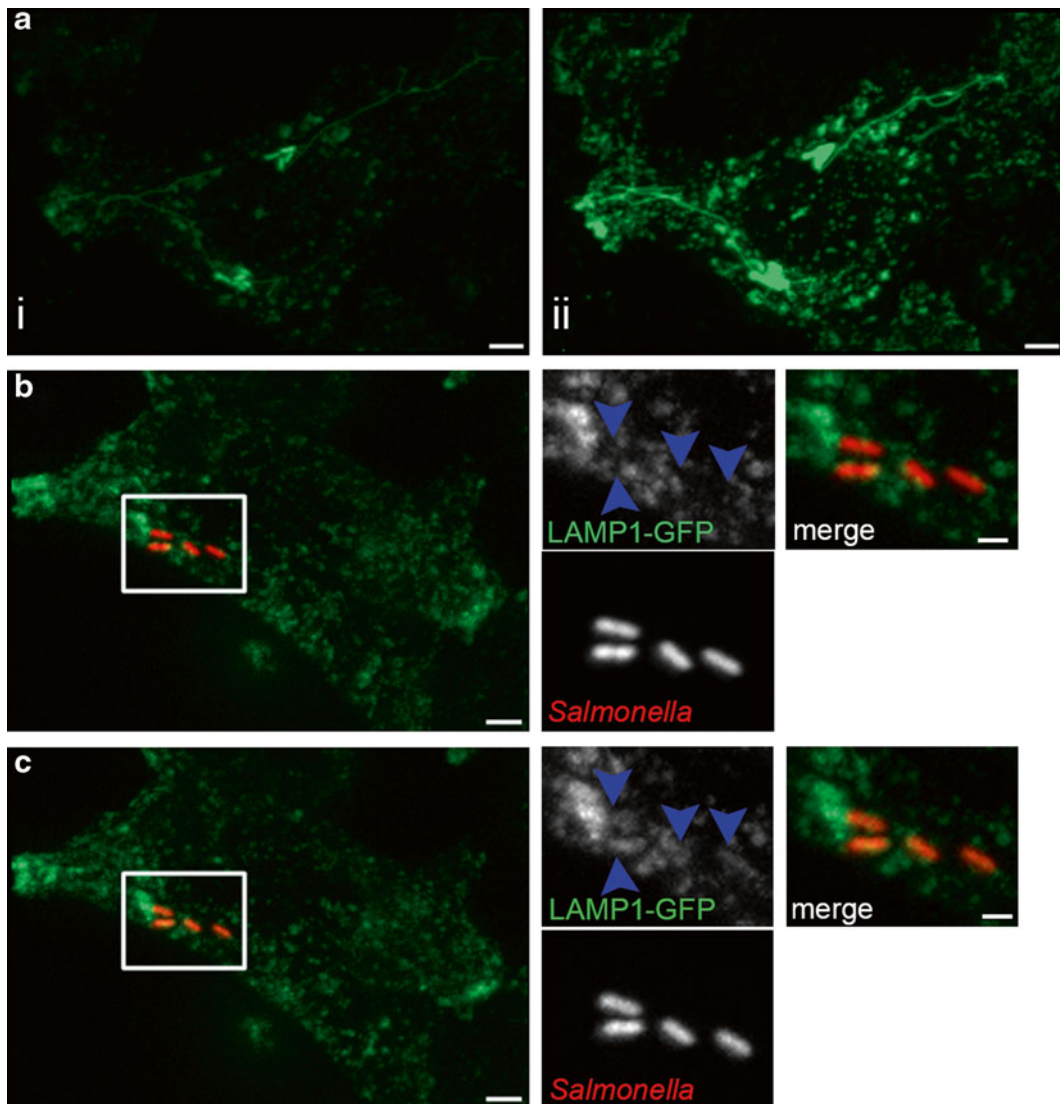


Fig. 2 Use of various fluorescent proteins in *Salmonella* infection models. **(a–c)** HeLa cells stably transfected with LAMP1-GFP were infected with wild-type *Salmonella* expressing different FPs and imaged by SDCM (see **Note 10**). Shown is a maximum intensity projection (MIP) of a 4.56 μ m Z-stack displayed with “Best Fit” parameters. **(a)** Cells harboring GFP-expressing *Salmonella* were imaged 5 h postinfection using 1 % 488 nm laser and 100 ms (*i*), or 1,000 ms (*ii*) camera exposure time for GFP, demonstrating underestimation of cellular signals if excitation is adjusted to bacterial signal (*i*), or overexposure of bacteria if adjusted to cellular signal (*ii*). Scale bar, 5 μ m. **(b, c)** Cells harboring TagRFP-T-expressing *Salmonella* were imaged 3 h post infection using 5 % 488 nm laser and 200 ms camera exposure time for GFP and 10 % 561 nm and 100 ms for TagRFP-T, respectively, using separate 525/50 nm BP and LP 580 nm filters (**b**), or a 527/54 nm and 645/60 nm DBP filter (**c**) for GFP and RFP detection. An overview of the imaged cell with the indicated area enlarged in GFP, RFP, and merge images is shown. Blue arrowheads indicate absence (**b**) or presence (**c**) of bacterial signal in the GFP channel due to the use of the different emission filters. Scale bars, 5 and 2 μ m in overview and detail images, respectively

experiment to show the extremes of morphological changes of the cell during acquisition. The Z-stack software nowadays also allows to differently acquire the single channels, i.e., acquiring a full Z-stack with the fluorescence channels and only a single slice with the BF channel, e.g., the center.

If aiming for multi-position experiments LCI is accompanied by another set of obstacles. Often one wants to image several positions over time (time-lapse acquisition), which can be cumbersome depending on the sample carrier and therefore the objective applied. Higher magnification objectives require immersion oils, which can dry out over time if too many positions are approached or if the sample carrier is too large. Therefore, the use of standard multiwell plates is normally excluded with oil objectives. Instead, small dishes (35 mm) or chamber slides (which are available in diverse variants from different suppliers) are often employed. If nevertheless a multiwell plate needs to be used, e.g., for screens, relatively low magnification (10–20 \times) air objectives or rather expensive so-called long distance (LD) air objectives (available for 40 \times) are inevitable. In any case, the objectives should include temperature correction rings to compensate for spherical alterations if imaging at 37 °C, which is by the way another essential factor to consider.

Connected to multi-position experiments is the requirement for proper focus strategies. Nowadays most microscope operating software include some form of software autofocus (SAF), which determines independent of the hardware components the sharp focal plane guided by certain software parameters. Major disadvantage of SAFs is the use of the actual lasers virtually scanning a Z-stack for this purpose, thereby already exciting the sample before the acquisition. This might not be elementary for fixed samples but with living samples this can be crucial. In addition, this procedure is rather slow, with too many positions possibly disabling a desired time interval.

Recently a new type of focus was introduced by several microscope suppliers: infrared-based focus (IRF). The principle is the determination of the distance between objective and the border between sample and slide via an infrared light-emitting LED. This measurement is then used to continuously adjust either other positions or the same position over time, in case drifts of mechanical or thermal nature occur (with the latter less pronounced with proper incubation). This method offers the advantage of being exceptionally gentle to the samples since a significantly less powerful LED is employed (with the infrared excitation additionally being out of range of normal chromophores). As a limitation of IRF, it is not possible to compensate for cell movements in Z, so that an SAF on top might still be indispensable.

Should the sample carrier by itself exhibit drifts or variations of the bottom surface (and therefore the focal plane) over its area, some software are also able to calculate a compensation if supported

with the focal planes for some points randomly distributed over the vessel. All of these focus strategies alone or to some degree in combination (as for the cell movements) can be the proper choice (if software allow combinations), depending on the exact experimental setup. One essential point with regard to focus strategies though is the nature of the sample carrier employed. For high-resolution oil-immersion imaging a glass or glass-like bottom with a thickness of ca. 0.17 mm is imperative (which is commonly available for the above mentioned smaller sample carriers), whereas with lower magnification plastic bottom (1 mm) carriers like standard multiwell plates normally are sufficient. But one specific task might be the scanning of multiwell plates with a relatively high magnification, which could demand multiwell plates with glass bottom. The reason is the possible failure of focus strategies, whether the SAF or IRF, due to not only the variation in distance between the objective and the bottom but also the comparably high variation in bottom thickness itself. In addition to an LD air objective this could necessitate another correction ring for bottom thickness at the objective, calling for a highly sophisticated product.

Apart from these hardware-specific considerations, some major factors specifically concerning LCI pertain to the biological samples themselves. Connected to the above mentioned FP tags is the way of introduction of these tags into the cells of interest. In infection biology, in most cases this is done via transfection (TF) of the eukaryotic host cells with plasmid DNA bearing a marker gene or gene of interest (GOI) tagged with an FP. Basically, two different outcomes can be achieved: (1) transient TF leading to the expression of the FP-tagged GOI for a certain period of time (depending on a range of factors), (2) or stable TF with constant expression of the FP-tagged GOI (mostly via integration into the genome). Both feature mutual advantages/disadvantages.

A diverse range of methods is available to achieve TF, including chemical, physical, or viral ones. Basically all of the methods employing chemical agents aim at increasing the probability of closer contact between the negatively charged DNA and the equally negatively charged cell membrane, mostly by surrounding the DNA with a net positive charge, with subsequent uptake of the DNA by the cell. One such type of agents are cationic polymers, like diethylaminoethyl (DEAE)-dextran (one of the first chemical agents used for TF at all) [27] or the successively developed polybrene, polyethyleneimine, and the so-called dendrimers. Another well-established chemical agent for TF (since it is inexpensive, effective with a range of cell lines, and easy-to-use) is calcium phosphate, causing co-precipitation and consecutive uptake of the DNA [28, 29]. Third of the widespread chemical ones are lipid-based transfection reagents (this process also called lipofection) [30, 31], with newer developments utilizing cationic lipids with the inclusion of neutral ones [32]. Some of these agents build

liposomes leading to actual fusion with the cell membrane; others simply encapsulate the DNA before uptake.

Even if transient TF is successful, care still has to be taken to choose cells in the actual imaging that do not exhibit unnatural traits, such as uncommon FP aggregation. This for sure represents cellular stress, whether as a stress response itself or due to the overexpression of the FP/FP-tagged GOI in highly expressing cells. In addition, effects possibly not directly visible (such as potentially detrimental metabolic burden due to high expression) have to be considered. Ideally, the construct used displays an expression level comparable to the endogenous one. Because this is not always clear, generally selecting a moderate or low level will likely not be disadvantageous since high levels might again induce stress.

Whereas transient TF is more or less independent of the cell line employed (with the misfortune of not all cell lines being accessible to transient TF or at least only to some degree), the major disadvantages of it include first a TF efficiency that is often not reliably predictable and second the frequent result of cells with a highly heterogeneous GOI expression which is illustrated in Fig. 3b, c for TF of LAMP1-GFP with calcium phosphate and FuGene (see Note 6), respectively. Both is exceptionally undesirable for LCI since this elongates the search procedure for appropriate cells and thus can significantly reduce the time to analyze certain time points or prohibit analysis completely. The alternative would be to establish stable TF, in which notably the latter two of the above mentioned chemical agent types provide adequate success, in most cases exploiting antibiotic selection (e.g., with Geneticin/G418). But since this is laborious and

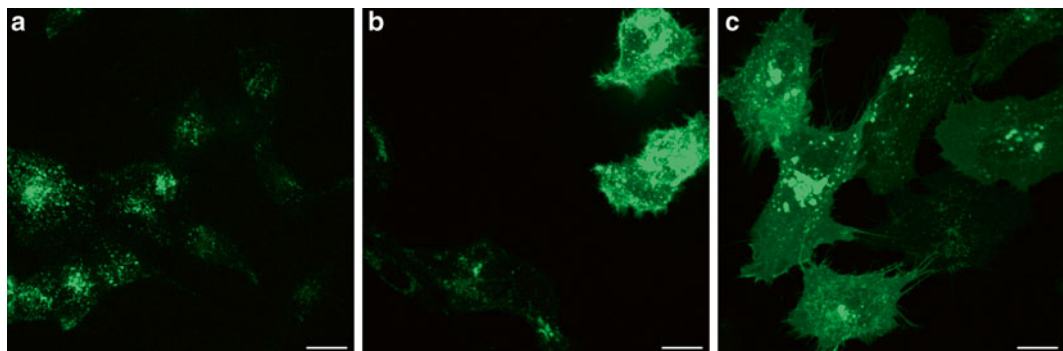


Fig. 3 Comparison of stable and transient transfection. (a–c) HeLa cells expressing LAMP1-GFP were imaged by SDCM (see Note 10) using 1 % 488 nm laser and 200 ms camera exposure time for GFP. Shown are single Z-slices indicating the heterogeneity of LAMP1-GFP expression. Scale bar, 20 μ m. (a) Stably transfected HeLa cells imaged 48 h after seeding showing overall moderate expression and low heterogeneity. (b) HeLa cells transiently transfected using calcium phosphate (see Subheading 3.2) imaged 48 and 24 h after seeding and transfection, respectively, show highly variable expression levels. (c) HeLa cells transiently transfected using FuGene (see Subheading 3.2) imaged 48 and 24 h after seeding and transfection, respectively, show higher heterogeneity and an overall higher expression leading to a higher cytosolic background signal

unfortunately also yields recurrently negative results another approach for stable TF is the use of viral vectors, with adenoviral or lentiviral ones being well established by now [33, 34]. Of course these methods can likewise be used for transient TF, which is particularly beneficial for cell lines inaccessible to other methods, but its full potential lies in its rather easy employment for stable TF. Taking safety considerations into account (an issue not to be underestimated with viral vectors) especially the lentiviral transfer applying a three-plasmid system proved to be suitable, where enveloping, packaging, and integrating (with the GOI incorporated) parts of the viral genome are separated. If successful, subsequent sorting via flow cytometry allows selecting for an appropriate level of fluorescence, thus with the reliable expression taken altogether abolishing several of the problems of transient TF, which also is illustrated in Fig. 3a with a stably transfected HeLa LAMP1-GFP cell line. Still such stably transfected cell lines have to be thoroughly tested for possible alterations of the examined phenotypes.

LCI certainly does not forbid the inclusion of other microscopic techniques if the acquired setup is open to. These might comprise for example fluorescence recovery after photobleaching (FRAP) as well as total internal reflection fluorescence (TIRF) techniques, but will not be discussed here in detail.

1.4 Imaging Setups for *Salmonella*

Apart from requirements necessary for LCI infection experiments with *Salmonella* call for yet another set of considerations. First, *Salmonella* has to be visualized during imaging, in most cases accomplished by using some standard plasmid simply bearing an FP gene. Aside from the same parameters important for the use of FPs in LCI in general (see Subheading 1.3), which have to be tested and possibly optimized in *Salmonella*, another critical one here is the choice of the promoter located before the FP gene (a parameter separate from the copy number of the plasmid). Together with the inherent brightness of the FP this factor controls the overall intensity of the fluorescence signal. For *Salmonella* theoretically a diverse set of promoters can be employed, ranging from natural enterobacterial or *Salmonella* specific to artificial ones. Naturally a promoter with constitutive expression would be chosen. But though also a bright signal is usually desirable, a combination of promoter and FP (and plasmid copy number) giving the highest signal intensity will unlikely be the preferred choice (see Subheading 1.3). After all it has to be ensured that the FP expression does not alter traits of *Salmonella*, here especially that it does not impair the virulence (e.g., due to metabolic burden or FP aggregation), which will more probably be achieved with moderate levels of fluorescence. One such suitable combination is the mid-copy plasmid pFPV25.1 with a GFPmut3a variant controlled by the ribosomal *rpsM* promoter [35–37], concurrently providing a backbone to introduce other FPs like mCherry [11]. These plasmids were used for imaging shown in Figs. 1 and 2a.

Concerning methods of TF, one has to bear in mind that lipid-based methods may alter a phenotype examined in general, and in particular lipid-related phenotypes. It is therefore pivotal to carefully determine the effect of the TF reagent for *Salmonella*-induced phenotypes, such as tubular membrane structures like SIF.

Furthermore, if using transient TF one empirical observation is the preference of *Salmonella* to invade non-transfected cells, complicating again the search for proper cells suitable for imaging. Although increasing the multiplicity of infection (MOI, i.e., the ratio of bacteria to cells) might alleviate this problem, this also results in an increased amount of cells with a high number of bacteria invaded, which can lead to such a high bacterial load that *Salmonella* escapes from the SCV and massively replicates in the cytosol (a phenomenon termed “hyper replication”), representing only in part a natural situation. Hence this also strongly argues for the use of stably transfected cell lines if available. However as mentioned above alterations of in this case *Salmonella*-induced virulence phenotypes have to be excluded by any means in such cell lines and correspondingly tested. Another empirical observation is the occasional appearance of “hyper replication” independent of elevated MOIs (i.e., regardless of the starting bacterial load) in moderately infected cells, again representing a possible hindrance in analysis. All in all these obstacles have to be taken into account when planning infection experiments.

Normally, the host cells and the *Salmonella* will be tagged with different FPs to allow precise intracellular localization of the bacteria and to avoid possible confusion with cellular compartments or complexes. Nevertheless if speed is of utmost importance the same tag can be applied (so one excitation laser can be omitted), since *Salmonella* normally can be distinguished rather well from cellular elements due to their size and form. In combination with LAMP1-tagging however one disadvantage would be the loss of discrimination between *Salmonella* and the SCV membrane. Additionally, since the fluorescence signal in *Salmonella* is comparatively condensed and bright, another problem might be overexposure of the *Salmonella* if the signal of the cell is adjusted to suitable levels or vice versa. This is illustrated in Fig. 2a by adjusting the acquisition of the signal with the camera exposure time to either the bacterial signal or the cellular, in the first case underestimating the cellular signal and in the second overexposing the bacterial.

2 Materials

2.1 Seeding of Cells for LCI

1. Cell line: we routinely use the non-polarized epithelial cell line HeLa, transfected with LAMP1-GFP or -mCherry either transiently (see Subheading 2.2) or stably using lentiviral vectors (see Note 1).

2. Cell culture medium (for HeLa cells): Dulbecco's Modified Eagle's Medium (DMEM), supplemented with 1 mM sodium pyruvate, 4 mM stable glutamine, and 10 % inactivated fetal calf serum (FCS) (*see Note 2*).
3. Phosphate buffered saline (PBS): 1.06 mM KH_2PO_4 , 2.97 mM Na_2HPO_4 , 155.2 mM NaCl, pH 7.4; Accutase (*see Note 3*).
4. Culture vessels/sample carriers for LCI: high-resolution compatible 35 mm dishes or chamber slides for regular imaging, or standard multiwell plates for screening approaches (*see Note 4*).

2.2 Transient Transfection

Transfection using calcium phosphate

1. DNA constructs of interest.
2. Solution A: 250 mM CaCl_2 .
3. Solution B: 1.4 mM phosphate (H_2PO_4^- or HPO_4^{2-}), 140 mM NaCl, 50 mM HEPES; adjust to pH 7.05 using HCl/NaOH (*see Note 5*).
4. Cell culture medium DMEM with FCS.
5. Optional: 10 % Glycerol in PBS.

Transfection using FuGENE HD transfection reagent

1. DNA constructs of interest.
2. FuGENE HD (*see Note 6*).
3. Cell culture medium DMEM without FCS.
4. Cell culture medium DMEM with FCS.

2.3 Infection of Cells

1. Luria-Bertani (LB) broth: 10 g/L tryptone, 5 g/L yeast extract, 10 g/L NaCl, adjusted to pH 7.0–7.5; LB agar plates (with 15 g/L agar); both with appropriate antibiotics if necessary (*see Note 7*).
2. Desired *Salmonella* strains (*see Note 8*).
3. PBS.
4. Cell culture medium DMEM without FCS.
5. Cell culture medium DMEM with FCS.
6. Gentamicin (Sigma-Aldrich): 10 mg/mL in $\text{H}_2\text{O}_{\text{dd}}$.

2.4 LCI Using Confocal Microscopy

1. Imaging medium (IM): MEM without sodium pyruvate, glutamine, phenol red, and bicarbonate; 30 mM HEPES pH 7.4 and 10 $\mu\text{g}/\text{mL}$ added (*see Note 9*).
2. Confocal Microscope: either a CLSM or an SDCM system (*see Note 10*).
3. Heating device for 37 °C incubation (*see Note 11*).

2.5 Fixation of Cells After LCI

1. 3 % paraformaldehyde (PFA) in PBS (see Note 12).
2. PBS.

3 Methods

3.1 Seeding of Cells for LCI

1. Seed PBS-washed and Accutase-detached cells (following standard cell culture procedures) into the culture vessel/sample carrier of choice (see Note 13).
2. Incubate for 1–2 days at 37 °C, 90 % humidity, 5 % CO₂.

3.2 Transient Transfection (See Note 14)

Transfection using calcium phosphate

1. Dissolve DNA in Solution A (see Note 15).
2. Add the same volume of Solution B to this mixture, homogenize shortly by pipetting.
3. Incubate for 1 min at room temperature (RT).
4. Apply the complete transfection mixture to the well/dish.
5. Incubate cells for 4 h at 37 °C, 90 % humidity, 5 % CO₂.
6. Remove old and add fresh medium (see Note 16).
7. Incubate for 24 h at 37 °C, 90 % humidity, 5 % CO₂ (see Note 17).

Transfection using FuGENE HD transfection reagent (Promega)

1. Dissolve DNA in medium without serum (see Note 18).
2. Add FuGENE HD in the desired reagent:DNA ratio (see Note 19).
3. Incubate for 5–15 min at RT (see Note 20).
4. Apply the transfection mixture to the well/dish.
5. Incubate for 24–48 h at 37 °C, 90 % humidity, 5 % CO₂ (see Note 21).

3.3 Infection of Cells

1. Inoculate liquid LB cultures (with antibiotics if required) in glass test tubes with single colonies from plates of the desired *Salmonella* strains.
2. Grow cultures overnight at 37 °C with aeration (see Note 22).
3. Dilute the culture 1:31 in fresh LB (with antibiotics if required, “subculture”) and incubate for another 3.5 h at 37 °C with aeration (see Note 23).
4. Measure OD₆₀₀ and adjust to an OD₆₀₀ of 0.2 with PBS (see Note 24).
5. Add the appropriate amount of bacteria for a specific MOI to the culture and distribute by gently pipetting up and down (see Note 25).
6. Incubate for 25 min at 37 °C, 90 % humidity, 5 % CO₂.

7. Wash cells 2–3 times with PBS (*see Note 26*).
8. Add medium without serum containing 100 µg/mL gentamicin; this is time point 0 h (*see Note 27*).
9. Incubate for 1 h at 37 °C, 90 % humidity, 5 % CO₂.
10. Change to medium with serum containing 10 µg/mL gentamicin (*see Note 28*).
11. Incubate until imaging at 37 °C, 90 % humidity, 5 % CO₂.

3.4 LCI Using Confocal Microscopy

The following procedure describes the generic steps to be applied to any confocal microscope system, although specific references to our systems described in Subheading 3.4 are inevitable.

1. Preheat the microscope system so that it can sufficiently equilibrate to 37 °C (*see Note 29*).
2. After desired time of infection, change cell culture medium to IM (*see Note 30*).
3. Transport the samples to the microscope (*see Note 31*).
4. Choose a high-resolution objective and add immersion medium as appropriate (*see Note 32*).
5. Search through the eyepiece for one or more suitable infected cells for imaging phenotypes under study using mercury, xenon, or metal halide arc lamp illumination with appropriate FITC/GFP and TRITC/RFP filters (*see Note 33*).
6. Switch to define appropriate settings for acquisition with lasers:
 - (a) For a CLSM system:
 - Mode of acquisition: dimensions, scanning order, tiles or multiple positions, size/resolution, speed, zoom, line/frame averaging, pinhole size (*see Note 34*).
 - Beam path settings: laser power, PMT emission setting (*see Note 35*).
 - Signal adjustment: smart gain, smart offset (*see Note 36*).
 - (b) For an SDCM system:
 - Channel configuration and light path settings: laser power, emission filters, camera exposure time and EM gain, dual camera settings (*see Note 37*).
 - Further acquisition parameters: binning, ROI, camera orientation, focus strategy and devices (*see Note 38*).
 - Multidimensional acquisition: Z-stack, time-lapse, tiles or multiple positions (*see Note 39*).
7. Start the acquisition of your defined experiment (*see Note 40*).
8. After acquisition finished save the generated files (*see Note 41*).

3.5 Fixation of Cells After LCI (See Note 42)

1. Remove medium and incubate for 15 min at RT with 3 % PFA (see Note 43).
2. Wash thrice with PBS and store in PBS (see Note 44).

4 Notes

1. Various other cell lines can be used to study the infectious cycle of *Salmonella*, including macrophages and polarized epithelial cell lines Caco-2 or MDCK. We record the passage number of cells and use cells up to a maximal passage number.
2. We routinely use cell culture media from PAA (GE Healthcare) or Biochrom (Merck Millipore). Considering the instability of L-glutamine if heated continuously or repeatedly most suppliers offer now media containing stable glutamine, i.e. a dipeptide of L-alanyl-L-glutamine (in some cases also glycyl-L-glutamine), which withstands heating (also called GlutaMAX from Gibco/Life Tech). Many suppliers of FCS do no longer recommend inactivating FCS, since destruction of beneficial components might prevail over inactivation of the complement system. Nevertheless we still complement inactivate serum to avoid undesired effects on *Salmonella*.
3. For detachment of adherent cells, Accutase (PAA) is routinely used. Alternatively, trypsin-EDTA solutions may be used.
4. Use 35 mm dishes with glass bottom (FluoroDishes World Precision Instruments or ibidi) for one-condition experiments. For sequential imaging of conditions, e.g., *Salmonella* strains, chamber slides are recommendable, ranging from 2- to 8-well slides (ibidi, with glass-like bottom; Nunc, glass bottom). For high-throughput analyses, 96-well plates may be used (TPP, Nunc).
5. The TF procedure is extremely dependent on the stable and precise pH of this solution [29].
6. We gained decent results especially regarding possible interference with *Salmonella*-induced phenotypes with this lipid-based but nonetheless non-liposomal TF reagent from Promega. Of course, there is a whole range of other renowned TF reagents, such as Lipofectamine from Life Tech (liposomal) or PolyFect from Qiagen (dendrimer).
7. Alternatively, use premixed LB media (Difco, BD).
8. *S. enterica* serovar Typhimurium NCTC12023 (identical to ATCC14028s) and SL1344 are used as wild-type (WT) strains, usually harboring the plasmid pFPV25.1 or derivatives for constitutive expression of GFP and alternative fluorescent proteins, complementary to the respective LAMP1-tagging (except if only one FP is used). Strains with these plasmids

show stable fluorescent signals and acceptable impairment of virulence traits. Nevertheless, other vector/FP combinations are possible.

9. This medium proved to be suitable for LCI, main aims being to exclude bicarbonate as buffer system and phenol red from microscopy (*see* Subheading 1.3) [12].
10. A Leica TCS SP5 II with a DMI6000 B stand and automated stage, operated via the Leica Application Suite Advanced Fluorescence (LAS AF) software, was used as CLSM. SDCM was performed on a Zeiss Cell Observer stand with a spinning disk Confocal Scanner Unit (CSU)-X1, an automated PZ-2000 stage from Applied Scientific Instrumentation (USA), two Evolve EMCCD cameras from Photometrics (USA), an IRF device called “Definite Focus” directly from Zeiss, a UNIBLITZ transmitted light (TL) shutter from Vincent Associates (USA), and an optional DirectFRAP device, operated via the ZEN 2012 software. Both systems are capable of multicolor imaging and are part of the Center for Advanced Light Microscopy of the University of Osnabrück (CALMOS); exact details including images of the systems can be looked up at the following address: <http://www.biologie.uni-osnabrueck.de/Calm-OS/index.php?cat=Home>. The Leica system is a rather basic, but highly stable system for standard CLSM applications adapted for LCI with an additional heating device, whereas the Zeiss system is specifically equipped for high-speed imaging, also combined with a heating device for LCI (*see* Note 11).
11. For environmental control, the CLSM was equipped with a large incubation chamber, “The Box,” by Life Imaging Services (Switzerland), with “The Cube” heating unit, and gas mixer “The Brick,” which delivers gas via a water-filled column (*see* Note 9). The SDCM uses a stage top incubation P Lab-Tek S1 heating insert and a PM S1 incubator lid from PeCon (Germany), which enables to insert 35 mm dishes or chamber slides. It is also capable of supplying CO₂ and humidity (via a water-filled bottle). Additionally, this system is equipped with a heated “working plate” where samples can be deposited temporarily.
12. We routinely use 3 % PFA; other laboratories also use 4 % PFA or additives such as 4 % sucrose.
13. If using stably transfected cells we normally seed 1 day before infection 4–6 × 10⁴ cells in 0.3 mL per well of an 8-well chamber slide (ibidi, 1 cm² growth area) or 3–4 × 10⁵ cells in 2–3 mL per FluoroDish (WPI, ca. 8.5 cm²). If cells are additionally transiently transfected, we seed 2 days before infection with half of the cell number stated above. In our hands these number give sufficient, but not too dispersed cells suitable for LCI (and if desired for TF). Nevertheless, cell numbers can be varied for specific tasks or depending on personal preferences.

14. This step may be skipped if using stably transfected cell lines, except if a second marker shall be introduced. Independent of the actual TF method used cells in general should be kept at optimal conditions during the whole experiment avoiding amongst others temperature shifts, e.g., by using aluminum heating plates while working outside the incubator to maintain 37 °C. With the cell numbers given in **Note 13** cells seeded 1 day before TF (and 2 days before infection) should show 70–80 % confluence at the time point of TF, being optimal for this process.
15. Optionally, medium can be changed directly or 30 min before TF, sometimes resulting in higher efficiency. The optimal amount of DNA has to be standardized for each combination of plasmid and cell line. We typically use 0.5 µg per well in an 8-well chamber slide or 2 µg in a 35 mm dish (thus not completely adjusting to the bigger growth area/higher cell number) of our LAMP1-GFP or LAMP1-mCherry plasmids with HeLa cells. Usually we use per well of 8-well chamber slides (or 24-well plates) 25 µL of Solution A and B, each, for dishes accordingly 200 µL.
16. Optionally, replace medium by pre-warmed 10 % glycerol in PBS for 1 min before adding fresh medium.
17. Exact times may vary dependent on constructs, but for most constructs the highest expression level can be observed after 24 h (as for our LAMP1 constructs).
18. Volumes of the serum-free medium correspond to the ones of the single solutions in calcium phosphate TF, i.e., 25 and 200 µL, respectively (*see Note 15*).
19. Basically, the manufacturer's instructions were applied. Minor modifications are reagent:DNA ratio of 2:1 for LAMP1 constructs, i.e., 1 µL FuGENE HD to 0.5 µg DNA or 4 µL to 2 µg in 8-well chamber slides or 35 mm dishes, respectively. It is important to avoid contact of FuGENE HD reagent with the walls of mixing tube, reagent must be added directly into the medium.
20. As mentioned these are the manufacturer's instructions, we generally incubate for 10 min.
21. Standard is 24 h.
22. We use a roller drum for optimal growth of bacterial cultures regarding aeration in glass test tubes. Alternatively, a platform shaker with tilted test tubes may be used. Alternatively, a culture grown overday can be used as long as it is stationary (grown at least for 8 h).
23. We empirically determined the highest expression of SPI1 genes (needed for invasion) with subcultures prepared this way (late logarithmic growth phase). Other laboratories use different

times and dilutions, partly due to the devices used. Independent of the exact growth conditions used one has to ensure optimal SPI1 gene expression. In our hands it is also possible to use time-controlled climate fridges/incubators. Inoculated culture tubes kept at 4 °C with shift to incubation at 37 °C is timed in a manner that allows start of host cell infection in the morning.

24. An $OD_{600}=0.2$ correlates empirically with roughly 3×10^8 bacteria/mL, allowing estimations of the MOI applied.
25. This procedure is the most convenient one for a single dish or well. If the same condition is applied to several dishes or wells an infection master mix can be prepared, i.e., an appropriate amount of bacteria in medium adjusted to the volume per dish/well needed. In such a mix medium without serum can be used, since it is discarded afterwards and thus does not remain long enough on the cells to induce serum hunger. Optionally, if possible (e.g., with standard multiwell plates), the infection can be synchronized by centrifugation for 5 min, $500 \times g$ at RT, thus increasing the contact frequency between bacteria and cells.
26. On the one hand excessive non-internalized bacteria should be removed; on the other hand care should be taken that cells do not detach from the bottom at this step.
27. The procedure described here is also called gentamicin protection assay: since eukaryotic cells are impermeable to gentamicin, after some time given for infection, only the non-internalized and non-washed-away bacteria should be killed by gentamicin, so that the ones that invaded the cells successfully are protected. In doing so initially, a rather high gentamicin concentration is chosen to effectively eradicate extracellular bacteria. Afterwards concentration is lowered, so again (as with the infection master mixes, *see Note 25*) medium without serum can be applied due to the short time of exposure.
28. A moderate antibiotic pressure is maintained to account for bacteria that still adhered to the outside of the cells despite the washing and the ones that get loose from bursting cells due to hyper-replication at early time points or normal replication at later time points.
29. Preheating of a large incubation box takes longer, normally 0.5–1 h, whereas a stage top incubation takes only several minutes (except the relatively large working plate, *see Note 11*).
30. One washing step with PBS may be included, but is not essential.
31. Again ideally, the cells are transported heated, e.g., using heating plates (*see Note 14*).

32. For the CLSM, HCX PL APO 40 \times /1.25–0.75 Oil or HCX PL APO 100 \times /1.40–0.70 Oil CS objectives are routinely used. The 40 \times objective might be the better choice in combination with zoom if resolution is not critical, because it is more light sensitive than the 100 \times and thus imaging of the sample can be designed more gentle (since with similar numerical apertures (NA) the magnification has a higher impact on the light collection efficiency of an objective). At the Zeiss system we normally use a α Plan-Apochromat 63 \times /1.46 Oil Corr (with a cover glass correction ring) or a Plan-Apochromat 40 \times /1.4 Oil DIC objective (both equipped with a DIC slider). Alternatively an LD Plan-Neofluar 40 \times /0.6 Corr air objective with a bottom thickness correction ring proved to be highly useful for multiwell plates and multi-position experiments since oil loss is omitted. For further details of the objectives refer to the website in **Note 10**.
33. Searching for suitable positions is usually done using the eyepiece with an arc lamp (thus being basically wide-field microscopy), primarily because laser illumination is prohibited at this step and it is gentler to the sample. But if for example using FRAP the filter wheel is replaced by a fast beam path switch, so one is forced to search with laser illumination. In both, the Leica system with the EL6000 and the Zeiss system with the HXP 120 C lamp, alignment-free metal halide type lamps are integrated, which are superior to mercury and xenon lamps with regard to LCI due to lower power and less spectral UV components. Whereas in LAS AF all concerning acquisition is arranged in one window or tab, “Acquire,” in ZEN the software is conveniently sorted by superior tabs, with the “Locate” tab being the one for manipulating the eyepiece observation. Depending on the exact FP-tagging of the cells and the bacteria other filters might be necessary, but here we mostly use a GFP filter to identify cells and an RFP filter for bacteria (or vice versa), which are the filter sets A and N2.1 at the Leica, and 38 HE and 43 HE at the Zeiss system (for detailed properties refer to the website in **Note 10**). From most suppliers a range of filters is available for the same spectral range and one has to decide which to choose depending on the exact preferences and requirements. For eyepiece observation emission longpass (LP) filters (i.e., from a designated wavelength onwards) are perfectly fine (as our Leica filters), even if FP crosstalk/bleed-through appears, as long as one can sufficiently distinguish the signals to choose suitable cells/positions and as long as acquisition settings are different from that. Otherwise BP filters (as our Zeiss filters) can be chosen. At this point it is especially useful to have the bacteria differently FP-tagged than the cells, so that searching for infected cells is rather straightforward with another fluorescence.

Searching for cells in BF is of course another possibility. Many like to use it for finding the focus since it is even gentler to the sample, albeit the general intensity of the lamp can mostly be adjusted or decreased, respectively, so that searching with fluorescence might again be acceptable. Additionally notably in transient TF finding cells using BF does not guarantee also transfected cells; hence one has to use fluorescent settings anyway at some step.

34. In LAS AF in the first tab, “Acquisition Mode,” first the dimensions are set: different combinations of x, y, z, and t are possible, whereupon using z or t opens additional tabs. The same holds true for using the “Sequential Scanning” (*see Note 35*) and “Tile Scan” or “Mark and Find” options (the latter two work only if the motorized stage was initialized, which is asked for during the start-up of LAS AF). In the next tab, “XY,” most of the image quality-influencing parameters can be modified. The default settings are a format of 512×512 and 400 Hz speed, which are basically fully sufficient for LCI. If resolution is increased to $1,024 \times 1,024$ (which we normally do), correspondingly the speed should be, especially for LCI, increased to account for slower scanning speed (e.g., to 700 Hz). Additionally “Bidirectional” should be checked so that scanning meanders instead of combing, also increasing the overall speed. Furthermore, a digital zoom can be applied accommodating for lower-resolution objectives (*see Note 32*). Moreover, the averaging of lines or complete frames can be chosen to reduce background noise. However due to the considerable loss of speed, elevated photobleaching/-toxicity, and possible cell movement, frame averaging is not advisable for LCI, and some even resign line averaging, but we nonetheless use 2–4 line averages. Along this it is possible to open the pinhole, thus increasing sensitivity (which might be beneficial for LCI) but also losing some axial resolution, but again we nevertheless stick to the default setting (i.e., 1 Airy Unit). If acquiring Z-stacks the beginning and end can be defined in the homonymous tab with the “Live” mode turned on. For the z-step size/number of z-steps either “System Optimized” can be checked or they can be defined individually; normally we stick to the latter and define somewhat bigger Z-steps (0.3–0.5 μm size) to increase speed, depending on the exact requirements. Similarly if acquiring a time-lapse experiment either a certain number of steps with a certain interval or a fixed duration (or even simply continuously until stopped) can be defined in the “t” tab, which is completely sample-dependent. If we analyze the overall development of the SIF network, we acquire for example for several hours with 30–60 min intervals. For SIF movements (highly dynamic events) we try to image as fast as possible (or switch to the Zeiss system since it is more suitable for such analyses).

If using “Tile Scan” a mosaic-like acquisition of neighboring fields of view can be designated in the corresponding tab, with “Mark and Find” being the analogous option for individual/separated positions.

35. In the main panel of LAS AF the beam path settings are adjusted. To avoid possible crosstalk/bleed-through of the FPs applied, sequential scans should be performed, i.e., acquisition of the channels one after the other. After choosing the appropriate number of scans each one of them can be altered separately. Switching between the scans during acquisition can be done between lines, frames, or even stacks, but again due to cell movement line switching should be preferred to frames (let alone stacks). Now the PMT settings can be defined for each of the scans (after clicking “Visible”), by first choosing a proper fluorophore (e.g., Alexa488 or Alexa568, respectively, as GFP and mCherry/RFP surrogates), then turning up/adjusting the laser power/percentage of the acousto-optical tunable filters (AOTF), and adapting the slider bar to the emission spectrum. Last an appropriate filter is selected for this channel setup, where we normally use the double dichroic (DD) 488/543 polychromic mirror for GFP/RFP acquisition (theoretically a triple dichroic (TD) 488/543/633 could also be employed, without actually using the additional band). In LCI we generally try to decrease laser powers as much as possible to avoid photobleaching/-toxicity, so we typically do not exceed 15 % 488 nm laser (20 mW Ar) and 30 % 543 nm laser (1 mW He-Ne) with the 100× objective. Besides we normally expand the emission slider bar a little bit to increase the overall signal intensity. Additionally here in the main panel a freely definable “ROI Scan” selection can be included, if desired, e.g., if not the complete field of view is necessary to image (thus also being beneficial for LCI).
36. To acquire with an optimized S/N start the “Live” mode (after choosing the intensity scale display mode with the “Quick Loop Up Table” (LUT) button) and first adjust the smart offset so that the background appears green, which means in this mode no signal. Then adjust the smart gain so that most areas appear orange to white and only some blue (the latter meaning saturated signal). We typically define an offset of -0.2 to 0.0 % and a relatively high gain of ca. 800 V for 488 nm and ca. 1,000 V for 543 nm lasers (rather high voltages, but which are also generally recommendable for LCI to increase sensitivity even if the S/N is lowered to some degree). If acquiring with cells and bacteria tagged with the same FP here specifically the bacteria will inevitably become saturated to get sufficient signal for the cells since their FP signal is highly condensed compared to the cells.

37. In ZEN, channel configuration can be done in two ways. Either by using the smart setup or by setting up channels from scratch. Smart setup is rather convenient, you simply choose the FPs used and decide between different light path setups (if several equivalent microscope components are available), which can include “Fastest,” “Best Signal,” or “Best Compromise.” The software automatically chooses the appropriate hardware components, depending on the chosen setup. The settings can then be checked and/or modified, if desired, at the “Light Path Settings” tab at the “Setup Manager” block and the “Channels” tab at the “Acquisition Parameters” block. But since these settings still might not be optimal and additionally might not recognize custom-altered parts (e.g., if Zeiss-external parts are not definable in the Micro Tool Box (MTB), the hardware-determining background software of Zeiss ZEN), we prefer to define channels from scratch via the “Channels” tab in combination with the Light Path Settings tab. This, albeit more error prone, gives higher flexibility in configuring proper channels. A standard configuration we use comprises channels with a 488 nm laser (100 mW optically pumped semiconductor) in combination with a 525/50 nm BP filter and a 561 nm laser (40 mW diode) with a LP 580 nm filter. With the 63 \times oil objective and a sufficiently bright FP signal 1–2 % 488 nm with an exposure time of the Evolve camera of 100 ms or even less is satisfactory. For the 561 nm we use about 5 % with 100–300 ms exposure time. Both holds true if the EM gain (also located here) is near 500. It ranges from 0 to 1,000 and can be increased independent of laser power/exposure time to raise the overall signal intensity. However, the so-called “sweet spot” of the camera is at a gain of ca. 500, which should result in a decent S/N compromise. For smaller magnification objectives, all these parameters have to be adjusted accordingly. Commonly adjustments of the fluorescence signal are monitored with the “Live” mode, where similar to LAS AF (*see Note 36*) over-/underexposed areas are marked as red or blue, respectively, by choosing the “Range Indicator” (in the “Dimensions” tab below the image). Additionally, ZEN shows a display curve of the gray values beneath the image which can be fluently adjusted for brightness, contrast, and gamma online. Generally, signal intensity is a point where a balance has to be found between laser power and exposure time. Raising laser power allows reducing the exposure time and thus increases speed, but conversely risks more photobleaching/-toxicity, and vice versa. This way or the other ideally exposure times of different channels should be synchronized so that the Nipkow disk shows the same rotation speed (we determined this empirically, reported at the “Light Path Settings” tab) and no speed is lost in accelerating or

decelerating the disk. As described in Subheading 1.3 different actions can be taken to further increase speed. For example we also use a 527/54 nm and 645/60 nm DBP for GFP/RFP acquisition (which is more suitable for a GFP/mCherry combination than for GFP with DsRed or TagRFP-T, respectively, since the latter exhibit a second excitation maximum at 488 nm and thus cause crosstalk and bleed-through with this filter). Another possibility is to use a dual camera option, where a 629/62 nm beamsplitter in the CSU unit separates the signal onto two different cameras (with only red signal detected with the second camera due to this specific beamsplitter, whereas with the first camera any filter of the normal CSU filter wheel can be used). However, the cameras have to be aligned each time in a separate menu opening thereupon. This is best done with botanical samples (such as from *Convallaria majalis*), which normally show a uniform image almost all over the spectral range. Additionally, one has to bear in mind that by splitting up the beam signal intensity for the individual channels is lost, so laser power/exposure time has to be adjusted (again increasing photobleaching/-toxicity risk).

38. Additional adjustments regarding the cameras are done in the “Acquisition Mode” tab at the “Acquisition Parameter” block, with one being the definition of an “Acquisition ROI,” where the rectangular shape is freely adjustable in size and position. Moreover, here binning can be adjusted and the orientation or the “Live” speed of the cameras altered, if desired. In the “Focus Strategy” tab different choices are available: none, Absolute Fixed Z-Position (e.g., if for several positions individual z-positions are defined, *see Note 36*), Definite Focus, SAF, Global Focus Surface (the strategy to define several focal support points to account for drift/variation in the sample carrier bottom, *see Subheading 1.3*), or different combinations of these. In the “Focus Devices” tab reference channels, exact settings of the SAF and time points of execution are hereupon adjustable. If Z-stacks are acquired (covering most of the cell) and cell movement is limited we stick in multi-position experiments to “Absolute Fixed Z-Position” with “Use Z-Position from Tiles Setup” checked (*see Note 39*). After all this works rather well and reduces the risk of failure of additional devices (only the motorized movement of the objective remains to be controlled). Otherwise the “Definite Focus” proved to be useful for LCI, especially because the SAF uses laser and (similar to the “Global Focus Surface”) appeared to be problematic in multi-position experiments if the sample carrier shows too much bottom variation, such as standard plastic bottom multiwell plates (*see also Subheading 1.3*).

39. At the “Multidimensional Acquisition” block additional tabs appear only if checked at the heading of the blocks. Comparable to LAS AF (see Note 34) Z-stacks can be defined at the homonymous tab via beginning/end, but also simply by a center. Here using the “Optimal” button fulfills the Nyquist criterion, but similar to the Leica system 0.3–0.5 μm is often sufficient. With the “Time Series” tab again either a certain number of steps or a fixed duration (or simply as long as possible), each also with a certain interval, can be defined with similar considerations as for the CLSM, only that the SDCM is generally much faster, if desired. Furthermore, in the “Tiles” tab (this being different from LAS AF) both “Tiles Regions” and independent “Positions” can be designated. If using a defined sample carrier (several templates are available, but new ones can also be defined from scratch), which was properly calibrated (using again a separate menu opening thereupon), it is also possible to define “Position Arrays” for automated screening of the sample carrier (with several possibilities to arrange the single positions, exhibiting an astounding position stability). Unfortunately the selectable “Options” (such as combining vs. meandering or optimized stage travel) apply only to tiles and not positions. If all these options do not suffice the use of the “Experiment Designer” allows the setup of acquisitions with complete liberty in design (e.g., if one wants to acquire every hour for 5 min at full speed).
40. In both LAS AF and ZEN settings can be saved (or even be retrieved from previous files/experiments) so that they do not have to be established from scratch every time.
41. The lite version of LAS AF allows opening, display of metadata, conversion and basic editing of images. Open source software such as ImageJ or Fiji may be used and incorporate routines of opening LAS files. In contrast, the ZEN lite version allows remarkably extensive image processing.
42. This step is optional if one wants to postpone certain analysis not dependent on LCI or to freeze an interesting phenotype, time point, etc.
43. This is our standard procedure. Additional washing steps with PBS might be included, but are not necessary, might even interfere with cellular phenotypes before they can be fixed. Additionally, depending on the phenotype observed some extend the fixation time to 1 h and/or fix at 37 °C (e.g., for actin cytoskeleton analysis temperature stability is crucial).
44. Samples fixed in such a way can be stored for several weeks without significant fluorescence signal loss.

Acknowledgements

We thank all the members of our laboratory for fruitful discussion and feedback especially Viktoria Krieger for additional hints for FuGENE TF and the CLSM system. Furthermore, we thank Rainer Kurre at CALMOS for constant and invaluable support of our microscope systems. Work was supported by Deutsche Forschungsgemeinschaft (DFG) through grants HE1964 and SFB944, project P4, and the Bundesministerium für Bildung und Forschung (BMBF).

References

1. Haraga A, Ohlson MB, Miller SI (2008) *Salmonellae* interplay with host cells. *Nat Rev Microbiol* 6:53–66
2. Fabrega A, Vila J (2013) *Salmonella enterica* serovar Typhimurium skills to succeed in the host: virulence and regulation. *Clin Microbiol Rev* 26:308–341
3. Van Der Heijden J, Finlay BB (2012) Type III effector-mediated processes in *Salmonella* infection. *Future Microbiol* 7:685–703
4. Gerlach RG, Claudio N, Rohde M et al (2008) Cooperation of *Salmonella* pathogenicity islands 1 and 4 is required to breach epithelial barriers. *Cell Microbiol* 10:2364–2376
5. Bakowski MA, Braun V, Brumell JH (2008) *Salmonella*-containing vacuoles: directing traffic and nesting to grow. *Traffic* 9:2022–2031
6. Figueira R, Holden DW (2012) Functions of the *Salmonella* pathogenicity island 2 (SPI-2) type III secretion system effectors. *Microbiology* 158:1147–1161
7. Garcia-Del Portillo F, Zwick MB, Leung KY et al (1993) Intracellular replication of *Salmonella* within epithelial cells is associated with filamentous structures containing lysosomal membrane glycoproteins. *Infect Agents Dis* 2:227–231
8. Garcia-Del Portillo F, Zwick MB, Leung KY et al (1993) *Salmonella* induces the formation of filamentous structures containing lysosomal membrane glycoproteins in epithelial cells. *Proc Natl Acad Sci U S A* 90:10544–10548
9. Garcia-Del Portillo F, Finlay BB (1995) Targeting of *Salmonella typhimurium* to vesicles containing lysosomal membrane glycoproteins bypasses compartments with mannose 6-phosphate receptors. *J Cell Biol* 129:81–97
10. Schroeder N, Mota LJ, Meresse S (2011) *Salmonella*-induced tubular networks. *Trends Microbiol* 19:268–277
11. Drecktrah D, Levine-Wilkinson S, Dam T et al (2008) Dynamic behavior of *Salmonella*-induced membrane tubules in epithelial cells. *Traffic* 9: 2117–2129
12. Rajashekhar R, Liebl D, Seitz A et al (2008) Dynamic remodeling of the endosomal system during formation of *Salmonella*-induced filaments by intracellular *Salmonella enterica*. *Traffic* 9:2100–2116
13. Mironov AA, Beznoussenko GV (2009) Correlative microscopy: a potent tool for the study of rare or unique cellular and tissue events. *J Microsc* 235:308–321
14. Muller T, Schumann C, Kraegeloh A (2012) STED microscopy and its applications: new insights into cellular processes on the nanoscale. *Chemphyschem* 13:1986–2000
15. Henriques R, Griffiths C, Hesper Rego E et al (2011) PALM and STORM: unlocking live-cell super-resolution. *Biopolymers* 95:322–331
16. Herbert S, Soares H, Zimmer C et al (2012) Single-molecule localization super-resolution microscopy: deeper and faster. *Microsc Microanal* 18:1419–1429
17. Conchello JA, Lichtman JW (2005) Optical sectioning microscopy. *Nat Methods* 2: 920–931
18. Rai V, Dey N (2011) The basics of confocal microscopy. In: Wang C-C (ed) *Laser scanning, theory and applications*. InTech, Winchester, pp 75–96
19. Swedlow JR, Platani M (2002) Live cell imaging using wide-field microscopy and deconvolution. *Cell Struct Funct* 27:335–341
20. Rines DR, Thomann D, Dorn JF et al (2010) Live cell imaging of yeast. In: Goldman RD, Swedlow JR, Spector DL (eds) *Live cell imaging: a laboratory manual*. Cold Springer Harbor Laboratory Press, Cold Spring Harbor, NY, pp 333–350
21. Stehbens S, Pemble H, Murrow L et al (2012) Imaging intracellular protein dynamics by spinning disk confocal microscopy. *Methods Enzymol* 504:293–313

22. Tanaami T, Otsuki S, Tomosada N et al (2002) High-speed 1-frame/ms scanning confocal microscope with a microlens and Nipkow disks. *Appl Optics* 41:4704–4708
23. Frigault MM, Lacoste J, Swift JL et al (2009) Live-cell microscopy – tips and tools. *J Cell Sci* 122:753–767
24. Rizzo MA, Davidson MW, Piston DW (2010) Fluorescent protein tracking and detection. In: Goldman RD, Swedlow JR, Spector DL (eds) *Live cell imaging: a laboratory manual*. Cold Spring Harbor Laboratory Press, Cold Spring Harbor, NY, pp 3–34
25. Kremers GJ, Gilbert SG, Cranfill PJ et al (2011) Fluorescent proteins at a glance. *J Cell Sci* 124:157–160
26. Stepanenko OV, Stepanenko OV, Shcherbakova DM et al (2011) Modern fluorescent proteins: from chromophore formation to novel intracellular applications. *Biotechniques* 51:313–314, 316, 318 *passim*
27. Vaheri A, Pagano JS (1965) Infectious poliovirus RNA: a sensitive method of assay. *Virology* 27:434–436
28. Graham FL, Van Der Eb AJ (1973) A new technique for the assay of infectivity of human adenovirus 5 DNA. *Virology* 52:456–467
29. Jordan M, Wurm F (2004) Transfection of adherent and suspended cells by calcium phosphate. *Methods* 33:136–143
30. Fraley R, Subramani S, Berg P et al (1980) Introduction of liposome-encapsulated SV40 DNA into cells. *J Biol Chem* 255: 10431–10435
31. Felgner PL, Gadek TR, Holm M et al (1987) Lipofection: a highly efficient, lipid-mediated DNA-transfection procedure. *Proc Natl Acad Sci U S A* 84:7413–7417
32. Felgner JH, Kumar R, Sridhar CN et al (1994) Enhanced gene delivery and mechanism studies with a novel series of cationic lipid formulations. *J Biol Chem* 269: 2550–2561
33. Douglas JT (2007) Adenoviral vectors for gene therapy. *Mol Biotechnol* 36:71–80
34. Cockrell AS, Kafri T (2007) Gene delivery by lentivirus vectors. *Mol Biotechnol* 36: 184–204
35. Cormack BP, Valdivia RH, Falkow S (1996) FACS-optimized mutants of the green fluorescent protein (GFP). *Gene* 173:33–38
36. Valdivia RH, Falkow S (1996) Bacterial genetics by flow cytometry: rapid isolation of *Salmonella typhimurium* acid-inducible promoters by differential fluorescence induction. *Mol Microbiol* 22:367–378
37. Valdivia RH, Hromockyj AE, Monack D et al (1996) Applications for green fluorescent protein (GFP) in the study of host-pathogen interactions. *Gene* 173:47–52

Chapter 14

In Vitro Modeling of Gallbladder-Associated *Salmonella* spp. Colonization

Geoffrey Gonzalez-Escobedo and John S. Gunn

Abstract

The host-pathogen interactions occurring in the gallbladder during *Salmonella* Typhi colonization contribute to typhoid fever pathogenesis during the acute and chronic stages of disease. The gallbladder is the primary reservoir during chronic typhoid carriage. In this organ, *Salmonella* encounters host-barriers including bile, immunoglobulins, and mucus. However, the bacterium possesses mechanisms to resist and persist in this environment, in part by its ability to attach to and invade into the gallbladder epithelium. Such persistence in the gallbladder epithelium contributes to chronic carriage. In addition, patients harboring gallstones in their gallbladders have increased risk of becoming carriers because these abnormalities serve as a substrate for *Salmonella* biofilm formation. Our laboratory has studied the *Salmonella* interactions in this specific environment by developing in vitro methods that closely mimic the gallbladder and gallstones niches. These methods are reproducible and provide a platform for future studies of acute and chronic bacterial infections in the gallbladder.

Key words *Salmonella*, Gallbladder, Canine gallbladder epithelial cells, Invasion, Biofilms

1 Introduction

The gallbladder is a pear-shaped organ that stores and concentrates bile, a complex fluid involved in the emulsification of lipids after ingestion of food [1]. Histologically, the gallbladder consists of three layers: mucosa, muscularis, and adventitia or serosa. The gallbladder has no muscularis mucosae or submucosa. The mucosa consists of a single layer of columnar epithelial cells and the underlying lamina propria that contains loose connective tissue, blood vessels, and some diffuse lymphatic tissue [2, 3]. The gallbladder epithelium produces mucus as a response to the presence of bile and lipopolysaccharide [4–6]. Thus, mucus induction represents an innate response of the gallbladder for initial protection against pathogens and bile. Bile itself has been demonstrated to be an environmental signal that alters the expression of many *Salmonella* genes [7, 8], including a downregulation of SPI-1 gene expression

which decreases epithelial cell invasion [9]. Bile has also been shown to enhance *Salmonella* biofilm formation [10].

Intracellular persistence and biofilm formation into/on the gallbladder epithelium have been shown to participate in *Salmonella* chronic carriage in the gallbladder of mice and humans [11]. This was determined by performing in vitro methods that closely mimic the gallbladder environment. These in vitro results were validated in our mouse model of chronic carriage [11, 12].

In this chapter, we describe the materials and methods used to study the host–pathogen interactions between *Salmonella enterica* serovar Typhimurium and canine gallbladder epithelial cells (CGEC), which are physiologically similar to human gallbladder epithelial cells [13–15]. These cells were a donation from the Sum P. Lee laboratory at the University of Washington. Emphasis is given to invasion and attachment assays to directly quantify and monitor these mechanisms by confocal and electron microscopy.

2 Materials

1. DMEM-GEC medium: Dulbecco's modified Eagle's medium supplemented with high glucose, L-glutamine, and sodium pyruvate (DMEM-high glucose, Gibco|Life Technologies, CA), 10 % of fetal bovine serum (FBS), 1× of 10 mg/mL streptomycin/10,000 IU/mL penicillin, 1× of MEM non-essential amino acids. Mix the components and filter the entire solution and keep at 4 °C for less than 2 weeks.
2. Bile solution (30 %): Dissolve 7.5 mg of ox-bile (sodium cholate, Sigma, MO) in DMEM-high glucose to a final volume of 25 mL. Filter to sterilize. This stock solution has to be made the same day of use. Do not store.
3. Transwell Inserts: All described methods have been optimized using 24-mm collagen-coated Transwell-COL inserts, 3 μ M membrane pore size (six-wells) (Corning, MA).
4. Trypsin/EDTA 0.25 %.
5. Trypan blue 0.4 %.
6. Luria Bertani (LB) broth.
7. Gentamicin.
8. Triton X-100.
9. Cell Tracker Red CMPTX (Invitrogen, CA).
10. 4 % paraformaldehyde in 0.1 M sodium phosphate, pH 7.4.
11. 2.5 % glutaraldehyde in 0.1 M phosphate buffer–0.1 M sucrose (pH 7.4).

12. Hexamethyldisilazane (HDMS) (Ted Pella, CA).
13. 1.5 % paraformaldehyde–1.5 % glutaraldehyde in 0.1 M cacodylate buffer, pH 7.2–7.4.
14. 0.1 M cacodylate buffer–0.1 M sucrose.
15. 1 % osmium tetroxide in 0.1 M cacodylate buffer, pH 7.2–7.4
16. 2 % uranyl acetate.
17. 2-hydroxypropyl methacrylate (HPMA).
18. Eponate resin.
19. 1× Phosphate buffered saline (PBS).
20. Millicell Electrical Resistance System (Millipore, MA).
21. Neubauer chamber.

3 Methods

3.1 Growth of CGEC

1. Thaw frozen cells in a 37 °C water bath for 1 min.
2. Inoculate in a 75 cm² flask containing DMEM-GEC medium.
3. Incubate at 37 °C in 5 % CO₂ until a confluent monolayer is formed (approximately 7–10 days).
4. Scale up to a 150 cm² flask by trypsinization and subculture of the epithelial cells (*see* below).
5. Incubate at 37 °C in 5 % CO₂ until a confluent monolayer is formed (approximately 3–5 days). Exchange DMEM-GEC medium every 2 days.

3.2 Subculturing Monolayer Cell Cultures from Flasks

Subculturing and cell counting methods were performed according to standard tissue culture using Corning's guidelines [16]. Briefly, medium is aspirated and then monolayers are rinsed with 1× PBS before incubation with 10 mL of 0.25 % trypsin/EDTA at 37 °C 5 % CO₂ until cells are completely detached (approx. 20 min). Then, add 10 mL of medium to inactivate the trypsin and collect the cell suspension. Centrifuge cells at 259 $\times g$ for 6 min. Dilute the pellet in 12 mL of medium (normally a confluent monolayer from a 150 cm² flask has the adequate number of cells to inoculate 12 Transwell inserts). Count the cells in the microscope by mixing 10 µL of trypan blue and 10 µL of cell suspension in a Neubauer chamber.

3.3 Growth and Differentiation of CGEC in Transwell Inserts

1. Start an equilibrium period to improve cell attachment by adding 1.5 mL of medium to the Transwell insert and 2.5 mL of medium into the chamber below the insert (*see Note 1*). These volumes are Corning's recommendation. Incubate O/N at 37 °C in 5 % CO₂.

2. Inoculate 2×10^6 epithelial cells in each Transwell. Prepare the cell suspension in 1.5 mL of fresh medium. Replace the medium from the Transwell insert with this cell suspension.
3. Spin the plate down for 10 min at $59.7 \times g$ and incubate at 37 °C in 5 % CO₂.
4. Monitor the polarization of cells by measuring the trans-epithelial electrical resistance (TEER) (require a resistance of $>700 \Omega \text{ cm}^{-2}$) using a Millicell Electrical Resistance System. CGEC usually polarize and differentiate after 8–10 days. Medium needs to be exchanged at least every 2 days.
5. Remove the medium from the insert well and exchange it with 1.5 mL of DMEM-high glucose $\pm 0.3\%$ ox bile (see Note 2). Add 2.5 mL of DMEM-high glucose to the chamber below the insert. Incubate overnight (O/N) at 37 °C in 5 % CO₂.

3.4 Infection of CGEC with *Salmonella* spp.

1. Grow *Salmonella* spp. O/N at 37 °C in LB broth with aeration at 225 rpm.
2. On the next day, back-dilute the bacterial culture 1:100 in LB broth and incubate at 37 °C with aeration at 225 rpm until an optical density (OD) of 0.6 at 600 nm is reached (OD₆₀₀ of 0.6 represents approximately 1×10^9 bacteria) (see Note 3).
3. Trypsinize two wells (\pm bile) to count the epithelial cells. Calculate the amount of inoculum needed to have a multiplicity of infection (MOI) of 100 (100 bacteria for every epithelial cell; see Note 4).
4. Aspirate the medium from the Transwell inserts and bottom wells. In the case of bile exposed cells (apical surface), wash twice with pre-warmed 1× PBS.
5. Add 1 mL of bacterial suspension/well (MOI of 100) to the Transwell insert and to the chamber below the insert (see Note 5). Include three technical replicates per bacterial strain or condition. Keep inoculum on ice, perform tenfold dilutions in 1× PBS, plate on LB agar (10^{-4} , 10^{-5} , and 10^{-6} dilutions), and incubate at 37 °C for exact bacterial enumeration.
6. Incubate at 37 °C in 5 % CO₂ for the desired time of infection (see Note 6).
7. Remove the supernatant from wells and wash twice (1 mL of pre-warmed 1× PBS to insert well and 1 mL to the bottom well). Do not let cells dry during washes and be careful when adding the solutions.

3.5 Gentamicin Protection Assays (for Attachment and Invasion Assays)

1. Add 1 mL of DMEM-high glucose with or without gentamicin (50 µg/mL) to both insert and bottom wells. Incubate at 37 °C in 5 % CO₂ for 30 min (see Note 7).
2. Remove medium with gentamicin and wash two times with 1× PBS (insert and bottom wells).

3. Add 1 mL of 0.1 % Triton X-100 in 1× PBS per well and incubate at 37 °C in 5 % CO₂ for 10 min. Vigorously pipette up and down 20 times. Check under the microscope to see if detachment is complete.
4. Perform tenfold dilutions of the lysate in 1× PBS (keep dilutions on ice until use) (*see Note 8*).
5. Plate each dilution in duplicate on LB agar and incubate at 37 °C O/N.
6. Enumerate bacteria.
7. Calculate invasiveness with the following formula:

$$\% \text{ invasion} = \frac{\text{average number of bacteria invaded} \times 100}{\text{average of original inoculum}}$$

8. Calculate number of attached bacteria by subtracting the number of total bacteria recovered from wells not treated with gentamicin from the number in wells treated with gentamicin.

3.6 Monitoring by Confocal Microscopy

1. Before infection, stain epithelial cells (grown on Transwell inserts) with 5 M Cell Tracker Red CMPTX according to the manufacturer's directions (*see Note 9*).
2. Perform infections as above.
3. After the respective postinfection time points, wash twice with 1× PBS to remove the medium which is autofluorescent.
4. Fix CGEC in 4 % paraformaldehyde in 0.1 M sodium phosphate, pH 7.4, for 15 min at room temperature (RT).
5. Rinse twice with 1× PBS.
6. Rinse once with sterile water.
7. Prepare a glass slide by applying mounting medium.
8. Carefully remove the membrane from the Transwell with a razor blade.
9. Mount membrane inserts on the mounting medium on the glass slides. Add a coverslip. Dry at RT O/N.
10. Observe in a confocal microscope (*see Fig. 1*).

3.7 Monitoring by Scanning Electron Microscopy

1. After the desired time of infection, rinse the epithelial cells twice by adding 1× PBS to the Transwell insert and to the chamber below the insert.
2. Fix infected cells O/N at 4 °C in 2.5 % glutaraldehyde in 0.1 M phosphate buffer–0.1 M sucrose (pH 7.4). Add 1 mL of fixative to both apical and basolateral chambers.
3. Remove the fixative and rinse twice with 0.1 M phosphate buffer–0.1 M sucrose (pH 7.4) for 5 min.

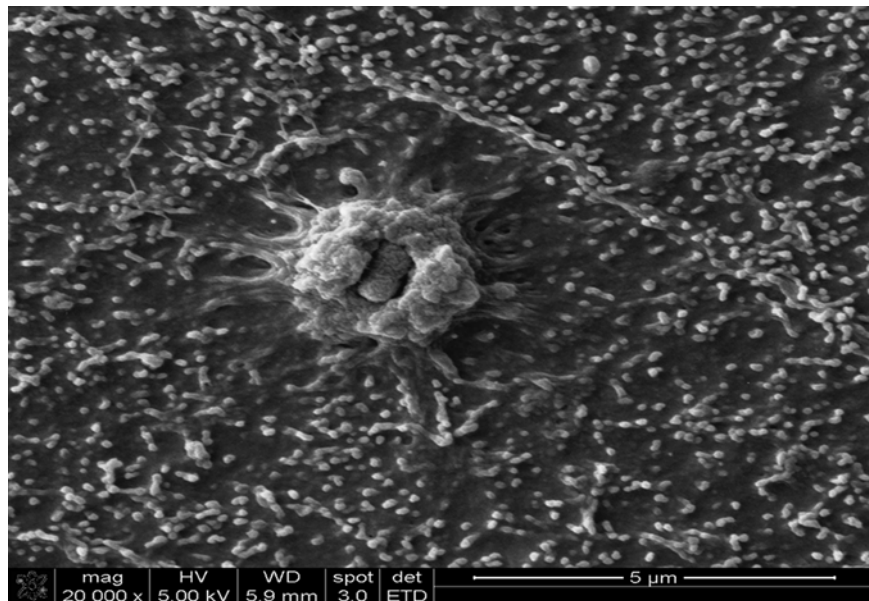


Fig. 1 Representative SEM image of *S. Typhimurium* invading CGEC. Note the membrane ruffling which is an SPI-1 mediated mechanism for *Salmonella* invasion into epithelial cells. Cells were fixed and processed at 2 h postinfection

4. Remove the buffer and dehydrate by addition of 1 mL of solutions of ethanol in a graded series, as follows: 35, 50, 70, 80, 95, and 100 % (twice). Keep every solution for 10 min. Do not let the membrane dry out during the procedure.
5. Chemically dry samples with consecutive washes of 1 mL of 25, 50, 75, and 100 % (twice) hexamethyldisilazane (HDMS). Incubate the sample in every solution for 15 min (see Note 10).
6. Remove HDMS and dry samples O/N in a fume hood.
7. Put the Transwell inserts on the sticky tape of aluminum stubs, and remove the excess of membrane that does not attach to the tape.
8. Store samples in a desiccator if they are not coated immediately.
9. Sputter coat with argon or gold for SEM observation (see Fig. 2).

3.8 Monitoring by Transmission Electron Microscopy (Adapted from Corning's Guidelines with Some Modifications)

1. After the desired time of infection, remove the medium and rinse the infected cells twice by adding 1× PBS to insert and bottom wells.
2. Fix epithelial cells O/N at 4 °C in 1.5 % paraformaldehyde–1.5 % glutaraldehyde in 0.1 M cacodylate buffer, pH 7.2–7.4
3. Rinse three times in 0.1 M cacodylate buffer–0.1 M sucrose for 5 min each rinse.

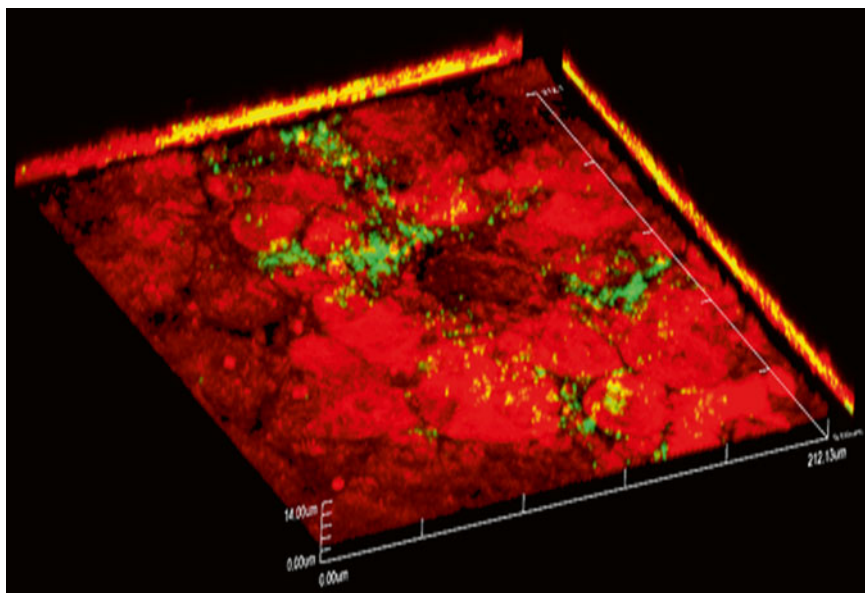


Fig. 2 Representative image showing CGEC infected with wild-type *S. Typhimurium* at 2 h postinfection in the presence of bile. Bacteria harbor the plasmid pFPV25.1 constitutively expressing GFP. DGEC are stained with Cell Tracker™ Red CMPTX. Magnification is 60 \times and the y-projection of the image is shown at the *right side*. Extracellular bacteria (green) can be seen on the surface whereas intracellular bacteria (yellow) can be seen in the y-projection (Color figure online)

4. Post-fix in 1 % osmium tetroxide in 0.1 M cacodylate buffer, pH 7.2–7.4 for 1 h at 4 °C (*see Note 9*).
5. Rinse three times in 0.1 M cacodylate buffer–0.1 M sucrose for 5 min each rinse.
6. Stain the entire block of tissue with 2 % uranyl acetate in 10 % ethanol.
7. Consecutively wash with increasing concentrations of 1 mL of ethanol as follows: 35, 50, 70, 80, 95, and 100 % (twice). Each rinse is for 10 min.
8. Replace ethanol with 2-hydroxypropyl methacrylate (HPMA) to cover the membrane and incubate for 15 min at RT on a rotator. Repeat.
9. Incubate in 1:1 HPMA/Eponate resin for 1 h at RT on a rocker.
10. After removing the previous resin, incubate in 1:2 HPMA/Eponate resin O/N on a rotator at RT.
11. After removing the previous resin, incubate in 100 % Eponate resin for 2–6 h at RT on a rotator. Repeat.
12. Embed in Eponate resin (on latex embedding molds) and polymerize at 60 °C for 16–24 h.

13. Remove the area of the resin containing the membrane using a fine jeweler's saw.
14. Section samples at 80 nm on a Reichert Ultracut E ultramicrotome at RT.
15. Observe on a TEM microscope.

4 Notes

1. All the reported volumes in this chapter apply to 24 mm six-well Transwell inserts (Corning).
2. This bile concentration was determined based on tolerance assays in which the TEER and viability of polarized CGEC were not altered. This concentration should not cause sloughing of the cells but increased mucus production should be evident (viscous appearance of the monolayers) in comparison with cells not exposed with bile.
3. Microaerophilic conditions were also performed and the results were not significantly different compared with those obtained with aeration conditions.
4. After calculation of the right amount of inoculum needed for an MOI of 100, centrifuge the required volume of bacterial culture ($9,931 \times g$ for 5 min) and then resuspend the pellet in DMEM-high glucose (without antibiotics). Final volume depends on the inoculum needed (number of wells). Do not vortex.
5. Invasion assays (lysed epithelial cells) are usually performed at 1 or 2 h postinfection. For microcolony/biofilm observation, cells need to be incubated at least for 8 h with an MOI of 10, exchanging the medium at least two times.
6. During and after infection, monitor the appearance of the cells in terms of number of detached cells and presence of abnormalities such as an increased amount of vacuoles. Compare with uninfected epithelial cells and with wild-type bacteria infected cells (when using mutant strains).
7. For intracellular survival assays, 10 μ g/mL of gentamicin needs to be included in the medium after the 2 h postinfection time point.
8. To save time and materials, dilutions can be made in 96-well plates and using a multichannel pipette; 10 μ L of each dilution can be inoculated on a single plate by dripping the volume down the length of the pre-dried agar plate. A maximum of six dilutions can be inoculated on a plate in this manner.

9. For immunofluorescence, all bacterial strains need to harbor the plasmid pFPV25.1, which constitutively expresses *gfp* [17].
10. Osmium tetroxide and HMDS are hazardous agents. Always manipulate them in a fume hood and dispose of them properly.

References

1. Center SA (2009) Diseases of the gallbladder and biliary tree. *Vet Clin North Am Small Anim Pract* 39(3):543–598, doi:S0195-5616(09)00022-9 [pii] 10.1016/j.vet.2009.01.004
2. Eroschenko VP (2008) DiFiore's atlas of histology with functional correlations, 11th edn. Lippincott Williams & Wilkins, Baltimore, MD
3. Henrikson RC, Mazurkiewicz JE (1997) Histology, vol 518. Lippincott Williams & Wilkins, Baltimore, MD
4. Savard CE, Blinman TA, Choi HS, Lee SK, Pandol SJ, Lee SP (2002) Expression of cytokine and chemokine mRNA and secretion of tumor necrosis factor-alpha by gallbladder epithelial cells: response to bacterial lipopolysaccharides. *BMC Gastroenterol* 2:23
5. Zen Y, Harada K, Sasaki M, Tsuneyama K, Katayanagi K, Yamamoto Y, Nakanuma Y (2002) Lipopolysaccharide induces overexpression of MUC2 and MUC5AC in cultured biliary epithelial cells: possible key phenomenon of hepatolithiasis. *Am J Pathol* 161(4):1475–1484. doi:10.1016/S0002-9440(10)64423-9
6. Klinkspoor JH, Yoshida T, Lee SP (1998) Bile salts stimulate mucin secretion by cultured dog gallbladder epithelial cells independent of their detergent effect. *Biochem J* 332(Pt 1):257–262
7. Prouty AM, Brodsky IE, Manos J, Belas R, Falkow S, Gunn JS (2004) Transcriptional regulation of *Salmonella enterica* serovar Typhimurium genes by bile. *FEMS Immunol Med Microbiol* 41(2):177–185. doi:10.1016/j.femsim.2004.03.002, S0928824404000495 [pii]
8. Prouty AM, Brodsky IE, Falkow S, Gunn JS (2004) Bile-salt-mediated induction of antimicrobial and bile resistance in *Salmonella* Typhimurium. *Microbiology* 150(Pt 4):775–783
9. Prouty AM, Gunn JS (2000) *Salmonella enterica* serovar Typhimurium invasion is repressed in the presence of bile. *Infect Immun* 68(12):6763–6769
10. Crawford RW, Gibson DL, Kay WW, Gunn JS (2008) Identification of a bile-induced exopolysaccharide required for *Salmonella* biofilm formation on gallstone surfaces. *Infect Immun* 76(11):5341–5349
11. Gonzalez-Escobedo G, Gunn JS (2013) Gallbladder epithelium as a niche for chronic *Salmonella* carriage. *Infect Immun* 8:2920–2930. doi:10.1128/IAI.00258-13
12. Crawford RW, Rosales-Reyes R, Ramirez-Aguilar Mde L, Chapa-Azuela O, Alpuche-Aranda C, Gunn JS (2010) Gallstones play a significant role in *Salmonella* spp gallbladder colonization and carriage. *Proc Natl Acad Sci U S A* 107(9):4353–4358, doi:1000862107 [pii]10.1073/pnas.1000862107
13. Morton MF, Pyati J, Dai H, Li L, Moreno V, Shankley NP (2005) Molecular cloning, expression and pharmacological characterization of the canine cholecystokinin 1 receptor. *Br J Pharmacol* 145(3):374–384. doi:10.1038/sj.bjp.0706196
14. Seo DW, Choi HS, Lee SP, Kuver R (2004) Oxysterols from human bile induce apoptosis of canine gallbladder epithelial cells in monolayer culture. *Am J Physiol Gastrointest Liver Physiol* 287(6):G1247–G1256. doi:10.1152/ajpgi.00013.2004
15. Tauscher A, Kuver R (2003) ABCG5 and ABCG8 are expressed in gallbladder epithelial cells. *Biochem Biophys Res Commun* 307(4):1021–1028
16. Ryan J (2012) Subculturing monolayer cell cultures. Corning Life Science, Tewksbury, MA
17. Valdivia RH, Hromockyj AE, Monack D, Ramakrishnan L, Falkow S (1996) Applications for green fluorescent protein (GFP) in the study of host-pathogen interactions. *Gene* 173(1):47–52, doi:0378111995007067 [pii]

Chapter 15

Salmonella Phages and Prophages: Genomics, Taxonomy, and Applied Aspects

Andrea I. Moreno Switt, Alexander Sulakvelidze, Martin Wiedmann, Andrew M. Kropinski, David S. Wishart, Cornelis Poppe, and Yongjie Liang

Abstract

Since this book was originally published in 2007 there has been a significant increase in the number of *Salmonella* bacteriophages, particularly lytic virus, and *Salmonella* strains which have been fully sequenced. In addition, new insights into phage taxonomy have resulted in new phage genera, some of which have been recognized by the International Committee of Taxonomy of Viruses (ICTV). The properties of each of these genera are discussed, along with the role of phage as agents of genetic exchange, as therapeutic agents, and their involvement in phage typing.

Key words Bacteriophage, Temperate, Lytic, Prophage, Genome analysis, Genetic map, Genome evolution, *Autographivirinae*, *Chilikevirus*, *Epsilon15likevirus*, *Felixounalikevirus*, *Jerseylikevirus*, Lambdoid phages, *Myoviridae*, *P2likevirus*, *P22likevirus*, *Phieco32likevirus*, *Podoviridae*, *Siphoviridae*, *Sp03likevirus*, *Sp058likevirus*, *Sp06likevirus*, *Sp6likevirus*, *T5likevirus*, *T7likevirus*, *V5likevirus*, *Viunalikevirus*

1 Introduction

Bacteriophages are the most abundant “life form” on this planet [1] and because their diversity represents an incredible gene pool, they have contributed significantly to host bacterial evolution. Bacteriophages are basically bacterial parasites, which cannot grow or replicate except in bacterial cells. These viruses may go through either of two life cycles: the lytic and the lysogenic cycle. A phage in the lytic cycle converts a bacterial cell to a factory and produces many progeny viruses. Phages adsorb to a specific receptors on the bacterial surface (flagella, pili, outer membrane proteins, capsules, lipopolysaccharides, lipoteichoic acids, proteins etc.) [2], and in the case of tailed viruses, inject their DNA through the bacterial cell wall. Once in the cell, the lytic phage’s genome prevents bacterial replication and transcription and subverts the cell to

produce viral nucleic acids and proteins. The latter include catalytic and structural proteins involved in DNA replication, packaging, and morphogenesis. Ultimately the new phage particles are released through the lysis of the host cell brought about by the combined action of a membrane pore-forming protein (holin) and a peptidoglycan-degrading lysin. A phage capable of only lytic growth is called a virulent or lytic phage.

Temperate phages can develop either by the lytic route or via the lysogenic cycle. A phage in the lysogenic cycle often synthesizes an integration enzyme (integrase), turns off further viral transcription (repressor), and usually inserts itself into the DNA of the bacterium, which continues to grow and multiply. The phage genes replicate as part of the bacterial chromosome. A bacterium that contains a complete set of phage genes is called a lysogen, while the integrated viral DNA is called a prophage. A lysogen often cannot be reinfected (superinfected) with a phage of the kind that first lysogenized the cell; it is immune to “superinfection” by virtue of the repressor. A lysogen may replicate the associated prophage continuously and stably. However, when its DNA is damaged by ultraviolet light or other inducing agents such as mitomycin C, the phage becomes derepressed and initiates a lytic cycle. This is called prophage induction. Most temperate phages form lysogens by integration at a unique attachment (*att*) site in the host chromosome. Lysogenization may result in changes to the host's phenotype (lysogenic conversion) such as the acquisition of toxigenicity or change in antigenicity [3–6]. Some phages can package host DNA and are called transducing phages. Generalized transducing phages produce particles that contain only bacterial DNA while specialized transducing phages occasionally produce particles containing both phage and bacterial DNA sequences. Both types of transducing particles can inject their DNA into a host and transfer DNA from one bacterium to another.

In addition to playing a significant role in the development of the field of “molecular biology” [7], *Salmonella* phages have practical significance: strain construction through transduction; phage typing for epidemiological purposes [8–10]; and the application of phage as therapeutic agents [11]. Lastly, phage genes and their products have contributed significantly to vector development (cosmids, integrative vectors, promoters, etc.) and as sources of molecular biologicals (DNA and RNA polymerases, ligase, nucleases, recombinases, restriction endonucleases, etc.).

Bringing Hans-Wolfgang Ackermann's [12] list of *Salmonella* phages observed by electron microscopy up to date, we now have almost 250 morphologically characterized viruses. Among the tailed viruses of the order *Caudovirales* [13] the breakdown is as follows: *Myoviridae* (phages with contractile tails), 64; *Siphoviridae* (viruses with long noncontractile tails), 94; and *Podoviridae* (short noncontractile tails), 71. In addition, we have seen a major

increase in the numbers of *Salmonella* phages fully sequenced: 14 myoviruses, 12 siphoviruses, and an equal number of podoviruses. This we believe is primarily due to the renewed interest in the use of phages as biocontrol and therapeutic agents (see Subheading 7). But, the impact of these developments has been broader than that—resulting in the classification of many of these phages into new viral genera which have been proposed to the International Committee on Taxonomy of Viruses (ICTV).

This review will concentrate on the properties of the fully sequenced members of the *Caudovirales*. In the first section we will describe the lytic phages active against *Salmonella*, while in the second we will deal with temperate phage and prophages. The last sections of this chapter address the practical use of phages in typing and therapy.

2 Diversity of Lytic Phages Infecting the Genus *Salmonella*

An orthocluster analysis was used to cluster the currently sequenced lytic phages infecting *Salmonella* in a similar manner to that which was used to classify 22 newly sequenced *Salmonella* phages [14]. In this section of the chapter sequences of *Salmonella* phages representing phages belonging to (1) currently ICTV recognized phage genera, (2) ICTV non-approved genera, and (3) phages not yet classified in a phage genus were clustered using a neighbor-joining tree according to the presence/absence of families of orthologous genes. Orthologous genes were identified with OrthoMCl v1.4 [15] and the tree was prepared with Splits Tree4 [16] (Fig. 1).

2.1 Diversity of Myoviridae

2.1.1 *Viunalikevirus*

The phage genus *Viunalikevirus* was proposed in 2012 to harbor seven phages that infected several bacteria of the family *Enterobacteriaceae* [17]. At that time, this genus included three *Salmonella* phages (i.e., Vi1, SFP10, and ΦSH19), two *E. coli* phages (i.e., CBA120, Phax1), a *Shigella* phage (ΦSboM-AG3), and a *Dickeya* bacteriophage (LIMESTONE1) [17–23]. As of June 2013, four other *Salmonella* phages (FSL SP-029, FSL SP-063, SKML-39, and STML-13-1) [14] (Table 1 and Fig. 1) had been isolated from northern New York State, and fully characterized. This revealed that they also belong to the genus *Viunalikevirus*. Genome-wide nucleotide identity with each other revealed >59 % identity, along with distinctive genomic and morphological features that characterize Vi1-like viruses. Genomic features included gene synteny, a genome size of approximately 157 kb, mol.% G+C of ca. 44.5 %, putative presence of a modified base (possibly HMdU), conserved early and late promoter sequences, and major rearrangements in the tailspikes [17]. Distinctive morphological features include icosahedral heads of ca. 90 nm and contractile tails

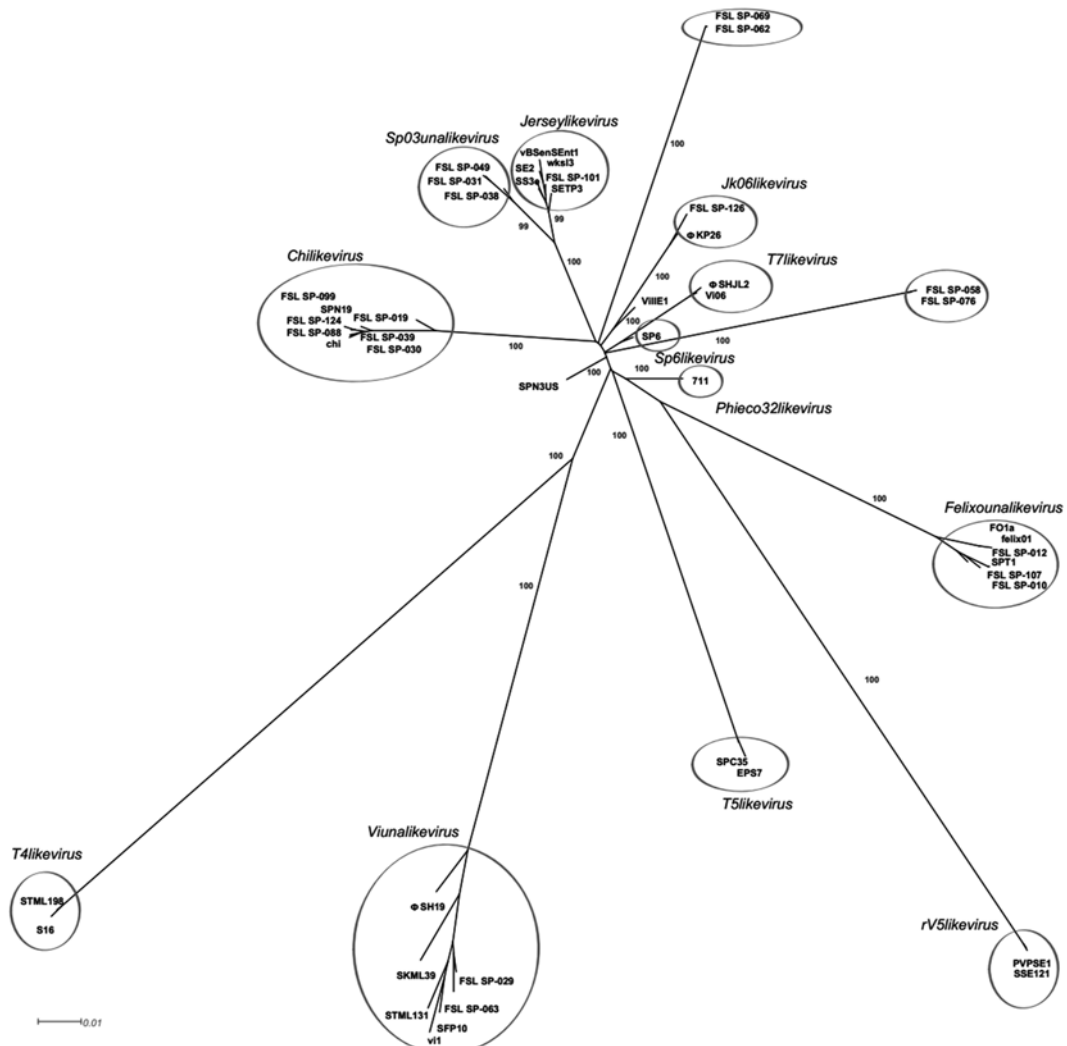


Fig. 1 Neighbor joining tree that was generated based on presence/absence of orthologous gene families. Lytic *Salmonella* phages representing the diversity of phage genera were clustered. Circles indicate the phages genera. Bootstrap values of 1,000 replicates supporting the clusters are indicated

of ca. 110×18 nm. In addition, a unique adsorption organelle was described for *Viunalikevirus*, and specifically, phage in this genus contain six tailspikes that experience structural changes; when the tailspikes are in unfolded conformation, an umbrella-like structure is observed [17]. Importantly, gene synteny is disrupted in the four genes encoding the tailspikes which is an important feature of the *Viunalikevirus* [14, 17]. Tailspikes in this genus were found to contain a conserved N-terminal (137–360 amino acids) and a highly variable C-terminal (161–1,044 amino acids); while the N-terminal might attach to the baseplate (this need to be experimentally validated), the variable C-terminal contains the residues

associated with bacterial receptor recognition [17, 19, 20]. Rearrangements in the tailspikes appear to facilitate infection of different *Enterobacteriaceae* by Vi1-like viruses, as is illustrated in their wide range of hosts (e.g., different *Salmonella* serovars, *Dickeya*, and *Shigella*) (shown in Table 1). For example, Phage Vi1, which infects *S. Typhi*, contains in one of the tailspikes an acetyl esterase domain that was found to target and hydrolyze the capsule polysaccharides of *S. Typhi* [19].

Table 1
Lytic phages infecting the genus *Salmonella*

Genus ^a	GenBank acc. no.	Name	Host	Reference
<i>Myoviridae</i>				
<i>Viunalikevirus</i>	JN126049	ϕSH19	<i>S. Typhimurium</i>	[23]
<i>Viunalikevirus</i>	NC_016073	SFP10	<i>S. Typhimurium</i>	[20]
<i>Viunalikevirus</i>	NC_015296	Vi01	<i>S. Typhi</i>	[19]
<i>Viunalikevirus</i>	KC139560	FSL SP-029 ^b	<i>S. Dublin</i>	[14]
<i>Viunalikevirus</i>	KC139522	FSL SP-063 ^b	<i>S. Dublin</i>	[14]
<i>Viunalikevirus^a</i>	NC_019910	SKML-39	<i>Salmonella^c</i>	Unpublished
<i>Viunalikevirus^a</i>	JX181828	STML-13-1	<i>Salmonella^c</i>	Unpublished
<i>Felixounalikevirus</i>	NC_005282	Felix01	<i>S. Typhi</i>	[28]
<i>Felixounalikevirus</i>	JF461087	FO1a	<i>Salmonella^c</i>	Unpublished
<i>Felixounalikevirus</i>	JX181822	SPT-1 ^b	<i>Salmonella^c</i>	[29]
<i>Felixounalikevirus</i>	KC139526	FSL SP-010 ^b	<i>S. Mbandaka</i>	[14]
<i>Felixounalikevirus</i>	KC139543	FSL SP-012 ^b	<i>S. Mbandaka</i>	[14]
<i>Felixounalikevirus</i>	KC139638	FSL SP-107 ^b	<i>S. Mbandaka</i>	[14]
<i>Felixounalikevirus^a</i>	JX181814	SBA-1781 ^b	<i>Salmonella^c</i>	Unpublished
<i>V5likevirus^a</i>	NC_016071	PVP-SE1	<i>S. Enteritidis</i>	[36]
<i>V5likevirus^a</i>	JX181824	SSE-121	<i>Salmonella^c</i>	Unpublished
<i>T4likevirus</i>	NC_020416	vB_SenM-S16	<i>S. Typhimurium</i>	[46]
<i>T4likevirus</i>	JX181825	STML-198	<i>Salmonella^c</i>	Unpublished
Unclassified	JN641803	SPN3US ^d	<i>S. Typhimurium</i>	[47]
<i>Siphoviridae</i>				
<i>T5likevirus</i>	NC_015269	SPC35	<i>S. Typhimurium</i>	[47]
<i>T5likevirus</i>	NC_010583	EPS7	<i>S. Typhimurium</i>	[52]
<i>Jerseylikevirus</i>	NC_021777	Jersey	<i>S. Paratyphi B</i>	[53]
<i>Jerseylikevirus</i>	NC_016763	SE2	<i>S. Enteritidis</i>	[57]
<i>Jerseylikevirus</i>	NC_009232	SETP3	<i>S. Enteritidis</i>	[58]
<i>Jerseylikevirus</i>	EF212163	SETP7 ^b	<i>S. Enteritidis</i>	[58]
<i>Jerseylikevirus</i>	EF212170	SETP13 ^b	<i>S. Enteritidis</i>	[58]
<i>Jerseylikevirus</i>	NC_006940	SS3e	<i>S. Typhimurium</i>	[56]
<i>Jerseylikevirus</i>	KC139511	FSL SP-101	<i>S. Dublin</i>	[14]
<i>Jerseylikevirus</i>	JX202565	wksl3	<i>S. Enteritidis</i>	[55]
<i>Jerseylikevirus</i>	HE775250	vB_SenS-Ent1	<i>S. Enteritidis</i>	[54]
<i>Jerseylikevirus</i>		vB_SenS-Ent2	<i>S. Enteritidis</i>	[54]
<i>Jerseylikevirus</i>		vB_SenS-Ent3	<i>S. Enteritidis</i>	[54]
<i>Jerseylikevirus</i>	KC832325	L3 ^e	<i>S. Gallinarum</i>	Unpublished
<i>Jerseylikevirus</i>	JX233783	ST4 ^e	<i>S. Typhimurium</i>	Unpublished
<i>Jerseylikevirus</i>	AJ277754	MB78 ^f	<i>S. Typhimurium</i>	[247]

(continued)

Table 1
(continued)

Genus ^a	GenBank acc. no.	Name	Host	Reference
<i>Jerseylikevirus</i>	JX297445	vB_SenS_AG11	<i>S. Enteritidis</i>	Unpublished
<i>Sp03unalikevirus^a</i>	KC139518	FSL SP-031	<i>S. Cerro</i>	[14]
<i>Sp03unalikevirus^a</i>	KC139652	FSL SP-038 ^b	<i>S. Cerro</i>	[14]
<i>Sp03unalikevirus^a</i>	KC139557	FSL SP-049 ^b	<i>S. Cerro</i>	[14]
<i>Chilikevirus</i>	JX094499	X (Chi)	<i>S. Typhimurium</i>	[67]
<i>Chilikevirus</i>	NC_019417	SPN19	<i>S. Typhimurium</i>	Unpublished
<i>Chilikevirus^a</i>	KC139571	FSL SP-019 ^b	<i>S. Newport</i>	[14]
<i>Chilikevirus^a</i>	KC139519	FSL SP-030	<i>S. Dublin</i>	[14]
<i>Chilikevirus^a</i>	KC139514	FSL SP-039	<i>S. Cerro</i>	[14]
<i>Chilikevirus^a</i>	KC139512	FSL SP-088	<i>S. Typhimurium</i>	[14]
<i>Chilikevirus^a</i>	KC139667	FSL SP-099 ^b	<i>S. Newport</i>	[14]
<i>Chilikevirus^a</i>	KC139515	FSL SP-124	<i>S. Cerro</i>	[14]
<i>Jk06likevirus</i>	KC579452	φKP26	<i>S. Oranienburg</i>	[248]
<i>Jk06likevirus</i>	KC139513	FSL SP-126	<i>S. Kentucky</i>	[14]
<i>Sp062likevirus^g</i>	KC139632	FSL SP-062 ^b	<i>S. Newport</i>	[14]
<i>Sp062likevirus^g</i>	KC139649	FSL SP-069 ^b	<i>S. Newport</i>	[14]
Unclassified	NC_010495	Vi II-E1	<i>S. Typhi</i>	[69]
Unclassified	JQ288021	SPN3UB ^h	<i>S. Typhimurium</i>	[159]
<i>Podoviridae</i>				
<i>Sp6likevirus</i>	NC_004831	SP6	<i>S. Typhimurium</i>	[79]
<i>T7likevirus</i>	NC_010807	φSG-JL2	<i>S. Gallinarum</i>	[78]
<i>T7likevirus</i>	NC_015271	Vi06	<i>S. Typhi</i>	[19]
<i>Phieco32likevirus</i>	NC_015938	7-11	<i>S. Newport</i>	[83]
<i>Phieco32likevirus^a</i>	Not sequenced	φSPB	<i>S. Paratyphi B</i>	[84]
<i>N4likevirus</i>	KC139517	FSL SP-058	<i>S. Dublin</i>	[14]
<i>N4likevirus</i>	KC139520	FSL SP-076	<i>S. Dublin</i>	[14]
Unclassified	NC_016761	SPN1S ^h	<i>S. Typhimurium</i>	[159]

^aGenus needs to be validated^bGenomes in several contigs that all together show similar size as compared with phages of the same genus^cSerovar information of the host is not available^dThis phage shows homology to: JX316028 (*Erwinia* phage φEaH2) which is described as a member of the *Siphoviridae*^eOnly one contig representing approximately a half size compared with phages of the same genus^fSeveral small contigs representing a fraction of the whole genome^gGenus needs to be proposed^hPhage contains an integrase, which indicate a lysogenic cycle

2.1.2 *Felixounalikevirus*

Originally known as phage O1, this virus was originally isolated by Felix and Callow [24]. Since this phage infects almost all *Salmonella* isolates it has been used as a diagnostic reagent [25]. In addition, a derivative of Felix O1 carrying the *luxAB* genes has been constructed to examine *Salmonella* in food samples [26]. Furthermore, because of its broad-host range it has been investigated as a way of reducing contamination of foodstuffs by *Salmonella* [27].

Currently, there are genome sequences for ten phages which belong to this genus, including seven phages infecting *Salmonella* (i.e., FelixO1, FO1a, FSL SP-010, FSL SP-012, FSL SP107, SPT-1, and SBA-171) (see Table 1 and Fig. 1) [14, 28, 29], two phages

infecting *E. coli* (i.e., wV8 and EC6) [30, 31], and a virus infecting *Erwinia* (Φ Ea21-4) [32]. Genomic characteristics of the *Felixounalikevirus* include (1) genome size of ca. 86 kb (range from 84 kb for Φ Ea21-4 to 88 kb for wV8), (2) mol.% G+C of ca. 39 %, except for Φ Ea21-4 which is significantly higher (43.8 %), (3) the presence of >20 tRNAs, and (4) presence of numerous homing endonucleases (six in Felix01) [28, 30–32]. Among all fully sequenced Felix01-like viruses, *Erwinia* phage Φ Ea21-4 is the most distant exhibiting only 69 common protein homologs to proteomic content of Felix01 (131 proteins; 52.7 % identity [33]). This represents a nucleotide identity over these genes that ranged from 40 to 86 % [32].

Morphologically phage Felix01 has an icosahedral head of ca. 73 nm and a 17×113 nm contractile tail, which contains six straight tail fibers that are typically folded along the tail [12, 28]. Slight variations in morphology have been reported for other phages in this genus; for example, the head of phage wV8 is 70.4 nm and the tail is 112.8×16.8 nm with four instead of six tail fibers [30]. One phenotypic characteristic of Felix01 is a very broad-host range. In one study Felix01 infected the 98.2 % of *Salmonella* strains tested (>600 strains) and only 1.4 % of other *Enterobacteriaceae* [34]. However, this broad-host range is not true for other *Salmonella* phages in this genus. FSL SP-010, FSL SP-012, and FSL SP-107 only infected 17, 30, and 13 % of the *Salmonella* strain tested (23 strains, representing 17 serovars), respectively, while Felix01 infected 100 % [14]. Its surface receptor is the terminal *N*-acetylglucosamine residue of the LPS core. Therefore, deep rough mutants of this genus are Felix01 resistant [35]. Interestingly, two receptors were reported for phage wV8, LPS, and a membrane protein [30]. Importantly, the mechanism underlying Felix01 broad-host range needs to be investigated.

2.1.3 *V5likevirus*

Salmonella phages PVP-SE1 and SSE-121 (Table 1, and Fig. 1) along with five *E. coli* phages (rV5, vB_EcoM-FV3, phAPEC8, Delta, and phi92), and *Cronobacter sakazakii* phage vB_CsaM_GAP31 [36–41] have been proposed as members of the *V5likevirus* genus. They share (1) genome sizes ranging from 136 kb (phage vB_EcoM-FV3) to 148 kb (phage phi92), (2) similar number of protein coding sequences (CDSs) ranging from 233 (rV5) to 269 (vB_CsaM_GAP31), (3) mol.% G+C ranging from 37.4 % (phi92) to 46.3 % (vB_CsaM_GAP31), and (4) number of tRNAs ranging from five (vB_EcoM-FV3) to 26 (vB_CsaM_GAP31) [36–41]. Recently, doubt has been cast on whether this grouping represents a genus or subfamily (“V5virinae”) containing three genera—the “V5likevirus” (rV5, FV3), the “Pvplikevirus” (PVP-SE1, GAP31, and SSE-121), and the “Phi92likevirus” (phi92 and phAPEC8) [37].

Morphologically, *Salmonella* phage PVP-SE1 has an icosahedral head 85 nm in diameter and a contractile tail (120×18 nm) that terminates in short tail fibers [36]. Cryo-electron microscopy

of phage phi92, at a very high resolution [41], showed that *V5likevirus* have four tailspikes or tail fibers, as well as a complex baseplate structure comparable to an “open Swiss army knife” [41]. Phages of this genus show a wide host range infecting several *E. coli* strains and strains representing numerous *Salmonella* serovars [36, 41]. Whereas the inner core region of the LPS was recognized as the receptor for PVP-SE1, another uncharacterized receptor was also proposed for this phage [36]; in addition, capability of infecting encapsulated and nonencapsulated bacteria was also reported for phi92 [41].

2.1.4 *T4likevirus*

Phages related to coliphage T4 [42, 43] are the most diverse group of viruses ecologically, morphologically, genomically, and proteomically including viruses infecting members of the Gammaproteobacteria (*Aeromonas*, *Escherichia*, *Pseudomonas*, *Salmonella*, *Vibrio*) and Epsilonproteobacteria (*Campylobacter*) [42–44]. These viruses show as much diversification as is seen in the order *Herpesvirales*.

Two *Salmonella* phages, STML-198 [45] and vB_SenM-S16 [46], share 57.6 and 60.0 % homologous proteins with T4 strongly suggesting that they are part of the *T4likevirus* genus (ICTV; <http://ictvonline.org/>). While a number of papers describing phage T4 are available [42–44], we will here describe in more detail *Salmonella* phages of this genus. Among the two *Salmonella* phages in this genus, only comparative analysis of phage vB_SenM-S16 has been reported. vB_SenM-S16 has a dsDNA genome of 160 kb, a mol.% G+C of 36.9, three tRNAs, and 269 CDSs [46]. Morphologically, vB_SenM-S16 has a head of approx. 117 nm length and 91 nm width that is slightly elongated, and a tail of approx. 120 nm that is terminated by long tail fibers [46].

When more than 150 *Salmonella* strains were tested for susceptibility, vB_SenM-S16 infected 76 % of all *Salmonella* isolates [46], but it does not infect other bacterial species. The receptor of vB_SenM-S16 is the *Salmonella* outer membrane protein OmpC which is recognized as the primary receptor [46].

2.1.5 *Unclassified Genera*

Salmonella phage SPN3US was isolated from chicken feces in South Korea and its genome was sequenced and released in 2011 [47]. However, this phage had not been assigned to a phage genus. While phage SPN3US was described as a myovirus, this phage shows homology to *Erwinia* phage phiEaH2, which was described as a member of the *Siphoviridae* [47, 48]. These two phages do not show homology to any other phage in the NCBI database as of June 2013. Phage SPN3US has the largest genome size reported for *Salmonella* phages (240 kb), and has a mol.% G+C of 48.5 [47]. Similarly, *Erwinia* phage phiEaH2 has a large genome size as well (243 kb) [48]. A total of 264 CDSs and two tRNAs were identified in phage SPN3US, though most (>79 %) of these were

annotated as hypothetical proteins. Functionally annotated CDSs include genes encoding proteins involved in phage morphogenesis (e.g., capsid, tail, terminase), in replication and transcription (e.g., helicase, RNA polymerase), and host lysis (i.e., endolysin) [47]. Importantly, phenotypic evidence shows that this phage's primary receptor is the *Salmonella* flagella [47].

2.2 Diversity of Siphoviridae

2.2.1 T5likevirus

Members of the genus *T5likevirus* include five *E. coli* phages (e.g., phage T5 and AKFV33), one *Vibrio* phage (phage 149), and two *Salmonella* phages (SPC35 and EPS7) (ICTV). Phage T5 is the type species of this genus, which is a very well-characterized siphovirus infecting enterobacterial hosts [49]. Genomic characteristics of this genus include (1) a genome that ranges in size from 108 kb (AKFV33) to 118 kb (SPC35), (2) approx. 10 kb direct repeats at both ends (terminally redundant), (3) a mol.% G+C of 39, (4) greater than 20 tRNAs, and (5) a genome that is divided in three regions (pre-early, early, and late) [49–51]. Phages in this genus have collinear genomes, as well as high genome conservation (approx. 80 % of nucleotide identity) [51]. The pre-early region contains genes encoding host enzyme inhibition proteins, the early region contains genes encoding proteins involved in DNA replication, transcription, DNA metabolism, and cell lysis, and the late region contains genes encoding structural proteins (e.g., capsid, tail) [49].

Morphologically, members of the *T5likevirus* genus possess an icosahedral head approx. 70 nm in diameter and a long noncontractile tail of 185 nm, which contains terminal fibers [50, 51]. A number of studies have investigated the receptors for this phage genus. Interestingly, T5-like-viruses bind reversible first to the LPS, and then the different members of this genus bind irreversibly to different outer membrane proteins (e.g., FepA, FluA, BtuB) [50–52]. The binding to different surface proteins could be related with the host range of these phages; while some of them infect *E. coli* and *Salmonella* (SPC35, EPS7), other are specific to *E. coli* O157:H7 (AKFV33) [51].

2.2.2 Jerseylikevirus

A number of phages representing *Jerseylikeviruses* have been sequenced (e.g., wksl3, VB_SenS_Ent1 etc. (see Table 1)). Phage Jersey was originally one of the phages used for the *Salmonella* Paratyphi B typing scheme [53]. Most of the currently sequenced *Jerseylikeviruses* lyse the globally distributed *Salmonella* serovar Enteritidis. Genomic characteristics of this genus include a terminally redundant and circularly permuted genome of approx. 42 kb [54], a mol.% G+C of around 49, and a number of encoded CDSs ranging from 58 to 64. Four transcriptional clusters, two early and two late, were described for the Jersey-like viruses [54–57]. Early transcript genes encode DNA replication and regulatory proteins and late transcript genes encode packaging, morphogenesis, and

lysis proteins [54]. Jersey-like phages appear to be specific for *Salmonella*, or to some serovars within *Salmonella*. For example, phage SETP3 was found only to be adsorbed by *Salmonella* belonging to the serogroups B and D1 [58]. Distinguishable morphological characteristics include a head of approx. 63–64 nm, a long noncontractile tail of approx. 120 nm × 7 nm, and a 20 nm baseplate with spikes. Importantly, a high level of nucleotide identity (up to 93 % of identity between wksl3 and SS3e) is a distinctive feature of this phage genus [55].

2.2.3 *Sp03unalikevirus*

This phage genus needs to be proposed to ICTV; currently only three *Salmonella* phages (e.g., FSL SP-031, FSL SP-038, and FSL SP-049) belong to this genus, and all of them were isolated from dairy farms in New York State [59]. Genomic characteristics of this phage genus include a genome size of approx. 44 kb and a mol.% G+C of 51. A total of 67 CDSs are encoded, including genes encoding structural proteins (e.g., head morphogenesis protein, tail tape measure protein), genes encoding proteins involved in DNA recombination (e.g., DNA helicase), and genes encoding proteins involved in lysis (lysozyme) [14]. Phages in this genus resemble *Jerseylikevirus*; however, nucleotide identity between the phage Jersey and the *Sp03unalikevirus* FSL SP-031 is only 53.4 %. Morphologically, FSL SP-031 is a lambda-like siphovirus. One phenotypic characteristic that is distinguishable for the phages in this genus is a very narrow host range. When 25 *Salmonella* serovars were tested, only one strain representing *Salmonella* Cerro was infected [59].

2.2.4 *Tunalikevirus*

Bacteriophage T1, originally called α , was isolated by Milislav Demerec [60]. It was one of the viruses first singled out for intense study by Max Delbrück. Bacteriophage T1 is one of the most efficient bacterial killing machines and can withstand drying. Because of this many biotechnology companies have produced T1-resistant (*tonB*) *E. coli* strains for molecular cloning experiments. Morphologically it possesses an icosahedral head 60 nm in diameter and a long tail (ca. 200 nm) terminated by four short kinked fibers [61]. The 50.7 kb genome (45.6 % G+C) is a terminally redundant and circularly permuted sequence that contains 48,836 bp of nonredundant nucleotides, and encodes 77 CDSs [62, 63]. Since it was first sequenced a number of members of this genus have been proposed (ICTV). Two of the interesting properties of these phages are that the small early region genes tend not to be conserved, and these phages possess homologs to coliphage lambda gpH, gpL, gpI, gpFII, gpU, and gpV indicating a phylogenetic relationship between the tail modules of the T1 and lambdoid phages.

Recently, a number of T1-like phages, active against *E. coli* O157:H7, have been isolated from ruminants including JK06

(DQ121662) from Israel; vB_EcoS_Rogue1 [64] from Canada; phiKP26 (KC579452) and phiJLA23 (KC333879) from Mexico; and *Salmonella* phage FSL SP-126, isolated from cattle manure in the USA [14]. While these viruses resemble T1 at the proteomic level, BLASTN analyses reveal that their sequence is considerably different from that of T1. This leads to our suggestion that the taxonomic status of the *Tunalikevirus* genus should be reassessed, with the creation of several new genera including the *Jk06likevirus*.

2.2.5 *Chilikevirus*

Phage X (Chi) was isolated in 1935 by Sertic and Boulgakov and shown to only attack motile *Salmonella* strains [65]. Further studies revealed its host range to include *Serratia marcescens* and *E. coli* [66]. “Bacteriophage chi attaches to the filament of a bacterial flagellum by means of a tail fiber, but the ultimate receptor site for the phage is located at the base of the bacterial flagellum” [66]. Schade and Adler [66] observed circular DNA molecules by electron microscopy indicating cohesive termini.

The phage head is an icosahedron measuring 65.0–67.5 nm between the parallel sides. The tail is a flexible rod about 220–230 nm × 12.5–14 nm wide, displaying approximately 55 cross-striations. This is terminated by an extremely long tail fiber measuring 2.0–2.5 nm in width and approximately 200–220 nm in length [66].

Recently the genome of phage X was sequenced by three laboratories Denyes and Kropinski (Canada), Hendrix and Casjens (USA), and Ryu et al. (Korea [67]). Its genome is about 59 kb with a mol.% G+C content to 56.6. Unpublished work by Hendrix and Casjens revealed 5'-GCTCTGCGCACC cohesive termini. Ryu and colleagues also identified two other related phages SPN19 (JN871591) and iEPS5 [68] which are also flagella specific. Phage iEPS5 features an isometric capsid (59 nm) and a noncontractile tail (216 nm). These three phages share a high degree of DNA identity (89–90 %) and shared proteins (91–93 %) and thus belong to the same genus.

2.2.6 *Sp062likevirus*

Sp062likevirus is a phage genus not yet proposed to ICTV. FSL SP-062 and FSL SP-069, the two phages in this genus, were isolated recently by Moreno Switt et al. from manure samples of dairy farms with history of *Salmonella* isolation [59]. Sp062-like viruses morphologically resemble coliphage lambda, possess a 56 kb genome (mol.% G+C of 42.8), and encode 102 CDSs [14]. Since only four SNPs differentiate FSL SP-062 and FSL SP-069 these phages were considered to be phage variants. The host range of these phage variants are distinct; while FSL SP-062 infects two *Salmonella* serovars (i.e., serovars Newport and Kentucky), FSL SP-069 only infects *Salmonella* Newport. Importantly, three of the SNPs described above are in a gene encoding a tail fiber.

2.2.7 Unclassified Genera

Vi-typing bacteriophage E1 is one of the phages that have the *Salmonella* Typhi capsule antigen as primary receptor [69]. Phage ViIE1 has a genome size of approx. 45 kb, a mol.% G+C of 47, and encodes for 56 CDSs. Comparative genomic analyses showed similarity with orthologs of ES18 (encoding head morphogenesis proteins) and T1 (encoding proteins involved in replication and recombination); however, the amino acid identity of these orthologs is quite low (e.g., 28–36 % for the orthologs shared with ES18) [69]. EM images showed an icosahedral head of 55 nm in diameter, and a noncontractile tail 205 nm in length and 11 nm wide.

2.3 Diversity of Podoviridae

2.3.1 Autographivirinae

This group of phages is characterized by possessing 37–50 kb terminally redundant genomes which encode large single-subunit RNA polymerases which are used in the switch from early to middle and late transcription of these viruses. The taxonomic status of the “T7-superfamily” was reexamined by Lavigne et al. [70] who recommended the creation of a subfamily, the *Autographivirinae*, containing three genera based upon protein similarity. The genera (*T7likevirus*, *Sp6likevirus*, and *Phikmvlikevirus*) are now ICTV ratified genera with the subfamily, *Autographivirinae*. One of the interesting features of this group of phages is the underrepresentation of certain common restriction sites, e.g., both T7 and SP6 which are similar in mass and mol.% GC content but show no DNA homology and lack sites for BamHI, PstI, SacI, SacII, SalI, SmaI, and SphI. The biotechnological significance of this group of phages, and SP6, in particular is that their promoters and polymerases have been used in an extensive array of general cloning (e.g., pGEM) and protein expression (pET, PALTER) vector systems as well as the production of RNA hybridization probes and RNA interference, synthesis of mRNA for in vitro translation.

T7likevirus

Coliphage T7 is one of the best studied virulent (lytic) bacteriophages and one of the first to have been completely sequenced [71]. Its life cycle is described here briefly: After binding to its cell receptor, lipopolysaccharide, viral DNA is translocated into the cell through a virus-derived pore in a novel transcription-dependent process [72]. Host RNA polymerase (*EcRNP*) transcribes the left-most 20 % of the T7 genome. The product of early gene *0.3* (*Ocr*) is a small protein which mimics B-form DNA and binds to, and inhibits, type I restriction endonucleases [73, 74]. The product of early gene *0.7* functions in host gene shutoff [75] and as a protein kinase which phosphorylates host elongation factors G and P and ribosomal protein S6 [76]. The other, highly significant early gene is *1* which encodes the rifampicin-resistant phage-specific RNA polymerase (φ RNP; Fig. 2). This protein recognizes specific promoters and is responsible for middle (DNA replication) and late (morphogenesis and lysis) gene expression. At the molecular level

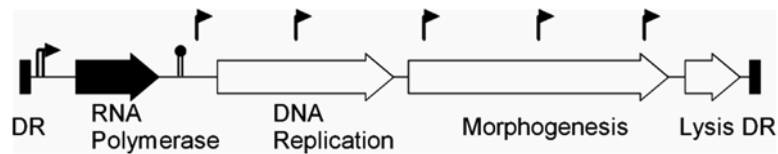


Fig. 2 Gene diagram of T7-like phages showing genome terminated by direct repeats (DR), the presence of host-dependent (vertical lines with right-sided arrowhead) and phage-dependent (vertical line with right-sided arrowhead) promoters and the rho-independent terminator at which the host RNP transcription terminates (vertical lines with filled circle)

it is the possession of φ RNP and their cognate promoters which have been used to define the “T7 group” of phages [77]. Two *Salmonella*-specific phages belong to this genus *S. Gallinarum* phage φ SG-JL2 [78] and *S. Typhi* phage Vi06 [19].

Sp6likevirus

SP6 has a 43.8 kb (47.2 % G + C) genome with 174 bp direct terminal repeats [79, 80]. Scholl et al. [80] described it as belonging to “an estranged subgroup of the T7 supergroup” showing the closest relationship to coliphage K1-5. The work of Lavigne et al. [70], based largely on proteomic analysis using CoreGenes [81], showed that this phage only shared nine proteins in common with T7 indicating that they are related but distinct. An interesting property of SP6 is that gp49 is an acidic 59 kDa protein with homology to the C-termini of gp9 of *Salmonella* phages ST104, ST64T, and P22; and to Orf49 of KS7. The P22 homolog has been demonstrated to be the tailspike protein and possesses endorhamnosidase activity at its carboxyl terminus, the portion of gp49 which shares 48.3 % sequence identity. *S. Typhimurium* phage UAB_Phi78 (NC_020414) is another member of this genus. So far no member of the *Phikmvlikevirus* genus has been isolated which infects *Salmonella*.

2.3.2 *Phieco32likevirus*

Phage phiEco32 is a novel coliphage with C3 morphology possessing a head 145 nm \times 44 nm and short (\sim 13 nm \times 8 nm) tail terminated by short tail fibers [82]. It harbors a 77.6 kb genome mol.% G + C with 193 bp direct repeats (G + C content of 42.3 %). *S. Newport* phage 7-11 is very similar in size (head: 154 \times 40 nm; tail: 12 \times 9 nm). Its genome is 89.9 kb long (44.1 mol.% G + C) and encodes 151 CDSs and six tRNAs [83]. While currently classified as a member of the *Phieco32likevirus* genus its genome exhibits minimal sequence similarity to phiEco32, and possess only 41 homologous proteins. The result (32 % homologous proteins) suggests that these two phages are most likely members of the same subfamily, rather than of the same genus. Another possible member of this genus is *Salmonella* phage φ SPB [84].

2.3.3 *N4likevirus*

On the basis of host specificity, this is a very diverse group of phages infecting *E. coli* (N4, vB_EcoP_G7C, EC1-UPM, KBNP21), *Enterobacter* (EcP1, IME11), *Erwinia* (vB_EamP-S6), *Pseudomonas* (LIT1, LUZ7), *Roseovarius* (phage 1), *Ruegeria* (DSS3φ2), and *Sulfitobacter* (EE36φ1). To this we can now add two *Salmonella* phage FSL SP-058 and FSL SP-076 [14]. With one notable exception, phage EcP1, the genomes range from 69.9 to 74.9 mol.% G+C. Coliphage N4 has an icosahedral head ~70 nm in diameter with short tail fibers originating between the head and the tail [85]. The unique feature of these phages is the presence of 1–2 copies of a large (3,500 amino acid residues; 382,495 Da) rifampicin-resistant single-subunit RNA polymerase within the phage particles, which is responsible for early transcription [85]. The two *Salmonella* phages, FSL SP-058 and FSL SP-076, were both isolated from manure samples in New York State [59]. A genome size of 72 kb, with a mol.% G+C of 39.5, encoding for ten tRNAs and a 97 CDSs are characteristics of this genus [14]. FSL SP-058 and FSL SP-076 show an average overall amino acid identity of 89 %; while they show a genome synteny, the two tailspikes encoded show a relatively conserved N-terminal (60–72 % of amino acid identity) and a very distinct C-terminal (7–33 % of amino acid identity). Since these two phages differ considerably in DNA identity to N4 they may be considered part of a new genus, *Sp058likevirus*, which together with the *N4likevirus* is part of a new subfamily.

3 Diversity of Temperate Phages Infecting the Genus *Salmonella*

In the organization of this part of the chapter the temperate, but plaque-forming phages will be distinguished from phage identified as part of host genome studies, or those which are inducible but cannot form plaques, i.e., cryptic prophages.

3.1 *Podoviridae*

3.1.1 *P22likevirus*

In 1952, Zinder and Lederberg demonstrated the transfer (generalized transduction) of genetic material between *Salmonella enterica* serovar Typhimurium mutants involving a phage intermediary [86]. The temperate phage vector, originally called PLT 22, is now commonly referred to as P22 and has continued to be the virus of choice for investigating the genetics of this bacterium. It is also one of the best studied bacterial viruses. Many studies have suggested that P22, in spite of its morphology, is a member of the lambdoid family. Indeed, the layout of its genes is very similar to that of other lambdoid phages (see Figs. 3 and 4), viable λ -P22 hybrids exist, and 15 of its genes show close λ analogues. But, largely because of the morphological difference between λ and P22, the latter is considered the archetype of the P22-like phage genus by NCBI. The *P22likevirus* genus also includes coliphage HK620 [87, 88];

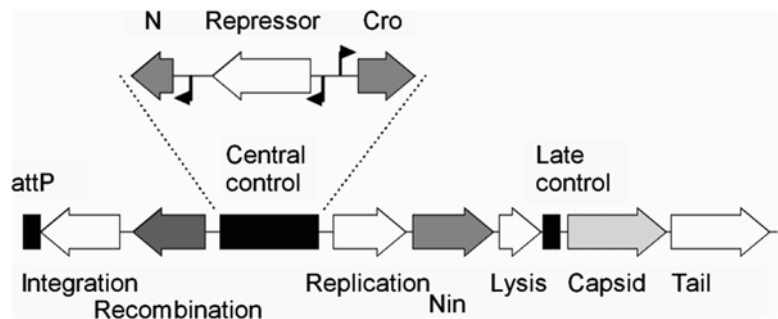


Fig. 3 Diagram of the gene layout of coliphage λ . For comparative purposes in all the genomic diagrams for the temperate phages, the integration features (*int* and *attP*) are presented on the *left*. The central control region specifies the repressor and its cognate operators, promoters, and those adjacent genes which control the lysis-lysogeny switch

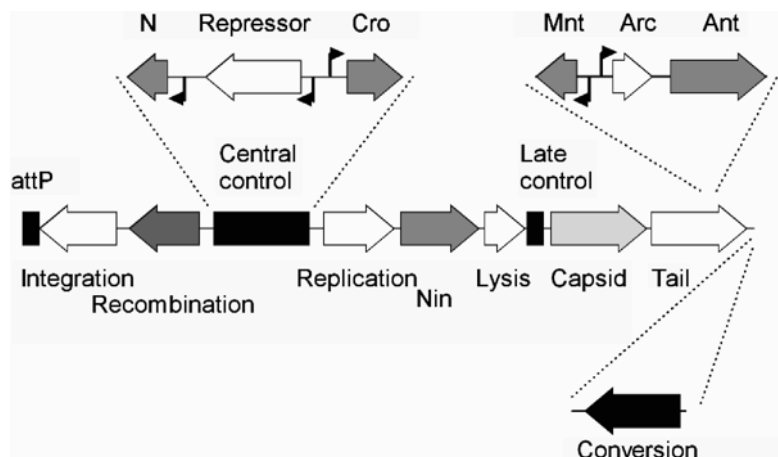


Fig. 4 Diagrammatic genetic map of *Salmonella* phage P22. Please note that the major differences between this and λ are the presence of the lysogenic conversion module (*gtrABC*) downstream of the integration cassette and the presence of the additional regulatory region, *imml*, inserted into the tail morphogenesis gene cluster

Salmonella phages ε34 [89], g341c (NC_013059), Phi20 (GQ422450), SE1 (NC_011802), ST64T [90], ST160 [91], and vB_SemP_Emek [92]; and *Shigella* phage Sf6 [93]. BLASTN analysis reveals that *Salmonella* Heidelberg strains CFSAN002069, 41578, B182, and SL476 harbor prophages which are related to P22 (74 % query coverage).

P22 adsorption is a multistep process [94] which is initiated by phage binding to its receptor (lipopolysaccharide [LPS] O side chains of *Salmonella* serovars A, B, and D1) via the virion tailspike proteins [95]. The latter possess endorhamnosidase activity, which digests the O antigen, permitting diffusion of the phage through

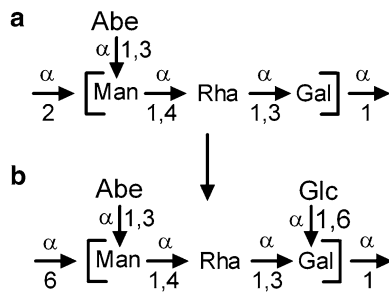


Fig. 5 The sequence of the O-antigen repeat in *S. Typhimurium* is composed of a branched tetrasaccharide of Abe (abequose: 3,6-dideoxy-D-galactose), Man (mannose), Rha (rhamnose), and Gal (Galactose). The phage gtrABC cluster is responsible for the O1 antigen: a glucosyl side chain (Glc) on the terminal Gal residue

the LPS barrier to the surface of the outer membrane, where tight binding occurs. The linear viral genome enters the host cell and circularizes, a reaction involving (1) the terminally redundant ends of the molecules, (2) the phage-encoded protein Erf, and (3) the host RecA and gyrase. This is the substrate for replication or integration into the host chromosome. The phage integration site, like that of many prophages, maps within a tRNA gene—*thrW*. Unlike coliphage λ integration, the integration of P22 does not require integration host factor (IHF) even though IHF-recognition sites are present within *attP* [96].

In the lysogenic state, P22 expresses three different systems that may interfere with superinfection by homologous phages. These are immunity conferred by the prophage repressor ($\epsilon 2$; N.B. unfortunately the genetic designations for proteins of identical function in P22 and λ are frequently different: the lambda homolog in this case is *cI*), superinfection exclusion mediated by the *sieA* and *sieB* genes, and serovar conversion. The presence of the C2 protein represses the replication of homoimmune phage genomes, while the *sie* genes appear to function in preventing phage DNA injection [97, 98]. Lysogenization by P22 also results in a chemical change to the LPS O-antigen which results in a change in the antigenic formula of serovar Typhimurium from 4,5,12 to 1,4,5,12 and prevents the binding of P22 (see Fig. 5 [99, 100]). Sequence analysis [101] and cloning [102] have shown three membrane-bound phage products involved in serovar conversion (i.e., GtrA, GtrB, and GtrC). GtrA is a 120 amino acid glucosyl undecaprenyl phosphate flippase, GtrB is a 310 amino acid bactoprenyl glucosyl transferase, and GtrC is a 486 amino acid conversion protein responsible for adding glucosyl residues to the side chain repeat precursor.

Upon induction of lysogens, specialized transducing particles arise, carrying genes adjacent to the *attBP* sites, as well as a generalized transducing particle carrying only host DNA. This was demonstrated experimentally by Ebel-Tsipis and coworkers [103].

Early events mimic those observed with coliphage λ in that transcription is initiated from two promoters, P_L and P_R , that flank the repressor ($c2$) gene. The early proteins are gp24, a λ N homolog which functions as a transcriptional antiterminator, and Cro, which functions to inhibit transcription from P_{RM} and generally downregulate transcription from P_L and P_R , thereby favoring lytic development. Another early transcript is initiated from P_{ant} in the unique *immI* region, giving rise to an antirepressor, Ant, which functions to inhibit $c2$ repressor function. The synthesis of Ant is negatively regulated by Mnt binding to an operator (O_{Mnt}) and preventing expression from P_{Ant} . Late gene expression is regulated, as it is in λ in an antitermination-dependent mechanism involving gp23, a Q homolog [104]. The late genes include a holin (gp13), a lysozyme homolog (gp19), and the genes involved in morphogenesis. The last have been extensively studied, revealing that, unlike the situation with λ phage morphogenesis, a unique scaffolding protein (gp8) is involved in the formation of a morphogenic core together with portal protein (gp1) and pilot proteins (gp16, gp20, and gp7) [105–109]. The virus surface is composed almost exclusively of a single protein (gp5). The scaffold is reutilized in subsequent rounds of capsid assembly [110]. Cryo-electromicrographs of the P22 tail structure [111, 112] have redefined our understanding of the tail machine showing the spatial relationship of tail associated multimeric proteins gp4 and gp10, tailspike protein gp9, and the needle (gp26). A dodecamer of gp4 subunits provides for binding of gp10 (hexamer) to form the tail tube. To this six tailspike trimers bind, and the tail is complete by the addition of a trimer of gp26 which forms a 12.4×3.8 nm plug in the tail preventing leakage of DNA from the head and possibly, because it protrudes, playing a role in adsorption and/or injection [111].

DNA replication is initiated from an origin (Ori) located within the primase gene [18] (gp18) and a helicase (gp12). Replication leads to the formation of concatemeric molecules as a result of rolling-circle replication [48]. DNA packaging in P22 proceeds from a unique site (*pac*) located within gene 3 on the concatemeric substrate, resulting in the head-full packaging of a limited series of terminally redundant and circularly permuted genomes [113]. P22 packages about 43.4 kb of DNA that is terminally redundant (0.9 kb, 2.2 %) [114].

ε34

This phage possesses an isometric head 62.5 nm in length, a neck 11 nm in width, and a short tail 4.4 nm in width by 5.5 nm in length [115], and is characterized by its ability to infect, lysogenize, and seroconvert *Salmonella enterica* serovar Anatum ε15 lysogens.

The receptor and probable mechanisms of serovar conversion are shown in Fig. 6. A further common characteristic to its relative P22 is that the 60 kDa tailspike protein (if unheated) migrates in SDS-polyacrylamide gels as a trimer and possesses

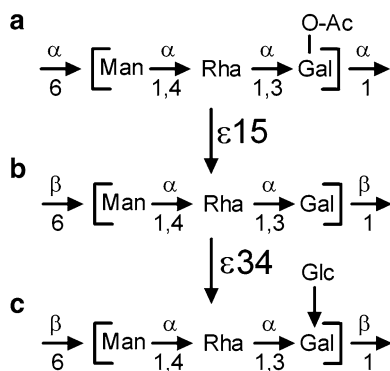


Fig. 6 Structure of the trimeric O-antigenic repeat in *S. Anatum* by phages $\varepsilon 15$ (see below) and $\varepsilon 34$. The O-Ac moiety is an O-acetyl group on the galactosyl residue

LPS-depolymerizing activity [115]. The first 113 amino acids of the tailspike protein (TSP) of this phage show a high level of sequence identity to analogous proteins of phages Sf6, HK620, P22, ST64T, and ST104. The conservation of the N-terminal region is a common feature among related phages since this region is associated with binding to the tail machine [111]. It is noteworthy that the TSP ε_{34} competes with TSP P_{22} for binding to P22 TSPless particles suggesting similar sites. But, noninfectious particles are formed.

The sequence of the genome of this bacteriophage is 43.0 kb and 47.3 % G+C. As expected it shows considerable overall sequence and spatial similarity to P22. This phage integrates into the host *argU* tRNA gene [116].

ST64T

This phage was mitomycin C induced, along with ST64B, from *S. Typhimurium* DT64 and, like P22, is a generalized transducer with a capsid 50 nm in diameter (M.W. Heuzenroeder, personal communication) [90]. It is also a serovar-converting phage possessing homologs of the P22 *gtrABC* operon. Lysogenization by this phage is probably also responsible for converting *S. Typhimurium* phage type (DT) 9–64, 135–16, and 41–29 [117]. Its genome is 40.7 kb with a G+C content of 47.5 %. The region of 348 bp between *int* and *gtrA* is 99 % identical to the similar region in ST104 and 93 % to P22. Furthermore the 128 bp proximal to the *int* gene of phage ES18 are 99 % identical suggesting that the integration sites (*attP*) of these four phages are identical.

Like P22, downstream of the late control protein (Q-homolog) we find the lysis cassette—the lysin exhibits 99 % amino acid sequences identity to gp19 of *Salmonella* phage PS3 (CAA09701) and to a variety of other prophage and phage putative lysins, including those of the myoviruses RB49 and RB43, and the siphovirus T5. The annotation of its homologs suggests that this protein may be

an L-alanyl-D-glutamate peptidase. Downstream, ST64Tp47 possesses (1) an N-terminal transmembrane domain, (2) high level sequence identity to gp15 of PS34, and (3) Orf66 from P22 and is most probably the Rz homolog. If one truncates the version of the annotated locus ST64Tp48 to represent a better initiation site and homologs it (*orf243*) and subsequent gene products (ST64Tp49 and ST64Tp50) exhibit 100 % sequence identity to the products of contiguous ST104 genes (YP_006401, YP_006402, and YP_006403). Interestingly, the latter protein has been shown to be a capsid decoration protein by homology to *Salmonella* phage L (AAX21524) [118]. While its genomics are clearly related to P22, the *immI* region differs in that it lacks *arc* and *ant* genes.

ST104

Mitomycin C treatment of *S. Typhimurium* DT104 resulted in the induction and isolation of phage ST104, which, based upon its close homology to phage P22 and the lack of a gene for a tail tape measure protein, is a member of the *Podoviridae* [119]. The prophage is probably the same as the generalized transducer PDT17 identified by Schmieger and Schicklmaier in this bacterial strain [120]. Its genome is 41.4 kb (47.3 % G+C) and it encodes for at least 65 proteins. A high percentage of these proteins are homologous to proteins in phages ϵ 34, P22, and ST64T. These include conserved antirestriction (*abc*), conversion (*gtr*), superinfection exclusion (*sie*), *nin*, and *immC* loci. Furthermore, the putative *pac* site of this phage (GAAGACTTATCTGAGGTCGTTA) is identical to that of phages ϵ 34, ST64T, PS119 (GenBank accession number BPS011581), PS3 (BPS011579), L [118], and LP7 [121]. Antitermination protein gp24 (N-analog) exhibits 96 % sequence identity with gp24 of P22 suggesting that the early controls of both phages are similarly controlled. The Q-analog (gp23) exhibits only 41 % sequence identity with highest degree of identity being associated with the N-terminal part of the protein.

3.1.2 *Epsilon15likevirus*

The receptor for phage ϵ 15 is the O-antigen of *S. Anatum* which belongs to serogroup E1 expressing serovar factors 3 and 10. The receptor structure is shown in Fig. 6a. Lysogenization of cells resulted in a serological change to serogroup E2 (Fig. 6b) a phenomenon first explored by Luria and Uetake [122–124], and then Robbins et al. [125–130]. Electron micrographs of this phage reveal an isometric head 50 nm in diameter [131]. The tail, like that of phage P22, possesses endorhamnosidase activity, capable of degrading Group E1 *S. enterica* O-polysaccharide polymers down to a D-O-acetyl-Galactosyl- α 1 → 4-D-Mannosyl- β 1 → 4-L-Rhamnose trisaccharide end-product [132, 133]. The function of this enzymatic activity is probably to allow a closer access of the virus particle to the surface of the outer membrane, prior to tight binding and DNA injection [134].

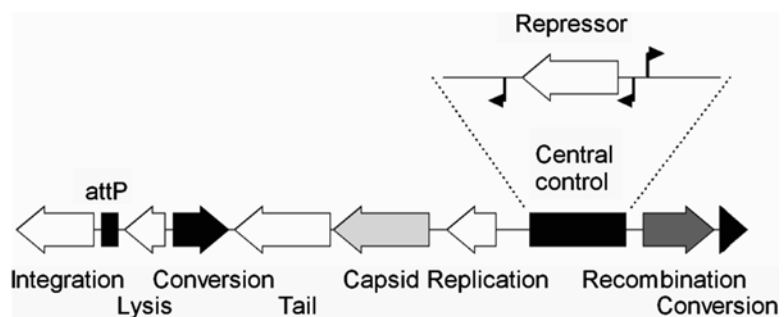


Fig. 7 Gene map of phage $\epsilon 15$. Please note that the conversion genes are not clustered and that *attP* is upstream of *int*

The unique genome sequence of $\epsilon 15$ is 39.7 kb and 50.8 mol.% G+C [135] (Fig. 7). Since the original estimation of mass, based upon restriction analysis, was 40.3 kb the genome is circularly permuted with a terminal redundancy of ~0.6 kb [131]. This phage shows few homologs to its 50 potential gene products amongst existing *Salmonella* phage proteins. Until recently, the nearest phage relatives of $\epsilon 15$ appeared to be *Photobacterium profundum* prophage P ϕ Ppr1 (11 genes in common [136]), *Burkholderia cepacia* phage BcepC6B (10 genes in common [137]), and *Bordetella bronchiseptica*-specific phage, BPP-1 (9 genes in common [138]). In each case the homologs are to other known or putative members of the *Podoviridae*. In the case of all three homologous phages, it is the morphogenic genes which are conserved. Perry and Applegate sequenced the *E. coli* O157:H7-specific phage V10 [139], misnamed φ V10, and showed that it displays considerable sequence similarity to $\epsilon 15$, but lacks the conversion genes of this phage [140].

Although the protein product of gene 38 exhibits poor sequence similarity with other known phage repressors, it is similar in size (198 amino acids) and contains a helix-turn-helix motif of the type that typically serves in operator recognition. A clear plaque mutation ($\epsilon 15vir$) maps within this gene. Like the repressor genes of Lambda, D3 [141], and phage r1t [142]; $\epsilon 15$ gene 38 lacks an identifiable ribosome binding site (RBS). This phage is not UV-inducible, in spite of containing a potential cleavage site (Ala120-Gly121) for the RecA protein stimulated autodigestion of the major repressor proteins [143–145]. Interestingly we have identified ten 17 bp, hyphenated, inverted repeats, which are represented by the consensus sequence ATTACCWDWWNGGTAAT. Of particular interest was our observation that three of the putative operator sites lie to the left of gene 38 and two to its right. This suggests that as with λ divergent transcription is modulated by protein binding to sites on either side of the repressor gene. The significance of the other sites is, as yet, unknown. We have no biochemical,

homology, or protein motif data to support the notion that either of the upstream genes (gp39 or 40) encodes a Cro homolog.

The two other noteworthy features of $\epsilon 15$ are putative presence of an upstream *attP* site and the genes involved in conversion. The phage integration site *attP* is almost always located downstream of the *int* gene. The only known exceptions are *Myxococcus xanthus* phage Mx8, where *attP* is located within *int* [146], and enterobacterial phages HK620 [87] and Sf6 [93] where *attP* is located upstream of *int*. Interestingly there is no evidence for a Xis homolog.

Lysogenic conversion is brought about through the concerted activity of three intimate membrane proteins gp21, gp22, and gp28. The latter 60 amino acid protein acts to inhibit the trans-acetylase activity found in the wild-type cells, while the 66 amino acid encoding gene 22 inhibits the α -polymerase activity responsible to adding the repeat units in an $\alpha 1 \rightarrow 6$ pattern. The 43 kDa product of gene 21 encodes a new $\beta 1 \rightarrow 6$ polymerase. Interestingly only two of these genes are linked. The small size of the membrane inhibitors mimics that of the *Pseudomonas aeruginosa* serovar converting phage D3 LPS polymerase inhibitor [4].

In a brilliant study by Jiang and colleagues, the structure of the entire $\epsilon 15$ virion was studied by cryo-electron microscopy and proteomics [147]. The latter analysis revealed the virus particles contain capsid protein (gp7), which is partially proteolytically processed and may also be, in part, cross-linked, a 12 subunit portal complex (gp4), six bulbous tailspikes (gp20), and a tail hub, probably composed of gp15, 16, and 17.

3.1.3 Other Serovar Conversions Induced by Prophages

In addition to the ability of phage P22 to induce serovar conversion, this property is carried by other undefined phages [148–150]. O-antigen 5 of *S. Typhimurium* strain LT2 is encoded by the prophage Sty-cPP2 *oafA* gene, which specifies an O-antigen acetylase [151, 152]. Other O-antigens are also phage encoded, including 6 [153], 14 [154, 155], 20, and 27 [156–158], but the phage genes responsible for them are currently unidentified, except for those carried by phage P27.

3.1.4 Orphan Podoviruses

Three unclassified *Salmonella* temperate phages include the serovar converting phage SPN9CC (JF900176) and the closely related phages SPN1S [159] (JN391180) and SPN9TCW (JQ691610).

3.2 Temperate Members of the Siphoviridae

3.2.1 ES18

Originally isolated in 1953, bacteriophage ES18 is a temperate, broad-host range, generalized transducing virus of O-antigen-containing (smooth) and lacking (rough) strains of *S. enterica* [160, 161]. As such it differs from other transducing phages for this genus which all require smooth lipopolysaccharide. The cellular receptor for ES18 is FhuA, the outer membrane protein involved in ferrichrome transport [162].

Morphologically this phage possesses an isometric head 56 nm in diameter and a long tail (121 \times 12 nm) making it a member of the *Siphoviridae* [163]. One unusual property of the phage is the observation that it does not band in CsCl equilibrium gradients at the expected density of approximately 1.5 g/ml.

Using pulsed-field gel electrophoresis (PFGE) Casjens and colleagues [163] demonstrated that the genome of ES18 formed a broad band at 51.5 kb, suggestive of variation in the lengths of the packaged genomes. Since the finished sequence of the DNA indicated a circular molecule of 46.9 kb (48.6 % G+C) its genome must be circularly permuted and terminally redundant (ca. 10 %). These features are a result of headful packaging. Detailed analysis of the process in ES18 reveals that the *pac* site is, as with other phages, located in the gene for the small subunit of terminase, but the cleavage reactions which are a precursor to packaging from the concatemeric substrate occur from 300 bp upstream to 700 bp downstream of this site. The consequence is that restriction digestion, coupled by agarose gel electrophoresis and ethidium bromide staining, fails to reveal a cluster of submolar fragments as are observed with phage P22. Hybridizations are required to reveal their presence.

As with all temperate phages the ES18 genome is mosaic in nature (ES18 has been shown to recombine with both Fels-1 and P22 [164]). The genome layout though follows the lambdoid model with its 79 genes arrayed in the following order: packaging, heads, tails, integration, recombination, central regulation, replication, and lysis. BLASTX and CoreGenes analysis [81] reveals that 18 of the first 29 ES18 gene products, i.e., those involved in packaging, capsid, and tail formation, are related to prophage proteins in *Actinobacillus pleuropneumoniae* serovar 1 str. 4074 (GenBank Accession number: NZ_AACK01000018). The remainder of the genome is largely related to P22. Capsid morphogenesis has been used to subdivide the lambdoid phages into five types: HK97, Gifsy-2, 933 W, λ , and P22. The analysis of its genome reveals that ES18 is the sole representative of a new group. The capsids of ES18, like those of coliphage λ , are composed of a major head protein plus a decorator protein. In the case of ES18, the major capsid protein (gp9) undergoes proteolytic removal of 51 amino acids, while the portal (gp5) is also shortened, by in this case ten residues [163].

Transcription is regulated by repressor (gp55) and Cro (gp56) interactions with operators O_L (three sites) and O_R (three sites) affecting transcription from P_L , P_R , and the promoter for repressor maintenance (P_{RM}). All of these show sequence similarity to homologous sites and proteins in phage P22. Delayed early and late transcriptions are controlled by N- and Q-type antiterminators (gp54 and gp73 respectively). They display 63.3 and 37.8 % identity to their P22 homologs. The excisionase (*xis*, gp35), integrase (*int*,

gp34), and integration site (*attP*) show 96 % sequence identity to the homologous region in phage P22 suggesting that ES18 and P22 share a common bacterial insertion site (*attB*) [163].

3.2.2 Lambdoid Group

Three complete lambda-related prophages belonging to the family *Siphoviridae* (Fels-1, Gifsy-1, and Gifsy-2) have been identified in the sequenced *Salmonella* genomes [165–169].

Fels-1

Induction of *S. Typhimurium* LT2 led Yamamoto to discover two serologically and morphologically different phages (Fels-1 and Fels-2). Fels-1 with a genome of 41.7 kb is clearly a member of the lambdoid *Siphoviridae* (see Fig. 2). A preliminary analysis of its sequence suggests that as many as a dozen CDSs may have been missed during the annotation of *S. Typhimurium* LT2 (Kropinski, unpublished results). It is integrated between host genes *ybjP* and *STM0930*, and carries two potential virulence genes: *nanH* (neuraminidase), *sodC3* (superoxide dismutase) [166, 167]. BLASTN analysis reveals that the complete phage only exists in the *S. Typhimurium* LT2 genome.

Gifsy-1

This mitomycin C and UV-inducible 47.8 kb prophage is integrated into the 5' end of the host *lepA* gene which encodes a ribosome-binding GTPase [170]. The capsid measures approximately 60 nm in diameter and it possesses a flexible tail ca. 133 nm in length. Gifsy-1 derivatives exhibiting differing susceptibilities to superinfection have been identified in various *S. Typhimurium* isolates suggesting that the immunity regions are different. Since phages commonly evolve through the horizontal exchange of gene modules or cassettes this observation is not unexpected. The surface receptor for this phage and for Gifsy-2 is OmpC, and therefore these phages propagate most easily on rough mutants of *Salmonella* in which this outer membrane protein is surface exposed rather than obscured by a coating of LPS [171]. The annotated prophage contains a number of missed or potentially incorrectly annotated genes. *STM2628* encodes a protein of 136 amino acids containing a helix-turn-helix (HTH) motif. This is separated from a 79 amino acid protein with a HTH motif with homology to phage Cro-like proteins. It is quite possible that *STM2627* represents a CII-like protein. This requires experimental verification. Interestingly, the putative repressor *STM2628* lacks the Ala-Gly or Cys-Gly sites associated with RecA-dependent UV induction [144, 145] yet both Gifsy prophages are UV-inducible [167]. Both of these prophages also carry *dinI* homologs which negatively regulate induction. Gifsy-1 carries a number of potential virulence modulating genes including *gipA* in what is equivalent to the lambda *b2* region. The latter gene is involved in colonization of the small intestine, and its deletion results in reduced bacterial virulence. BLASTN (90–100 % coverage) analysis reveals related sequence in *S. Typhimurium*

strains LT2, 798, 14028S, UK-1, U288, T000240, D23580, ST4/74, SL1344, 08-1736, and *S. Newport* strains USMARC-S3124.1 and SL254. At 85 % coverage an analog can be found in *S. Choleraesuis* SC-B67, while at 70 % it can be found in *S. Bareilly* strain CFSAN000189.

Gifsy-2

This 45.5 kb prophage, integrated between *pncB* (nicotinate phosphoribosyl-transferase) and *pepN* (an aminopeptidase of peptidase family M1 [pfam01433]), is probably defective in strain LT2 but active in ATCC14028s [167]. Induction results in the release of a siphovirus with a head diameter of approximately 55 nm. As with Gifsy-1 the 693 amino acid containing major capsid gene (STM1033) contains an amino-terminal Clp protease domain (pfam00574). The C-terminus shows homology to proteins from prophages Fels-1 (STM0912) CP-1639 (CAC83157) and CP-933K (NP_286515) and represents a novel head/scaffold/protease composite. Amino acid sequence analysis of the mature capsid protein suggests cleavage near residue 399 [167]. In contrast in Gifsy-1 STM2604 is probably a head-decoration protein analogous to GpD in coliphage lambda and STM2603 is the λ GpE homolog (pfam03864). Gifsy-2 also carries a range of potential virulence determinant two of which *gtgA* (identical to Gifsy-1 *gogA*) and *sodC1* (periplasmic superoxide dismutase) have been implicated in the host pathogenesis. Deletion of *gtgA* results in a sevenfold reduction in virulence, while removal of *sodC1* attenuates virulence by fivefold [172].

Gifsy-2 is also broadly distributed being found in *S. Typhimurium* strains LT2, SL254, 08-1736, 14028S, UK-1, U228, 798, T000240, ST4/74, SL1344, D23580; *S. Newport* USMARC-S3124.1; *S. Paratyphi* C; and *S. Dublin* CT 02021853 (92–100 % coverage). *S. Choleraesuis* SC-B67 contains an analog (84 % coverage), while *S. Weltevreden* strain 2007-60-3289-1 possesses a related prophage (77 % homology).

3.3 Temperate *Myoviridae*

3.3.1 P2likevirus Group

PSP3

The P2-like phages are temperate members of the *Myoviridae* and include coliphages P2 and 186, *Pseudomonas* phage φ CTX, *Haemophilus* phages HP1 and HP2, and *Salmonella* phages PSP3 and SopE φ [173].

The genomic layout is indicated in Fig. 8. The central control region of P2 contains the lysogeny repressor (C) and Cox. The latter protein, which is analogous to Cro of the lambdoid phages, is involved with inhibition of the lysogenic promoter, but unlike Cro it is not essential for lytic development. Integration into the *E. coli* K12 genome occurs at *attB*_{P2} located between genes *yegQ* and *b2083*, and is catalyzed, as with coliphage λ , by Int and IHF. Interestingly, in P2 the function of excisionase (Xis) during excision is provided by Cox. Lysogens also express three conversion genes (also known as morons): *fun(Z)*, *old* (a predicted

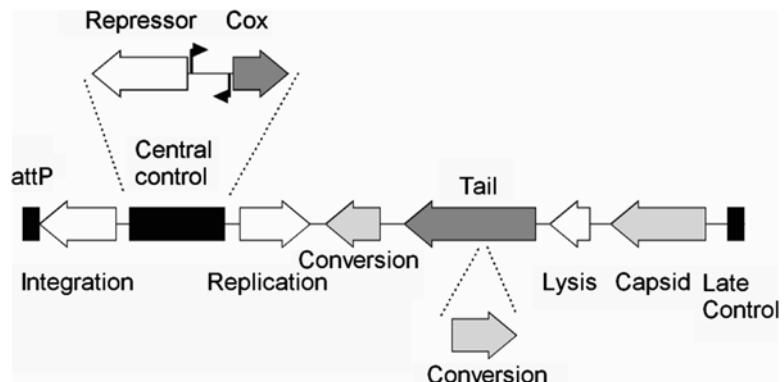


Fig. 8 Diagram of the gene layout of coliphage P2

ATP-dependent endonuclease), and *tin* which result in the cell becoming resistant to coliphages T5, λ , and T4, respectively. Replication involves a complex of protein A and B and results in single circular molecules (rather than concatemers) which are the substrate for packaging. Late gene expression is under positive regulation by Ogr from four promoters which display limited sequence homology to RpoD-dependent *E. coli* promoters and possesses novel imperfect 17 bp inverted repeats at -55 [174]. Experimental evidence suggests that Ogr interacts with the RpoA subunit of the host RNA polymerase complex to enable recognition of these promoters [174]. An interesting feature of P2 is that the usually collocated terminase genes (*terS* and *terL*) are in reverse order and interspersed with scaffold and capsid-encoding genes.

Phage PSP3 was originally isolated from *Salmonella* Potsdam but can lysogenize *E. coli* [173]. The 30.6 kb genome (52.8 % G+C) has 19 bp 5'-extended cohesive termini and encodes 42 proteins, 30 of which are P2 homologs. This phage is a closer relative of 186 and possesses no homologs to *old*, *tin*, or *fun*.

Fels-2

The Fels-2 phage has a head 55 nm in diameter and a contractile tail 110 \times 20 nm [168]. The prophage genome is 33.7 kb (52.5 % G+C) and appears to be bounded by 47 bp direct repeats. As a prophage it is located in *S. Typhimurium* LT2; it shares 32 homologs with PSP3 and 29 with P2. The prophage contains several unannotated and miss-annotated genes including an open reading frame which is related to PSP3 TumB (NP_958095). The prophage integrates into the 3' end of the host *ssrA* genes. A unique feature of this phage is the presence of a gene encoding a DAM methylase (STM2730). The host is also Dam-positive. Lastly, Yamamoto [168] demonstrated that the Fels-2 prophage could recombine with the morphologically unrelated P22 phage to give rise to F22 which is morphologically and serologically related to Fels-2 but carries the P22 *c* genes [175]. Prophages related to Fels-2 have been found in

the genomes of several *Salmonella* serovars, including *S. Javiana*, *S. Agona*, and *S. Dublin* (80–82 % coverage); *S. Typhi* (79 %) and *S. Paratyphi A* (74 %).

SopE φ

SopE φ also has the same *attB* site as Fels-2 [176] and shares many genes in common with the latter phage, and 25 with P2. Induction, with mitomycin C, from *S. Typhimurium* strain DT204 resulted in particles with heads 58 nm in diameters and contractile tails 133 \times 19 nm [177]. These particles infect sensitive *Salmonella* strains in an FhuA, TonB-independent manner and exhibit a burst size of approximately 8. The genome is approximately 34.7 kb (51.3 % G+C) and carries the type III effector protein SopE which binds to, and transiently activates, eukaryotic RhoGTPases [178]. *Salmonella* mutants lacking this protein show reduced invasiveness.

4 Diversity of *Salmonella* Prophages

Recognition that *S. Typhimurium* carried “symbiotic bacteriophages” was first noted by Boyd [179]. It is noteworthy that most salmonellae carry the genomes of temperate phages—*S. Typhimurium* strains usually carry 4–5 complete prophages while *S. Typhi* strains Ty2 and CT18 both possess seven prophages [180].

There are two methods to identify prophages: (1) experimental and (2) computational. Experimental methods involve inducing the bacterial host to release phage particles by exposing them to UV light or other DNA-disruptive conditions. This approach is widely used to prove the existence of viable phages but will not reveal defective prophages. Another limitation to standard experimental approaches is that not all viable phages can be induced under the same conditions and that in many cases, the conditions required to induce phage activation cannot be known *a priori*. Given the ease with which bacterial genomes can now be sequenced, the computational identification of prophages (both viable and non-viable) from genomic sequence data has become the preferred route.

Prophage regions within bacterial genomes can often be recognized by certain characteristic sequence features, such as the presence of disrupted or interrupted genes, their proximity to bacterial tRNA genes, unique sequence patterns (such as phage attachment sites), and long stretches of atypical DNA sequence content. These sequence features can be used to computationally identify possible prophage genes and genomes. However, prophage regions do not always exhibit atypical nucleotide content, nor do phages always integrate into the same coding regions nor do they always use tRNAs as their target site for integration. As a result these simplified rules do not always yield reliable prophage “hits.” To address these shortcomings, improved methods that rely on a more

integrated approach to prophage identification have started to appear. These methods combine sequence alignments to known phage or prophage genes with comparisons to known bacterial genes. They also combine tRNA site recognition and dinucleotide analysis with advanced pattern-matching methods (hidden Markov scanning) for attachment site recognition. These more advanced methods are now available in a number of programs and web servers including Phage_Finder [181], Prophinder [182], Prophage Finder [183], PhiSpy [184], PHACTS (<http://www.phantome.org/PHACTS/>), and PHAST [185].

Phage_Finder and Prophinder require that the input genome sequence must be well annotated with all CDSs and/or tRNA sites pre-identified. On the other hand, PHAST and Prophage Finder are able to work with unannotated DNA sequence data (as well as GenBank annotated data) and use gene prediction methods to identify all relevant sites. Most prophage identification tools are relatively slow, with the average run time being about 1–2 h per genome sequence. The exception is PHAST, which is able to perform its analyses in less than 5 min (using multiple processors and specially developed rapid annotation techniques). PHAST is the newest addition to a long line of computational prophage tools and it exploits, extends, or borrows from many of the best features of previously developed prophage software. In particular, PHAST combines genome-scale ORF prediction and translation (using GLIMMER 3.02), protein identification (using BLAST matching and annotation by homology), phage sequence identification (using BLAST matching to a large phage-specific sequence database), tRNA identification, attachment site recognition, and gene clustering density measurements using DBSCAN [5]. In addition to these integrated phage identification operations, PHAST also evaluates the completeness of the putative prophage, generates tables on the phage or phage-like features, and creates colorful graphs and charts.

In addition to its speed (10–20× faster), PHAST is also somewhat more accurate than other phage identification tools. Using a “gold standard” of 54 carefully annotated phage-containing genomes from different bacterial species, PHAST achieved 85.4 % sensitivity and 94.2 % positive predictive value (PPV) using annotated GenBank information compared with Prophinder (sensitivity 77.5 %, PPV 93.6 %) and Phage_Finder (sensitivity 68.5 %, PPV 94.3 %). PHAST also exhibited 79.4 % sensitivity and 86.5 % PPV using only raw DNA sequences data [4]. Within these 54 test genomes, there were three *Salmonella* genomes: NC_003198, NC_004631, and NC_003197. PHAST achieved 90 % sensitivity and 100 % PPV using annotated GenBank information compared with Prophinder (Sn 85 %, PPV 100 %) and Phage_Finder (Sn 85 %, PPV 94 %). PHAST also achieved 90 % sensitivity and 85.7 % on the raw *Salmonella* DNA sequence data.

Since it was first published in 2011, PHAST has undergone several upgrades and its phage sequence databases have more than doubled in size. Likewise improvements in its annotation, phage feature displays, and phage classification protocols along with many enhancements suggested by users have been made. Because of its superior performance and speed PHAST was used to perform a large-scale analysis of all sequenced *Salmonella* genomes and to identify and classify all of the prophages found in these genomes. The results of this global analysis can be found at the following web page http://phast.wishartlab.com/z_salmon_all.html.

In general terms, the presence of prophages may impact not only the serotype but also the phage sensitivity pattern (phage type) and pulsed-field gel electrophoretic (PFGE type) pattern. In *S. Typhimurium* strains that have been sequenced a total of 15 intact or cryptic prophages have been identified. This diversity has found application in the development of subtyping systems based upon prophages [186, 187].

5 *Salmonella* Phages: Practical Aspects

5.1 Genetic Manipulations

One of the prime uses of P22 is based upon its ability to transfer host DNA (i.e., generalized transduction). These transducing particles are normally present at 1–3 % of the plaque-forming particles, but high transducing derivatives (P22HT) have been isolated in which 50 % of the particles can transduce [188–190]. Classically this was used for genetic mapping but it is now more often used for strain construction. Other derivatives of P22 include the hybrid Mud-P22 phages which contain the termini of transposable coliphage Mu with the packaging features of P22 [191, 192]. These randomly insert into the host genome and upon induction specifically package DNA adjacent to the integration site.

The function of the *ImmI* region has been exploited by Stanley Maloy and coworkers to create the challenge phage system for studying protein–DNA interactions [193–196]. A *mnt*::Km derivative engineered to carry a specific DNA-binding motif rather than *O_{Mnt}* is tested for its ability to lysogenize, i.e., generate kanamycin-resistant colonies. Expression of the cognate DNA-binding protein will result in repression of *Ant* expression and enhanced lysogenization.

5.2 Phage Typing

5.2.1 Reasons for Characterization of *Salmonella* Isolates by Phage Typing

Phage typing entails a detailed subtyping of *Salmonella* isolates belonging to a particular *Salmonella* serovar. Further characterization of *Salmonella* isolates is of great benefit since it enables the investigator to trace cases and outbreaks of salmonellosis to its source and to recommend measures to eliminate the source and prevent reoccurrence of the disease. More than 2,600 *Salmonella* serovars are now recognized [197, 198]. However, human and

animal infections are primarily caused by a small subset of commonly occurring serovars that almost all belong to *Salmonella enterica* subsp. *enterica*.

5.2.2 The Necessity to Serotype *Salmonella* Isolates Before Phage Typing Is Attempted

Phage typing is a well-established, effective and commonly used diagnostic technique producing reliable results and maximum differentiation of *Salmonella* isolates [10]. Before phage typing is attempted some certainty must be obtained that the isolate indeed belongs to the *Salmonella* species. Therefore, isolates are first characterized as *Salmonella* by their ability to grow in selective enrichment broths such as tetrathionate brilliant green broth or Rappaport-Vassiliadis broth [199] and by displaying specific biochemical reactions when grown on brilliant green sulfa agar or lysine decarboxylase agar, when streaked on urea slants, and when stabbed into a triple sugar iron and Simmons citrate slants. Identity of *Salmonella* may be surmised based on a characteristic colony morphology and color when grown on media to distinguish *Salmonella* from other Enterobacteriaceae. It is often confirmed by picking a colony, preferably from a non-selective agar, and performing a slide agglutination reaction with polyvalent *Salmonella* antisera. When agglutinating, the isolate is likely a *Salmonella* strain and submitted to a *Salmonella* reference laboratory for serotyping. Serotyping is a method of subtyping of *Salmonella* isolates by examining the antigenic properties of the isolate. It is carried out by determining the O or somatic antigens and the H or flagellar antigens with the aid of group and serovar-specific O and H antisera. Serotyping the *Salmonella* isolate is a prerequisite and is generally carried out before phage typing is being attempted. The interaction of bacteriophages with their bacterial host is more or less specific for the *Salmonella* serovar. Serotyping often identifies surface structures of the *Salmonella* isolate that are unique for attachment by specific bacteriophages.

5.2.3 Phage Typing Procedures

Phage typing is carried out by infecting a *Salmonella* isolate of a serovar, e.g., *S. Typhi* or *S. Typhimurium*, with a number of phages listed in the phage typing scheme for that serovar. The media employed in phage typing are phage broth consisting of 20 g Difco Nutrient Broth and 8.5 g sodium chloride that are mixed in 1 L distilled water and boiled to dissolve the ingredients, and then dispensed in 3.5 mL amounts in tubes and autoclaved. To prepare a solid medium, 13 g Difco Bacto Agar is added to the phage broth and after mixing, boiling, autoclaving, and cooling to 50 °C, poured into scored square 15 × 15 cm Petri plates. The pH of both media should be about 6.8. The plates are dried before use. To type a *Salmonella* strain, the isolate is first grown in broth to a barely visible turbidity. The broth is flooded onto the agar surface with the aid of a sterile plastic pipette, and the broth is then sucked up with the same pipette and returned to its tube. The plate is



Fig. 9 Examples of phage typing from the OIE Reference Laboratory for Salmonellosis, Laboratory for Foodborne Zoonoses (Public Health Agency of Canada; courtesy of Dr. A. Muckle): left (*Salmonella* Heidelberg) and right (*Salmonella* sp. 1:4, 12:i)

dried again and the typing phages are dropped with the aid of a set of loops dipped into each of the typing phages or from a set of syringes containing the phages onto the surface of the phage agar. The plates are incubated overnight at 37 °C. The phage typing plates are usually read after 24 h incubation. The readings are done with a 10× hand lens through the bottom of the plates using transmitted oblique illumination. The method of recording degrees of lysis on the *Salmonella* phage typing plates including identification criteria of the plaque sizes, plaque numbers, and the kind of lysis has been described [200, 201]. The spots where the phages have been dropped and where they caused lysis are described as CL (confluent lysis), SCL (semi-confluent lysis), <CL and <SCL (intermediate degrees of lysis), and OL (opaque lysis, a confluent lysis with a heavy central opacity due to secondary growth of lysogenized bacteria) [201] (Fig. 9). The phages used for typing are in the routine test dilution (R.T.D.). The R.T.D. of a phage is the highest dilution which produces confluent or semi-confluent lysis on its homologous type strain, the strain on which the phage had been propagated. If the phages were to be used undiluted many of the reactions might be nonspecific [202]. Some of the phages producing small or minute plaques may only have to be diluted to 10⁻³, whereas others that produce large plaques can be diluted to 10⁻⁵ or 10⁻⁶ to obtain the R.T.D. Different sets of phages are being used for the phage typing of different *Salmonella* serovars.

5.2.4 Specificity of *Salmonella* Bacteriophages

The specificity of the phages for a serovar or for isolates of the same serovar may differ dramatically. As discussed above, specificity of a phage for the bacterium depends on a number of factors including

the ability of the phage to adsorb to the surface structures of the host. Some phages display a high degree of host specificity whereas others have a wide host range. A phage with high specificity is phage φX174 which grows well on *E. coli* strain C but fails to grow on most other *E. coli* laboratory strains. A phage with a very wide host range for *Salmonella* is the Felix O1 bacteriophage [24]. It lyses more than 99 % of all *Salmonella* isolates [202, 203] and is used to distinguish *Salmonella* isolates of *S. enterica* subspecies *enterica*, *salamae*, *diarizonae*, and *indica* which are lysed, from those belonging to *S. enterica* subspecies *arizona* and *houtenae* which are not lysed [197]. Many of the *Salmonella* serovar or serogroup specific phages attach to receptors in the O side chain, the lipo-polysaccharide (LPS) of the outer membrane of Gram-negative bacteria and a striking relationship has been observed in *Salmonella* between O antigens and phage susceptibility [204]. Phage typing of *Salmonella* is mostly performed with sets of phages that are more or less specific for the serovar to which the isolates belong.

5.2.5 Phage Typing Schemes for *Salmonella* Serovars

Phage typing of *Salmonella* has been employed since the late 1930s. The phage typing method and the first phage typing scheme, the Vi-phage typing system, were developed by Craigie and Yen [205, 206]. The Vi antigen is a virulence capsular exopolysaccharide consisting of an acetylated polymer of galactosaminuronic acid. Other bacteria that are known to express this antigen are *S. Paratyphi C*, some strains of *S. Dublin*, and a few strains of *Citrobacter freundii* [207]. The Vi antigen is encoded by the *viaB* operon. Nair et al. [208] showed that *S. Typhi* strains that possess the Vi antigen were lysed with adapted Vi II phages and with unadapted Vi I+IV phages, all of which use the Vi antigen for adsorption to the cell by Vi specific phages, but that strains that lacked the Vi antigen were not lysed by these phages. They further noticed that 112 of 120 *S. Typhi* strains with the Vi antigen contained a 137 Kb *Salmonella* Pathogenicity Island 7 (SPI7) encoding the *viaB* operon and possessing genes for type IVB pili, for putative conjugal transfer, and for *sopE* bacteriophage. The eight remaining strains had a complete or partial deletion of SPI7 and did neither possess the *viaB* locus for Vi exopolysaccharide nor the associated genes, and were not lysed by the Vi specific phages. The *S. Typhi* phage typing scheme was followed by the development of a typing scheme for *S. Paratyphi B* by Felix and Callow [24]. These schemes were instrumental in the identification of chronic fecal carriers and contaminated food products [24]. A phage typing scheme for *S. Typhimurium* was developed in the 1940s and 1950, and an extended scheme recognized 80 phage types [201]. *S. Typhimurium* has been the predominant cause of salmonellosis in humans and has also been the most frequently isolated *Salmonella* serovar from cattle and pigs, food products, animal feeds, and environmental sources [201, 209]. The *S. Typhimurium* typing scheme was again extended and definitive

numbers were given to the phage types; the present scheme consists of 34 phages and identifies 207 phage types [9]. Large egg-associated outbreaks of *S. Enteritidis* infection in humans have occurred worldwide during the late 1980s and 1990s and prompted the development of a phage typing scheme for this serovar [210]. Presently it consists of 16 typing phages that distinguish 77 phage types. A few of the phage types may account for more than 80 % of the isolates [211]. The acquisition of plasmids may cause a phage type conversion and associated antimicrobial resistance. An example thereof is the conversion of *S. Enteritidis* PT4 to PT24 following acquisition of an incompatibility group N (incN) drug resistance encoding plasmid [212]. Disconcerting is the observation that wild-type phage-mediated transduction may contribute to the dissemination of antimicrobial resistance genes, including those encoding extended spectrum β -lactamases (ESBLs) among commonly occurring *Salmonella* serovars that often cause salmonellosis in animals and humans [213]. During the last 15 years, *S. Heidelberg* has caused a large number of infections in chickens and humans in Canada and the United States. A *S. Heidelberg* phage typing scheme has recently been developed [214]. It employs 11 typing phages and distinguishes 49 phage types. Many phage typing schemes including those for typing *S. Typhimurium* and *S. Enteritidis* and associated techniques have been developed at the Central Public Health Laboratory at Colindale, London, United Kingdom. This laboratory is the World Health Organization (WHO) Reference Laboratory for the phage typing of *Salmonella*.

6 Phagotherapy

Recent advances in understanding the genomics and life cycles of various *Salmonella* phages have raised intriguing and far-reaching possibilities for their practical applications, both as research tools and for “phage therapy” or “phage biocontrol.” This section includes a brief overview of the use of *Salmonella* phages and their possible practical applications in various clinical (“phage therapy”) or agricultural/food safety (“phage biocontrol”) settings.

6.1 Initial Studies of Therapy with *Salmonella* Phages

Salmonella phages were the first phages examined for their ability to prevent and treat bacterial infections in various settings. The studies were conducted by Felix d’Hérelle in 1919, a few years after the independent discovery of bacteriophages by Frederick Twort and Felix d’Hérelle in 1915 and 1917, respectively [215]. During the initial pilot experiment, d’Hérelle isolated *Salmonella* bacteriophages from chickens, and he used them to treat birds experimentally infected with “*Salmonella gallinarum*.” It was a very small-scale study: only four birds were included in the phage-treated group, and two birds served as phage-untreated controls.

Nonetheless, the results were promising: the phage-treated birds survived, but the untreated birds died from, the experimental infection. D'Hérelle extended his phage therapy studies almost immediately after the completion of his initial pilot study, by conducting major field trials during 1919–1920. The phage preparations for the field trials were prepared by propagating *Salmonella* phages having the most potent lytic activity against *Salmonella* *Gallinarum*. The resulting phage lysates were packaged (0.5 ml volumes in sealed ampoules) and distributed to veterinarians in various regions of France, with instructions to administer them to chickens by subcutaneous (s.c.) injection. The treatment resulted in cessation of the epidemic and the recovery of most of the sick chickens [216]. Encouraged by these results, d'Hérelle expanded his therapy studies with other phages and other animals and humans. The success of d'Hérelle's early phage therapy studies also prompted other investigators to begin examining the value of various bacteriophages in dealing with various infections of bacterial origin. Some of those studies in which *Salmonella*-specific bacteriophages were used are briefly reviewed below. A more extensive review of various agricultural applications of *Salmonella* and non-*Salmonella* phages is available in the literature [217].

6.2 *Salmonella* Phages for Preventing and Treating *Salmonellosis* in Laboratory Animals

D'Hérelle's early phage therapy studies triggered strong initial interest in the possibility of using *Salmonella* phages to prevent and treat salmonellosis in animals. To give just a few examples, Topley and colleagues [218, 219] orally administered *Salmonella* phages in order to evaluate their efficacy in mice experimentally infected with *S. Typhimurium*. However, in contrast to d'Hérelle's observations with *Salmonella*-infected chickens, phage administration did not reduce mortality of mice. One possible explanation for the discrepancy between these studies and d'Hérelle's earlier observations is that *Salmonella* phages with weak lytic activity were used by Topley and colleagues, whereas d'Hérelle used phages with very strong lytic activity against the targeted bacteria. In this context, when Fisk [220] injected antityphoid phages possessing strong in vitro activity against the challenge *Salmonella* strain into mice before challenge with typhoid bacilli, phage administration strongly protected the mice. Also, in another study [221], when phages that specifically recognized the Vi antigen (a major virulence factor of *S. Typhi*) were injected into mice challenged with *S. Typhi*, the mortality rate was reduced from 93 % in the phage-untreated control group to 6 % in the phage-treated group (452 mice were included in that part of the study). Interestingly, the study further emphasized the importance of using phages with good lytic activity against the challenge bacterium. For example, the mortality rates after treatment with boiled culture supernatant fluids and after treatment with a non-*S. Typhi* phage were not significantly different, and they ranged from 93 to 100 % (200 mice

were included in that part of the study). The protection afforded by the *S. Typhi* phage treatment was concentration-dependent, and it was best when preparations containing $>1 \times 10^5$ viable “phage particles”/mouse were employed.

The results of the above-described studies were encouraging, and, together with the apparent discrepancy in results obtained by various investigators, they normally would have prompted additional research. However, the initially strong interest in phage therapy gradually decreased in the West after antibiotics became increasingly available, and research examining the ability of *Salmonella* phages to prevent or treat salmonellosis in animals was not actively pursued during the 1950s–1980s. This situation began to change in the 1990s, when a renewal of interest in phage therapy prompted several investigators to revisit the idea of using *Salmonella* phages to deal with *Salmonella* infections. One example is the study by Berchieri et al. [222] who used *Salmonella* bacteriophages to treat chickens experimentally infected with *S. Typhimurium*. The treatment significantly reduced mortality compared to the mortality of phage-untreated control birds. The efficacious phage treatment required using concentrated phage preparations (ca. 10^{10} PFU/ml), and phage administration shortly after bacterial challenge was significantly more effective than was delaying the treatment.

6.3 *Salmonella* Phages for Preventing and Treating Salmonellosis in Humans

Although enteric infections arguably have been the most common targets for traditional phage therapy applications, using *Salmonella* phages to prevent or treat human salmonellosis has been relatively limited, even in countries where phage therapy continued to be utilized during the antibiotic era (e.g., the former Soviet Union and some Eastern European countries) [223]. An example of such studies [224] examined the efficacy of intravenously administered *Salmonella* phages (in an isotonic glucose solution) in treating 56 typhoid patients at Los Angeles County General Hospital (patients were infected with *S. Typhi*, previously known as *S. typhosa* and *Eberthella typhosa*). The authors used the same phages previously reported [221] to be effective in treating mice experimentally infected with *S. Typhi*, and efforts were made to select phages possessing strong in vitro lytic activity against the strain of *S. Typhi* isolated from each patient. The treatment reduced patient mortality from 20 % to approximately 5 %, and the authors concluded that treatment with bacteriophages offers a “promising and safe procedure against typhoid fever.”

Shortly after the study by Knouf et al. [224], Desranleau [225] successfully used Vi antityphoid bacteriophages to treat 20 typhoid patients. He used a cocktail of at least four distinct *Salmonella* bacteriophages, and the phages were administered by intravenous (i.v.) injection in an isotonic glucose solution. During a larger subsequent study [226], he used an expanded version of the previous phage cocktail (which now included two additional *Salmonella*

phages, for a total of six phages in the preparation) to treat *S. Typhi* infections in approx. 100 typhoid patients in the province of Quebec, Canada. The treatment continued to be effective, reducing the mortality from approx. 20 % to approx. 2 %. An interesting aspect of the latter study was that *Salmonella* antigens (released by phage-mediated lysis while preparing phage lysates *in vitro* and during the lysis of *Salmonella* *in vivo*) in the phage cocktail were proposed to be directly responsible for the observed clinical improvement, whereas direct antibacterial action of bacteriophages *in vivo* was proposed to be only an “indirect cause of the cure as regards symptoms.” The idea of using phages to prepare phage lysates with strong immunostimulating activity has been advanced by several investigators since the 1920s, and it has received some renewed attention recently, including the development of “ghost vaccines” for preventing bacterial infections (including *Salmonella* infections), in various agriculturally important animals. More information dealing with this subject is available in the literature [217, 227].

In the former Soviet Union, *Salmonella* phages have been effectively used to prevent salmonellosis in children [228]. Clinical applications for *Salmonella* phages also have been reported by investigators at the Hirschfeld Institute of Immunology and Experimental Therapy in Poland. Since its founding in 1952, the institute has used its large collection of bacteriophages to treat various bacterial infections in several hospitals in Poland. The most commonly targeted bacterial pathogens included *Staphylococcus aureus*, *Pseudomonas aeruginosa*, and *E. coli*, but phages lytic for *Salmonella* also were employed successfully to treat human infections [229]. At the present time, therapeutic *Salmonella* bacteriophages are commercially produced by at least one company in Russia: ImBio currently manufactures several phage-based therapeutics, including a *Salmonella* phage cocktail (“Bacteriophagum salmonellae gr.ABCDE liquidum”) targeting ca. 10 different *Salmonella* serovars (<http://home.sinn.ru/~imbio/Bakteriofag.htm>).

6.4 *Salmonella* Phages for Improving Food Safety: Phage Biocontrol

A possible and novel application of bacteriophages, which recently has been generating increased interest, is to apply them directly onto food products, in order to reduce the levels of foodborne bacterial pathogens in foods. The first report in which this approach was studied with *Salmonella* was published by Leverentz et al. in 2001 [230]. The authors examined the ability of phages to reduce experimental *Salmonella* contamination of fresh-cut melons and apples stored at various temperatures mimicking real-life settings. Treatment of the experimentally contaminated fruit with aliquots (25 µl per fruit slice, applied with a pipette) of a *Salmonella*-specific phage preparation reduced *Salmonella* populations by ca. 3.5 logs on honeydew melon slices stored at 5 and 10 °C, and by ca. 2.5 logs on slices stored at 20 °C (Fig. 10), which was superior to the

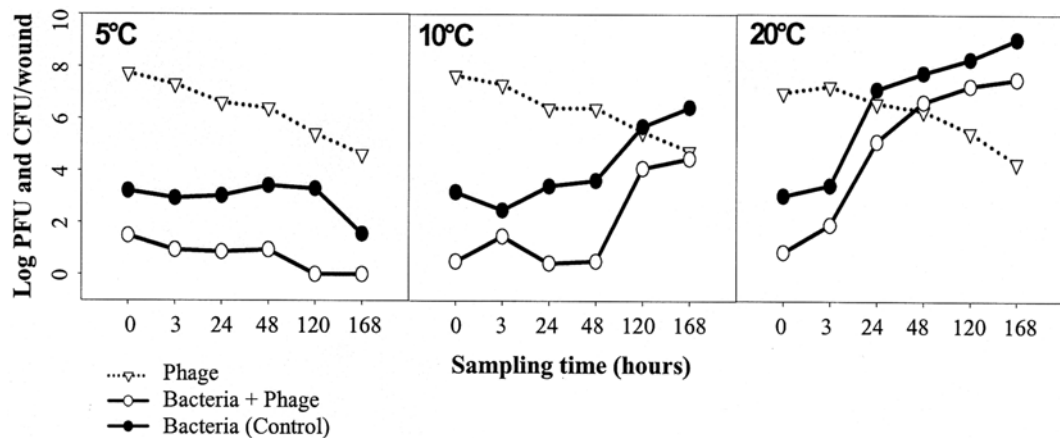


Fig. 10 Reduction of *Salmonella* serovar Enteritidis levels on honeydew melon slices treated with *Salmonella*-specific bacteriophages (from ref. 14). Reprinted with permission from the *Journal of Food Protection* (Copyright held by A. Sulakvelidze)

reduction usually achieved with commonly used chemical sanitizers. However, the phage preparation was significantly less effective on fresh-cut Red Delicious apples, possibly because of the phages' rapid inactivation by the apple slices' more acidic pH (pH 4.2, as opposed to pH 5.8 for the melon slices). A description of one of the *Salmonella* phages (designated SPT-1) used in the above study was recently published [29]. SPT-1 is an O1 species phage possessing broad-spectrum lytic activity against several *Salmonella* serovars. It is a member of the family *Myoviridae*, and it contains abnormal tails that do not appear to result from in vitro assembly of dissociated phages. The phage's genome has been fully sequenced, is 87,069 base pairs in size, and contains 129 open reading frames, 95 (ca. 74 %) of which encode genes of unknown function (A. Sulakvelidze, unpublished data).

A similar phage biocontrol approach also may be of value in the poultry industry; e.g., to reduce contamination of raw chicken carcasses with salmonellae prior to packaging. The results of one study [231] supporting that idea indicated that applying *Salmonella* phages onto chicken skin experimentally contaminated with *Salmonella* significantly reduced (by ca. 99 %, $p=<0.01$) the number of salmonellae on the skin, compared to that on phage-untreated control skin. In addition, when the level of initial *Salmonella* contamination was low, phage treatment yielded *Salmonella*-free skin. Another study [27] found that applying Felix O1 bacteriophage, or its mutant possessing increased in vitro lytic activity against *S. Typhimurium* strain DT104, onto chicken frankfurters experimentally contaminated with the bacterium reduced its concentration by ca. 1.8 logs and 2.1 logs, respectively, compared to that on phage-untreated control frankfurters ($p=0.0001$).

The efficacy of directly applying *Salmonella* phages to other foods also has been examined. For example, Modi et al. [232] reported that adding *Salmonella* phages to milk during the production of raw and pasteurized cheeses reduced their *S. Enteritidis* concentrations by 1–2 logs. In contrast, the *Salmonella* viable counts in cheeses made from milk to which phages were not added increased by about 1 log. Another adaptation of *Salmonella* “phage biocontrol” has been to use *Salmonella* phages to limit the growth of *Salmonella* on various growing plants before they are harvested for food. For example, Ye et al. [233] observed that antagonistic bacteria combined with lytic anti-*Salmonella* bacteriophages significantly reduced the levels of *Salmonella* in sprouting mung beans and alfalfa seeds.

The results of the studies briefly described in this subsection support the idea that using phages to reduce *Salmonella* contamination of various foods has merit. However, the practical applicability of that approach may be complicated by various factors, including the narrow host range of phages. The latter may be of particular concern for *Salmonella*, a very heterogeneous genus comprising >2,600 serovars [234]. Thus, future research in this area may focus on developing phage preparations specifically targeting the *Salmonella* strains or serovars known to be most often responsible for human salmonellosis or to be most virulent, such as *Salmonella* serovars Enteritidis and Typhimurium (including *S. Typhimurium* definitive phage type 104/DT104 strains). In that context, and encouragingly, the first commercial *Salmonella* phage preparation (developed and marketed by Intralytix, Inc., and designated SalmoFreshTM) recently cleared by the FDA for direct food applications has been reported [45] to be effective against *Salmonella* strains belonging to the most common and highly pathogenic serovars Typhimurium, Enteritidis, Heidelberg, Newport, Hadar, Kentucky, Thompson, Georgia, Agona, Grampian, Senftenberg, Alachua, Infantis, Reading, and Schwarzengrund. The preparation received a GRAS (Generally Recognized As Safe) affirmation from the FDA in 2013 (GRAS Notice No. GRN 000435), for direct application onto poultry, fish, and shellfish, and fresh and processed fruits and vegetables. Also, SalmoFresh has been included, in FSIS Directive 7120.1, as a safe and suitable antimicrobial processing aid during the production of poultry-based products. SalmoFresh, at concentrations ranging from 10^6 to 10^7 PFU/g of food, has been reported (GRAS Notice No. GRN 000435) to reduce significantly ($P < 0.05$) the level of *Salmonella* in various foods, with viable count reductions ranging from 65 % in raw turkey breast trim (before grinding) to 98 % in ready-to-eat deli meat. At least one other company, Mirceos, recently announced that its *Salmonella*-specific phage preparation, designated SalmonelexTM, is undergoing field trials

(<http://www.micreosfoodsafety.com/en/Salmonellex.aspx>; last visited on 7 December 2013).

Another adaptation of the phage biocontrol approach for *Salmonella* is to use *Salmonella*-specific phages as nonchemical, environmentally friendly “microbial biopesticides” for significantly reducing or eliminating *Salmonella* contamination of various hard surfaces found in household kitchens and commercial food processing facilities. The rationale for that adaptation is based on the idea that the phage treatment can significantly reduce the number of viable salmonellae on the surfaces, so foods coming in contact with them would be less likely to be contaminated with a level of *Salmonella* required to elicit disease. Recently, using lytic bacteriophages to remove specific foodborne and non-foodborne bacterial pathogens from hard surfaces has been gaining increased attention. For example, some studies have focused on determining the efficacy of phages targeting some major foodborne bacterial pathogens, such as *Listeria monocytogenes* [235, 236] and *E. coli* O157:H7 [237, 238], as well as some non-foodborne pathogens of high bioterrorism concern [239]. Also, a phage-based preparation (ListShield™) was recently granted registration by the U.S. Environmental Protection Agency (EPA) as an antimicrobial for significantly reducing *L. monocytogenes* contamination of nonfood-contact surfaces in food processing plants and food handling establishments (EPA Registration # 74234-1). Therefore, similar applications may also be envisioned for *Salmonella* phages. In this context, a recent study [45] reported that bacteriophages lytic for *Salmonella* rapidly reduced (by 2.1–4.3 logs) *Salmonella* contamination of glass and stainless steel surfaces. Two additional observations reported in the same study were that (1) spot-test susceptibility of the contaminating strains to the *Salmonella* phage cocktail was indicative of efficacy in subsequent surface decontamination studies, and (2) the *Salmonella* phage cocktail could be rapidly customized and adapted to achieve lytic activity against *Salmonella* strains/serovars not previously lysed with the original phage cocktail. If such upgrades can be implemented in real-life settings, they may offer an unprecedented opportunity to renew/upgrade phage preparations as and when needed, in order to maintain their efficacy against newly emerging *Salmonella* strains and highly pathogenic serovars. Studies on the use of phages to reduce *Salmonella* and *Campylobacter* in food have recently been reviewed by Carvalho et al. [240].

6.5 Safety Considerations

Phage-based intervention strategies may be some of the most environmentally friendly approaches for controlling *Salmonella* contamination in various settings. Phages are very specific for their bacterial hosts, and they do not infect eukaryotic cells and strains of unrelated bacteria. The total number of phages on earth is estimated to be 10^{30} – 10^{32} [241], and, although it is difficult to

estimate what percentage of this phage population consists of *Salmonella* phages, it is likely that they are some of the most common phages in the environment. For example, the amount of F-specific phages for *S. Typhimurium* strain WG49 in U.S. sewage has been roughly estimated [217] to be 1×10^{18} PFU/day.

Although the history of phage therapy strongly suggests that phages are very safe for humans, various strategies may be employed to ensure further the safety and consistency of modern therapeutic phage preparations. One concern with phages used for either “phage therapy” or “phage biocontrol” applications is the possible presence of undesirable, potentially harmful genes (e.g., bacterial toxin-encoding genes) in their genomes. Although such genes are very unlikely to endanger individual patients treated with phages, it is sensible to exclude phages containing them from commercial phage preparations, in order to limit their release into the environment. Thus, it is prudent to ensure that *Salmonella* phage preparations do not contain bacterial toxin genes in their genomes, before they are used for traditional phage therapy or to improve food safety. From a practical standpoint, this should be feasible. For example, the increasing availability of high-throughput sequencing techniques should permit full-genome sequencing of all phages considered for therapeutic applications, and their rapid screening for the presence of undesirable genes.

7 Concluding Remarks

Illnesses caused by *Salmonella* are a significant worldwide health burden. For example, the Centers for Disease Control has estimated that foodborne *Salmonella* in the USA causes more than one million people to become sick annually, ca. 19,000 of whom are hospitalized and ca. 400 of whom die (<http://www.cdc.gov/foodborneburden/> PDFs/FACTSHEET_A_FINDINGS_updated4-13.pdf). Also, the illnesses have been estimated [242] to result in ca. \$2.4 billion in medical costs annually. Furthermore, a recent (2010) report from the FoodNet indicated that, although there was an encouraging overall downward trend in the occurrence of most foodborne bacterial diseases during 2010, the morbidity rates for *Salmonella* and *Vibrio* spp. continued to increase. Specifically, all foodborne bacterial diseases were found to have declined except for those caused by vibrios (a 115 % increase) and salmonellae (a 3 % increase). Although the percent increase in morbidity was larger for *Vibrio* than for *Salmonella*, the occurrence of foodborne diseases caused by salmonellae was significantly higher than that of vibrios. In fact, salmonellae were the most common cause of foodborne diseases (ca. 1.2 million cases in the USA) and the most common cause of hospitalization and death tracked during 2010 by the FoodNet. Also, an alarming recent development was

the observation (<http://www.cdc.gov/salmonella/typhimurium-groundbeef/index.html>) that a *S. Typhimurium* strain that contaminated ground beef and caused at least 20 clinical cases of salmonellosis was resistant to several commonly prescribed antibiotics. This is a troubling development because diseases caused by such multi-antibiotic-resistant strains are associated with an increased risk of hospitalization or possible treatment failure.

Despite the increasing rate of foodborne salmonellosis and the importance of salmonellae as human pathogens, published studies evaluating the efficacy of *Salmonella*-specific phages in preventing or treating human salmonellosis are relatively rare. Several reasons may account for this phenomenon. One likely reason is that *Salmonella* infections have low fatality rates and, when necessary, they can be relatively easily controlled by commonly available antibiotics. Thus, the lack of a pressing need for an alternative treatment modality may explain the lack of a strong interest in developing therapeutic *Salmonella* phages for human salmonellosis, even in countries where phage therapy has continued to be utilized during the antibiotic era. However, that situation may drastically change if antibiotic-resistant strains of *Salmonella* similar to those involved in the above-mentioned outbreak become increasingly prevalent. Another possible explanation is that since salmonellae are intracellular pathogens, they must be targeted by therapeutic bacteriophages in the gut before they have been internalized and protected from the phages' lytic effect. Therefore, initiating phage treatment *after* the onset of clinical symptoms may be of limited value, and such approaches have not been actively pursued. On the other hand, *Salmonella* phages may provide an intriguing tool for *preventing* salmonellosis in humans, e.g., as a food safety intervention tool. Indeed, as briefly discussed in this chapter, the "phage biocontrol" approach (i.e., applying *Salmonella*-specific bacteriophages to various foods and food preparation surfaces) may provide a natural means for significantly reducing *Salmonella* contamination of various foods and, thereby, significantly improving public health.

The recent increase in the incidence of human salmonellosis, which is due to the ingestion of contaminated poultry and other foods, indicates that developing and implementing novel approaches for reducing contamination of foods with *Salmonella* are of clear public health importance. A *Salmonella* phage-based approach may be an important part of an overall program for *Salmonella* control. Therefore, additional research in this area is indicated, and it is likely to generate critical data needed for the design and implementation of phage-based intervention strategies that optimally reduce the occurrence of human salmonellosis. In addition, improving our understanding of the genetic makeup and lytic cycles of various *Salmonella* phages (whose major groups were discussed earlier in this chapter) is likely to provide us with the

tools and knowledge required to formulate lytic phage preparations optimal for the prevention and treatment of salmonellosis. A good example of the potential findings resulting from such research is the extensive characterization of the broad-range *S. Typhimurium* phage IRA by investigators at the George Eliava Institute of Bacteriophage, Microbiology and Virology in Georgia [243]. They cloned selected genes of the IRA phage into a plasmid vector, and they found that the recombinant plasmid pKI71's expression elicited lethal structural changes in the *Salmonella* cell wall. Similar studies (albeit not for *Salmonella* phages) have been recently gaining increased popularity in the United States [244–246], and further characterizing this and similar mechanisms is likely to yield new information about phage-bacterial host cell interactions. On a more long-term basis, they are also likely to aid in developing effective phage-based preparations and intervention strategies for *Salmonella* control, and in identifying novel phage-encoded gene products of potential diagnostic or therapeutic value.

Acknowledgements

A.M.K. would like to thank the Laboratory for Foodborne Zoonoses and Health Canada's Genomic Research and Development Initiative for funding this research. Work on *Salmonella* phages by A.I.M.S. and M.W. was supported through a USDA-NIFA Special Research Grant to M.W. (2009-34459-19750).

References

1. Rohwer F (2003) Global phage diversity. *Cell* 113:141
2. Kropinski AM (2009) Measurement of the bacteriophage inactivation kinetics with purified receptors. *Methods Mol Biol* 501: 157–160
3. Brody TB, Fischetti VA (2003) *In vivo* lysogenic conversion of Tox(–) *Streptococcus* pyogenes to Tox(+) with lysogenic *Streptococci* or free phage. *Infect Immun* 71:3782–3786
4. Newton GJ, Daniels C, Burrows LL, Kropinski AM, Clarke AJ, Lam JS (2001) Three-component-mediated serotype conversion in *Pseudomonas aeruginosa* by bacteriophage D3. *Mol Microbiol* 39: 1237–1247
5. Zhou Y, Sugiyama H, Johnson EA (1993) Transfer of neurotoxigenicity from *Clostridium butyricum* to a nontoxigenic *Clostridium botulinum* type E-like strain. *Appl Environ Microbiol* 59:3825–3831
6. Los M, Kuzio J, McConnell M, Kropinski AM, Wegrzyn G, Christie GE (2010) Lysogenic conversion in bacteria of importance to the food industry. In: Sabour P et al (eds) *Bacteriophages in the detection and control of foodborne pathogens*. ASM Press, Washington, DC, pp 157–198
7. Cairns J, Stent GS, Watson JD (1966) *Phage and the origins of molecular biology*. Cold Spring Harbor Laboratory Press, Cold Spring Harbor, NY
8. Nicolle P, Vieu JF, Diverneau G (1970) Supplementary lysotyping of Vi-positive strains of *Salmonella typhi*, insensitive to all the adapted preparations of Craigie's Vi II phage (group I+IV). *Arch Roum Pathol Exp Microbiol* 29:609–617
9. Anderson ES, Ward LR, De Saxe MJ, De Sa JDH (1977) Bacteriophage-typing designations of *Salmonella* typhimurium. *J Hygiene* 78:297–300
10. Anderson ES (1964) The phage typing of *Salmonella* other than *S typhi*. In: Van Oye E (ed) *The world problem of salmonellosis*. Dr. W. Junk Publishers, The Hague, pp 89–109

11. Fischetti VA (2001) Phage antibacterials make a comeback. *Nat Biotechnol* 19:734–735
12. Ackermann H-W (2007) *Salmonella* phages examined in the electron microscope. *Methods Mol Biol* 394:213–234
13. Ackermann H-W (1998) Tailed bacteriophages: the order *Caudovirales*. *Adv Virus Res* 51:135–201
14. Moreno Switt AI, Orsi RH, den Bakker HC, Vongkamjan K, Altier C, Wiedmann M (2013) Genomic characterization provides new insight into *Salmonella* phage diversity. *BMC Genomics* 14:481
15. Li L, Stoeckert CJ Jr, Roos DS (2003) OrthoMCL: identification of ortholog groups for eukaryotic genomes. *Genome Res* 13:2178–2189
16. Huson DH, Bryant D (2006) Application of phylogenetic networks in evolutionary studies. *Mol Biol Evol* 23:254–267
17. Adriaenssens EM, Ackermann HW, Anany H, Blasdel B, Connerton IF, Goulding D, Griffiths MW, Hooton SP, Kutter EM, Kropinski AM, Lee JH, Maes M, Pickard D, Ryu S, Sepehrzadeh Z, Shahrbabak SS, Toribio AL, Lavigne R (2012) A suggested new bacteriophage genus: "Viunalikevirus". *Arch Virol* 157:2035–2046
18. Adriaenssens EM, Van Vaerenbergh J, Vandenheuvel D, Dunon V, Ceyssens PJ, De Proft M, Kropinski AM, Noben JP, Maes M, Lavigne R (2012) T4-related bacteriophage LIMEstone isolates for the control of soft rot on potato caused by 'Dickeya solani'. *PLoS One* 7:e33227
19. Pickard D, Toribio AL, Petty NK, van Tonder A, Yu L, Goulding D, Barrell B, Rance R, Harris D, Wetter M, Wain J, Choudhary J, Thomson N, Dougan G (2010) A conserved acetyl esterase domain targets diverse bacteriophages to the Vi capsular receptor of *Salmonella enterica* serovar Typhi. *J Bacteriol* 192:5746–5754
20. Park M, Lee JH, Shin H, Kim M, Choi J, Kang DH, Heu S, Ryu S (2012) Characterization and comparative genomic analysis of a novel bacteriophage, SFP10, simultaneously inhibiting both *Salmonella enterica* and *Escherichia coli* O157:H7. *Appl Environ Microbiol* 78:58–69
21. Anany H, Lingohr EJ, Villegas A, Ackermann HW, She YM, Griffiths MW, Kropinski AM (2011) A *Shigella boydii* bacteriophage which resembles *Salmonella* phage ViI. *Virol J* 8(242):242
22. Kutter EM, Skutt-Kakaria K, Blasdel B, El-Shibiny A, Castano A, Bryan D, Kropinski AM, Villegas A, Ackermann HW, Toribio AL, Pickard D, Anany H, Callaway T, Brabban AD (2011) Characterization of a ViI-like phage specific to *Escherichia coli* O157:H7. *Virol J* 8:430
23. Hooton SP, Timms AR, Rowsell J, Wilson R, Connerton IF (2011) *Salmonella typhimurium*-specific bacteriophage Φ SH19 and the origins of species specificity in the Vi01-like phage family. *Virol J* 8:498. doi:10.1186/1743-422X-8-498,498
24. Felix A, Callow BR (1943) Typing of paratyphoid B bacilli by means of Vi bacteriophage. *Br Med J* 2:4308–4310
25. Hirsh DC, Martin LD (1983) Rapid detection of *Salmonella* spp. by using Felix-O1 bacteriophage and high-performance liquid chromatography. *Appl Environ Microbiol* 45:260–264
26. Kuhn J, Suissa M, Wyse J, Cohen I, Weiser I, Reznick S, Lubinsky-Mink S, Stewart G, Ulitzur S (2002) Detection of bacteria using foreign DNA: the development of a bacteriophage reagent for *Salmonella*. *Int J Food Microbiol* 74:229–238
27. Whichard JM, Sriranganathan N, Pierson FW (2003) Suppression of *Salmonella* growth by wild-type and large-plaque variants of bacteriophage Felix O1 in liquid culture and on chicken frankfurters. *J Food Prot* 66: 220–225
28. Whichard JM, Weigt LA, Borris DJ, Li LL, Zhang Q, Kapur V, Pierson FW, Lingohr EJ, She YM, Kropinski AM, Sriranganathan N (2010) Complete genomic sequence of bacteriophage Felix O1. *Viruses* 2:710–730
29. Voelker R, Sulakvelidze A, Ackermann HW (2005) Spontaneous tail length variation in a *Salmonella* myovirus. *Virus Res* 114: 164–166
30. Villegas A, She YM, Kropinski AM, Lingohr EJ, Mazzocco A, Ojha S, Waddell TE, Ackermann HW, Moyles DM, Ahmed R, Johnson RP (2009) The genome and proteome of a virulent *Escherichia coli* O157:H7 bacteriophage closely resembling *Salmonella* phage Felix O1. *Virol J* 6:41
31. Tiwari BR, Kim J (2013) Complete genome sequence of bacteriophage EC6, capable of lysing *Escherichia coli* O157:H7. *Genome Announc* 1:e00085-12
32. Lehman SM, Kropinski AM, Castle AJ, Svircev AM (2009) Complete genome of the broad-host-range *Erwinia amylovora* phage ϕ Ea21-4 and its relationship to *Salmonella* phage felix O1. *Appl Environ Microbiol* 75:2139–2147

33. Celamkoti S, Kundeti S, Purkayastha A, Mazumder R, Buck C, Seto D (2004) GeneOrder3.0: software for comparing the order of genes in pairs of small bacterial genomes. *BMC Bioinformatics* 5:52

34. Welkos S, Schreiber M, Baer H (1974) Identification of *Salmonella* with the O-1 bacteriophage. *Appl Microbiol* 28:618–622

35. Hudson HP, Lindberg AA, Stocker BA (1978) Lipopolysaccharide core defects in *Salmonella typhimurium* mutants which are resistant to Félix O phage but retain smooth character. *J Gen Microbiol* 109:97–112

36. Santos SB, Kropinski AM, Ceysens PJ, Ackermann HW, Villegas A, Lavigne R, Krylov VN, Carvalho CM, Ferreira EC, Azeredo J (2011) Genomic and proteomic characterization of the broad-host-range *Salmonella* phage PVP-SE1: creation of a new phage genus. *J Virol* 85:11265–11273

37. Kropinski AM, Waddell T, Meng J, Franklin K, Ackermann HW, Ahmed R, Mazzocco A, Yates J, Lingohr EJ, Johnson RP (2013) The host-range, genomics and proteomics of *Escherichia coli* O157:H7 bacteriophage rV5. *J Virol* 87:10:76

38. Truncaite L, Simoliunas E, Zajanckauskaite A, Kaliniene L, Mankeviciute R, Staniulis J, Klausas V, Meskys R (2012) Bacteriophage vB_EcoM_FV3: a new member of "rV5-like viruses". *Arch Virol* 157:2431–2435

39. Tsinos J, Adriaenssens EM, Klumpp J, Hernalsteens JP, Lavigne R, De Greve H (2012) Complete genome sequence of the novel *Escherichia coli* phage phAPEC8. *J Virol* 86:13117–13118

40. Abbasifar R, Kropinski AM, Sabour PM, Ackermann HW, Alanis VA, Abbasifar A, Griffiths MW (2012) Genome sequence of *Cronobacter sakazakii* myovirus vB_CsaM_GAP31. *J Virol* 86:13830–13831

41. Schwarzer D, Buettner FF, Browning C, Nazarov S, Rabsch W, Bethe A, Oberbeck A, Bowman VD, Stummeyer K, Muhlenhoff M, Leiman PG, Gerardy-Schahn R (2012) A multivalent adsorption apparatus explains the broad host range of phage phi92: a comprehensive genomic and structural analysis. *J Virol* 86:10384–10398

42. Edgell DR, Gibb EA, Belfort M (2010) Mobile DNA elements in T4 and related phages. *Virol J* 7:290

43. Miller EC, Kutter E, Mosig G, Arisaka F, Kunisawa T, Rüger W (2003) Bacteriophage T4 genome. *Microbiol Mol Biol Rev* 67:86–156

44. Petrov VM, Ratnayaka S, Nolan JM, Miller ES, Karam JD (2010) Genomes of the T4-related bacteriophages as windows on microbial genome evolution. *Virol J* 7:292

45. Parks A, Abuladze T, Anderson B, Li M, Carter C, Hanna L, Heyse S, Charbonneau D, Sulakvelidze A, Woolston J (2013) Bacteriophages lytic for *Salmonella* rapidly reduce *Salmonella* contamination on glass and stainless steel surfaces. *Bacteriophage* 3:e25697

46. Marti R, Zurfluh K, Hagens S, Pianezzi J, Klumpp J, Loessner MJ (2013) Long tail fibres of the novel broad-host-range T-even bacteriophage S16 specifically recognize *Salmonella* OmpC. *Mol Microbiol* 87:818–834

47. Lee JH, Shin H, Kim H, Ryu S (2011) Complete genome sequence of *Salmonella* bacteriophage SPN3US. *J Virol* 85:13470–13471

48. Dömöör D, Becságh P, Rákely G, Schneider G, Kovács T (2012) Complete genomic sequence of *Erwinia amylovora* phage PhiEaH2. *J Virol* 86:10899–10912

49. Wang J, Jiang Y, Vincent M, Sun Y, Yu H, Wang J, Bao Q, Kong H, Hu S (2005) Complete genome sequence of bacteriophage T5. *Virology* 332:45–65

50. Kim M, Ryu S (2011) Characterization of a T5-like coliphage, SPC35, and differential development of resistance to SPC35 in *Salmonella enterica* serovar typhimurium and *Escherichia coli*. *Appl Environ Microbiol* 77:2042–2050

51. Niu YD, Stanford K, Kropinski AM, Ackermann HW, Johnson RP, She YM, Ahmed R, Villegas A, McAllister TA (2012) Genomic, proteomic and physiological characterization of a T5-like bacteriophage for control of Shiga toxin-producing *Escherichia coli* O157:H7. *PLoS One* 7:e34585

52. Hong J, Kim KP, Heu S, Lee SJ, Adhya S, Ryu S (2008) Identification of host receptor and receptor-binding module of a newly sequenced T5-like phage EPS7. *FEMS Microbiol Lett* 289:202–209

53. Ackermann HW, Berthiaume L, Kasatiya SS (1972) Morphology of lysotypic phages of *Salmonella paratyphi* B (Felix and Callow chart). *Can J Microbiol* 18:77–81

54. Turner D, Hezwani M, Nelson S, Salisbury V, Reynolds D (2012) Characterization of the *Salmonella* bacteriophage vB_SenS-Ent1. *J Gen Virol* 93:2046–2056

55. Kang HW, Kim JW, Jung TS, Woo GJ (2013) wksl3, a new biocontrol agent for *Salmonella enterica* serovars Enteritidis and Typhimurium in foods: characterization, application, sequence analysis, and oral acute toxicity study. *Appl Environ Microbiol* 79:1956–1968

56. Kim SH, Park JH, Lee BK, Kwon HJ, Shin JH, Kim J, Kim S (2012) Complete genome sequence of *Salmonella* bacteriophage SS3e. *J Virol* 86:10253–10254

57. Tiwari BR, Kim S, Kim J (2012) Complete genomic sequence of *Salmonella enterica* serovar Enteritidis phage SE2. *J Virol* 86:7712

58. De Lappe N, Doran G, O'Connor J, O'Hare C, Cormican M (2009) Characterization of bacteriophages used in the *Salmonella enterica* serovar Enteritidis phage-typing scheme. *J Med Microbiol* 58:86–93

59. Moreno Switt AI, den Bakker HC, Vongkamjan K, Hoelzer K, Warnick LD, Cummings K, Wiedmann M (2013) *Salmonella* bacteriophage diversity reflects host diversity on dairy farms. *Food Microbiol* 36:275–285

60. Delbrück M, Luria SE (1942) Interference between bacterial viruses. I. Interference between two bacterial viruses acting upon the same host, and the mechanism of virus growth. *Arch Biochem* 1:111–114

61. Roberts MD, Kropinski AM (2011) T1-like viruses: Siphoviridae. In: Tidona CA et al (eds) *The Springer index of viruses*. Springer, New York, pp 1821–1830

62. Roberts MD (2001) T1-like viruses. In: Tidona CA et al (eds) *The Springer index of viruses*. Springer, Heidelberg, pp 1–10

63. Roberts MD, Martin NL, Kropinski AM (2004) The genome and proteome of coliphage T1. *Virology* 318:245–266

64. Kropinski AM, Lingohr EJ, Moyles DM, Ojha S, Mazzocco A, She YM, Bach SJ, Rozema EA, Stanford K, McAllister TA, Johnson RP (2012) Endemic bacteriophages: a cautionary tale for evaluation of bacteriophage therapy and other interventions for infection control in animals. *J Virol* 9:207

65. Sertic V, Boulgakov N (1935) Classification et identification des typhi-phages. C R Séances Soc Biol Ses Fil 119:1270–1272

66. Schade SZ, Adler J, Ris H (1967) How bacteriophage chi attacks motile bacteria. *J Virol* 1:591–598

67. Lee JH, Shin H, Choi Y, Ryu S (2013) Complete genome sequence analysis of bacterial-flagellum-targeting bacteriophage chi. *Arch Virol* 158(10):2179–2183

68. Choi Y, Shin H, Lee JH, Ryu S (2013) Identification and characterization of a novel flagellum-dependent *Salmonella*-infecting bacteriophage, iEPS5. *Appl Environ Microbiol* 79(16):4829–4837

69. Pickard D, Thomson NR, Baker S, Wain J, Pardo M, Goulding D, Hamlin N, Choudhary J, Threfall J, Dougan G (2008) Molecular characterization of the *Salmonella enterica* serovar Typhi Vi-typing bacteriophage E1. *J Bacteriol* 190:2580–2587

70. Lavigne R, Seto D, Mahadevan P, Ackermann H-W, Kropinski AM (2008) Unifying classical and molecular taxonomic classification: analysis of the *Podoviridae* using BLASTP-based tools. *Res Microbiol* 159:406–414

71. Dunn JJ, Studier FW (1983) Complete nucleotide sequence of bacteriophage T7 DNA and the locations of T7 genetic elements. *J Mol Biol* 166:477–535

72. Molineux IJ (2001) No syringes please, ejection of phage T7 DNA from the virion is enzyme driven. *Mol Microbiol* 40:1–8

73. Walkinshaw MD, Taylor P, Sturrock SS, Atanasiu C, Berge T, Henderson RM, Edwardson JM, Dryden DT (2002) Structure of Ocr from bacteriophage T7, a protein that mimics B-form DNA. *Mol Cell* 9:187–194

74. Sturrock SS, Dryden DT, Atanasiu C, Dornan J, Bruce S, Cronshaw A, Taylor P, Walkinshaw MD (2001) Crystallization and preliminary X-ray analysis of ocr, the product of gene 0.3 of bacteriophage T7. *Acta Crystallogr D Biol Crystallogr* 57:1652–1654

75. Marchand I, Nicholson AW, Dreyfus M (2001) High-level autoenhanced expression of a single-copy gene in *Escherichia coli*: overproduction of bacteriophage T7 protein kinase directed by T7 late genetic elements. *Gene* 262:231–238

76. Robertson ES, Aggison LA, Nicholson AW (1994) Phosphorylation of elongation factor G and ribosomal protein S6 in bacteriophage T7-infected *Escherichia coli*. *Mol Microbiol* 11:1045–1057

77. Chen Z, Schneider TD (2005) Information theory based T7-like promoter models: classification of bacteriophages and differential evolution of promoters and their polymerases. *Nucleic Acids Res* 33:6172–6187

78. Kwon HJ, Cho SH, Kim TE, Won YJ, Jeong J, Park SC, Kim JH, Yoo HS, Park YH, Kim SJ (2008) Characterization of a T7-like lytic bacteriophage (φSG-JL2) of *Salmonella enterica* serovar gallinarum biovar gallinarum. *Appl Environ Microbiol* 74:6970–6979

79. Dobbins AT, George M Jr, Basham DA, Ford ME, Houtz JM, Pedulla ML, Lawrence JG, Hatfull GF, Hendrix RW (2004) Complete genomic sequence of the virulent *Salmonella* bacteriophage SP6. *J Bacteriol* 186:1933–1944

80. Scholl D, Kieleczawa J, Kemp P, Rush J, Richardson CC, Merril C, Adhya S, Molineux

IJ (2004) Genomic analysis of bacteriophages SP6 and K1-5, an estranged subgroup of the T7 supergroup. *J Mol Biol* 335:1151–1171

81. Zafar N, Mazumder R, Seto D (2002) CoreGenes: a computational tool for identifying and cataloging "core" genes in a set of small genomes. *BMC Bioinformatics* 3:12

82. Savalia D, Westblade LF, Goel M, Florens L, Kemp P, Akulenko N, Pavlova O, Padovan JC, Chait BT, Washburn MP, Ackermann H-W, Mushegian A, Gabisonia T, Molineux I, Severinov K (2008) Genomic and proteomic analysis of phiEco32, a novel *Escherichia coli* bacteriophage. *J Mol Biol* 377:774–789

83. Kropinski AM, Lingohr EJ, Ackermann HW (2011) The genome sequence of enterobacterial phage 7-11, which possesses an unusually elongated head. *Arch Virol* 156:149–151

84. Ahiwale SS, Bankar AV, Tagunde SN, Zinjarde S, Ackermann HW, Kapadnis BP (2013) Isolation and characterization of a rare water-borne lytic phage of *Salmonella enterica* serovar Paratyphi B. *Can J Microbiol* 59:318–323

85. Kazmierczak KM, Rothman-Denes LB (2006) Bacteriophage N4. In: Calendar R (ed) *The bacteriophages*. Oxford University Press, New York, pp 302–314

86. Zinder ND, Lederberg J (1952) Genetic exchange in *Salmonella*. *J Bacteriol* 64:679

87. Clark AJ, Inwood W, Cloutier T, Dhillon TS (2001) Nucleotide sequence of coliphage HK620 and the evolution of lambdoid phages. *J Mol Biol* 311:657–679

88. Dhillon TS, Poon AP, Chan D, Clark AJ (1998) General transducing phages like *Salmonella* phage P22 isolated using a smooth strain of *Escherichia coli* as host. *FEMS Microbiol Lett* 161:129–133

89. Villafane R, Zayas M, Gilcrease EB, Kropinski AM, Casjens SR (2008) Genomic analysis of bacteriophage ϵ 34 of *Salmonella enterica* serovar Anatum (15+). *BMC Microbiol* 8:227

90. Mmolawa PT, Schmieger H, Tucker CP, Heuzenroeder MW (2003) Genomic structure of the *Salmonella enterica* serovar Typhimurium DT 64 bacteriophage ST64T: evidence for modular genetic architecture. *J Bacteriol* 185:3473–3475

91. Price-Carter M, Roy-Chowdhury P, Pope CE, Paine S, De Lisle GW, Collins DM, Nicol C, Carter PE (2011) The evolution and distribution of phage ST160 within *Salmonella enterica* serotype Typhimurium. *Epidemiol Infect* 139:1262–1271

92. Ho N, Lingohr EJ, Villegas A, Cole L, Kropinski AM (2012) Genomic characterization of two new *Salmonella* bacteriophages: vB_SosS_Oslo and vB_SemP_Emek. *Ann Agrarian Sci* 10:18–23

93. Casjens S, Winn-Stapley DA, Gilcrease EB, Morona R, Kuhlewein C, Chua JE, Manning PA, Clark AJ (2004) The chromosome of *Shigella flexneri* bacteriophage Sf6: complete nucleotide sequence, genetic mosaicism, and DNA packaging. *J Mol Biol* 339:379–394

94. Venza Colon CJ, Vasquez Leon AY, Villafane RJ (2004) Initial interaction of the P22 phage with the *Salmonella typhimurium* surface. *P R Health Sci J* 23:95–101

95. Steinbacher S, Miller S, Baxa U, Weintraub A, Seckler R (1997) Interaction of *Salmonella* phage P22 with its O-antigen receptor studied by X-ray crystallography. *Biol Chem* 378:337–343

96. Cho EH, Nam CE, Alcaraz R Jr, Gardner JF (1999) Site-specific recombination of bacteriophage P22 does not require integration host factor. *J Bacteriol* 181:4245–4249

97. Hofer B, Ruge M, Dreiseikelmann B (1995) The superinfection exclusion gene (*sieA*) of bacteriophage P22: identification and overexpression of the gene and localization of the gene product. *J Bacteriol* 177:3080–3086

98. Ranade K, Poteete AR (1993) Superinfection exclusion (*sieB*) genes of bacteriophages P22 and lambda. *J Bacteriol* 175:4712–4718

99. Iseki S, Kashiwagi K (1955) Induction of somatic antigen 1 by bacteriophage in *Salmonella* group B. *Proc Jpn Acad* 31:558–564

100. Rundell K, Shuster CW (1975) Membrane-associated nucleotide sugar reactions: influence of mutations affecting lipopolysaccharide on the first enzyme of O-antigen synthesis. *J Bacteriol* 123:928–936

101. Pedulla ML, Ford ME, Karthikeyan T, Houtz JM, Hendrix RW, Hatfull GF, Poteete AR, Gilcrease EB, Winn-Stapley DA, Casjens SR (2003) Corrected sequence of the bacteriophage P22 genome. *J Bacteriol* 185:1475–1477

102. Vander BC, Kropinski AM (2000) Sequence of the genome of *Salmonella* bacteriophage P22. *J Bacteriol* 182:6472–6481

103. Ebel-Tsipis J, Botstein D, Fox MS (1972) Generalized transduction by phage P22 in *Salmonella typhimurium*. I Molecular origin of transducing DNA. *J Mol Biol* 71:433–448

104. Poteete AR (1988) Bacteriophage P22. In: Calendar R (ed) *The bacteriophages*. Plenum, New York, pp 647–682

105. Parent KN, Doyle SM, Anderson E, Teschke CM (2005) Electrostatic interactions govern

both nucleation and elongation during phage P22 procapsid assembly. *Virology* 340:33–45

106. Weigle PR, Sampson L, Winn-Stapley D, Casjens SR (2005) Molecular genetics of bacteriophage P22 scaffolding protein's functional domains. *J Mol Biol* 348:831–844

107. Kang S, Prevelige PE Jr (2005) Domain study of bacteriophage p22 coat protein and characterization of the capsid lattice transformation by hydrogen/deuterium exchange. *J Mol Biol* 347:935–948

108. Anderson E, Teschke CM (2003) Folding of phage P22 coat protein monomers: kinetic and thermodynamic properties. *Virology* 313:184–197

109. Cingolani G, Moore SD, Prevelige PE Jr, Johnson JE (2002) Preliminary crystallographic analysis of the bacteriophage P22 portal protein. *J Struct Biol* 139:46–54

110. Casjens S, Weigle P (2005) DNA packaging by bacteriophage P22. In: Catalano CE (ed) *Viral genome packaging machines: genetics, structure, and mechanisms*. Landes Bioscience, Georgetown, TX, pp 80–88

111. Tang L, Marion WR, Cingolani G, Prevelige PE, Johnson JE (2005) Three-dimensional structure of the bacteriophage P22 tail machine. *EMBO J* 24:2087–2095

112. Andrews D, Butler JS, Al-Bassam J, Joss L, Winn-Stapley DA, Casjens S, Cingolani G (2005) Bacteriophage P22 tail accessory factor GP26 is a long triple-stranded coiled-coil. *J Biol Chem* 280:5929–5933

113. Wu H, Sampson L, Parr R, Casjens S (2002) The DNA site utilized by bacteriophage P22 for initiation of DNA packaging. *Mol Microbiol* 45:1631–1646

114. Casjens SR, Thuman-Commike PA (2011) Evolution of mosaically related tailed bacteriophage genomes seen through the lens of phage P22 virion assembly. *Virology* 411:393–415

115. Greenberg M, Dunlap J, Villafane R (1995) Identification of the tailspike protein from the *Salmonella newington* phage epsilon 34 and partial characterization of its phage-associated properties. *J Struct Biol* 115:283–289

116. Villafane R, Casjens SR, Kropinski AM (2005) Sequence of *Salmonella enterica* serovar Anatum-specific bacteriophage Epsilon34. Unpublished results

117. Mmolawa PT, Willmore R, Thomas CJ, Heuzenroeder MW (2002) Temperate phages in *Salmonella enterica* serovar Typhimurium: implications for epidemiology. *Int J Med Microbiol* 291:633–644

118. Gilcrease EB, Winn-Stapley DA, Hewitt FC, Joss L, Casjens SR (2005) Nucleotide sequence of the head assembly gene cluster of bacteriophage L and decoration protein characterization. *J Bacteriol* 187:2050–2057

119. Tanaka K, Nishimori K, Makino S, Nishimori T, Kanno T, Ishihara R, Sameshima T, Akiba M, Nakazawa M, Yokomizo Y, Uchida I (2004) Molecular characterization of a pro-phage of *Salmonella enterica* serotype Typhimurium DT104. *J Clin Microbiol* 42:1807–1812

120. Schmieger H, Schicklmaier P (1999) Transduction of multiple drug resistance of *Salmonella enterica* serovar Typhimurium DT104. *FEMS Microbiol Lett* 170:251–256

121. Petri JB, Schmieger H (1990) Isolation of fragments with pac function for phage P22 from phage LP7 DNA and comparison of packaging gene 3 sequences. *Gene* 88:47–55

122. Uetake H, Uchita T (1959) Mutants of *Salmonella* ε15 with abnormal conversion properties. *Virology* 9:495–505

123. Uetake H, Luria SE, Burrous JW (1958) Conversion of somatic antigens in *Salmonella* by phage infection leading to lysis or lysogeny. *Virology* 5:68–91

124. Uetake H, Nakagawa T, Akiba T (1955) The relationship of bacteriophage to antigenic changes in group E Salmonellas. *J Bacteriol* 69:571–579

125. Bray D, Robbins PW (1967) Mechanism of ε15 conversion studied with bacteriophage mutants. *J Mol Biol* 30:457–475

126. Losick R, Robbins PW (1967) Mechanism of ε15 conversion studied with a bacterial mutant. *J Mol Biol* 30:445–455

127. Robbins P, Uchida T (1962) Studies on the chemical basis of the phage conversion of O-antigens in the E-group Salmonellae. *Biochemistry* 1:325–335

128. Robbins P, Uchida T (1965) Chemical and macromolecular structure of O-antigens from *Salmonella anatum* strains carrying mutants of bacteriophage Epsilon 15. *J Biol Chem* 240:375–383

129. Robbins P, Keller JM, Wright A, Bernstein RL (1965) Enzymatic and kinetics studies on the mechanism of O-antigen conversion by bacteriophage Epsilon 15. *J Biol Chem* 240:384–390

130. Uchida T, Robbins PW, Luria SE (1963) Analysis of the serological determinant groups of the *Salmonella* E-group O-antigens. *Biochemistry* 2:663–668

131. McConnell M, Walker B, Middleton P, Chase J, Owens J, Hyatt D, Gutierrez H, Williams M, Hambright D, Barry M Jr (1992) Restriction endonuclease and genetic mapping

studies indicate that the vegetative genome of the temperate, *Salmonella*-specific bacteriophage, epsilon 15, is circularly-permuted. *Arch Virol* 123:215–221

132. Kanegasaki S, Wright A (1973) Studies on the mechanism of phage adsorption: Interaction between Epsilon 15 and its cellular receptor. *Virology* 52:160–173

133. Takeda K, Uetake H (1973) *In vitro* interaction between phage and receptor lipopolysaccharide: a novel glycosidase associated with phage Epsilon 15. *Virology* 52:148–159

134. McConnell MR, Reznick A, Wright A (1979) Studies on the initial interactions of bacteriophage Epsilon 15 with its host cell, *Salmonella anatum*. *Virology* 94:10–23

135. Kropinski AM, Kovalyova IV, Billington SJ, Butts BD, Patrick AN, Guichard JA, Hutson SM, Sydlaske AD, Day KR, Falk DR, McConnell MR (2007) The genome of ε15, a serotype-converting, Group E1 *Salmonella enterica*-specific bacteriophage. *Virology* 369:234–244

136. Vezzi A, Campanaro S, D'Angelo M, Simonato F, Vitulo N, Lauro F, Cestaro A, Malacrida G, Simonati B, Cannata N, Bartlett D, Valle G (2004) Genome analysis of *Photobacterium profundum* reveals the complexity of high pressure adaptations. GenBank Accession Number: NC_006370. Unpublished results

137. Summer EJ, Gonzalez CF, Bomer M, Carlile T, Morrison W, Embry A, Kucherka AM, Lee J, Mebane L, Morrison WC, Mark L, King MD, LiPuma MJ, Vidaver AK, Young R (2006) Divergence and mosaicism among virulent soil phages of the *Burkholderia cepacia* complex. *J Bacteriol* 188:255–268

138. Liu M, Gingery M, Doulatov SR, Liu Y, Hodes A, Baker S, Davis P, Simmonds M, Churcher C, Mungall K, Quail MA, Preston A, Harvill ET, Maskell DJ, Eiserling FA, Parkhill J, Miller JF (2004) Genomic and genetic analysis of *Bordetella* bacteriophages encoding reverse transcriptase-mediated tropism-switching cassettes. *J Bacteriol* 186:1503–1517

139. Ahmed R, Bopp C, Borczyk A, Kasatiya S (1987) Phage-typing scheme for *Escherichia coli* O157:H7. *J Infect Dis* 155:806–809

140. Perry LL, SanMiguel P, Minocha U, Terekhov AI, Shroyer ML, Farris LA, Bright N, Reuhs BL, Applegate BM (2009) Sequence analysis of *Escherichia coli* O157:H7 bacteriophage φV10 and identification of a phage-encoded immunity protein that modifies the O157 antigen. *FEMS Microbiol Lett* 292:182–186

141. Kropinski AM (2000) Sequence of the genome of the temperate, serotype-converting, *Pseudomonas aeruginosa* bacteriophage D3. *J Bacteriol* 182:6066–6074

142. van Sinderen D, Karsens H, Kok J, Terpstra P, Ruiters MH, Venema G, Nauta A (1996) Sequence analysis and molecular characterization of the temperate lactococcal bacteriophage r1t. *Mol Microbiol* 19:1343–1355

143. Craig NL, Roberts JW (1980) *E. coli* *recA* protein-directed cleavage of phage lambda repressor requires polynucleotide. *Nature* 283:26–30

144. Little JW (1991) Mechanism of specific LexA cleavage: autodigestion and the role of RecA coprotease. *Biochimie* 73:411–421

145. Roberts JW, Roberts CW, Mount DW (1977) Inactivation and proteolytic cleavage of phage lambda repressor in vitro in an ATP-dependent reaction. *Proc Natl Acad Sci U S A* 74:2283–2287

146. Magrini V, Storms ML, Youderian P (1999) Site-specific recombination of temperate *Myxococcus xanthus* phage Mx8: regulation of integrase activity by reversible, covalent modification. *J Bacteriol* 181:4062–4070

147. Jiang W, Chang J, Jakana J, Weigele P, King J, Chiu W, Jiang W, Chang J, Jakana J, Weigele P, King J, Chiu W (2006) Structure of epsilon15 bacteriophage reveals genome organization and DNA packaging/injection apparatus. *Nature* 439:612–616

148. Le Minor L (1962) Conversion par lysogenisation de quelques sérotypes de *Salmonella* des groupes A, B et D normalement dépourvus du facteur 027 en cultures 27 positives. *Ann Inst Pasteur* 103:684–706

149. Le Minor L (1963) Conversion antigénique chez les *Salmonella*: IV. Acquisition du facteur 01 par les *Salmonella* des groupes R et T sous l'effet de la lysogenisation. *Ann Inst Pasteur* 105:879–896

150. Le Minor L, Ackermann H-W, Nicolle P (1963) Acquisition simultanée des facteurs 01 et 037 par les *Salmonella* du groupe G sous l'effet de la lysogénisation. *Ann Inst Pasteur* 104:469–475

151. Kim ML, Slauch JM (1999) Effect of acetylation (O-factor 5) on the polyclonal antibody response to *Salmonella typhimurium* O-antigen. *FEMS Immunol Med Microbiol* 26:83–92

152. Slauch JM, Lee AA, Mahan MJ, Mekalanos JJ (1996) Molecular characterization of the *oafA* locus responsible for acetylation of *Salmonella typhimurium* O-antigen: *oafA* is a member of a family of integral membrane trans-acylases. *J Bacteriol* 178:5904–5909

153. Barrow PA (1986) Bacteriophages mediating somatic antigenic conversion in *Salmonella*

cholerae-suis: their isolation from sewage and other *Salmonella* serotypes possessing the somatic 6 antigen. *J Gen Microbiol* 132: 835–837

154. Nnalue NA, Newton S, Stocker BA (1990) Lysogenization of *Salmonella choleraesuis* by phage 14 increases average length of O-antigen chains, serum resistance and intraperitoneal mouse virulence. *Microb Pathog* 8:393–402

155. Le Minor L (1965) Conversions antigéniques chez les *Salmonella*. VII. Acquisition du facteur 14 par les *Salmonella* du sous groupe C1 (6, 7) après lysogénisation par un phage tempère isolé des cultures du sous groupe C4 (6, (7), (14)). *Ann Inst Pasteur* 109:505–515

156. Le Minor L, Le Minor S, Nicolle P (1961) Conversion des cultures de *S. schwarzengrund* et *S. bredeney* dépourvues de l'antigène 27 en cultures 27 positives par lysogénisation. *Ann Inst Pasteur* 101:571–589

157. Bagdian G, Mäkelä PH (1971) Antigenic conversion by phage P27. I Mapping of the prophage attachment site on the *Salmonella* chromosome. *Virology* 43:403–411

158. Lindberg AA, Hellerqvist CG, Bagdian-Motta G, Mäkelä PH (1978) Lipopolysaccharide modification accompanying antigenic conversion by phage P27. *J Gen Microbiol* 107:279–287

159. Shin H, Lee JH, Lim JA, Kim H, Ryu S (2012) Complete genome sequence of *Salmonella enterica* serovar *typhimurium* bacteriophage SPN1S. *J Virol* 86:1284–1285

160. Kuo TT, Stocker BA (1970) ES18, a general transducing phage for smooth and nonsmooth *Salmonella typhimurium*. *Virology* 42: 621–632

161. Le Minor L, Chalon AM (1975) Sensitivity to bacteriophage ES18 of strains of "S. dublin", "S. enteritidis" and "S. blegdam" and related serotypes. *Ann Microbiol* 126:327–331

162. Killmann H, Braun M, Herrmann C, Braun V (2001) FhuA barrel-cork hybrids are active transporters and receptors. *J Bacteriol* 183: 3476–3487

163. Casjens SR, Gilcrease EB, Winn-Stapley DA, Schicklmaier P, Schmieger H, Pedulla ML, Ford ME, Houtz JM, Hatfull GF, Hendrix RW (2005) The generalized transducing *Salmonella* bacteriophage ES18: complete genome sequence and DNA packaging strategy. *J Bacteriol* 187:1091–1104

164. Yamamoto N (1978) A generalized transducing salmonella phage ES18 can recombine with a serologically unrelated phage Fels 1. *J Gen Virol* 38:263–272

165. Figueroa-Bossi N, Coissac E, Netter P, Bossi L (1997) Unsuspected prophage-like elements in *Salmonella typhimurium*. *Mol Microbiol* 25:161–173

166. Figueroa-Bossi N, Uzzau S, Maloriol D, Bossi L (2001) Variable assortment of prophages provides a transferable repertoire of pathogenic determinants in *Salmonella*. *Mol Microbiol* 39:260–271

167. Bossi L, Figueroa-Bossi N (2005) Prophage arsenal of *Salmonella enterica* serovar *Typhimurium*. In: Waldor MK et al (eds) *Phages: their role in bacterial pathogenesis and biotechnology*. ASM Press, Washington, DC, pp 165–186

168. Yamamoto N (1969) Genetic evolution of bacteriophage. I. Hybrids between unrelated bacteriophages P22 and Fels 2. *Proc Natl Acad Sci U S A* 62:63–69

169. Yamamoto N (1967) The origin of bacteriophage P22. *Virology* 33:545–547

170. Caldon CE, Yoong P, March PE (2001) Evolution of a molecular switch: universal bacterial GTPases regulate ribosome function. *Mol Microbiol* 41:289–297

171. Ho TD, Slauch JM (2001) OmpC is the receptor for Gifsy-1 and Gifsy-2 bacteriophages of *Salmonella*. *J Bacteriol* 183: 1495–1498

172. Ho TD, Figueroa-Bossi N, Wang M, Uzzau S, Bossi L, Slauch JM (2002) Identification of GtGE, a novel virulence factor encoded on the Gifsy-2 bacteriophage of *Salmonella enterica* serovar *Typhimurium*. *J Bacteriol* 184: 5234–5239

173. Bullas LR, Mostaghimi AR, Arensdorf JJ, Rajadas PT, Zuccarelli AJ (1991) *Salmonella* phage PSP3, another member of the P2-like phage group. *Virology* 185:918–921

174. Nilsson AS, Haggård-Ljungquist E (2006) The P2-like bacteriophages. In: Calendar R (ed) *The bacteriophages*. Oxford University Press, New York, pp 365–390

175. Yamamoto N, McDonald RJ (1986) Genomic structure of phage F22, a hybrid between serologically and morphologically unrelated *Salmonella typhimurium* bacteriophages P22 and Fels 2. *Genet Res* 48:139–143

176. Pelludat C, Mirold S, Hardt WD (2003) The SopEPhi phage integrates into the *ssrA* gene of *Salmonella enterica* serovar *Typhimurium* A36 and is closely related to the Fels-2 prophage. *J Bacteriol* 185:5182–5191

177. Mirold S, Rabsch W, Rohde M, Stender S, Tschape H, Russmann H, Igwe E, Hardt WD (1999) Isolation of a temperate bacteriophage encoding the type III effector protein

SopE from an epidemic *Salmonella typhimurium* strain. Proc Natl Acad Sci U S A 96:9845–9850

178. Rudolph MG, Weise C, Mirol S, Hillenbrand B, Bader B, Wittinghofer A, Hardt WD (1999) Biochemical analysis of SopE from *Salmonella typhimurium*, a highly efficient guanosine nucleotide exchange factor for RhoGTPases. J Biol Chem 274:30501–30509

179. Boyd JS (1950) The symbiotic bacteriophages of *Salmonella typhi-murium*. J Pathol Bacteriol 62:501–517

180. Thomson N, Baker S, Pickard D, Fookes M, Anjum M, Hamlin N, Wain J, House D, Bhutta Z, Chan K, Falkow S, Parkhill J, Woodward M, Ivens A, Dougan G (2004) The role of prophage-like elements in the diversity of *Salmonella enterica* serovars. J Mol Biol 339:279–300

181. Fouts DE (2006) Phage_Finder: automated identification and classification of prophage regions in complete bacterial genome sequences. Nucleic Acids Res 34:5839–5851

182. Lima-Mendez G, van Helden J, Toussaint A, Leplae R (2008) Prophinder: a computational tool for prophage prediction in prokaryotic genomes. Bioinformatics 24:863–865

183. Bose M, Barber R (2006) Prophage Finder: a prophage loci prediction tool for prokaryotic genome sequences. In Silico Biol 6:0020

184. Akhter S, Aziz RK, Edwards RA (2012) PhiSpy: a novel algorithm for finding prophages in bacterial genomes that combines similarity- and composition-based strategies. Nucleic Acids Res 40:e126

185. Zhou Y, Liang Y, Lynch KH, Dennis JJ, Wishart DS (2011) PHAST: a fast phage search tool. Nucleic Acids Res 39:W347–W352

186. Cooke FJ, Wain J, Fookes M, Ivens A, Thomson N, Brown DJ, Threlfall EJ, Gunn G, Foster G, Dougan G (2007) Prophage sequences defining hot spots of genome variation in *Salmonella enterica* serovar Typhimurium can be used to discriminate between field isolates. J Clin Microbiol 45:2590–2598

187. Rychlik I, Hradecka H, Malcova M (2008) *Salmonella enterica* serovar Typhimurium typing by prophage-specific PCR. Microbiology 154:1384–1389

188. Maloy SR, Stewart VP, Taylor RK (1996) Genetic analysis of pathogenic bacteria. Cold Spring Harbor Laboratory Press, Cold Spring Harbor, NY

189. Davis RW, Botstein D, Roth JR (1980) Advanced bacterial genetics: a manual for genetic engineering. Cold Spring Harbor Laboratory Press, Cold Spring Harbor, NY

190. Schmieger H (1972) Phage P22-mutants with increased or decreased transduction abilities. Mol Gen Genet 119:75–88

191. Benson NR, Goldman BS (1992) Rapid mapping in *Salmonella typhimurium* with Mud-P22 prophages. J Bacteriol 174:1673–1681

192. Youderian P, Sugiono P, Brewer KL, Higgins NP, Elliott T (1988) Packaging specific segments of the *Salmonella* chromosome with locked-in Mud-P22 prophages. Genetics 118:581–592

193. Chen LM, Goss TJ, Bender RA, Swift S, Maloy S (1998) Genetic analysis, using P22 challenge phage, of the nitrogen activator protein DNA-binding site in the Klebsiella aerogenes put operon. J Bacteriol 180: 571–577

194. Szegedi SS, Gumpert RI (2000) DNA binding properties in vivo and target recognition domain sequence alignment analyses of wild-type and mutant RsrI [N6-adenine] DNA methyltransferases. Nucleic Acids Res 28: 3972–3981

195. Ashraf SI, Kelly MT, Wang YK, Hoover TR (1997) Genetic analysis of the *Rhizobium meliloti* nifH promoter, using the P22 challenge phage system. J Bacteriol 179:2356–2362

196. Pfau JD, Taylor RK (1996) Genetic footprint on the ToxR-binding site in the promoter for cholera toxin. Mol Microbiol 20:213–222

197. Grimont PAD, Weill F-X (2007) Antigenic formulae of the *Salmonella* serovars, 9th edn. WHO Collaborating Centre for Reference and Research on Salmonella, Pasteur Institute, Paris

198. Guibourdenche M, Roggentin P, Mikoleit M, Fields PI, Bockemühl J, Grimont PA, Weill FX (2010) Supplement 2003–2007 (no. 47) to the White-Kauffmann-Le Minor scheme. Res Microbiol 161:29

199. Rhodes P, Quesnel LB (1986) Comparison of Muller-Kauffmann tetrathionate broth with Rappaport-Vassiliadis (RV) medium for the isolation of salmonellas from sewage sludge. J Appl Bacteriol 60:161–167

200. Anderson ES, WILLIAMS RE (1956) Bacteriophage typing of enteric pathogens and staphylococci and its use in epidemiology. J Clin Pathol 9:94–127

201. Callow BR (1959) A new phage-typing scheme for *Salmonella typhi-murium*. J Hygiene 57:346–359

202. Kallings LO (1967) Sensitivity of various salmonella strains to felix 0-1 phage. Acta Pathol Microbiol Scand 70:446–454

203. Poppe C, McFadden KA, Demczuk WH (1996) Drug resistance, plasmids, biotypes and susceptibility to bacteriophages of *Salmonella* isolated from poultry in Canada. *Int J Food Microbiol* 30:325–344

204. Lindberg AA (1973) Bacteriophage receptors. *Annu Rev Microbiol* 27:205–241

205. Craigie J, Yen CH (1938) The demonstration of types of *B. typhosus* by means of preparations of type II Vi phage. I. Principles and technique. *Can J Public Health* 29:448–484

206. Craigie J, Yen CH (1938) The demonstration of types of *B. typhosus* by means of preparations of type II Vi phage. II. The stability and epidemiological significance of V form types of *B. typhosus*. *Can J Public Health* 29:484–496

207. Selander RK, Smith NH, Li J, Beltran P, Ferris KE, Kopecko DJ, Rubin FA (1992) Molecular evolutionary genetics of the cattle-adapted serovar *Salmonella dublin*. *J Bacteriol* 174:3587–3592

208. Nair S, Alokam S, Kothapalli S, Porwollik S, Proctor E, Choy C, McClelland M, Liu SL, Sanderson KE (2004) *Salmonella enterica* serovar Typhi strains from which SPI7, a 134-kilobase island with genes for Vi exopolysaccharide and other functions, has been deleted. *J Bacteriol* 186:3214–3223

209. Mitchell E, O'Mahony M, Lynch D, Ward LR, Rowe B, Uttley A, Rogers T, Cunningham DG, Watson R (1989) Large outbreak of food poisoning caused by *Salmonella typhimurium* definitive type 49 in mayonnaise. *BMJ* 298:99–101

210. Ward LR, de Sa JD, Rowe B (1987) A phage-typing scheme for *Salmonella enteritidis*. *Epidemiol Infect* 99:291–294

211. Khakhria R, Duck D, Lior H (1991) Distribution of *Salmonella enteritidis* phage types in Canada. *Epidemiol Infect* 106:25–32

212. Frost JA, Ward LR, Rowe B (1989) Acquisition of a drug resistance plasmid converts *Salmonella enteritidis* phage type 4 to phage type 24. *Epidemiol Infect* 103:243–248

213. Zhang Y, LeJeune JT (2008) Transduction of bla(CMY-2), tet(A), and tet(B) from *Salmonella enterica* subspecies enterica serovar Heidelberg to *S. typhimurium*. *Vet Microbiol* 129:418–425

214. Demczuk W, Soule G, Clark C, Ackermann HW, Easy R, Khakhria R, Rodgers F, Ahmed R (2003) Phage-based typing scheme for *Salmonella enterica* serovar Heidelberg, a causative agent of food poisonings in Canada. *J Clin Microbiol* 41:4279–4284

215. Duckworth DH (1976) Who discovered bacteriophage? *Bacteriol Rev* 40:793–802

216. Summers WC (1999) The hope of phage therapy. In: Felix d'Herelle and the origins of molecular biology, Anonymouspp. Yale University Press, New Haven, CT, pp 108–124

217. Sulakvelidze A, Barrow P (2005) Phage therapy in animals and agribusiness. In: Kutter E et al (eds) *Bacteriophages: biology and application*. CRC Press, Boca Raton, FL, pp 335–380

218. Topley WWC, Wilson J (1925) Further observations of the role of the Twort-d'Herelle phenomenon in the epidemic spread of murine typhoid. *J Hygiene* 24:295–300

219. Topley WWC, Wilson J, Lewis ER (1925) Role of Twort-d'Herelle phenomenon in epidemics of mouse typhoid. *J Hygiene* 24:17–36

220. Fisk RT (1938) Protective action of typhoid phage on experimental typhoid infection in mice. *Proc Soc Exp Biol Med* 38:659–660

221. Ward WE (1942) Protective action of VI bacteriophage in *Enterobacter typhi* Infections in mice. *J Infect Dis* 172–176

222. Berchieri AJ, Lovell MA, Barrow PA (1991) The activity in the chicken alimentary tract of bacteriophages lytic for *Salmonella typhimurium*. *Res Microbiol* 142:541–549

223. Sulakvelidze A, Kutter E (2005) Bacteriophage therapy in humans. In: Kutter E et al (eds) *Bacteriophages: biology and application*. CRC Press, Boca Raton, FL, pp 381–436

224. Knouf EG, Ward WE, Reichle PA, Bower AW, Hamilton PM (1946) Treatment of typhoid fever with type-specific bacteriophage. *JAMA* 132:134–136

225. Desranleau JM (1948) The treatment of typhoid fever by the use of Vi antityphoid bacteriophages. *Can J Public Health* 39:317

226. Desranleau JM (1949) Progress in the treatment of typhoid fever with Vi phages. *Can J Public Health* 40:473–478

227. Jalava K, Hensel A, Szostak M, Resch S, Lubitz W (2002) Bacterial ghosts as vaccine candidates for veterinary applications. *J Control Release* 85:17–25

228. Kiknadze GP, Gadua MM, Tsereteli EV, Mchedlidze LS, Birkadze TV (1986) Efficiency of preventive treatment by phage preparations of children's hospital salmonellosis. In: Kiknadze GP (ed) *Intestinal infections*. Soviet Medicine, Tbilisi, GA, pp 41–44

229. Slopek S, Weber-Dabrowska B, Dabrowski M, Kucharewicz-Krukowska A (1987) Results of bacteriophage treatment of suppurative bacterial infections in the years 1981–1986. *Arch Immunol Ther Exp (Warsz)* 35:569–583

230. Leverentz B, Conway WS, Alavidze Z, Janisiewicz WJ, Fuchs Y, Camp MJ, Chighladze E, Sulakvelidze A (2001) Examination of bacteriophage as a biocontrol method for salmonella on fresh-cut fruit: a model study. *J Food Prot* 64:1116–1121

231. Goode D, Allen VM, Barrow PA (2003) Reduction of experimental *Salmonella* and *Campylobacter* contamination of chicken skin by application of lytic bacteriophages. *Appl Environ Microbiol* 69:5032–5036

232. Modi R, Hirvi Y, Hill A, Griffiths MW (2001) Effect of phage on survival of *Salmonella enteritidis* during manufacture and storage of cheddar cheese made from raw and pasteurized milk. *J Food Prot* 64:927–933

233. Ye J, Kostrzynska M, Dunfield K, Warriner K (2010) Control of *Salmonella* on sprouting mung bean and alfalfa seeds by using a biocontrol preparation based on antagonistic bacteria and lytic bacteriophages. *J Food Protect* 73:9–17

234. Popoff MY, Bockemuhl J, Brenner FW (2000) Supplement 1999 (no. 43) to the Kauffmann–White scheme. *Res Microbiol* 151:893–896

235. Roy B, Ackermann HW, Pandian S, Picard G, Goulet J (1993) Biological inactivation of adhering *Listeria monocytogenes* by listeria-phages and a quaternary ammonium compound. *Appl Environ Microbiol* 59: 2914–2917

236. Hibma AM, Jassim SA, Griffiths MW (1997) Infection and removal of L-forms of *Listeria monocytogenes* with bred bacteriophage. *Int J Food Microbiol* 34:197–207

237. Abuladze T, Li M, Menetrez MY, Dean T, Senecal A, Sulakvelidze A (2008) Bacteriophages reduce experimental contamination of hard surfaces, tomato, spinach, broccoli, and ground beef by *Escherichia coli* O157:H7. *Appl Environ Microbiol* 74: 6230–6238

238. Sharma M, Ryu JH, Beuchat LR (2005) Inactivation of *Escherichia coli* O157:H7 in biofilm on stainless steel by treatment with an alkaline cleaner and a bacteriophage. *J Appl Microbiol* 99:449–459

239. Rashid MH, Revazishvili T, Dean T, Butani A, Verratti K, Bishop-Lilly KA, Sozhamannan S, Sulakvelidze A, Rajanna C (2012) A *Yersinia pestis*-specific, lytic phage preparation significantly reduces viable *Y. pestis* on various hard surfaces experimentally contaminated with the bacterium. *Bacteriophage* 2:168–177

240. Carvalho CM, Santos SB, Kropinski AM, Ferreira EC, Azeredo J (2012) Phages as therapeutic tools to control major foodborne pathogens: *Campylobacter* and *Salmonella*. In: Kurtböke I (ed) *Bacteriophages*. InTech, Rijeka, pp 179–214

241. Brüssow H, Hendrix RW (2002) Phage genomics: small is beautiful. *Cell* 108:13–16

242. Mead PS, Slutsker L, Dietz V, McCaig LF, Bresce JS, Shapiro C, Griffin PM, Tauxe RV (1999) Food-related illness and death in the United States. *Emerg Infect Dis* 5:607–625

243. Adamia RS, Matitashvili EA, Kvachadze LI, Korinteli VI, Matoyan DA, Kutateladze MI, Chanishvili TG (1990) The virulent bacteriophage IRA of *Salmonella typhimurium*: cloning of phage genes which are potentially lethal for the host cell. *J Basic Microbiol* 30:707–716

244. Garcia P, Garcia E, Ronda C, Lopez R, Tomasz A (1983) A phage-associated murein hydrolase in *Streptococcus pneumoniae* infected with bacteriophage Dp-1. *J Gen Microbiol* 129:489–497

245. Nelson D, Loomis L, Fischetti VA (2001) Prevention and elimination of upper respiratory colonization of mice by group A streptococci by using a bacteriophage lytic enzyme. *Proc Natl Acad Sci U S A* 98:4107–4112

246. Schuch R, Nelson D, Fischetti VA (2002) A bacteriolytic agent that detects and kills *Bacillus anthracis*. *Nature* 418:884–889

247. Zargar MA, Pandey B, Sharma R, Chakravorty M (1997) Identification of a strong promoter of bacteriophage MB78 that lacks consensus sequence around minus 35 region and interacts with phage specific factor. *Virus Genes* 14:137–146

248. Amarillas L, Chaidez-Quiroz C, Sanudo-Barajas A, Leon-Felix J (2013) Complete genome sequence of a polyvalent bacteriophage, phiKP26, active on *Salmonella* and *Escherichia coli*. *Arch Virol* 158(11): 2395–2398

INDEX

A

Acousto-optic tuneable filter (AOTF) 169, 184, 192, 220
Acquisition speed 202, 204
A/C replicons 56
Actin 175, 176, 181–182
 cytoskeleton 166, 171, 199, 223
Actinobacillus pleuropneumoniae serovar 1 str. 4074 258
Adenylate cyclase 94
Adenylate cyclase domain of CyaA 94
Adventitia 227
Aeromonas 244
Agar-coated coverslips 177
Agar disks 185, 186, 193
 imaging 178, 180, 185, 186
AKFV33 245
Alfalfa seeds 273
Amoxicillin–clavulanic acid 48
AmpC 49, 53, 55, 60
Ampicillin 52, 53, 84, 89, 91, 94, 134, 135, 158
 resistance 48, 97
Antibiotic resistance 73, 77, 83
 genes 64–66, 82, 99, 102
Antibiotic-resistant strains 276
Antibiotic selection 208
Antibodies 81, 106, 107, 118–120, 122,
 124, 125, 153, 172–174, 179, 182, 183, 188, 190
 assay 118, 119, 121
 labeling 162, 173
Antigenicity 142, 144, 147, 148, 238
Antigens 2, 6, 8, 9, 19, 21, 24, 26, 66, 67, 118–120,
 122, 123, 125, 139, 140, 143, 145–148, 166, 179, 188,
 248, 251, 252, 255, 257, 265, 267, 269, 271
Antimicrobial agent 49
Antimicrobial resistance 47–60, 268
Antimicrobials 2, 47–60, 105–115, 273, 274
Antimicrobial therapy 2
Anti-OmpA antibody 129, 134, 136
Anti-TAG capture probes 5
Aortic aneurysms 117
Array technology 1–26
Asymptomatic infections 121
Atomic force microscopy (AFM) 167
Attachment 41, 151–162, 176, 228–231, 265
Attachment (*att*) site 238, 262, 263
Autodisplay plasmid vector (pJM22) 154, 156,
 158, 161, 162

Autodisplay vector system 161
Autographivirinae 248
Autolytic enzymes 48
Axial resolution 169, 170, 191, 219

B

B182 251
Bacteria 1, 31, 58, 73, 81, 93,
 118, 129, 139–148, 152, 166, 204, 230, 237
Bacterial-based therapies 152, 271
Bacterial behavior 173
Bacterial cell wall 237
Bacterial chromosome 83, 97, 238
Bacterial colony 50, 96, 98
Bacterial division 177, 185
Bacterial DNA 48, 50, 238
Bacterial fitness 82, 173
Bacterial infection 49, 120, 167, 175, 268, 271
Bacterial interactions with host cells 176
Bacterial invasion 172, 173
Bacterial isolates 49
Bacterial membrane 153, 154, 156, 160, 161
Bacterial morphology 167
Bacterial motility 167, 177
Bacterial parasites 1, 5, 6, 9, 237
Bacterial pathogenesis 175
Bacterial populations 173, 181
Bacterial replication 166, 217, 237
Bacterial surface 140, 160, 237
Bacterial vector 209, 210
Bacterial vitality 178
Bacteriophage 237, 239, 254, 262,
 265–274, 276, 277
 chi 247
 E1 248
 ES18 257
 λ 94, 102
 T1 246
Bacteriotherapy 151–162
Band pass (BP) emission filters 204
Bead arrays 3, 5
Bead hybridization 8, 13, 20–21
Bead suspension array 1–26
Beamsplitter 204, 222
 β-lactamases 48, 53, 55, 268
 enzymes 49, 52–53

BF/DIC acquisition 204
BHI broth. *See* Brain Heart Infusion (BHI) broth
Bifidobacteria bacteriotherapy 152
 Bile 227, 228, 230, 233, 234
 Bile solution 228
 Binning 204, 213, 222
 Biocompatibility 152
 Biocontrol 239, 268, 271–276
 Biofilm 170, 234
 formation 167, 228
 structure 168
 Biotin 154, 156, 158, 160, 161
 label 5, 6
 ligase peptide 161
 molecules 154
 Biotin Ligase (BirA) 154–161
 peptide target site 154, 161
 target peptide 156, 158, 160
 target sites 154–156, 161
 Biotin-streptavidin approach 154
 Biotin-streptavidin bond 154
 Biotin-streptavidin complex 154, 155, 160
 BirA. *See* Biotin Ligase (BirA)
*bla*_{CTX-M} 53–55
*bla*_{OXA-1} group 53, 54
*bla*_{SHV} 53
 BLASTN program 51, 55, 247, 251, 259
 Blood vessels 227
 Bochner-Maloy plates 66, 68, 74, 75, 78
 Bone marrow toxicity 48
Bordetella
 B. bronchiseptica 256
 B. pertussis 94, 96
 Brain Heart Infusion (BHI) broth 52
 B/O replicons 56
 Bright field (BF) 204, 206, 219
Burkholderia cepacia phage BcepC6B 256

C

Caco-2 178, 214
 Calmodulin 94
 cAMP. *See* Cyclic AMP (cAMP)
Campylobacter 2, 6, 17, 119, 121, 124, 244, 274
 C. fetus 17
 C. spp. 119
 Cancer 151–153
 cells 152
 therapies 151, 152
 Canine 228
 Canine gallbladder epithelial cells (CGEC) 227–234
 Capsules 237, 241, 248
 Carbenicillin resistance 75
 Cassette, kanamycin 84
Caudovirales 238, 239
 CBA120 239
 CCD cameras. *See* Charge-coupled device (CCD) cameras
 Ceftriaxone 49, 57–58, 60
 Cell fractionation 31
 Cell lines 187, 207–210, 214, 216
 Cell membrane protein fraction 128, 130–131
 Cell morphology 174, 175, 204
 Cell proteome 30, 175
 Cellular fractionation 31
 Cellular proteins 170, 175
 Cellular proteomes 30
 Cellular responses 166, 174–177
 Cell wall architecture 168
 Cephalosporin 49
 CFSAN002069 251
 CGEC. *See* Canine gallbladder epithelial cells (CGEC)
 Charge-coupled device (CCD) cameras 168, 179, 180, 185, 202, 204, 215
Chilikevirus 242, 247
 Chloramphenicol 64, 68, 69, 75
 resistance 48
 Chloramphenicol acetyl transferase 48, 64, 68, 71, 75, 76
 Chloramphenicol resistance gene (CAT) 64, 68
 Chromophores 206
 Chromosomal *cyaA* fusion 94–98, 101–103
 Chromosomal *cyaA* translational fusions 93–104
 Chromosome 66, 77, 78, 82–84, 89, 90, 94, 97, 102, 238, 252
 Ciprofloxacin 48
 resistance 49
 Clavulanic acid 48
 Clinical and Laboratory Standards Institute (CLSI) 49
 CLSM systems. *See* Confocal laser scanning microscopy (CLSM) systems
¹³C¹⁵N-arginine 31, 33–34
¹³C¹⁵N-lysine-labeling 31, 33–34
 Co-infection 2, 3, 16, 173
 Coliphage
 HK620 250
 lambda (λ) 246, 247, 251–253, 258, 260, 261
 Mu 264
 N4 250
 T4 244
 T7 248
 Collinear genomes 245
 Colloidal instability 152, 159
 Confocal 169, 170, 172, 177, 191, 193, 202
 Confocal aperture “optical sectioning” 169
 Confocal laser scanning microscopy (CLSM) systems
 fluorophores 169
 photomultiplier tube (PMT) 202
 spinning (or Nipkow) disk systems, pinholes 169
 Confocal microscopes 90, 91, 167, 169, 175, 189, 201, 211, 213, 231

Confocal microscopy 167, 175

Connective tissue 227

Correlative light electron microscopy (CLEM) 172, 200

COS cells 178

Cosmids 238

CO₂ supply 203

Cronobacter sakazakii phage vB_CsaM_GAP31 243

Cryo-electron microscopy 243, 257

Cryptic prophages 250, 264

CyaA 93–104

CyaA activity assay 99–101

CyaA'-encoding sequence 93, 102

CyaA' fusion 93–104

CyaA' translational fusions 93–104

Cyclic AMP (cAMP) 94–96, 100, 101, 103

Cytokinesis 41, 168

Cytoskeletal proteins ruffles 175

Cytotoxicity 173

D

Deconvolution 170–172, 175, 187, 189, 202, 204

Decreased ciprofloxacin susceptibility (DCS) 48, 59

Delivery of drugs 48

Delivery system 140, 153

Delta 243

Dendritic cells 140, 168

Detection 1–26, 52–55, 65, 82, 105–115, 118–120, 124, 130, 136, 141, 152, 169, 170, 174, 192, 201, 204, 205

of class 1 integrons in NTS 57

and identification of *Salmonella* 14–17

translocation, CyaA' fusion 94

for xTAG GPP 13

Diagnostic procedures 2

Diagnostic reagent 242

Diagnostic yield 3

Diarrhea 1, 2

DIC imaging. *See* Differential interference contrast (DIC) imaging

Dickeya 241

Dickeya bacteriophage 239

Differential antibody staining 182–183

Differential fluorescence induction technique 174

Differential interference contrast (DIC) imaging 184, 193, 204, 218

Dihydrofolate reductase 48

Dihydropteroate synthase 48

Direct hybridization 4

Division 177, 185

DNA

- double-stranded 64, 68, 74–76
- extraction and quantification 9
- gyrase 49, 50
- gyrase-mediated resistance 49

ligases 4, 83–87

polymerases 4, 55, 83, 86, 95, 96, 98

repair machinery 168

topoisomerase IV 50

Drug for treatment 48

DT104 255, 272, 273

E

EC6 243

E. coli. *See* *Escherichia coli* (*E. coli*)

EcRNP 248

Effector proteins 170, 174, 175, 199, 262

- translocation 174, 199

Effectors 81, 82, 90, 93, 94, 98, 174, 200

- delivery 174
- SseK1 94

Electron microscopy (EM) 129, 132, 133, 142, 143, 147, 167, 168, 172, 175, 200, 213, 221, 228, 238, 247, 248.

- See also* Scanning electron microscopy (SEM); Transmission electron microscopy (TEM)

Electroporation 64, 72–75, 89, 95, 97, 102

ELISA. *See* Enzyme-linked immunosorbent assay (ELISA)

EMCCD cameras 202, 215

Endonucleases 66, 71, 75, 238, 243, 248, 261

Endosomal system 200

Enhanced green fluorescent protein (EGFP) 203

Enteric fever 49, 117, 199

Enteric pathogens rotavirus 2

Enterobacteriaceae 239, 241, 243, 265

Enterobacterial genomes 63–78, 245, 259, 262–264

Enterobacterial Repetitive Intergenic Consensus (ERIC PCR) 58–59

Enteropathogen, gasteroenteritis 165

Enterotoxic activity 127, 128

- stn* gene 127

Enzymatic chemistry 4

Enzyme 6, 12, 48, 49, 52–54, 65, 75, 83–87, 159, 161, 174, 238, 245

Enzyme-linked immunosorbent assay (ELISA) 117–125

Epithelium 166, 168, 172, 199, 227, 228

Epitope tags 65–66, 174

$\epsilon34$ 251, 253–255

$\epsilon15$ virion 257

Epsilon15likevirus 255–257

Epsilonproteobacteria 244

Erwinia (vB_EamP-S6) 250

Erwinia phage Φ Ea21-4 243

Erwinia phage phiEaH2 244

ES18 248, 254, 257–259

ESBLs. *See* Extended-spectrum β -lactamases (ESBLs)

Escherichia 93, 244

Escherichia coli (*E. coli*) 2, 6, 16, 17, 64, 83, 85, 86, 88, 94, 102, 119, 129, 134, 135, 137, 139, 153, 167, 239, 243–247, 250, 256, 260, 261, 267, 271, 274

Expression 5, 64, 66, 67, 76, 82, 89, 90, 98, 137, 156–158, 166, 167, 173, 174, 177, 185, 207–209, 214, 216, 217, 227, 248, 253, 261, 264, 277

Extended-spectrum β -lactamases (ESBLs) 49, 53, 60, 268

F

FACS. *See* Fluorescence-activated cell sorting (FACS)

F-actin 181–182

Far-western blotting 130, 135–137

Fecal specimens 2

Felix O1 242, 243, 267, 272

FelixO1-like viruses 243

Felixounalikevirus 241–243

Fels-1 258–260

Fels-2 259, 261–262

FIA replicons 56

FIB replicons 56

FIIs replicons 56

Fimbrial adhesion SiiE 199–200

Flagella 167, 237, 245, 247

Flagellar dynamics 177

Flagellin gene (*flxC*), ceftriaxone resistant *S. Typhi* 57–58

FlAsH tag 174

Flow cytometry 174, 209

Fluorescence 155, 160, 167–172, 174–177, 179, 184, 187–189, 191, 193, 204, 206, 209, 210, 218, 219, 221, 223, 235

- microscopy 174, 179, 181–183, 187, 193
- signal 193, 209, 210, 221, 223
- WFM 176

Fluorescence-activated cell sorting (FACS) 154–156, 160–162, 174

Fluorescence recovery after photobleaching (FRAP) 170, 209, 218

Fluorescent dyes 5, 160, 177

Fluorescent labeling 179, 190

Fluorescent probes 176

Fluorescent protein-based reporters 166

Fluorescent proteins (FPs) 65, 203–205, 209, 210, 214, 220, 221

- aggregation 208, 209
- expression 173, 209
- gene 209
- tags 207

Fluorescent staining 172, 177, 181–183, 189

Fluorochromes 3, 179

Fluorophore 4, 155, 156, 169, 173, 177, 182–184, 188, 189, 192, 220

- nanoparticle cargo 154

Fluoroquinolones (FQ) 48

- resistance 49, 59

FO1a 241, 242

Folate metabolism 48

Foodborne illness 1

Food-borne zoonotic pathogens 48

Food safety 21, 121, 165, 268, 271–276

4–16 nm sucrose-gold nanoparticles 154, 156–159

41578 251

FP/FP-tagged GOI 208

FPs. *See* Fluorescent proteins (FPs)

FP-tagged GOI 207

FRAP. *See* Fluorescence recovery after photobleaching (FRAP)

FrepB replicons 56

FSL SP-010 242, 243

FSL SP-012 242, 243

FSL SP-029 239, 241

FSL SP-058 242, 250

FSL SP-062 247

FSL SP-063 239, 241

FSL SP-069 247

FSL SP-076 242, 250

FSL SP107 242

FSL SP-126 242, 247

G

Gallbladder 227–235

- epithelium 227, 228

Gammaproteobacteria 244

GAP31 243

Gastroenteritis 1, 3, 5, 48, 117, 127, 199

- typhoid fever 48, 117, 127

Gastroenteritis-causing bacteria 1, 3, 5

Gastrointestinal infections 1, 16

Gastrointestinal pathogen 2, 3

Gastrointestinal symptoms 119

g341c (NC_013059) 251

Gel electrophoresis 37, 38, 105–115

Gel electrophoresis system 32, 37

Gene cassettes 65–67, 75, 76

Gene fusions 65, 76, 78, 174

Gene induction 174

Gene microarray 53

Gene of interest (GOI) 66, 68, 83, 101, 207–209

- expression 208

Gene pool 237

Gene-specific mutant strains 64

GeneStrings 76

Gene synteny 239, 240

Gene synteny *Viunalikevirus* 239, 240

Genetic exchange 259

Genetic manipulations 64, 173, 264

Genetic transplantation 66, 78

Genome 63–78, 207, 209, 237, 239, 242–250, 252–256, 258–264, 272, 275

- sequences 63, 242, 256, 263

Genomics 139, 237–277

Genotypic characterization, antimicrobial resistance 59

Genotyping 58–59

Gentamicin 96, 100, 103, 172, 173, 211, 213, 217, 228, 230–231, 234

Gentamicin-protection assays 172, 173, 217, 230–231

Gentamycin 31, 33, 41

GFP. *See* Green fluorescent protein (GFP)

GFP-actin 171, 176

GFP-based reporters 166

GFP-FYVE 176

GFPmut3a variant 209

GFP-promoter constructs 174

GFP-tagged cellular proteins 170

GFP-tagged proteins 176

Gifsy-1 259–260

Gifsy-2 258–260

Gifsy prophages 259

GOI. *See* Gene of interest (GOI)

Gold 118, 129, 134, 136, 152, 154, 156–159, 161, 180, 186, 188, 232, 263

Gold nanoparticles 152, 154, 156–159, 161 conjugation 154

Golgi 38, 43, 200

Golgi apparatus 35

Golgi-enriched fraction 31–32, 35–36, 38, 43

Golgi-enriched fraction coronaviruses 31

Golgi-enriched membranes 37

Golgi membrane enrichment 37

gp49 249

Green fluorescent protein (GFP) 91, 173, 174, 184, 192, 193, 201, 203–205, 208, 213, 214, 218, 220, 222, 233 expression 173, 185, 208 fluorescence 174 labeling 173

Growth 40, 74, 75, 78, 102, 140, 142, 148, 152, 158, 159, 167, 178, 187, 190, 193, 215–217, 229–230, 238, 266, 273 patterns 177 rates 177

gyrA 50 mutations 51, 59

gyrase 49, 50, 252

gyrB 50, 51, 59, 60

H

HeLa cells 31–35, 40, 41, 90, 91, 95, 99, 100, 103, 175, 178, 201, 205, 208–211, 216

Helicobacter pylori 120

Hep-2 178

Herpesvirales 244

Heterogeneous infection of cells 175

HI1. *See* HI incompatibility group (HI1)

High resolution TEM 167

H1 incompatibility group (HI1) 48

HK620 250, 254, 257

Holin 238, 253

Homologous recombination 64, 74, 75, 77, 82, 83, 88–89, 131

Host–pathogen interactions 30, 168, 228

Hosts 152, 241, 245, 274 bacterial evolution 237

cells 30, 63, 81, 93, 94, 103, 127, 166, 167, 174–176, 199, 200, 207, 210, 217, 238, 252, 277 proteins 175 chromosome 238, 252 factors 29–44 proteins 81, 173 expression 173 secretory pathway 31

HotStarTaq Master Mix 8, 19

Huygens software 171

Hybrid detectors 177

Hybridization 6, 8, 12–14, 20–21, 248, 258 assay 4 of labeled amplicons 9

Hyper replication 210, 217

I

ICTV. *See* International Committee of Taxonomy of Viruses (ICTV)

Identification 2, 3, 14–17, 29–44, 49, 93, 106, 139, 172, 176, 262, 266, 267 of proteins 44, 263

iEPS5 247

Illumination 168–170, 179, 192, 213, 218, 266

Image acquisition 168–170, 175, 179, 203

Image analysis 176, 189

Image processing deconvolution algorithms 170

Image resolution 172, 175

Imaging live bacteria, agar-disk imaging technique 185

Imaging software autofocus (SAF) 206

Imaging techniques 168, 175, 177, 180, 185, 186

Immunoassays 96, 100

Immunofluorescence microscopy 179, 181

Immunogold labeling 134, 167

Immunogold stain 129, 133

Immunolabeling 162, 172–174

IMTEC-Salmonella-Antibodies Screen (IgG/IgA/IgM)/ Antibodies IgA 119

Inactivation, selected target genes 64

Incubation chamber 179, 203, 215

Indicators, signalling events 176

Indirect immunofluorescence 188

Infected 29, 31, 33, 35, 40–42, 81, 90, 91, 94, 100, 103, 166, 171, 174, 185–186, 201, 205, 210, 213, 218, 231–234, 239, 243, 244, 246, 268–270

Infection 1–3, 16, 29–44, 47–49, 96, 100, 103, 117–121, 124, 127, 165–168, 170, 172–178, 181, 186, 187, 190, 193, 194, 200, 201, 205, 207, 209–213, 215–217, 230–234, 238, 241, 265, 268–271, 276

Infection cycle 29–44
 Infectious diseases 3
 surveillance 118
 In-frame deletion 63, 68, 74–76
 Infrared-based focus (IRF) 206, 207, 209, 215
 Infrared light-emitting LED 206
 InstaGene matrix by vortex 17
 Integrase 238, 242, 258
 Integrative vectors 238
 Integrity 42, 127–138, 142, 147, 177
 International Committee of Taxonomy of Viruses (ICTV) 239, 244–248
 Intestinal epithelial cells 127
 Intestine 166, 172, 199, 259
 Intracellular infection 30
 Intracellular pathogen 30, 81, 276
 Intracellular trafficking 177
 Invasion 127, 153, 166, 172, 173, 175–177, 181, 199, 216, 228, 230–232, 234
 In vivo epithelia 175
 In vivo infection 175
*I*I replicons 56
 IRF. *See* Infrared-based focus (IRF)
 Isoelectric focusing of β -lactamase enzymes 52–53
 Isogenic mutant strains 63
 Isolates 2, 3, 16, 17, 19, 21–23, 26, 48, 49, 2, 53, 57–58, 63, 89, 120, 242, 244, 259, 264–268
 Isotope forms 29

J

Jersey-like phages 246
Jerseylikevirus 241, 242, 245–246
 JK06 (DQ121662) 246–247
Jk06likevirus 242, 247

K

*K*B replicons 56

L

lacZ gene fusions 174
 λ -P22 hybrids 250
 λ Red recombinase 75, 77, 82, 84, 88, 89
 λ Red system 64
 Lambdoid group 259–260
 Lambdoid phages 246, 250, 258, 260
 Lambdoid *Siphoviridae* 258
 Lamina propria 227
 LAMP1. *See* Lysosomal-associated membrane protein 1 (LAMP1)
 LAMP1-negative tubules (LNTs) 200
 LAMPs. *See* Lysosome-associated membrane proteins (LAMPs)
 Laser therapies 152
 Late endosomes (LE)/lysosomes 200
 Lateral flow rapid tests (LFRTs) 118
 LCI. *See* Live cell imaging (LCI)
 LC-MS/MS analysis 38
 Leaky vasculature 152
 LE markers 200
Les 200
 Light 13, 26, 29–31, 33, 35, 41, 42, 66, 95, 99, 146, 167–170, 172, 175, 183, 191–193, 200–202, 204, 206, 213, 215, 218, 221, 238, 262
 Light microscopy (LM) 167, 168, 175, 177–178, 200, 201, 215
 Limit of detection 15
 Lipopolysaccharide (LPS) 118–120, 122–124, 140–141, 144, 227, 237, 243–245, 248, 251, 252, 257, 259, 267
 FelixO1 243
 LPS-based ELISA 118, 120
 LPS-specific immunoglobulin G (IgG) 118
 Lipoteichoic acids 237
Listeria 152, 153, 274
 Live cell and fixed cell microscopy 166
 Live cell imaging (LCI) 169, 170, 173, 174, 176, 177, 179, 184–185, 190–193, 199–223
 dynamics of infection 166, 176, 193
 time-lapse phase contrast microscopy 184–185
 LIVE/DEAD[®] *bacLight*TM viability kit 193
 Live/dead staining 177
 Living cells 168, 176
 Living samples 206
 LM. *See* Light microscopy (LM)
 LNTs. *See* LAMP1-negative tubules (LNTs)
 Loss of an OMP 48
 LPS. *See* Lipopolysaccharide (LPS)
 Luciferase reporter gene fusion 65
 Luminex analyzer 6–9, 13, 14, 20, 21, 26
 Luminex 100/200 analyzer 8, 9, 20, 21, 26
 Luminex 200 analyzer 21
 Luminex beads 26
 Luminex[®] multiplex 1–26
 Luminex reader 4
 Luminex[®] xMAP[®] multiplexing system 3
 Luminex xPONENT software 13
luxAB genes 242
 Lymphatic tissue 227
 Lymphoid tissue 166
 Lysis 7, 9, 11, 41, 50, 103, 141, 238, 245, 246, 248, 254, 258, 266, 271
 Lysis Buffer 7, 9, 11, 41, 141
 Lysogen 99, 103, 238, 252, 253, 260
 Lysogenic 237, 238, 242, 251, 252, 257, 260
 Lysogenic conversion 238, 251, 257
 Lysogenic cycle 237, 238, 242
 Lysosomal-associated membrane protein 1 (LAMP1) 91, 200, 216
 LAMP1-GFP 201, 205, 208–210, 216
 LAMP1-tagging 210, 214

Lysosome-associated membrane proteins (LAMPs) 200, 218

Lytic 237–248, 253, 260, 269–274, 276, 277

Lytic cycle 237, 238, 276

Lytic phages 239–250, 277

Lytic virus 248

M

Macrophages 95, 99, 100, 103, 127, 153, 166, 178, 214

Madin-Darby canine kidney (MDCK)
epithelial cells 167, 171, 176, 178, 183, 187

MAGPIX System 7, 14

MagPlex®-TAG™ Microspheres 5

MALDI-TOF-TOF analysis 35, 41

Mannose-6-phosphate receptor (M6PR) 200

Mass spectrometry (MS) 29, 30, 35, 37–39, 44

Mass spectrometry (MS)-based quantitative proteomic analyses 29

Maximum intensity projection (MIP) 201, 205

mCherry 173, 201, 209, 210, 220, 222

MDCK cells. *See* Madin-Darby canine kidney (MDCK)
epithelial cells

Membrane bound biotin target sites 160

Membrane composition 127–162, 200
and integrity 127–162

Membrane pore-forming protein (holin) 238

Membrane protein fraction 128, 130, 131

Membrane ruffles(ing) 166, 167, 175, 176, 184, 232

Metabolic status 177

Microarrays 53, 118

Microbial protein synthesis 488

Microfluidics apparatus 177

Micropatterned cells 175

Microscopy 2, 90, 91, 129, 132, 142, 143, 147, 159, 165–193, 200, 201, 211, 213, 215, 218, 228, 231–234, 238, 243, 247, 257

Microscopy techniques 167–169

Microsphere or bead-based suspension arrays 3

Microtubule (MT), cytoskeleton 200

Microtubule-organizing center (MTOC) 200

Mini-transposon 97

MIP. *See* Maximum intensity projection (MIP)

Mitomycin C 238, 254, 255, 259, 262

MOIs. *See* Multiplicity of infections (MOIs)

Molecular detection, β -lactamase genes 53–55

Morphology 132, 147, 167, 172, 174, 175, 204, 249, 250, 265

Motility 2, 9, 26, 167, 175, 177

MS-MS spectra 29

Mucosa 140, 227

Mucus 227, 234

Mucus induction 227

Multidrug resistance (MDR) 48

Multiphoton (MP) microscopy 168

Multiple infections 3

Multiplexed bead sets 4

Multiplexed molecular assays 3

Multiplexing 3

Multiplex molecular bead array (assays) 3, 5

Multiplex PCR 6, 9, 54–56

Multiplex RT-PCR 8, 11–12

Multiplex RT-PCR/PCR 11–12

Multiplex test 3

Multiplicity of infections (MOIs) 33, 35, 40, 41, 100, 181, 210, 212, 217, 230, 234

Mung beans 273

Murine ileal loop model 127

Muscularis 227

Muscularis mucosae 227

Mutagenesis 63–64, 66–68, 76, 77
approaches 63, 68

Mutations 49–51, 59, 60, 63, 64, 67, 68, 75, 77, 78, 90, 103, 256

Myoviridae 238–245, 260–262, 272

Myoviruses 239, 254

N

Nalidixic acid resistance 49

Nanoparticle-coated *Salmonella* strain CRC2631
nanoparticles 153

Nanoparticles 139–148, 151–162
aggregation 161
cargo 151–162
construct 160
delivery 140, 160
load 159, 160
therapeutic approaches 154

Nipkow disk 169, 202, 221

Nomarski imaging 204

Non-infected cells 29

Non-phagocytic M cells 166

Non-typhoid 53, 58, 117–125

Non-typhoidal *Salmonellae* 53, 58, 119

Non-typhoidal *Salmonella* spp. 2

Non-typhoid human *Salmonella* infections
diagnosis 121

Non-typhoid human salmonellosis 120, 121

Non-typhoid *Salmonella* antibodies 119, 120

Non-typhoid *Salmonella* ELISA 117, 119

Norovirus 2, 6

Nucleic acids 3–5, 12, 24, 238
amplification 3
detection 4
extraction 7–9, 11
sequences 3

NucliSENS 7, 11, 15, 16

NucliSENS easyMAG system 15, 16

Nyquist sampling 170, 171, 192, 202

O

O and H antigens 8
 Oligonucleotide 64, 67–69, 74–76,
 78, 94, 96, 98, 101, 102
 capture probes 4, 6
 ligation 4
 primers 50–58
 sequences 4, 65, 66
 OMP. *See* Outer membrane protein (OMP)
 OmpA 134–137
 protein 129–130, 134, 135, 137
 Orphan podovirus 257
 Orthocluster analysis 239
 Orthologous genes 239, 240
 Outer membrane lipopolysaccharide 118–120,
 122–124, 141, 144, 237, 243–245, 251, 252, 254,
 257, 259, 267
 Outer membrane protein (OMP) 48, 167, 237,
 244, 245, 257, 259

P

P22 73, 77, 95, 99, 103, 249–255, 257–259, 261, 264
 PALM. *See* Photo-activated localization microscopy
 (PALM)
 Paraformaldehyde (PFA) 160, 173, 179,
 181, 182, 188, 212, 214, 215, 228, 229, 231, 232,
 260
 Parasites 1, 2, 5, 6, 9, 16, 237
 Paratyphoid fever 47
parC 50, 51, 59
parE 51
 Pathogenesis 63, 139, 166, 175, 260
 Pathogen–host interactions 30, 168, 228
 Pathogenicity 199
 Pathogenic lifestyle 63, 77, 200
 Pathogens 1–3, 5, 6, 14–17, 30, 48,
 81, 93, 124, 127, 139, 166, 200, 227, 271, 274,
 276
 Patient management 2
 pCold-TF plasmid 129, 134, 137
 PCR 4, 5, 7, 8, 11–13, 17, 19–21, 24, 25,
 50–60, 68–71, 73–78, 82–89, 95–98, 102,
 133–135
 products 51
 protocols 53
 targeting, flagellin 27–28
 Peptidoglycan-degrading lysin 238
 Peptidoglycan synthesis 48
 Peyer's patch tissue 172
 PFA. *See* Paraformaldehyde (PFA)
 PFGE. *See* Pulsed field gel electrophoresis (PFGE)
 pH 31, 32, 36, 37, 40–42, 49, 51–59, 69,
 90, 94, 95, 106, 108, 109, 113, 114, 122, 128–130,
 136, 141, 142, 144, 146, 157, 158, 166, 174, 179, 180,
 186, 187, 203, 211, 214, 228, 229, 231–233, 265, 272
 PHACTS 263

Phage_Finder 263
 Phages
 biocontrol 268, 271–276
 X(Chi) 242, 247
 FelixO1 243
 genera 239, 240
 genes 237, 238, 257, 262, 263
 λ Red recombination system 64, 94
 O1 242
 particles 238, 250, 262, 270
 phi92 243, 244
 PVP-SE1 241, 243, 244
 SETP3 241, 246
 Sf6 251, 254, 257
 SPN3US 241, 244
 SSE-121 243
 T4 241, 244, 261
 T5 245, 254, 261
 transduction 73, 77, 153, 238, 250,
 264, 268
 vB_EcoM-FV3 243
 vB_SenM-S16 241, 244
 Vi1 239, 241
 wV8 243
 Phage typing 238, 264–268
 procedures 265–266
 schemes 245, 265, 267–268
 Phagotherapy 268–275
 phAPEC8 243
 Phase contrast 167, 176–178, 193, 204
 Phase contrast microscopy 184–185
 PHAST 53, 263, 264
 Phax1 239
 Phi20 (GQ422450) 251
 phi92 243, 244
Phieco32likevirus 242, 249
 ΦEa21-4 243
 phiJLA23 (KC333879) 247
Phikmvlikevirus 248, 249
 phiKP26 (KC579452) 247
 Phi92likevirus 243
 φRNP 248, 249
 φSG-JL2 242, 249
 φSPB 242, 249
 ΦSboM-AG3 239
 ΦSH19 239, 241
 PhiSpy 263
 Photo-activated localization microscopy
 (PALM) 168, 201
 Photo-activation 170
Photobacterium profundum prophage
 PφPpr1 256
 Photobleaching 170, 182, 188,
 192, 193, 202–204, 209, 219–222
 Photodamage 169, 177
 Photomultiplier tubes (PMT) 169, 184, 192,
 202, 213, 220

Phototoxicity 191, 193, 202–204, 219–222
 Pili 167, 237, 267
 Pinholes 191, 192, 202, 213, 219
 aperture 169, 183, 201
 PI(3)P 176
 pJM22-BirA autodisplay vector construction 155, 156, 162
 pJM22-BirA plasmid 160
 Plasmids 48, 49, 51, 56–57, 64, 66–69, 71, 74–76, 78, 82–90, 94, 96, 97, 102, 103, 134, 135, 137, 156, 158, 160–162, 173, 207, 209, 214, 216, 233, 235, 268, 277
 pFPV25.1 209, 214, 233, 235
 pKD46 64, 71, 73–75, 83, 84, 88, 89, 94, 96, 102
 types 56, 60
 vectors 94, 154, 158, 277
P22likevirus 250–255
 PMT. *See* Photomultiplier tubes (PMT)
Podoviridae 238, 242, 248–257
 Podoviruses 239, 257
 Point mutations 49, 67
 Point-scanning systems 170
 Polarised epithelial cells 175, 187, 200, 210, 214, 230, 234
 Polarized epithelia tissue 172
 Population heterogeneity 166
 Post-infection complications septicemia 117
 Primer extension 4, 55
 Progeny viruses 237
 Prokaryotic 50S ribosomal subunit 48
 Promoters 64–67, 71, 76, 82–84, 102, 173, 174, 209, 238, 239, 248, 249, 251, 253, 258, 260, 261
 Prophage Finder 263
 Prophages 77, 237–277
 genes 262, 263
 induction 238
 regions 262
 Prophinder 263
 Prostate cancer cells 152, 153
 Protein profile changes 30
 Proteins 29, 48, 63, 81, 93, 106, 127–138, 140, 154, 166, 199, 237
 Erf 252
 secretion 65, 167
 Proteome changes 30
 Proteomic approach 29, 30
 Proteomic identification 29–44
Pseudomonas 93, 244, 257, 260, 271
Pseudomonas (LIT1, LUZ7) 250
 PSP3 260–262
 Pulsed field gel electrophoresis (PFGE) 49–50, 58, 59, 258, 264
 Pvplikevirus 243
 PVP-SE1 241, 243, 244

Q

QE. *See* Quantum efficiencies (QE)
 QRDR. *See* Quinolone resistance-determining region (QRDR)
 Quantification of *Salmonella* isolate DNA 17–19
 Quantitative immunolabelling 174
 Quantitative proteomics 29–44
 Quantum efficiencies (QE) 202
 Quantum yield (QY) 188, 203
 Quinolone resistance 49–51, 59
 Quinolone resistance-determining region (QRDR) 49–51, 59
 QY. *See* Quantum yield (QY)

R

Rab7 200
 Rapid diagnosis 3
 Reactive arthritis 117, 119, 120
 Real-time 3, 173, 176
 RecA 252, 259
 protein 256
 Receptors 237, 241, 243–245, 247, 248, 251, 253, 255, 257, 259, 267
 Recombinant OmpA protein 129–130, 135, 137
 Recombinant Stn protein 129, 130, 133–135, 137, 138
 Recombineering 63–78, 153
 of epitope tags 65
 procedure 64–65
 Redistribution of proteins 176
 Red-mediated mutagenesis 76
 RedoxSensor™ kit 178
 Red recombination 64, 73, 77, 94
 Region of interest (ROI) 74, 204, 213, 220, 222
 Relapse rate 48
 Replication 81, 89, 97, 102, 166, 175, 210, 217, 237, 238, 245, 248, 252, 253, 258, 261
 Reporter fusion 64, 65
 Resistance 47–60
 to ampicillin 89, 97
 cassette 64, 66, 68, 73, 77, 82–84
 genes 53, 64–67, 82, 83, 88, 99, 102, 268
 to nalidixic acid 49
 profiling 2
 Resolution 106, 167–172, 175, 177, 183, 185, 187, 191, 200–204, 207, 211, 213, 218, 219, 244
 Respiratory viral pathogens 3
 Restriction fragment length polymorphisms (RFLP) analysis 51, 59
 Reverse transcription PCR (RT-PCR) 3, 8, 11–12
 RFLP analysis. *See* Restriction fragment length polymorphisms (RFLP) analysis
 RFP 205, 213, 218, 220, 222

Ribosomal *rpsM* promoter 209
 Rifampicin-resistant 248, 250
ROI. *See* Region of interest (ROI)
Roseovarius 250
 RT-PCR. *See* Reverse transcription PCR (RT-PCR)
Ruegeria (DSS3φ2) 250
rV5 243

S

SAF. *See* Software autofocus (SAF)
 Safety considerations 209, 274–275
Salmonella 1–26, 29–44, 47–60, 63–78, 81–91, 93–104, 117–125, 127–140, 143, 146, 151–162, 165–193, 199–223, 227–235, 237–277
 adherence 166, 176
 antibodies 119–121, 171, 183
 antigen gene target sequences 6
 bacteria 41, 42, 154
 bacteriophages 266–268, 270, 271, 273
 biofilms 167, 170, 228
 detection 1–26, 120
 ELISAs 119–121
 flagella 245
 infection 29, 33, 42, 48, 117–121, 165–166, 168, 170, 172–177, 205, 270, 271, 276
 invasion 172, 175, 176, 181, 232
 isolates 2, 17–19, 21, 22, 120, 242, 244, 247, 264–265, 267
 membrane 154, 156–161
 morphology 132
 outer membrane protein OmpC 244
 phages 237–277
 Potsdam 261
 prophages 237–277
S. enterica, serovar Anatum ε15 lysogens 253
 therapy 153
 viability macrophages 178
 virulence 77, 78, 127
 gene expression 166
Salmonella-AuNP conjugates 161
Salmonella-containing vacuole (SCV) 81, 166, 176, 177, 200, 210
 biogenesis 166
 membrane 210
Salmonella effector
 SseK1 94
 translocation 82
Salmonella enterotoxin (Stn) 127–140
Salmonella–host cell interactions 166
Salmonella–host interactions 130
Salmonella-induced filaments (SIFs) 81, 170, 199–201, 210, 219
 dynamics 200, 201
Salmonella-induced “membrane ruffles,” 166, 167, 175
Salmonella-induced secretory carrier membrane protein 3 (SCAMP3) tubules (SIST) 200
Salmonella-induced virulence 210
Salmonella-infected cells 35, 175
Salmonella pathogenicity island 1 (SPI-1) 93, 166, 175, 232
 gene expression 227
Salmonella pathogenicity island 2 (SPI2) 93, 94, 200
 effectors 200
Salmonella pathogenicity island 4 (SPI4) 200
Salmonella pathogenicity islands (SPI) 63, 199
 gene expression 177
Salmonella-specific ELISAs salmonellosis 118
Salmonella typhimurium infection 29–44
 Salmonellosis 117–121, 264, 266–271, 273, 276, 277
 SAPE reporter 9, 26
 SBA-171 242
 Scanning electron microscopy (SEM) 142, 147, 167, 172, 175, 180, 185–186, 231–232
 Scarless chromosomal modifications 78
 Scarless chromosomal mutations 64
 Scarless mutagenesis 66–67, 77
 Screening
 for *aac(6')*-*Ib-cr* gene 52
 for plasmids in non-typhoidal *Salmonellae* 56–57
 for *qnr* genes 51–52
 SCV. *See* *Salmonella*-containing vacuole (SCV)
 SCV-associated compartments 177
 SDCM. *See* Spinning disk confocal microscopy (SDCM)
 SE1 (NC_011802) 251
 Secondary bacteremia 165
 Secondary infections 3
 Secretion 65, 81, 89, 90, 93, 94, 127, 167, 174
 Secretory pathway 30, 31
 SEM. *See* Scanning electron microscopy (SEM)
 Septation 177, 178
 Sequence analysis 55, 137, 252, 267
 of *gyrA* 51
 Seroconversion 120, 121
 Sero-diagnosis 120
 Widal test 118
 Sero-incidence 121
 Serological antibody assays 118
 Serological diagnosis 118
 Serological methods 118, 119
 Serological tests 118
 Serology 117–121
 Serosa 227
 Serotypes 2, 8, 16–19, 21–23, 26, 59, 117, 264, 265
 determination 3
 Serotype-specific antigens 6
 Serotype-specific markers 8
 Serotyping 1–26
Serratia marcescens 247

SFP10.....239
*Shigella*2.....6, 17, 93, 239, 241
Shigella phage.....239, 251
Shigella phage Sf6.....251
SIFs. *See* *Salmonella*-induced filaments (SIFs)
Signal-to-noise ratios (S/N).....21, 171, 172, 202
Signal transduction pathways.....93
SiiE.....77, 199, 200
SILAC. *See* Stable isotope labeling by amino acids in cell culture (SILAC).....
Simplex PCR.....56
SipA.....174
Siphoviridae.....238, 241, 242, 244–248, 257–260
Siphoviruses.....239, 245, 246, 254, 260
Site-directed mutagenesis.....76
Skimming motility.....175
SKML-39.....239, 241
SL476.....251
SNX1-GFP.....177
Software autofocus (SAF).....206, 207, 222
SopE2.....174
SopE φ260, 262
Sorting nexin (SNX) tubules.....200
SP6.....242, 248, 249
Spacious vacuole-associated tubules (SVAT).....200
SPC35 EPS7.....245
Specificity, *Salmonella* bacteriophages.....266–267
Spectral characteristics.....3
Spectral identities.....3
Spectra stable isotopes.....31
SPI. *See* *Salmonella* pathogenicity islands (SPI)
SPI2-encoded T3SS.....200
Spinning disk.....177
 microscopes.....175
 systems.....170
Spinning disk confocal microscopy
 (SDCM).....201, 202, 205, 208, 211, 213, 215, 223
SPI-1 T3SS.....175, 199, 200
Sp03unalikevirus.....242, 246
Sp6likevirus.....242, 248, 249
Sp058likevirus.....250
Sp062likevirus.....250
Split GFP method.....174
SPN19 (JN871591).....247
SPN3US.....244
SPT-1.....241, 242, 272
SptP.....174
SSE-121.....241, 243
ST104.....149, 254, 255
ST160.....251
Stable isotope labeling by amino acids in cell culture
 (SILAC).....29–31, 33–36, 39, 41, 42, 44
 approach.....31
 experiments.....29, 30, 33, 35–36, 41, 42
 quantitative analysis.....39
Stably transfected cell lines.....209, 210, 215, 216
Standardised ELISA.....119–122
StatQuant program.....39
Stimulated emission depletion microscopy (STED).....200
STML-13-1.....239, 241
STML-198.....241, 244
Stn activities.....127, 128
Stn function.....128
Stn gene-deleted *Salmonella*.....131, 132, 134
Stn-OmpA complex.....137
Stn protein.....127–138
Stochastic optical reconstruction microscopy
 (STORM).....201
Stool culture.....2
Stool sample.....11
Stool sample preparation and pretreatment.....8
Stool specimens.....5, 15, 24
Stool testing.....3
STORM. *See* Stochastic optical reconstruction microscopy
 (STORM)
Strain CRC631.....153
Strain CRC2631.....153, 156, 157
Streptavidin-associated nanoparticles.....154–161
Streptavidin-conjugated cargo.....161
Streptavidin-conjugated fluorophores.....154, 156
Streptavidin-conjugated nanoparticles.....154, 160
Streptomycin.....31, 33, 41, 48, 93, 228
Structural information.....167, 200
Structural proteins.....238, 245, 246
Structured illumination microscopy.....168
ST64T.....249, 251, 254–255
Submucosa.....227
Sucrose-coated gold nanospheres.....157
Sucrose-coated nanoparticles.....159
Sucrose-conjugated gold nanoparticle load.....159
Sucrose conjugation.....154, 156–159
Sucrose-gold nanoparticles.....154, 156–159, 161
Sulfamethoxazole.....48
Sulfitobacter (EE36 φ 1).....250
Sulfonamides.....48
Superinfection.....238, 252, 255, 259
Superparamagnetic beads.....5
Super-resolution microscopy techniques.....168, 200
Surface biotinylation.....154–161
Symbiotic bacteriophages.....262
Synthetic DNA.....68, 76–78

T

Tagging, effector proteins.....174
TagRFP-T.....204, 205, 222
TAG sequences.....4, 5
Tailspikes.....239–241, 244, 249–251, 253, 254, 257
Target DNA.....4, 78
Target sequence.....4–6, 67, 82
Target-specific PCR.....4, 5

Target-specific primers 5
 Target strain 65, 74–77
 Taxonomy 237–277
 TEM-1 beta-lactamase 174
 Temperate *Myoviridae* 260–262
 Temperate phages 238, 239, 250–262
 TEM-1-tagged proteins 174
 Tetracyclines 48
 resistance 66, 68
 TF. *See* Transfection (TF)
 Therapeutic agents 238, 239
 Therapeutic nanoparticles 152, 153
 Therapeutic properties 152
 Therapeutic *Salmonella* 153, 154, 160, 271, 276
 Therapy 2, 151–153, 160, 239, 268–271, 275, 276
 Time-lapse acquisition 201, 206
 Time-lapse phase contrast 176, 184–185
 Time-lapse SIF 201
 Time-lapse studies 177
 T1-like phages 246
T4likevirus 241, 244
T5likevirus 245
T7likevirus 248
T4likevirus genus 244
T5likevirus genus 245
T5likevirus phage T5 245
 Total internal reflection fluorescence (TIRF) 209
 Toxicity 48, 152, 153, 160, 202, 204, 219–222
 Toxigenicity 238
 Transcription 3, 237, 238, 245, 248–250, 253, 256, 258
 Transducing particles 238, 252, 264
 Transducing phages 238, 257
 Transduction 73, 77, 93, 153, 238, 250, 264, 268
 Transfection (TF) 129, 134, 137,
 207–209, 211, 212, 214–216, 219
 Transgenic adenocarcinoma of mouse prostate
 (TRAMP) 153
 Translational fusions 93–104
 Translocated effector proteins 174
 Translocation 81, 90–91, 93, 94, 103, 167, 174, 200
 of effector proteins, immunolabelling 174
 pores 167
 Transmission electron microscopy (TEM) 49, 53,
 132, 147, 154, 159, 167, 172, 174, 175, 200,
 232–234
 Transposons 63, 94
 Trimethoprim–sulfamethoxazole 48
 co-trimoxazole 48
 resistance 48
 TRITC-phalloidin 188
 T3SS. *See* Type III secretion systems (T3SS)
 T3SS1 93, 98, 103
 T3SS2 93, 94, 98
 Tumors 151–162
 cells 152
 destruction 153
Tunalikevirus 246–247
 Type III secretion systems (T3SS) 81, 93, 127,
 166, 167, 175, 199, 200
 effectors 93, 94
 Type I secretion system (T1SS) 200
 Typhoidal *Salmonella* (TS) 49, 58–60
 Typhoid fever 47, 48, 118, 119,
 121, 127, 165, 166, 199, 270
 Typhoid (enteric) fever 117
 Typhoid non-typhoid types 117
 Typing 15, 238, 239, 245, 264–268

U

UAB_Phi78 (NC_020414) 249
 Uncaging 170

V

Vacuolar escape 175
 vB_CsaM_GAP31 243
 vB_EcoM-FV3 243
 vB_EcoS_Rogue1 247
 vB_SenM-S16 241, 244
 Vector development 238
 Vi1 239
 Viability 177, 178, 185, 193, 234
Vibrio 6, 244, 275
Vibrio phage 245
 Vi capsular polysaccharide 167
 Vi1-like viruses 239, 241
 Viral nucleic acids 238
 Viral transcription 238
 Viral vectors 209, 210
 Virulence
 factors 93, 127
 functions 63
 gene expression 166
 genes 63, 166, 259
 phenotype 63, 210
 properties 63, 77
 Virulent (lytic) phage 238, 248, 273
 Viruses 1, 5, 6, 16, 237–239, 241,
 243–248, 250
Viunalikevirus 239–242
V5likevirus 241, 243–244
V5likevirus (rV5, FV3) 241, 243–244
 V5virinae 243
 vW8 243

W

WFM. *See* Widefield microscopy (WFM)
 White–Kauffmann–Le Minor scheme 2, 21
 Widal tube agglutination test 118

Widefield microscopy (WFM).....168–172,
175–177, 189, 191, 192, 201, 202

CCD camera168

deconvolution172

live cell imaging (*Salmonella* infection).....169, 177, 179

wV8243

X

xMAP bead-based array5

xMAP Salmonella Serotyping Assay
(SSA)5, 8, 9, 17–24, 26

data acquisition protocols21

xTAG Gastrointestinal Pathogen Panel
(GPP)5–7, 9–18, 23–25

clinical studies.....14

data acquisition protocols13

target regions15

xTAG GPP Kit Package Insert14, 23, 25

xTAG GPP (LX) protocol14

xTAG GPP (MP) protocol14

xTAG universal array system5

Y

Yersinia93

Y. enterocolitica6, 119, 120, 124

Z

Zoonotic disease, *Campylobacter*121

Zoonotic serovars117

Z-stacks201, 204–206, 213,
219, 222, 223

Z-stack software206

